(2)

Ocean Engineering Studies

Compiled 1990

Volume II: Acrylic Submersibles

J. D. Stachiw

PUBLISHED BY
NAVAL OCEAN SYSTEMS CENTER
SAN DIEGO, CALIFORNIA

Foreword

Exploration of hydrospace requires manned and unmanned underwater vehicles capable of carrying observers and/or electro-optical devices to the very bottom of the sea. In either case, the vehicles must be provided with viewports through which the occupants can observe, and the cameras can record, the environment around them. Windows in these viewports must not only be clear but also strong enough to withstand the external hydrostatic pressure exerted by a column of water extending from the vehicle to the water's surface.

Pressure-resistant, acrylic-plastic windows were introduced into submersibles in 1947 by Professor Piccard. Since then, these windows have seen extensive service on undersea vehicles where they provided the occupants a clear, but limited view of hydrospace. However, even vehicles equipped with multiple viewports do not afford the occupants the desired panoramic view of the environment outside the vehicle. On the contrary, they accentuate the occupants' feelings of being enclosed in an opaque box with multiple peepholes that allow only tantalizing glimpses of the colorful environment.

This burdensome obstacle to unimpeded visual exploration of hydrospace could be eliminated by providing the crew of the submersible with a pressure-resistant, transparent cockpit. This cockpit would be mounted on top or in front of the opaque housing that encloses the functional subsystems of the submersible. To convert this concept into reality, many technical problems had to be solved. A transparent material with desirable structural properties had to be selected; a pressure-resistant enclosure, compatible with the structural characteristics of the material, had to be designed; and one, or several, economical fabrication techniques had to be developed.

The Navy achieved the goal of a crew compartment that was transparent with panoramic visibility, when, in 1970, the Naval Facilities Engineering Command launched the world's first two-man transparent submersible, *Nemo*, that had an operational depth of 600 feet. The pioneering transparent cockpit design gave rise to a whole class of oceanographic submersibles with transparent compartments and with a depth rating that has gradually been extended to 3000 feet by improving the structural performance of the transparent enclosure.

To preserve and disseminate the new engineering knowledge gained during the development of the transparent, pressure-resistant crew compartments for oceanographic submersibles, all the technical reports published on this subject have been collected. They are presented to the ocean engineering community in Volumes 1 and 2 of this monograph. This information should prove very helpful to any engineer contemplating the design of transparent, pressure-resistant, spherical hulls for submersibles.

J. D. Stachiw
Marine Materials Office
Ocean Engineering Division

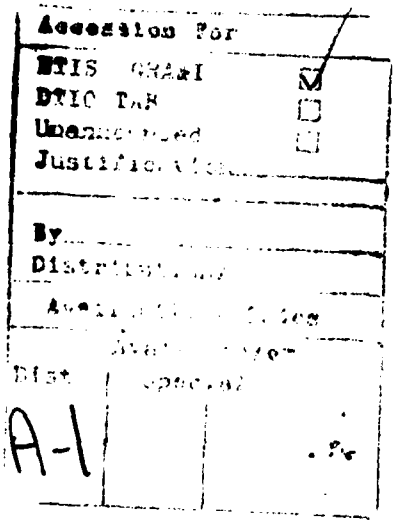

TABLE OF CONTENTS: VOLUME II

NUC TP 493

IMPROVED FABRICATION PROCESS FOR SPHERICAL ACRYLIC PLASTIC SUBMERSIBLE HULLS

by

J. D. Stachiw
OCEAN TECHNOLOGY DEPARTMENT

December 1975

NAVAL UNDERSEA CENTER, SAN DIEGO, CA. 92132

AN ACTIVITY OF THE NAVAL MATERIAL COMMAND

R. B. GILCHRIST, CAPT, USN
Commander

HOWARD L. BLOOD, PhD
Technical Director

ADMINISTRATIVE INFORMATION

The work described in this report was performed between June 1972 and June 1973 as part of an investigation into man-rated transparent submersibles for deep operation. It was funded through the Independent Research and Independent Exploratory Development Program at the Naval Undersea Center under subproject task area number ZF-61-412-001.

Released by
H. R. TALKINGTON, Head
Ocean Technology Department

ACKNOWLEDGMENTS

The fabrication and testing of the model 2000B spherical acrylic plastic hull represent the combined efforts of Adroit Engineering, San Diego, Calif., who designed the hatches and molds; Polymer Products, Oakland, Calif., who made the acrylic castings; and Southwest Research Institute, San Antonio, Texas, who tested the finished assembly. The successful completion of this work is due to the support of H. R. Talkington, Head of the Ocean Technology Department at the Naval Undersea Center, and Dr. W. B. McLean, retired technical director of the Naval Undersea Center. The report was reviewed for technical accuracy by K. O. Gray.

UNCLASSIFIED

SECURITY CLASSIFICATION OF THIS PAGE (When Data Entered)

REPORT DOCUMENTATION PAGE		READ INSTRUCTIONS BEFORE COMPLETING FORM
1 REPORT NUMBER TP 493	2 GOVT ACCESSION NO.	3 RECIPIENT'S CATALOG NUMBER
4 TITLE (and Subtitle) Improved Fabrication Process for Spherical Acrylic Pressure Hulls		5 TYPE OF REPORT & PERIOD COVERED R&D, June 72-June 73 6 PERFORMING ORG. REPORT NUMBER
7 AUTHOR(s) J. D. Stachiw		8 CONTRACT OR GRANT NUMBER(s)
9 PERFORMING ORGANIZATION NAME AND ADDRESS Nayal Undersea Center San Diego, Ca. 92132		10 PROGRAM ELEMENT, PROJECT, TASK AREA & WORK UNIT NUMBERS ZF-61-412-001
11 CONTROLLING OFFICE NAME AND ADDRESS Naval Undersea Center San Diego, Ca. 92132		12 REPORT DATE December 1975 13 NUMBER OF PAGES 152
14 MONITORING AGENCY NAME & ADDRESS(if different from Controlling Office)		15 SECURITY CLASS (of this report) Unclassified 15a DECLASSIFICATION/DOWNGRADING SCHEDULE

16 DISTRIBUTION STATEMENT (of this Report)

Approved for public release; distribution unlimited.

17 DISTRIBUTION STATEMENT (of the abstract entered in Block 20, if different from Report)

18 SUPPLEMENTARY NOTES

19 KEY WORDS (Continue on reverse side if necessary and identify by block number)

20 ABSTRACT (Continue on reverse side if necessary and identify by block number)

This report describes an improved process for fabricating spherical acrylic plastic pressure hulls within close dimensional tolerances. The process consists of casting acrylic plastic hemispheres in a precision mold assembly, machining their equatorial edge and cutting polar penetrations, bonding them together with a cast-in-place equatorial joint, polishing their inner and outer surfaces, and installing an aluminum hatch and penetration plate. The cost of the improved process is approximately 50 percent less than that of the standard process, which

DD FORM 1 JAN 73 1473 EDITION OF 1 NOV 65 IS OBSOLETE

UNCLASSIFIED

SECURITY CLASSIFICATION OF THIS PAGE (When Data Entered)

20. Abstract (continued)

consists of bonding together 12 thermoformed and machined spherical pentagonal shell sections. In addition, 90 percent fewer bonded joints are required, resulting in an order-of-magnitude improvement in optical qualities. A full-scale prototype with an outside diameter of 66.500 inches and an inside diameter of 58.000 inches has been constructed and shown to be acceptable for manned service to a depth of 2500 feet by hydrostatic testing under sustained loading at pressures of 900, 1350, 1800, and 4000 lb/in^2. Implosion occurred after 13 minutes of sustained loading at 4000 lb/in^2 and 75°F (simulated depth of 9000 feet).

SUMMARY

This report describes an improved process for fabricating spherical acrylic plastic pressure hulls within close dimensional tolerances. The process consists of casting acrylic plastic hemispheres in a precision mold assembly, machining their equatorial edge and cutting polar penetrations, bonding them together with a cast-in-place equatorial joint, polishing their inner and outer surfaces, and installing an aluminum hatch and penetration plate. The cost of the improved process is approximately 50 percent less than that of the standard process, which consists of bonding together 12 thermoformed and machined spherical pentagonal shell sections. In addition, 90 percent fewer bonded joints are required, resulting in an order-of-magnitude improvement in optical qualities. A full-scale prototype with an outside diameter of 66.500 inches and an inside diameter of 58.000 inches has been constructed and shown to be acceptable for manned service to a depth of 2500 feet by hydrostatic testing under sustained loading at pressures of 900, 1350, 1800, and 4000 lb/in^2. Implosion occurred after 13 minutes of sustained loading at 4000 lb/in^2 and 75°F (simulated depth of 9000 feet).

CONTENTS

INTRODUCTION

Since the spherical shape provides optimal resistance to external hydrostatic pressure (ref. 1-6), it was chosen for the first acrylic plastic pressure hull, used on the manned submersible NEMO (ref. 7-11). Though limited to an operational depth of 600 ft, NEMO proved the feasibility of this kind of hull and the value of panoramic visibility underwater (ref. 12). MAKAKAI, the second Navy submersible of this class, used the same hull design as NEMO and also had an operational depth limitation of 600 ft (ref. 13). When the Smithsonian Institution built JOHNSON SEA LINK I, a spherical acrylic plastic pressure hull similar to those used on NEMO and MAKAKAI was chosen; the design of hull and hatches was modified, however, to permit operation to a depth of 1000 ft (ref. 14-15). Finally, during design of JOHNSON SEA LINK II for the Harbor Branch Foundation, hull and hatches were further improved, and a depth capability of 3000 ft was obtained (ref. 16).

The only shortcoming of the model 600, 1000, and 2000 hulls used on NEMO, MAKAKAI, and JOHNSON SEA LINK was their fabrication from multiple spherical pentagonal units (figure 1a). This method of fabrication resulted in more than 50 feet of bonded joints, requiring a large amount of hand labor and producing frequent optical discontinuities in the hull (ref. 17). For this reason an experimental study was undertaken jointly by the Naval Undersea Center and the Harbor Branch Foundation to develop a method of fabricating spherical acrylic plastic hulls from two hemispherical sections with a single equatorial joint (figure 1b).

The development of the improved fabrication process was planned to proceed in two steps. The objective of the first step was to show the feasibility of a precision casting process that would produce hemispheres requiring no machining of their spherical surfaces. This objective was accomplished by casting hemispherical windows with an inside diameter of 10 inches and outside diameter of 18 inches and testing them to show that they were acceptable for manned submersibles (ref. 4).

The second part of the study addressed itself to applying the casting process developed in the first part to full-sized spherical hulls. This report describes the work performed, which resulted in the model 2000B spherical acrylic plastic pressure hull with an operational depth rating of 2500 feet.

DESIGN AND FABRICATION

The focus of the study was the model 2000 hull developed for JOHNSON SEA LINK II. This hull, shown in figure 2, represented the most advanced model in the series and therefore had the greatest potential value to prospective users. In addition, the Harbor Branch Foundation had a requirement for two pressure hulls with at least a 2000-foot depth capability. Thus, if tooling could be developed for casting the model 2000 hull in hemispherical rather than pentagonal sections, it would be available without additional cost for fabrication of these hulls.

HULL DESIGN

The objective was to develop a hull design whose performance under hydrostatic loading would be identical to that of the model 2000 hull assembled from 12 thermoformed plexiglas-G spherical pentagons of four-inch thickness. This presented a problem, since tests conducted in phase I of the study showed that although the acrylic plastic resulting from the precision casting process developed by Polymer Products met Navy and ASME specifications (ref. 18) for man-rated acrylic windows and hulls, it had approximately 10 percent lower yield strength than Plexiglas G.

To approximate the structural performance of the model 2000 hull it became necessary to increase its minimum four-inch wall thickness by at least 10 percent (figure 3). Since decreasing the inner diameter of the hull would make the interior more cramped for the crew, most of the increase was accomplished by increasing the outer diameter of the spherical shell. No other changes were made at that time to the original design. As a result both the hatch and bottom penetration assemblies designed previously for the model 2000 capsule could be utilized in the model 2000B hull with only minor modifications. The modifications consisted of increasing the width of the polycarbonate insert from 4.875 inches to 5.000 inches and decreasing the thickness of the insert flange from 0.905 to 0.750 inch. These minor modifications accommodated the polycarbonate insert originally designed for a four-inch wall thickness to the 4.4-inch wall thickness of the model 2000B hull.

TOOLING

Tooling for the precision casting of acrylic plastic hemispheres for the model 2000B hull consisted of a mold assembly, an autoclave cart, and a strongback. All tooling components were designed by Adroit Engineering, San Diego, California.

Mold Assembly

The mold assembly consisted of a matched set of male and female molds (figure 4). Considerable thought went into the design of the mold assembly. It was to serve as the form for gelling and polymerization of the acrylic plastic and as a power assisted jig for separating the polymerized casting from the mold. In addition, the mold assembly had to fit into the autoclave, where polymerization took place under elevated temperature and pressure.

The mold assembly was patterned after the mold developed during phase I for the hemispherical window castings. The major components were the female mold (serving as the foundation for four flanged wheels), the male mold (serving as the foundation for six hydraulic lifting jacks and six elevation adjusting screws), and a manually operated hydraulic pump (for pressurization of the hydraulic jacks). The whole assembly was fabricated from welded low-carbon steel. The nominal wall thickness of the female mold was 0.5 inch and of the male mold 0.75 inch. Both molds were reinforced with meridional and circumferential stiffeners to maintain their sphericity during and after machining (figures 5 and 6). The male mold was made from thicker steel than the female mold because it was thought that it might buckle under external pressure, exerted by the shrinking plastic, during the polymerization process inside the autoclave.

The hydraulic jacks mounted on the extensions of the male mold served to separate it from the polymerized casting (figure 7). Since the shrinkage of the casting was known to be in the 5 to 10 percent range, a substantial grip would be exerted on the male mold. To overcome this grip each of the jacks was designed to exert up to 10 tons of thrust against the equatorial edge of the casting. A manually operated hydraulic pump provided pressurized oil through flexible hoses to the jacks.

The thrust of the hydraulic jacks was augmented by air pressure applied through a fitting in the bottom of the mold to the interface between mold and casting (figure 8a). This provision was found to be very helpful, since the jacks alone could not always insure separation between the mold and the casting.

The separation of the female mold from the casting was accomplished by pressurized water pumped into the annular space between mold and casting through a fitting located at the very bottom of the mold. After the separation was accomplished, further influx of water made the casting float up in the mold till a lifting jig could be attached to it (figure 8b).

The elevation adjusting screws, located on the extensions of the male mold, were used for adjusting the clearance between the bottom of the male mold and the female mold. They also helped to locate the center of the male mold in the center of the female mold. With the help of these screws it was possible to center the male mold within 0.030 inch of the desired location.

Flanged wheels, attached to the lower external circumferential stiffener on the female mold, were designed for moving the mold assembly on rails in and out of the autoclave located at Polymer Products. In this manner, the mold assembly could be easily filled with casting mix outside the autoclave and then moved on rails into the autoclave without disturbing the gelling mixture.

Autoclave Cart

The autoclave cart consisted of a box frame supported by four flanged wheels whose spacing matched that of the narrow track extending from the interior of the autoclave into the general work area. The cart was designed to support the assembled castings during bonding of the equatorial joint and subsequent polymerization of the adhesive inside the autoclave (figure 9).

Strongback

The strongback consisted of a circular frame with a lifting sling. The diameter of the circular frame was smaller than the outer diameter of the casting, permitting the casting to be lifted from the female mold after it was partially raised by water (figure 10). The strongback was attached to the casting by disassembling it into two halves, placing them around the casting, and clamping them together with bolts.

CASTING AND INSPECTION

Casting Process

The casting process developed previously for this purpose by Polymer Products of Oakland, California, consisted of five distinct steps: (1) mixing of resin with additives; (2) pouring of resin mix into the mold assembly; (3) gellation of resin mix in the mold at atmospheric pressure and temperature; (4) polymerization of gelled resin mix inside the autoclave under elevated temperature and pressure; and (5) removal of the polymerized casting from the mold.

Mixing of acrylic (figure 11) with the required additive took place under atmospheric pressure and temperature. The same ratio of acrylic to polymer powder, catalyst, and cross-linking initiator was used as in phase I of the study. The mixing was performed by hand with an electric rotary mixer in five gallon batches (figure 12), followed by degassing under vacuum. The degassed resin mix was then, after some further manual mixing (figure 13), poured into the mold assembly whose surfaces were scrupulously cleaned (figures 14, 15, 16) and protected from dust by plastic sheets. The mixing of batches was repeated until the mold was filled.

Gellation of the casting inside the mold assembly took place under atmospheric pressure and temperature. The length of time required for gellation varied with temperature, but as a rule several hours were sufficient.

Polymerization of the gelled resin mixture took place inside a horizontal autoclave. The resin-filled mold assembly was rolled into the autoclave on tracks extending from the general assembly area. The pressurization and heating schedule was the one developed (ref. 17) previously for this purpose by Polymer Products in phase I of the study. Record was kept of the pressures and temperatures during the polymerization process so that any malfunction of the autoclave system could be detected and its effect on the physical properties of the castings noted.

The crucial step in the polymerization process was the separation of the male mold from the already polymerized but still hot casting. The separation was achieved by simultaneously applying air pressure to the fitting in the bottom of the mold and hydraulic pressure to the six hydraulic jacks spaced around its circumference. After the mold had been raised about two inches, it was placed on wedges resting on the rim of the female mold. Upon completion of this step the door to the autoclave was closed again and the gradual lowering of ambient temperature initiated.

The lifting of the male mold generated a small clearance between it and the interior surface of the casting. Because of this clearance, cooling of the casting could take place without the generation of tensile hoop stresses in the rim of the casting. If the casting had been cooled to ambient atmospheric temperature without prior release of the male mold, tensile cracks would have appeared. Opening of the autoclave door and rolling out of the mold assembly completed the polymerization process (figure 17).

Removal of the casting from the mold assembly was accomplished in the general work area outside the autoclave. First, the male mold was removed with a forklift. Second, the casting was partially raised inside the female mold by injecting tap water through the

bottom of the mold into the interface between mold and casting (figure 18). Third, the split strongback frame was clamped around the casting protruding from the mold, and the casting was lifted with the forklift from the mold (figure 19).

Inspection

After removal from the mold, the casting was subjected to an inspection whose objectives were to determine its quality. The inspection included visual observation, dimensional measurement, and testing of material specimens to determine their physical properties.

Visual observation was conducted utilizing transmitted sunlight as the source of illumination. The observation focused on the smoothness of the casting surfaces, the clarity of the casting, and the size and number of voids.

The concave and convex surfaces possessed the same surface roughness (about 64 microinches rms) as the Teflon-coated metallic molds, and no further finishing was required except fine sanding and polishing (figure 20). Of the five hemispheres cast, only one exhibited surface irregularities caused by separation of the casting from the mold during the polymerization process (figure 21). The surface irregularity was repaired by casting a thin overlay followed by rough sanding that brought the finished surface to the required thickness and sphericity. One of the castings exhibited meridional cracks. They were caused by failure of temperature control in the autoclave, resulting in sudden cooling of the casting prior to removal of the male mold (figure 22).

The equatorial edge of the castings was in the form of a meniscus with two-inch depth caused by shrinking of the resin mix during the polymerization process (figure 23). This was as expected and allowed for in the design of the mold assembly.

The clarity of the casting was equivalent to that of Plexiglas G of similar thickness. After fine sanding and polishing of inner and outer surfaces, the casting was found to satisfy the proposed ASME requirement for clarity in acrylic plastic viewports.*

The number of voids varied from one casting to another. Some castings had none, while others had more than ten. The voids were in almost every case located in the midplane of the shell thickness and several inches below the equator. They varied in shape but as a rule were elongated, about one inch diameter and two to four inches long.

Since the presence of such voids (figure 24) was unacceptable from the structural and optical viewpoints, small holes were drilled from the equatorial edge of the casting and the voids filled with standard casting mix. The mix was subsequently polymerized by placing the casting back in the autoclave and subjecting it to the required pressure and temperature regimen. Visual inspection after polymerization showed a significant improvement (figure 25). Before the repair, the voids reflected most of the incident light; now they transmitted it in a largely coherent manner. However, even though the refilled voids represented an order-of-magnitude optical improvement, they still were not deemed acceptable. As a result, they were routed out completely and refilled again, utilizing the standard casting mix and polymerization process.

**Clear print of size 7 lines per column inch and 16 letters to the linear inch shall be clearly visible when viewed from a distance of 20 inches through the thickness of the casting with opposite faces polished (ref. 19, 20).*

The improvement achieved by the second recasting was still more significant (figure 26). The repair could now be detected only by moving a printed newspaper page along one surface while the observer watched for minute distortion of the print image at the boundary of the recast void. The credit for this result was given to routing, which created large cavities with smooth vertical walls and large openings. The vertical walls prevented entrapment of gas bubbles during pouring of the casting mix, while the large opening allowed for adequate degassing of the mix once it was poured.

Dimensional measurements were aimed at determining the actual wall thickness of the castings at all locations. There was little need to check sphericity, which always closely conforms to that of the mold. Since the mold surfaces were machined within ±0.060 inch of the specified radius, the sphericity of the castings was more than adequate to meet U.S. Navy specifications for man-rated spherical pressure hulls of acrylic plastic.*

The reason for checking wall thickness was that the male mold might not have been aligned properly with the female mold. If the alignment was not proper, the wall thickness would vary from point to point on the hemisphere even though the sphericity of the surfaces was within specification.

The wall thickness of the hemispheres was found to vary from one location to another, with the largest deviation found at the pole. Thus, the minimum thickness at the pole was found to be 4.107 inches, while around the circumference at the equator it varied from 4.370 to 4.210 inches. Since the variation in thickness around the equator was less than the specified tolerance of 0.200 inch, it was considered to be within the range of permissible thickness tolerances imposed by machining tolerances of the molds, and thus acceptable. The variation in thickness between the equator and the pole of the hemisphere, however, was considered not to be acceptable, since it was approximately 0.093 inch below the minimum specified thickness of 4.200 inches.

To avoid this problem in future hemispherical castings produced in the existing 66-inch mold by Polymer Products, the elevation of the male mold inside the female mold will be raised by 0.125 inch. Thus, new castings will have a thickness that does not exceed the 4.200-to-4.400-inch range at any location.

The physical properties of the castings were determined by testing material specimens cut from the poles, the future location of metallic hatches. Two specimens were used per test for each hemisphere. The results of the tests (summarized in table 1) were satisfactory, and in every case the physical properties of the material met or surpassed Navy and ASME specifications for acrylic plastic in man-rated pressure resistant structures (appendix A).

**For spherical hulls with 66-inch outside diameter, the maximum permitted deviation in sphericity is ±0.165 inch (ref. 19, 20).*

Table 1. Properties of Acrylic Plastic Casting.

Property	Specified value	Actual value (average)
Ultimate tensile strength	9,000 lb/in^2 min	9,670 lb/in^2
Tensile elongation at fracture	2 percent min	3.85 percent
Tensile modulus of elasticity	400,000 lb/in^2 min	497,500 lb/in^2
Test method: ASTM D638		
Compressive yield strength	15,000 lb/in^2 min	16,150 lb/in^2
Compressive modulus	400,000 lb/in^2 min	515,000 lb/in^2
Test method: ASTM D695		
Shear strength	8,000 lb/in^2 min	9,775 lb/in^2
Test method: ASTM D732		
Ultimate flexural strength	14,000 lb/in^2 min	15,150 lb/in^2
Flexural modulus	420,000 lb/in^2 min	490,000 lb/in^2
Test method: ASTM D790		
IZOD Impact strength	0.20 ft-lb/in min	0.29 ft-lb/in
Test method: ASTM D256		
Deformation under load at 4,000 lb/in^2 and 122°F	1.0 percent max	0.385 percent
Test method: ASTM D621		
Rockwell M hardness	90 min	105
Test method: Rockwell		
Water absorption in 24-hour submersion	0.25 percent max	0.20 percent
Test method: ASTM D570		
Heat distortion temperature	205°F min	216°F
Test method: ASTM D648		
Refractive index	1.48–1.50	1.491
Test method: ASTM D542		
Specific gravity	1.18–1.20	1.182
Test method: ASTM D792		
Coefficient of linear thermal expansion	4.3×10^{-5} in/in at 80°F	4.6×10^{-5} in/in °F 77–105°F range
Test method: ASTM D696		

Table 1. Continued.

Property	Specified value	Actual value (average)
Resistance to stress Test method: Table 1 of ASTM Methods	N.A.	2,000 lb/in^2; no visual evidence of crazing or cracking
Residual monomer (methyl methacrylate) Test method: SPE Trans. 1962	1.5 percent max	0.40 percent

ASSEMBLY

Assembly of the model 2000B hull consisted of the machining and bonding together of two hemispherical castings, followed by polishing and inspection of the completed sphere. The finished hull was then fitted with aluminum inserts that served as hatch and penetration plate.

Machining of the hemispherical castings was preceded by rough grinding of the equatorial edge with a rotary file (figure 27). After the edge was ground to within an inch of its final dimension, the casting was mounted in a vertical mill and the polar opening machined (figure 28). It was then turned over in the mill and the equatorial edge machined to its final dimension.

Bonding of the hemispheres into a single structural entity was begun by placing one hemisphere on top of the other (figure 29). The width of the joint was controlled by placing small acrylic plastic spacers of 1/4-inch thickness between the hemispheres. The joint was subsequently covered with adhesive aluminum foil tape. To facilitate pouring of the bonding mix into the joint cavity, three pouring spouts were plumbed to openings in the tape covering provided for this purpose (figure 30).

The bonding mix was prepared by combining the same ingredients that made up the basic casting mix. The mix was poured concurrently into the three pouring spouts around the circumference of the sphere and into a separate test block joint. This block served later as a source of specimens for determination of joint strength. As soon as the mix gelled, the sphere assembly with the associated test block was placed in the autoclave and subjected to temperature and pressure until polymerization of the joint was completed (figure 31).

Upon removal of the assembly from the autoclave, extensive voids were found on the inner surface of the joint (figure 32). Careful examination of joint and polymerization procedure established shrinkage of the mix during polymerization to be the cause. The voids were not present on the outer surface of the joint because extra mix was provided by an outward bulge in the tape. This bulge was absent on the inner surface of the joint, resulting in the observed shrinkage voids. Such voids will be prevented in the future by forming the tape over the joint in such a manner that a bulge is present.

The voids in the joint decreased its bearing surface to such a degree (about 25 percent) that it became structurally unacceptable. This problem was corrected by removing the tape, rotating the sphere until the equatorial joint was in the vertical plane, and filling

the voids with room-temperature-polymerizing PS-30 adhesive. Since the adhesive could be placed properly only in the void at the lowest point of the vertically oriented joint, the sphere had to be rotated between fillings.

The resulting joint was still far from completely void free, but the cross section and number of remaining voids were so small that it could be considered structurally acceptable (figure 33). Because the room-temperature-polymerized PS-30 adhesive was somewhat softer than the high-temperature and high-pressure polymerized casting mix, differential compression of the joint was expected when the sphere was subjected to hydrostatic testing.

Polishing of the completed sphere consisted of rough sanding of the edges of the joint followed by fine sanding and polishing of both the internal and external surfaces (figure 34). Inspection consisted of detailed visual observation, dimensional measurements, and testing of bond samples. The objective of the visual observation was to ascertain the effect of the joint and repaired voids in the castings on the optical properties of the hull. The dimensional measurements were performed to determine the conformance of the completed sphere assembly to specified dimensional tolerances. The testing of bond samples served as quality control for the bonding technique used for joining the hemispheres.

The visual inspection showed that the optical properties of the sphere were generally more than adequate for underwater search, salvage, or work missions where panoramic visibility is of paramount importance. The only areas that showed optical distortion were the equatorial joint and the repaired voids in the castings (figure 35), both of which distorted images at their boundaries. The distortion was not severe enough to significantly lower the value of the sphere as a panoramic observation capsule. It was, however, sufficient to preclude photography through the sphere at those locations.

Dimensional measurements (figure 36) showed that the diameter and angle of the top and bottom polar openings, as well as the outside diameter of the capsule, were within specified tolerances. The thickness of the hull was found, however, to fall below the minimum specified thickness by 0.093 inch. As noted previously, the excessive variation in thickness was caused by improper centering of the male mold within the female mold during casting. The result was that the shell of the capsule was thinnest at the edges of penetrations, where the stresses are highest during external hydrostatic loading. Better alignment of the male mold within the female mold will forestall the recurrence of this problem.

Installation of polar inserts consisted of placing the top hatch and bottom penetration plate with associated polycarbonate gaskets into their respective polar openings and locking them in place by bolting on split retaining rings. The hatch and penetration plate assemblies used for testing the model 2000B hull were those used in the previous model 2000 hull test and evaluation program (figures 37 through 46). This meant that they had been previously pressurized to 1800 lb/in^2 and as a result might have experienced some local yielding.

Only minor modification was required to the polycarbonate gasket even though the cast hemispheres of the model 2000B hull were about 0.100 inch thicker at the polar opening than those of the model 2000 hull. This was feasible, however, only because the wall thickness at the polar opening was in the 4.1-to-4.2-inch range rather than the 4.2-to-4.4-inch range specified. If the wall thickness of the castings had been within the specified range, the model 2000 polycarbonate gasket would have had to be replaced with a new one (figure 46). The modified gasket actually used in the test is shown in figure 47.

HYDROSTATIC TESTING

The objective of hydrostatic testing was to determine the strains, displacements, and failure mode of the model 2000B hull so that its performance under pressure could be compared with that of the model 2000 hull. Since the polar inserts were the same for both hulls, differences in performance would be attributable only to the physical properties of the material and the slight difference in wall thickness.

TESTS AND INSTRUMENTATION

Hydrostatic testing was conducted in a 90-inch-diameter pressure vessel at the Southwest Research Institute, San Antonio, Texas (figure 48) in four discrete steps, each consisting of sustained loading and relaxation phases. By making the length of the loading and relaxation phases equal, viscoelastic strains were given an opportunity to return to zero before the material was subjected to higher strain levels. Prior to testing, the interior of the hull assembly was filled with water to mitigate the shock of implosion and to provide a means of determining the rate of volumetric contraction under loading. To maintain zero atmospheric pressure inside the sphere, a tube was connected to both the top hatch and the pressure vessel closure. As the acrylic sphere contracted, the water was forced out through this tube and its volume measured at the outlet with a 2000 ml graduate.

Pressure Test 1. The model 2000B assembly was pressurized to 900 lb/in^2 at 100 lb/in^2/min at room temperature and maintained at this pressure for 24 hours; it was then depressurized to 0 lb/in^2 at 100 lb/in^2/min and maintained at this pressure for 24 hours. Strains and displacements were recorded at 100 lb/in^2 intervals during pressurization and at 6 hour intervals during depressurization.

Pressure Test 2. Identical to test 1 except that the maximum pressure was 1350 lb/in^2.

Pressure Test 3. Identical to test 1 except that the maximum pressure was 1800 lb/in^2.

Pressure Test 4. The assembly was pressurized to 4000 lb/in^2 at 50 lb/in^2/min and maintained at this pressure to implosion. Strains were recorded until the 4000-lb/in^2 pressure was reached, and displacements were recorded to the moment of implosion.

Instrumentation consisted of 90-degree biaxial strain rosettes bonded at critical locations to the acrylic hull and polar aluminum inserts (figures 49 and 50). The gage locations chosen for the model 2000B assembly were identical to those chosen for the model 2000 assembly tested previously. Because of this, direct comparison between strains on both assemblies could be made.

The acrylic hull was instrumented only on the equator and at the edges of the polar penetrations. Both locations were important; the magnitude of creep at the equator would give a fair indication of viscoelastic deformation over most of the hull, while that at the edge of penetrations would represent the maximum on the hull.

The aluminum inserts were instrumented only at locations that previous tests on the model 2000 hull had shown to be areas of high stress. Strains measured at these locations would indicate the onset of yielding as the model 2000B hull was pressurized to implosion.

STRAIN RESULTS

Strains measured on the model 2000B assembly, as expected, varied widely from one location to another, but in all cases they were very active (figures 51 through 62 and appendix B). In the hull itself the highest strains were recorded on the interior surface at the edges of polar openings. The maximum strain was in the longitudinal direction, and its magnitude was approximately 50 percent larger than that of strains measured on the interior surface at the equator.

During short term loading, the maximum strains at the polar openings were found to increase linearly with external hydrostatic pressure to about 1350 lb/in^2; at higher pressures the strains increased faster than the external pressure. Their magnitudes were measured to be 4500, 9250, 14600, and 20300 microinches/inch at 450, 900, 1350, and 1800 lb/in^2 respectively. However, on the interior surface at the equator the maximum strains (hoop orientation) were only 2825, 5800, 9050, 12250, and 32500 microinches/inch at 150, 900, 1350, 1800, and 4000 lb/in^2 respectively.

During long term loadings of 24-hour duration there took place some viscoelastic creep whose magnitude varied with the location on the hull. On the interior surface at the equator, viscoelastic creep was approximately 15 percent of the short term strain at 900 and 1350 lb/in^2, while at 1800 lb/in^2 it increased to about 25 percent of the short term strain. At the polar penetrations, the magnitude was larger than at the equator, but in terms of short term strain the percentage was about the same. At the conclusion of the 24-hour sustained pressure loadings strains returned almost to zero. The difference between strain readings at the conclusion of relaxation and zero can be attributed to permanent deformation and errors in the strain recording system. Since the magnitude of permanent residual strains did not increase with the magnitude of sustained pressure, it can be postulated that the magnitude of residual strains measured on the sphere at 900, 1350, and 1800 lb/in^2 is not only a function of pressure but also of other unknown test variables. It is also interesting to note that the longitudinal strain measured on the equatorial bond was significantly higher than near the joint. The difference in readings indicates that the adhesive used in the bond had a lower modulus of elasticity and probably a lower compressive yield point than the hull material.

When the model 2000B assembly was tested to destruction, the magnitude of compressive strains measured on the interior at the equator was approximately 32500 microinches/inch. Since strain readings were not taken after the 4000-lb/in^2 pressure loading was reached, the magnitude of creep that took place during this test is not exactly known. However, by converting the change in displaced volume to strains on the acrylic hull, it is possible to calculate the average strains near the equator on the interior surface of the hull at the moment of failure. The magnitude of strain calculated in such a manner is 44500 microinches/inch.

The strains measured on the aluminum inserts (hatch and penetration plate) were similar to those measured when the inserts were tested as part of the model 2000 assembly, indicating that no yielding had taken place during the previous testing to 1800 lb/in^2.

Even when the model 2000B assembly was pressurized to 4000 lb/in^2, very little yielding was noted, though compressive strains in excess of 3000 microinches/inch were measured on the interior of the top hatch. When the maximum strain measured on the top hatch was converted to stress, it was found that it amounted to 39,423 lb/in^2.

DISPLACEMENT RESULTS

Displacement of water from the interior of the model 2000B assembly increased under load. The relationship between external pressure applied at 50 lb/in^2/min and the volume of displaced water was linear to about 1350 lb/in^2 (figure 63). At higher pressures the relationship became markedly nonlinear, with the volume of displaced water increasing at a higher rate than the external pressure.

Under sustained loading, the displacement increased further than under short-term pressurization. The volume of displaced water under long-term loading was a function of both pressure and time. For the three nondestructive sustained pressure loadings of 24-hour duration at 900, 1350, and 1800 lb/in^2 the total volume of displaced water was 1.8, 3.0, and 4.2 percent, respectively, of the original volume. At the termination of each sustained loading test, the sphere returned to its original dimensions after the 24-hour relaxation period at 0 lb/in^2. The only sustained loading test that culminated in failure of the assembly took place at 4000 lb/in^2. The total volume of displaced water due to contraction of the sphere prior to failure was 13.5 percent of the original volume.

FAILURE MODE

The model 2000B assembly imploded by general plastic instability after being subjected to an external hydrostatic pressure of 4000 lb/in^2 for 13 minutes. Because of unforeseen mechanical problems with pumps, the average pressurization rate was 50 lb/in^2/min instead of the 100 lb/in^2/min specified.

The acrylic hull was fragmented into many irregularly shaped pieces whose size, as a rule, did not exceed three feet in length or width (figures 64 and 65). There was no indication that the bonded joint constituted a plane of weakness. As a matter of fact, most cleavage planes crossed the bonded joint at right angles rather than following it.

No crazing or radial cracks were found in the acrylic surfaces bearing against the polycarbonate gaskets (figure 66). This constitutes a significant improvement over the model 600 and 1000 hulls, which did not utilize polycarbonate gaskets and therefore exhibited many radial cracks after being tested to implosion.

The polycarbonate gasket for the penetration plate was found to be full of small cracks but intact, while the one for the hatch was fragmented into small pieces (figures 67 and 68). The high bearing stresses between the gasket and the aluminum inserts made the polycarbonate flow into the O-ring grooves on the outer circumference of the hatch ring and penetration plate (figure 69).

The aluminum inserts survived the implosion without any visible deformation (figures 70 and 71). This was significantly different from the results obtained for the model 600, assembly numbers 0 and 3, where the hatches buckled plastically at a pressure lower than the implosion pressure of the hull.

EVALUATION OF TEST RESULTS

The above test results show that the performance of the model 2000B assembly is comparable to that of the model 2000 assembly in distribution and magnitude of strains as well as in implosion depth. The basic difference is in the magnitude of permanent strains in the hull after sustained 24-hour pressure loadings. While in the model 2000 assembly the permanent strains were on the order of 50 to 100 microinches/inch, in the model 2000B they were about 200 to 1000 microinches/inch. Although some fraction of the permanent strains can be discounted as experimental error, it is impossible to discount them completely in this manner. In view of this, it appears that the model 2000B should be certified to a lesser depth than 3000 feet, the maximum operational depth of the model 2000. In order to arrive rationally at a safe maximum operational depth, however, it is necessary to review the pertinent design, fabrication, material, and test results involved in the evaluation of the model 2000B assembly.

The design of the model 2000B is identical to that of the model 2000 except for the location of bonded joints and hull thickness. While on the latter there is a multitude of bonded joints between the 12 spherical pentagons, on the former there is only a single bonded equatorial joint. The model 2000B hull is also thicker, 4.210 inches minimum thickness versus 4.050 inches for the model 2000.

Since both the single equatorial joint and additional hull thickness represent structural advantages, the total effect of design on the operational depth of the model 2000B is beneficial. If the acrylic castings of the model 2000B had the properties of Plexiglas G, from which the hull of the model 2000 was fabricated, the maximum operational depth could be increased by four percent to 3120 feet.

Although the fabrication techniques for the model 2000 and 2000B differ, the sphericity tolerances for the finished acrylic hull are the same. It can thus be postulated that the difference in fabrication technique would neither increase nor decrease the potential maximum operational depth capability of 3120 feet.

Although the materials used in constructing the model 2000 and 2000B possess physical properties that meet Navy specifications for acrylic plastics used in manned systems, there is a significant difference between their compressive yield strengths. Where, for example, the average compressive yield strength of the acrylic plastic pentagons used in the model 2000 was 18,416 lb/in^2, the hemispherical castings used in the model 2000B were found to have an average compressive strength of only 16,300 lb/in^2. The 11.5 percent lower yield strength of the hemispherical castings should decrease the potential maximum operational depth capability from 3120 to 2761 feet.

The compressive creep (time dependent strain under sustained constant loading) measured on the model 2000B was found to be approximately equal to that measured on the model 2000. For example, the values measured on the interior surface of the hull at the equator in the hoop direction were found to be 900, 1350, and 3000 microinches/inch for the model 2000B at 900, 1350 and 1800 lb/in^2 sustained loadings of 24-hour duration. This is approximately equal to the values of 500, 1850, and 3100 microinches/inch measured on the model 2000. Because the magnitude of the creep was approximately equal in both assemblies, it would appear that in this respect the maximum operational depth of the model 2000B assembly should be the same as that of the model 2000, that is 3000 feet.

Permanent deformation of the model 2000B was significantly higher than that of the model 2000 after identical sustained pressure loadings. For the former the deformations measured after 24 hours of sustained pressure loadings of 900, 1350, and 1800 lb/in^2 were -950, -700, +75 microinches/inch respectively. In contrast, the model 2000 showed a permanent deformation of only -100, -50, -150 microinches/inch after sustained pressure loadings of 900, 1350, and 1800 lb/in^2. Since there is no known well defined relationship between the magnitude of permanent deformation at the equator after several tests at different pressures and the fatigue life of the acrylic bearing surface at the polar penetration, the maximum operational depth of the model 2000B cannot be established on the basis of this data at some lesser depth than that of the model 2000 assembly. Instead, only an indirect approach can be used here, influenced to a large degree by other data not generated in the test program for the model 2000B hull.

The basic assumption underlying the indirect approach to the problem of permanent deformation is that the maximum operational depth of the model 2000B should be substantially less than that of the model 2000 until cyclic fatigue data is experimentally generated by tests of model 2000B scale models similar to those conducted during evaluation of the model 2000 pressure hull assembly. When such data is generated at some future time, it will be possible to establish with confidence the maximum operational depth at which fatigue cracks appear in the acrylic bearing surface at the polar penetrations after 1000 standard dives (four hours at maximum operational depth followed by four hours of relaxation). Until such cyclic fatigue data is generated, the maximum operational depth will of necessity be based on the cyclic pressure tests performed previously on cast acrylic hemispheres with a thickness-to-inside-radius (t/R_i) ratio of 0.8. Extrapolating the safe operational cyclic pressure of approximately 6100 lb/in^2 for hemispheres with $t/R_i = 0.8$ to $t/R_i = 0.147$ for the model 2000B, one arrives at a predicted safe cyclic pressure of approximately 1120 lb/in^2 (equivalent to an operational depth of 2500 feet). Since extrapolating data from high to low t/R_i ratios is inherently conservative, the extrapolated cyclic fatigue depth for the model 2000B can be used without reservations until it can be increased on the basis of more complete cyclic fatigue tests.

The implosion pressure of the model 2000B system was found to be approximately the same as that of the model 2000 assembly. The comparison of implosion pressures could not be made directly as the model 2000B and 2000 assemblies tested to destruction were not of the same size, the former being a full-scale prototype and the latter a 1:4.4 scale model. Implosion of the model 2000 scale model took place after 23 minutes at 4000 lb/in^2, while that of the model 2000B full-scale assembly after only 13 minutes (figures 72). Since the hull thickness of the scale model was approximately 10 percent greater than specified, the projected time to implosion for the full-scale model 2000 is probably only about 15 minutes. In such a case there appears to be no significant difference between the model 2000B and 2000 in resisting external hydrostatic pressure under sustained long-term loading. In effect, then, the static fatigue of the model 2000B is comparable to that of the model 2000 and cannot be used as a factor for increasing or decreasing the maximum operational depth.

This discussion of the physical parameters and test results pertaining to the structural response of the model 2000B shows that, while in comparison to the model 2000 the hull is four percent thicker, has stronger bonded joints, and has approximately the same time-dependent strains, the residual strains observed at the conclusion of simulated dives are

significantly higher. In the absence of cyclic fatigue data for the model 2000B assembly at this time, the conservative approach is to consider the large residual strains as adequate reason for assigning the assembly temporarily an operational depth that is less than 3000 feet.

The temporary operational depth of 2500 feet (1120 lb/in^2) assigned to the model 2000B is based on previously generated cyclic fatigue data for spherical sector windows cast by Polymer Products, Inc, utilizing the same resin mix and polymerization process as used in production of the model 2000B. If at some future time cyclic pressure testing of the model 2000B assembly establishes its ability to withstand 1000 simulated dives to 3000 feet without generation of cracks in the hull at the polar openings, the current operational depth limit of 2500 feet will be raised to 3000 feet.

FINDINGS AND CONCLUSIONS

The following are the specific findings of this study:

1. It is technically feasible to fabricate spherical pressure hulls of any size by bonding together acrylic plastic hemispheres precision cast in metallic mold assemblies composed of a male and a female component.

2. Precision cast hemispheres do not require any subsequent machining of spherical surfaces in order to satisfy Navy specified tolerances for sphericity and thickness.

3. The physical properties of the acrylic plastic castings produced by Polymer Products satisfy Navy and ASME specifications for acrylic plastic used in man-rated external or internal pressure vessels.

4. Bonding with the same resin mix that was used in casting the hemispheres produces joints with a tensile strength in excess of 9000 lb/in^2.

5. Voids in the acrylic plastic hemispheres can be successfully recast by filling them with standard casting resin mix and subjecting the hemisphere to the polymerization process for a second time.

6. The repaired hemisphere is structurally as strong under external hydrostatic loading as a hemisphere without recast voids.

7. The repaired voids are optically objectionable if located in the crew's main field of vision.

8. The model 2000B assembly, fabricated by bonding two precision cast acrylic plastic hemispheres with 66.5-inch outside diameter and 57.85-inch inside diameter, successfully withstood 24-hour simulated dives to 2000, 3000, and 4000 feet.

9. The model 2000B assembly imploded after 13 minutes of sustained loading at a simulated 9000-foot depth.

10. The aluminum polar inserts (hatch and penetration plate) withstood the simulated 9000-foot depth without losing their structural integrity.

On the basis of these findings it is concluded that the model 2000B assembly meets the applicable certification criteria for manned service. The maximum recommended safe operational depth of 2500 feet is based on a conservative interpretation of existing cyclic fatigue data for the acrylic plastic material used in the tested prototype.

OPERATIONAL RECOMMENDATIONS

The following operational recommendations are based on the conservative interpretation of limited cyclic fatigue data. Thus the maximum operational depth and number of crack-free cycles at that depth, as well as the duration of individual cycles, are to be considered as temporary minimums, to be increased later when more definitive cyclic fatigue data is generated.

1. The model 2000B assembly during its operational life should never be subjected to depths greater than 2500 feet. The proof test should preferably utilize a test depth of less than or equal to 3000 feet. Under no conditions should the proof test depth exceed 3000 feet.

2. The cyclic crack-free fatigue life of the model 2000B assembly is considered to be in excess of 10,000,000 foot-hours (1000 cycles X 2500-foot depth X 4 hours duty). At the conclusion of each dive, the recorded foot-hours should be subtracted from the initial 10,000,000 foot-hour fatigue life. When the sum of foot-hour subtotals generated by dives equals 10,000,000, inserts and gaskets should be removed from the capsule and the entire hull subjected to a detailed visual examination. If no cracks are observed at the polar penetrations, the assembly should be strain-gaged, reassembled, proof-tested to the required depth, and recorded strains at the equator and penetrations compared to those generated during the first proof test conducted immediately after fabrication. Significant differences in strain behavior will be considered indicators of hull deterioration and should result in a significantly reduced depth rating. Cracks in the bonded joint originating at inclusions will be repaired if their length exceeds 0.5 inch. Severely cracked polycarbonate gaskets will be replaced with new gaskets.

If no significant difference in strain behavior is observed, the capsule assembly will be returned to service with a 2500-foot operational depth rating and an additional 10,000,000-foot-hour fatigue life. When the second 10,000,000-foot-hour life has been completed, the assembly will be subjected to the same inspection and proof-testing procedures conducted at the conclusion of the first 10,000,000-foot-hour period. If the results of the new inspection and proof-testing are satisfactory, the capsule will again return to service with a 2500-foot depth rating and additional 10,000,000-foot-hour life.

The recertification process will be repeated until cracks are observed in the bearing surfaces of the acrylic hull during one of the inspections or the strains change significantly. If cracks are observed, they will either be repaired by routing and recasting with resin prior to retesting of the hull, or they will be left in place and the hull's depth rating reduced to 600 feet.

Subsequently, the hull will be inspected without disassembly for signs of crack propagation every 100 dives. When the depth of any crack exceeds one inch, the capsule will be taken out of service immediately and the cracks repaired either by enlarging the polar opening or by recasting the cracked areas. If not repaired, such a hull can be recertified for service to 120 feet. If, during periodic inspections conducted every 100 dives, the depth of the crack at the penetration is found to exceed two inches, the acrylic hull will either be repaired or declared unfit for manned operation at any depth.

3. For applications where the presence of a bonded joint in the visual field of the crew is objectionable, the pair of polar penetrations should be moved from their present location to a new location, preferably close to the circumferential joint.

4. Attempts should be made to ensure that operators are seated inside the hull as close as possible to the center of the sphere in order to minimize optical distortion (ref. 21). Camera mountings should be located at the center of the hull if wide angle panning is to be performed.

5. Many functions of equipment mounted outside the pressure hull can be controlled by modulated light beams projected from the interior of the hull by the crew (ref. 22). This type of arrangement will eliminate the need for electrical connections through the penetration plate and make the control of externally stored scientific equipment an operationally easy matter.

REFERENCES

1. Naval Civil Engineering Laboratory. Technical Report R-631, Windows for External or Internal Hydrostatic Pressure Vessels; Part 3, Critical Pressure of Acrylic Spherical Shell Windows Under Short Term Pressure Application, by J. D. Stachiw, F. W. Brier. June 1969 (AD689789).
2. Naval Undersea Center. Technical Publication 383, Cast Acrylic Dome for Undersea Applications, by J. D. Stachiw. January 1974.
3. Naval Undersea Center. Technical Publication 315, Acrylic Plastic Hemispherical Shells for NUC Undersea Elevator, by J. D. Stachiw. September 1972 (AD 749029).
4. Naval Undersea Center. Technical Publication 355, Flanged Acrylic Plastic Hemispherical Shells for Undersea Systems, by J. D. Stachiw. August 1973 (AD 769213).
5. Naval Undersea Center. Technical Publication 393, Glass or Ceramic Spherical Shell Window Assembly for 20,000 psi Operational Pressure, by J. D. Stachiw. May 1974.
6. Naval Undersea Center. Technical Publication 486, Acrylic Plastic Spherical Shell Windows Under Point Impact Loading, by J. D. Stachiw, O. Burnside. July 1975.
7. Naval Civil Engineering Laboratory. Technical Report R-749, NEMO, A New Concept in Submersibles, P. K. Rockwell, R. E. Elliott, M. R. Snoey. November 1971 (AD 735103).

8. Naval Civil Engineering Laboratory. Technical Report R-676, Development of a Spherical Acrylic Plastic Pressure Hull for Hydrospace Application, by J. D. Stachiw. April 1970 (AD 707363).

9. Naval Civil Engineering Laboratory. Technical Note N-1113, The Spherical Acrylic Pressure Hull for Hydrospace Application; Part 2, Experimental Stress Evaluation of Prototype NEMO Capsule, by J. D. Stachiw, K. L. Mack. October 1970 (AD 715772).

10. Naval Civil Engineering Laboratory. Technical Note N-1094, The Spherical Acrylic Pressure Hull for Hydrospace Application; Part 3, Comparison of Experimental and Analytical Stress Evaluations for Prototype NEMO Capsule, by H. Ottsen. March 1970 (AD 709914).

11. Naval Civil Engineering Laboratory. Technical Note N-1134, The Spherical Acrylic Pressure Hull for Hydrospace Application; Part 4, Cyclic Fatigue of NEMO Capsule #3, by J. D. Stachiw. October 1970 (AD 715345).

12. American Society of Mechanical Engineers. Paper No. 70-WA/UnT-3, Spherical Acrylic Pressure Hulls for Undersea Exploration, by J. D. Stachiw. Journal of Engineering for Industry, May 1971.

13. American Society of Mechanical Engineers. Paper No. 72-WA/OCT-8, Transparent Hull Submersible MAKAKAI, by D. W. Murphy, W. F. Mazzone. December 1972.

14. American Society of Mechanical Engineers. Paper No. 70-WA/UnT-6, The JOHNSON SEA-LINK – The First Deep Diving Welded Aluminum Submersible, by R. A. Kelsey, R. B. Dolan. December 1970.

15. American Society of Mechanical Engineers. Paper No. 71-WA/UnT-6, Acrylic Pressure Hull for JOHNSON SEA-LINK Submersible, by J. R. Maison, J. D. Stachiw. December 1971.

16. Naval Undersea Center. Technical Publication 451, NEMO Module 2000 Acrylic Plastic Spherical Hull for Manned Submersible Operation, by J. D. Stachiw. December 1974.

17. Naval Undersea Center. Technical Publication 410, Development of a Precision Casting Process for Acrylic Plastic Spherical Shell Windows Applicable to High Pressure Service, by J. D. Stachiw. May 1974.

18. American Society of Mechanical Engineers. Paper No. 70-WA/UnT-4, Fabrication of NEMO-Type Spherical Acrylic Capsules for Underwater Vehicles, K. Tsuji, R. Shelton. December 1970.

19. Naval Undersea Center. Technical Publication 378, Recommended Practices for the Design, Fabrication, Prooftesting and Inspection of Windows in Man-Rated Hyperbaric Chambers, by J. D. Stachiw. December 1973 (AD 773737).

20. American Society of Mechanical Engineers. Paper No. 73-WA/OCT-18, Recommended Practices for the Design, Fabrication, and Prooftesting of Acrylic Plastic Windows in Man-Rated Hyperbaric Chambers, by J. D. Stachiw et al. December 1973.

21. American Society of Mechanical Engineers. Paper No. 70-UnT-A, Optical Properties of a Spherical Plastic Underwater Observatory NEMO, by T. Trowbridge. December 1970.

22. American Society of Mechanical Engineers. Paper No. 72-WA/OCT-11, Modulated Light Beam Information Transmission System for Transparent Pressure Hulls, by J. E. Holzschuh, G. R. Beaman. December 1972.

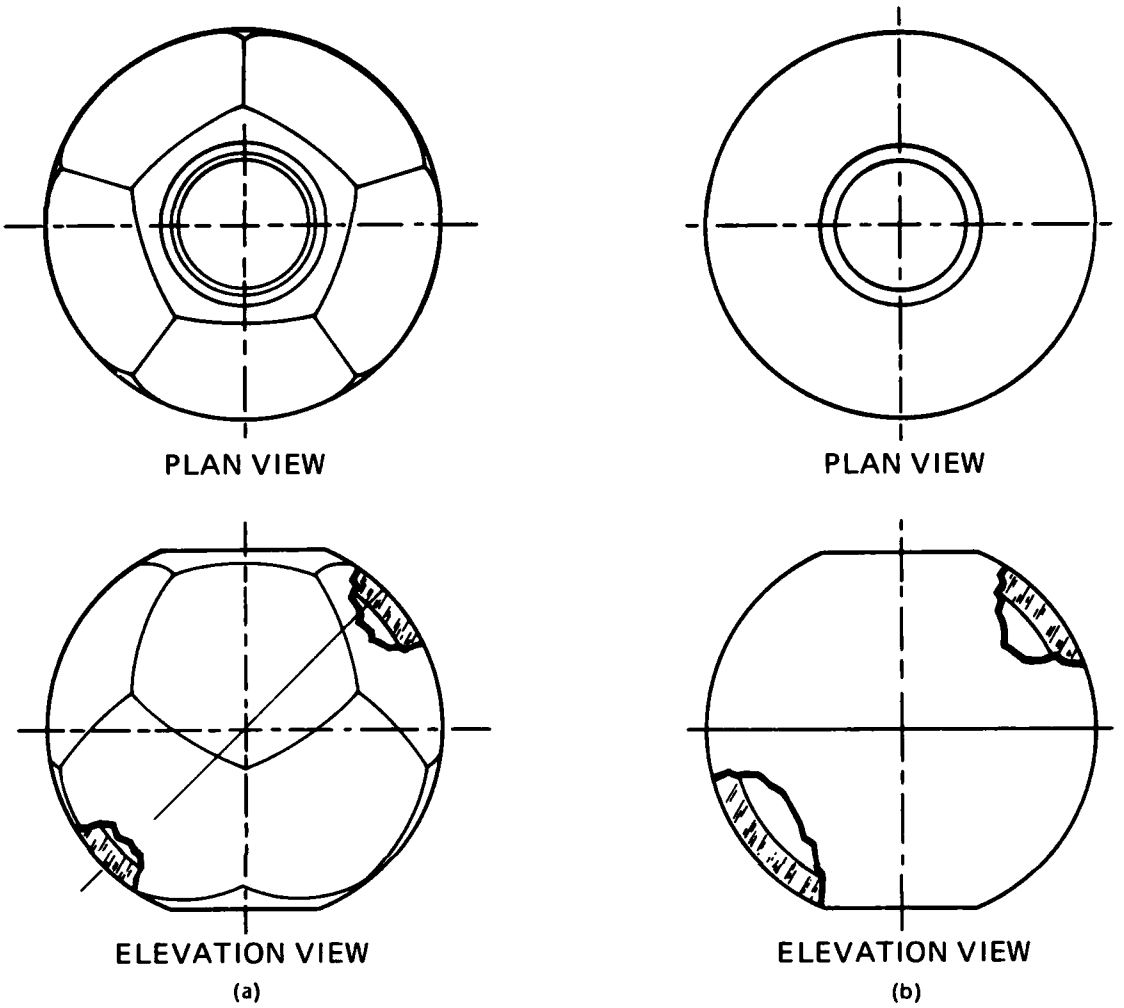

Figure 1. Two approaches to the fabrication of spherical acrylic plastic hulls. (a) Assembly of twelve spherical pentagonal shell sections. (b) Assembly of two hemispherical shell sections.

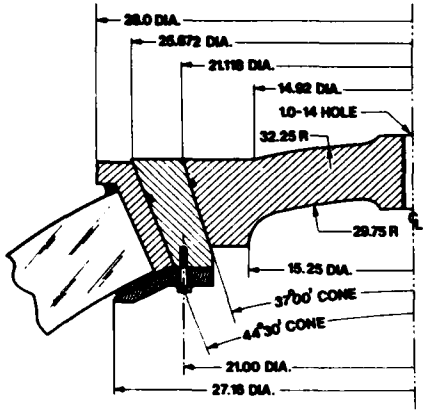

TOP HATCH DETAIL

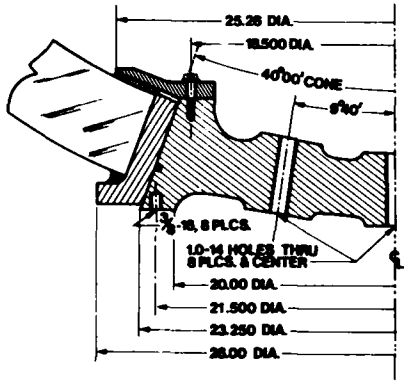

BOTTOM PLATE DETAIL

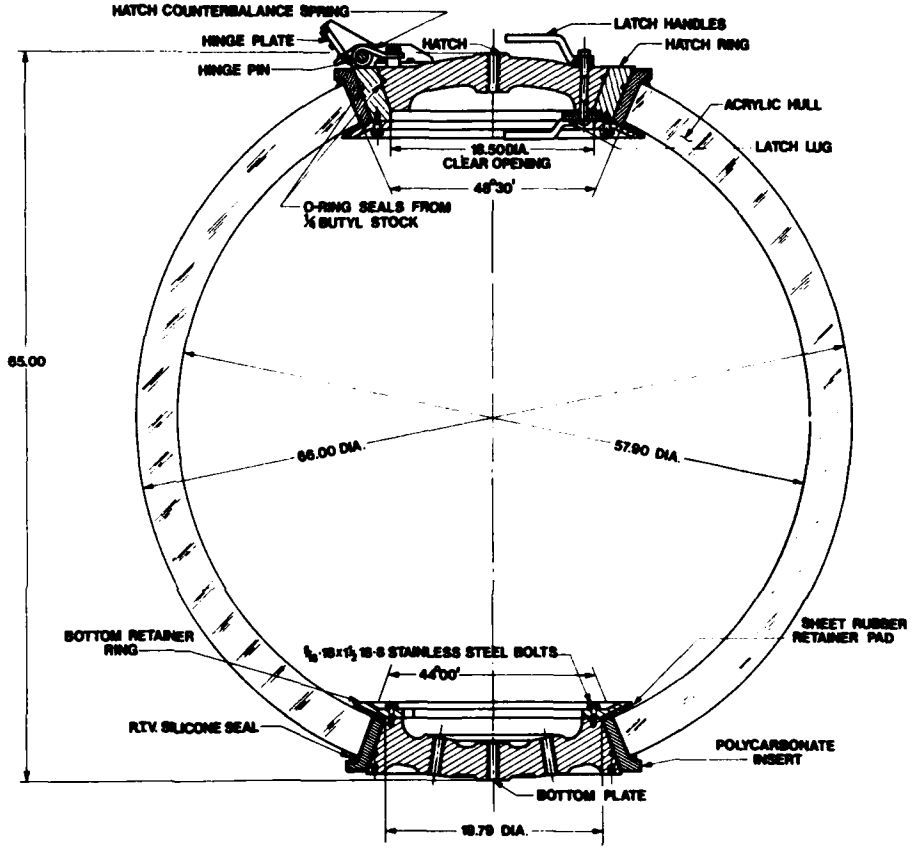

NAVAL UNDERSEA CENTER **ACRYLIC PLASTIC SUBMERSIBLE HULL** **MODEL 2000** material: plexiglas G acrylic plastic construction: bonded spherical pentagons	weight: 2500 lb *displacement*: 5600 lb cyclic fatigue life: 1000 dives of 4 hr duration to 3000 ft minimum	operational depth: 3000 ft proof test depth: 3600 ft implosion depth: 10,500 ft positive buoyancy: 3100 lb weight/displacement: 0.44

Figure 2. Model 2000 spherical acrylic plastic hull assembled from 12 spherical pentagonal shell sections.

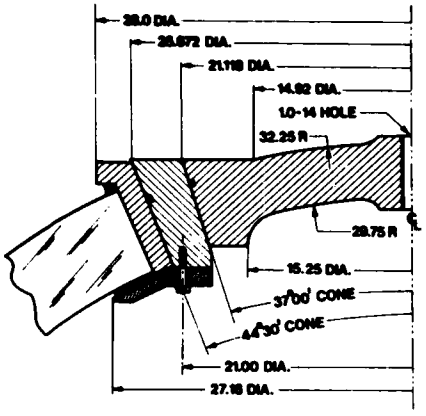

TOP HATCH DETAIL

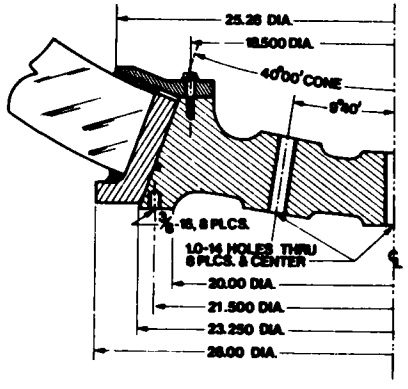

BOTTOM PLATE DETAIL

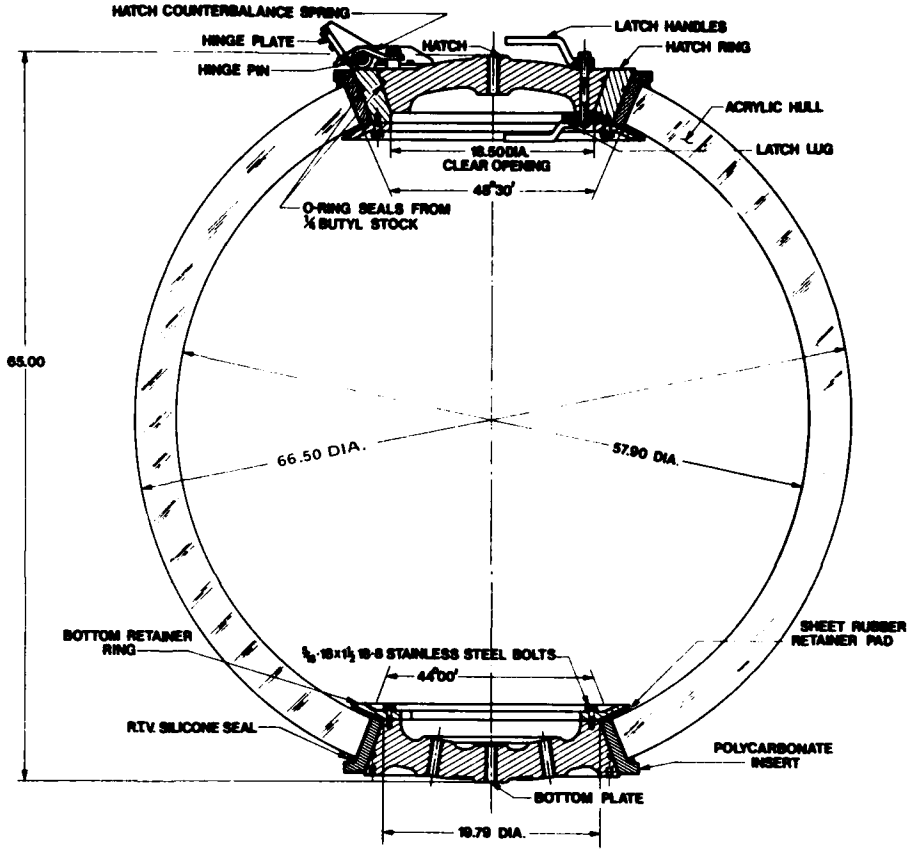

NAVAL UNDERSEA CENTER **ACRYLIC PLASTIC SUBMERSIBLE HULL** **MODEL 2000 B** material: Polymer Products casting construction: bonded hemispheres	weight: 2700 lb displacement: 5700 lb cyclic fatigue life: in excess of 1000 dives of 4 hr duration to 2000 ft	operational depth: 2,000 ft proof test depth: 3,000 ft implosion depth: 10,500 ft positive buoyancy: 3000 lb weight/displacement: 0.47

Figure 3. Model 2000B spherical acrylic plastic hull assembled from two hemispherical shell sections.

(a)

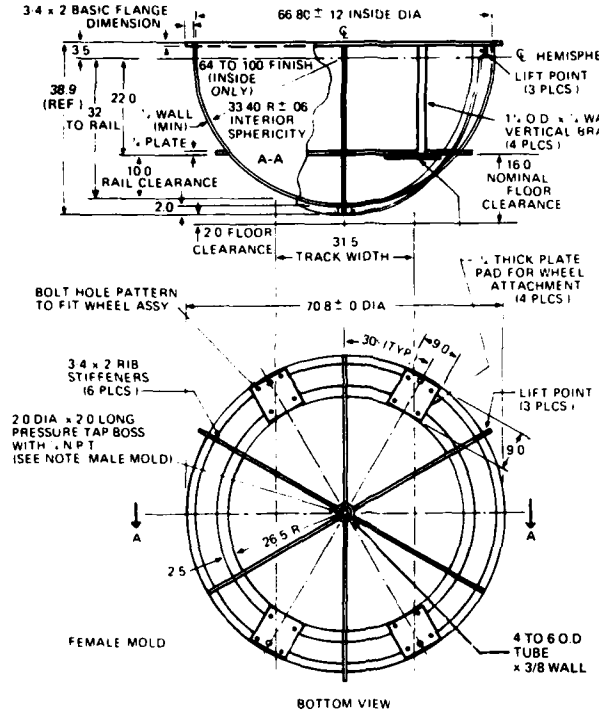

BOTTOM VIEW

(b)

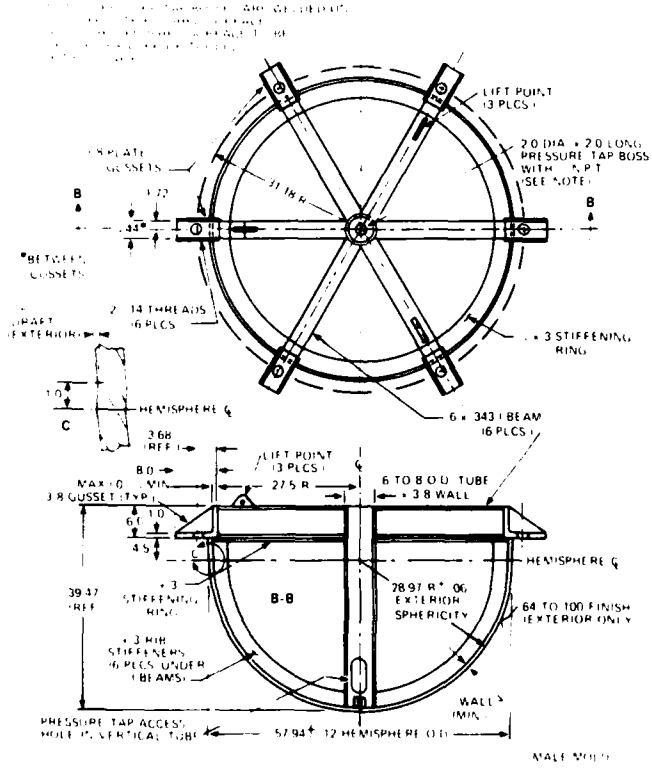

MALE MOLD

Figure 4. Steel molds for precision casting of hemispherical shells for model 2000B acrylic plastic hull. (a) Female mold with pads for mounting wheels. (b) Male mold.

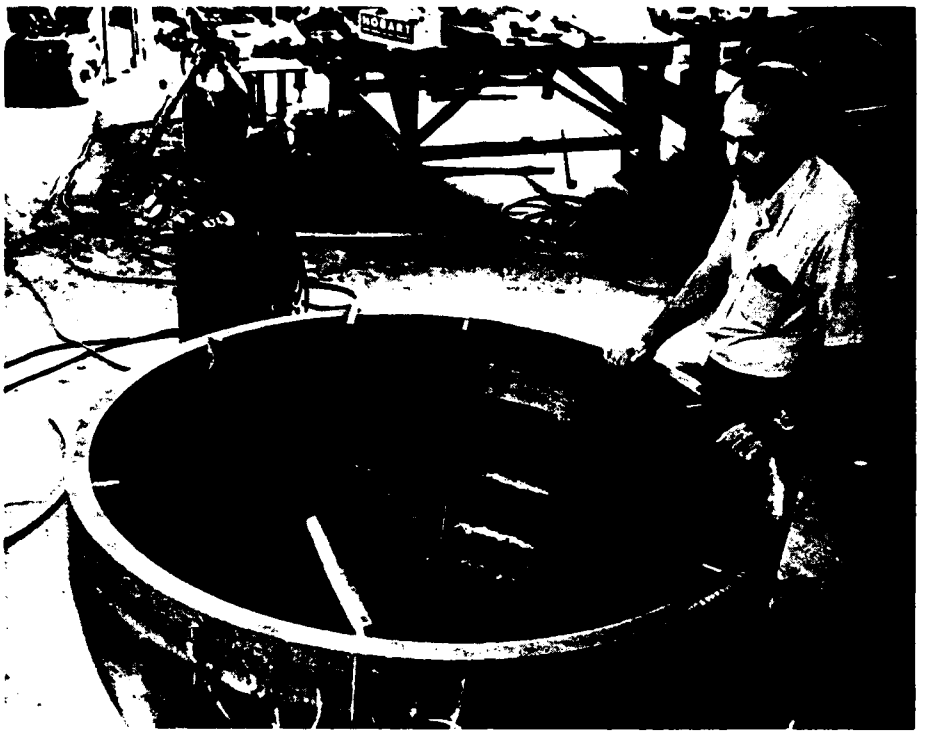

Figure 5. Male mold with inner stiffener rings tacked in place for welding.

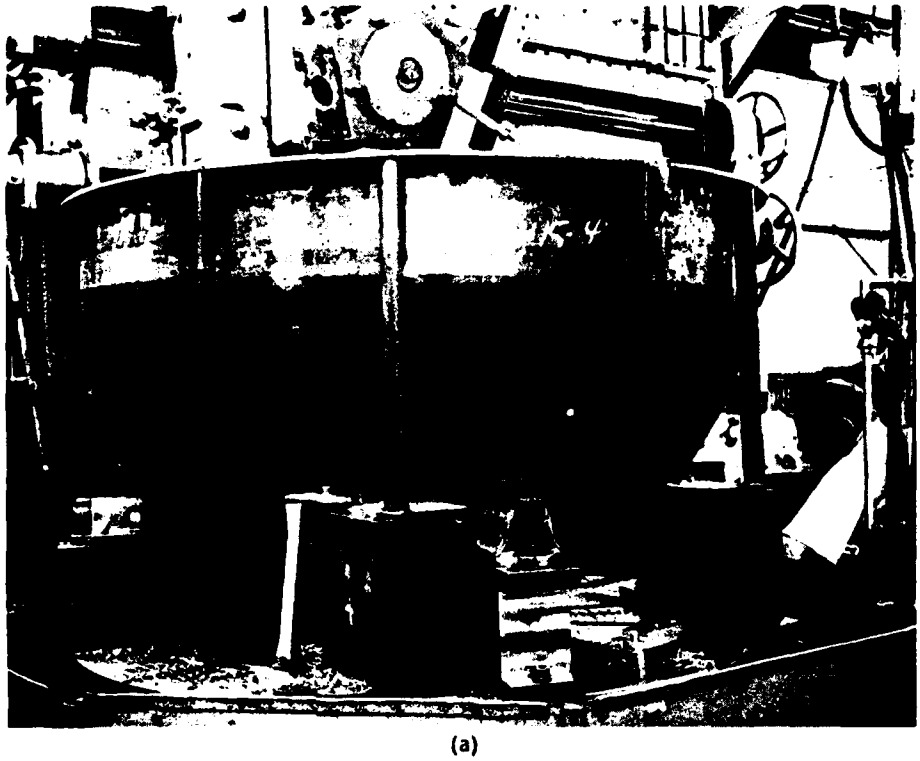

(a)

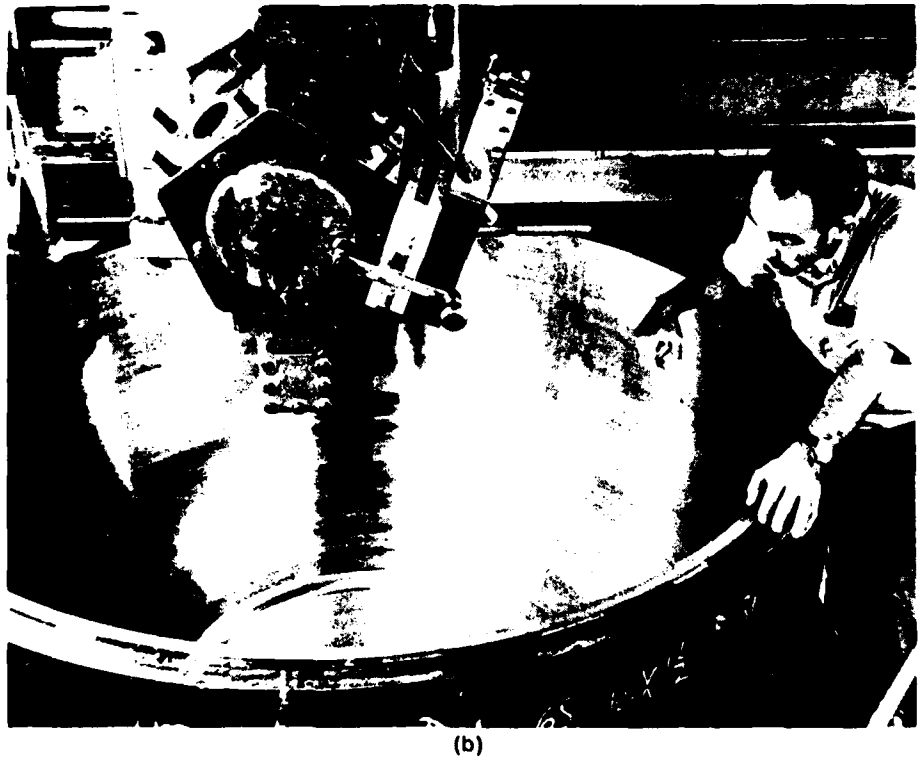

(b)

Figure 6. Female mold. (a) Ready for machining; note external longitudinal and circumferential stiffeners. (b) During machining.

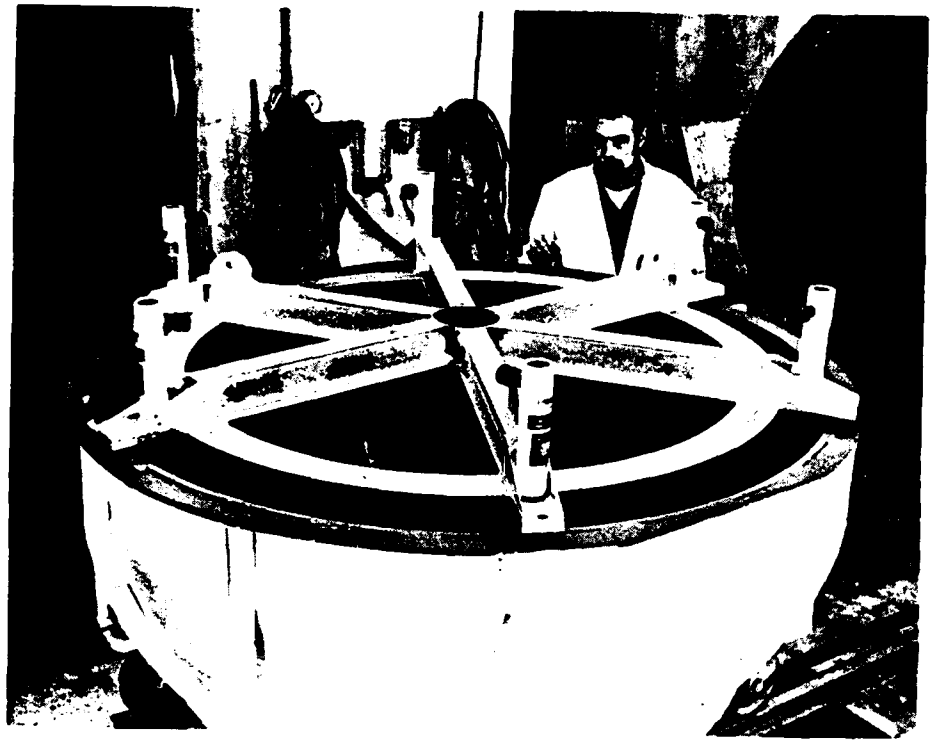

Figure 7. Completed mold assembly with hydraulic jacks and wheels in place.

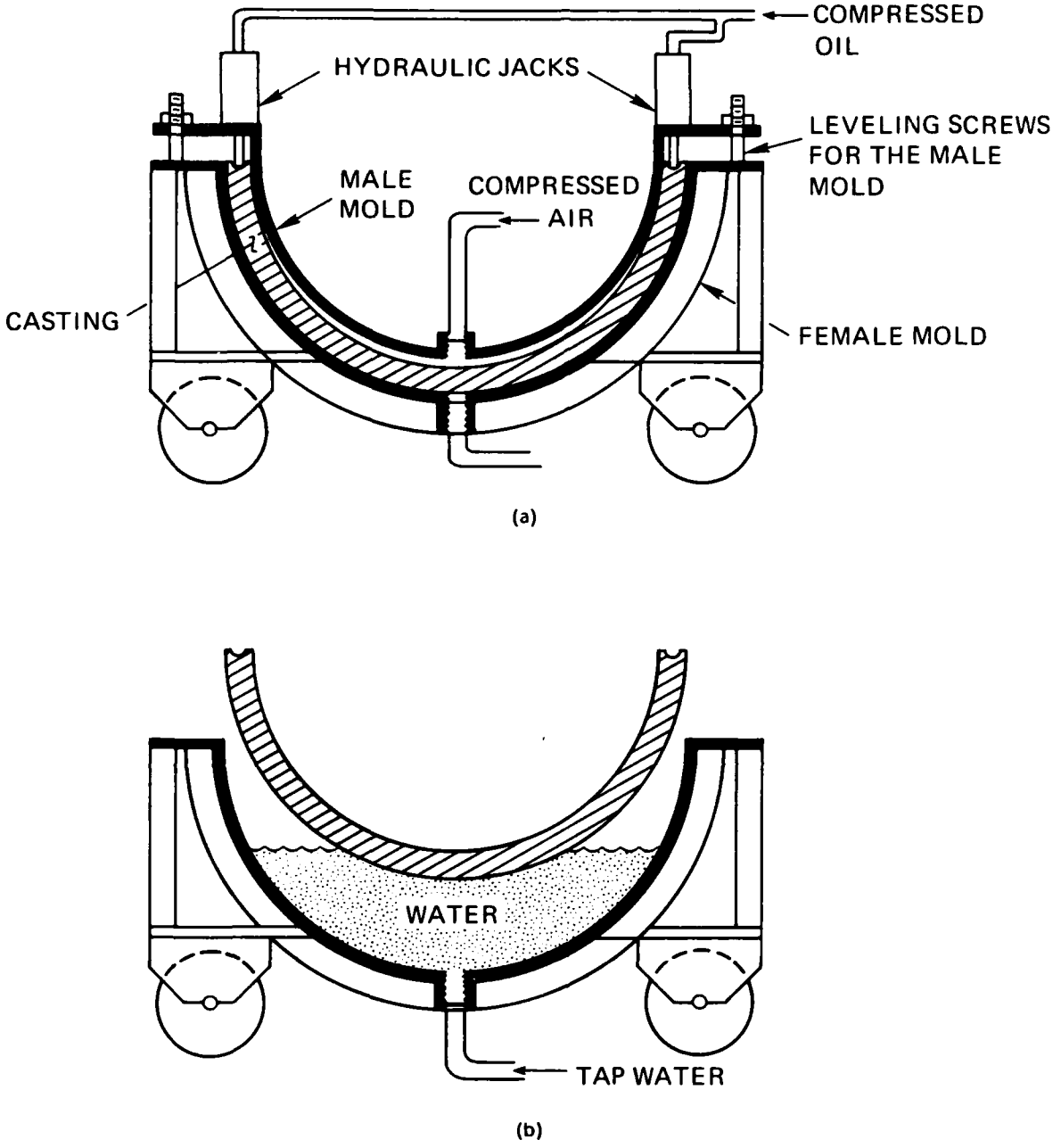

Figure 8. Method of separating molds from casting. (a) Separation of male mold with compressed air and hydraulic jacks. (b) Separation of female mold with compressed water.

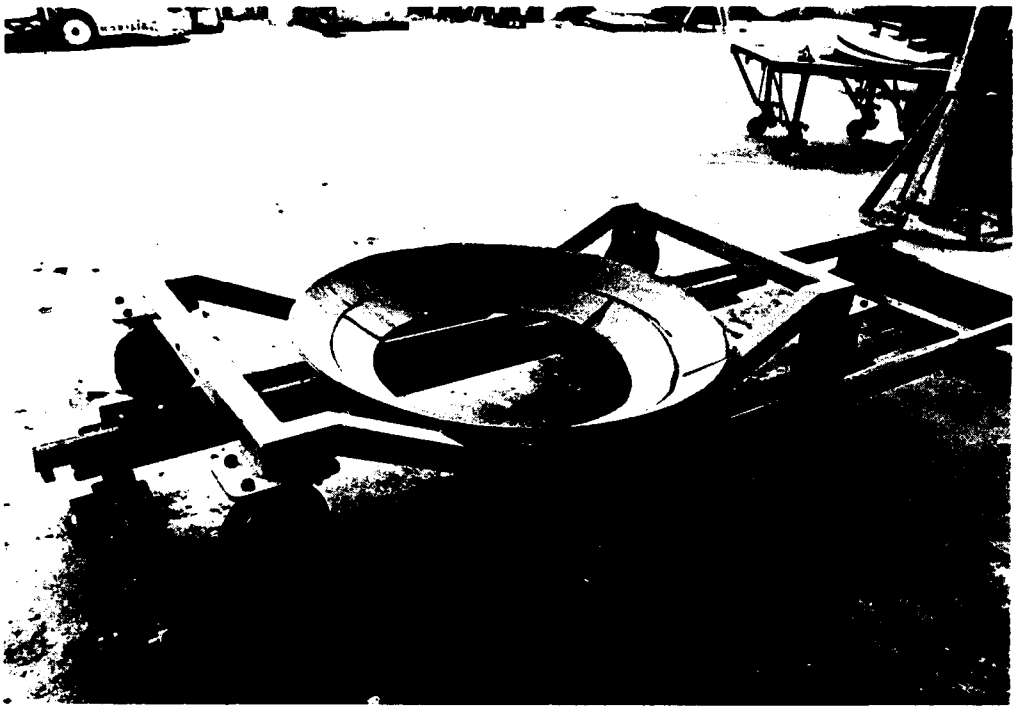

Figure 9. Cart for transporting mold assembly into autoclave.

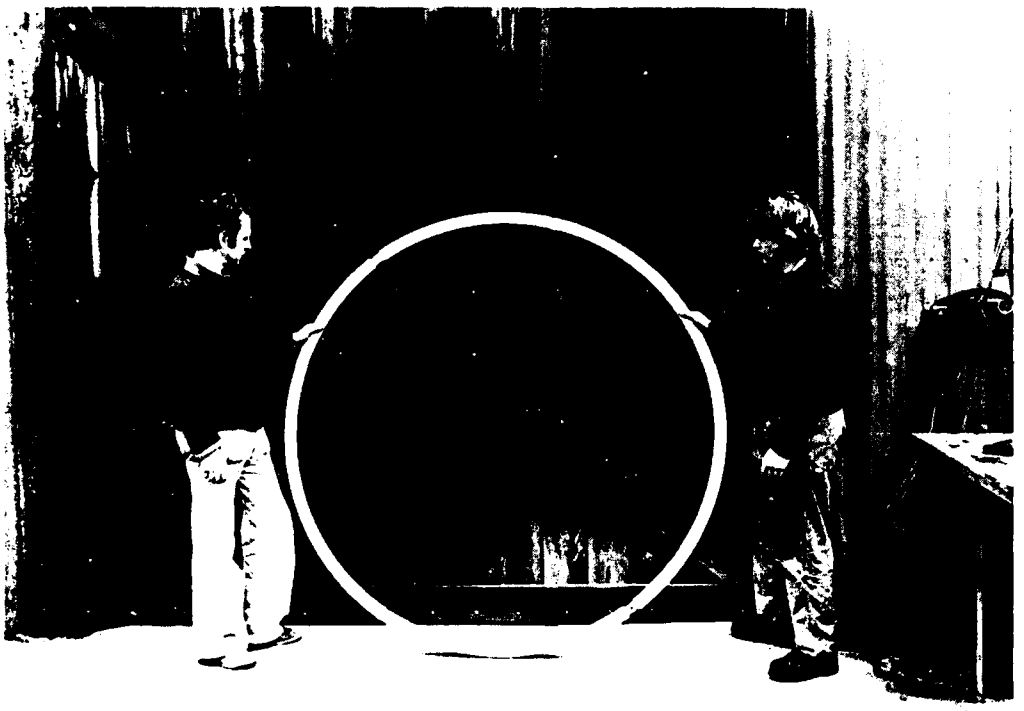

Figure 10. Circular strongback for lifting casting from mold.

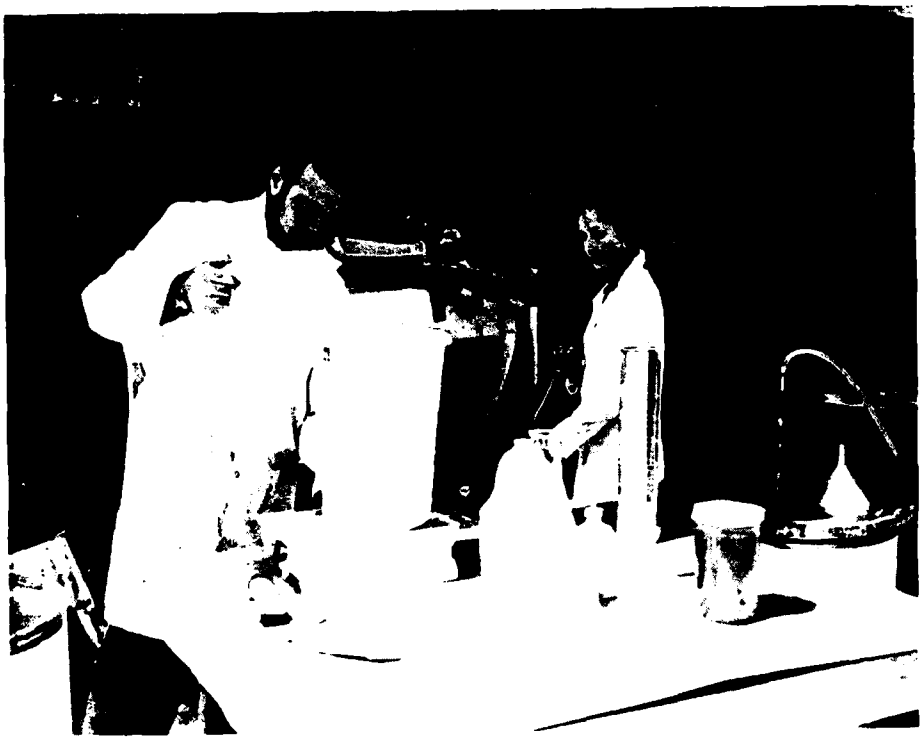

Figure 11. Weighing acrylic polymer powder for a typical casting mix batch.

Figure 12. Mixing of ingredients used in a typical casting mix batch.

Figure 13. Stirring casting mix batch to the verge of gelling.

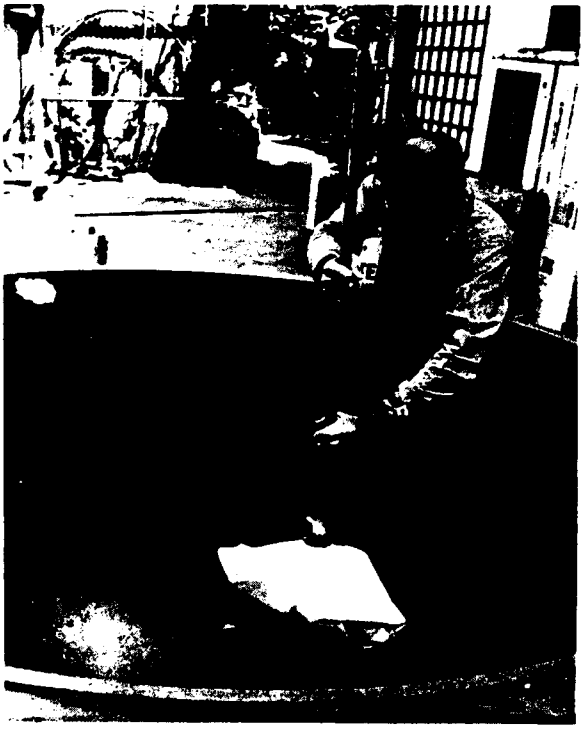

Figure 14. Cleaning of female mold.

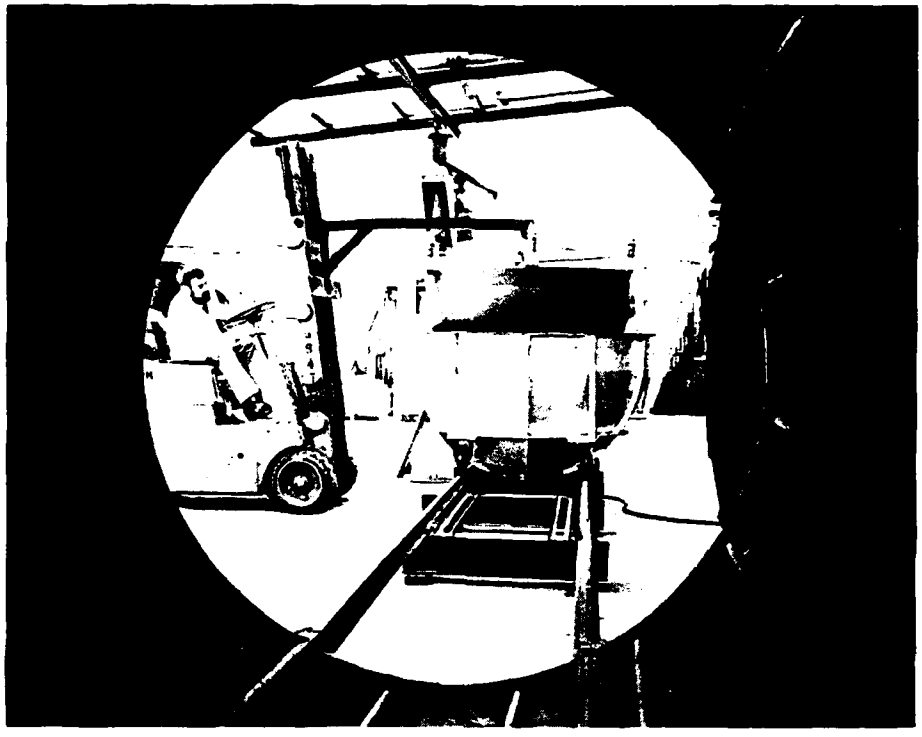

Figure 15. Assembly of cleaned molds to receive casting mix.

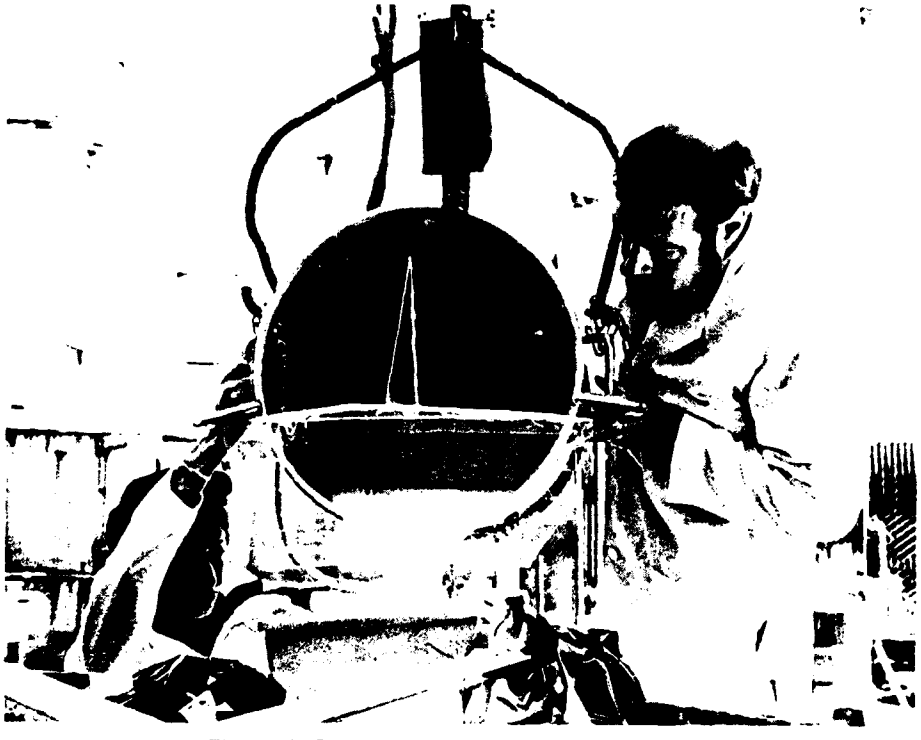

Figure 16. Pouring of casting mix into mold assembly.

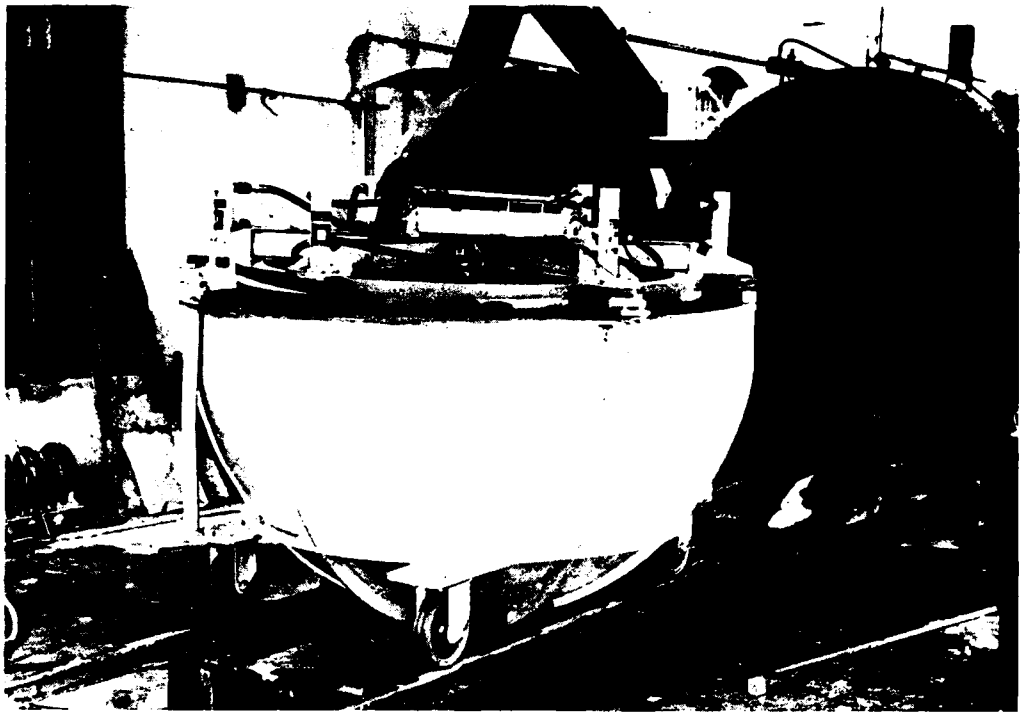

Figure 17. Mold assembly leaving autoclave after polymerization of casting, note hydraulic pump for applying pressure to hydraulic jacks and wooden blocks for keeping raised male mold from resting on casting.

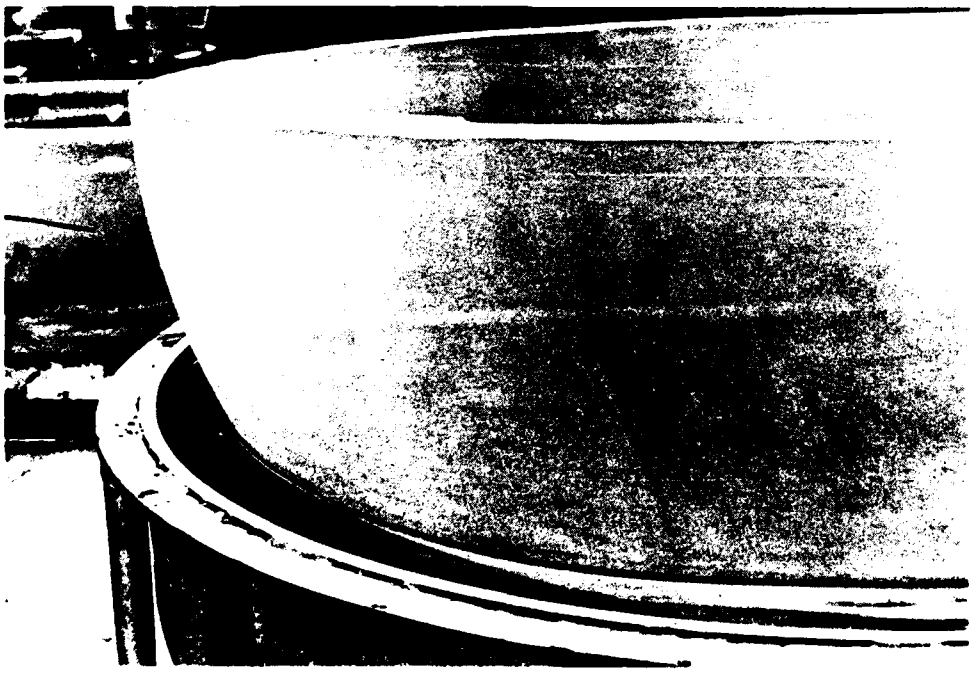

Figure 18. Casting floating on water injected into female mold.

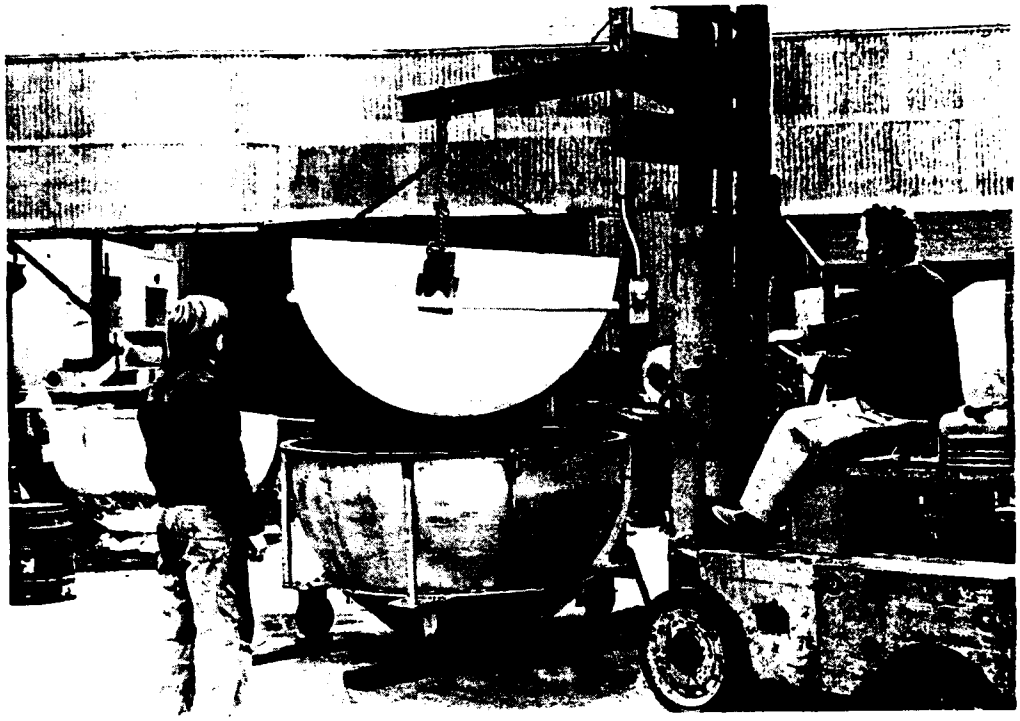

Figure 19. Lifting of casting with strongback.

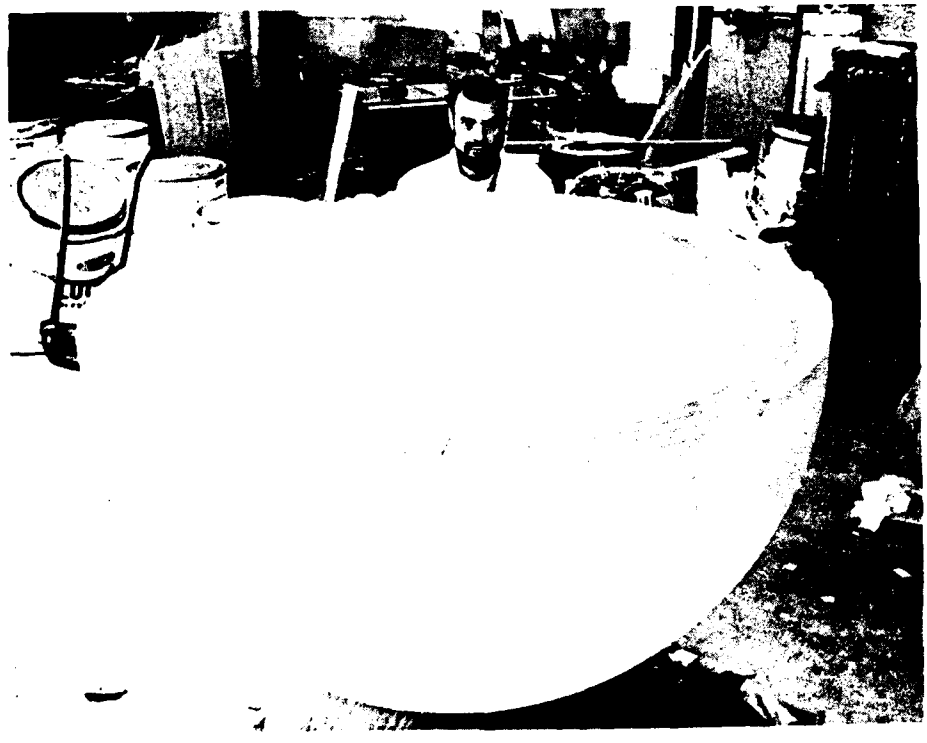

Figure 20. Typical casting after removal from mold.

Figure 21. Separation on surface of casting.

Figure 22. Meridional crack on casting subjected to interrupted polymerization cycle (temperature lowered to room temperature without removing male mold).

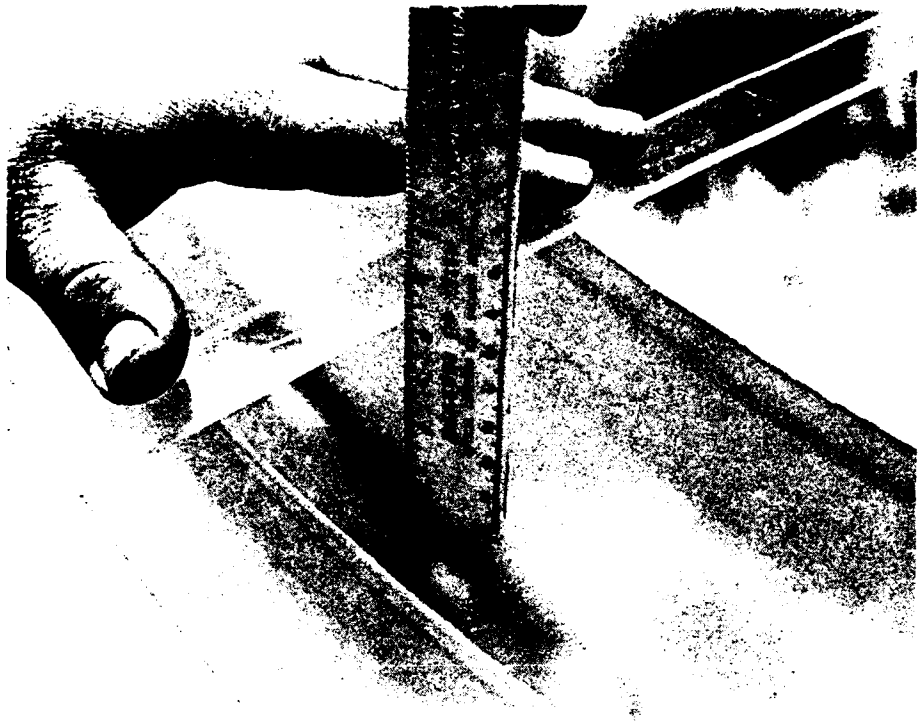

Figure 23. Typical two-inch meniscus on equatorial edge of casting.

Figure 24. Typical voids in castings.

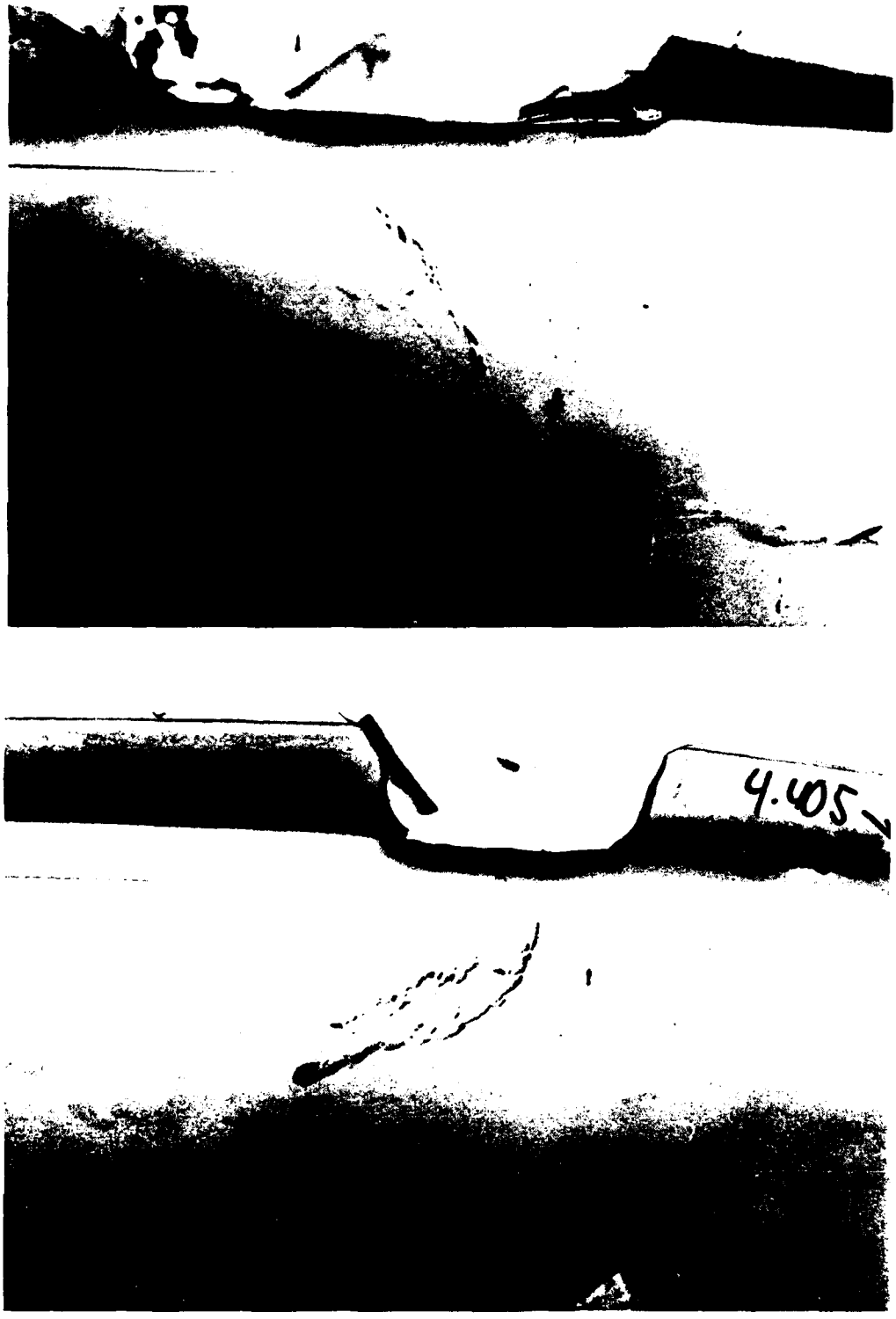

Figure 25. Typical voids after first repair, note numerous small voids.

Figure 26. Typical voids after second repair.

Figure 27. Grinding equatorial edge of casting before machining.

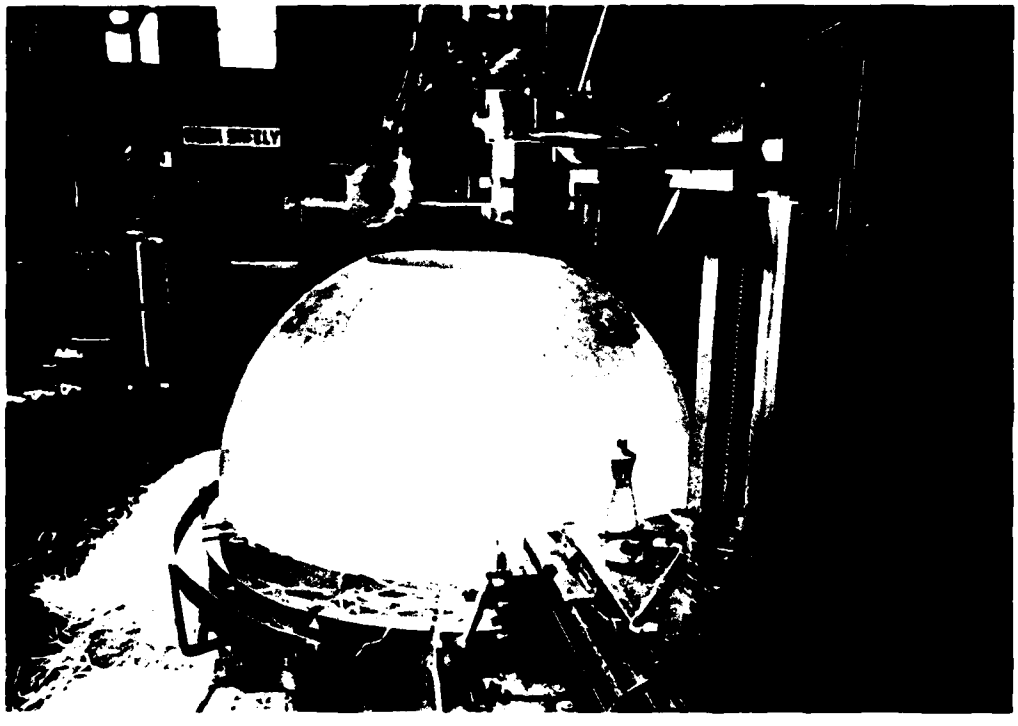

Figure 28. Casting after machining of polar opening.

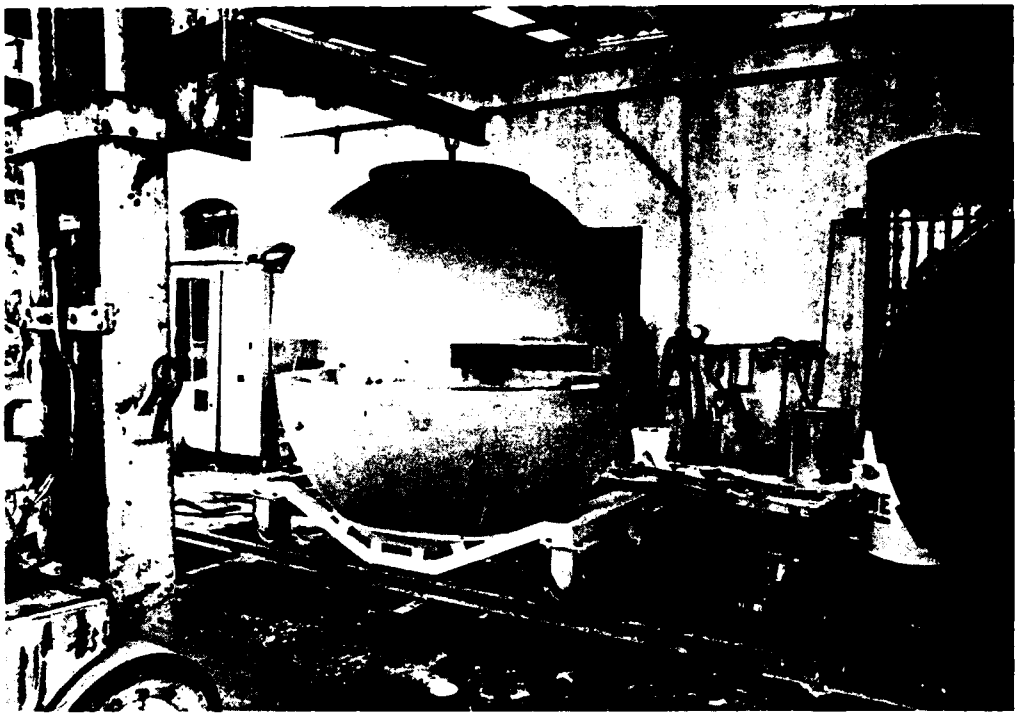

Figure 29. Assembly of castings for bonding together at equatorial joint.

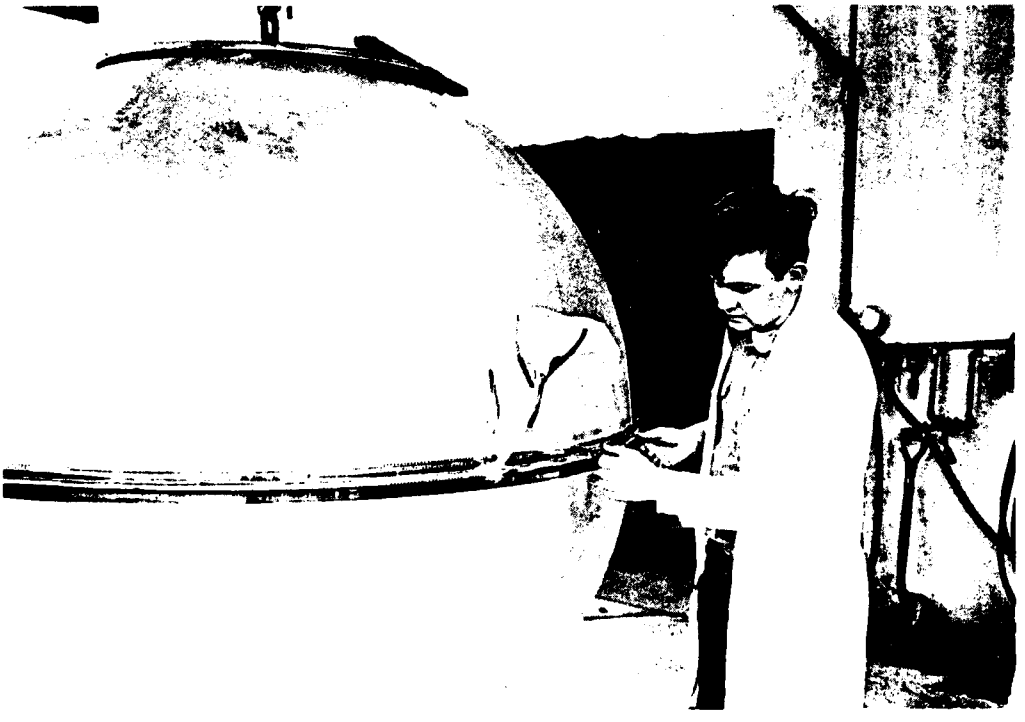

Figure 30. Taped equatorial joint ready for pouring of casting mix.

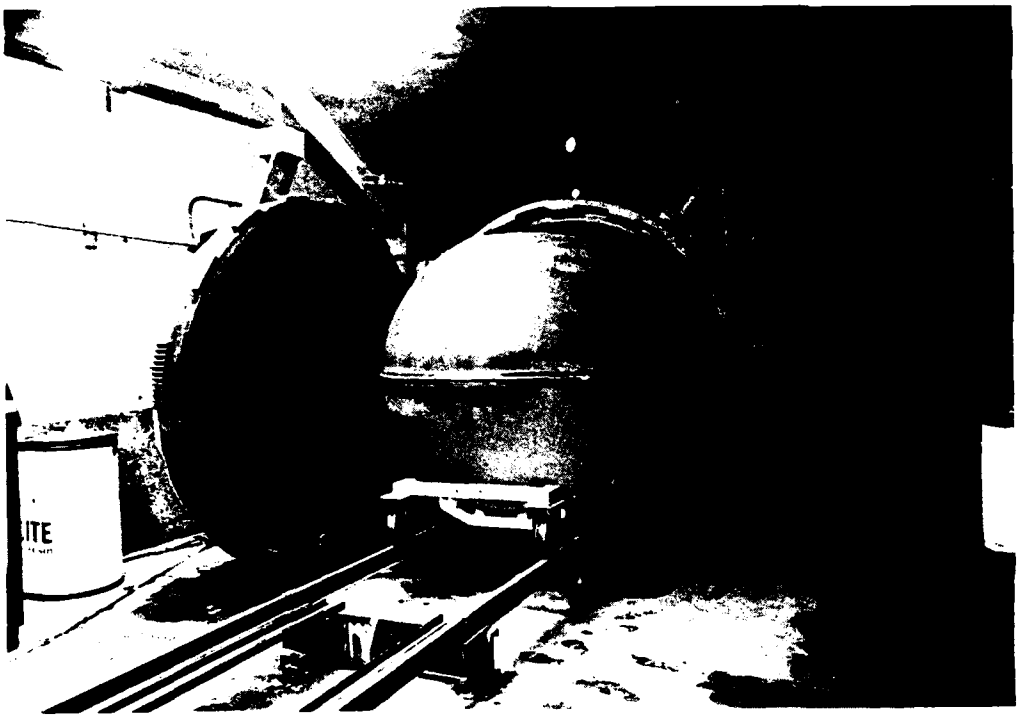

Figure 31. Gelled casting mix in equatorial joint ready for polymerization in autoclave.

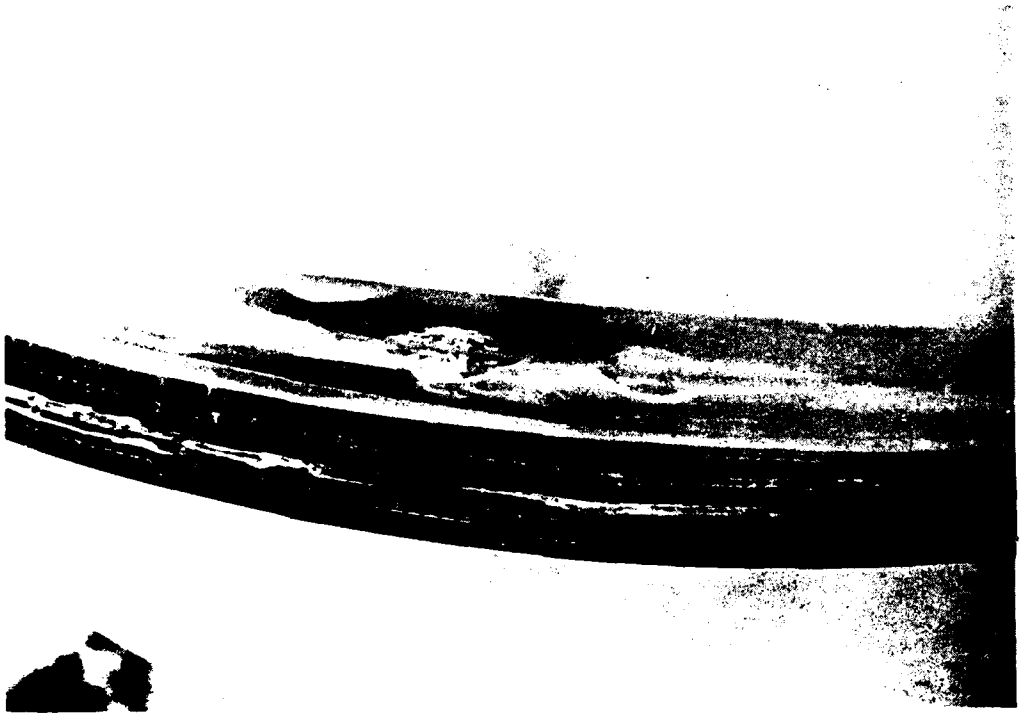

Figure 32. Polymerized equatorial joint with shrinkage voids on inner surface.

Figure 33. Equatorial joint after repair with room-temperature-polymerizing PS-30 adhesive.

Figure 34. Completed acrylic plastic sphere ready for inspection.

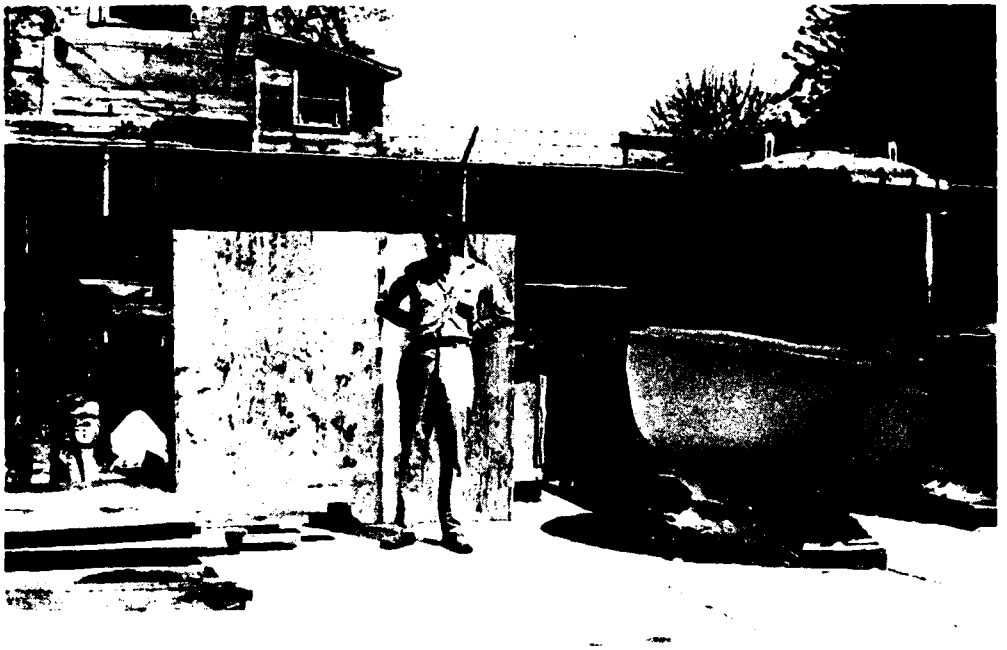

(a)

(b)

Figure 35. View through assembled sphere. (a) Above equatorial joint. (b) At equatorial joint.

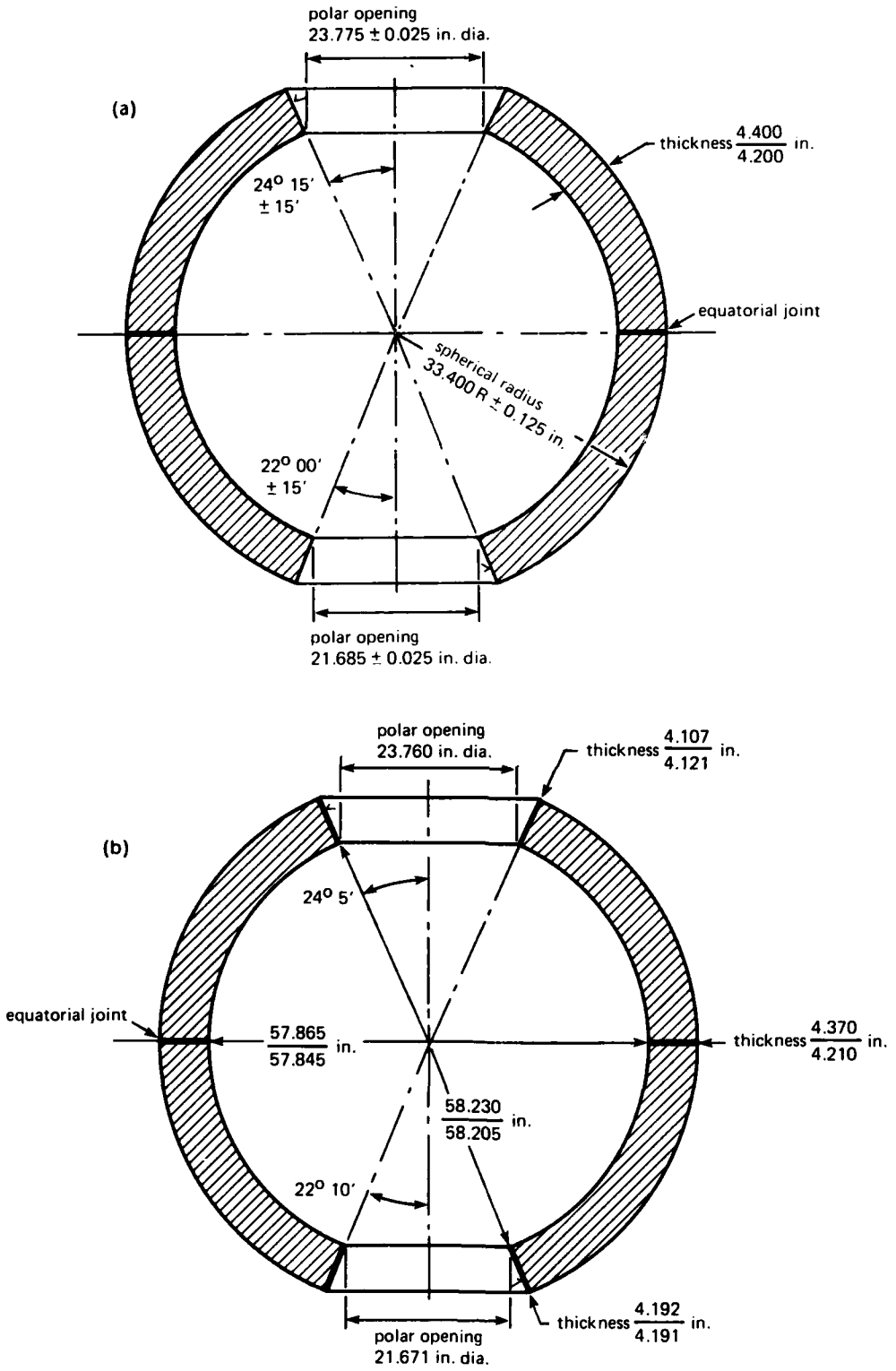

Figure 36. Dimensions of assembled sphere. (a) Specified dimensions. (b) Actual dimensions.

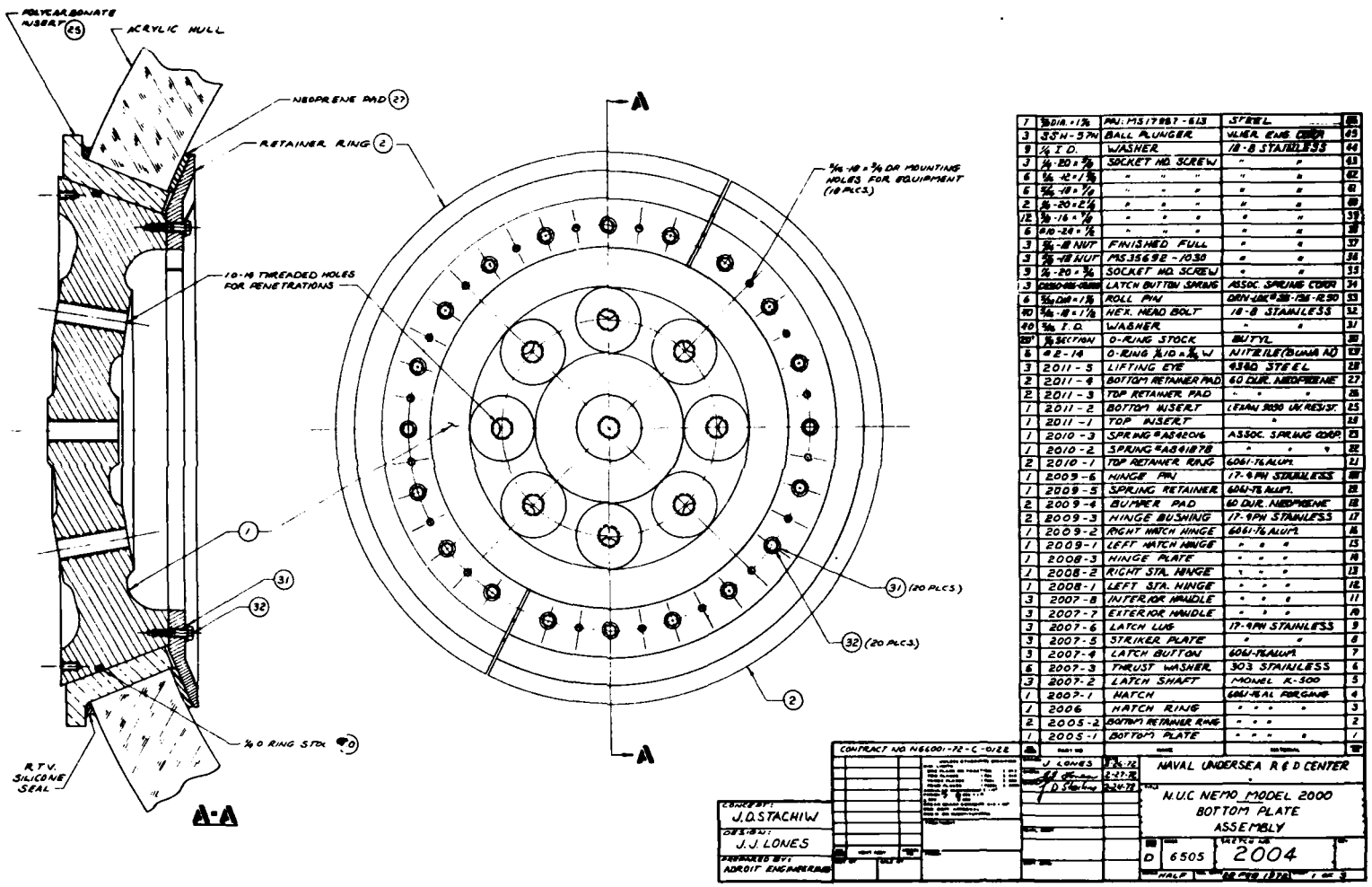

1	3" DIA. x 1 3/8	PAT. MS17987-613	STEEL	65
3	3.5 N-3 PH	BALL PLUNGER	VLIER. ENG. CORP.	64
9	1/4 I.D.	WASHER	18-8 STAINLESS	63
3	1/4-20 x 5/8	SOCKET HD. SCREW	" "	61
6	1/4-20 x 1 3/4	" " "	" "	62
6	5/16-18 x 1/2	" " "	" "	61
2	1/4-20 x 2 1/4	" " "	" "	60
12	1/2-16 x 1/2	" " "	" "	59
6	#10-24 x 1/2	" " "	" "	58
3	5/16-18 NUT	FINISHED FULL	" "	57
3	5/16-18 NUT	MS35692-1030	" "	56
3	1/4-20 x 3/4	SOCKET HD. SCREW	" "	55
3	[illegible]	LATCH BUTTON SPRING	ASSOC. SPRING CORP.	54
6	3/16 DIA x 1 1/8	ROLL PIN	DRIV-LOK #38-188-1250	53
90	3/16-18 x 1 1/8	HEX. HEAD BOLT	18-8 STAINLESS	52
90	3/16 I.D.	WASHER	" "	51
220'	1/8 SECTION	O-RING STOCK	BUTYL	50
6	#2-14	O-RING 1/4 I.D. x 3/8 W	NITRILE (BUNA N)	49
3	2011-5	LIFTING EYE	4340 STEEL	28
2	2011-4	BOTTOM RETAINER PAD	60 DUR. NEOPRENE	27
2	2011-3	TOP RETAINER PAD	" " "	26
1	2011-2	BOTTOM INSERT	(FORM 9030 UV RESIST.	25
1	2011-1	TOP INSERT	"	24
1	2010-3	SPRING #AS42016	ASSOC. SPRING CORP.	23
1	2010-2	SPRING #AS41878	" " "	22
2	2010-1	TOP RETAINER RING	6061-T6 ALUM.	21
1	2009-6	HINGE PIN	17-4 PH STAINLESS	20
1	2009-5	SPRING RETAINER	6061-T6 ALUM.	19
2	2009-4	BUMPER PAD	60 DUR. NEOPRENE	18
2	2009-3	HINGE BUSHING	17-4 PH STAINLESS	17
1	2009-2	RIGHT HATCH HINGE	6061-T6 ALUM.	16
1	2009-1	LEFT HATCH HINGE	" " "	15
1	2008-3	HINGE PLATE	" " "	14
1	2008-2	RIGHT STA. HINGE	" " "	13
1	2008-1	LEFT STA. HINGE	" " "	12
3	2007-8	INTERIOR HANDLE	" " "	11
3	2007-7	EXTERIOR HANDLE	" " "	10
3	2007-6	LATCH LUG	17-4 PH STAINLESS	9
3	2007-5	STRIKER PLATE	" "	8
3	2007-4	LATCH BUTTON	6061-T6 ALUM.	7
6	2007-3	THRUST WASHER	303 STAINLESS	6
3	2007-2	LATCH SHAFT	MONEL K-500	5
1	2007-1	HATCH	6061-T6 AL FORGING	4
1	2006	HATCH RING	" " "	3
2	2005-2	BOTTOM RETAINER RING	" " "	2
1	2005-1	BOTTOM PLATE	" " "	1

CONTRACT NO. N66001-72-C-0122

DRAWN BY: J. LONES 8-24-72
CHECKED BY: J.D. STACHIW 8-24-72
DESIGN BY: J.J. LONES
APPROVED BY: ADROIT ENGINEERING

NAVAL UNDERSEA R & D CENTER

N.U.C. NEMO MODEL 2000
BOTTOM PLATE
ASSEMBLY

SIZE D | CODE 6505 | DRAWING NO. 2004

Figure 37. Penetration plate assembly.

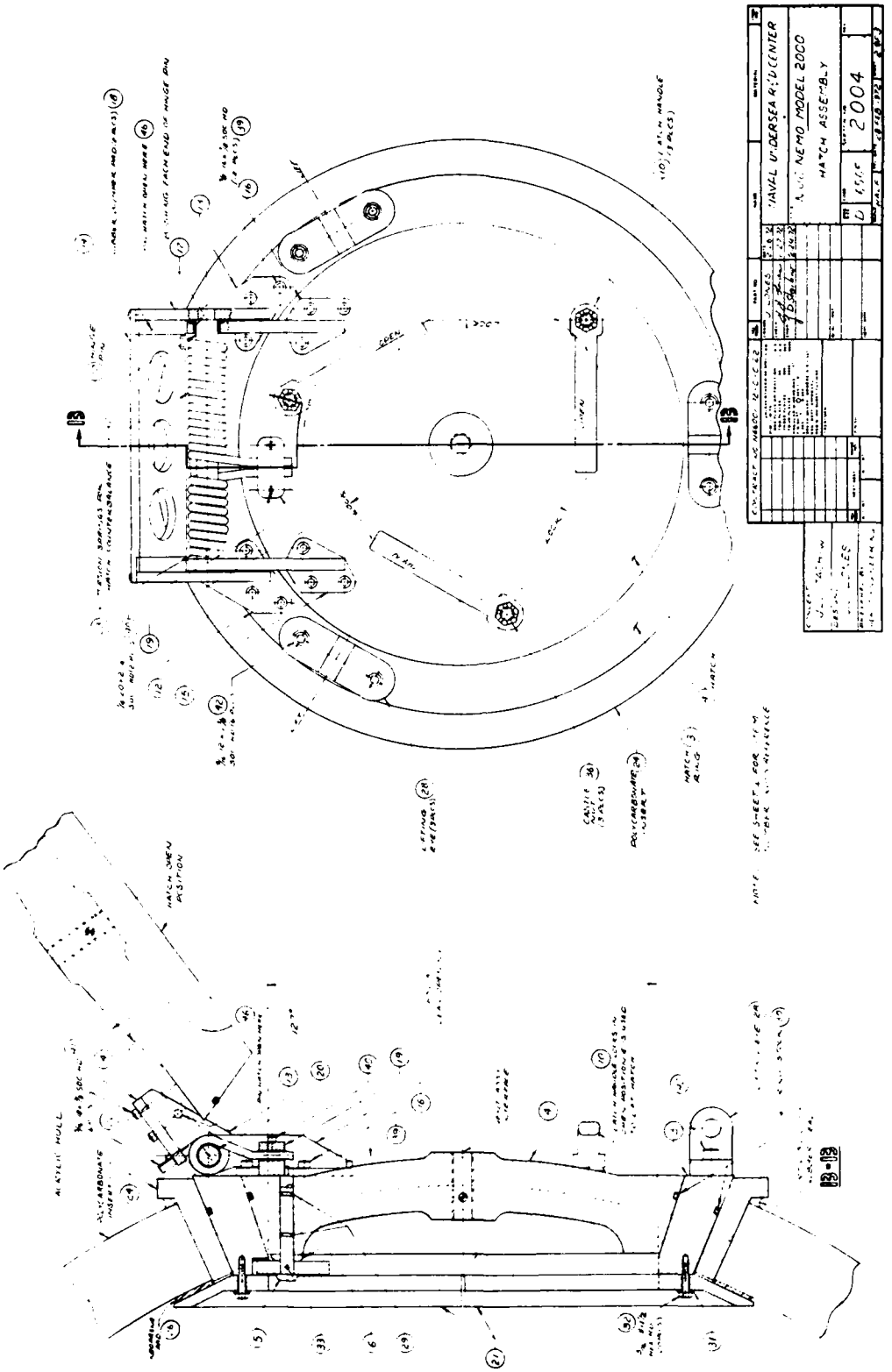

Figure 38. Hatch assembly.

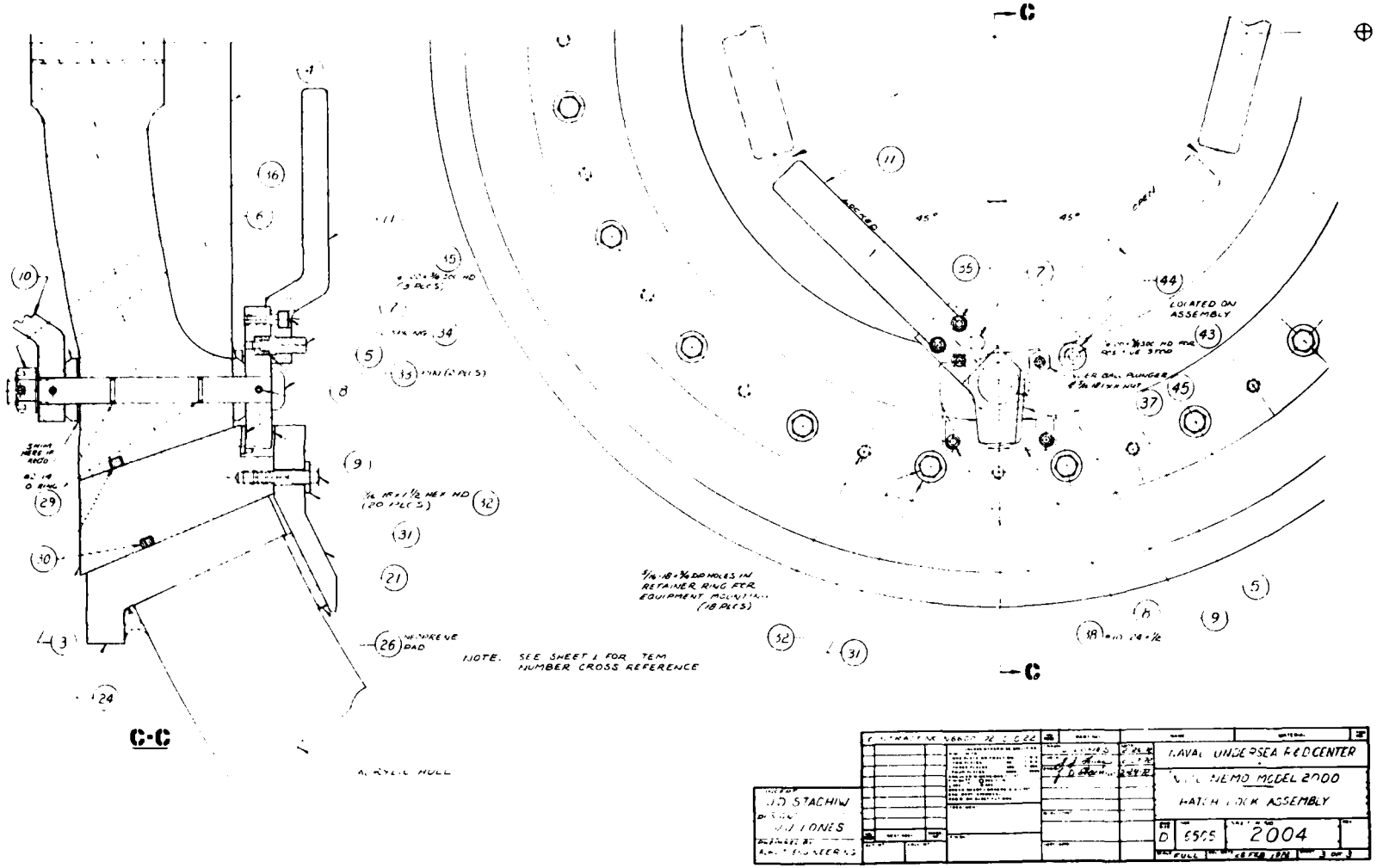

Figure 39. Hatch lock assembly.

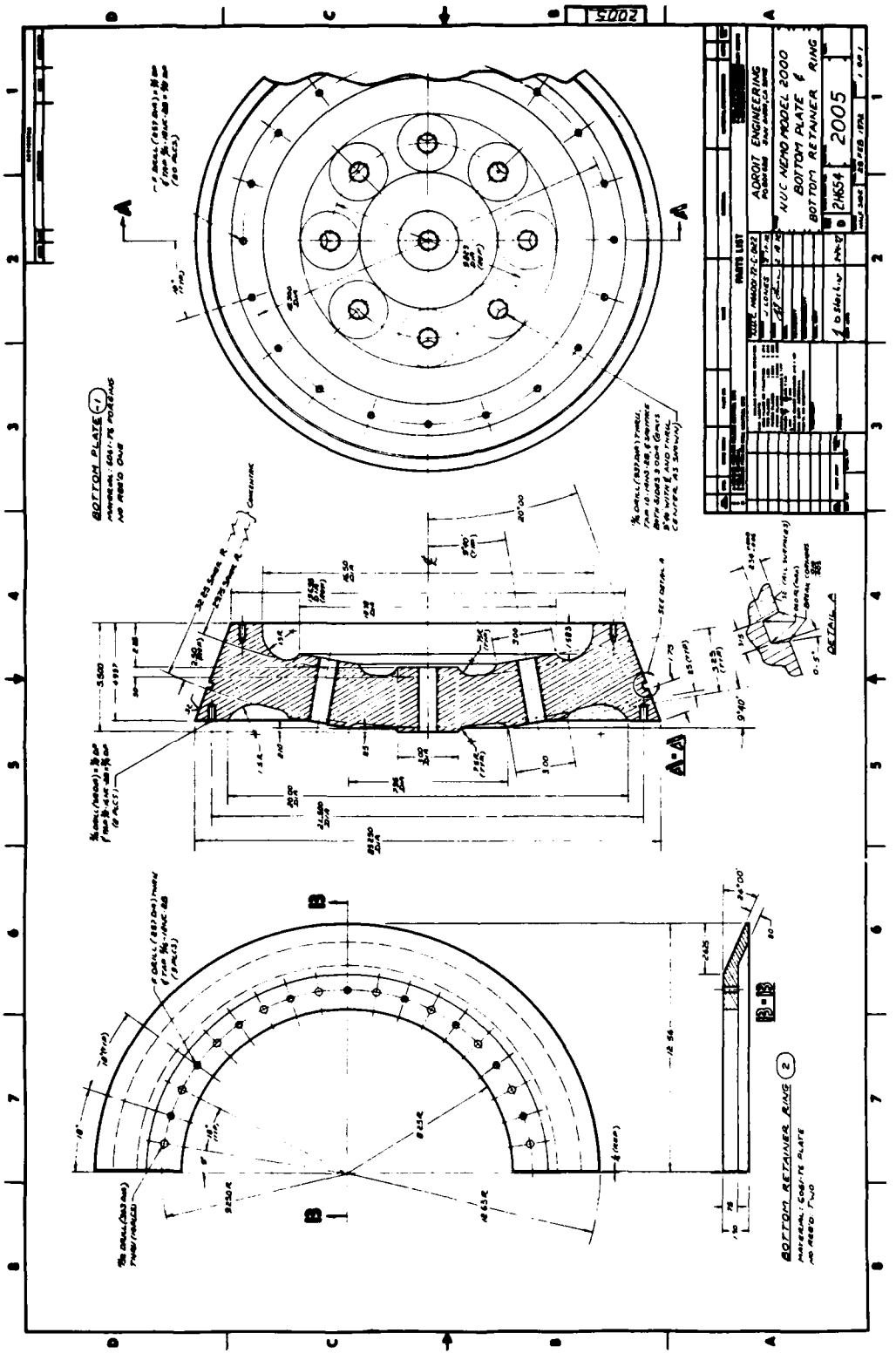

Figure 40. Penetration plate and retainer ring.

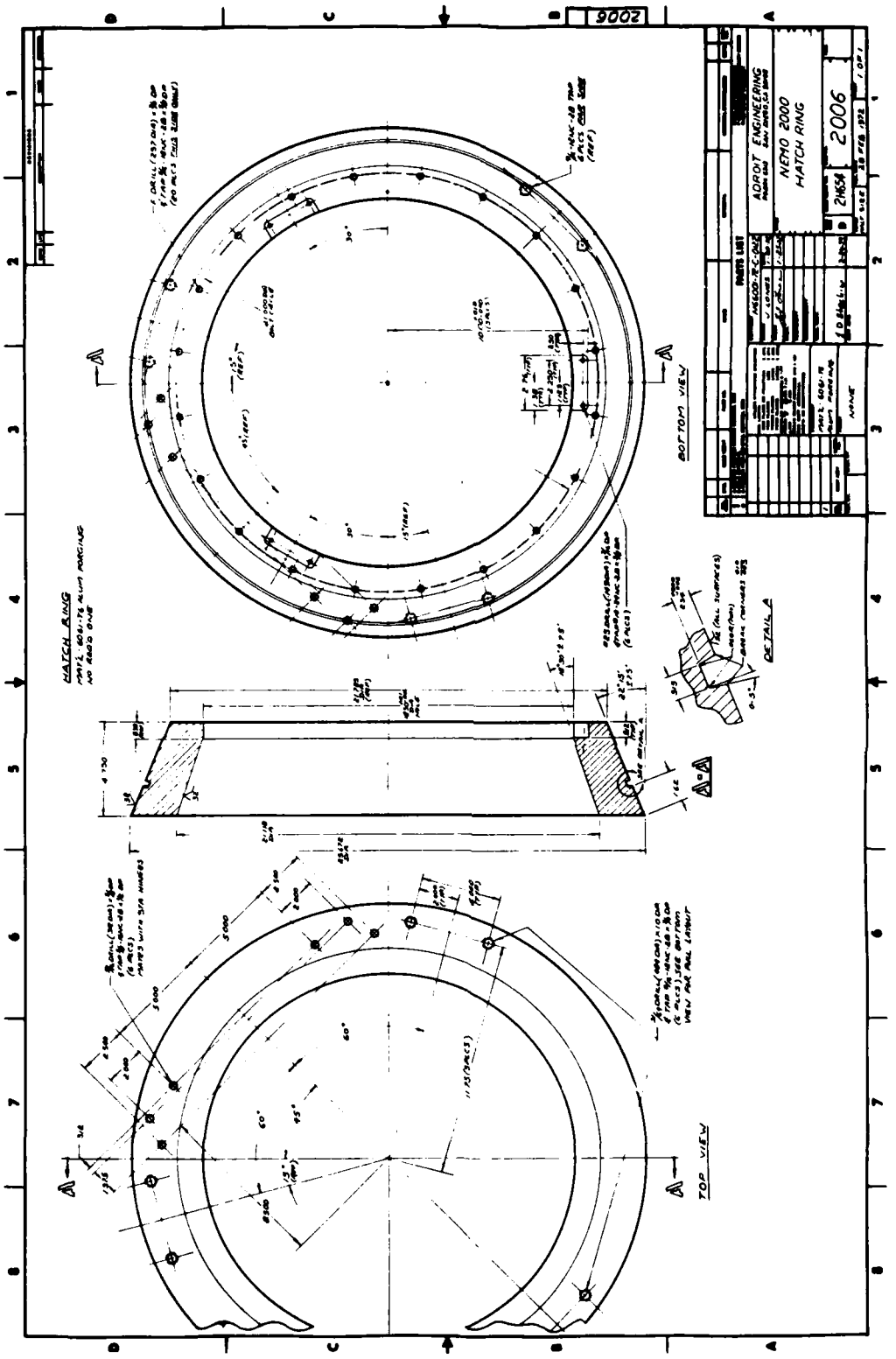

Figure 41. Hatch ring.

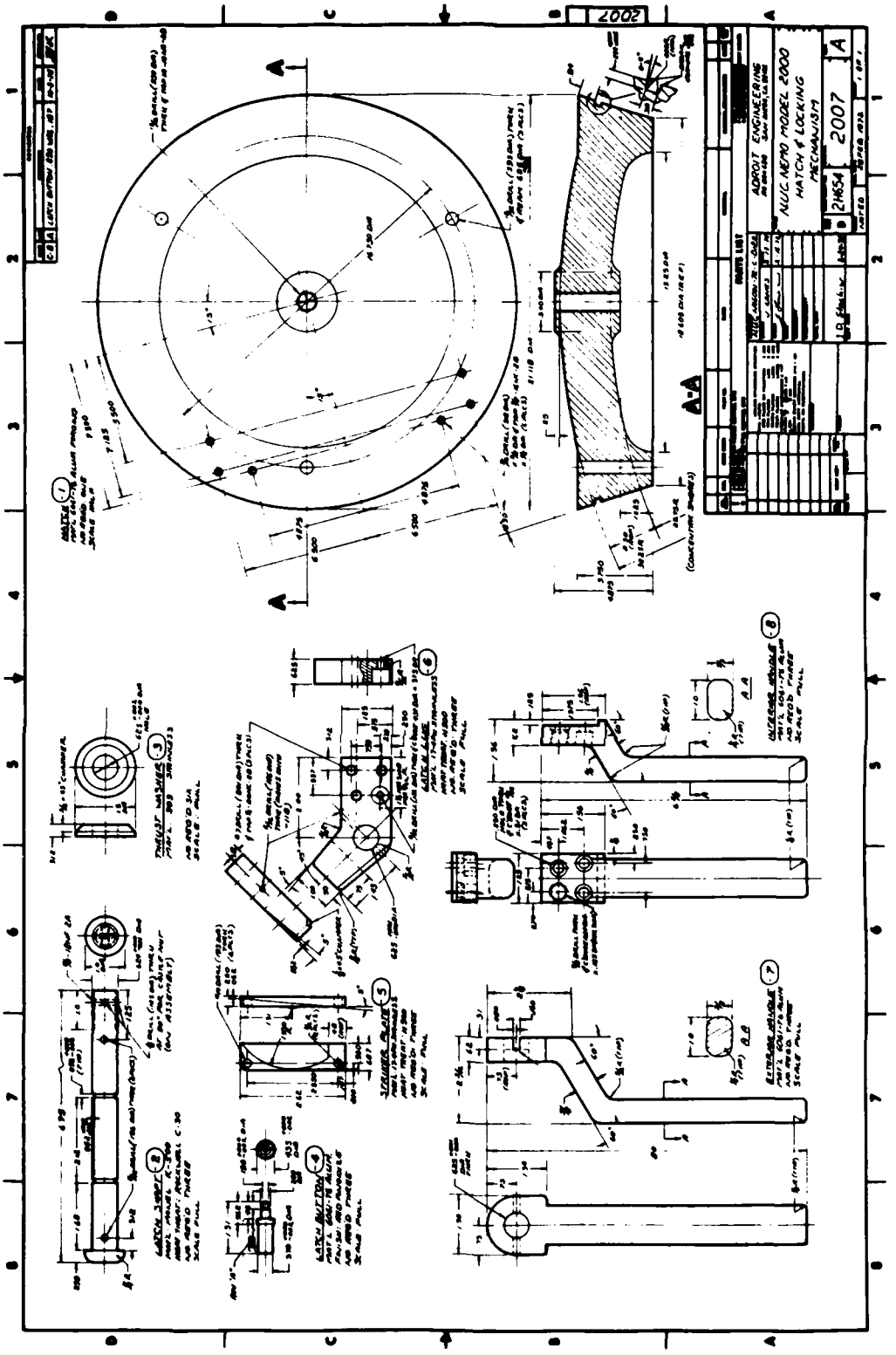

Figure 42. Hatch and locking mechanism.

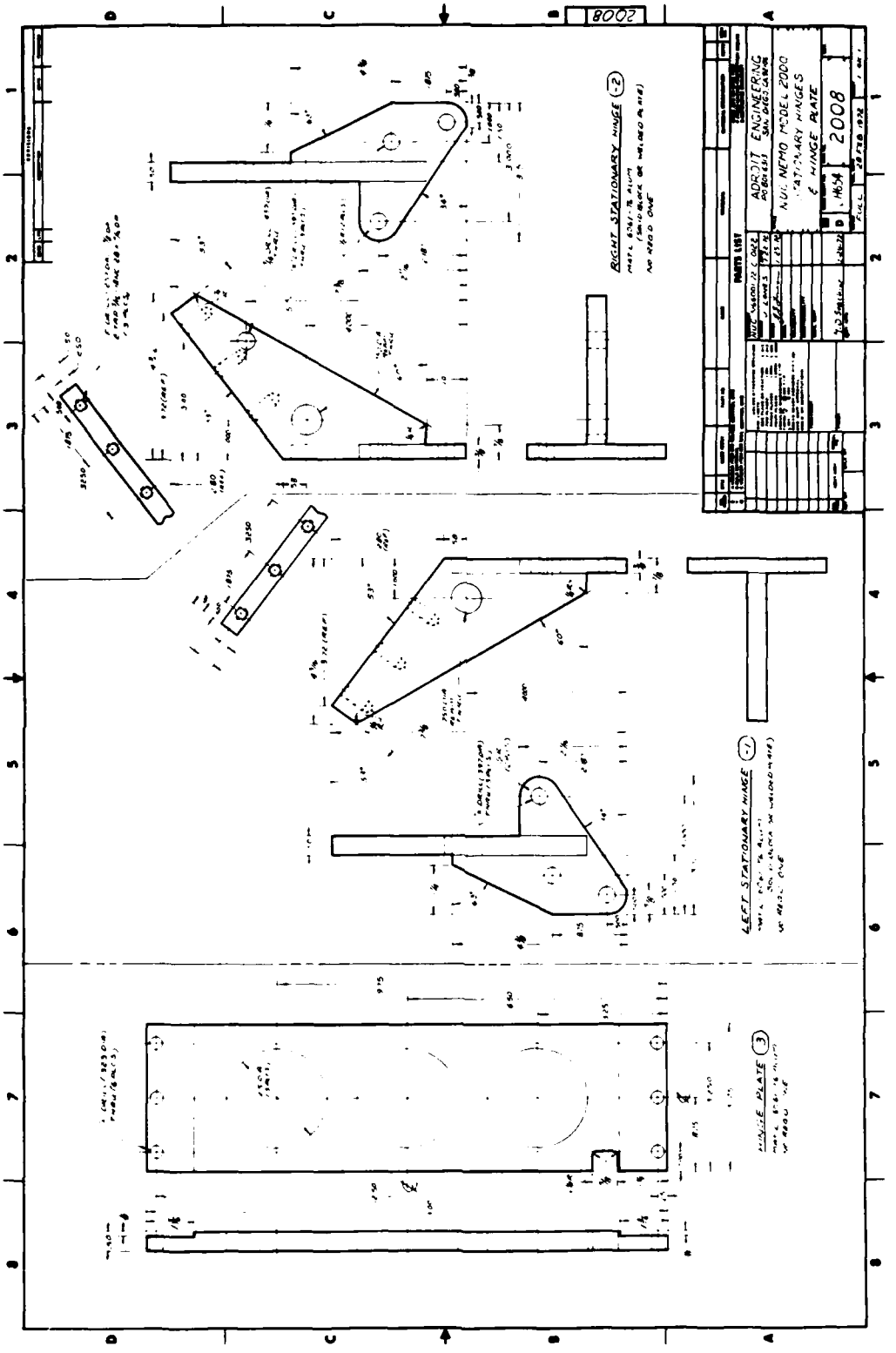

Figure 43. Stationary hinges and hinge plate.

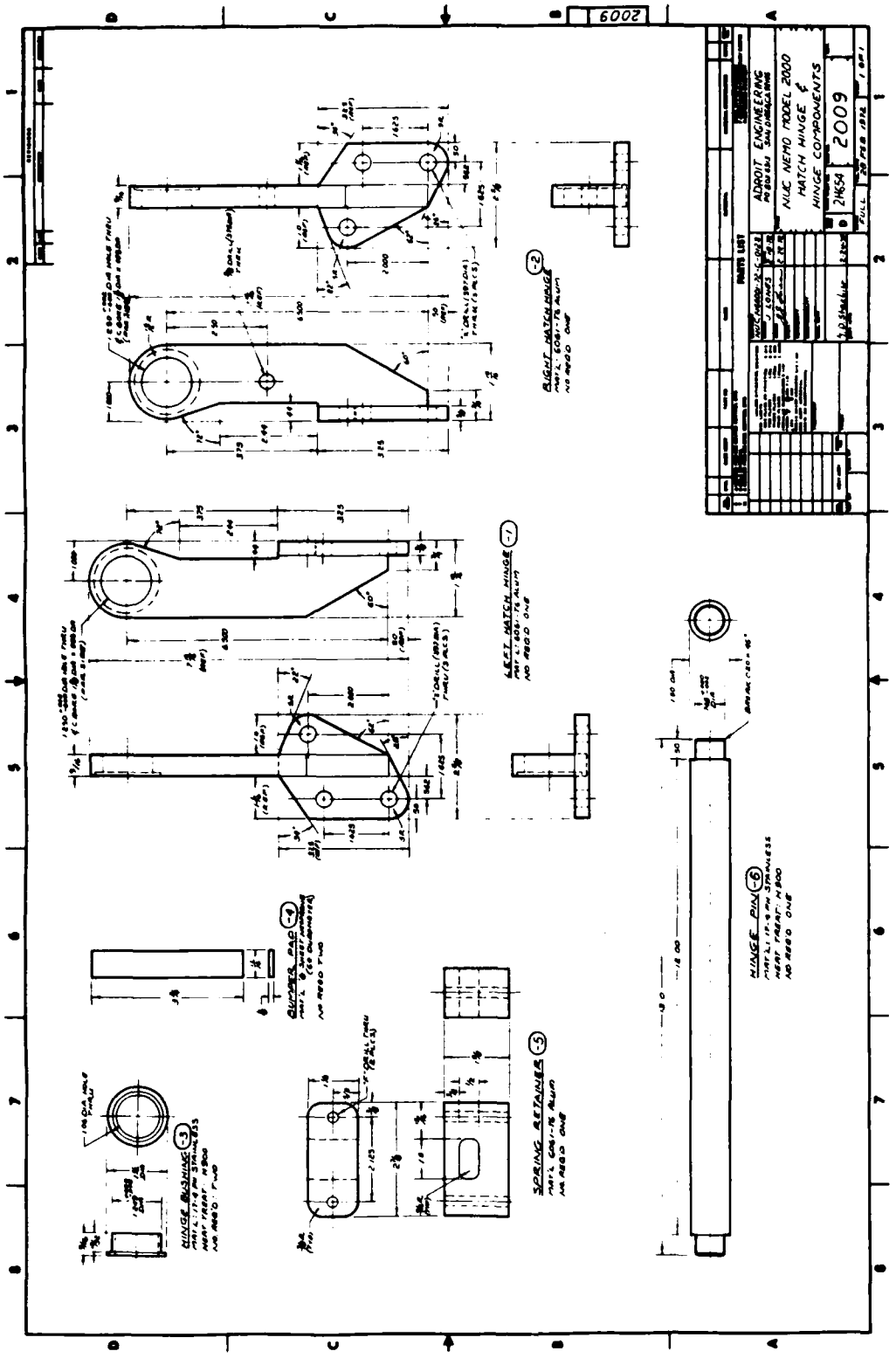

Figure 44. Hatch hinge and hinge components.

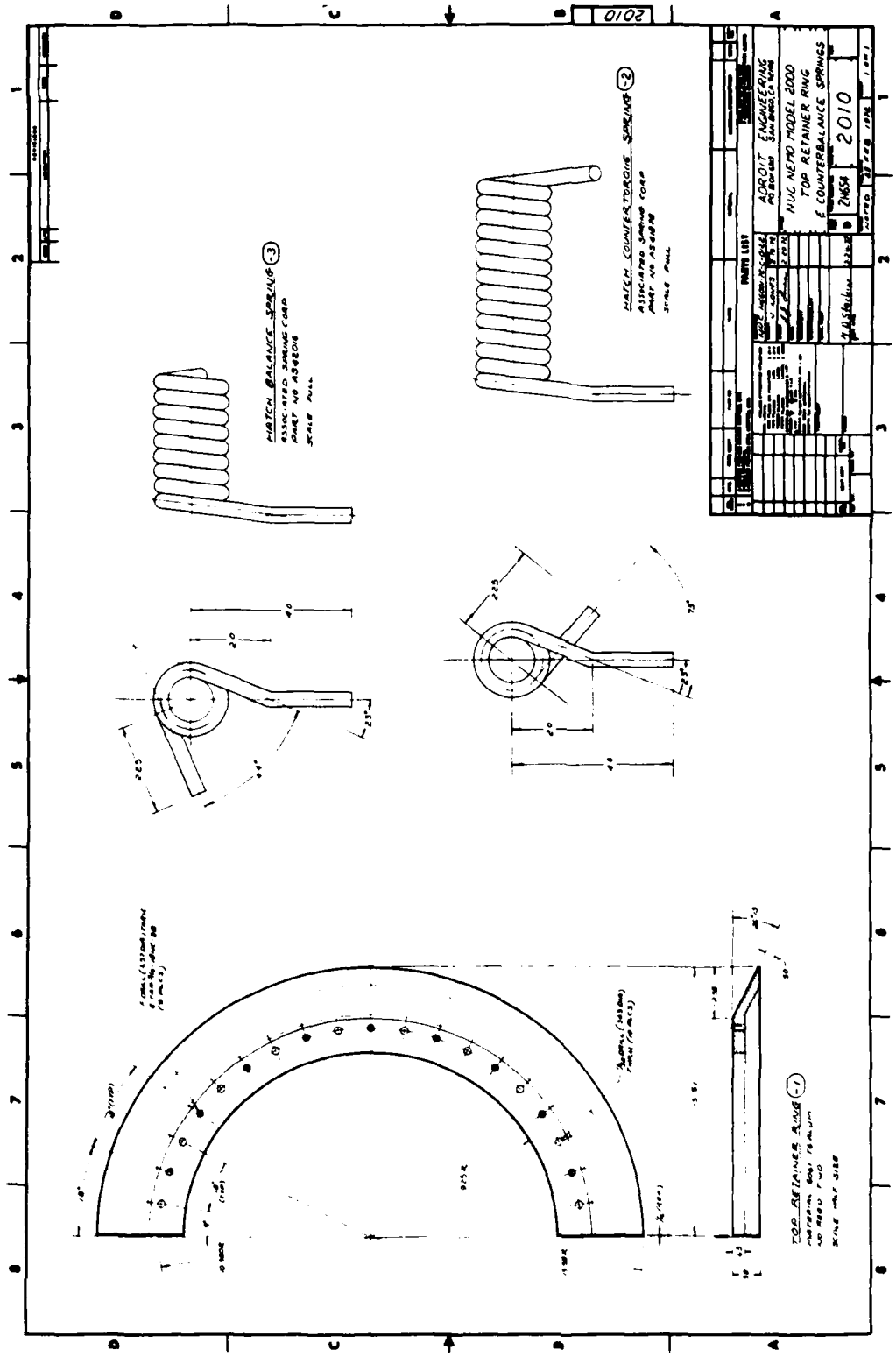

Figure 45. Hatch retainer ring and counterbalance springs.

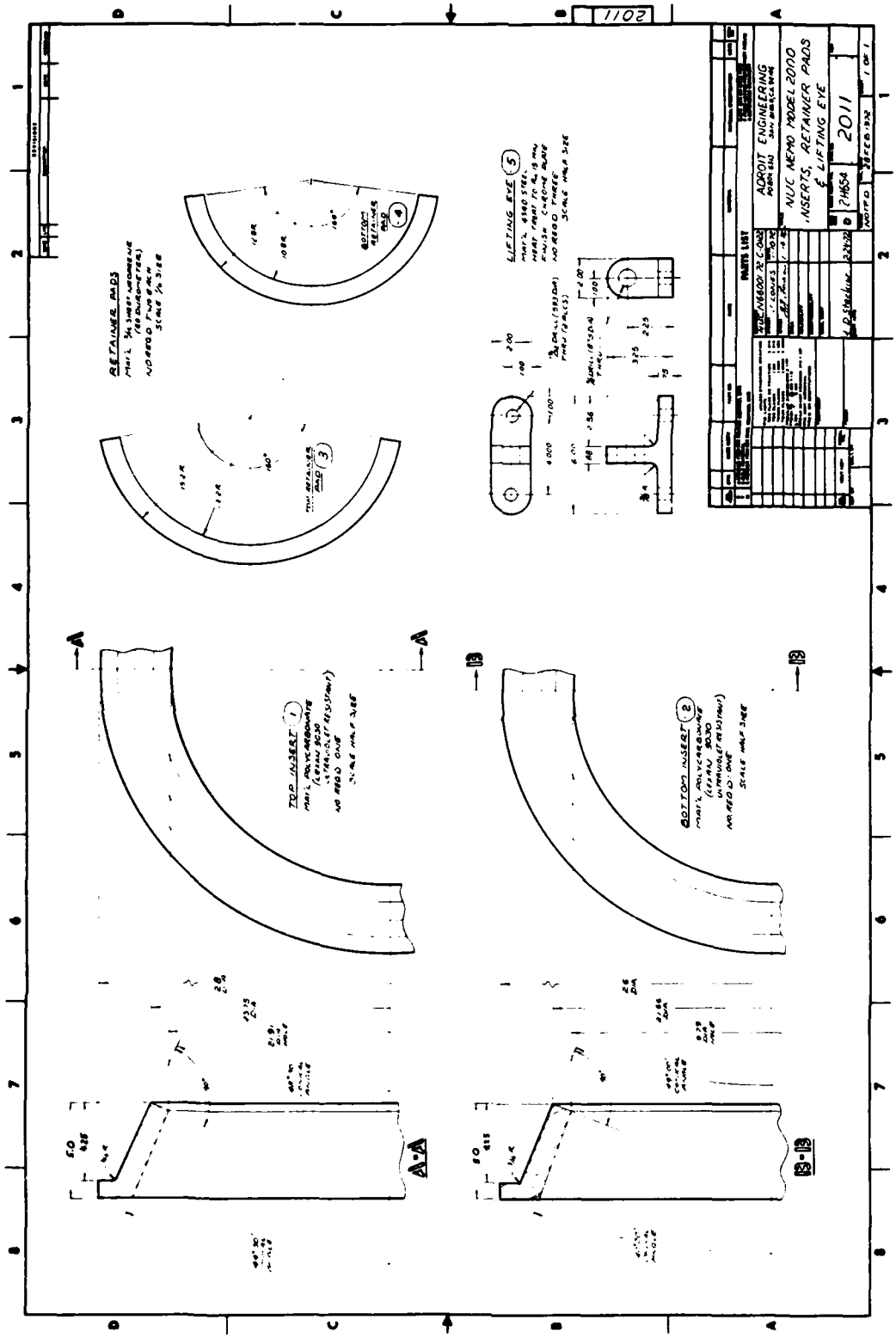

Figure 46. Inserts, retainer pads, and lifting eye.

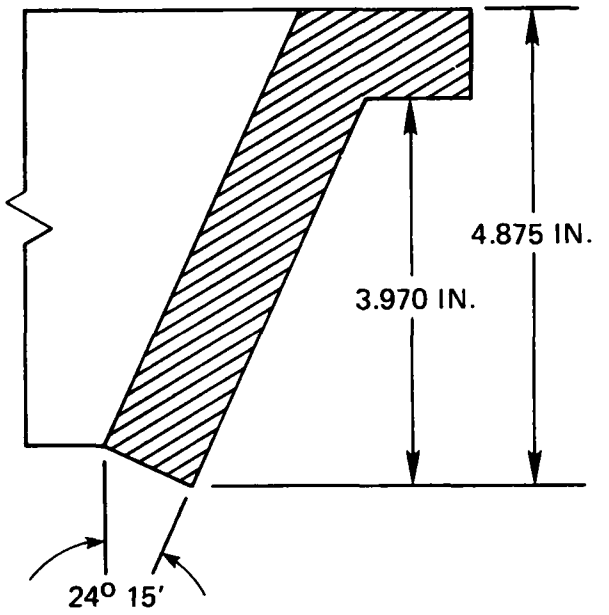

(a)

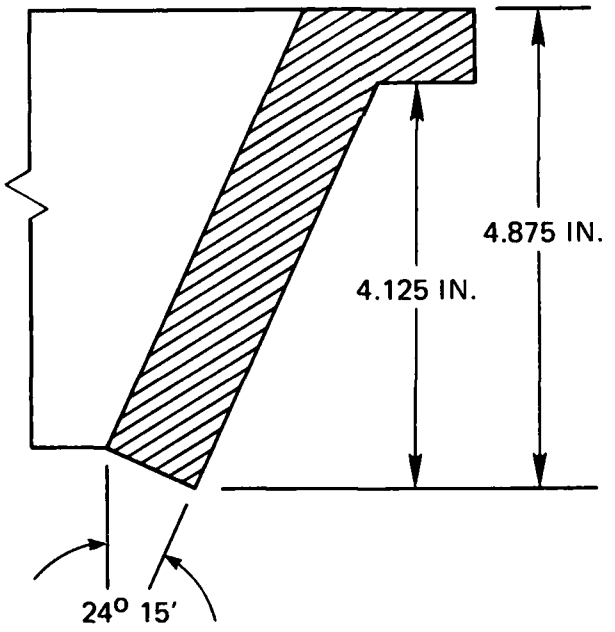

(b)

Figure 47. Polycarbonate gasket. (a) Before modification. (b) After modification.

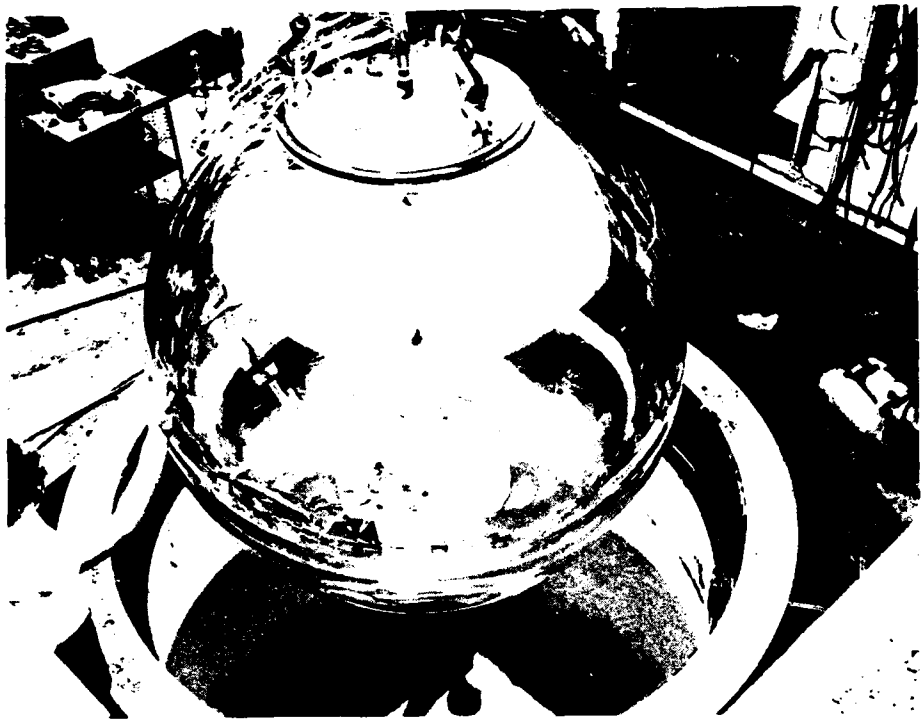

Figure 48. Placing the model 2000B assembly in the 90-inch-diameter pressure vessel at Southwest Research Institute.

Figure 49. Model 2000B assembly instrumented with electrical resistance strain gages and water displacement measurement tubing.

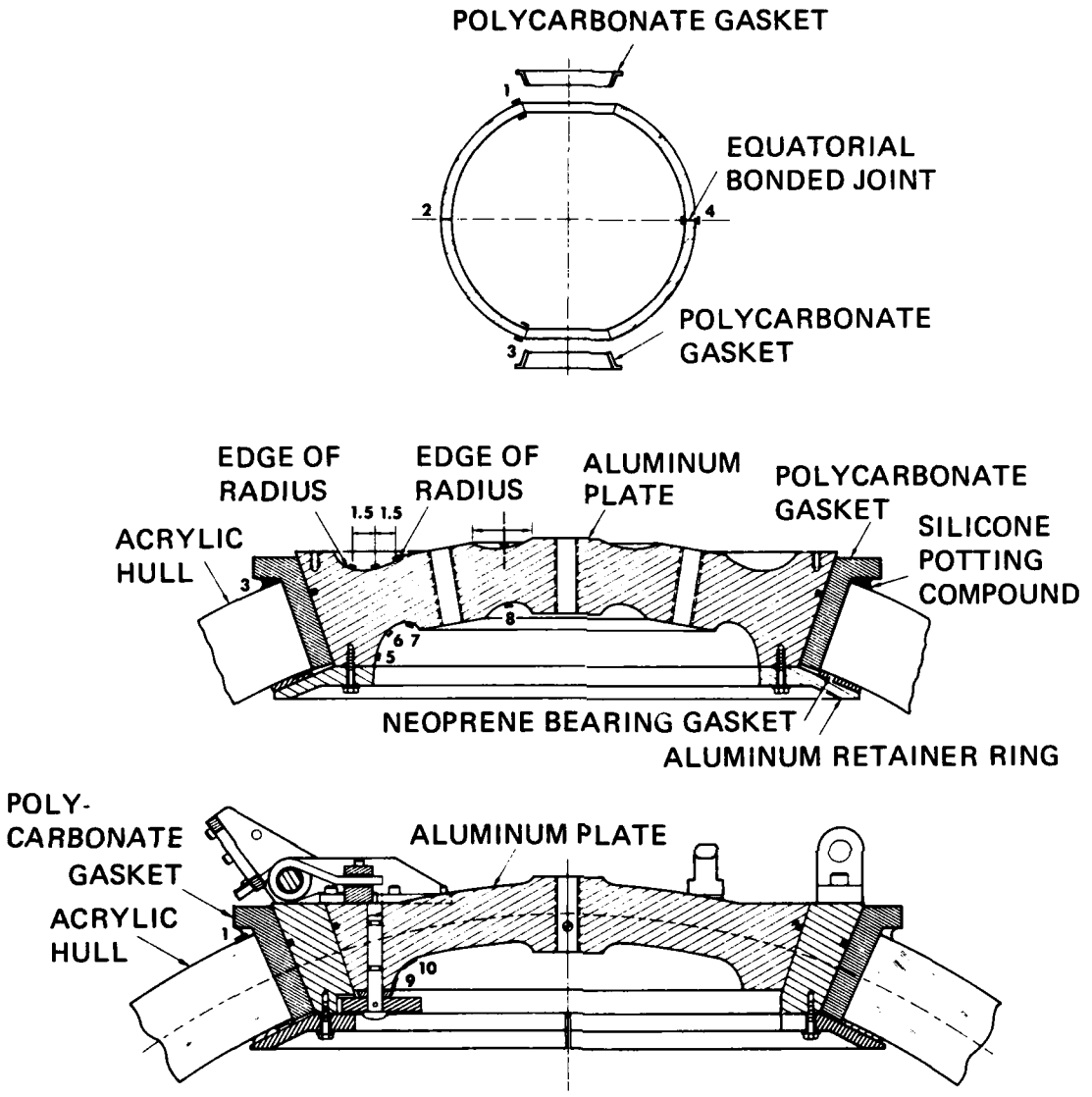

Figure 50. Location of electrical resistance strain gages on model 2000B assembly.

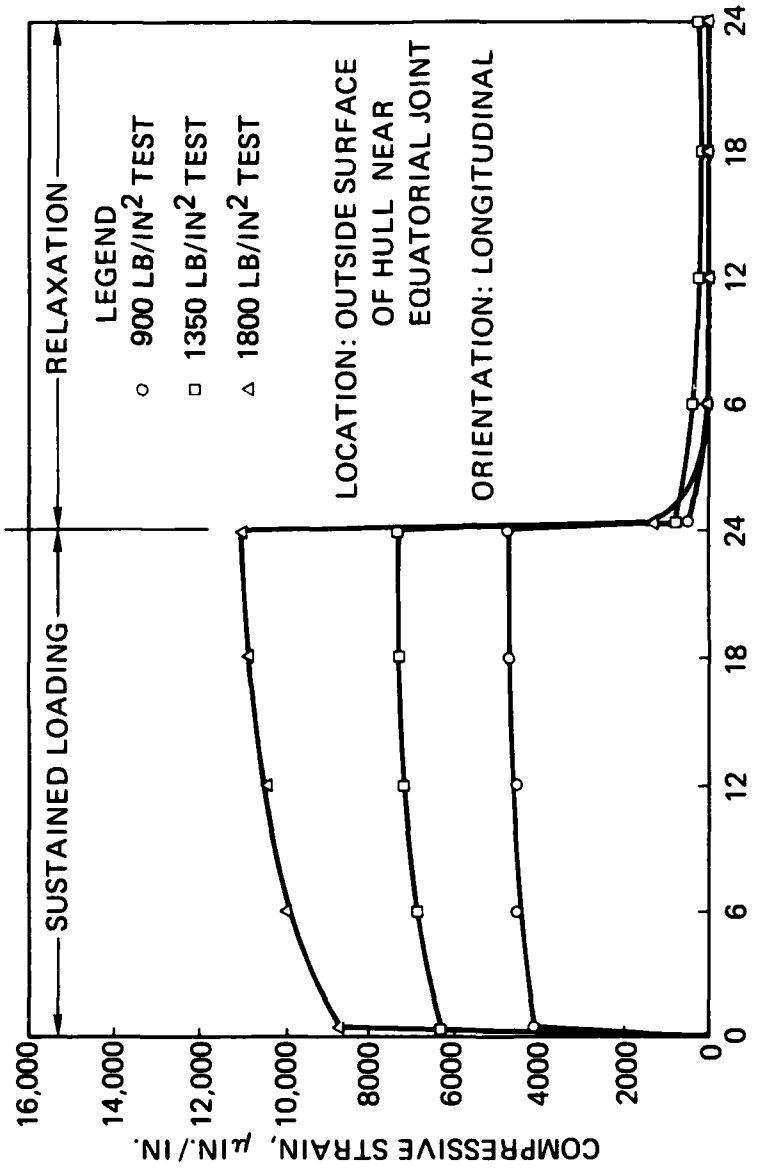

Figure 51. Longitudinal strain on outside surface of hull near equatorial joint (gage location 2).

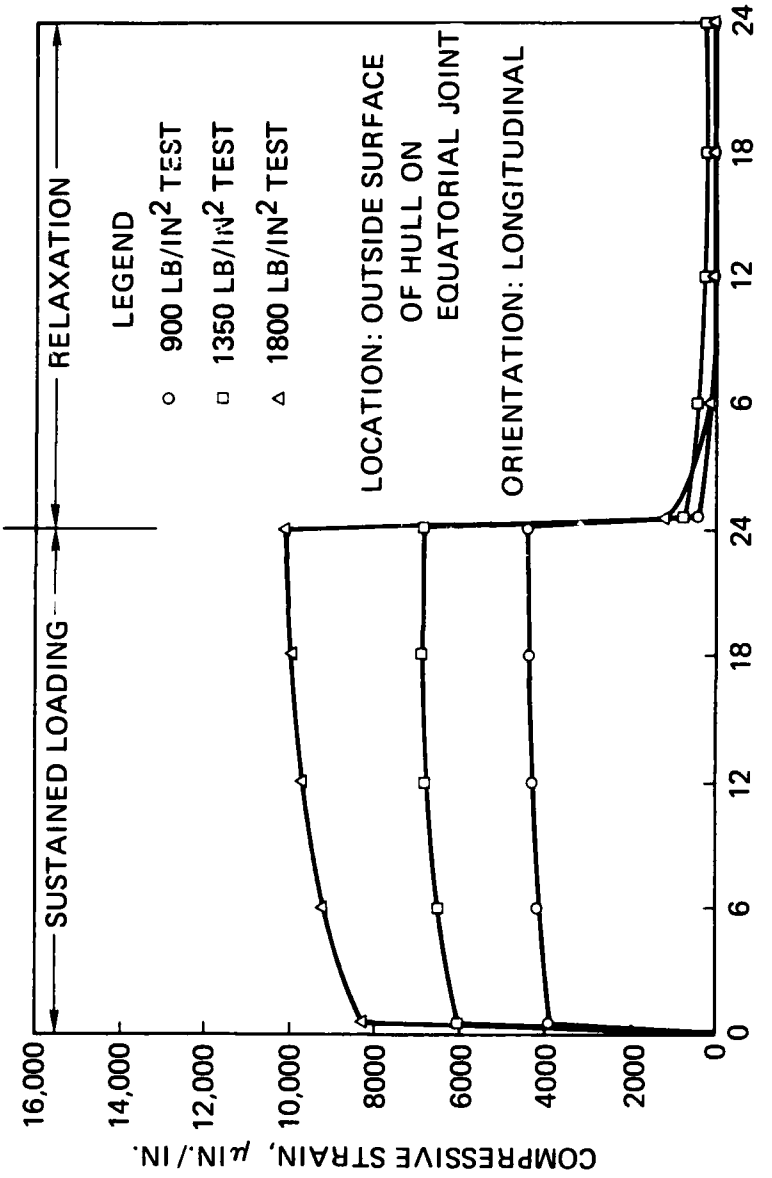

Figure 52. Longitudinal strain on outside surface of hull at equatorial joint (gage location 4).

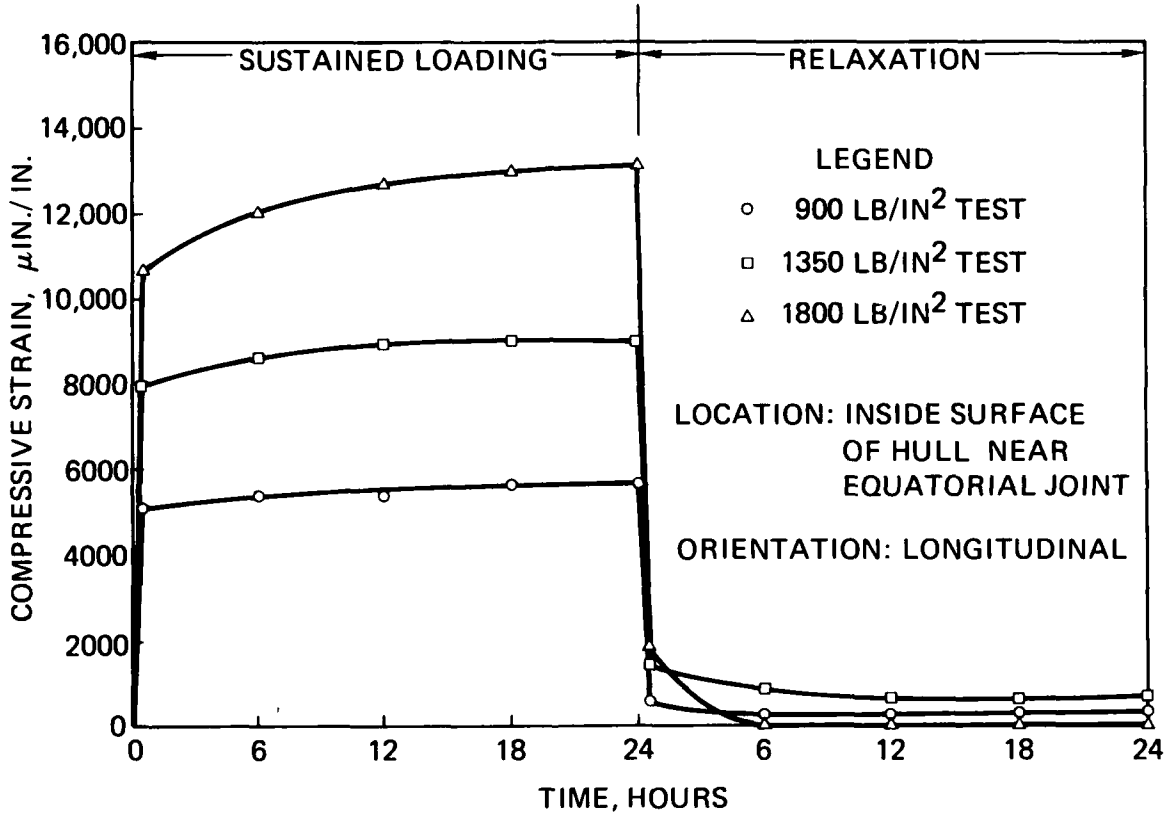

Figure 53. Longitudinal strain on inside surface of hull near equatorial joint (gage location 2).

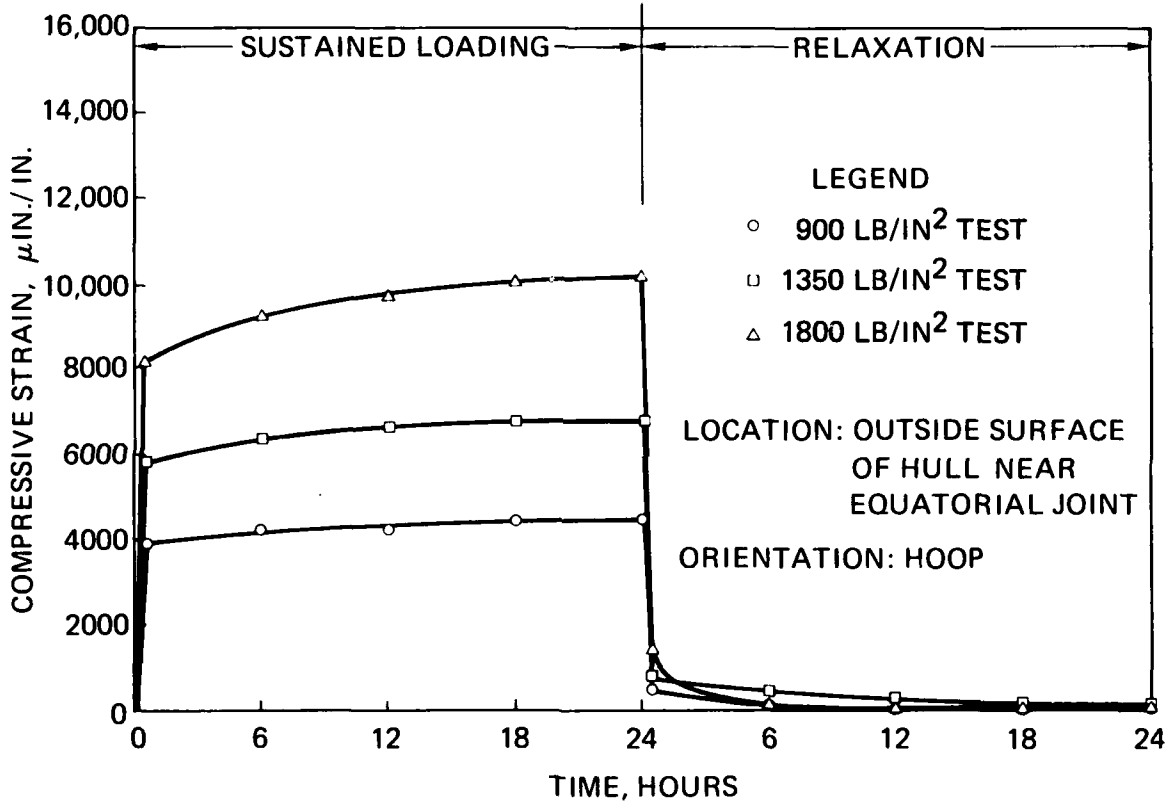

Figure 54. Hoop strain on outside surface of hull near equatorial joint (gage location 2).

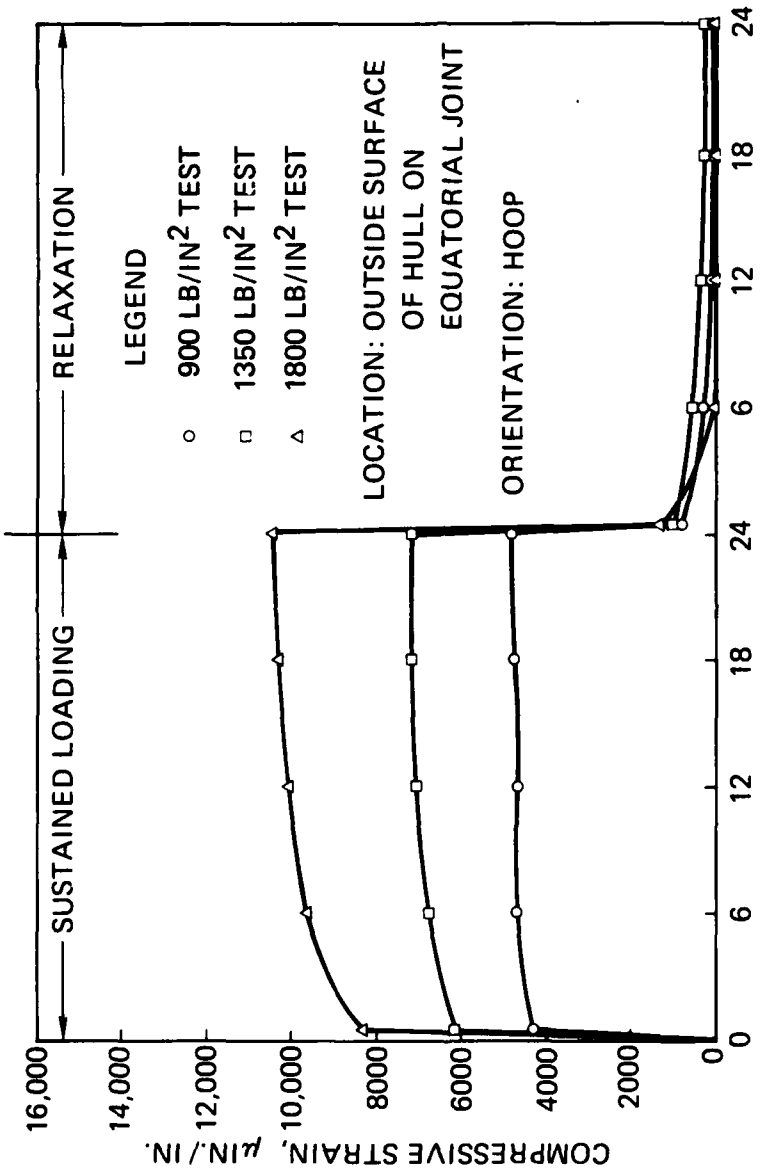

Figure 55. Hoop strain on outside surface of hull at equatorial joint (gage location 4).

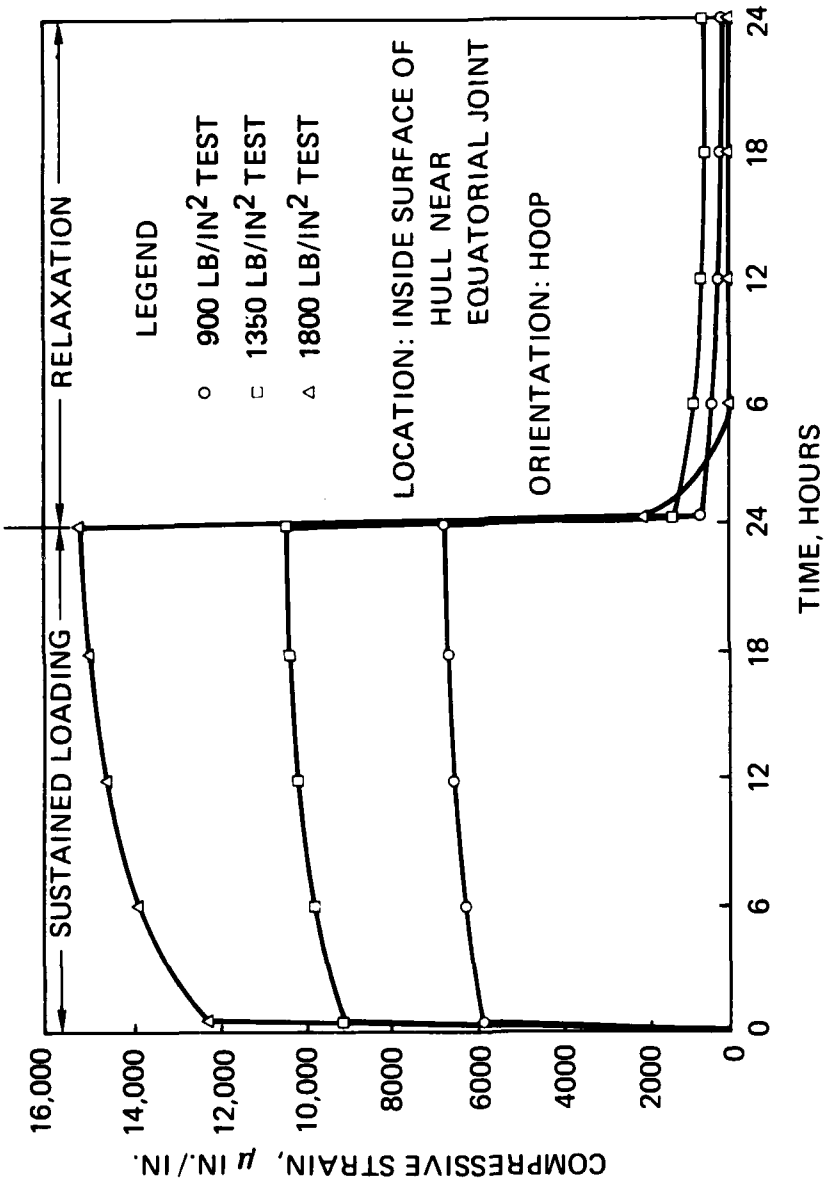

Figure 56. Hoop strain on inside surface of hull near equatorial joint (gage location 2).

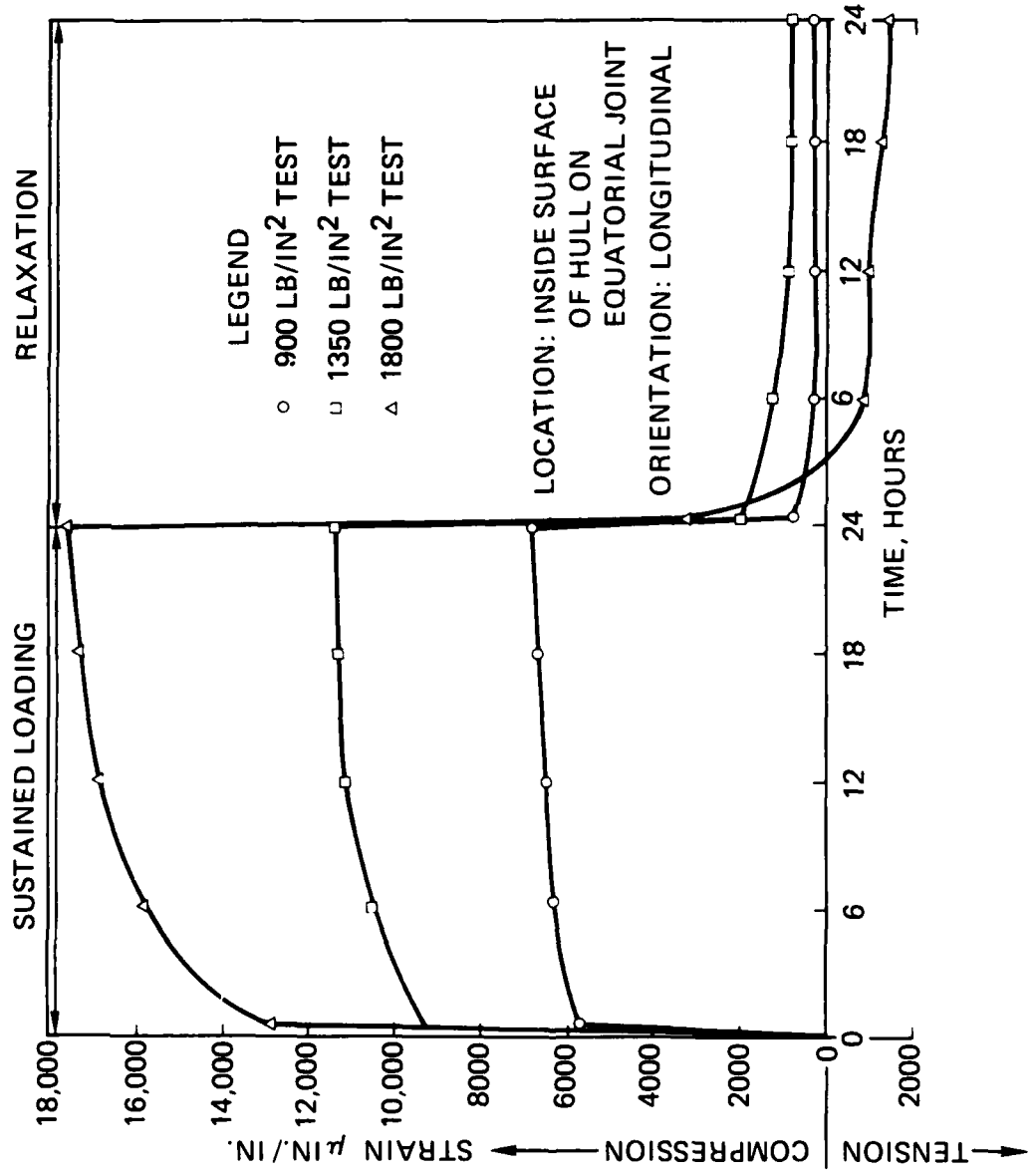

Figure 57. Longitudinal strain on inside surface of hull at equatorial joint (gage location 4).

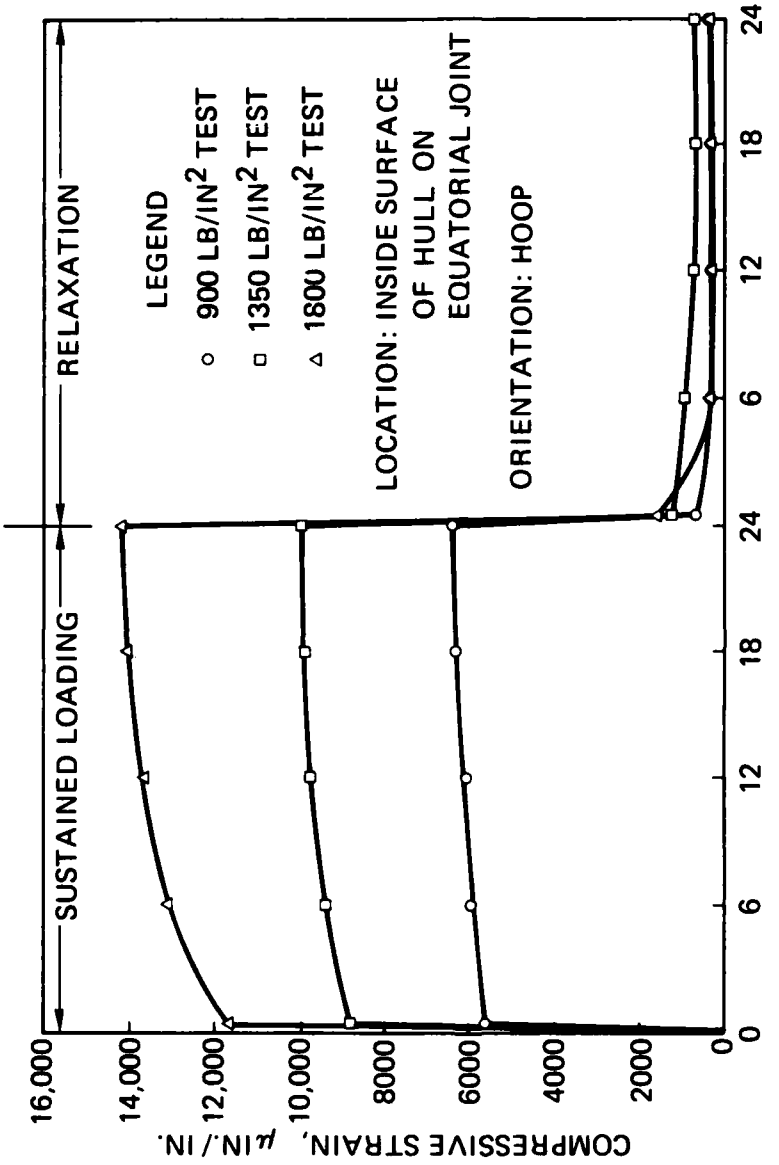

Figure 58. Hoop strain on inside surface of hull at equatorial joint (gage location 4).

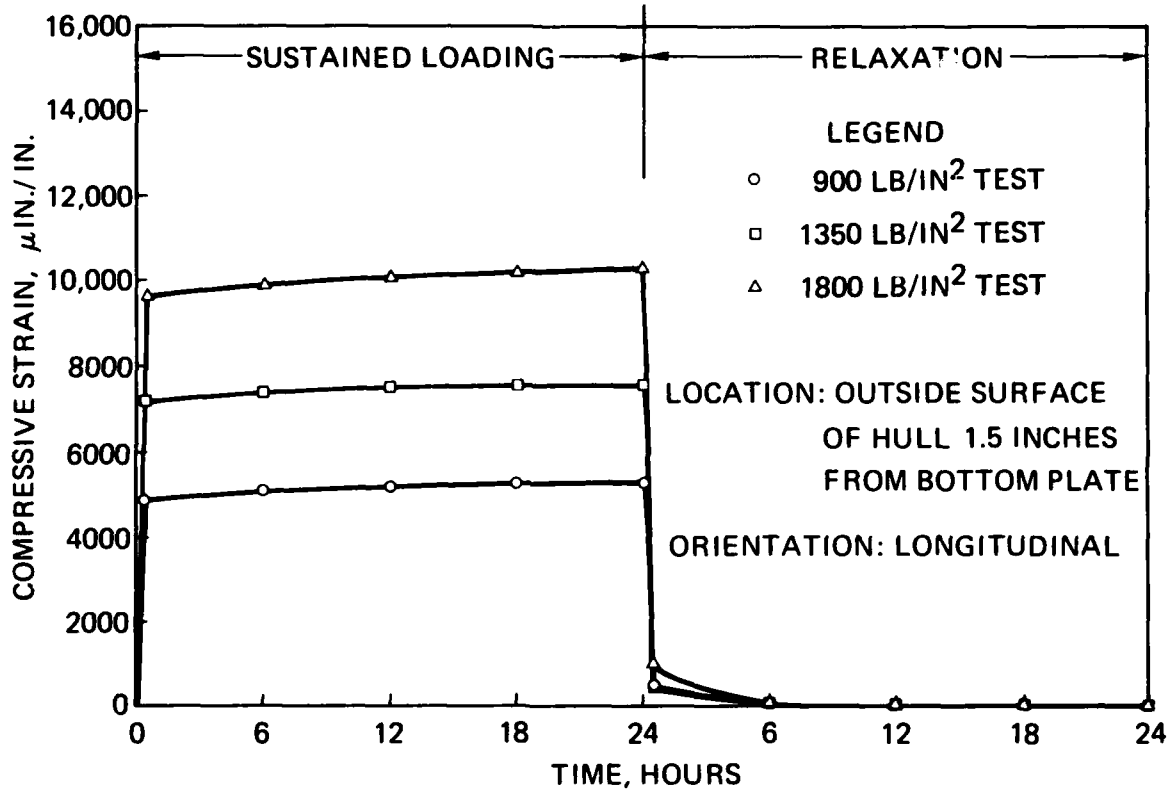

Figure 59. Longitudinal strain on outside surface of hull 1.5 inches from edge of penetration plate (gage location 3).

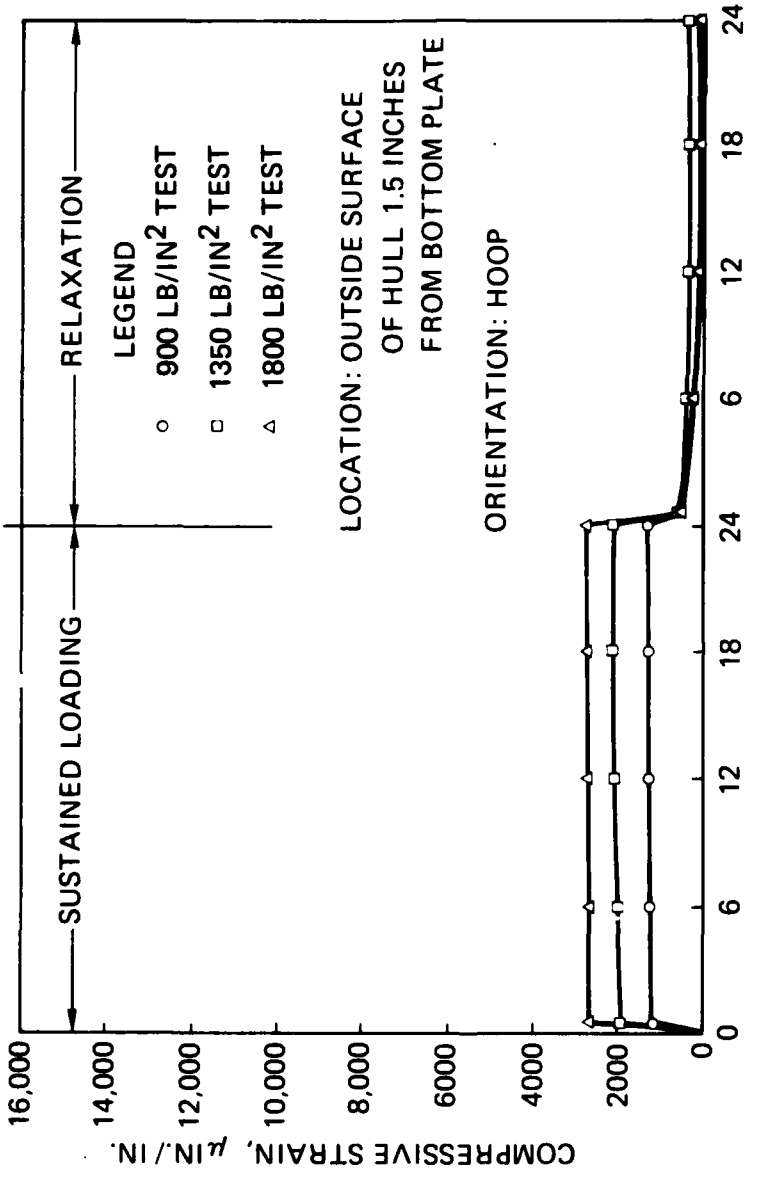

Figure 60. Hoop strain on outside surface of hull 1.5 inches from edge of penetration plate (gage location 3).

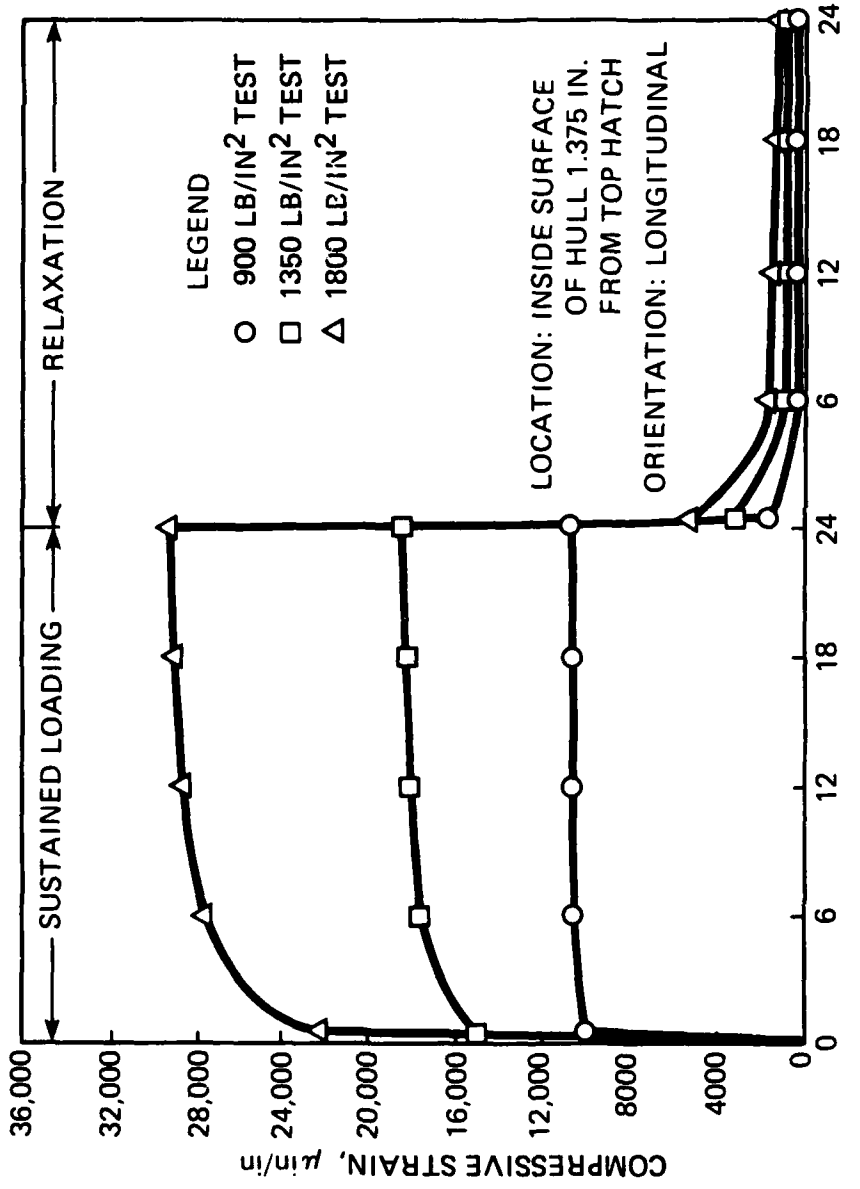

Figure 61. Longitudinal strain on inside surface of hull 1.375 inches from edge of hatch (gage location 1).

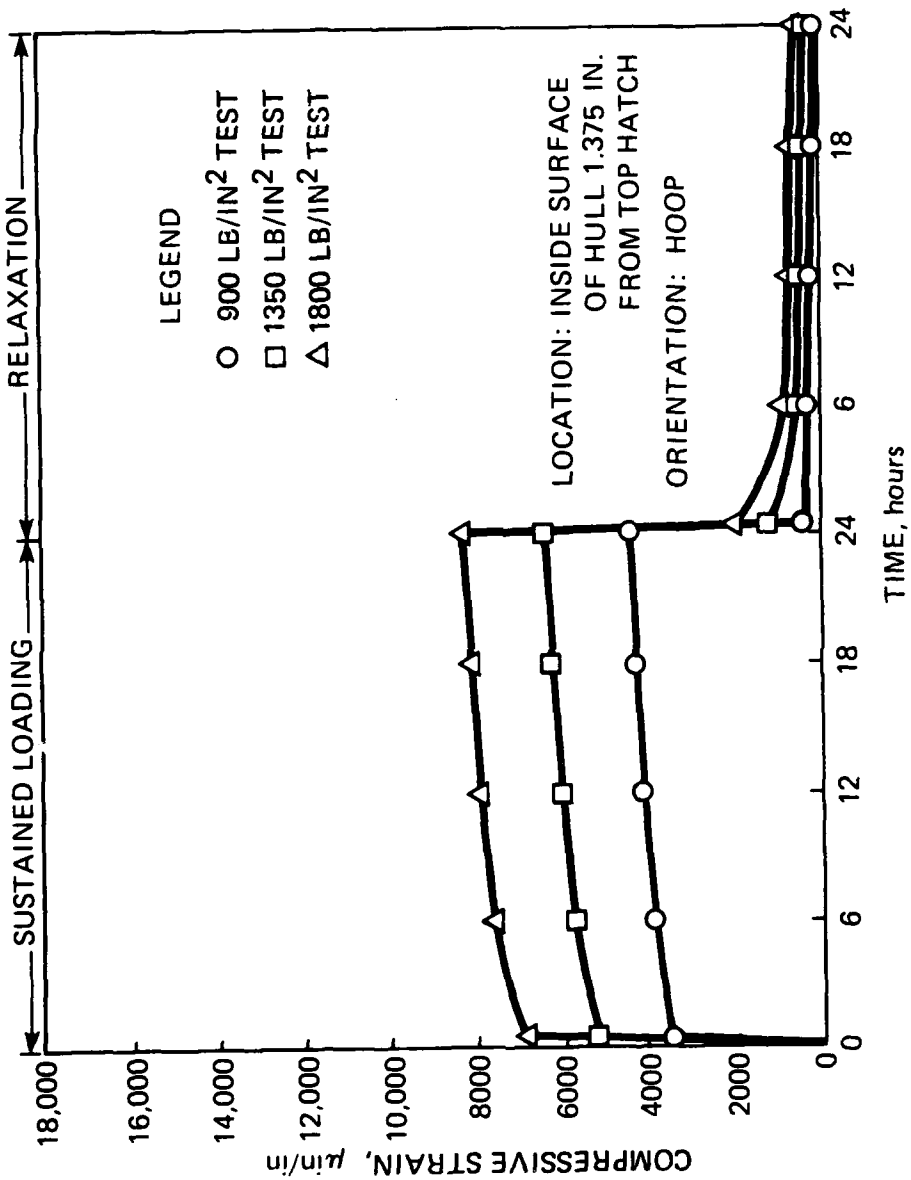

Figure 62. Hoop strain on inside surface of hull 1.375 inches from edge of hatch (gage location 1).

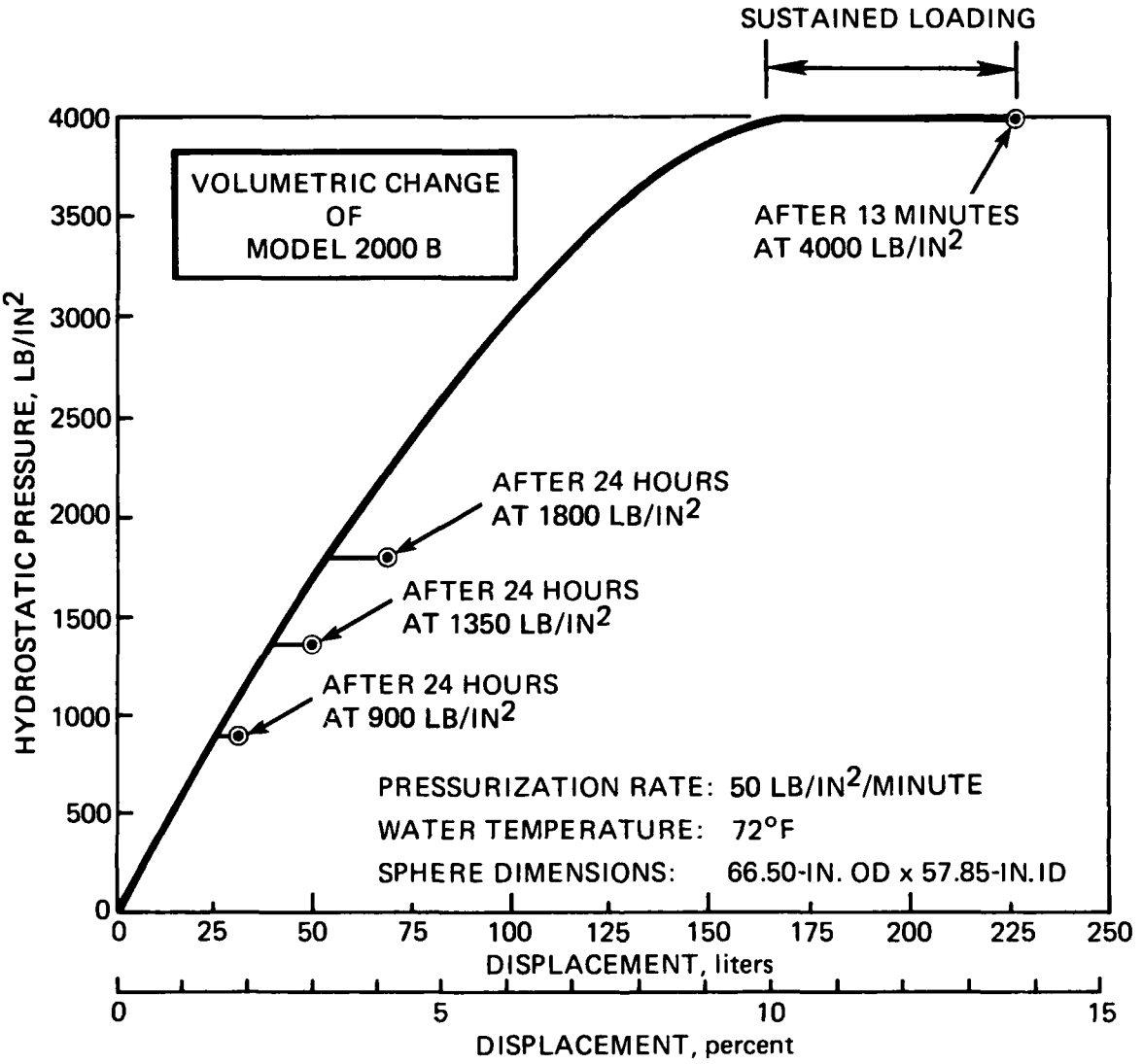

Figure 63. Displacement as a function of time and pressure.

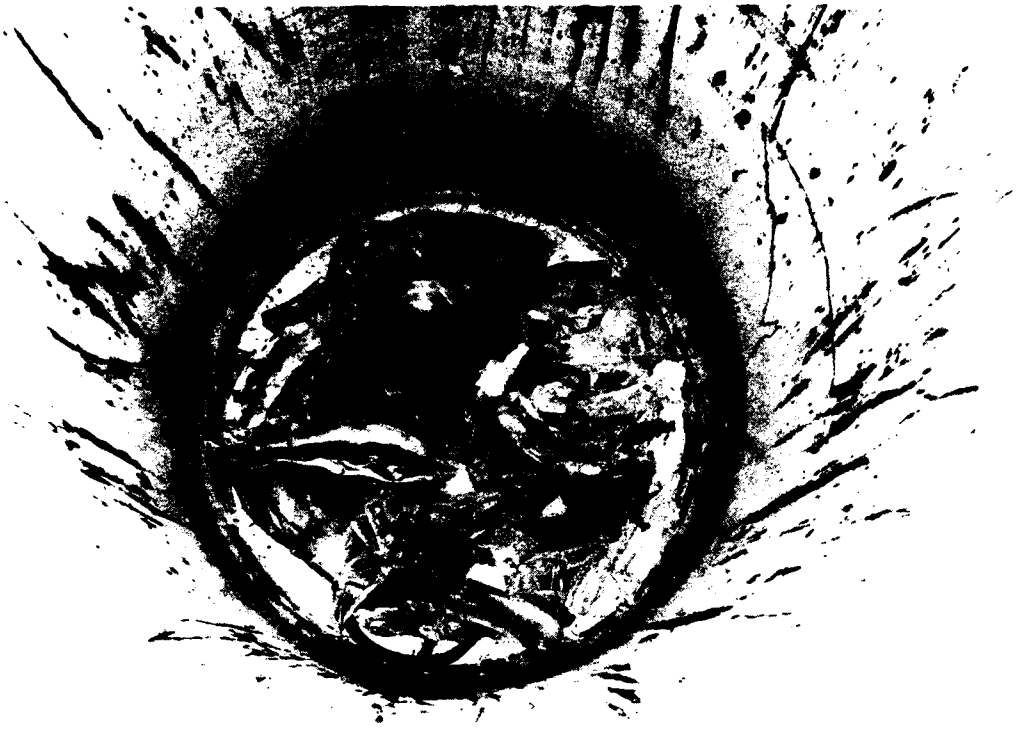

Figure 64. Model 2000B hull assembly after implosion.

Figure 65. Fragments of imploded hull assembly.

Figure 66. Cross section of acrylic plastic bearing surface at bottom polar penetration.

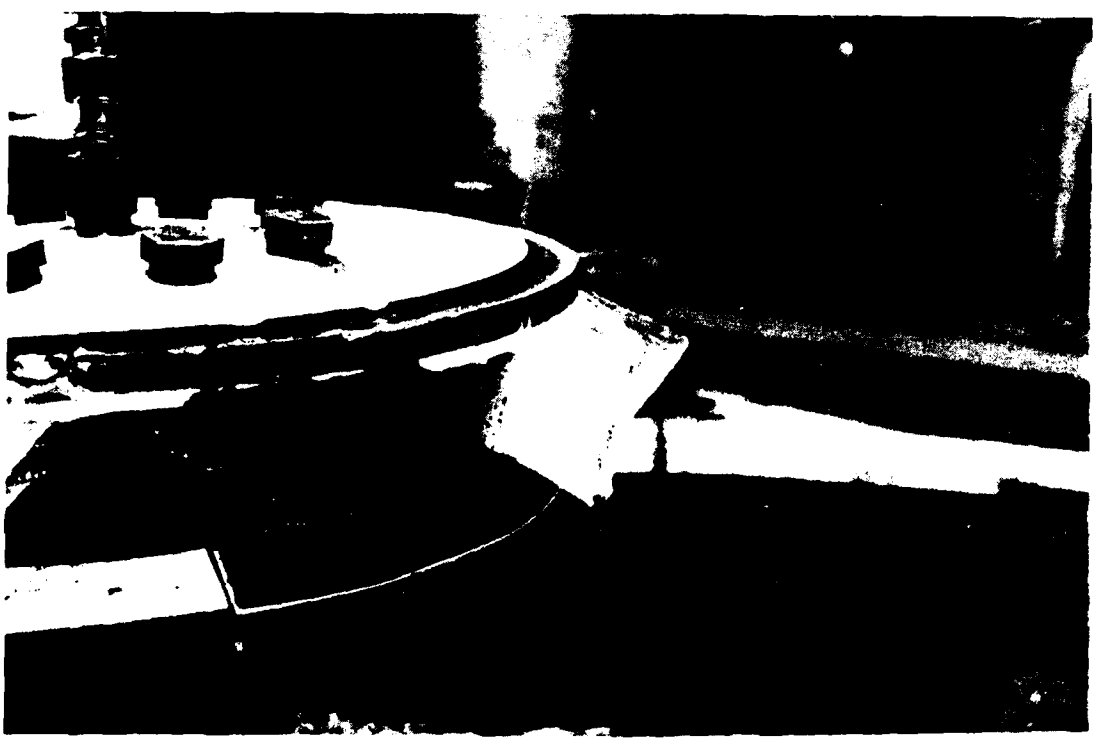

Figure 67. Penetration plate with piece of hull clinging to polycarbonate gasket.

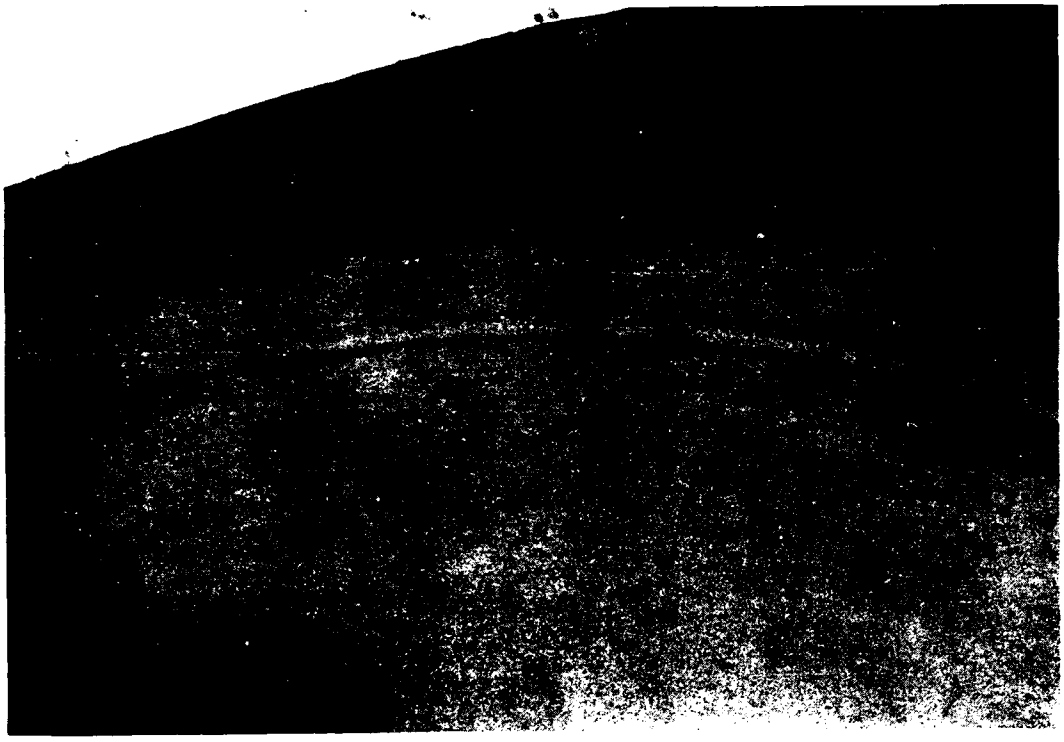

Figure 68. Typical shear cracks in bearing surface of polycarbonate gasket.

Figure 69. Polycarbonate gasket after intrusion into O-ring groove of hatch ring.

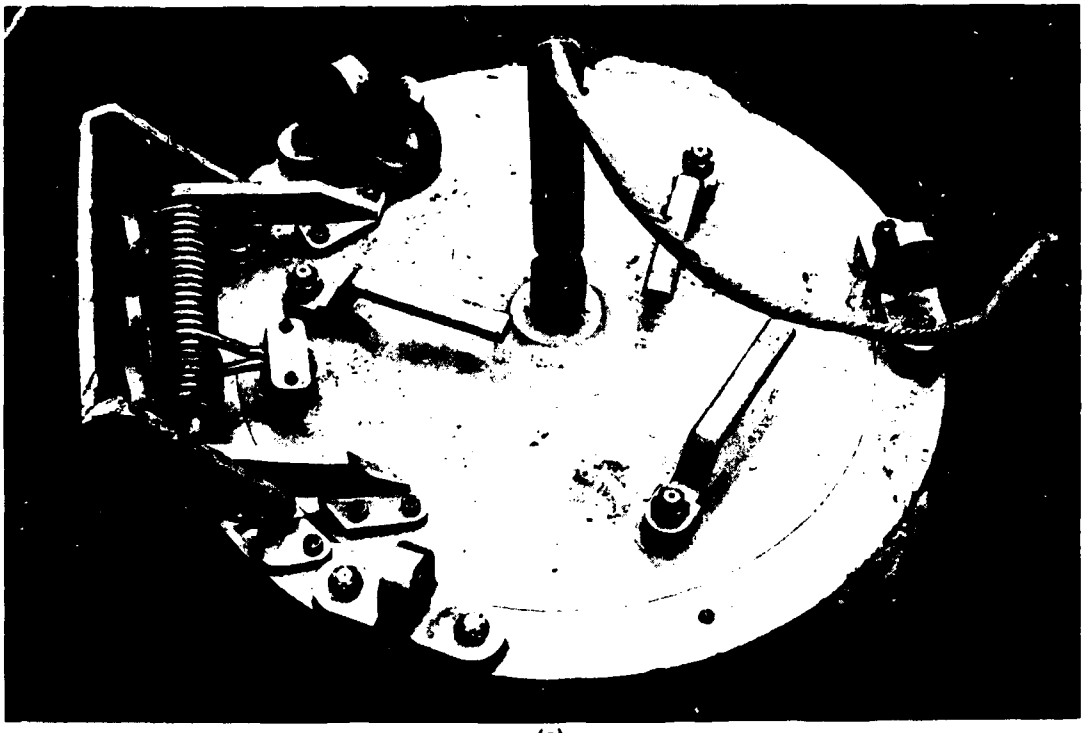

(a)

(b)

Figure 70. Undamaged aluminum hatch. (a) Top view. (b) Bottom view.

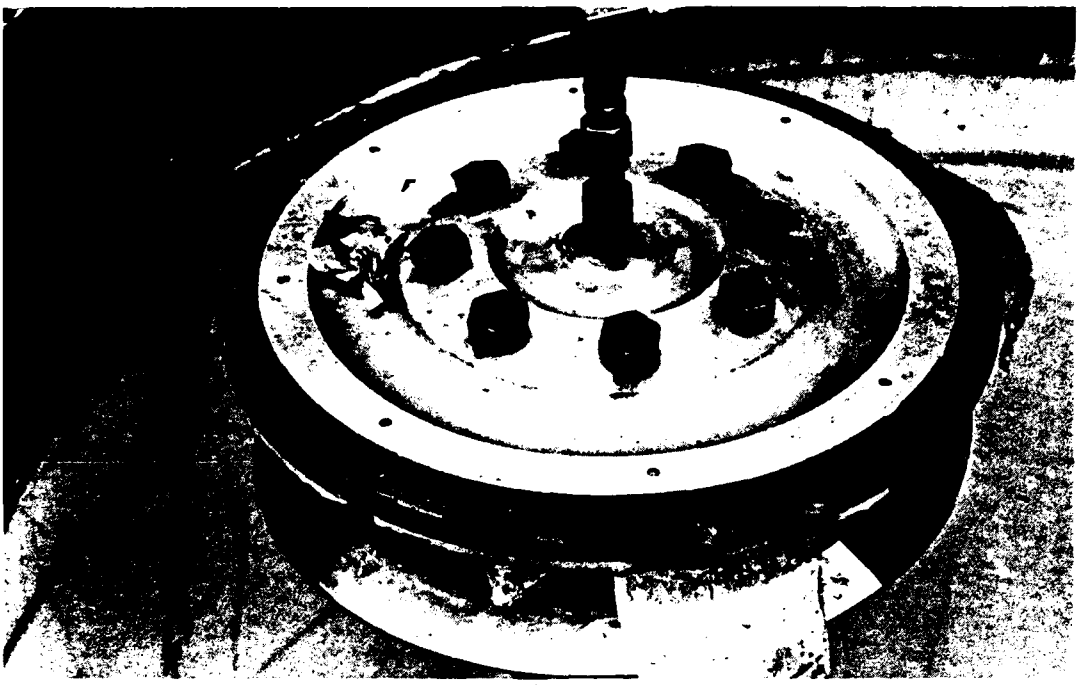

(a)

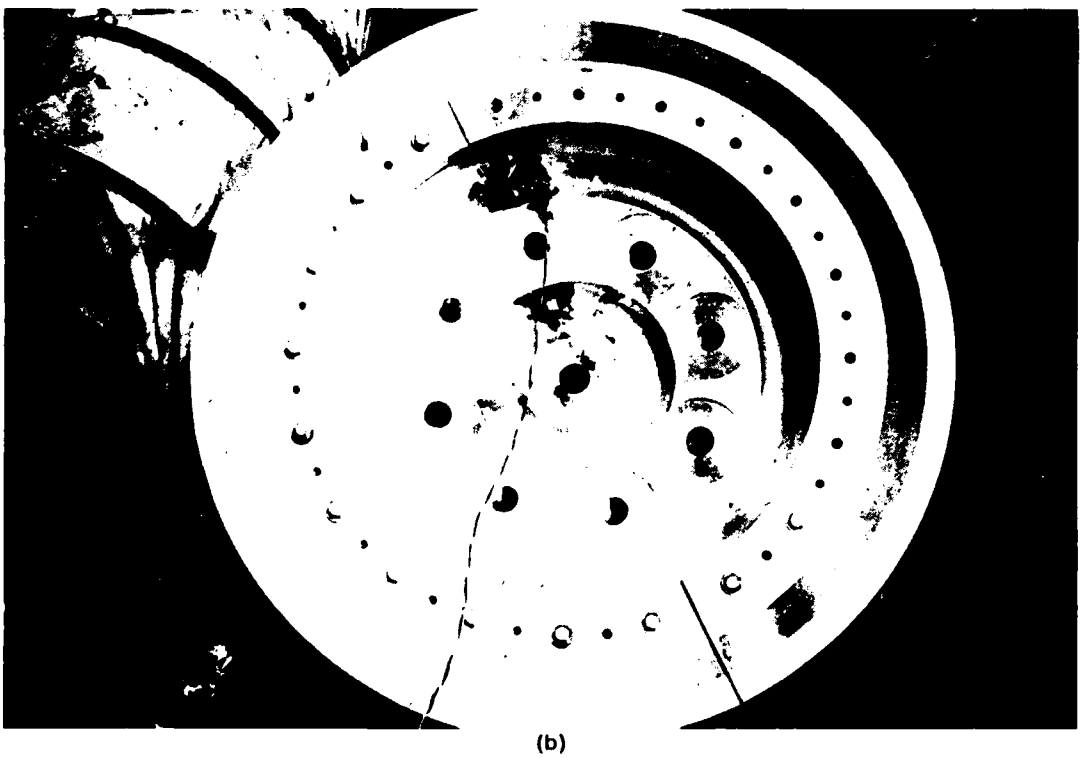

(b)

Figure 71. Undamaged aluminum penetration plate. (a) Top view. (b) Bottom view.

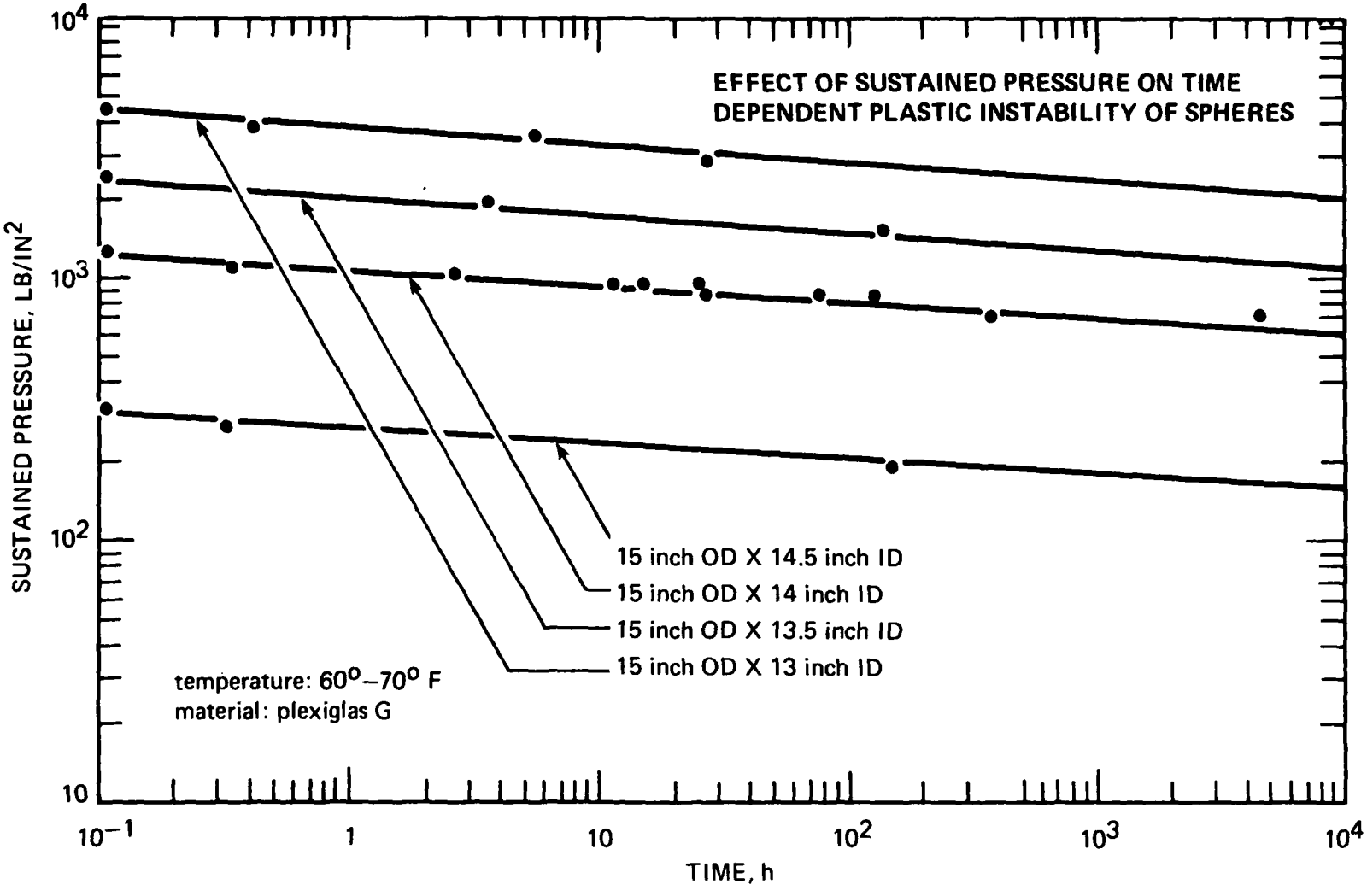

Figure 72. Implosion pressure of model 2000 hull assemblies as a function of time.

APPENDIX A
PHYSICAL PROPERTIES OF TEST SPECIMENS

This appendix presents data from the material tests described in the Casting and Inspection section of the report.

DELSEN corporation
TESTING LABORATORIES
1031 FLOWER ST. • GLENDALE, CALIFORNIA 91201

245-8517
245-4551

TEST REPORT

In account with	Date	Page 1 of 7 Pages
Naval Undersea Center South Rosecrans Street San Diego, California 92132	4/9/75	
	W.O. No T 11296	P.O. No N66001-75-M-V390
	Identification As noted	Shipper No number

IDENTIFICATION: Acylic Material

COMPRESSIVE YIELD STRENGTH AND MODULUS
Tested as Received at Room Temperature
Rate of Test: 0.05 Inch/Minute

TEST METHOD: ASTM D695

SPECIMEN	WIDTH INCHES	THICKNESS INCHES	YIELD LOAD POUNDS	COMPRESSIVE YIELD STRENGTH PSI	COMPRESSIVE MODULUS PSI x 10⁵
A					
1	0.492	0.490	3,960	16,400	5.3
2	0.493	0.491	3,770	15,600	5.1
			AVERAGE:	16,000	5.2
B					
1	0.504	0.501	4,160	16,500	5.1
2	0.505	0.504	4,110	16,100	5.0
			AVERAGE:	16,300	5.1
			REQUIREMENT:	15,000	4.0

DELSEN corporation
TESTING LABORATORIES
1031 FLOWER ST. • GLENDALE, CALIFORNIA 91201
245-8517
245-4551

TENSILE STRENGH, MODULUS AND ELONGATION
Tested at Room Temperature
Rate of Test: 0.05 Inch/Minute

TEST METHOD: ASTM D638

SPECIMEN	THICKNESS INCHES	WIDTH INCHES	MAXIMUM LOAD POUNDS	TENSILE MODULUS PSI x 10^5	TENSILE STRENGTH PSI	TENSILE ELONGATION %
A						
1	0.236	0.483	1,142	5.1	10,020	4.1
2	0.242	0.483	1,125	4.9	9,620	3.5
			AVERAGE:	5.0	9,820	3.8
B						
1	0.241	0.482	1,113	4.9	9,580	4.1
2	0.236	0.475	1,060	5.0	9,460	3.6
			AVERAGE:	4.6	9,520	3.9
			REQUIREMENT:	4.0 Min.	9,000 Min.	2.0 Min.

SHEAR STRENGTH
Tested as Received at Room Temperature
Rate of Test: 0.05 Inch/Minute
Punch Diameter: 1.000 Inches

TEST METHOD: ASTM D732

SPECIMEN	THICKNESS INCHES	MAXIMUM LOAD POUNDS	SHEAR STRENGTH PSI
A			
1	0.230	7,100	9,830
2	0.225	6,780	9,590
		AVERAGE:	9,710
B			
1	0.204	6,180	9,640
2	0.219	6,900	1,030
		AVERAGE:	9,840
		REQUIREMENT:	8,000 min.

DELSEN corporation
TESTING LABORATORIES
1031 FLOWER ST. • GLENDALE, CALIFORNIA 91201
245-8517
245-4551

W.O No T 11296 | Page 3 of 7 Pages

FLEXURAL STRENGTH AND MODULUS
Tested as Received at Room Temperature
Rate of Test: 0.2 Inch/Minute
Span: 7.180 Inch/Minute

TEST METHOD: ASTM D790

SPECIMEN	THICKNESS INCHES	WIDTH INCHES	MAXIMUM LOAD POUNDS	TYPE OF FAILURE	FLEXURAL STRENGTH PSI	FLEXURAL MODULUS PSI x 10^5
A						
1	0.492	0.492	164.5	Fracture	14,900	4.9
2	0.495	0.498	172.0	Fracture	15,200	4.9
				AVERAGE:	15,100	4.9
B						
1	0.502	0.501	170.5	Fracture	14,500	4.9
2	0.502	0.502	187.0	Fracture	15,900	4.9
				AVERAGE:	15,200	4.9
				REQUIREMENT:	14,000 Min.	4.2 Min.

IZOD IMPACT STRENGTH
Tested as Received at Room Temperature

TEST METHOD: ASTM D256, procedure B

SPECIMEN	WIDTH INCHES	BREAKING LOAD INCH-POUNDS	IZOD IMPACT STRENGTH FOOT-LBS/INCH OF NOTCH
A			
1	0.490	1.5	0.26
2	0.494	1.7	0.29
		AVERAGE:	0.28
B			
1	0.490	1.8	0.31
2	0.493	1.9	0.32
		AVERAGE:	0.32
		REQUIREMENT:	0.20 Min.

DELSEN corporation
TESTING LABORATORIES
1031 FLOWER ST. • GLENDALE, CALIFORNIA 91201
245-8517
245-4551

DEFORMATION UNDER LOAD
Tested at 24 Hours at 122°F ± 20°F

TEST METHOD: ASTM D621

SPECIMEN	THICKNESS INCHES	WIDTH INCHES	LENGTH INCHES	APPLIED LOAD POUNDS	DEFORMATION %
A					
1	0.500	0.502	0.499	1,000	0.38
2	0.505	0.495	0.496	1,000	0.40
			AVERAGE:		0.39
B					
1	0.501	0.500	0.492	1,000	0.39
2	0.500	0.500	0.494	1,000	0.38
			AVERAGE:		0.38
			REQUIREMENTS:		1.0 Max.

SPECIFIC GRAVITY
Tested as Received at Room Temperature

TEST METHOD: ASTM D792

SPECIMEN	INITIAL WEIGHT GRAMS	APPARENT WEIGHT LOSS GRAMS	SPECIFIC GRAVITY 23/23°C
A			
1	10.3149	8.7247	1.182
		REQUIREMENT:	1.18 - 1.20

DELSEN corporation
TESTING LABORATORIES
1031 FLOWER ST. • GLENDALE, CALIFORNIA 91201
245-8517
245-4551

W.O No. T 11296 | Page 5 of 7 Pages

COEFFICIENT OF LINEAR THERMAL EXPANSION

TEST METHOD: ASTM D696

SPECIMEN	TEMPERATURE RANGE °F	COEFFICIENT OF LINEAR THERMAL EXPANSION INCHES/INCH °F
A	-25 to +77	3.4×10^{-5}
1	77 to 105	4.6×10^{-5}
REQUIREMENT:	80°F	4.3×10^{-5}

ROCKWELL "M" HARDNESS

Tested as Received at Room Temperature

A	104
	105
	105
	105
	105
AVERAGE:	105
REQUIREMENT:	90

WATER ABSORBTION

Tested at Room Temperature in Distilled Water for 24 Hours

TEST METHOD: ASTM D570

SPECIMEN	INITIAL WEIGHT GRAMS	WEIGHT GAIN GRAMS	WATER ABSORBTION %
A			
1	10.3149	0.021	0.20
		REQUIREMENT:	0.25 Max.

DELSEN corporation
TESTING LABORATORIES
1031 FLOWER ST. • GLENDALE, CALIFORNIA 91201
245-8517
245-4551

W.O. No. T 11296 | Page 6 of 7 Pages

HEAT DISTORTION TEMPERATURE
Span: 4 Inches

TEST METHOD: ASTM D648

SPECIMEN	THICKNESS INCHES	WIDTH INCHES	APPLIED LOAD POUNDS	HEAT DISTORTION °F
A 1	0.507	0.505	2,409	216
			REQUIREMENT:	205 Min.

RESISTANCE TO STRESS
Tested at 75°F

TEST METHOD: Table I of ASTM methods

SPECIMEN	WIDTH INCHES	THICKNESS INCHES	LOAD LBS.	STRESS PSI
A 1	1.010	0.232	4.53	2,000

Result: There was no visual evidence of crazing, cracking, or other chemical degradation.

Note: Applied Fiber Stress of 2,000 PSI.

DELSEN corporation
TESTING LABORATORIES
1031 FLOWER ST. • GLENDALE, CALIFORNIA 91201

245-8517
245-4551

W.O. No. T 11296 | Page 7 of 7 Pages

REFRACTIVE INDEX

TEST METHOD: ASTM D542

Refractive Index was taken on sample A, per the above test method and was found to be 1.491.

RESIDUAL MONOMER

Sample A, methyl methacrylate monomer 0.40 ± 0.005 %.

Respectfully submitted,

DELSEN CORPORATION

APPENDIX B
STRAIN DATA

The strain data generated by the electrical resistance strain gages mounted on the model 2000B assembly during hydrostatic testing is reproduced in this appendix for the benefit of personnel who may be involved in certification of the model 2000B and engineers interested in the design of acrylic plastic submersibles. The data is presented in order of increasing pressure (900, 1350, 1800, and 4000 lb/in^2). The gage numbers correspond to locations on the assembly indicated in figure 50. Some of the readings at interior locations 1 and 3 are irregular, and it is surmised that they were caused by sliding of the compressed neoprene gasket on the gage.

STRAIN REDUCTION OF A TWO GAGE ROSETTE

E= .40 POISSONS RATIO= .40 GAGE NO.= 1=OUTSIDE

LOAD	EPI	EP2	SIGMA MAX	SIGMA MIN	TAU MAX
0	0	0	0	0	0
100	-500	-125	-262	-155	-54
200	-500	-550	-343	-357	7
300	-600	-1050	-486	-614	64
400	-600	-1450	-562	-805	121
500	-600	-1900	-648	-1019	186
600	-650	-2350	-757	-1243	243
700	-650	-2800	-843	-1457	307
800	-650	-3200	-919	-1648	364
900	-650	-3650	-1005	-1862	429
900	-625	-3750	-1012	-1905	446
900	-600	-3750	-1000	-1900	450
900	-600	-3900	-1029	-1971	471
900	-600	-3950	-1038	-1995	479
600	-600	-2600	-781	-1352	286
300	-550	-1300	-510	-724	107
0	-100	-400	-105	-162	29
0	-50	-150	-52	-81	14
0	50	-250	-24	-110	43
0	100	-150	19	-52	36
0	150	-100	52	-19	36

STRAIN REDUCTION OF A TWO GAGE ROSETTE

E = .40 POISSONS RATIO= .40 GAGE NO.= 2=OUTSIDE

LOAD	EP1	EP2	SIGMA MAX	SIGMA MIN	TAU MAX
0	0	0	0	0	0
100	-400	-500	-286	-314	14
200	-850	-1000	-595	-638	21
300	-1300	-1450	-895	-938	21
400	-1700	-1900	-1171	-1229	29
500	-2150	-2300	-1462	-1505	21
600	-2600	-2800	-1771	-1829	29
700	-3000	-3200	-2038	-2095	29
800	-3450	-3700	-2348	-2419	36
900	-3900	-4150	-2648	-2719	36
900	-4200	-4500	-2857	-2943	43
900	-4200	-4500	-2857	-2943	43
900	-4400	-4650	-2981	-3052	36
900	-4400	-4700	-2990	-3076	43
600	-3300	-3300	-2200	-2200	0
300	-1900	-2050	-1295	-1338	21
0	-500	-500	-333	-333	0
0	-150	-50	-81	-52	-14
0	-50	-50	-33	-33	0
0	-100	0	-48	-14	-14
0	-100	0	-48	-14	-14

STRAIN REDUCTION OF A TWO GAGE ROSETTE

E= .40 POISSONS RATIO= .40 GAGE NO.= 2-INSIDE

LOAD	EP1	EP2	SIGMA MAX	SIGMA MIN	TAU MAX
0	0	0	0	0	0
100	-600	-500	-381	-352	-14
200	-1300	-1100	-829	-771	-29
300	-1900	-1700	-1229	-1171	-29
400	-2500	-2200	-1610	-1524	-43
500	-3150	-2800	-2033	-1933	-50
600	-3800	-3350	-2448	-2319	-64
700	-4450	-3900	-2862	-2705	-79
800	-5100	-4450	-3276	-3090	-93
900	-5800	-5050	-3724	-3510	-107
900	-6200	-5425	-3967	-3717	-125
900	-6500	-5350	-4114	-3786	-164
900	-6600	-5400	-4210	-3924	-143
900	-6700	-5675	-3319	-3598	139
600	-3900	-3950	-2610	-2624	7
300	-2700	-2300	-1724	-1610	-57
0	-700	-500	-429	-371	-29
0	-1000	-250	-524	-310	-107
0	-1050	-200	-538	-295	-121
0	-1000	-250	-524	-310	-107
0	-950	-300	-510	-324	-93

STRAIN REDUCTION OF A TWO GAGE ROSETTE

E= .40 POISSONS RATIO= .40 GAGE NO.= 3=OUTSIDE

LOAD	EP1	EP2	SIGMA MAX	SIGMA MIN	TAU MAX
0	0	0	0	0	0
100	-200	-550	-200	-400	50
200	-250	-1050	-319	-548	114
300	-350	-1600	-471	-829	179
400	-400	-2150	-600	-1100	250
500	-500	-2700	-752	-1381	314
600	-600	-3250	-905	-1662	379
700	-700	-3900	-1076	-1990	457
800	-1000	-4300	-1295	-2238	471
900	-1150	-4850	-1471	-2529	529
900	-1200	-5000	-1524	-2610	543
900	-1200	-5100	-1543	-2657	557
900	-1200	-5200	-1562	-2705	571
900	-1250	-5250	-1595	-2738	571
600	-1100	-3950	-1276	-2040	407
300	-900	-2400	-886	-1314	214
0	-300	-550	-248	-319	36
0	-100	-50	-57	-43	-7
0	-100	0	-48	-19	-14
0	-75	0	-36	-14	-11
0	-25	-50	-21	-29	4

STRAIN REDUCTION OF A TWO GAGE ROSETTE

E= .40 POISSONS RATIO= .40 GAGE NO.= 3-INSIDE

LOAD	EP1	EP2	SIGMA MAX	SIGMA MIN	TAU MAX
0	0	0	0	0	0
100	-300	-675	-271	-379	54
200	-575	-1700	-598	-919	161
300	-825	-2825	-931	-1502	286
400	-1100	-3900	-1267	-2067	400
500	-1400	-5125	-1643	-2707	532
600	-1700	-6300	-2010	-3324	657
700	-2100	-7350	-2400	-3900	750
800	-2500	-8300	-2771	-4429	829
900	-2900	-9250	-3143	-4957	907
900	-3150	-9675	-3343	-5207	932
900	-3400	-9575	-3443	-5207	882
900	-2900	-9800	-3248	-5219	986
900	-2900	-9875	-3262	-5255	996
600	-2450	-6800	-2462	-3705	621
300	-1900	-3500	-1571	-2029	229
0	-2550	-2250	-1643	-1557	-43
0	-1200	-750	-714	-586	-64
0	-900	-400	-505	-362	-71
0	-650	-300	-367	-267	-50
0	-450	0	-214	-86	-64

STRAIN REDUCTION OF A TWO GAGE ROSETTE

E= .40 POISSONS RATIO= .40 GAGE NO.= 4=OUTSIDE

LOAD	EP1	EP2	SIGMA MAX	SIGMA MIN	TAU MAX
0	0	0	0	0	0
100	-650	-500	-705	-362	-21
200	-1100	-950	-705	-662	-21
300	-1600	-1400	-1029	-971	-29
400	-2000	-1800	-1295	-1238	-29
500	-2500	-2300	-1629	-1571	-29
600	-2900	-2700	-1895	-1838	-29
700	-3300	-3100	-2162	-2105	-29
800	-3800	-3500	-2476	-2390	-43
900	-4300	-3900	-2790	-2676	-57
900	-4700	-4200	-3038	-2895	-71
900	-4650	-4250	-3024	-2910	-67
900	-4750	-4400	-3100	-3000	-50
900	-4800	-4400	-3124	-3010	-57
600	-3450	-3100	-2233	-2133	-50
300	-2150	-1750	-1357	-1243	-57
0	-750	-400	-433	-333	-50
0	-250	-100	-138	-95	-21
0	-200	-50	-105	-62	-21
0	-150	0	-71	-29	-21
0	-100	0	-48	-14	-14

STRAIN REDUCTION OF A TWO GAGE ROSETTE

E= .40 POISSONS RATIO= .40 GAGE NO.= 4=INSIDE

LOAD	EP1	EP2	SIGMA MAX	SIGMA MIN	TAU MAX
0	0	0	0	0	0
100	-600	-650	-410	-424	7
200	-1250	-1300	-843	-857	7
300	-1875	-1900	-1255	-1262	4
400	-2500	-2500	-1667	-1667	0
500	-3150	-3200	-2110	-2124	7
600	-3700	-3900	-2605	-2562	29
700	-4400	-4550	-2962	-3005	21
800	-5050	-5150	-3386	-3414	14
900	-5650	-5800	-3795	-3838	21
900	-6000	-6400	-4076	-4190	57
900	-6050	-6500	-4119	-4248	64
900	-6300	-6800	-4295	-4438	71
900	-6350	-6900	-4338	-4495	79
600	-4450	-4900	-3052	-3181	64
300	-2500	-2850	-1733	-1833	50
0	-600	-800	-438	-495	29
0	-300	-350	-210	-224	7
0	-300	-350	-210	-224	7
0	-350	-400	-243	-257	7
0	-350	-400	-243	-257	7

STRAIN REDUCTION OF A TWO GAGE ROSETTE

E= 10,00 POISSONS RATIO= ,30 GAGE NO,= 5=OUTSIDE

LOAD	EP1	EP2	SIGMA MAX	SIGMA MIN	TAU MAX
0	0	0	0	0	0
100	-100	0	-1099	-330	-385
200	-100	0	-1099	-330	-385
300	-100	0	-1099	-330	-385
400	-150	0	-1648	-495	-577
500	-200	0	-2198	-659	-769
600	-200	0	-2198	-659	-769
700	-200	0	-2198	-659	-769
800	-250	50	-2582	-275	-1154
900	-250	0	-2747	-824	-962
900	-200	100	-1868	440	-1154
900	-250	100	-2418	275	-1346
900	-250	50	-2582	-275	-1154
900	-150	0	-1648	-495	-577
600	0	0	0	0	0
300	0	0	0	0	0
0	0	0	0	0	0
0	0	0	0	0	0
0	0	0	0	0	0
0	0	0	0	0	0
0	0	0	0	0	0

STRAIN REDUCTION OF A TWO GAGE ROSETTE

E= 10.00 POISSONS RATIO= .30 GAGE NO.= S=INSIDE

LOAD	EP1	EP2	SIGMA MAX	SIGMA MIN	TAU MAX
0	0	0	0	0	0
100	-600	-50	-6758	-2527	-2115
200	-1300	-100	-14615	-5385	-4615
300	-1900	-125	-21291	-7637	-6827
400	-2500	-150	-27967	-9890	-9038
500	-3150	-200	-35275	-12582	-11346
600	-3750	-200	-41868	-14560	-13654
700	-4400	-225	-49093	-16978	-16058
800	-5000	-325	-56014	-20055	-17981
900	-5650	-400	-63407	-23022	-20192
900	-6000	-300	-66923	-23077	-21923
900	-6000	-300	-66923	-23077	-21923
900	-6250	-300	-69670	-23901	-22886
900	-6300	-325	-70302	-24341	-22981
600	-4450	-275	-49808	-17692	-16058
300	-2450	-200	-27582	-10275	-8654
0	-550	0	-6044	-1813	-2115
0	-250	0	-2747	-824	-962
0	-250	0	-2747	-824	-962
0	-250	0	-2747	-824	-962
0	-250	0	-2747	-824	-962

STRAIN REDUCTION OF A TWO GAGE ROSETTE

E= 10,00 POISSONS RATIO= ,30 GAGE NO.= 6=INSIDE

LOAD	EP1	EP2	SIGMA MAX	SIGMA MIN	TAU MAX
0	0	0	0	0	0
100	-200	-100	-2527	-1758	-385
200	-250	-125	-3159	-2198	-481
300	-275	-150	-3516	-2555	-481
400	-300	-175	-3874	-2912	-481
500	-400	-225	-5137	-3791	-673
600	-500	-275	-6401	-4670	-865
700	-525	-300	-6758	-5027	-865
800	-550	-300	-7033	-5110	-962
900	-625	-400	-8187	-6456	-865
900	-475	-375	-6456	-5687	-385
900	-500	-350	-6648	-5495	-577
900	-525	-400	-7088	-6126	-481
900	-575	-400	-7637	-6291	-673
600	-275	-250	-3846	-3654	-96
300	-50	-150	-1044	-1813	385
0	50	-50	385	-385	385
0	0	-50	-165	-549	192
0	0	-50	-165	-549	192
0	0	-50	-165	-549	192
0	0	-50	-165	-549	192

STRAIN REDUCTION OF A TWO GAGE ROSETTE

t= 10.00 POISSONS RATIO= .30 GAGE NO.= 7=OUTSIDE

LOAD	EP1	EP2	SIGMA MAX	SIGMA MIN	TAU MAX
0	0	0	0	0	0
100	-50	0	-549	-165	-192
200	-50	0	-549	-165	-192
300	-100	-50	-1264	-879	-192
400	-100	-50	-1264	-879	-192
500	-100	-50	-1264	-879	-192
600	-150	-50	-1813	-1044	-385
700	-150	-50	-1813	-1044	-385
800	-200	-50	-2363	-1209	-577
400	-200	-50	-2363	-1209	-577
900	-200	-50	-2363	-1209	-577
900	-200	-50	-2363	-1209	-577
900	-200	-50	-2363	-1209	-577
900	-100	-100	-1429	-1429	0
600	-100	-100	-1429	-1429	0
300	0	-100	-330	-1099	385
0	0	0	0	0	0
0	0	0	0	0	0
0	0	0	0	0	0
0	0	0	0	0	0
0	-50	0	-549	-165	-192

STRAIN REDUCTION OF A TWO GAGE ROSETTE

E= 10.00 POISSONS RATIO= .30 GAGE NO.= 7-INSIDE

LOAD	EP1	EP2	SIGMA MAX	SIGMA MIN	TAU MAX
0	0	0	0	0	0
100	-50	0	-549	-165	-192
200	-150	0	-1648	-495	-577
300	-200	0	-2198	-659	-769
400	-275	0	-3022	-907	-1058
500	-325	0	-3571	-1071	-1250
600	-400	0	-4396	-1319	-1538
700	-450	0	-4945	-1484	-1731
800	-475	0	-5220	-1566	-1827
900	-525	0	-5769	-1731	-2019
900	-525	0	-5769	-1731	-2019
900	-525	0	-5769	-1731	-2019
900	-550	0	-6044	-1813	-2115
900	-575	0	-6319	-1896	-2212
600	-400	0	-4396	-1319	-1538
300	-200	0	-2198	-659	-769
0	0	0	0	0	0
0	0	0	0	0	0
0	0	0	0	0	0
0	0	0	0	0	0
0	0	0	0	0	0

STRAIN REDUCTION OF A TWO GAGE ROSETTE

E= 10.00 POISSONS RATIO= .30 GAGE NO.= B=OUTSIDE

LOAD	EP1	EP2	SIGMA MAX	SIGMA MIN	TAU MAX
0	0	0	0	0	0
100	0	0	0	0	0
200	0	-50	-165	-549	192
300	-50	-100	-879	-1264	192
400	-50	-100	-879	-1264	192
500	-100	-100	-1429	-1429	0
600	-100	-100	-1429	-1429	0
700	-100	-150	-1593	-1978	192
800	-100	-200	-1758	-2527	385
900	-100	-200	-1758	-2527	385
900	-150	-150	-2143	-2143	0
900	-100	-175	-1676	-2253	288
900	-100	-200	-1758	-2527	385
900	-150	-225	-2390	-2967	288
600	-200	-150	-2692	-2308	-192
300	-50	-75	-797	-989	96
0	0	0	0	0	0
0	0	0	0	0	0
0	0	0	0	0	0
0	0	0	0	0	0
0	0	0	0	0	0

STRAIN REDUCTION OF A TWO GAGE ROSETTE

E= 10,00 POISSONS RATIO= .30 GAGE NO.= R-INSIDE

LOAD	EP1	EP2	SIGMA MAX	SIGMA MIN	TAU MAX
0	0	0	0	0	0
100	-75	-100	-1154	-1346	96
200	-200	-125	-2610	-2033	-288
300	-250	-200	-3407	-3022	-192
400	-325	-275	-4478	-4093	-192
500	-400	-400	-5714	-5714	0
600	-475	-450	-6703	-6511	-96
700	-550	-600	-8022	-8407	192
800	-800	-750	-11264	-10879	-192
900	-850	-800	-11778	-11593	-192
900	-675	-600	-9396	-8819	-288
900	-600	-550	-8407	-8022	-192
900	-500	-500	-7143	-7143	0
900	-450	-500	-6593	-6978	192
600	-400	-200	-5055	-3516	-769
300	0	-50	-165	-549	192
0	-250	-100	-3077	-1923	-577
0	-200	-100	-2527	-1758	-385
0	-200	-100	-2527	-1758	-385
0	-75	50	-659	302	-481
0	100	150	1593	1978	-192

STRAIN REDUCTION OF A TWO GAGE ROSETTE

E= .40 POISSONS RATIO= .40 GAGE NO.= 1=OUTSIDE

LOAD	EP1	EP2	SIGMA MAX	SIGMA MIN	TAU MAX
0	0	0	0	0	0
100	-150	-100	-90	-76	-7
200	-150	-200	-110	-124	7
300	-150	-600	-186	-314	64
400	-150	-1050	-271	-529	129
500	-180	-1500	-371	-749	189
600	-200	-1950	-467	-967	250
700	-220	-2400	-562	-1185	311
800	-280	-2800	-667	-1387	360
900	-280	-3300	-762	-1625	431
1000	-300	-3700	-848	-1819	486
1100	-350	-4450	-1014	-2186	586
1200	-380	-4950	-1124	-2430	653
1300	-300	-5400	-1171	-2629	729
1350	-320	-5650	-1229	-2761	761
1350	-420	-5700	-1286	-2794	754
1350	-450	-5860	-1330	-2876	773
1350	-460	-5850	-1333	-2873	770
1350	-470	-5850	-1338	-2875	769
900	-400	-4000	-952	-1981	514
600	-350	-2700	-681	-1352	336
300	-300	-1500	-429	-771	171
0	50	-100	5	-38	21
0	0	-180	-34	-86	26
0	0	160	30	76	-23
0	-50	180	10	76	-33
0	-50	180	10	76	-33
0	-100	160	-17	57	-37

STRAIN REDUCTION OF A TWO GAGE ROSETTE

E= .40 POISSONS RATIO= .40 GAGE NO.= 2=OUTSIDE

LOAD	EP1	EP2	SIGMA MAX	SIGMA MIN	TAU MAX
0	0	0	0	0	0
100	-150	-350	-138	-195	29
200	-620	-900	-467	-547	40
300	-1080	-1300	-762	-825	31
400	-1480	-1800	-1048	-1139	46
500	-1950	-2300	-1367	-1467	50
600	-2350	-2700	-1633	-1733	50
700	-2750	-3180	-1915	-2038	61
800	-3200	-3650	-2219	-2348	64
900	-3780	-4180	-2596	-2710	57
1000	-4150	-4650	-2862	-3005	71
1100	-4600	-5100	-3162	-3305	71
1200	-5100	-5550	-3486	-3614	64
1300	-5500	-6020	-3766	-3914	74
1350	-5750	-6350	-3948	-4119	86
1350	-6350	-6850	-4329	-4471	71
1350	-6650	-7220	-4542	-4705	81
1350	-6700	-7300	-4581	-4752	86
1350	-6750	-7320	-4609	-4771	81
900	-5100	-5600	-3495	-3638	71
600	-3820	-4150	-2610	-2704	47
300	-2500	-2750	-1714	-1786	36
0	-700	-800	-486	-514	14
0	-480	-480	-320	-320	0
0	-200	-250	-143	-157	7
0	-200	-300	-152	-181	14
0	-150	-250	-119	-148	14
0	-380	-220	-242	-225	-9

STRAIN REDUCTION OF A TWO GAGE ROSETTE

E= .40 POISSONS RATIO= .40 GAGE NO.= 2-INSIDE

LOAD	EP1	EP2	SIGMA MAX	SIGMA MIN	TAU MAX
0	0	0	0	0	0
100	-720	-650	-467	-447	-10
200	-1350	-1200	-871	-829	-21
300	-1920	-1750	-1248	-1199	-24
400	-2600	-2250	-1667	-1567	-50
500	-3250	-2900	-2100	-2000	-50
600	-3950	-3500	-2548	-2419	-64
700	-4600	-4000	-2952	-2781	-86
800	-5250	-4600	-3376	-3190	-93
900	-5950	-5200	-3824	-3610	-107
1000	-6600	-5750	-4238	-3995	-121
1100	-7300	-6400	-4695	-4438	-129
1200	-7950	-6950	-5110	-4824	-143
1300	-8600	-7600	-5543	-5257	-143
1350	-9050	-7900	-5814	-5486	-164
1350	-9750	-8550	-6271	-5929	-171
1350	-10200	-8900	-6552	-6181	-186
1350	-10300	-8950	-6610	-6224	-193
1350	-10400	-9000	-6667	-6267	-200
900	-7950	-7000	-5119	-4848	-136
600	-5950	-5200	-3824	-3610	-107
300	-3950	-3450	-2538	-2395	-71
0	-1300	-1250	-857	-843	-7
0	-850	-820	-561	-552	-4
0	-650	-550	-414	-386	-14
0	-600	-600	-400	-400	0
0	-600	-650	-410	-424	7
0	-700	-650	-457	-443	-7

STRAIN REDUCTION OF A TWO GAGE ROSETTE

E= .40 POISSONS RATIO= .40 GAGE NO.= 3=OUTSIDE

LOAD	EP1	EP2	SIGMA MAX	SIGMA MIN	TAU MAX
0	0	0	0	0	0
100	-150	-570	-180	-300	60
200	-220	-1050	-305	-542	119
300	-350	-1600	-471	-829	179
400	-450	-2250	-643	-1157	257
500	-500	-2750	-762	-1405	321
600	-600	-3300	-914	-1686	386
700	-800	-3800	-1105	-1962	429
800	-900	-4300	-1248	-2219	486
900	-1100	-4850	-1448	-2519	536
1000	-1150	-5350	-1567	-2767	600
1100	-1400	-5950	-1800	-3100	650
1200	-1450	-6480	-1925	-3362	719
1300	-1900	-6850	-2210	-3624	707
1350	-1900	-7150	-2267	-3767	750
1350	-1950	-7300	-2319	-3848	764
1350	-2000	-7500	-2381	-3952	786
1350	-2000	-7500	-2381	-3952	786
1350	-2050	-7550	-2414	-3986	786
900	-1900	-5850	-2019	-3148	564
600	-1700	-4250	-1619	-2348	364
300	-1550	-2550	-1224	-1510	143
0	-420	-450	-286	-294	4
0	-320	-150	-181	-132	-24
0	-300	20	-139	-48	-46
0	-350	50	-157	-43	-57
0	-320	100	-133	-13	-60
0	-500	50	-229	-71	-79

STRAIN REDUCTION OF A TWO GAGE ROSETTE

t= .40 POISSONS RATIO= .40 GAGE NO.= 3-INSIDE

LOAD	EP1	EP2	SIGMA MAX	SIGMA MIN	TAU MAX
0	0	0	0	0	0
100	-550	-650	-386	-414	14
200	-800	-1700	-705	-962	129
300	-1100	-2800	-1057	-1543	243
400	-1350	-3950	-1395	-2138	371
500	-1650	-5100	-1757	-2743	493
600	-1950	-6300	-2129	-3371	621
700	-2150	-7350	-2424	-3910	743
800	-2400	-8500	-2762	-4505	871
900	-2700	-9600	-3114	-5086	986
1000	-2900	-10800	-3438	-5695	1129
1100	-3550	-11600	-3900	-6200	1150
1200	-3750	-13000	-4262	-6905	1321
1300	-4500	-13900	-4790	-7476	1343
1350	-4600	-14600	-4971	-7829	1429
1350	-5900	-15000	-5667	-8267	1300
1350	-10500	-14600	-7781	-8952	586
1350	-10000	-13200	-7276	-8190	457
1350	-9600	-8750	-6238	-5995	-121
900	-7350	-7500	-4929	-4971	21
600	-7000	-4900	-4267	-3667	-300
300	-6300	-3950	-3752	-3081	-336
0	-4800	-900	-2457	-1343	-557
0	-4150	-700	-2110	-1124	-493
0	-3200	-600	-1638	-895	-371
0	-3000	-550	-1533	-833	-350
0	-2700	-550	-1390	-776	-307
0	-2500	-550	-1295	-738	-279

STRAIN REDUCTION OF A TWO GAGE ROSETTE

E= .40 POISSONS RATIO= .40 GAGE NO.= 4=OUTSIDE

LOAD	EP1	EP2	SIGMA MAX	SIGMA MIN	TAU MAX
0	0	0	0	0	0
100	-450	-430	-296	-290	-3
200	-850	-870	-570	-576	3
300	-1300	-1300	-867	-867	0
400	-1750	-1750	-1167	-1167	0
500	-2200	-2150	-1457	-1493	-7
600	-2600	-2650	-1743	-1757	7
700	-3150	-3050	-2081	-2052	-14
800	-3550	-3500	-2357	-2343	-7
900	-4050	-3980	-2687	-2667	-10
1000	-4450	-4450	-2967	-2967	0
1100	-4950	-4900	-3290	-3276	-7
1200	-5400	-5300	-3581	-3552	-14
1300	-5850	-5800	-3890	-3876	-7
1350	-6150	-6050	-4081	-4052	-14
1350	-6750	-6500	-4452	-4381	-36
1350	-7050	-6850	-4662	-4605	-29
1350	-7100	-6850	-4686	-4614	-36
1350	-7150	-6900	-4719	-4648	-36
900	-5500	-5250	-3619	-3548	-36
600	-4150	-3920	-2723	-2657	-33
300	-2800	-2550	-1819	-1748	-36
0	-950	-720	-590	-524	-33
0	-600	-500	-381	-352	-14
0	-400	-350	-257	-243	-7
0	-350	-350	-233	-233	0
0	-350	-350	-233	-233	0
0	-380	-380	-253	-253	0

STRAIN REDUCTION OF A TWO GAGE ROSETTE

E= .40 POISSONS RATIO= .40 GAGE NO.= 4=INSIDE

LOAD	EP1	EP2	SIGMA MAX	SIGMA MIN	TAU MAX
0	0	0	0	0	0
100	-700	-800	-486	-514	14
200	-1320	-1400	-895	-918	11
300	-1950	-2000	-1310	-1324	7
400	-2600	-2700	-1752	-1781	14
500	-3200	-3200	-2133	-2133	0
600	-3850	-4000	-2595	-2638	21
700	-4500	-4700	-3038	-3095	29
800	-5200	-5400	-3505	-3562	29
900	-5850	-6100	-3948	-4019	36
1000	-6450	-6800	-4367	-4467	50
1100	-7100	-7500	-4810	-4924	57
1200	-7550	-8250	-5167	-5367	100
1300	-8400	-8950	-5705	-5862	79
1350	-8800	-9480	-5990	-6176	93
1350	-9400	-10700	-6514	-6886	186
1350	-9750	-11300	-6795	-7238	221
1350	-9850	-11400	-6862	-7305	221
1350	-9900	-11600	-6924	-7410	243
900	-7500	-9300	-5343	-5857	257
600	-5600	-7250	-4048	-4519	236
300	-3600	-5050	-2676	-3090	207
0	-1200	-2000	-952	-1181	114
0	-900	-1350	-686	-814	64
0	-700	-950	-514	-586	36
0	-700	-900	-505	-562	29
0	-750	-900	-529	-671	71
0	-800	-950	-562	-605	21

STRAIN REDUCTION OF A TWO GAGE ROSETTE

E= 10.00 POISSONS RATIO= .30 GAGE NO.= 5=OUTSIDE

LOAD	EP1	EP2	SIGMA MAX	SIGMA MIN	TAU MAX
0	0	0	0	0	0
100	-100	0	-1099	-330	-385
200	-100	0	-1099	-330	-385
300	-120	0	-1319	-396	-462
400	-150	0	-1648	-495	-577
500	-150	0	-1648	-495	-577
600	-180	50	-1813	-44	-885
700	-200	50	-2033	-110	-962
800	-200	50	-2033	-110	-962
900	-250	50	-2582	-275	-1154
1000	-300	50	-3132	-440	-1346
1100	-320	80	-3253	-176	-1538
1200	-350	100	-3516	-55	-1731
1300	-380	100	-3846	-154	-1846
1350	-380	100	-3846	-154	-1846
1350	-350	100	-3516	-55	-1731
1350	-400	100	-4066	-220	-1923
1350	-400	100	-4066	-220	-1923
1350	-400	100	-4066	-220	-1923
900	-220	100	-2088	374	-1231
600	-200	100	-1868	440	-1154
300	-150	100	-1319	604	-962
0	-50	0	-549	-165	-192
0	0	0	0	0	0
0	0	0	0	0	0
0	0	0	0	0	0
0	0	0	0	0	0
0	-100	0	-1099	-330	-385

STRAIN REDUCTION OF A TWO GAGE ROSETTE

E= 10,00 POISSONS RATIO= ,30 GAGE NO,= S-INSIDE

LOAD	EP1	EP2	SIGMA MAX	SIGMA MIN	TAU MAX
0	0	0	0	0	0
100	-200	-100	-2527	-1758	-385
200	-250	-100	-3077	-1923	-577
300	-300	-50	-3462	-1538	-962
400	-400	-100	-4725	-2418	-1154
500	-500	-150	-5989	-3297	-1346
600	-600	-150	-7088	-3626	-1731
700	-700	-200	-8352	-4505	-1923
800	-800	-220	-9516	-5055	-2231
900	-850	-350	-10495	-6648	-1923
1000	-900	-300	-10879	-6264	-2308
1100	-950	-500	-12088	-8626	-1731
1200	-1050	-500	-13187	-8956	-2115
1300	-1100	-450	-13571	-8571	-2500
1350	-1100	-450	-13571	-8571	-2500
1350	-1100	-400	-13407	-8022	-2692
1350	-1150	-400	-13956	-8187	-2885
1350	-1100	-350	-13242	-7473	-2885
1350	-1100	-350	-13242	-7473	-2885
900	-700	-300	-8681	-5604	-1538
600	-400	-200	-5055	-3516	-769
300	-200	-100	-2527	-1758	-385
0	-100	0	-1099	-330	-385
0	-100	0	-1099	-330	-385
0	-50	0	-549	-165	-192
0	-100	0	-1099	-330	-385
0	-50	0	-549	-165	-192
0	-100	0	-1099	-330	-385

STRAIN REDUCTION OF A TWO GAGE ROSETTE

E= 10.00 POISSONS RATIO= .30 GAGE NO.= 6=OUTSIDE

LOAD	EP1	EP2	SIGMA MAX	SIGMA MIN	TAU MAX
0	0	0	0	0	0
100	-30	0	-330	-99	-115
200	-50	0	-549	-165	-192
300	-100	0	-1099	-330	-385
400	-130	0	-1429	-429	-500
500	-150	0	-1648	-495	-577
600	-180	0	-1978	-593	-692
700	-180	0	-1978	-593	-692
800	-200	0	-2198	-659	-769
900	-220	0	-2418	-725	-846
1000	-280	0	-3077	-923	-1077
1100	-320	0	-3516	-1055	-1231
1200	-300	0	-3297	-989	-1154
1300	-350	0	-3846	-1154	-1346
1350	-350	0	-3846	-1154	-1346
1350	-350	0	-3846	-1154	-1346
1350	-350	0	-3846	-1154	-1346
1350	-350	0	-3846	-1154	-1346
1350	-350	0	-3846	-1154	-1346
900	-200	0	-2198	-659	-769
600	-150	0	-1648	-495	-577
300	-150	0	-1648	-495	-577
0	0	0	0	0	0
0	50	0	549	165	192
0	50	0	549	165	192
0	50	0	549	165	192
0	50	0	549	165	192
0	0	0	0	0	0

STRAIN REDUCTION OF A TWO GAGE ROSETTE

E= 10.00 POISSONS RATIO= .30 GAGE NO.= 6=INSIDE

LOAD	EP1	EP2	SIGMA MAX	SIGMA MIN	TAU MAX
0	0	0	0	0	0
100	-50	-50	-714	-714	0
200	-100	-50	-1264	-879	-192
300	-200	-100	-2527	-1758	-385
400	-300	-100	-3626	-2088	-769
500	-400	-150	-4890	-2967	-962
600	-450	-200	-5604	-3681	-962
700	-550	-250	-6868	-4560	-1154
800	-650	-300	-8132	-5440	-1346
900	-700	-350	-8846	-6154	-1346
1000	-800	-400	-10110	-7033	-1538
1100	-850	-450	-10824	-7747	-1538
1200	-900	-480	-11473	-8242	-1615
1300	-950	-500	-12088	-8626	-1731
1350	-950	-550	-12253	-9176	-1538
1350	-900	-500	-11538	-8462	-1538
1350	-950	-500	-12088	-8626	-1731
1350	-900	-500	-11538	-8462	-1538
1350	-900	-500	-11538	-8462	-1538
900	-600	-400	-7912	-6374	-769
600	-300	-280	-4220	-4066	-77
300	-100	-150	-1593	-1978	192
0	0	-50	-165	-549	192
0	0	0	0	0	0
0	50	-50	385	-385	385
0	50	-50	385	-385	385
0	50	-50	385	-385	385
0	0	-50	-165	-549	192

STRAIN REDUCTION OF A TWO GAGE ROSETTE

E= 10.00 POISSONS RATIO= .30 GAGE NO.= 7=OUTSIDE

LOAD	EP1	EP2	SIGMA MAX	SIGMA MIN	TAU MAX
0	0	0	0	0	0
100	-50	0	-549	-165	-192
200	-50	-50	-714	-714	0
300	-100	-50	-1264	-879	-192
400	-120	-80	-1582	-1275	-154
500	-150	-100	-1978	-1593	-192
600	-150	-100	-1978	-1593	-192
700	-150	-80	-1912	-1374	-269
800	-200	-100	-2627	-1758	-385
900	-250	-180	-3341	-2802	-269
1000	-250	-200	-3407	-3022	-192
1100	-300	-200	-3956	-3187	-385
1200	-350	-200	-4505	-3352	-577
1300	-380	-200	-4835	-3451	-692
1350	-400	-200	-5055	-3516	-769
1350	-380	-200	-4835	-3451	-692
1350	-400	-200	-5055	-3516	-769
1350	-400	-200	-5055	-3516	-769
1350	-400	-200	-5055	-3516	-769
900	-300	-180	-3890	-2967	-462
600	-200	-100	-2527	-1758	-385
300	-180	-100	-2308	-1692	-308
0	0	0	0	0	0
0	0	50	165	549	-192
0	50	50	714	714	0
0	0	50	165	549	-192
0	0	50	165	549	-192
0	0	0	0	0	0

E= 10.00 POISSONS RATIO= .30 GAGE NO.= 7=INSIDE

LOAD	EP1	EP2	SIGMA MAX	SIGMA MIN	TAU MAX
0	0	0	0	0	0
100	-100	-50	-1264	-879	-192
200	-150	-50	-1813	-1044	-385
300	-200	-50	-2363	-1209	-577
400	-300	-50	-3462	-1638	-962
500	-350	-50	-4011	-1703	-1154
600	-400	-100	-4725	-2418	-1154
700	-450	-100	-5275	-2582	-1346
800	-500	-150	-5989	-3297	-1346
900	-550	-150	-6538	-3462	-1538
1000	-600	-100	-6923	-3077	-1923
1100	-700	-150	-8187	-3956	-2115
1200	-750	-100	-8571	-3571	-2500
1300	-800	-200	-9451	-4835	-2308
1350	-800	-150	-9286	-4286	-2500
1350	-800	-150	-9286	-4286	-2500
1350	-850	-150	-9835	-4451	-2692
1350	-800	-150	-9286	-4286	-2500
1350	-800	-150	-9286	-4286	-2500
900	-550	-150	-6538	-3462	-1538
600	-350	-100	-4176	-2253	-962
300	-100	-50	-1264	-879	-192
0	-50	-50	-714	-714	0
0	0	0	0	0	0
0	-50	0	-549	-165	-192
0	-50	0	-549	-165	-192
0	-50	0	-549	-165	-192
0	-50	-50	-714	-714	0

STRAIN REDUCTION OF A TWO GAGE ROSETTE

E= 10.00 POISSONS RATIO= .30 GAGE NO.= 8=OUTSIDE

LOAD	EP1	EP2	SIGMA MAX	SIGMA MIN	TAU MAX
0	0	0	0	0	0
100	0	-50	-165	-549	192
200	0	-100	-330	-1099	385
300	-20	-100	-549	-1165	308
400	-50	-120	-945	-1484	269
500	-100	-150	-1593	-1978	192
600	-120	-120	-1714	-1714	0
700	-150	-150	-2143	-2143	0
800	-200	-200	-2857	-2857	0
900	-200	-200	-2857	-2857	0
1000	-220	-230	-3176	-3253	38
1100	-300	-300	-4286	-4286	0
1200	-320	-320	-4571	-4571	0
1300	-350	-350	-5000	-5000	0
1350	-380	-380	-5429	-5429	0
1350	-380	-380	-5429	-5429	0
1350	-380	-380	-5429	-5429	0
1350	-380	-380	-5429	-5429	0
1350	-380	-380	-5429	-5429	0
900	-280	-250	-4101	-3670	-115
600	-180	-200	-2637	-2791	77
300	-100	-180	-1692	-2308	308
0	0	0	0	0	0
0	0	0	0	0	0
0	0	0	0	0	0
0	0	0	0	0	0
0	0	0	0	0	0
0	0	0	0	0	0

STRAIN REDUCTION OF A TWO GAGE ROSETTE

E= 10.00 POISSONS RATIO= .30 GAGE NO.= 8=INSIDE

LOAD	EP1	EP2	SIGMA MAX	SIGMA MIN	TAU MAX
0	0	0	0	0	0
100	-250	-150	-3242	-2473	-385
200	-300	-250	-4121	-3736	-192
300	-200	-350	-3352	-4505	577
400	-300	-450	-4780	-5934	577
500	-350	-550	-5659	-7198	769
600	-500	-650	-7637	-8791	577
700	-450	-680	-7167	-8956	885
800	-600	-750	-9066	-10220	577
900	-650	-850	-9945	-11484	769
1000	-600	-900	-9560	-11868	1154
1100	-650	-950	-10275	-12582	1154
1200	-800	-1050	-12253	-14176	962
1300	-850	-1100	-12967	-14890	962
1350	-900	-1200	-13846	-16184	1154
1350	-900	-1050	-13352	-14505	577
1350	-800	-1000	-12088	-13626	769
1350	-800	-1000	-12088	-13626	769
1350	-750	-950	-11374	-12912	769
900	-350	-700	-6154	-8846	1346
600	-250	-600	-4396	-6319	962
300	-150	-300	-2637	-3791	577
0	-200	-250	-3022	-3407	192
0	-200	-200	-2857	-2857	0
0	0	-100	-330	-1099	385
0	-100	-160	-1593	-1978	192
0	-150	-250	-2473	-3242	385
0	-180	-200	-2637	-2791	77

STRAIN REDUCTION OF A TWO GAGE ROSETTE

E= 10.00 POISSONS RATIO= .30 GAGE NO.= 9=INSIDE

LOAD	EP1	EP2	SIGMA MAX	SIGMA MIN	TAU MAX
0	0	0	0	0	0
100	0	0	0	0	0
200	-100	50	-934	220	-577
300	-150	100	-1319	604	-962
400	-250	0	-2747	-824	-962
500	-350	150	-3352	495	-1923
600	-500	150	-5000	0	-2500
700	-550	150	-5549	-165	-2692
800	-700	150	-7198	-659	-3269
900	-750	150	-7747	-824	-3462
1000	-850	150	-8846	-1154	-3846
1100	-900	200	-9231	-769	-4231
1200	-950	300	-9461	165	-4808
1300	-1060	350	-10385	385	-5385
1350	-1100	300	-11099	-330	-5385
1350	-1100	350	-10934	220	-5577
1350	-1100	500	-10440	1868	-6154
1350	-1050	450	-10055	1484	-5769
1350	-1050	450	-10055	1484	-5769
900	-700	250	-6868	440	-3654
600	-480	100	-4615	-385	-2115
300	-150	0	-1648	-495	-577
0	0	0	0	0	0
0	0	50	165	549	-192
0	0	0	0	0	0
0	0	50	165	549	-192
0	0	-50	-165	-549	192
0	-50	-100	-879	-1264	192

STRAIN REDUCTION OF A TWO GAGE ROSETTE

E= 10.00 POISSONS RATIO= .30 GAGE NO.= 10-INSIDE

LOAD	EP1	EP2	SIGMA MAX	SIGMA MIN	TAU MAX
0	0	0	0	0	0
100	-50	-200	-1209	-2363	577
200	-100	-300	-2088	-3626	769
300	-150	-400	-2967	-4890	962
400	-250	-450	-4231	-5769	769
500	-350	-500	-5495	-6648	577
600	-400	-600	-6374	-7912	769
700	-450	-700	-7253	-9176	962
800	-600	-800	-9231	-10769	769
900	-650	-900	-10110	-12033	962
1000	-700	-1000	-10989	-13297	1154
1100	-750	-1050	-11703	-14011	1154
1200	-850	-1100	-12967	-14890	962
1300	-900	-1250	-14011	-16703	1346
1350	-950	-1300	-14725	-17418	1346
1350	-950	-1250	-14560	-16868	1154
1350	-900	-1250	-14011	-16703	1346
1350	-900	-1250	-14011	-16703	1346
1350	-900	-1250	-14011	-16703	1346
900	-650	-900	-10110	-12033	962
600	-400	-550	-6209	-7363	577
300	-150	-300	-2637	-3791	577
0	-50	0	-549	-165	-192
0	-50	0	-549	-165	-192
0	-50	0	-549	-165	-192
0	-50	0	-549	-165	-192
0	-50	0	-549	-165	-192
0	-50	-50	-714	-714	0

STRAIN REDUCTION OF A TWO GAGE ROSETTE

E= .40 POISSONS RATIO= .40 GAGE NO.= 2=INSIDE

LOAD	EP1	EP2	SIGMA MAX	SIGMA MIN	TAU MAX
0	0	0	0	0	0
100	-700	-500	-429	-371	-29
200	-1300	-1100	-829	-771	-29
300	-1925	-1700	-1240	-1176	-32
400	-2600	-2275	-1671	-1579	-46
500	-3600	-2825	-2252	-2031	-111
600	-4325	-3400	-2707	-2443	-132
700	-4600	-3950	-2943	-2757	-93
800	-5200	-4525	-3338	-3145	-96
900	-5900	-5150	-3790	-3576	-107
1000	-6525	-5725	-4198	-3969	-114
1100	-7200	-6350	-4638	-4395	-121
1200	-7925	-6975	-5102	-4831	-136
1300	-8675	-7550	-5569	-5248	-161
1400	-9550	-8200	-6110	-5724	-193
1500	-10000	-8725	-6424	-6060	-182
1600	-10800	-9400	-6933	-6533	-200
1700	-11450	-9950	-7348	-6919	-214
1800	-12250	-10650	-7862	-7405	-229
1800	-13950	-12100	-8948	-8419	-264
1800	-14575	-12700	-9360	-8824	-268
1800	-14800	-12850	-9495	-8938	-279
1800	-15250	-13150	-9767	-9167	-300
1500	-13550	-11700	-8681	-8152	-264
1200	-11700	-10100	-7495	-7038	-229
900	-9725	-8500	-6250	-5900	-175
600	-7450	-6500	-4786	-4514	-136
300	-4900	-4250	-3143	-2957	-93
0	-2000	-1800	-1295	-1238	-29
0	0	0	0	0	0
0	25	-50	2	-19	11
0	125	-50	50	0	25
0	125	-50	50	0	25
0	125	200	98	119	-11
0	75	0	36	14	11

STRAIN REDUCTION OF A TWO GAGE ROSETTE

E= .40 POISSONS RATIO= .40 GAGE NO.= 1=OUTSIDE

LOAD	EP1	EP2	SIGMA MAX	SIGMA MIN	TAU MAX
0	0	0	0	0	0
100	-500	-50	-248	-119	-64
200	-500	-450	-324	-310	-7
300	-500	-850	-400	-500	50
400	-600	-1400	-552	-781	114
500	-650	-1750	-643	-957	157
600	-650	-2250	-738	-1195	229
700	-650	-2650	-814	-1386	286
800	-650	-3650	-1005	-1862	429
900	-700	-3850	-1067	-1967	450
1000	-750	-4250	-1167	-2167	500
1100	-700	-4700	-1229	-2371	571
1200	-750	-5100	-1329	-2571	621
1300	-750	-5650	-1433	-2833	700
1400	-900	-6700	-1705	-3362	829
1500	-900	-7200	-1800	-3600	900
1600	-950	-7550	-1890	-3776	943
1700	-950	-8000	-1976	-3990	1007
1800	-900	-8450	-2038	-4195	1079
1800	-950	-8700	-2110	-4324	1107
1800	-900	-8700	-2086	-4314	1114
1800	-950	-8650	-2100	-4300	1100
1800	-1050	-8900	-2195	-4438	1121
1500	-1050	-7800	-1986	-3914	964
1200	-1050	-6550	-1748	-3319	786
900	-950	-5400	-1481	-2752	636
600	-900	-4100	-1210	-2124	457
300	-1050	-2200	-919	-1248	164
0	-500	-450	-324	-310	-7
0	-300	0	-143	-57	-43
0	-250	0	-119	-48	-36
0	-300	50	-133	-33	-50
0	-100	100	-29	29	-29
0	-300	100	-124	-10	-57
0	-100	150	-19	52	-36

STRAIN REDUCTION OF A TAU GAGE ROSETTE

E= .40 POISSONS RATIO= .40 GAGE NO.= 2=OUTSIDE

LOAD	EP1	EP2	SIGMA MAX	SIGMA MIN	TAU MAX
0	0	0	0	0	0
100	-400	-450	-276	-290	7
200	-850	-900	-576	-590	7
300	-1250	-1350	-852	-881	14
400	-1700	-1850	-1162	-1205	21
500	-2300	-2350	-1543	-1557	7
600	-2550	-2800	-1748	-1819	36
700	-3000	-3200	-2038	-2095	29
800	-3400	-3700	-2324	-2410	43
900	-3900	-4150	-2648	-2719	36
1000	-4300	-4650	-2933	-3033	50
1100	-4750	-5100	-3233	-3333	50
1200	-5200	-5600	-3543	-3657	57
1300	-5750	-6150	-3910	-4024	57
1400	-6200	-6650	-4219	-4348	64
1500	-6700	-7100	-4543	-4657	57
1600	-7150	-7675	-4867	-5017	75
1700	-8100	-8100	-5400	-5400	0
1800	-8100	-8650	-5505	-5662	79
1800	-9250	-9900	-6290	-6476	93
1800	-9650	-10350	-6567	-6767	100
1800	-9750	-10450	-6633	-6833	100
1800	-10200	-10900	-6933	-7133	100
1500	-9050	-9750	-6167	-6367	100
1200	-7800	-8600	-5352	-5581	114
900	-6550	-7100	-4471	-4629	79
600	-5050	-5450	-3443	-3557	57
300	-3500	-3500	-2333	-2333	0
0	-1400	-1300	-814	-886	-14
0	-200	0	-95	-38	-29
0	-150	0	-71	-29	-21
0	-50	0	-24	-10	-7
0	0	150	29	71	-21
0	0	200	38	95	-29
0	0	200	38	95	-29

STRAIN REDUCTION OF A TAU GAGE ROSETTE

E= .40 POISSONS RATIO= .40 GAGE NO.= 3=OUTSIDE

LOAD	EP1	EP2	SIGMA MAX	SIGMA MIN	TAU MAX
0	0	0	0	0	0
100	-200	-800	-248	-419	86
200	-300	-1350	-400	-700	150
300	-400	-1850	-543	-957	207
400	-500	-2400	-695	-1238	271
500	-600	-3000	-857	-1543	343
600	-800	-3450	-1038	-1795	379
700	-850	-4000	-1167	-2067	450
800	-1000	-4500	-1333	-2333	500
900	-1250	-4950	-1538	-2595	529
1000	-1350	-5500	-1690	-2876	593
1100	-1400	-6000	-1810	-3124	657
1200	-1500	-6600	-1971	-3429	729
1300	-1800	-7200	-2229	-3771	771
1400	-1850	-7650	-2338	-3995	829
1500	-1850	-8200	-2443	-4257	907
1600	-1950	-8700	-2586	-4514	964
1700	-2050	-9200	-2729	-4771	1021
1800	-2600	-9550	-3057	-5043	993
1800	-2600	-9900	-3124	-5210	1043
1800	-2700	-9950	-3181	-5252	1036
1800	-2600	-10000	-3143	-5257	1057
1800	-2700	-10300	-3248	-5419	1086
1500	-2600	-9100	-2971	-4829	929
1200	-2500	-7900	-2695	-4238	771
900	-2350	-6500	-2357	-3543	593
600	-2150	-4700	-1919	-2648	364
300	-1800	-2800	-1390	-1676	143
0	-950	-1000	-405	-562	79
0	-150	-50	-81	-52	-14
0	-100	0	-48	-19	-14
0	-75	100	-17	33	-25
0	-75	150	-7	67	-32
0	-80	150	5	62	-29
0	-150	150	-43	43	-43

STRAIN REDUCTION OF A TWO GAGE ROSETTE

E= .40 POISSON'S RATIO= .40 GAGE NO.= 4=OUTSIDE

LOAD	EP1	EP2	SIGMA MAX	SIGMA MIN	TAU MAX
0	0	0	0	0	0
100	-500	-450	-324	-310	-7
200	-1000	-900	-648	-619	-14
300	-1350	-1400	-910	-924	7
400	-1700	-1750	-1143	-1157	7
500	-2250	-2250	-1500	-1500	0
600	-2650	-2650	-1767	-1767	0
700	-3100	-3050	-2057	-2043	-7
800	-3550	-3500	-2357	-2343	-7
900	-4100	-3950	-2705	-2662	-21
1000	-4500	-4450	-2990	-2976	-7
1100	-4900	-4850	-3257	-3243	-7
1200	-5450	-5300	-3605	-3562	-21
1300	-5900	-5850	-3924	-3910	-7
1400	-6400	-6300	-4248	-4219	-14
1500	-6800	-6800	-4533	-4533	0
1600	-7250	-7250	-4833	-4833	0
1700	-7800	-7700	-5181	-5152	-14
1800	-8300	-8200	-5514	-5486	-14
1800	-9600	-9300	-6343	-6257	-43
1800	-10000	-9700	-6610	-6524	-43
1800	-12000	-9800	-7581	-6952	-314
1800	-15000	-10150	-9076	-7690	-693
1500	-9350	-9050	-6176	-6090	-43
1200	-8100	-7800	-5343	-5257	-43
900	-6800	-6450	-4467	-4367	-50
600	-5200	-4900	-3410	-3324	-43
300	-3350	-3150	-2195	-2138	-29
0	-1300	-1150	-838	-795	-21
0	0	-50	-10	-24	7
0	0	0	0	0	0
0	100	-100	29	-29	29
0	-100	50	-38	5	-21
0	-100	100	-29	29	-29
0	0	100	19	48	-14

STRAIN REDUCTION OF A TWO GAGE ROSETTE

E= .40 POISSONS RATIO= .40 GAGE NO.= 4=INSIDE

LOAD	EP1	EP2	SIGMA MAX	SIGMA MIN	TAU MAX
0	0	0	0	0	0
100	-650	-650	-433	-433	0
200	-1250	-1350	-852	-881	14
300	-1900	-1950	-1276	-1290	7
400	-2550	-2700	-1729	-1771	21
500	-3200	-3400	-2171	-2229	29
600	-3700	-4050	-2533	-2633	50
700	-4400	-4750	-3000	-3100	50
800	-5100	-5400	-3457	-3543	43
900	-5800	-6200	-3943	-4057	57
1000	-6350	-6900	-4338	-4495	79
1100	-7050	-7700	-4824	-5010	93
1200	-7700	-8400	-5267	-5467	100
1300	-8350	-9100	-5710	-5924	107
1400	-9000	-10000	-6190	-6476	143
1500	-9700	-10750	-6667	-6967	150
1600	-10400	-11500	-7143	-7457	157
1700	-11050	-12300	-7605	-7962	179
1800	-11750	-13100	-8090	-8476	193
1800	-13100	-16100	-9305	-10162	429
1800	-13600	-17200	-9752	-10781	514
1800	-13750	-17650	-9910	-11024	557
1800	-14150	-17800	-10129	-11171	521
1500	-12500	-16700	-9133	-10333	600
1200	-10750	-14800	-7938	-9095	579
900	-8800	-12650	-6600	-7700	550
600	-6600	-10200	-5086	-6114	514
300	-4250	-7000	-3357	-4143	393
0	-1500	-8200	-1324	-1810	243
0	-300	750	0	300	-150
0	-250	900	52	381	-164
0	-150	1200	157	543	-193
0	-200	1350	162	605	-221
0	-200	1500	190	676	-243
0	-250	1550	176	690	-257

STRAIN REDUCTION OF A TWO GAGE ROSETTE

E= 10,00 POISSONS RATIO= ,30 GAGE NO,= 5=OUTSIDE

LOAD	EP1	EP2	SIGMA MAX	SIGMA MIN	TAU MAX
0	0	0	0	0	0
100	-50	0	-[illegible]49	-165	-192
200	-150	0	-[illegible]98	-495	-577
300	-100	50	-934	220	-577
400	-100	50	-934	220	-577
500	-150	0	-1648	-495	-577
600	-200	50	-2033	-110	-962
700	-200	100	-1868	440	-1154
800	-200	50	-2033	-110	-962
900	-250	50	-2582	-275	-1154
1000	-250	50	-2582	-275	-1154
1100	-300	100	-2967	110	-1538
1200	-300	100	-2967	110	-1538
1300	-350	100	-3516	-55	-1731
1400	-350	150	-3352	495	-1923
1500	-350	150	-3352	495	-1923
1600	-400	150	-3901	330	-2115
1700	-400	150	-3901	330	-2115
1800	-450	200	-4286	714	-2500
1800	-450	150	-4451	165	-2308
1800	-400	200	-3736	879	-2308
1800	-400	150	-3901	330	-2115
1800	-450	150	-4451	165	-2308
1500	-350	200	-3187	1044	-2115
1200	-300	150	-2802	659	-1731
900	-250	150	-2253	824	-1538
600	-200	100	-1868	440	-1154
300	-150	100	-1319	604	-962
0	50	50	714	714	0
0	50	50	714	714	0
0	50	50	714	714	0
0	50	50	714	714	0
0	100	50	1264	879	192
0	100	50	1264	879	192
0	50	50	714	714	0

STRAIN REDUCTION OF A TWO GAGE ROSETTE

E= 10,00 POISSONS RATIO= ,30 GAGE NO.= 5=INSIDE

LOAD	EP1	EP2	SIGMA MAX	SIGMA MIN	TAU MAX
0	0	0	0	0	0
100	-50	50	-385	385	-385
200	-150	100	-1319	604	-962
300	-250	100	-2418	275	-1346
400	-400	150	-3901	330	-2115
500	-500	175	-4918	275	-2596
600	-550	0	-6044	-1813	-2115
700	-600	0	-6593	-1978	-2308
800	-700	0	-7692	-2308	-2692
900	-750	-200	-8901	-4670	-2115
1000	-800	-100	-9121	-3736	-2692
1100	-900	-100	-10220	-4066	-3077
1200	-1000	-150	-11484	-4945	-3269
1300	-1050	-250	-12363	-6209	-3077
1400	-1150	-300	-13626	-7088	-3269
1500	-1200	-350	-14341	-7802	-3269
1600	-1200	-350	-14341	-7802	-3269
1700	-1300	-300	-15275	-7582	-3846
1800	-1350	-150	-15330	-6099	-4615
1800	-1350	-50	-15000	-5000	-5000
1800	-1250	-100	-14066	-5220	-4423
1800	-1200	-100	-13516	-5055	-4231
1800	-1350	-200	-15496	-6648	-4423
1500	-1050	-150	-12033	-6110	-3462
1200	-800	-50	-8956	-3187	-2885
900	-500	50	-5330	-1099	-2115
600	-200	100	-1868	440	-1154
300	-100	50	-934	220	-577
0	50	50	714	714	0
0	200	0	2198	659	769
0	250	0	2747	824	962
0	300	100	3626	2088	769
0	350	50	4011	1703	1154
0	350	50	4011	1703	1154
0	350	50	4011	1703	1154

STRAIN REDUCTION OF A TWO GAGE ROSETTE

E= 10.00 POISSONS RATIO= .30 GAGE NO.= 6=OUTSIDE

LOAD	EP1	EP2	SIGMA MAX	SIGMA MIN	TAU MAX
0	0	0	0	0	0
100	0	0	0	0	0
200	-50	0	-549	-165	-192
300	-100	0	-1099	-330	-385
400	-100	0	-1099	-330	-385
500	-100	0	-1099	-330	-385
600	-150	0	-1648	-495	-577
700	-150	0	-1648	-495	-577
800	-200	0	-2198	-659	-769
900	-150	0	-1648	-495	-577
1000	-200	0	-2198	-659	-769
1100	-250	0	-2747	-824	-962
1200	-250	0	-2747	-824	-962
1300	-300	0	-3297	-989	-1154
1400	-350	0	-3846	-1154	-1346
1500	-350	0	-3846	-1154	-1346
1600	-350	0	-3846	-1154	-1346
1700	-400	0	-4396	-1319	-1538
1800	-400	0	-4396	-1319	-1538
1800	-350	0	-3846	-1154	-1346
1800	-400	-100	-4725	-2418	-1154
1800	-350	-100	-4176	-2253	-962
1800	-350	-150	-4341	-2802	-769
1500	-350	-50	-4011	-1703	-1154
1200	-200	0	-2198	-659	-769
900	-250	50	-2582	-275	-1154
600	-200	150	-1703	989	-1346
300	-200	250	-1374	2088	-1731
0	0	350	1154	3846	-1346
0	50	300	1538	3462	-962
0	50	350	1703	4011	-1154
0	100	400	2418	4725	-1154
0	100	350	2253	4176	-962
0	50	350	1703	4011	-1154
0	50	350	1703	4011	-1154

STRAIN REDUCTION OF A TWO GAGE ROSETTE

E= 10.00 POISSONS RATIO= .30 GAGE NO.= 6=INSIDE

LOAD	EP1	EP2	SIGMA MAX	SIGMA MIN	TAU MAX
0	0	0	0	0	0
100	0	0	0	0	0
200	-150	0	-1646	-495	-577
300	-250	0	-2747	-824	-962
400	-350	0	-3846	-1154	-1346
500	-400	-150	-4890	-2967	-962
600	-500	-200	-6154	-3846	-1154
700	-550	-250	-6868	-4560	-1154
800	-650	-300	-8132	-5440	-1346
900	-650	-350	-8297	-5999	-1154
1000	-750	-350	-9396	-6319	-1538
1100	-850	-400	-10659	-7198	-1731
1200	-900	-450	-11374	-7912	-1731
1300	-950	-450	-11923	-8077	-1923
1400	-950	-500	-12088	-8626	-1731
1500	-1050	-500	-13187	-8956	-2115
1600	-1150	-550	-14451	-9835	-2308
1700	-1200	-600	-15165	-10549	-2308
1800	-1200	-650	-15330	-11099	-2116
1800	-1150	-700	-14945	-11484	-1731
1800	-1100	-650	-14231	-10769	-1731
1800	-1100	-650	-14231	-10769	-1731
1800	-1200	-900	-16154	-13846	-1154
1500	-1000	-650	-12802	-9341	-1731
1200	-800	-600	-10110	-7033	-1538
900	-500	-250	-6319	-4396	-962
600	-300	-150	-3791	-2637	-577
300	-50	-200	-1209	-2363	577
0	0	0	0	0	0
0	0	-50	-165	-549	192
0	50	-50	385	-385	385
0	100	50	1264	879	192
0	50	0	549	165	192
0	100	50	1264	879	192
0	50	50	714	714	0

STRAIN REDUCTION OF A TWO GAGE ROSETTE

E= 10.00 POISSONS RATIO= .30 GAGE NO.= 7=OUTSIDE

LOAD	EP1	EP2	SIGMA MAX	SIGMA MIN	TAU MAX
0	0	0	0	0	0
100	0	0	0	0	0
200	-50	0	-549	-165	-192
300	-100	-50	-1264	-879	-192
400	-100	-50	-1264	-879	-192
500	-100	-50	-1264	-879	-192
600	-150	-100	-1978	-1593	-192
700	-150	-100	-1978	-1593	-192
800	-200	-100	-2527	-1758	-385
900	-250	-150	-3242	-2473	-385
1000	-250	-150	-3242	-2473	-385
1100	-200	-150	-2692	-2308	-192
1200	-300	-150	-3791	-2637	-577
1300	-350	-150	-4341	-2802	-769
1400	-350	-150	-4341	-2802	-769
1500	-350	-150	-4341	-2802	-769
1600	-400	-150	-4890	-2967	-962
1700	-400	-200	-5055	-3516	-769
1800	-450	-200	-5604	-3681	-962
1800	-450	-200	-5604	-3681	-962
1800	-400	-100	-4725	-2418	-1154
1800	-350	-100	-4176	-2253	-962
1800	-400	-100	-4725	-2418	-1154
1500	-300	-50	-3462	-1538	-962
1200	-250	-50	-2912	-1374	-769
900	-200	0	-2198	-659	-769
600	-200	0	-2198	-659	-769
300	-50	0	-549	-165	-192
0	100	50	1264	879	192
0	50	50	714	714	0
0	50	0	549	165	192
0	100	50	1264	879	192
0	100	50	1264	879	192
0	100	50	1264	879	192
0	50	50	714	714	0

STRAIN REDUCTION OF A TWO GAGE ROSETTE

E= 10.00 POISSONS RATIO= .30 GAGE NO.= 7=INSIDE

LOAD	EP1	EP2	SIGMA MAX	SIGMA MIN	TAU MAX
0	0	0	0	0	0
100	0	-50	-165	-549	192
200	-200	-50	-2363	-1209	-577
300	-300	-50	-3462	-1538	-962
400	-350	-100	-4176	-2253	-962
500	-350	-100	-4176	-2253	-962
600	-400	-100	-4725	-2418	-1154
700	-450	-100	-5275	-2582	-1346
800	-450	-100	-5275	-2582	-1346
900	-500	-150	-5989	-3297	-1346
1000	-550	-250	-6868	-4560	-1154
1100	-600	-150	-7088	-3626	-1731
1200	-800	-200	-9451	-4835	-2308
1300	-850	-200	-10000	-5000	-2500
1400	-900	-200	-10549	-5165	-2692
1500	-900	-200	-10549	-5165	-2692
1600	-1000	-200	-11648	-5495	-3077
1700	-1050	-200	-12198	-5659	-3269
1800	-1100	-200	-12747	-5824	-3462
1800	-1050	-200	-12198	-5659	-3269
1800	-1000	-150	-11484	-4945	-3269
1800	-1000	-150	-11484	-4945	-3269
1800	-1100	-250	-12912	-6374	-3269
1500	-900	-150	-10385	-4615	-2885
1200	-750	-150	-8736	-4121	-2308
900	-550	-100	-6374	-2912	-1731
600	-300	-100	-3626	-2088	-769
300	-100	-50	-1264	-879	-192
0	-150	-50	-1813	-1044	-385
0	-100	0	-1099	-330	-385
0	-50	-50	-714	-714	0
0	0	0	0	0	0
0	-50	0	-549	-165	-192
0	-50	0	-549	-165	-192
0	-50	0	-549	-165	-192

STRAIN REDUCTION OF A TWO GAGE ROSETTE

E= 10,00 POISSONS RATIO= ,30 GAGE NO.= R=OUTSIDE

LOAD	EP1	EP2	SIGMA MAX	SIGMA MIN	TAU MAX
0	0	0	0	0	0
100	-100	-50	-1264	-879	-192
200	-100	-100	-1429	-1429	0
300	-100	-200	-1758	-2527	385
400	-150	-250	-2473	-3242	385
500	-150	-150	-2143	-2143	0
600	-150	-150	-2143	-2143	0
700	-150	-150	-2143	-2143	0
800	-150	-150	-2143	-2143	0
900	-150	-150	-2143	-2143	0
1000	-150	-200	-2308	-2692	192
1100	-200	-200	-2857	-2857	0
1200	-225	-200	-3132	-2940	-96
1300	-250	-300	-3736	-4121	192
1400	-300	-350	-4451	-4835	192
1500	-300	-350	-4451	-4835	192
1600	-300	-350	-4451	-4835	192
1700	-325	-350	-4725	-4918	96
1800	-350	-400	-5165	-5549	192
1800	-425	-400	-5989	-5797	-96
1800	-400	-300	-5385	-4615	-385
1800	-350	-300	-4835	-4451	-192
1800	-350	-350	-5000	-5000	0
1500	-400	-250	-5220	-4066	-577
1200	-300	-300	-4286	-4286	0
900	-250	-150	-3242	-2473	-385
600	-200	-100	-2527	-1758	-385
300	-100	-50	-1264	-879	-192
0	-50	100	-220	934	-577
0	0	100	330	1099	-385
0	100	100	1429	1429	0
0	0	150	495	1648	-577
0	50	150	1044	1813	-385
0	100	150	1593	1978	-192
0	100	150	1593	1978	-192

STRAIN REDUCTION OF A TWO GAGE ROSETTE

E= 10.00 POISSONS RATIO= .30 GAGE NO.= R=INSIDE

LOAD	EP1	EP2	SIGMA MAX	SIGMA MIN	TAU MAX
0	0	0	0	0	0
100	-200	-150	-2692	-2308	-192
200	-225	-350	-3626	-4588	481
300	-275	-550	-4835	-6951	1058
400	-500	-800	-8132	-10440	1154
500	-500	-900	-8462	-11538	1538
600	-500	-1100	-9121	-13736	2308
700	-550	-1250	-10165	-15549	2692
800	-600	-1350	-11044	-16813	2885
900	-650	-1400	-11758	-17527	2885
1000	-700	-1450	-12473	-18242	2885
1100	-750	-1500	-13187	-18956	2885
1200	-800	-1550	-13901	-19670	2885
1300	-800	-1500	-13736	-19121	2692
1400	-850	-1550	-14451	-19835	2692
1500	-800	-1600	-14066	-20220	3077
1600	-900	-1550	-15000	-20000	2500
1700	-850	-1600	-14615	-20385	2885
1800	-900	-1600	-15165	-20549	2692
1800	-850	-1150	-13132	-15440	1154
1800	-700	-1000	-10989	-13297	1154
1800	-650	-1000	-10440	-13132	1346
1800	-650	-1050	-10604	-13681	1538
1500	-500	-900	-8462	-11538	1538
1200	-400	-650	-6538	-8462	962
900	-300	-450	-4780	-5934	577
600	-200	-300	-3187	-3956	385
300	-100	-100	-1429	-1429	0
0	-50	-75	-797	-989	96
0	0	100	330	1099	-385
0	50	100	879	1264	-192
0	0	-100	-330	-1099	385
0	-400	-250	-5220	-4066	-577
0	-250	-250	-3571	-3571	0
0	-225	-200	-3132	-2940	-96

STRAIN REDUCTION OF A TWO GAGE ROSETTE

E= 10.00 POISSONS RATIO= .30 GAGE NO.= 9=INSIDE

LOAD	EP1	EP2	SIGMA MAX	SIGMA MIN	TAU MAX
0	0	0	0	0	0
100	-50	75	-302	659	-481
200	-250	100	-2418	275	-1346
300	-200	200	-1538	1538	-1538
400	-275	50	-2857	-357	-1250
500	-400	100	-4066	-220	-1923
600	-500	150	-5000	0	-2500
700	-600	150	-6099	-330	-2885
800	-675	200	-6758	-27	-3365
900	-800	250	-7967	110	-4038
1000	-800	300	-7802	659	-4231
1100	-900	300	-8901	330	-4615
1200	-1000	300	-10000	0	-5000
1300	-1100	250	-11264	-879	-5192
1400	-1250	300	-12749	-824	-5962
1500	-1250	400	-12418	275	-6346
1600	-1250	425	-12335	549	-6442
1700	-1350	450	-13352	495	-6923
1800	-1450	400	-14615	-385	-7115
1800	-1400	500	-13736	879	-7308
1800	-1350	450	-13352	495	-6923
1800	-1300	425	-12885	385	-6635
1800	-1400	400	-14066	-220	-6923
1500	-1150	350	-11484	55	-5769
1200	-850	300	-8352	495	-4423
900	-650	250	-6319	604	-3462
600	-400	50	-4231	-769	-1731
300	-150	0	-1648	-495	-577
0	-50	-50	-714	-714	0
0	-100	0	-1099	-330	-385
0	-100	0	-1099	-330	-385
0	-50	-50	-714	-714	0
0	-50	0	-549	-165	-192
0	-100	0	-1099	-330	-385
0	-100	0	-1099	-330	-385

STRAIN REDUCTION OF A TWO GAGE ROSETTE

E= 10.00 POISSONS RATIO= .30 GAGE NO.= 10=INSIDE

LOAD	EP1	EP2	SIGMA MAX	SIGMA MIN	TAU MAX
0	0	0	0	0	0
100	-50	-150	-1044	-1813	385
200	-100	-200	-1758	-2527	385
300	-150	-300	-2637	-3791	577
400	-250	-400	-4066	-5220	577
500	-300	-450	-4780	-5934	577
600	-400	-550	-6209	-7363	577
700	-450	-650	-7088	-8626	769
800	-550	-775	-8599	-10330	865
900	-600	-850	-9396	-11319	962
1000	-650	-850	-9445	-11484	769
1100	-800	-950	-11923	-13077	577
1200	-850	-1050	-12802	-14341	769
1300	-950	-1200	-14396	-16319	962
1400	-950	-1300	-14725	-17418	1346
1500	-1000	-1300	-15275	-17582	1154
1600	-1050	-1350	-15989	-18297	1154
1700	-1100	-1450	-16868	-19560	1346
1800	-1200	-1600	-18462	-21538	1538
1800	-1200	-1550	-18297	-20989	1346
1800	-1200	-1400	-17802	-19341	769
1800	-1150	-1450	-17418	-19725	1154
1800	-1200	-1500	-18132	-20440	1154
1500	-950	-1250	-14560	-16868	1154
1200	-800	-1000	-12088	-13626	769
900	-550	-700	-8352	-9505	577
600	-300	-450	-4780	-5934	577
300	-100	-200	-1758	-2527	385
0	0	100	330	1099	-385
0	0	0	0	0	0
0	0	0	0	0	0
0	0	100	330	1099	-385
0	0	50	165	549	-192
0	0	50	165	549	-192
0	0	0	0	0	0

STRAIN REDUCTION OF A TWO GAGE ROSETTE

E= .40 POISSONS RATIO= .40 GAGE NO.= 1=OUTSIDE

LOAD	EP1	EP2	SIGMA MAX	SIGMA MIN	TAU MAX
0	0	0	0	0	0
500	-100	-1725	-376	-840	232
1000	-250	-4100	-900	-2000	550
1500	-400	-6700	-1467	-3267	900
2000	-450	-9350	-1995	-4538	1271
2500	-800	-12400	-2743	-6057	1657
3000	-900	-14950	-3276	-7290	2007
3500	-2025	-16675	-4140	-8326	2093
4000	-5450	-17100	-5852	-9181	1664

STRAIN REDUCTION OF A TWO GAGE ROSETTE

E= .40 POISSONS RATIO= .40 GAGE NO.= 2=OUTSIDE

LOAD	EP1	EP2	SIGMA MAX	SIGMA MIN	TAU MAX
0	0	0	0	0	0
500	-2000	-2250	-1381	-1452	36
1000	-4350	-4650	-2957	-3043	43
1500	-6600	-7150	-4505	-4662	79
2000	-9050	-9750	-6167	-6367	100
2500	-11850	-12600	-8043	-8257	107
3000	-14850	-15800	-10081	-10352	136
3500	-18300	-19450	-12419	-12748	164
4000	-23500	-24800	-15914	-16286	186

STRAIN REDUCTION OF A TWO GAGE ROSETTE

E= .40 POISSONS RATIO= .40 GAGE NO.= 2-INSIDE

LOAD	EP1	EP2	SIGMA MAX	SIGMA MIN	TAU MAX
0	0	0	0	0	0
500	-3200	-2700	-2038	-1895	-71
1000	-6500	-5500	-4143	-3857	-143
1500	-9400	-8650	-6362	-6005	-179
2000	-13600	-11750	-8714	-8186	-264
2500	-17800	-15400	-11410	-10724	-343
3000	-22000	-19200	-14133	-13333	-400
3500	-27450	-24300	-17700	-16800	-450
4000	-32500	-28900	-20981	-19952	-514

STRAIN REDUCTION OF A TWO GAGE ROSETTE

.40 POISSONS RATIO= .40 GAGE NO.= 3=OUTSIDE

LOAD	EP1	EP2	SIGMA MAX	SIGMA MIN	TAU MAX
0	0	0	0	0	0
500	-550	-3000	-833	-1533	350
1000	-1600	-5450	-1800	-2900	550
1500	-2300	-8150	-2648	-4319	836
2000	-2900	-10750	-3429	-5671	1121
2500	-3400	-13500	-4190	-7076	1443
3000	-3700	-16000	-4810	-8324	1757
3500	-4100	-17800	-5343	-9257	1957
4000	-4450	-18350	-5614	-9586	1986

STRAIN REDUCTION OF A TWO GAGE ROSETTE

E= .40 POISSONS RATIO= .40 GAGE NO.= 4=OUTSIDE

LOAD	EP1	EP2	SIGMA MAX	SIGMA MIN	TAU MAX
0	0	0	0	0	0
500	-2250	-2200	-1490	-1476	-7
1000	-4400	-4450	-2943	-2957	7
1500	-6800	-6800	-4533	-4533	0
2000	-9200	-9250	-6143	-6157	7
2500	-12250	-12100	-8138	-8096	-21
3000	-15400	-15100	-10210	-10124	-43
3500	-18250	-18400	-12195	-12238	21
4000	-21400	-24400	-14838	-15695	429

STRAIN REDUCTION OF A TWO GAGE ROSETTE

E= .40 POISSONS RATIO= .40 GAGE NO.= 4=INSIDE

LOAD	EP1	EP2	SIGMA MAX	SIGMA MIN	TAU MAX
0	0	0	0	0	0
500	-3125	-3400	-2136	-2214	39
1000	-6350	-7425	-4438	-4745	154
1500	-9850	-11750	-6929	-7471	271
2000	-13100	-16300	-9343	-10257	457
2500	-17000	-22100	-12305	-13762	729
3000	-21375	-27900	-15493	-17357	932
3500	-26600	-32200	-18800	-20400	800
4000	-31000	-37000	-21810	-23524	857

STRAIN REDUCTION OF A TWO GAGE ROSETTE

t= 10.00 POISSONS RATIO= .30 GAGE NO.= 5=OUTSIDE

LOAD	EP1	EP2	SIGMA MAX	SIGMA MIN	TAU MAX
0	0	0	0	0	0
500	-200	20	-2132	-440	-846
1000	-250	50	-2582	-275	-1154
1500	-400	125	-3984	55	-2019
2000	-500	175	-4918	275	-2596
2500	-600	200	-5934	220	-3077
3000	-700	225	-6951	165	-3558
3500	-900	300	-8901	330	-4615
4000	-1100	400	-10769	769	-5769

STRAIN REDUCTION OF A TWO GAGE ROSETTE

E= 10.00 POISSONS RATIO= .30 GAGE NO.= 5=INSIDE

LOAD	EP1	EP2	SIGMA MAX	SIGMA MIN	TAU MAX
0	0	0	0	0	0
500	-400	175	-3819	604	-2212
1000	-800	300	-7802	659	-4231
1500	-1275	150	-13516	-2555	-5481
2000	-1625	-100	-19187	-6456	-6868
2500	-2250	75	-24478	-6893	-8942
3000	-2425	325	-25577	-4423	-10577
3500	-2500	800	-24835	549	-12692
4000	-2550	775	-25467	110	-12788

STRAIN REDUCTION OF A TWO GAGE ROSETTE

E= 10.00 POISSONS RATIO= .30 GAGE NO.= 6=INSIDE

LOAD	EP1	EP2	SIGMA MAX	SIGMA MIN	TAU MAX
0	0	0	0	0	0
500	-375	-100	-4451	-2335	-1058
1000	-725	-350	-9121	-6236	-1442
1500	-1075	-550	-13626	-9588	-2019
2000	-1400	-725	-17775	-12582	-2596
2500	-1775	-900	-22473	-15742	-3365
3000	-2075	-1050	-26264	-18379	-3942
3500	-2325	-1175	-29423	-20577	-4423
4000	-2275	-1300	-29286	-21786	-3750

STRAIN REDUCTION OF A TWO GAGE ROSETTE

t= 10.00 POISSONS RATIO= .30 GAGE NO.= 7=OUTSIDE

LOAD	EP1	EP2	SIGMA MAX	SIGMA MIN	TAU MAX
0	0	0	0	0	0
500	-175	-75	-2170	-1401	-386
1000	-300	-100	-3626	-2088	-769
1500	-400	-175	-4973	-3242	-865
2000	-525	-225	-6511	-4203	-1154
2500	-625	-250	-7692	-4808	-1442
3000	-800	-300	-9780	-5934	-1923
3500	-1000	-425	-12390	-7967	-2212
4000	-1200	-550	-15000	-10000	-2500

STRAIN REDUCTION OF A TWO GAGE ROSETTE

10.00 POISSONS RATIO= .30 GAGE NO.= 7=INSIDE

LOAD	EP1	EP2	SIGMA MAX	SIGMA MIN	TAU MAX
0	0	0	0	0	0
500	-275	-50	-3187	-1456	-865
1000	-600	-125	-7005	-3358	-1827
1500	-875	-200	-10275	-5082	-2596
2000	-1150	-250	-13462	-6538	-3462
2500	-1400	-300	-16374	-7912	-4231
3000	-1625	-325	-18929	-8929	-5000
3500	-1800	-325	-20852	-9505	-5673
4000	-1750	-325	-20302	-9341	-5481

STRAIN REDUCTION OF A TWO GAGE ROSETTE

E= 10.00 POISSONS RATIO= .30 GAGE NO.= 8=OUTSIDE

LOAD	EP1	EP2	SIGMA MAX	SIGMA MIN	TAU MAX
0	0	0	0	0	0
500	-125	-150	-1868	-2060	96
1000	-225	-225	-3214	-3214	0
1500	-375	-350	-5275	-5082	-96
2000	-500	-450	-6978	-6593	-192
2500	-600	-550	-8407	-8022	-192
3000	-725	-700	-10275	-10082	-96
3500	-925	-900	-13132	-12940	-96
4000	-1200	-1200	-17143	-17143	0

STRAIN REDUCTION OF A TWO GAGE ROSETTE

E= 10.00 POISSONS RATIO= .30 GAGE NO.= 8=INSIDE

LOAD	EP1	EP2	SIGMA MAX	SIGMA MIN	TAU MAX
0	0	0	0	0	0
500	-300	-350	-4451	-4835	192
1000	-450	-750	-7418	-9725	1154
1500	-725	-1050	-11429	-13929	1250
2000	-900	-1300	-14176	-17253	1538
2500	-1225	-1900	-19725	-24918	2596
3000	-1425	-2100	-22582	-27775	2596
3500	-1900	-2600	-29451	-34835	2692
4000	-2000	-1500	-26923	-23077	-1923

STRAIN REDUCTION OF A TWO GAGE ROSETTE

F= 10.00 POISSONS RATIO= .30 GAGE NO.= 9=INSIDE

LOAD	EP1	EP2	SIGMA MAX	SIGMA MIN	TAU MAX
0	0	0	0	0	0
500	-325	100	-3242	27	-1635
1000	-800	200	-8132	-440	-3846
1500	-1200	325	-12115	-385	-5865
2000	-1600	500	-15934	220	-8077
2500	-1850	625	-18269	769	-9519
3000	-2075	725	-20412	1126	-10769
3500	-2075	700	-20495	852	-10673
4000	-2100	800	-20440	1868	-11154

STRAIN REDUCTION OF A TWO GAGE ROSETTE

E= 10.00 POISSONS RATIO= .30 GAGE NO.= 10-INSIDE

LOAD	EP1	EP2	SIGMA MAX	SIGMA MIN	TAU MAX
0	0	0	0	0	0
500	-300	-450	-4780	-5934	577
1000	-675	-900	-10385	-12115	865
1500	-1000	-1350	-15440	-18132	1346
2000	-1275	-1725	-19698	-23159	1731
2500	-1550	-2100	-23956	-28187	2115
3000	-1800	-2500	-28022	-33407	2692
3500	-1825	-2750	-29121	-36236	3558
4000	-1875	-3025	-30577	-39423	4423

NUC TP 505

SPHERICAL ACRYLIC PLASTIC HULLS UNDER EXTERNAL EXPLOSIVE LOADING

by

J. D. Stachiw

Ocean Technology Department

March 1976

NAVAL UNDERSEA CENTER, SAN DIEGO, CA. 92132

AN ACTIVITY OF THE NAVAL MATERIAL COMMAND

R. B. GILCHRIST, CAPT, USN
Commander

HOWARD L. BLOOD, PhD
Technical Director

ADMINISTRATIVE INFORMATION

This report describes research performed between June 1973 and June 1975 as part of the investigation into man-rated transparent submersibles. The program was funded under a Project Order from the Naval Material Command through the Independent Research and Independent Exploratory Development program at the Naval Undersea Center under Subproject Task Area Number ZF-61-412-001.

Released by

H. R. Talkington, Head,
Ocean Technology Department

ACKNOWLEDGEMENTS

The testing of model-size and full-size NEMO-type hulls was conducted at Southwest Research Institute. The experimental study owes its achievement to the administrative and moral support of H. R. Talkington, Head, NUC Ocean Technology Department, and Dr. Wm. B. McLean, retired NUC Technical Director.

UNCLASSIFIED

SECURITY CLASSIFICATION OF THIS PAGE (When Data Entered)

REPORT DOCUMENTATION PAGE		READ INSTRUCTIONS BEFORE COMPLETING FORM
1. REPORT NUMBER NUC TP 505	2. GOVT ACCESSION NO.	3. RECIPIENT'S CATALOG NUMBER
4. TITLE (and Subtitle) SPHERICAL ACRYLIC PLASTIC HULLS UNDER EXTERNAL EXPLOSIVE LOADING		5. TYPE OF REPORT & PERIOD COVERED Research Report June 1973 – June 1975 6. PERFORMING ORG. REPORT NUMBER
7. AUTHOR(s) J. D. Stachiw		8. CONTRACT OR GRANT NUMBER(s)
9. PERFORMING ORGANIZATION NAME AND ADDRESS Naval Undersea Center San Diego, California 92132		10. PROGRAM ELEMENT, PROJECT, TASK AREA & WORK UNIT NUMBERS ZF-61-412-001
11. CONTROLLING OFFICE NAME AND ADDRESS Naval Undersea Center San Diego, California 92132		12. REPORT DATE March 1976 13. NUMBER OF PAGES 78
14. MONITORING AGENCY NAME & ADDRESS(if different from Controlling Office)		15. SECURITY CLASS. (of this report) UNCLASSIFIED 15a. DECLASSIFICATION DOWNGRADING SCHEDULE

16. DISTRIBUTION STATEMENT (of this Report)

Approved for public release; distribution unlimited.

17. DISTRIBUTION STATEMENT (of the abstract entered in Block 20, if different from Report)

18. SUPPLEMENTARY NOTES

19. KEY WORDS (Continue on reverse side if necessary and identify by block number)

submersibles
transparent materials
underwater explosions

20. ABSTRACT (Continue on reverse side if necessary and identify by block number)

NEMO-type acrylic spherical hulls have been subjected to underwater explosions in order to determine their resistance to hydrodynamic impulse loading. Six 15-in.-OD and one 66-in.-OD spheres have been subjected to explosions of sufficient magnitude to initiate fracture in the hull. The tests were conducted at simulated depths of 10, 100, 1000, and 2000 ft with explosive charges of 1.1, 8.2, 14.6, 169.9, 387.8, and 688.6 grams.

DD FORM 1 JAN 73 1473 EDITION OF 1 NOV 65 IS OBSOLETE

UNCLASSIFIED

SECURITY CLASSIFICATION OF THIS PAGE (When Data Entered)

20. Continued.

The tests have shown that an acrylic sphere will fracture in the 0- to 50-ft depth range under dynamic peak overpressures that are smaller in magnitude than static pressures required for general implosion of the sphere. At the depth that is equal to 0.2 of static implosion pressure, the magnitude of dynamic peak overpressures must be in excess of the static implosion pressure before fracture of the acrylic sphere is initiated.

Fractures were generally initiated on the internal surface of the sphere at two locations; (a) at a point closest to the explosive and (b) at a point farthest from the explosive. The fractures were generally in the shape of a star.

SUMMARY

PROBLEM

Manned submersibles with spherical acrylic plastic hulls have been known since the NEMO hull was designed in 1961 to provide greater panoramic vision at lower cost and weight-to-displacement ratio than steel hulls (of the same shape, size, and depth capability) equipped with many small viewports. Several submersibles with NEMO-type hulls have been built since that time by the U. S. Navy. After more than 5 years of service, the acrylic hulls have been found to be virtually maintenance free and have shown no sign of weathering. There is, however one area of uncertainty that currently restricts the choice of missions for submersibles with acrylic hulls; it is not known how resistant the spherical acrylic hull is to hydrodynamic impulse loadings generated by explosive-actuated tools like cable cutters, stud guns, explosive anchors, corers, and others. If the resistance of NEMO-type hulls to underwater explosions were known, acrylic submersibles could be utilized in missions for which explosive tools are mandatory for meeting the mission objective.

RESULTS

An exploratory test program has shown that spherical hulls of acrylic plastic can withstand dynamic impulses of considerable magnitude before fracture of the hull is initiated. Increasing the depth of operations was found to increase significantly the resistance of the acrylic hull to fracture initiation by dynamic impulses. The NEMO Mod 2000 hull, with a 66-in. outside diameter and 4-in. shell thickness, has been found to withstand explosion-generated peak dynamic overpressure of 4,927 psi without initiation of fracture.

RECOMMENDATION

Manned submersibles with NEMO-type spherical hulls of acrylic plastic may be safely utilized in search, rescue, salvage, and work missions where explosive-actuated work tools are routinely utilized for achievement of mission objectives, provided that the peak dynamic overpressure impinging on the acrylic hull is less than 25 percent of static implosion pressure of the hull.

CONTENTS

INTRODUCTION

Underwater visibility is extremely important to crews of submersibles engaged in search, salvage, or work missions. Panoramic visibility can be provided in many ways, but large spherical acrylic plastic windows are considered to provide the most cost effective and reliable way of meeting this operational requirement (Ref. 1). An even better way is to use a transparent acrylic plastic hull of spherical shape (Ref. 2). Not only does it provide unlimited visibility in all directions, but it also generates a significant amount of buoyancy. Furthermore, such a hull is non-magnetic, provides unsurpassed thermal and sound insulation, and is virtually maintenance free. Because of its transparency, it can be inspected for incipient cracks visually by its crew at any time. This feature alone makes acrylic pressure hulls inherently safer than those fabricated from opaque materials that require expensive and time-consuming inspection procedures for detection of cracks.

The performance of spherical acrylic pressure hulls under short-term, long-term, and cyclic pressure loadings has been experimentally established over the years by U. S. Navy (Refs. 3-12) so that submersibles with spherical acrylic plastic hulls can be economically built and operated in the 0- to 3300-ft depth range. Several submersibles with acrylic plastic hulls have been already built and are operating in that depth range (Refs. 13, 14, 15). Their performance record is excellent, and acrylic plastic hulls that have been exposed to sun, seawater, and heat for 6 years still show no signs of deterioration.

In many undersea missions, the submersible may be exposed to explosions generated intentionally by, for example the firing of a stud gun or cable cutter during a typical underwater work sequence. During some missions, the submersible may be subjected to severe explosions unintentionally, e.g., during recovery or neutralization of underwater ordnance (Ref. 1). The effect of underwater explosions on submersible hulls made of steel is fairly well understood and the resistance to dynamic overpressures can be readily calculated. This is not the case with acrylic plastic pressure hulls or large spherical sector windows.

This report summarizes findings from the first exploratory study conducted by the U. S. Navy on the effect of underwater explosions on acrylic plastic spherical hulls of NEMO-type design and construction.

DESCRIPTION OF STUDY

The objective of the study was to provide operators of existing acrylic plastic submersibles (NEMO, Makakai, Johnson-Sea-Link I and Johnson-Sea-Link II) with operational guidelines for missions in which the submersible may be exposed to underwater explosions.

The approach selected for meeting the objective of the study was experimental in nature. It was felt that the experimental approach was, in this case, more direct, more reliable, and less expensive than an analytical approach, which would, subsequently, have to be experimentally validated before it could be used with confidence by operators of submersibles.

The scope of the study was limited to spherical hulls of NEMO design and construction with 1000 and 3000 ft maximum operational depths. Only two sizes of hulls were to be tested: the 66-in.-OD full-size and the 15-in.-OD scale-size spheres. The NEMO-type design uses a sphere with two penetrations located at opposite poles of the sphere; each penetration is closed with a metallic closure equipped with a conical seating surface. In NEMO-type construction, the sphere is assembled from 12 spherical-sector pentagons bonded together with self-polymerizing acrylic cement.

EXPERIMENTAL DESIGN

TEST SPECIMENS

Two NEMO capsules, one 66-in.-OD full-size and six 15-in.-OD scale-size, served as test specimens (Figs. 1 and 2). Both NEMO Mod 600 with 1000-ft operational depth and NEMO Mod 2000 with 3000-ft operational depth were utilized (Table 1 and Appendix A). Both the full-size and scale-size NEMO capsules have been exposed previously to cyclic fatigue testing and thus can be considered to be equivalent to submersibles with several years of field service (Ref. 11).

All specimens were fabricated from Plexiglas G, whose physical properties met the U. S. Navy and ASME requirements. The spherical hulls were assembled in every case from thermoformed spherical pentagons that were bonded together with either PS-18 or PS-30 self-polymerizing adhesive. The scale-size hulls had polar inserts machined either from stainless steel or titanium (Figs. 3–6), while the full-size hull utilized aluminum, both for top hatch and bottom penetration plate (Fig. 7).

TEST ARRANGEMENT

Scale-Size NEMO Capsules

The testing of scale-size models took place in a 30-in.-ID pressure vessel, 20 ft long, located at the Southwest Research Institute. The test specimen was placed in a test jig that held it approximately 120 in. below the end closure and 120 in. above the bottom closure (Fig. 8). To prevent point contact between the test specimen and the steel test jig, the specimen was wrapped in a wire net that, in turn, was fastened to the three longitudinal members of the test jig.

The explosive was suspended above the test specimen by means of two horizontal wires stretched between the longitudinal members of the test jig. It was centered directly above the center of the test specimen, with the standoff being defined as the distance between the center of explosive and the outer surface of the test specimen facing the charge (Fig. 9).

The instrumentation consisted solely of two tourmaline piezoelectric transducers for measurement of dynamic overpressures. The transducers were positioned adjacent to the model and were the same distance from the explosive charge as was the outer surface of the model. Transducer response was transmitted through differential amplifiers and displayed on a dual-beam oscilloscope, where it was photographed. It was considered advantageous to

use two transducer systems so that the validity of pulse characteristics could be ascertained by noting the similarity in response of the two independent monitoring systems.

The output of the piezoelectric transducers was displayed on an oscilloscope and recorded photographically by a Polaroid camera. The oscilloscope was triggered by a small breakwire wrapped around the charge. The breaking of the wire by the explosion generated a pulse which energized the oscilloscope for a single sweep. In initial tests, a time-delay pulse generator was not available, so the sweep speed of the oscilloscope had to be such that transducer response to shock overpressure was appropriately displayed during the single sweep. In later tests, by using a delayed trigger pulse, it was possible to eliminate the initial straight-line portion of the display and obtain greater detail of shock-pulse characteristics.

Full-Size NEMO Capsules

Testing of the full-size NEMO Mod 2000 capsule took place in a 12-ft-diameter, 100-ft-deep, water-filled well located on the premises of Southwest Research Institute (Fig. 10). The test specimen was securely wrapped with Nylon webbing and suspended within a steel cage by means of steel cables (Fig. 11). The cage itself was kept suspended at 50 ft depth by means of a cable attached to a large mobile crane.

For the first three shots, the explosive (Fig. 12) was held above the test specimen. For the subsequent two tests it was placed below the test specimen. Changing the location of the explosive was made necessary by the generation of large downward force upon the crane by pressure waves radiating from explosive held above the specimen. When the explosive was placed below the specimen, the pressure wave would tend to decrease the load on the crane, rather than increase it.

Instrumentation consisted of two electric resistance strain gages and two pressure-sensitive transducers. The strain gages were mounted on the interior of the hull midway between the polar inserts and directly below the explosive.

The pressure transducers, PCB Model 113A23 acceleration-compensated ultra-rigid quartz element pressure probes with built-in amplifiers, were positioned the same distance from the explosive charge as the apex of the test specimen (Fig. 13). Pressure gage outputs were displayed on a Tektronix Model 454 split-beam oscilloscope, and strain gage outputs were displayed on a Tektronix Model 502 dual-beam oscilloscope. Both scopes were set to trigger in a single sweep mode, with the trace being recorded on Polaroid film. A small-diameter breakwire, wrapped around the charge, broke when the charge detonated, thereby creating a voltage change and triggering the oscilloscopes; the scope sweeps were delayed by a time slightly less than the time required for an acoustic pulse in water to travel the distance between the charge and the apex of the model.

TEST PROCEDURE

Scale-Size NEMO Capsules

Each of the scale-size NEMO capsules were tested individually. Since the objective of the testing program for scale-size capsules was to determine the effect of the depth and capsule shell thickness on the resistance of capsules to damage caused by dynamic overpressure, some of the test parameters, like sizes of explosive charges and standoff distances, were

kept constant. The sizes of charges chosen were 1.1, 8.2 and 14.6 grams. Standoff distances were set at 48, 36, 24 and 12 in.

The procedure (Tables 2 and 3) followed during testing of any given test specimen was to start with the smallest charge (1.1 grams) placed at the longest standoff distance (48 in.). If no damage to the test specimen was observed, an identical charge would be placed at the next shorter standoff distance (36 in.). The standoff distances chosen for each shot were progressively shorter until the shortest standoff (12 in.) was reached.

If the smallest charge did not initiate failure of the test specimen at the shortest standoff distance, the next larger charge (8.2 grams) would be placed at the longest standoff. The larger charges would be set off following the test procedure already described for the smallest charge. If the larger charge did not initiate cracks at the shortest standoff, the series of tests would be repeated again, utilizing, however, the largest charge (14.6 grams).

The 15-in.-OD by 14-in.-ID scale-size NEMO test specimens were tested at simulated depths of 10, 100, or 1000 ft. The 10-ft depth represented the typical surface cruising depth of a submersible, while 1000 ft represented maximum operational depth of NEMO capsules with $t/R_o = 0.067$ ratio.

The 15-in.-OD by 13-in.-ID scale-size NEMO test specimens were tested at depths of 10, 100, or 2000 ft. Here again, 10 ft represented the typical surface cruising depth, while 1000 and 2000 ft represented depths of typical deep submergence operational missions.

Full-Size NEMO Capsules

The test procedure for full-size capsules (Table 4) differed from the test procedure used for scale-size capsules. While for scale-size capsules both the size of the charge and the standoff distance were experimental variables, for the full-size capsule only the charge size was varied, while the standoff was held constant at 52.8 in. This standoff distance was determined by multiplying the shortest standoff distance of 12 in. by 66/15, the ratio representing the relationship between the size of the full-size NEMO and that of the scale-size NEMO.

The charge weights used against the full-size NEMO capsule were 1.1, 5.6, 14.5, 169.9, 387.8, and 688.6 grams. The first three charges were of the same weight as those used in the explosive testing of scale-size NEMO capsules. They were used primarily to calibrate pressure transducers and strain gage readout equipment. The last three charges were scaled-up versions of charges previously used against scale-model NEMOs. Thus, the 169.9-gram charge is the scaled-up version of the 1.1-gram charge, the 387.8-gram charge is the scaled-up version of 4.6-gram charge, and the 688.6-gram charge is the scaled-up version of 8.25-gram charge. The scaled-up charges were supposed to generate the same peak overpressures on the full-scale NEMO from a $0.8R_o$ standoff as were generated previously on the scale-size NEMO capsules from a $0.8r_o$ standoff by 1.1-, 4.6-, and 8.2-gram charges.*

*R_o – *external radius of the full-size NEMO*

r_o – *external radius of the scale-size NEMO*

TEST OBSERVATIONS

Scale-Size NEMO Capsules

The testing of the scale-size NEMO capsules was very destructive to the 30-in. pressure vessel in which the testing was conducted. Seals in the vessel end closures as well as hydraulic piping were repeatedly damaged. Because of it, seals and hydraulic fittings had to be replaced every second or third shot.

Pressure transducers were also damaged repeatedly. After several days of testing, the project ran out of transducers, and further shots were conducted without any instrumentation. Thus, for some of the shots during which the capsules failed, both the peak overpressure and the impulse intensity had to be calculated. There is, however, a very high confidence in the calculated values, since it was found that during the shots in which instrumentation functioned, the correlation between calculated and experimental values was quite good (Figs. 14, 15, 16, and 17).

Failure of model-size NEMO capsules was manifested by formation of either tensile- or flexure-type cracks. As a rule, the flexure cracks were present on the interior surface of the equator directly facing the charge, on the opposite side, or on both sides, while the tensile cracks extended radially from the edges of penetrations. If the underwater explosion was severe, there would be several long flexure-type cracks joined together in a form of a star, very similar in appearance to the pattern of cracks observed in spherical sector windows under point impact loading (Ref. 16). Severe explosions would also generate tensile meridional cracks at the penetrations.

Light damage was observed on test specimens J and 26 (Figs. 18 and 19). In both cases, there were only one or two small flexure cracks at the equator, no leakage of water took place and the capsule was considered to have withstood the explosion without endangering its potential cargo. These capsules could have completed their mission successfully.

Medium severe damage was noted on test specimens M and 24 (Figs. 20 and 21). In both cases, there were several short flexure cracks present at the equator and at least one long tensile crack at the penetration. Only a few drops of water leaked into the interiors of the capsules, but not in sufficient quantity to endanger the potential cargo. Still, the missions of the capsules would have to be terminated immediately to avoid endangering the crew.

Very severe damage was observed on test specimens K and 25 (Figs. 22 and 23). In both cases, a large star-shaped flexure crack at the equator and several tensile cracks radiating from penetrations were produced. Because of the many cracks, water leaked into the interiors of these two capsules. There would have been severe jeopardy for any cargo. It is very probable that capsules in such condition could not return from their missions since they would fill with water prior to reaching the mother ship.

Full-Size NEMO Capsule

The full-size NEMO capsule withstood all the explosions without initiation of cracks in the acrylic plastic. However, during the last three shots, the capsule was torn loose from its fastenings. On the last shot, the capsule broke free of its 0.25-in. steel cable netting and

rose rapidly to the surface of the well shaft, where it struck a protruding steel beam. The point impact broke off a large chip from the capsule surface, thus terminating any further tests on this capsule (Fig. 24).

Dynamic strains measured on the interior of the capsule facing the 387.8-gram charge indicated considerable tension immediately followed by compression of approximately the same magnitude (Fig. 25). Still, the strains were not of such magnitude as to suggest failure during the following 688.6-gm shot.

Dynamic pressure readings were obtained only with the initial two small charges (Figs. 26 and 27). No experimental pressure readings were obtained with the following four larger charges because the breaking loose of the capsule destroyed, in every case, the pressure pickups and associated wiring. However, such a good correlation was obtained between the experimental and calculated peak overpressure values during the initial shots that peak overpressures for the last three shots could be calculated with confidence.

DISCUSSION OF TEST RESULTS

Although the data generated during the testing program are far from complete, several definite relationships between the force of explosion and capsule's resistance to failure can be formulated.

EFFECT OF SHELL THICKNESS

It appears that the resistance to fracture of acrylic plastic spheres subjected to underwater explosions is directly related to shell thickness, provided that the method of construction and outside radius remain the same. This postulate is based on the observation that to initiate cracking in 1-in.-thick scale-size NEMO capsules required a unit impulse and peak dynamic overpressure twice as large as those required to produce similar results in 0.5-in.-thick capsules. Both tests were conducted at the same depth. For example, test specimen No. 26 with a 0.5-in.-thick wall failed at 1000 ft under 0.1 psi.-sec unit impulse and 2816 psi peak dynamic overpressure, while test specimen No. K with 1.0-in.-thick wall required 0.206 psi-sec unit impulse and 6176 psi peak dynamic overpressure to initiate cracking at the same depth. A similar relationship can be seen, although less clearly, between specimen No. 25 and No. M.

EFFECT OF DEPTH

The data show quite clearly that the resistance to fracture of acrylic plastic spheres subjected to underwater explosions increases significantly with depth. This conclusion is based on the observation that it required a 3 to 5 times larger peak overpressure and unit impulse to fracture an identical test specimen at 1000 ft depth than it did at 10 ft. For example, test specimen No. M failed at 10 ft depth under 0.045 psi-sec unit impulse, and 1434 psi peak dynamic overpressure, while test specimen No. K at 1000 ft depth required 0.206 psi-sec unit impulse and 6176 psi peak dynamic overpressure to generate a fracture. Similar relationship can be seen between specimen No. 25 and No. 26.

EFFECT OF SCALING

There are insufficient experimental data to establish the validity of using scale-size models for determining the resistance of full-size NEMO capsules to underwater explosions. The few data points generated during the study seem to indicate, however, that extrapolating data from scale-size models is on the conservative side and, thus, acceptable. This conclusion is based on the observation that the full-size NEMO capsule did not crack when subjected to peak dynamic overpressure of 4927 psi generated by a 688.56-gm charge with $0.8R_o$ standoff, while the same peak dynamic overpressure generated by a scaled-down charge of 8.2 gm with $0.8\ r_o$ standoff would, without a doubt, have cracked the 15-in.-OD by 13-in.-ID scale-size NEMO capsule.

EFFECT OF MOUNTING

During the testing of model-size capsules, there was no problem with retaining the capsules inside the test jig to which they were mounted. The mounting, which consisted of chicken wire mesh wrapped around the capsule and fastened securely with wires to the jig frame, was substantial and capable of withstanding the thrust exerted upon the capsule by dynamic pressure. This was not the case with the full-size NEMO capsule. Although the nylon netting was substantial, and the net was fastened to the frame with 0.25-in. steel cables, the thrust exerted by dynamic pressure upon the 66-in.-diameter capsule was much higher than what the cables could withstand. As a result, the capsule was torn loose from its mounting during the firing of shots No. 4, 5, and 6. (Table 4)

The beneficial effect of depth on the resistance of pressure hulls to dynamic overpressure has been previously observed in other brittle materials besides acrylic plastic, materials whose tensile strength is significantly less than their compressive strength, e.g., glass, ceramics, and concrete. The beneficial effect of depth derives its action from the compressive membrane prestressing imposed on the hull by the static external pressure loading. The compressive prestress must be overcome by the tensile flexure stress generated by the underwater explosion before the brittle material can fail in tension on the interior surface of the hull.

Needless to say, imposing compressive prestress on the hull by static external pressure has its limits for all brittle materials. The limit for the beneficial depth effect is reached when the material in the pressure hull begins to fail during dynamic pressure loading in compression rather than in tension. This happens when the *sum of the dynamic compressive stress* (equal in magnitude to, and following immediately after, the tensile flexure stress phase) *and static compressive stress* exceeds either the yield or ultimate compressive strength (depending on which one is the smaller value) of the brittle material.

For acrylic plastic hulls designed to fail by general plastic instability, the maximum allowable depth for static precompression purposes is approximately 25 to 30 percent of their short-term critical pressure (based on compressive strains generated in the hull after 8 hours of sustained loading at maximum operational depth). Since the maximum operational depth of acrylic hulls is, as a rule, set at 25 to 30 percent of their short-term critical pressure, the beneficial depth effect is active through the whole depth range of operations for acrylic submersibles.

The breaking loose of the full-size NEMO from its mounting as a result of underwater explosion points up to a very serious practical problem for a submersible containing a NEMO capsule. It appears that unless the NEMO capsule is restrained in some very ingenious manner, the primary damage to the acrylic capsule will be caused either by impact against the framework of the submersible after the capsule has broken loose from a weak mounting, or by excessive dynamic stresses generated by very strong, but rigid mounting. Since the NEMO capsules are generally attached to the submersible framework by their metallic end closures, it is highly probable that when subjected to a severe underwater explosion, the capsule will crack around the penetrations because of unacceptably high bearing stresses. For this reason, it is desirable that the capsule also be supported at other locations by large elastomeric pads that would tend to distribute and absorb some of the capsule's thrust caused by impulse loading.

FINDINGS

1. Acrylic plastic spherical pressure hulls will fracture when exposed to underwater explosions whose peak dynamic overpressure may be less than the static critical pressure of the hull.

2. Underwater explosions generate cracks primarily on the interior surface of the sphere at locations directly facing and opposite the charge.

3. Cracks on the interior surface of the sphere indicate localized external dynamic pressure loading, very similar to a mechanical point-impact loading (Ref. 16).

4. Dynamic strains measured on the interior shell surface facing the charge alternate rapidly from tension to compression.

5. Increasing the thickness of the acrylic plastic sphere also increases its resistance to underwater explosions; doubling the thickness appears to double the unit impulse and peak dynamic overpressure required for crack initiation.

6. Increasing the depth of operation also increases the resistance of the acrylic plastic sphere to underwater explosions; increasing the depth by 1000 feet appears to at least triple the unit impulse and peak dynamic overpressure required for crack initiation.

7. Mountings for acrylic plastic spheres tend to fail sooner than the spheres themselves when subjected to underwater explosions.

CONCLUSIONS

Submersibles with NEMO-type acrylic plastic spherical hulls can successfully withstand underwater explosions of considerable magnitude. Increasing the depth of operation significantly increases the resistance of spherical acrylic plastic hull to underwater explosions.

RECOMMENDATIONS

Operational

Submersibles with spherical acrylic plastic pressure hulls should not be exposed to underwater explosions of such magnitude that cracks will be initiated in the hull, or the whole hull torn away from its mounting in the submersible structure. This means that (a) the explosive charges in cable cutters or stud drivers carried routinely by an acrylic plastic submersible should not exceed a certain size if the tools are to be activated in the immediate vicinity of the submersible, and (b) the submersible should not be involved in search missions for unexploded underwater ordnance whose warhead exceeds a critical size for given underwater visibility (i.e., good visibility allows discovery of an unexploded item of ordnance without getting close to it, while poor visibility requires the submersible to be almost in physical contact with the item of ordnance before it is recognized as such).

The maximum sizes of permissible explosive charges for work tools or devices carried routinely by a work submersible have been calculated (Ref. 19) on the basis of the largest charge used in the testing program against full-size NEMO Mod 2000 at 50 ft depth that did no damage to the hull or its mounting (Shot No. 3 of Table 4). Charges *equal to, or less than* those shown in Fig. 28 can be used repeatedly in performance of work missions in the 10- to 3000-ft depth range by a submersible equipped with NEMO Mod 2000 (Ref. 11) or 2000B *hull* (Ref. 12) ($t/R_o \geq 0.121$).

The minimum safe standoff distance for missions involving search and/or disposal of underwater ordnance have been calculated (Ref. 19) on the basis of the largest charge used in the testing program against full-size NEMO Mod 2000 at 50 ft depth that did no damage to the hull but considerable damage to the capsule mounting (Shot No. 6 of Table 4). Standoff distances *equal to or larger* than those shown in Fig. 29 must be maintained between the submersible with NEMO Mod 2000 or 2000B hull and the unexploded underwater ordnance in the 50- to 3000-ft depth range if fracture of the acrylic hull due to explosion is to be avoided. The standoff distances shown in Fig. 29 are very conservative for depths in excess of 1000 ft.

It is understood, however, that unless a mounting is provided that is capable of restraining the NEMO Mod 2000 hull against a thrust of at least 10^6 lb, the hull may be torn loose from its mounting when subjected to the explosions and standoff distances shown in Fig. 29.

Design

Typical mountings for work submersibles with NEMO Mod 2000 or 2000B acrylic hulls are generally configured (Fig. 30) to withstand forces generated only by vertical buoyancy or dead weight and horizontal hydrodynamic drag of the sphere. The magnitudes of these forces are low, approximately 3000 lb vertical static force and 1000 lb horizontal drag. Since, however, the submersible is also subjected to dynamic forces during docking and retrieval, a well-designed mounting will, as a minimum, restrain an acrylic hull against 100,000 lb of downward thrust, 100,000 lb horizontal thrust, and 10,000 lb vertical pull (for some types of mountings the vertical pull is also about 100,000 lb).

Unfortunately, even well-designed mountings for typical work missions do not provide adequate restraint against severe underwater explosions at the standoffs plotted in Fig. 29. To withstand the thrust of severe explosions, the mountings must be designed with this specific objective in mind. Unfortunately, proven mounting designs do not exist at the present time for submersibles with acrylic spheres routinely engaged in missions in which severe underwater explosions may be encountered. A conceptual design for such service has been prepared, however, and is shown in Fig. 31.

Although Figs. 28 and 29 have been developed specifically for NEMO Mod 2000 and 2000B acrylic plastic hulls, they are also applicable to other acrylic spheres with $t/R_o \geqslant 0.12$. There is sufficient structural similarity between spheres and spherical sectors with included angle $\alpha \geqslant 120^\circ$ to make Figs. 28 and 29 applicable also to spherical acrylic plastic sector bow windows in submersibles. Some experimental data exist which confirm this belief.

REFERENCES

1. Naval Civil Engineering Laboratory, Technical Report R-631, Windows for External or Internal Hydrostatic Pressure Vessels; Part 3. Critical Pressure of Acrylic Spherical Shell Windows Under Short-Term Pressure Application, by J. D. Stachiw, F. W. Brier, June 1969 (AD 689789).

2. American Society of Mechanical Engineers, Paper No. 65-WA/UNT-10, "The Design, Fabrication and Testing of Acrylic Pressure Hulls For Manned Vehicles", by J. G. Moldenhauer, J. D. Stachiw, K. Tsuji, November, 1965.

3. Naval Civil Engineering Laboratory, Technical Report R-676, Development of a Spherical Acrylic Plastic Pressure Hull for Hydrospace Application, by J. D. Stachiw, April 1970 (AD 707363).

4. Naval Civil Engineering Laboratory, Technical Note N-1113, The Spherical Acrylic Pressure Hull for Hydrospace Application; Part 2. Experimental Stress Evaluation of Prototype NEMO Capsule, by J. D. Stachiw, K. L. Mack, October 1970 (AD 715772).

5. Naval Civil Engineering Laboratory, Technical Note N-1094, The Spherical Acrylic Pressure Hull for Hydrospace Application; Part 3. Comparison of Experimental and Analytical Stress Evaluations for Prototype NEMO Capsule, by H. Ottsen, March 1970 (AD 709914).

6. Naval Civil Engineering Laboratory, Technical Note N-1134, The Spherical Acrylic Pressure Hull for Hydrospace Application; Part 4. Cyclic Fatigue of NEMO Capsule #3, by J. D. Stachiw, October 1970 (AD 715345).

7. American Society of Mechanical Engineers, Paper No. 70-WA/UnT-6, "The JOHNSON SEA-LINK – The First Deep Diving Welded Aluminum Submersible," by R. A. Kelsey and R. B. Dolan, December 1970.

8. Naval Undersea Center, NUC TP 315, Acrylic Plastic Hemispherical shells for NUC Undersea Elevator, by J. D. Stachiw, September 1972 (AD 749029).

9. Naval Undersea Center, NUC TP 383, Cast Acrylic Dome for Undersea Applications, by J. D. Stachiw, January 1974.

10. Naval Undersea Center, NUC TP 410, Development of a Precision Casting Process for Acrylic Plastic Spherical Shell Windows Applicable to High-Pressure Service, by J. D. Stachiw, May 1974.

11. Naval Undersea Center, NUC TP 451, NEMO Mod 2000 Acrylic Plastic Spherical Hull for Manned Submersible Operation At Depths to 3000 ft, by J. D. Stachiw, December 1974.

12. Naval Undersea Center, NUC TP 493, Development of Economical Casting Process for NEMO Type Acrylic Pressure Hulls, by J. D. Stachiw, December 1975.

13. Naval Civil Engineering Laboratory, Technical Report R-749, NEMO, A New Concept in Submersibles, P. K. Rockwell, R. E. Elliott, M. R. Snoey, November 1971 (AD 735103).

14. American Society of Mechanical Engineers, Paper No. 72-WA/OCT-8, "Transparent Hull Submersible MAKAKAI," by D. W. Murphy and W. F. Mazzone, December 1972.

15. American Society of Mechanical Engineers, Paper No. 71-WA/UnT-6, "Acrylic Pressure Hull for JOHNSON SEA-LINK Submersible," by J. R. Maison and J. D. Stachiw, December 1971.

16. Naval Undersea Center, NUC TP 486, Acrylic Plastic Spherical Shell Windows Under Point Impact Loading, by J. D. Stachiw and O. Burnside, July 1975.

17. Naval Undersea Center, NUC TP 393, Glass or Ceramic Spherical Shell Window Assembly for 20,000 psi Operational Pressure, by J. D. Stachiw, May 1974.

18. Naval Undersea Center, NUC TP 355, Flanged Acrylic Plastic Hemispherical Shells for Undersea Systems, by J. D. Stachiw, August 1973 (AD 769213).

19. R. H. Cole, *Underwater Explosions*, Dover Publications, Inc., New York, 1965.

TABLE 1. ACRYLIC PLASTIC SPHERES SERVING AS TEST SPECIMENS

	Outside Diameter, in.	Inside Diameter, in.	Top		Bottom		Short-term static critical pressure,* psi
			Penetration minor diameter (included angle)	Inserts	Penetration minor diameter (included angle)	Inserts	
Model 24	15	14	4.793 in. 40°	316 stainless steel hatch no gasket	4.793 in. 40°	316 stainless steel hatch no gasket	1,650
Model 25	15	14	5.150 in. 43°	316 stainless steel hatch polycarbonate gasket	5.150 in. 43°	acrylic plastic spherical sector no gasket	1,650
Model 26	15	14	5.150 in. 43°	acrylic plastic spherical sector no gasket	no penetration	no hatch no gasket	1,650
Model J	15	13	5.285 in. 48°	6A14V titanium hatch polycarbonate gasket	4.445 in. 40°	6A14V titanium hatch no gasket	4,750
Model K	15	13	5.285 in. 48°	6A14V titanium hatch polycarbonate gasket	4.445 in. 40°	6A14V titanium hatch no gasket	4,750

*Based on experimental data from previous studies (Refs. 3, 11).

TABLE 1. ACRYLIC PLASTIC SPHERES SERVING AS TEST SPECIMENS (Continued)

	Outside Diameter, in.	Inside Diameter, in.	Top		Bottom		Short-term static critical pressure,* psi
			Penetration minor diameter (included angle)	Inserts	Penetration minor diameter (included angle)	Inserts	
Model M	15	13	5.285 in. 48°	6A14V titanium hatch polycarbonate gasket	4.445 in. 40°	6A14V titanium hatch no gasket	4,750
Model NEMO MOD 2000	66	57.9	23.822 in. 48° 30′	6061-T6 aluminum hatch polycarbonate gasket	21.727 in. 44°	6061-T6 aluminum penetration plate polycarbonate gasket	4,750

**Based on experimental data from previous studies (Refs. 3, 11).*

TABLE 2. RESISTANCE OF 15-in.-O.D. BY 14-in.-I.D. NEMO SCALE MODELS TO DYNAMIC PRESSURE IMPULSES

Size of Charge, grams	Model 25 10 ft Depth	Model 24 100 ft Depth	Model 26 1000 ft Depth
	Standoff, in.		
1.1	48	48	48
	36	36	36
	24	24	24
	12	12	12
8.2	48.†	48	48
	1035. psi peak overpressure	36	36
	0.033 psi-sec unit impulse	24 **	24
	Severe cracking of hull at equator facing and opposite charge; also severe radial cracks around the penetrations (Fig. 23)	2250. psi peak overpressure 0.067 psi-sec unit impulse	
		Minor meridional cracks near penetrations facing and opposite charge. (Fig. 21)	
14.6			48
			36
			24 *
			2816 psi peak overpressure 0.1 psi-sec unit impulse
			Small crack on equator opposite charge. (Fig. 19)

Notes:
- *The standoff is measured between the tip of the charge and the surface of the NEMO model.*
- *Explosive used is cast explosive composed of 50% PETN and 50% TNT.*
- *Failure is indicated by presence of cracks.*
- *Shock wave parameters are calculated values.*

*Denotes light damage.
**Denotes medium severe damage.
†Denotes very severe damage.

TABLE 3. RESISTANCE OF 15-in.-O.D. BY 13-in.-I.D. NEMO SCALE MODELS TO DYNAMIC PRESSURE IMPULSES

Size of Charge, grams	Model M 10 ft Depth	Model K 1000 ft Depth	Model J 2000 ft Depth
	Standoff, in.		
1.1	48	48	48
	36	36	36
	24	24	24
	12	12	12
8.2	48	48	48
	36 **	36	36
	1434 psi peak overpressure	24	24
	0.045 psi-sec unit impulse		
	Cracks on equator facing charge; also radial crack at the penetration. (Fig. 20)		
14.6		48	48
		36	36
		24	24
		12 †	12 *
		6170. psi peak overpressure	6170 psi peak overpressure
		0.208 psi-sec unit impulse	0.208 psi-sec unit
		Star shaped cracks on equator facing charge; also radial crack at penetration. (Fig. 22)	Small incipient cracks on equator facing and opposite the charge. (Fig. 18)

Notes:
- *The standoff is measured between the tip of the charge and the surface of the NEMO model.*
- *Explosive used is cast explosive composed of 50% PETN and 50% TNT.*
- *Failure is indicated by presence of cracks.*
- *Shockwave parameters are calculated values.*

**denotes light damage; **denotes medium severe damage, †denotes very severe damage*

TABLE 4. RESISTANCE OF 66-in.-O.D. BY 57.90-in.-I.D. FULL-SIZE NEMO MOD 2000 TO DYNAMIC PRESSURE IMPULSES

Shot No.	Size of Charge, grams	Standoff, in.	Peak Overpressure, psi	Unit Impulse psi-sec	Comments
1	1.10*	52.9	435	0.0074	No damage
2	5.62*	52.9	805	0.0228	No damage
3	14.50*	52.9	1,150	0.0436	No damage
4	169.87*	52.9	2,906	0.2347	No damage; capsule broke loose from test jig.
5	387.77**	52.9	3,967	0.412	No damage, capsule broke loose from test jig.
6	688.56**	52.9	4,927	0.611	No damage, capsule broke loose from test jig.

Notes:
- *The standoff is measured between the tip of the charge and the surface of the NEMO capsule.*
- *Explosive used is cast explosive composed of 50% PETN and 50% TNT.*
- *Damage is indicated by presence of cracks.*
- *Shock wave parameters are calculated values.*
- *All tests were conducted at 50 ft depth.*

**Explosive located above the capsule.*
***Explosive located below the capsule.*

Figure 1. Scale-size NEMO-type hulls tested to destruction under dynamic impulse loading.

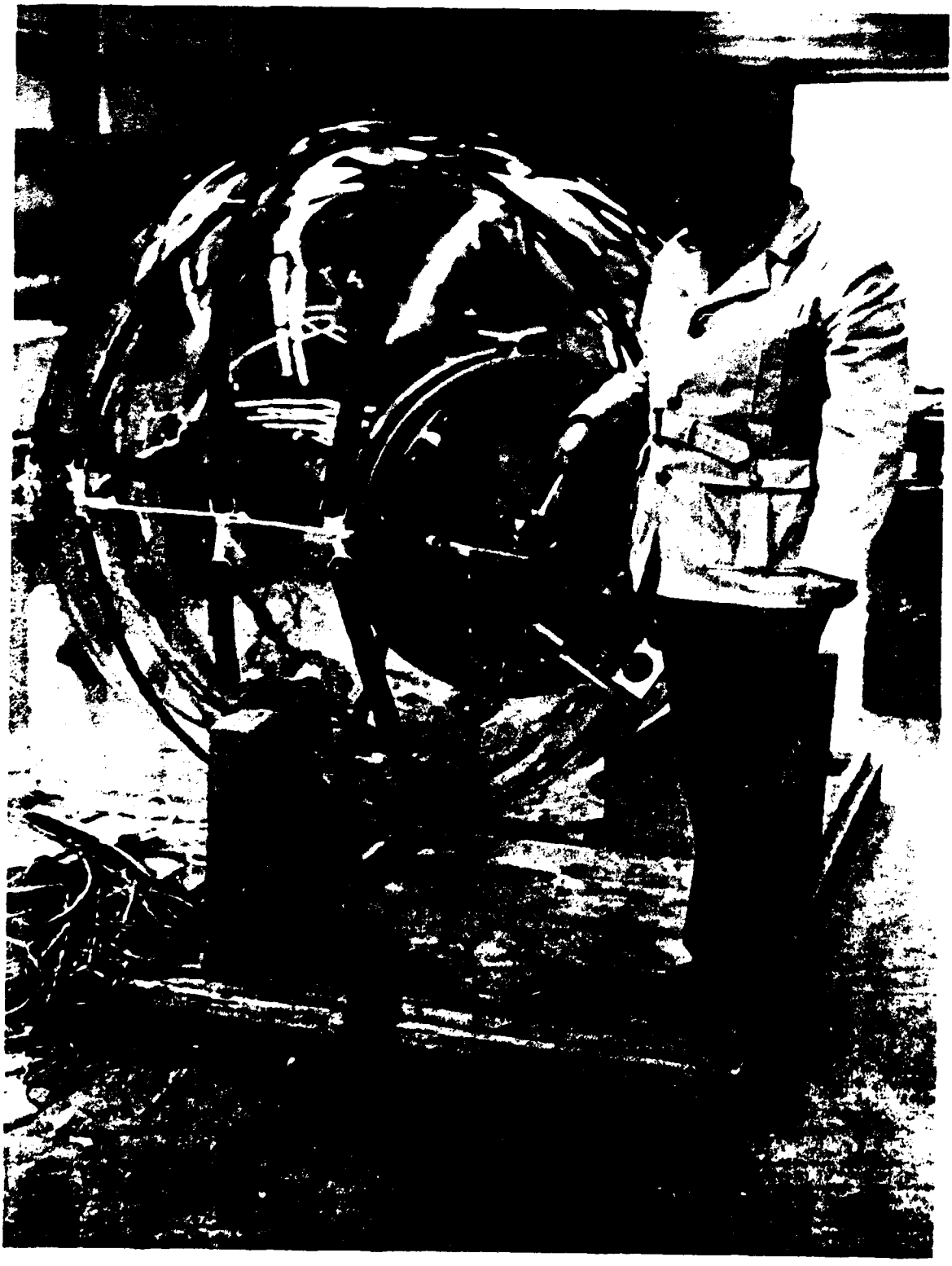

Figure 2. Full-size NEMO Mod 2000 hull tested to destruction under dynamic impulse loading.

APPLICATION				REVISIONS		
NEXT ASSY	USED ON	ZONE	LTR	DESCRIPTION	DATE	APPROVED

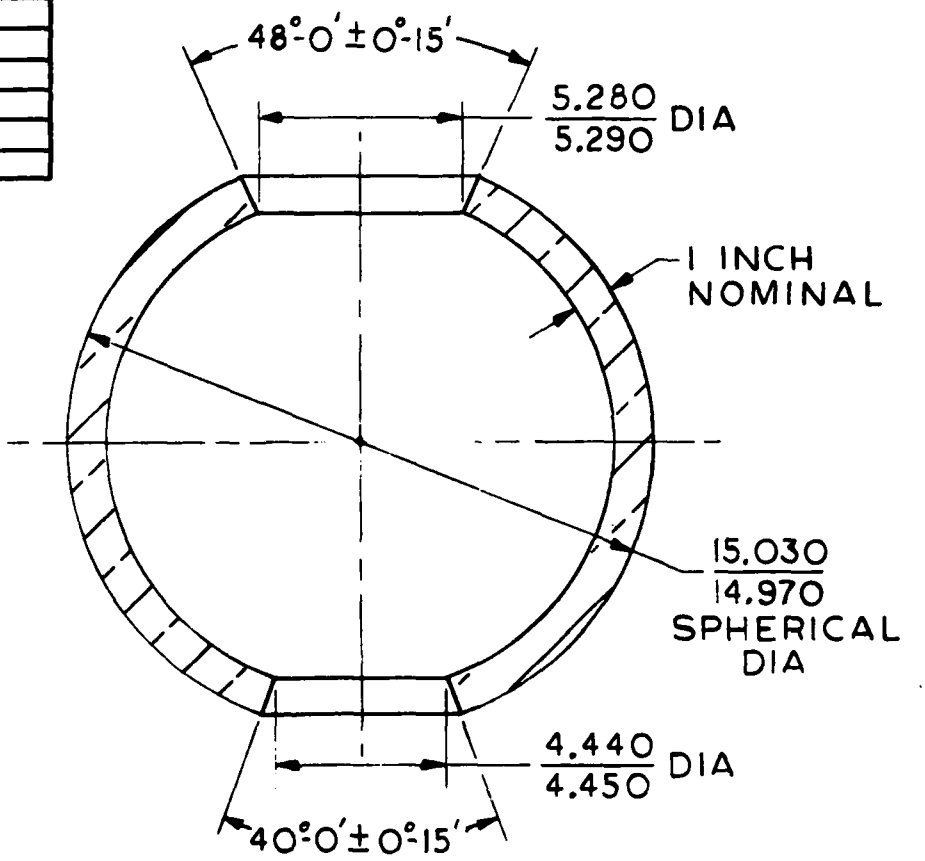

℄ SECTION

NOTES:
1. MATERIAL: PLEXIGLAS G, 1.0 INCH PLATE
2. ADHESIVE: PS-30
3. INSERTS: TOP OPENING - TYPE B TITANIUM HATCH WITH POLYCARBONATE GASKET
BOTTOM OPENING - TYPE A TITANIUM HATCH WITHOUT GASKET

UNLESS OTHERWISE SPECIFIED DIMENSIONS ARE IN INCHES TOLERANCES ANGLES : FRACTIONS : DECIMALS : PART SHALL BE FREE OF BURRS BROKEN EDGES MAX FILLETS MAX SURFACE ROUGHNESS ✓ DO NOT SCALE THIS DRAWING INTERPRET DRAWING IN ACCORDANCE WITH MIL-D-1000	NAVAL UNDERSEA CENTER SAN DIE J. CALIF. 92132 10-25-74 APPROVED FOR 197 BY DIRECTION	DEPARTMENT OF THE NAVY WASHINGTON, D.C. 20360 NEMO MOD 2000 ACRYLIC HULL 15 INCH NEMO SCALE MODELS #35, #36, & #37 SIZE A · CODE IDENT 30879 · DWG NO. SK6514-A-0139 SCALE NONE · WT. · SHEET 1 OF 1

11ND-NUC-3910/2A-(2) (11-72)

Figure 3. Typical dimensions of 15-in. OD by 13-in. ID scale-size NEMO-type hulls.

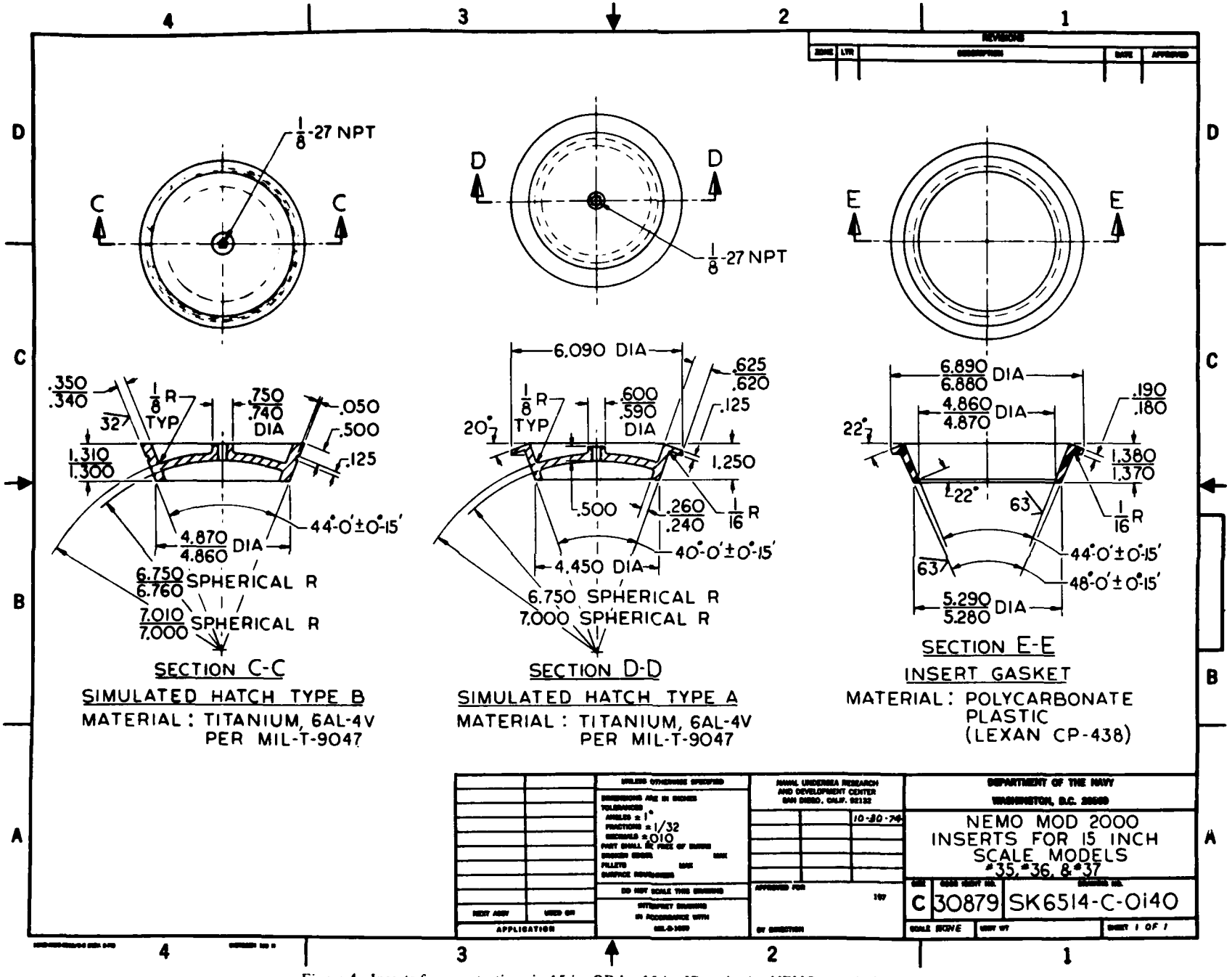

Figure 4. Inserts for penetrations in 15-in.-OD by 13-in.-ID scale-size NEMO-type hulls.

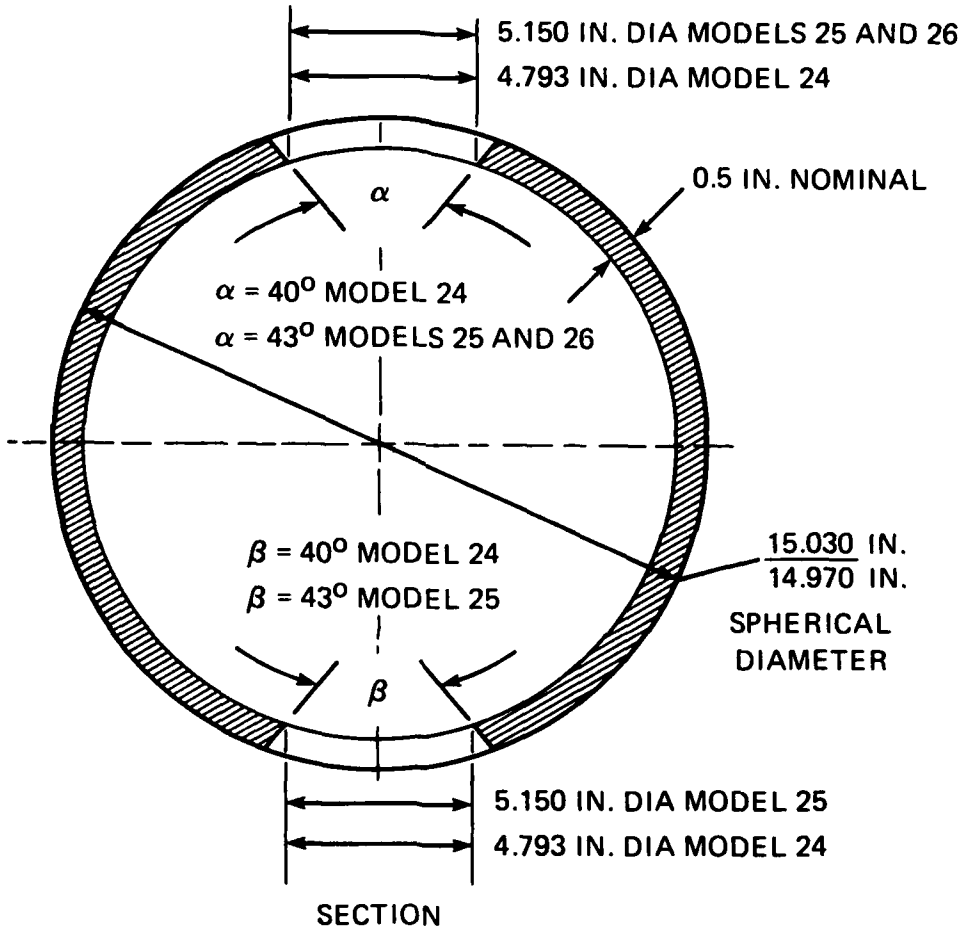

NOTES:

1. MATERIAL: PLEXIGLAS G, 0.5 IN. PLATE
2. ADHESIVE: PS-18

Figure 5. Typical dimensions of 15-in.-OD by 14-in.-ID scale-size NEMO-type hulls.

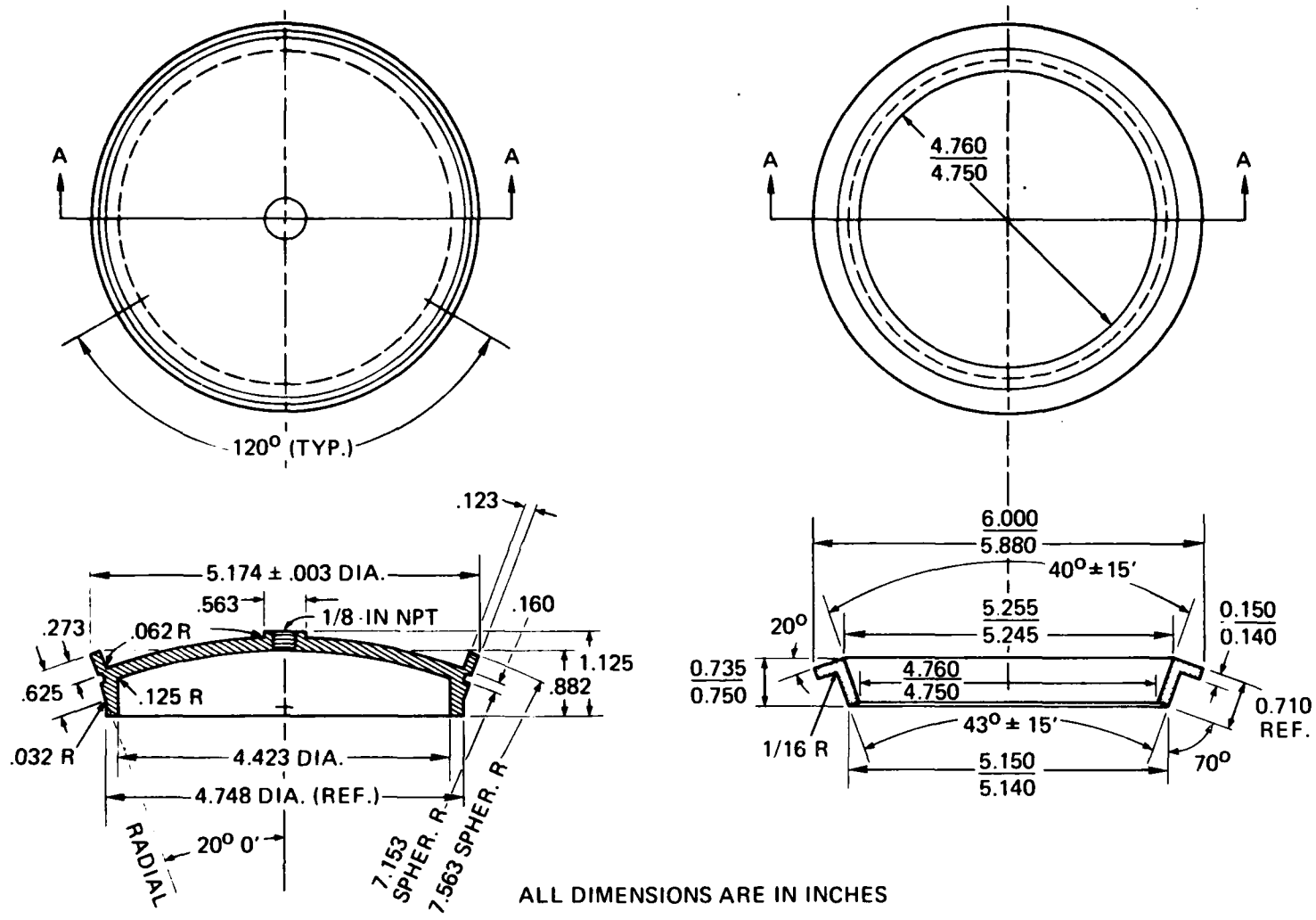

ALL DIMENSIONS ARE IN INCHES

SECTION A–A

SIMULATED HATCH – TYPE C
MATERIAL: 316 STAINLESS STEEL

SECTION A–A

INSERT GASKET
MATERIAL: POLYCARBONATE PLASTIC

Figure 6. Inserts for penetrations in 15-in.-OD by 14-in.-ID scale-size NEMO-type hulls.

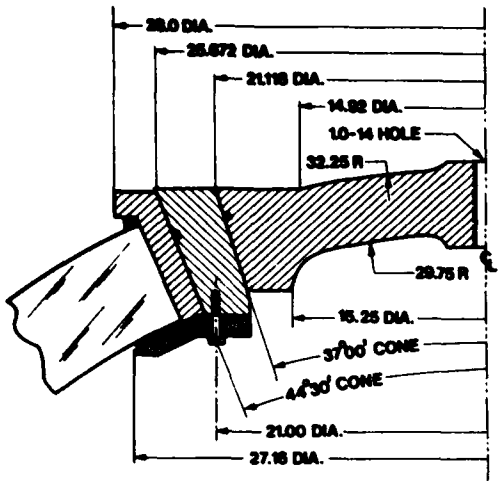

TOP HATCH DETAIL

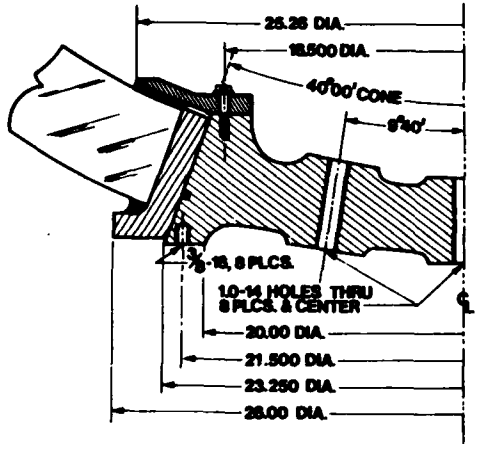

BOTTOM PLATE DETAIL

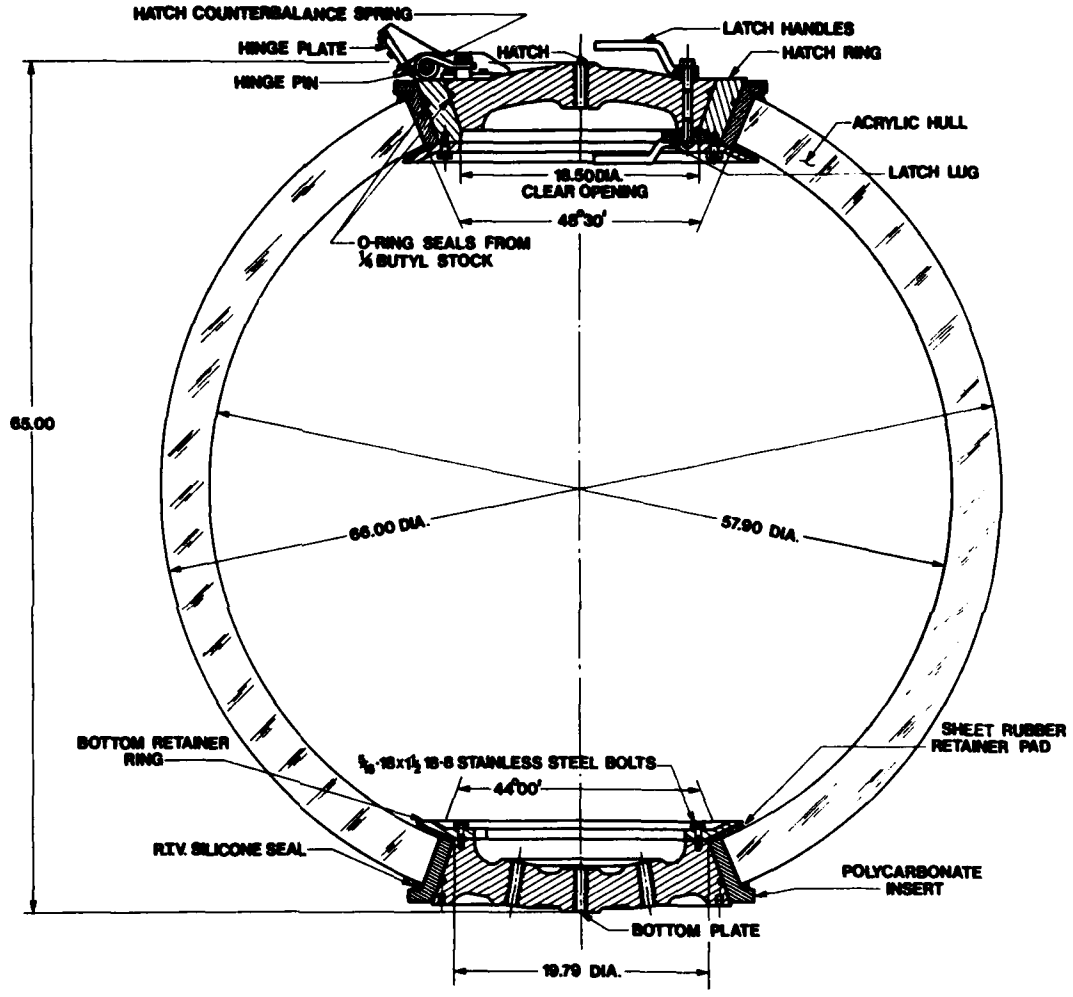

NAVAL UNDERSEA CENTER **ACRYLIC PLASTIC SUBMERSIBLE HULL** **NEMO MODEL 2000** material: plexiglas G acrylic construction: bonded spherical pentagons	weight: 2500 lbs displacement: 5600 lbs cyclic fatigue life: in excess of 1000 dives of 4 hr duration to 3000 ft	operational depth: 3000 ft proof test depth: 3600 ft implosion depth: 10,500 ft positive buoyancy: 3100 lbs weight/displacement: 0.44

Figure 7. Dimensions of 66-in.-OD by 57.9-in.-ID full-size NEMO Mod 2000 capsule.

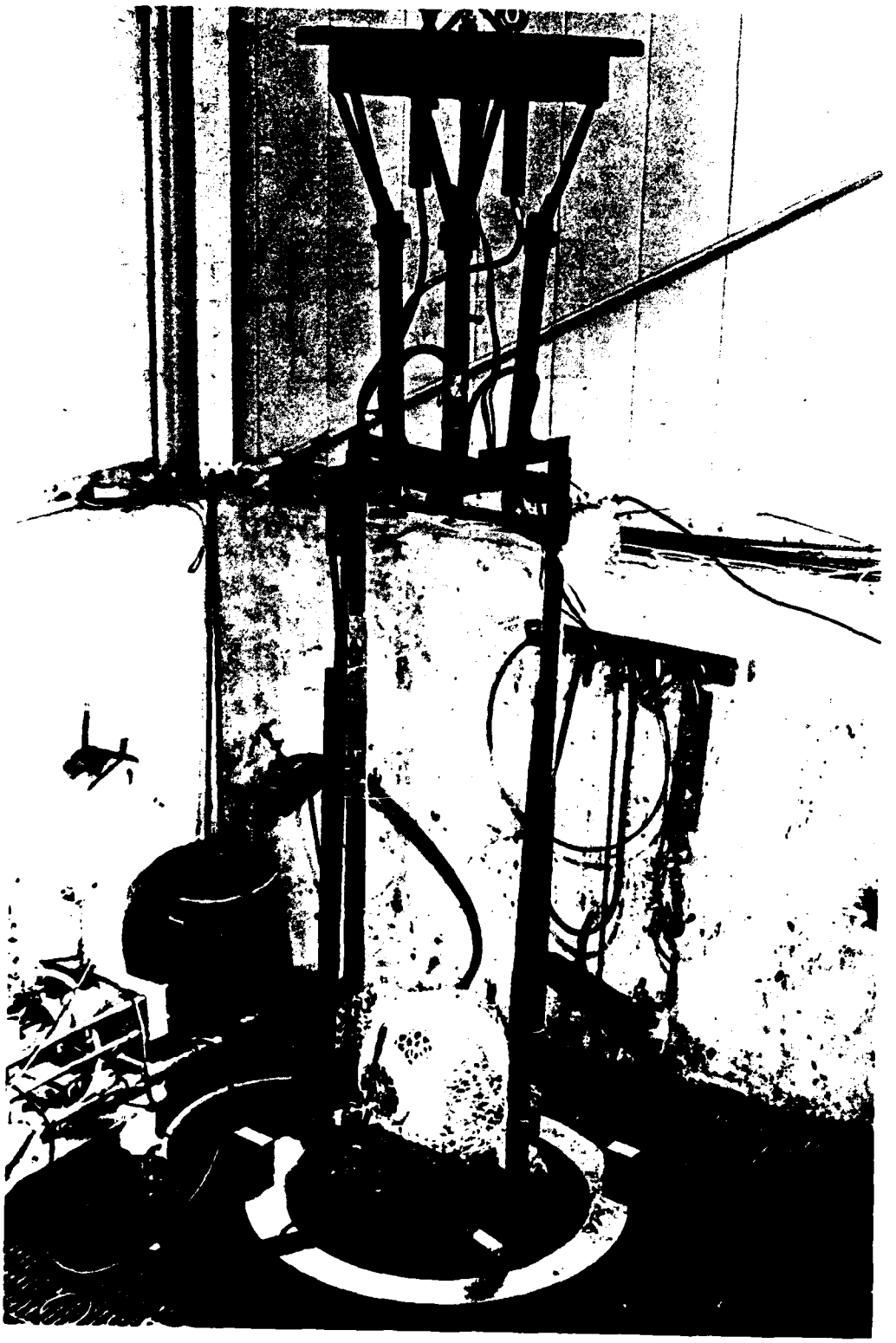

Figure 8. Test jig for holding the scale-size acrylic capsules in the pressure vessel during detonation of explosive.

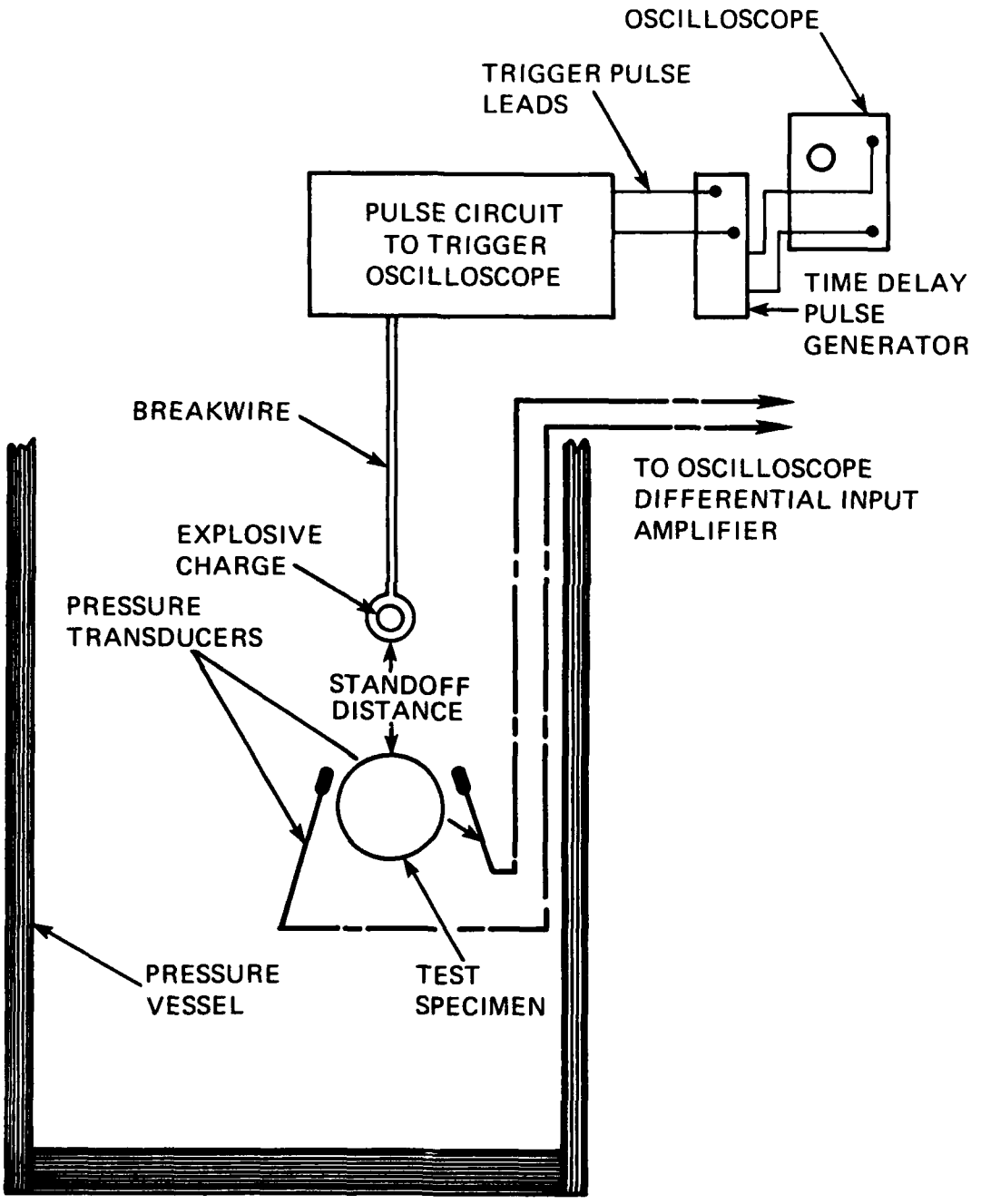

Figure 9. Schematic of instrumentation used for measurement of peak pressures impinging on the acrylic capsules.

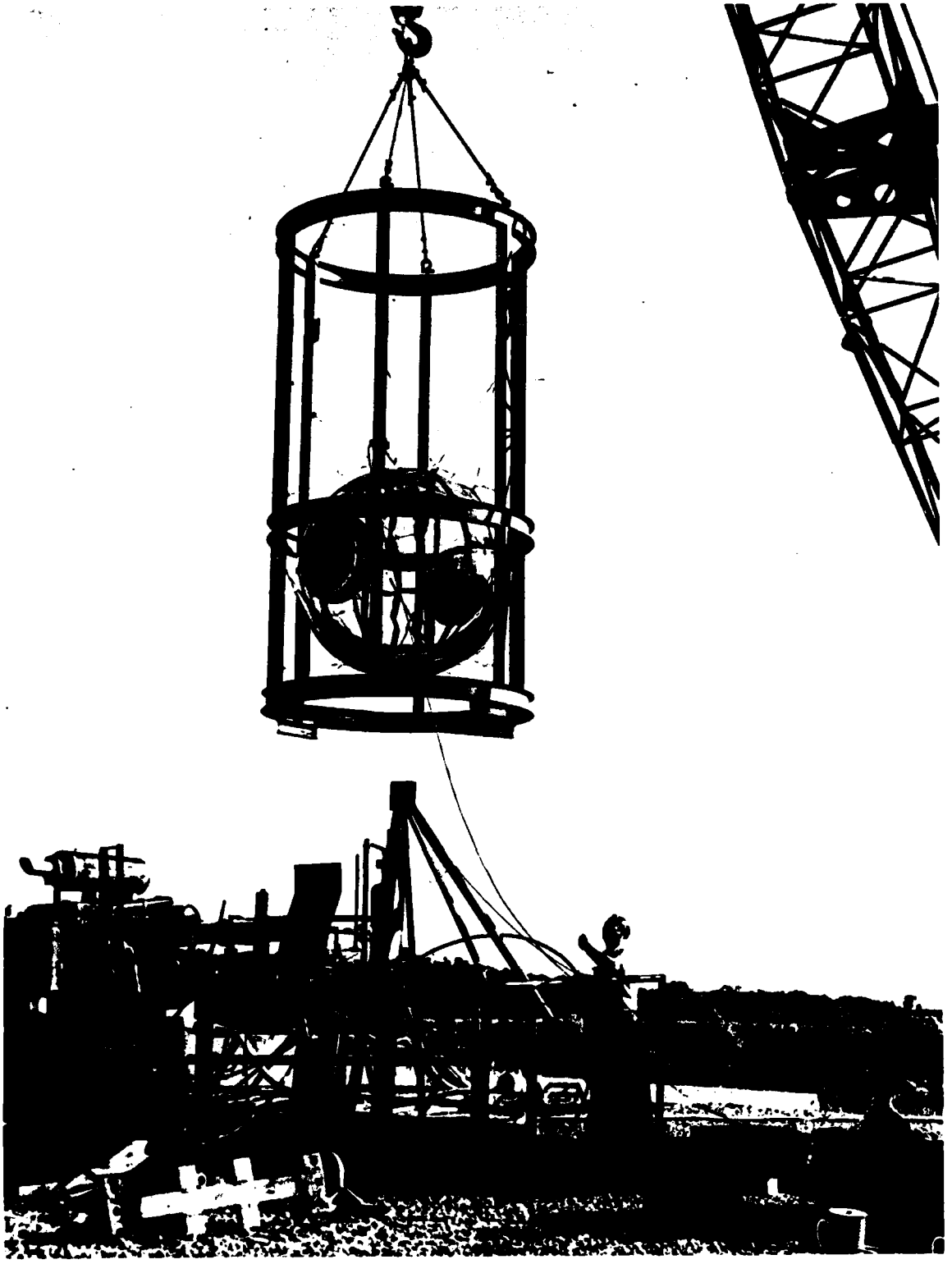

Figure 10. Test jig for holding the full-size NEMO Mod 2000 capsule in the well during detonation of explosive.

Figure 11. Mounting of the NEMO Mod 2000 capsule inside the test jig.

Figure 12. Typical size and shape of explosive charge used against full-size NEMO Mod 2000 capsule.

Figure 13. Closeup of pressure transducer used in tests with the full-size NEMO Mod 2000 capsule.

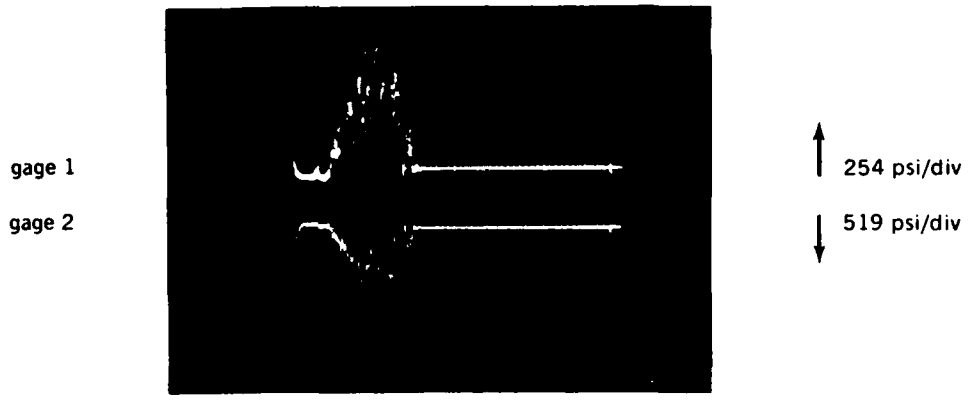

Model: 25 NEMO (15" X 14")

Charge: 8.2 grams

Standoff: 48 inches

Hydrostatic Pressure: 10 psi

	Gage 1	Gage 2	Calculated
Peak Shock Overpressure, psi	1,020	1,035	1,035
Unit Impulse, psi-sec	0.175	0.18	.0325
Duration, μsec	1,350	1,350	—

Note — Model failed.

Figure 14. Peak pressure measured at the scale-size capsule No. 25 during the explosion that fractured the capsule.

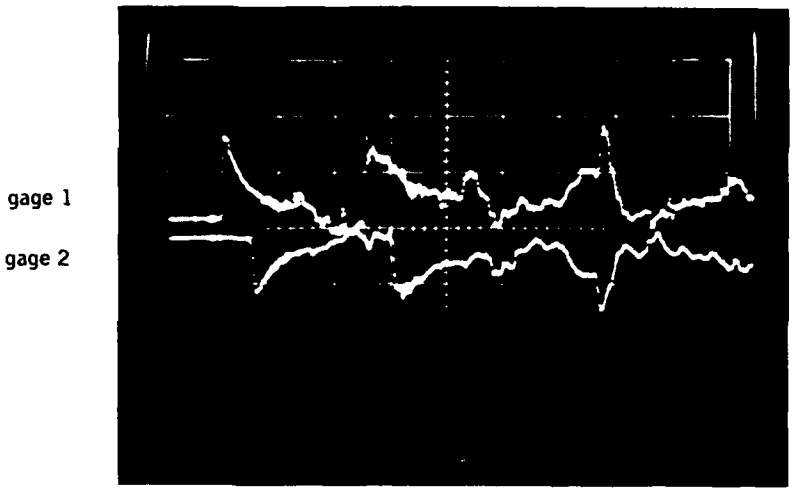

Model: NEMO 26 (15" X 14")

Charge: 14.6 grams

Standoff: 24" (gage 1), 26" (gage 2), 24" (model)

Hydrostatic Pressure: 450 psi

			Calculated	
	Gage 1	Gage 2	Gage 1	Gage 2
Peak Shock Overpressure, psi	2,820	2,250	2,810	2,580
Unit Impulse, psi-sec	.111	.0654	.101	.094
Duration, μsec	80	75	—	—

Note — Model failed. Gage 2 was farther from model and charge than gage 1 and gives a lower than anticipated value.

Figure 15. Peak pressure measured at the scale-size capsule No. 26 during the explosion that fractured the capsule

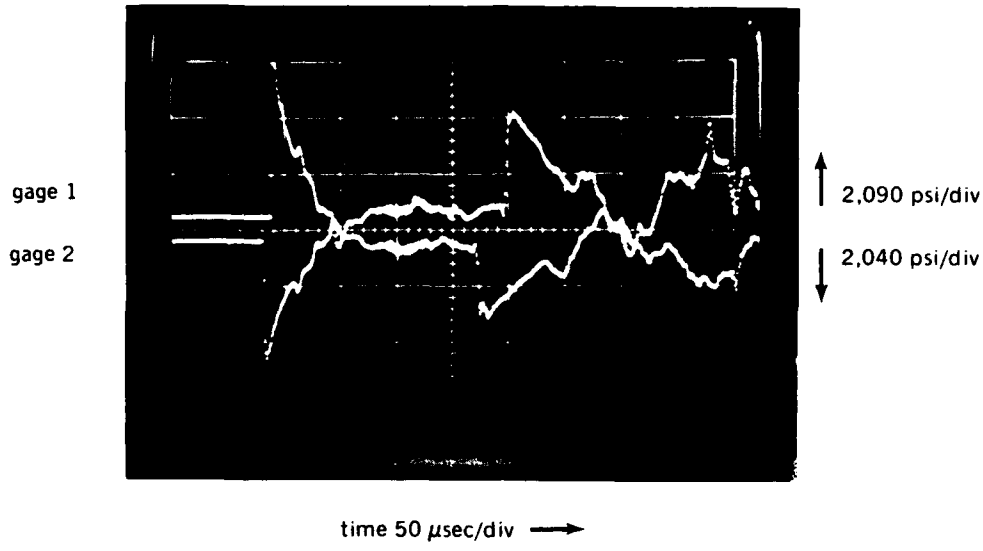

Model: NEMO J (15" X 13")

Charge: 14.6 grams

Standoff: 13" (gage 1), 12" (gage 2), 12" (model)

Hydrostatic Pressure: 1,000 psi

			Calculated	
	Gage 1	Gage 2	Gage 1	Gage 2
Peak Shock Overpressure, psi	5,660	4,480	5,660	6,200
Unit Impulse, psi-sec	.1276	.1108	.194	.215
Duration, μsec	50	47.5	—	—

Note — Model failed. Gage 2 gives lower than anticipated value.

Figure 16. Peak pressure measured at the scale-size capsule No. J during the explosion that fractured the capsule.

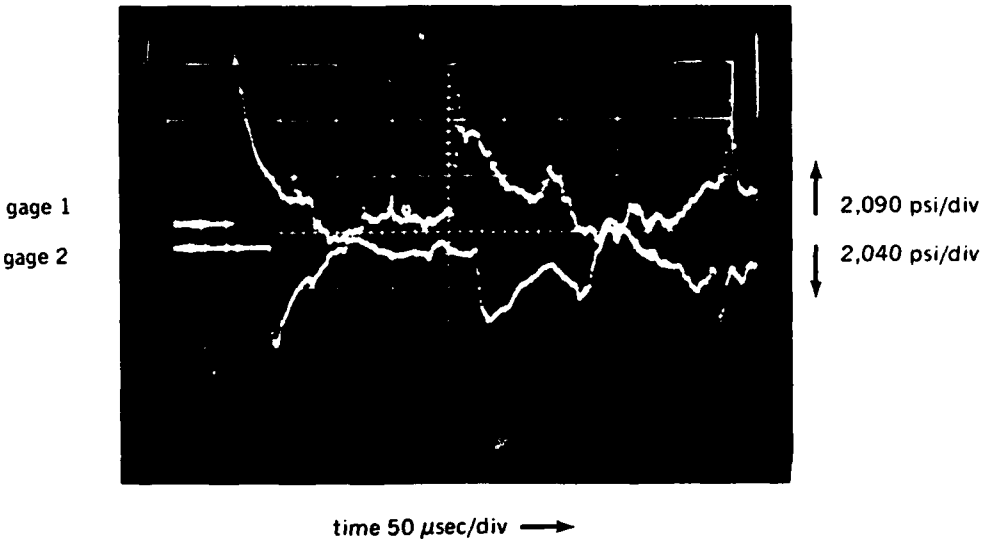

Model: NEMO K (15" X 13")

Charge: 14.6 grams

Standoff: 12" (gage 1), 13" (gage 2), 12" (model)

Hydrostatic Pressure: 450 psi

			Calculated	
	Gage 1	Gage 2	Gage 1	Gage 2
Peak Shock Overpressure, psi	6,280	4,080	6,200	5,660
Unit Impulse, psi-sec	.1856	.085	.215	.194
Duration, μsec	75	50	—	—

Note — Model failed. Gage 2 reads lower than anticipated.

Figure 17. Peak pressure measured at the scale-size capsule No. K during the explosion that fractured the capsule.

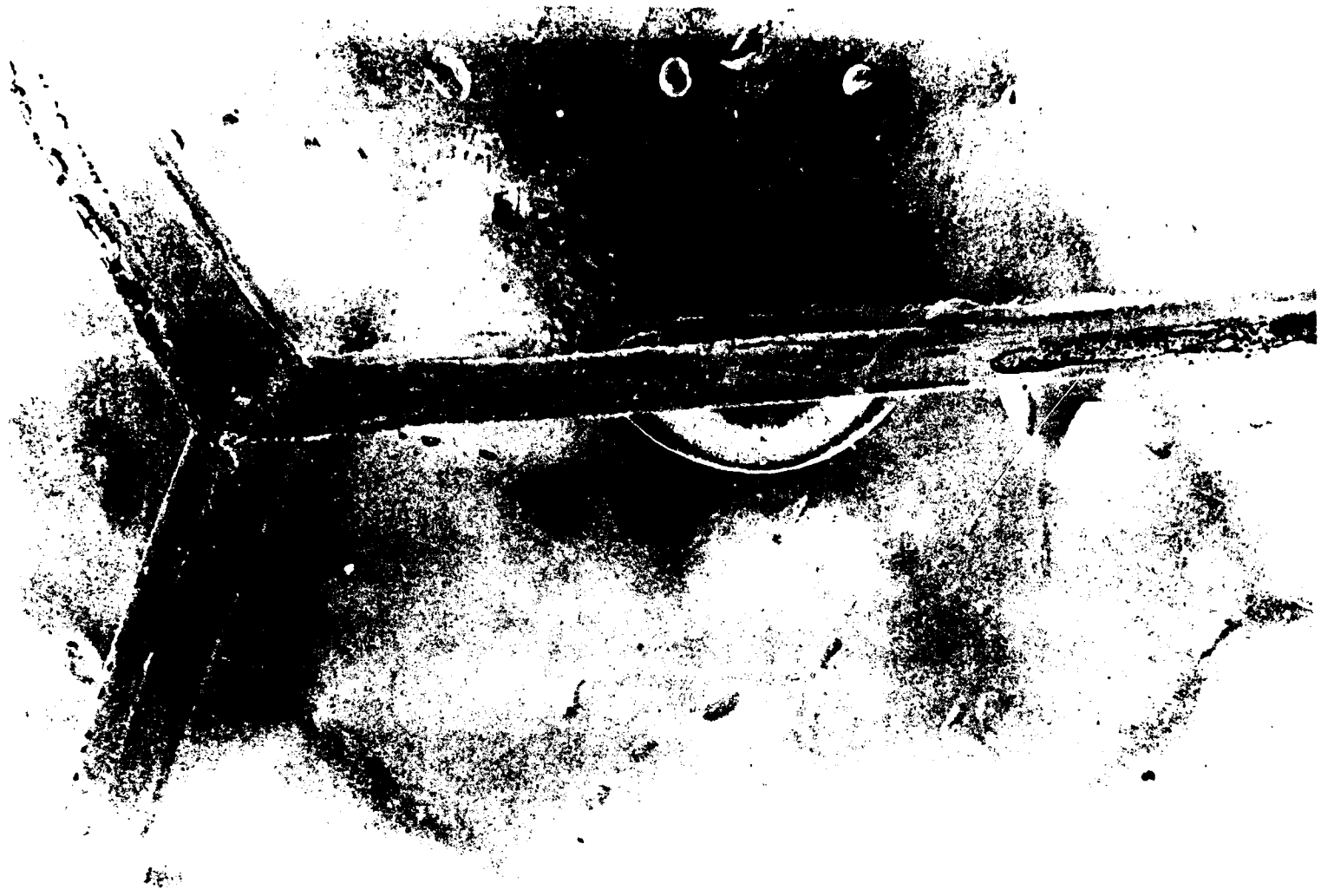

Figure 18. Fractures in capsule No. J after being subjected (at 2000-ft depth) to a 14.6-gram charge at 12 in. standoff: (a) crack is facing the explosive. (Sheet 1 of 2)

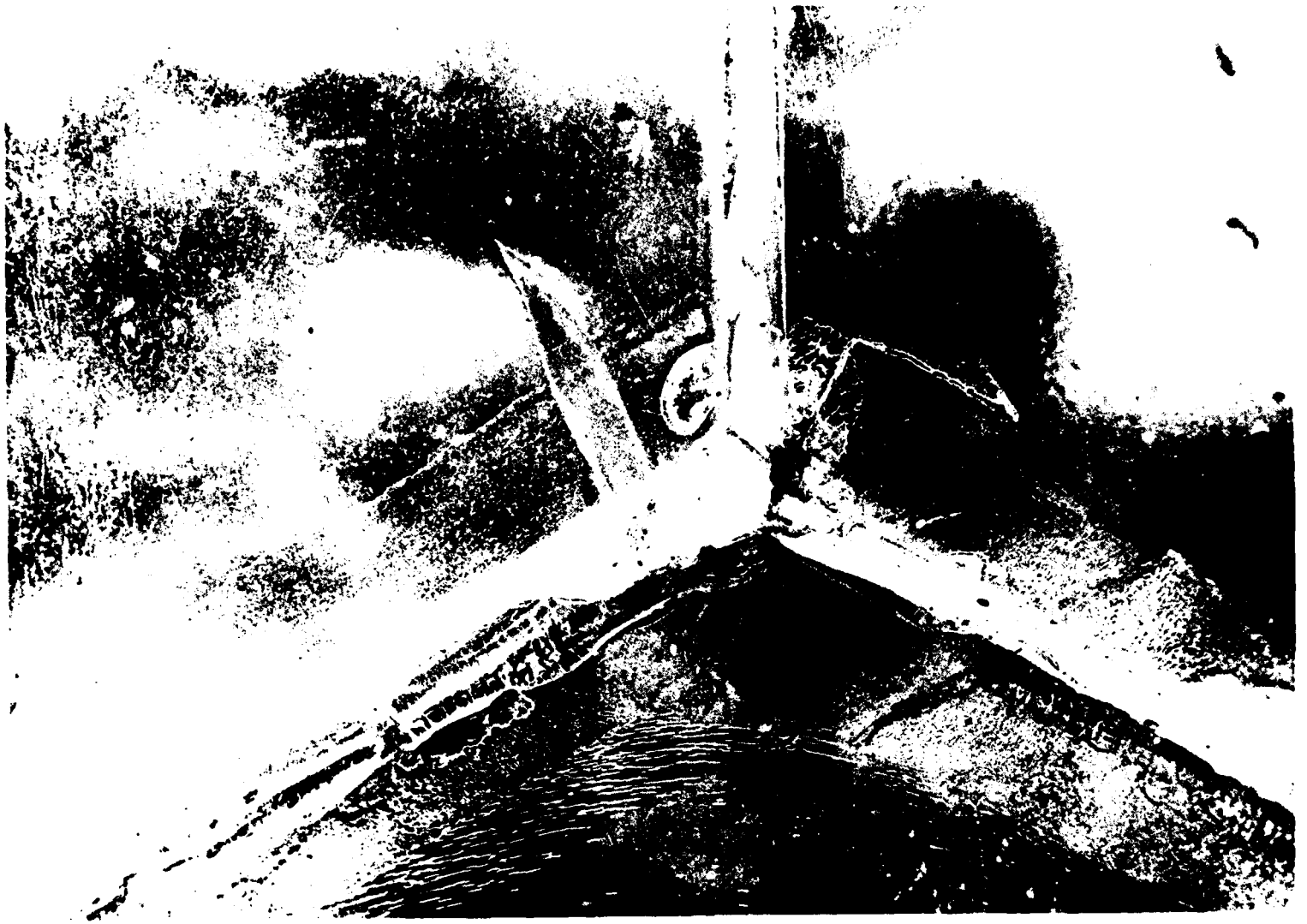

Figure 18. Fractures in capsule No. J after being subjected (at 2000-ft depth) to a 14.6-gram charge at 12 in. standoff: (b) crack is on the opposite side of capsule. (Sheet 2 of 2)

Figure 19. Fracture in capsule No. 26 after being subjected (at 1000-ft depth) to a 14.6-gram charge at 24 in. standoff. Crack is facing the explosive.

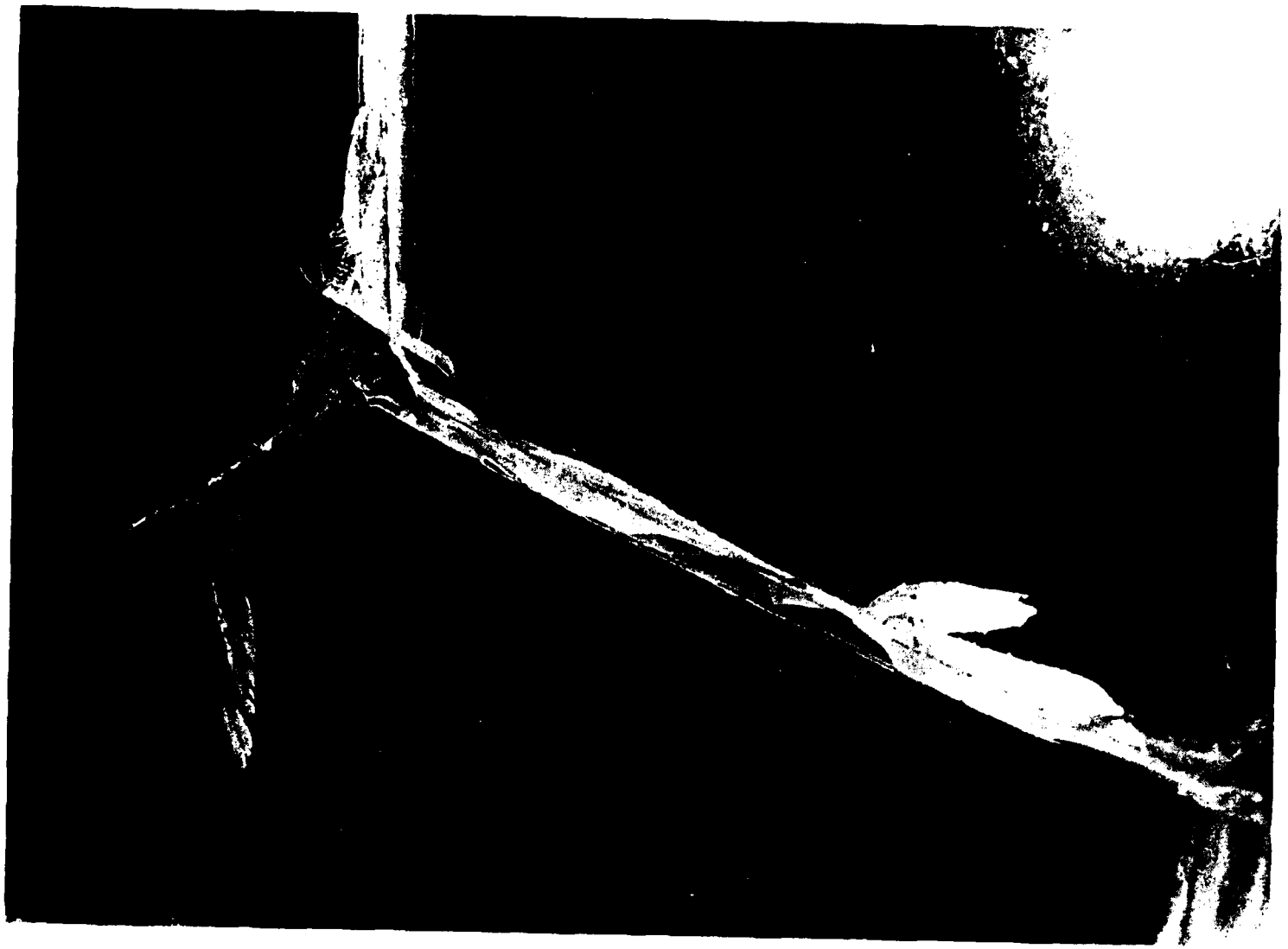

Figure 20. Fractures in capsule No. M after being subjected (at 10-ft depth) to a 14.6-gram charge at 36 in. standoff: (a) crack is facing the explosive. (Sheet 1 of 2)

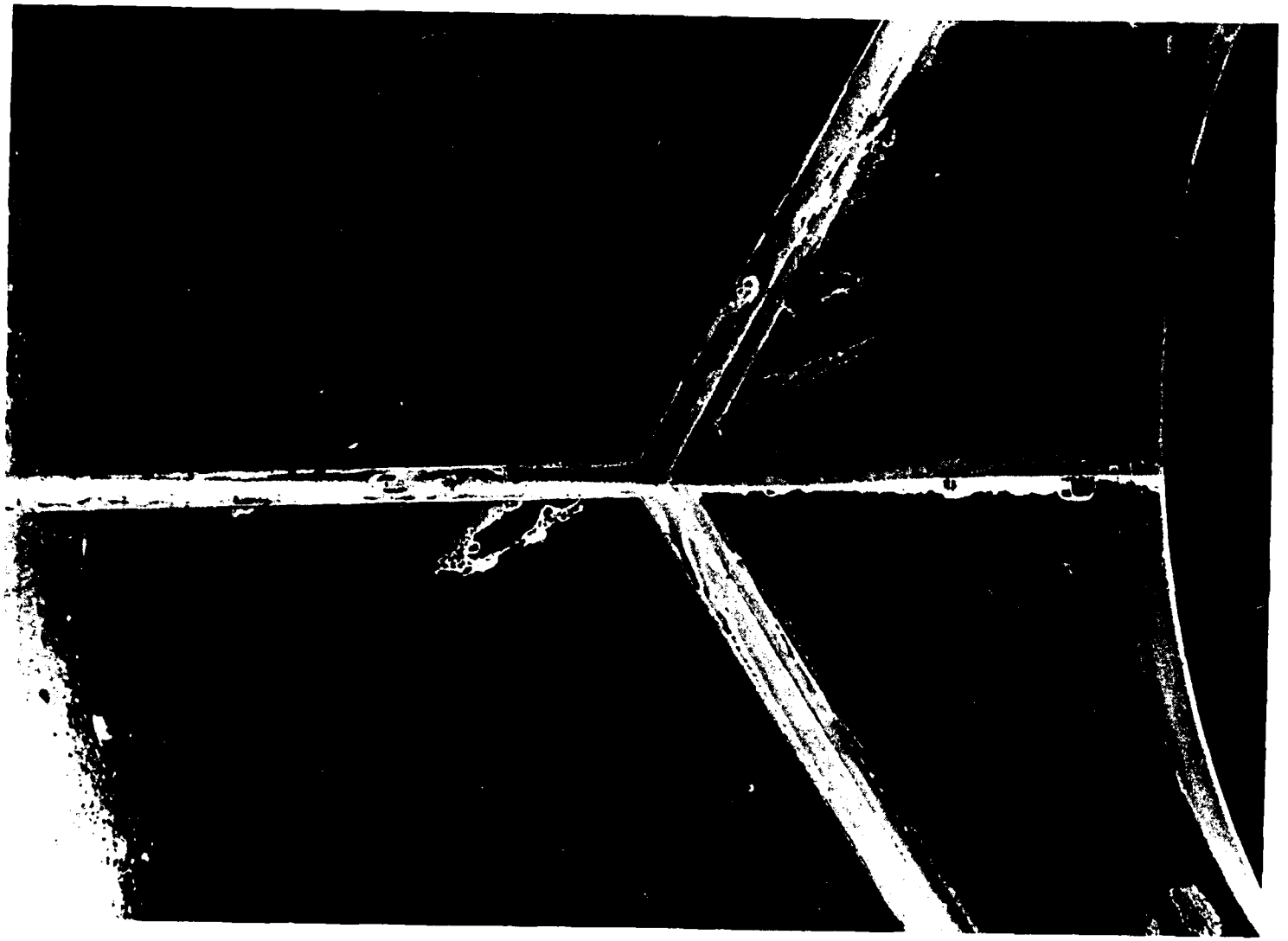

Figure 20. Fractures in capsule No. M after being subjected (at 10-ft depth) to a 14.6-gram charge at 36 in. standoff: (b) crack is at the penetration. (Sheet 2 of 2)

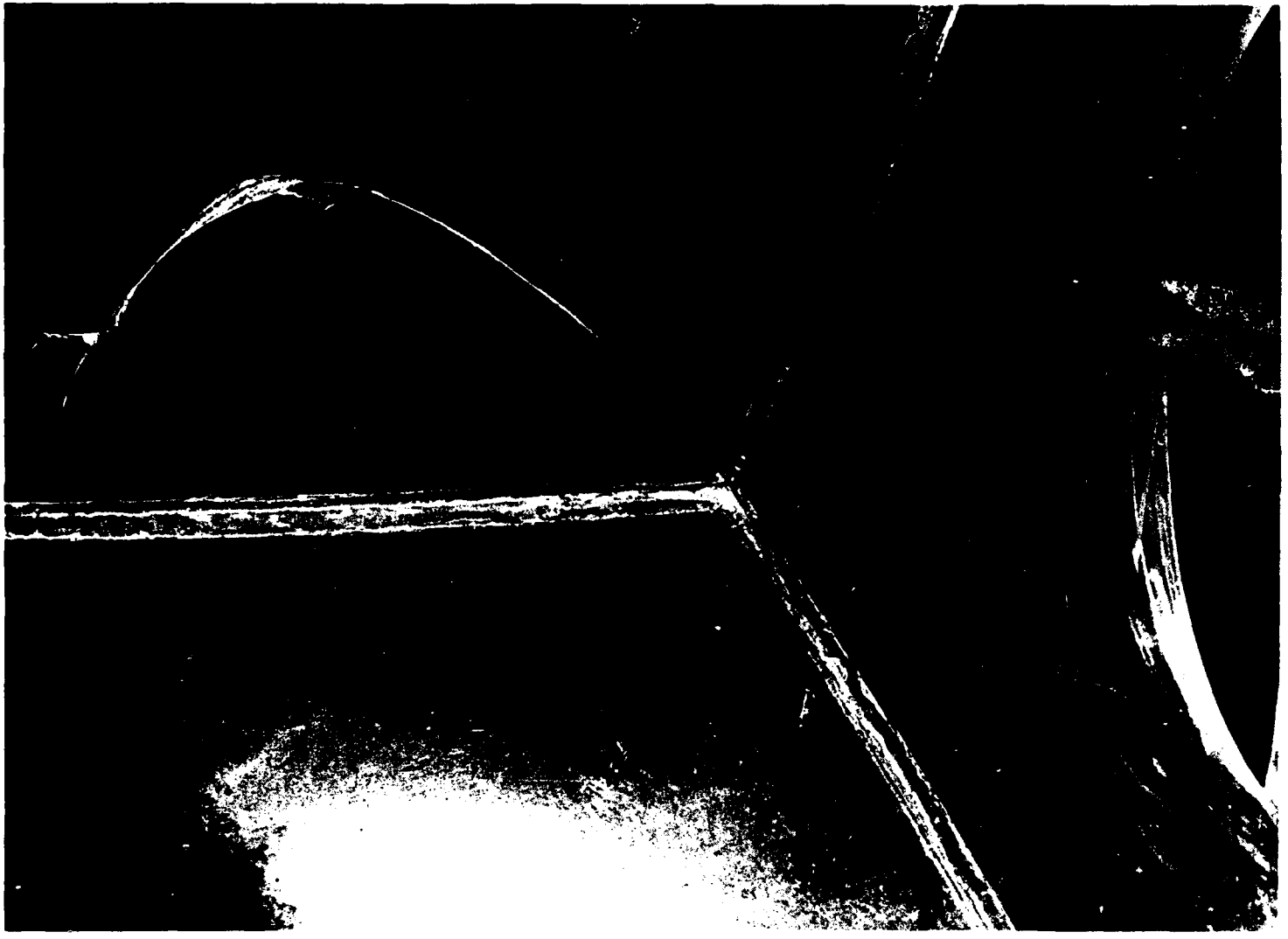

Figure 21. Fractures in capsule No. 24 after being subjected (at 10-ft depth) to a 8.2-gram charge at 24 in. standoff: (a) crack is facing the explosive. (Sheet 1 of 2)

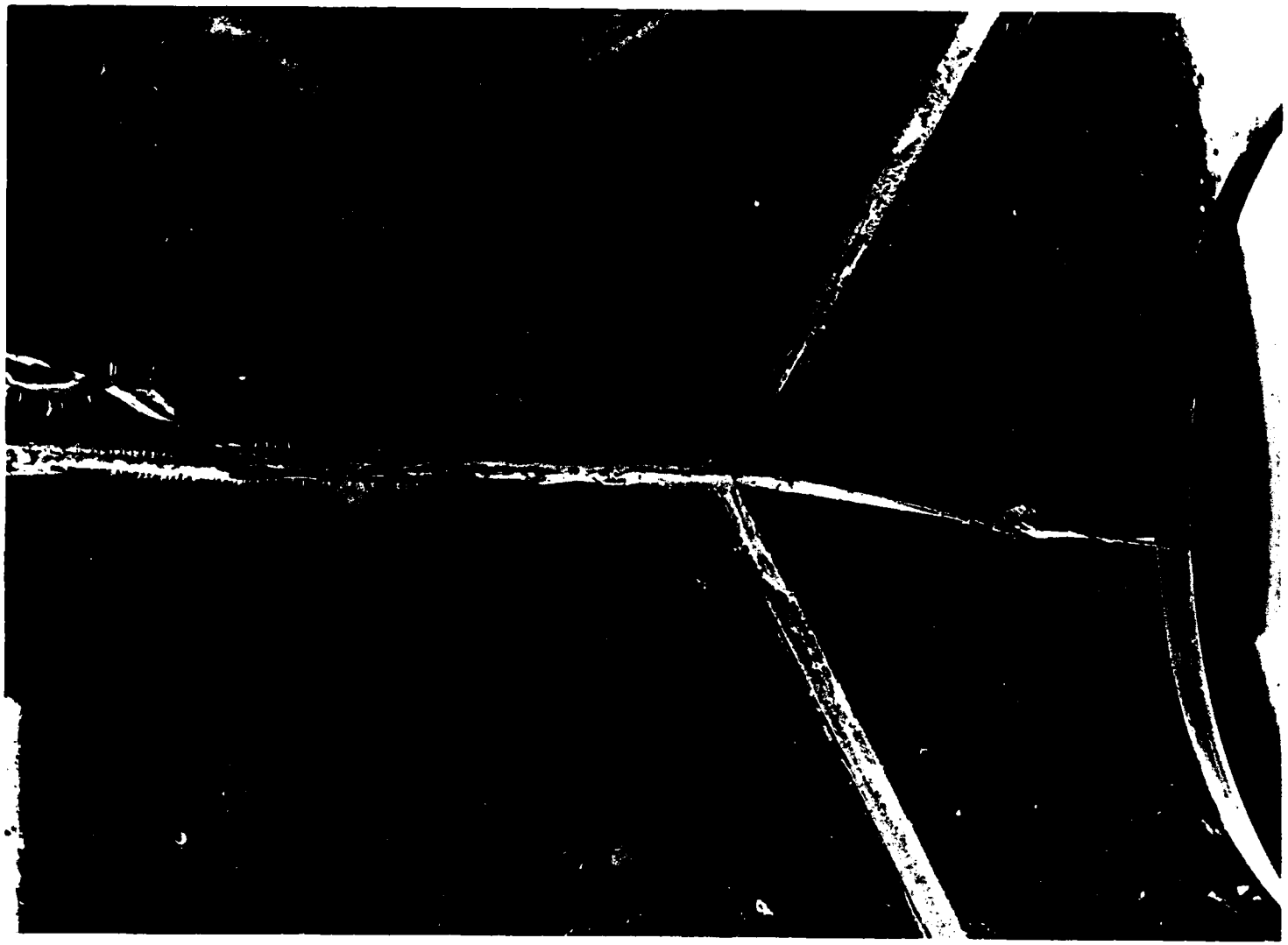

Figure 21. Fractures in capsule No. 24 after being subjected (at 10-ft depth) to a 8.2-gram charge at 24 in. standoff: (b) crack is on the opposite side of capsule near penetration. (Sheet 2 of 2)

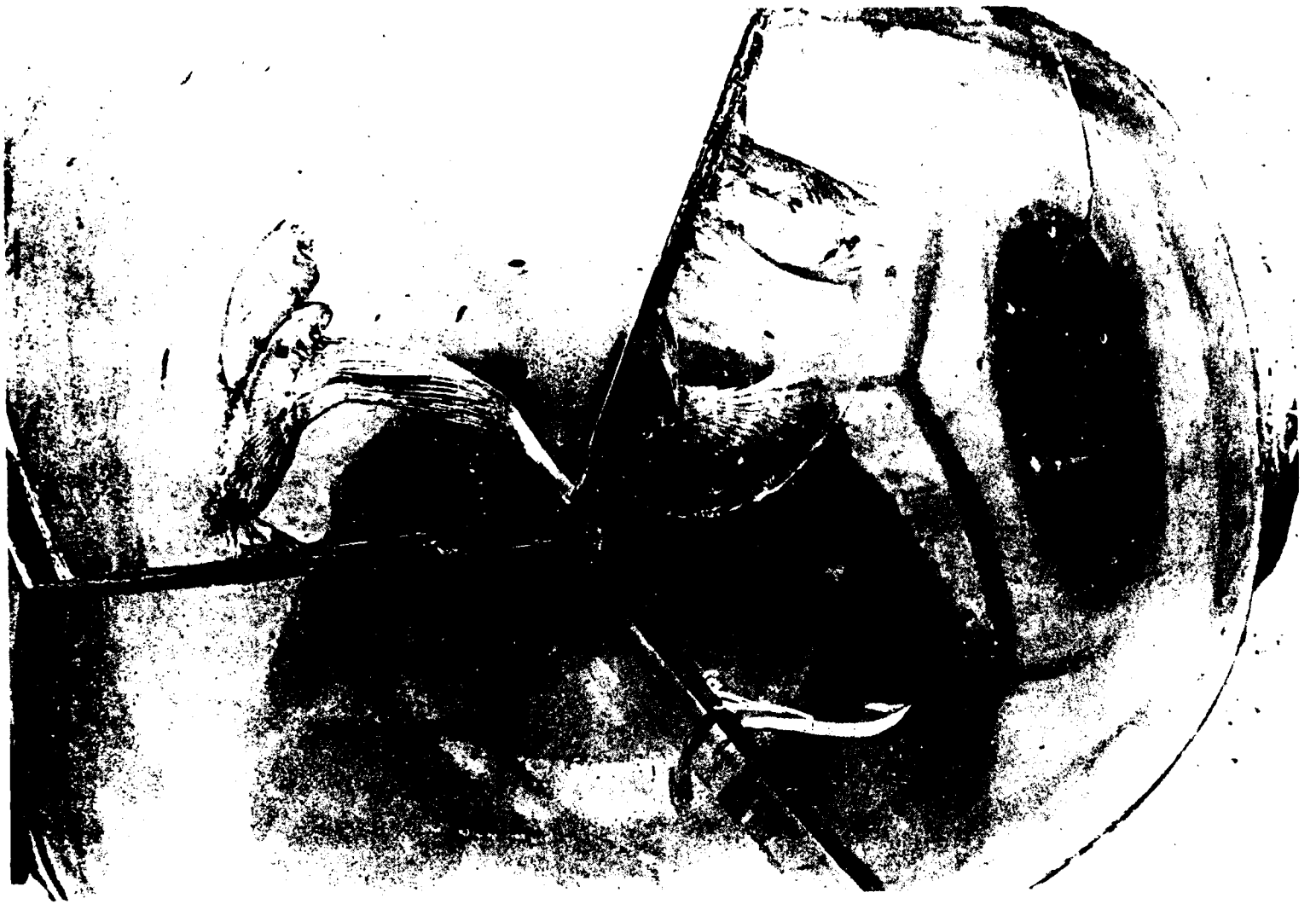

Figure 22. Fractures in capsule No. K after being subjected (at 1000-ft depth) to a 14.6-gram charge at 12 in. standoff: (a) crack is facing the explosive. (Sheet 1 of 2)

Figure 22. Fractures in capsule No. K after being subjected (at 1000-ft depth) to a 14.6-gram charge at 12 in. standoff: (b) crack is on the opposite side of capsule near penetration. (Sheet 2 of 2)

Figure 23. Fractures in capsule No. 25 after being subjected (at 10-ft depth) to a 8.2-gram charge at 48 in. standoff: (a) crack is facing the explosive. (Sheet 1 of 2)

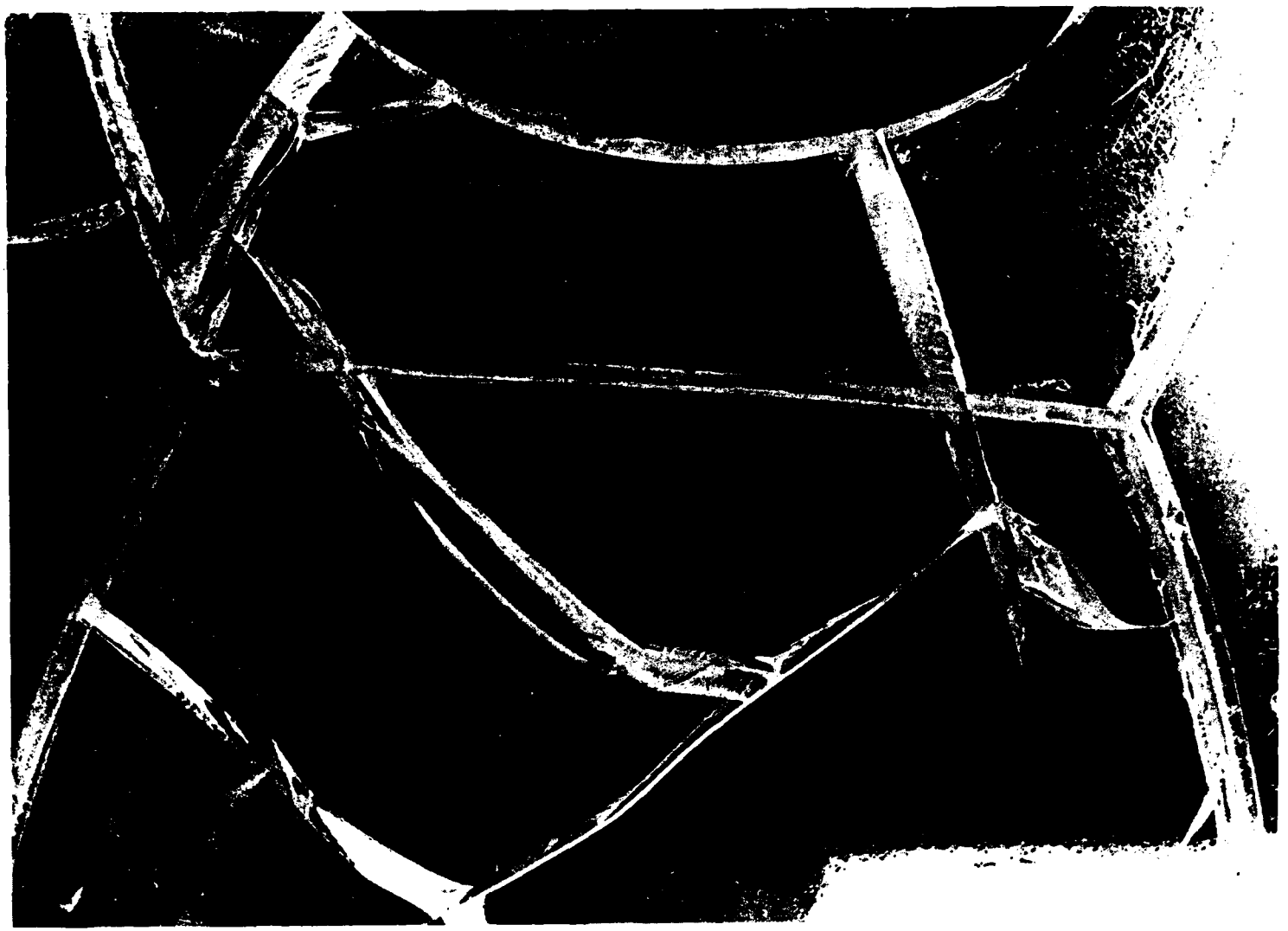

Figure 23. Fractures in capsule No. 25 after being subjected (at 10-ft depth) to a 8.2-gram charge at 48 in. standoff: (b) crack is on the opposite side of capsule near penetration. (Sheet 2 of 2)

Figure 24. Point-impact fracture in the NEMO Mod 2000 capsule after striking a steel beam in the test jig. The charge was 688.56 grams at 52.9 in. standoff in 50 ft of water.

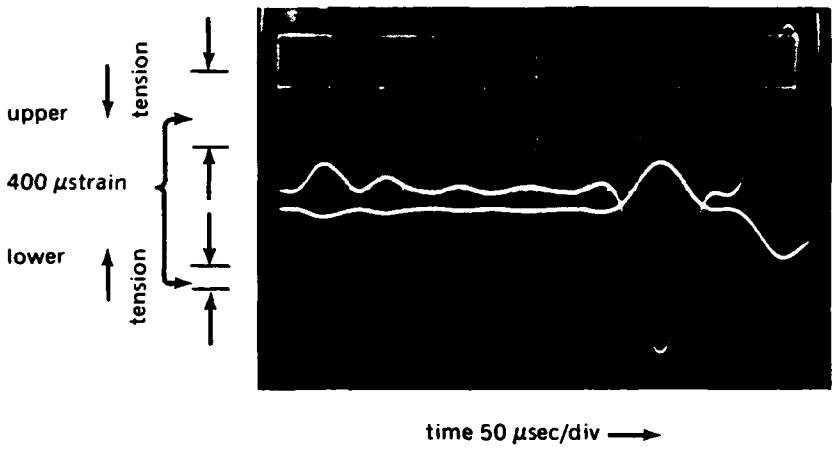

NOTES:

a) 1/4 inch strain gage was positioned internally on apex of sphere closest to point of detonation

b) Gage output was recorded at two voltage deflection levels on scope since strain level was was not known

c) 7/8 pound of pentolite was detonated 53 inches from outer surface of sphere

d) Maximum strain was initially 930 microinches in tension followed by an equal strain in compression

e) Scope trigger was delayed 500 microseconds after detonation

Figure 25. Dynamic strains measured on the interior surface of the NEMO Mod 2000 capsule directly below the charge of 387.8 grams at 52.9 in. standoff.

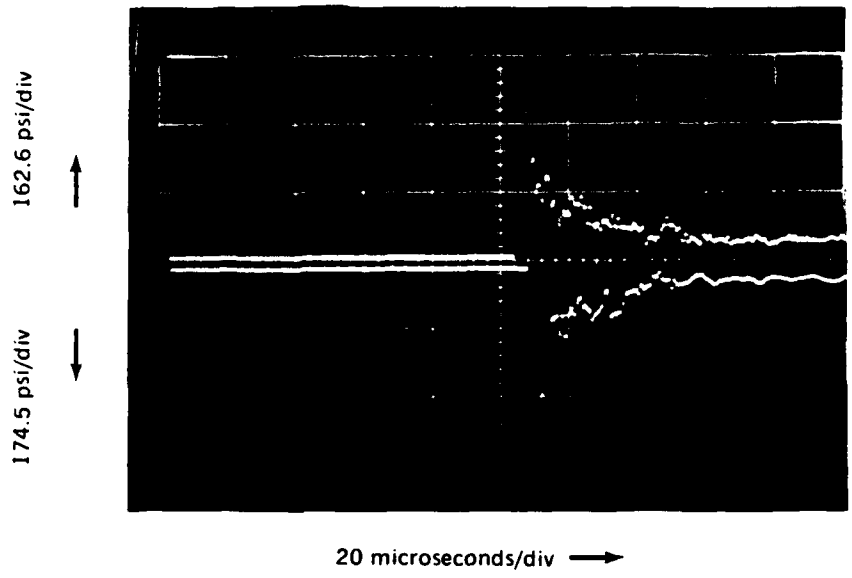

Charge:	E81 Electric Blasting Cap
Standoff:	4.41 Feet
Depth:	50 Feet
Peak Measured Pressure:	Upper Trace 504 Psi
	Lower Trace 502 Psi
Measured Unit Impulse:	Not Readable
Calculated Peak Pressure:	435 Psi
Calculated Unit Impulse:	.00745 Psi-Sec
Comments:	No Damage

Figure 26. Peak pressure measured at the full-size NEMO Mod 2000 capsule when the 1.1-gram charge was fired at 52.9 in. standoff.

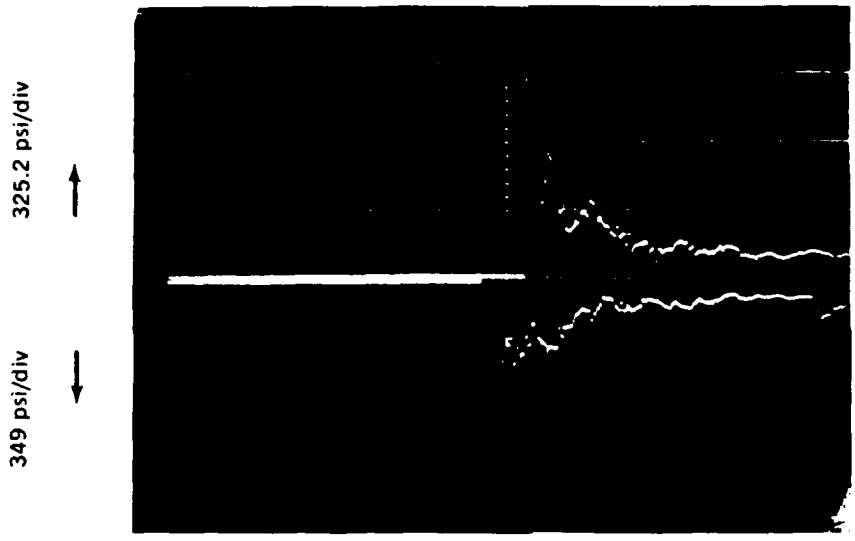

Charge:	.01242 lbs
Standoff:	4.41 Feet
Depth:	50 Feet
Peak Measured Pressure:	Upper Trace 975 Psi
	Lower Trace 1,012 Psi
Measured Unit Impulse:	Not Readable
Calculated Peak Pressure:	805 Psi
Calculated Unit Impulse:	0.0228 Psi-Sec
Comments:	Nos Damage

Figure 27. Peak pressure measured at the full-size NEMO Mod 2000 capsule when the 5.62-gram charge was fired at 52.9 in. standoff.

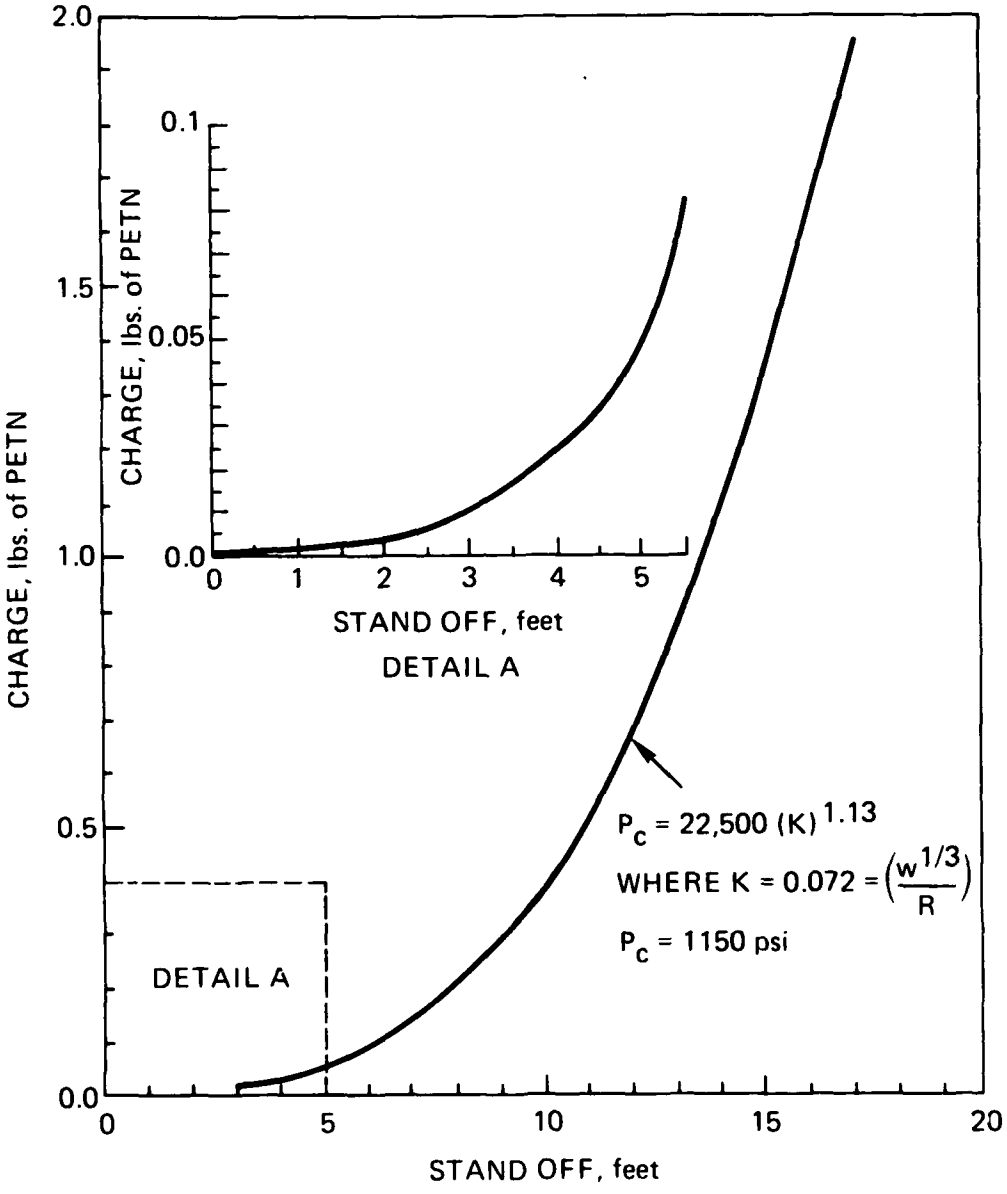

Figure 28. Weight of charges that can be repeatedly exploded underwater in the vicinity of NEMO Mod 2000 capsule without any damage to the acrylic hull or its mounting in the structure of the submersible.

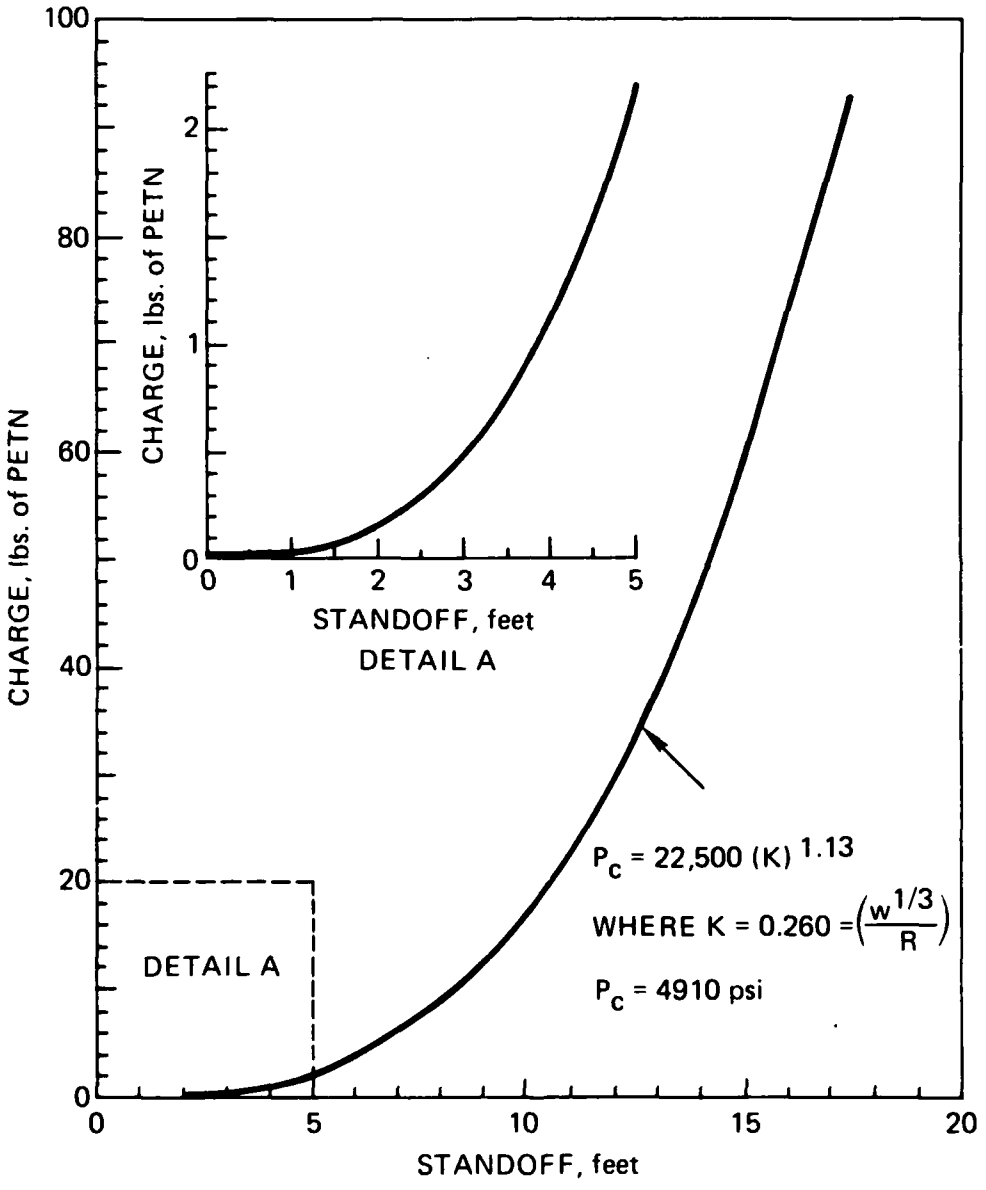

Figure 29. Maximum weight of charges that can be set off underwater in the vicinity of NEMO Mod 2000 without fracturing the hull. Such charges may, however, tear the capsule from its mounting in the structure of the submersible.

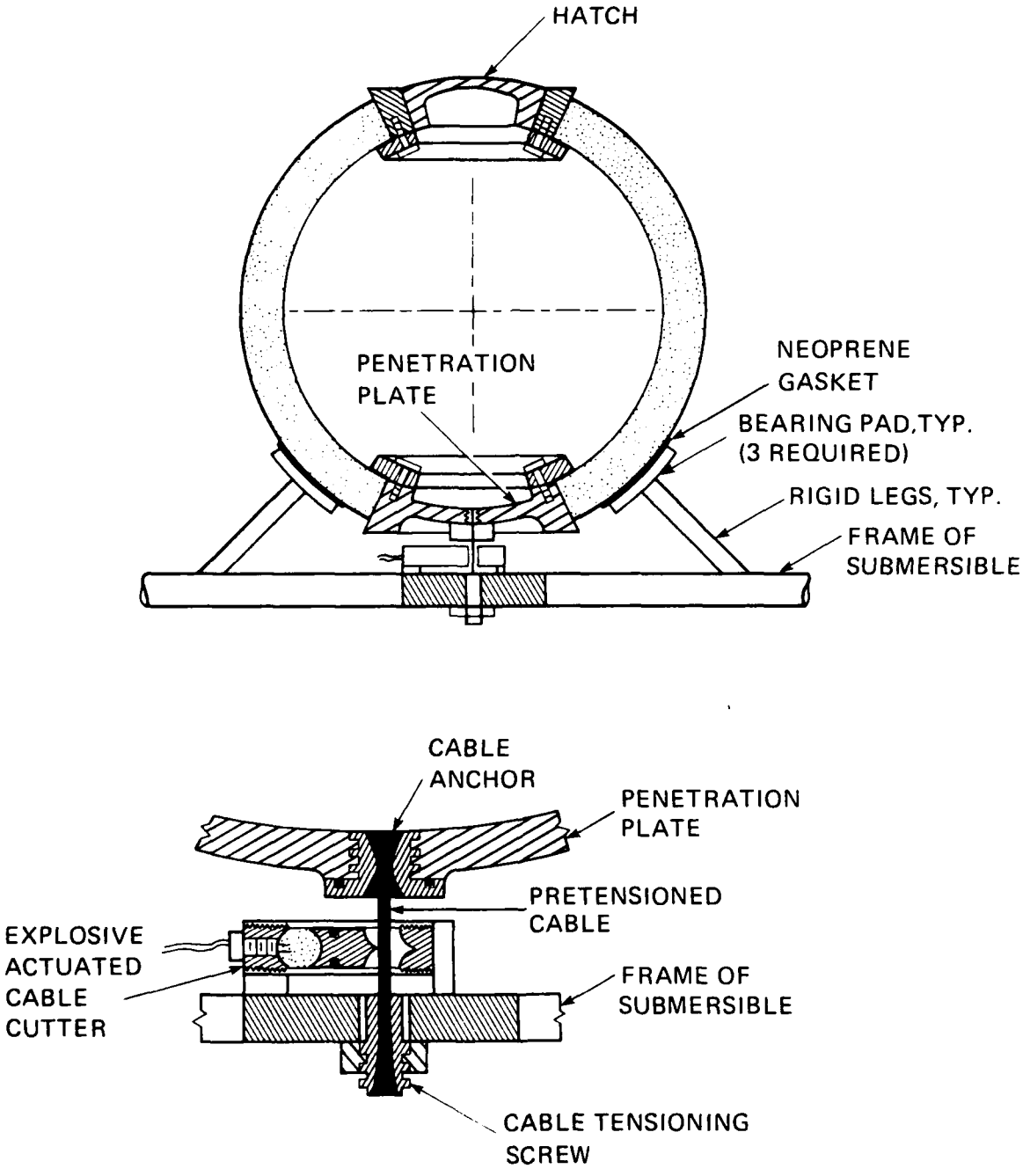

Figure 30. Typical mountings for NEMO type hulls. The single-pole mounting provides better upward visibility and is very suitable for emergency release of the capsule, while the twin-pole mounting provides a more secure attachment to the frame. (Sheet 1 of 2)

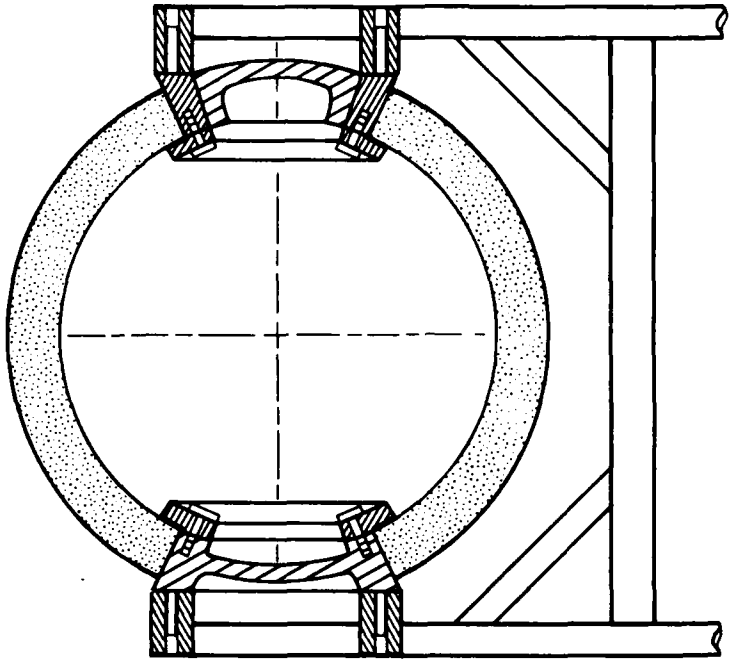

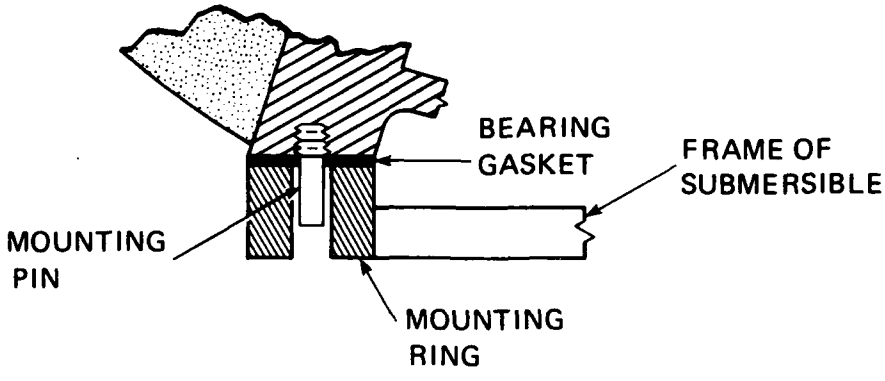

(b) TWIN-POLE MOUNTING

Figure 30. Typical mountings for NEMO type hulls. The single-pole mounting provides better upward visibility and is very suitable for emergency release of the capsule, while the twin-pole mounting provides a more secure attachment to the frame. (Sheet 2 of 2)

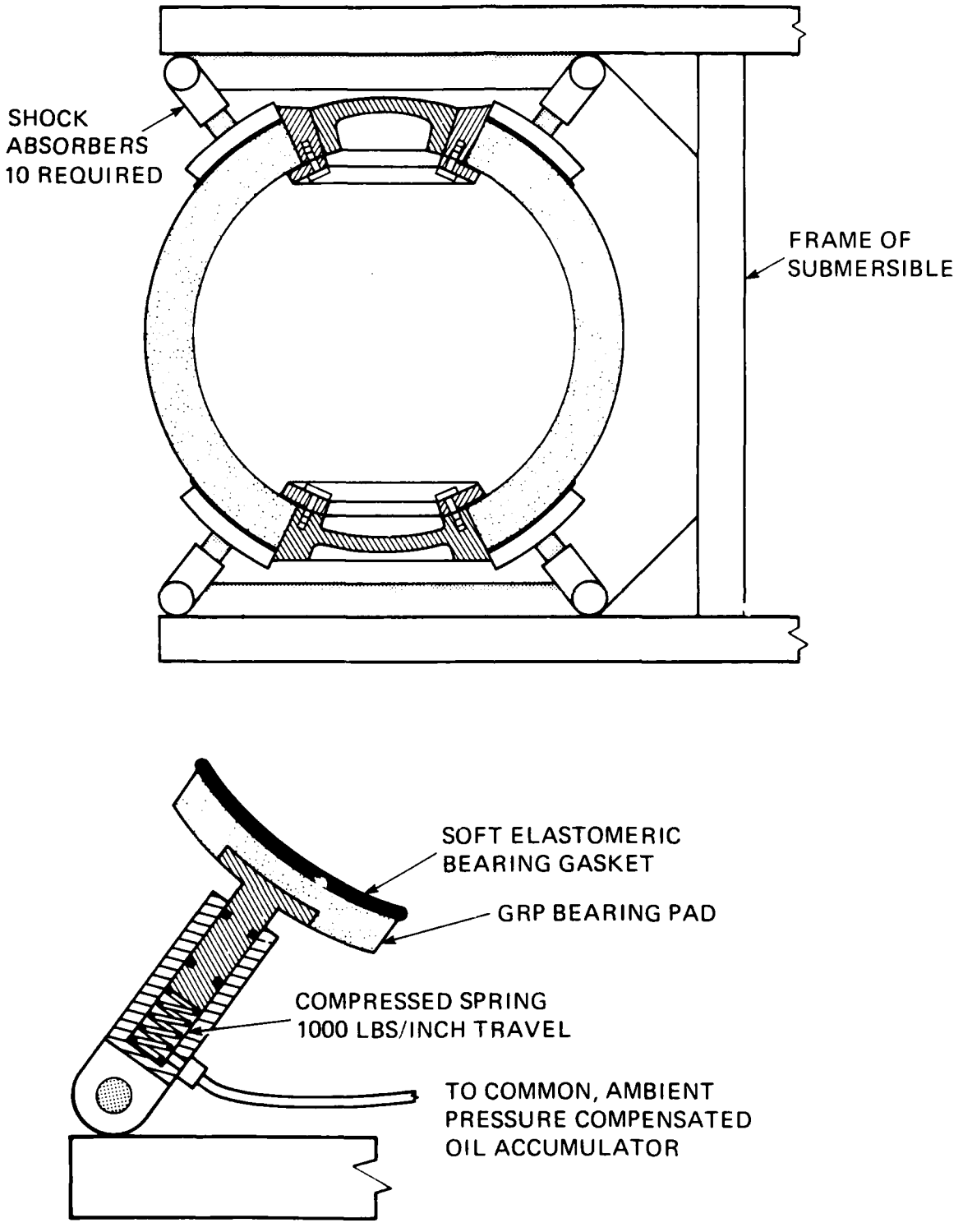

Figure 31. Concept of a mounting providing a secure, but shock-mitigating attachment to the frame.

APPENDIX

DESCRIPTION OF TEST SPECIMENS

MODEL J

Outside diameter:		15 in.
Inside diameter:		13 in.
Shell thickness:		0.040 – 0.980 in.
Material:		Plexiglas G
Construction:		Assembly of 12 thermoformed pentagons bonded with PS-30 adhesive (Fig. 3).
Penetrations:	top	– 5.285 in. minor diameter with 48° included angle
	bottom	– 4.445 in. minor diameter with 40° included angle
Inserts:	top	– Type B (Fig. 4), 6A14V titanium
	bottom	– Type A (Fig. 4), 6A14V titanium
Insert gasket:	top	– polycarbonate gasket (Fig. 4)
	bottom	– none
Life history:		– Pressure cycled 1000 times to 1000 psi in tap water at 61-74°F ambient temperature. Typical pressure cycle consisted of pressurizing to 1000 psi, holding at 1000 psi for 4 hours, depressurizing to 0 psi, and relaxing for 4 hours at 0 psi.

MODEL K

Outside diameter:	15 in.
Inside diameter:	13 in.
Shell thickness:	0.935 – 0.975 in.
Material:	Plexiglas G
Construction:	Assembly of 12 thermoformed pentagons bonded with PS-30 adhesive (Fig. 3)
Penetrations:	top – 5.285 in. minor diameter with 48° included angle bottom – 4.445 in. minor diameter with 40° included angle
Inserts:	top – Type B (Fig. 4) 6A14V titanium bottom – Type A (Fig. 4) 6A14V titanium
Insert gasket:	top – polycarbonate gasket (Fig. 4) bottom – none
Life history:	– Pressure cycled 1000 times to 1500 psi in tap water at 61-74°F ambient temperature. Typical pressure cycle consisted of pressurizing to 1500 psi, holding at 1500 psi for 4 hours, depressurizing to 0 psi, and relaxing for 4 hours at 0 psi.

MODEL M

Outside diameter:		15 in.
Inside diameter:		13 in.
Shell thickness:		0.930 – 0.990
Material:		Plexiglas G
Construction:		Assembly of 12 thermoformed pentagons bonded with PS-30 adhesive (Fig. 3)
Penetrations:	top –	5.285 in., minor diameter with 48° included angle
	bottom –	4.445 in., minor diameter with 40° included angle
Inserts:	top –	Type B (Fig. 4), 6A14V titanium
	bottom –	Type A (Fig. 4), 6A14V titanium
Insert gasket:	top –	polycarbonate gasket (Fig. 4)
	bottom –	none
Life history:		Pressure cycled 1056 times to 500 psi in tap water at 61-74°F ambient temperature. Typical pressure cycle consisted of pressurizing to 500 psi, holding at 500 psi for 4 hours, depressurizing to 0 psi, and relaxing for 4 hours at 0 psi.

MODEL 24

Outside diameter:	15 in.
Inside diameter:	14 in.
Shell thickness:	0.460 – 0.490 in.
Material:	Plexiglas G
Construction:	Assembly of 12 thermoformed pentagons bonded with PS-18 adhesive (Fig. 5).
Penetrations:	top – 4.793 in., minor diameter with 40° included angle
	bottom – 4.793 in., minor diameter with 40° included angle
Inserts:	top – Type C (Fig. 6), 316 stainless steel
	bottom – Type C (Fig. 6), 316 stainless steel
Insert gasket:	top – none
	bottom – none
Life history:	– Pressure cycled 1056 times to 500 psi in tap water at 61-74°F ambient temperature. Typical pressure cycle consisted of pressurizing to 500 psi, holding at 500 psi for 4 hours, depressurizing to 0 psi, and relaxing for 4 hours at 0 psi.

MODEL 25

Outside diameter:		15 in.
Inside diameter:		14 in.
Shell thickness:		0.460 – 0.490 in.
Material:		Plexiglas G
Construction:		Assembly of 12 thermoformed pentagons bonded with PS-18 adhesive (Fig. 5).
Penetrations:	top	– 5.150 in., minor diameter with 43° included angle
	bottom	– 5.150 in., minor diameter with 43° included angle
Inserts:	top	– Type C (Fig. 6), 316 stainless steel
	bottom	– Spherical shell sector, 0.5 in. thick with 43° included angle, acrylic plastic
Insert gasket:	top	– polycarbonate gasket, (Fig. 6)
	bottom	– none
Life history:		– Pressure cycled 1056 times to 500 psi in tap water at 61-74°F ambient temperature. Typical pressure cycle consisted of pressurizing to 500 psi, holding at 500 psi for 4 hours, depressurizing to 0 psi, and relaxing for 4 hours at 0 psi.

MODEL 26

Outside diameter:		15 in.
Inside diameter:		14 in.
Shell thickness:		0.460 – 0.500 in.
Material:		Plexiglas G
Construction:		Assembly of 12 thermoformed pentagons bonded with PS-18 adhesive (Fig. 5)
Penetrations:	top –	5.150 in., minor diameter with 43° included angle
	bottom –	none
Inserts:	top –	Spherical shell sector, 0.5 in. thick with 43° included angle, acrylic plastic
	bottom –	none
Insert gasket:	top –	none
	bottom –	none
Life history:	–	Was not subjected to any hydrostatic tests prior to explosive testing.

MODEL NEMO 2000

Outside diameter:		66 in.
Inside diameter:		57.900 in.
Shell thickness:		4.050 in.
Material:		Plexiglass G
Construction:		Assembly of 12 thermoformed pentagons bonded with PS-30 adhesive (Fig. 7).
Penetrations:	top	– 23.822 in., minor diameter with 48°30′ included angle
	bottom	– 21.727 in., minor diameter with 44° included angle
Inserts:	top	– Working hatch, 6061-T6 aluminum (Appendix A)
	bottom	– penetration plate, 6061-T6 aluminum (Appendix A)
Insert gasket:	top	– polycarbonate gasket (Appendix A)
	bottom	– polycarbonate gasket (Appendix A)
Life history:		– Pressure cycled one time each to 450 psi, 900 psi, 1350 psi, and 1800 psi. Each pressure cycle consisted of pressurizing to maximum pressure, holding at that pressure for 24 hours, depressurizing to 0 psi, and relaxing for 24 hours at 0 psi.

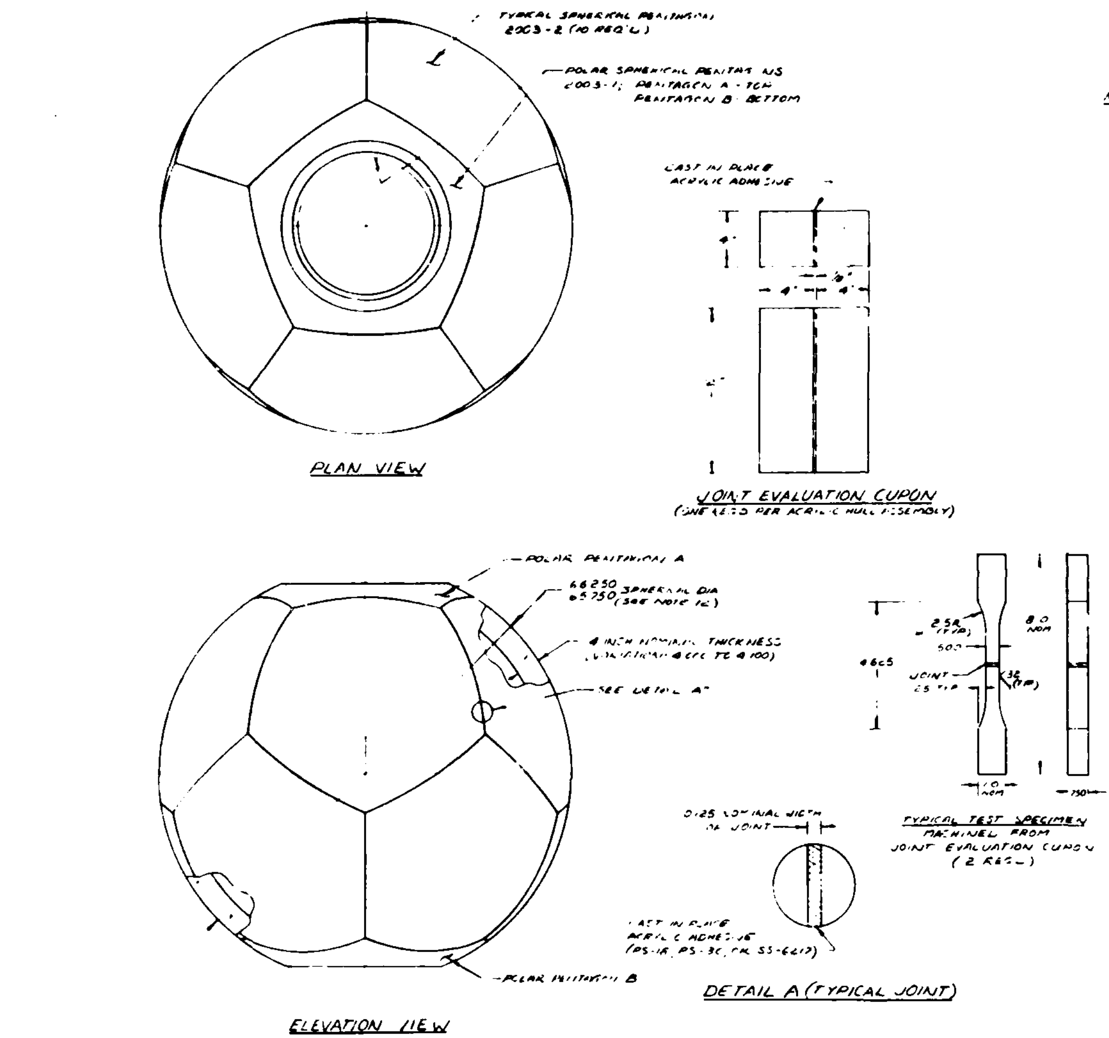

NOTES.

1. PENTAGONS MUST BE ANNEALED AT 160°F FOR 24 HRS SUBSEQUENT TO MACHINING OPERATIONS BUT PRIOR TO BONDING
2. PS 18, PS-30 OR SS 6217 ACRYLIC ADHESIVE WILL BE [illegible] THE PENTAGONS TOGETHER
3. NO UNDERCUTS IN THE BONDED JOINT WILL BE PERMITTED [illegible] THEY ARE DUE TO MISMATCH OF PENTAGON THICKNESS
4. THE TENSILE STRENGTH OF THE BONDED JOINT MUST BE A MINIMUM OF 5000 PSI AT 75°F [illegible]
5. WHEN BONDING IS COMPLETED THE INTERIOR AND EXTERIOR SURFACES OF THE HULL ARE TO BE POLISHED [illegible] THAT AN OBSERVER LOCATED IN THE CENTER OF THE HULL [illegible] NOT NOTICE ANY IMPERFECTIONS ON THE INTERIOR AND EXTERIOR SURFACES OF THE HULL
6. THE BONDED ACRYLIC HULL IS TO BE ANNEALED AFTER ALL [illegible] OPERATIONS HAVE BEEN COMPLETED
7. ANNEAL THE ACRYLIC HULL FOR A MINIMUM OF 24 HRS AT 16[illegible] °F AFTER ANNEALING DO NOT EXCEED [illegible]°F/HR COOLING RATE.
8. STRENGTH OF JOINTS WILL BE DETERMINED BY TENSILE TESTS OF JOINT EVALUATION SPECIMENS MACHINED FROM THE JOINT EVALUATION CUPON BONDED AND ANNEALED IN THE SAME MANNER AS THE PRESSURE HULL
9. THE BONDED JOINT WILL SHOW NO CRACKS OR CRAZING [illegible] AND CAVITIES MUST BE LESS THAN 1/8 INCH IN DIAMETER [illegible] OF SMALLER BUBBLES PERMITTED WILL BE ONE [illegible] FOR [illegible] AND 10 PER LINEAL FEET FOR [illegible] 1/16 INCH
10. BETWEEN THE SUCCEEDING POURS OF CEMENT THE SURFACE [illegible] PREVIOUSLY CAST CEMENT SHOULD BE REMOVED TO [illegible] BUBBLES THAT HAVE MIGRATED TO [illegible] DURING SETTING OF CEMENT
11. THE SPHERICITY OF THE HULL, AS [illegible] OF 33.000 INCH RADIUS, WILL NOT DEVIATE MORE THAN [illegible]
12. THE DIAMETER OF THE HULL AS MEASURED [illegible] METER, WILL NOT DEVIATE MORE THAN 0.250 INCHES FROM THE NOMINAL 66.000 INCH OUTSIDE DIAMETER
13. THE BONDED JOINTS IN THE HULL SHALL BE WATERTIGHT TO A DEPTH OF 2000 FEET OF SEA WATER

NUC [illegible] MODEL 2002
ACRYLIC HULL
ASSEMBLY

2002

REVISIONS				
LTR	SYM	DESCRIPTION	DATE	APPROVED
C-5	A	23 WAS 22 WAS 23 382	3-21-73	703

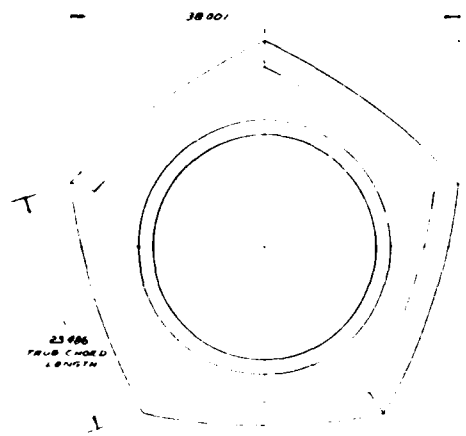

(1) POLAR SPHERICAL PENTAGON

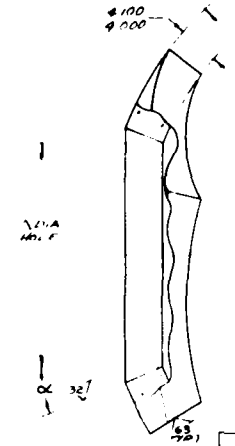

	Δ DIA	ANGLE α	NO REQ'D/ASSY
POLAR PENTAGON A	23.822 ± .010	24°15' ± 15'	ONE
POLAR PENTAGON B	21.727 ± .010	22°00' ± 15'	ONE

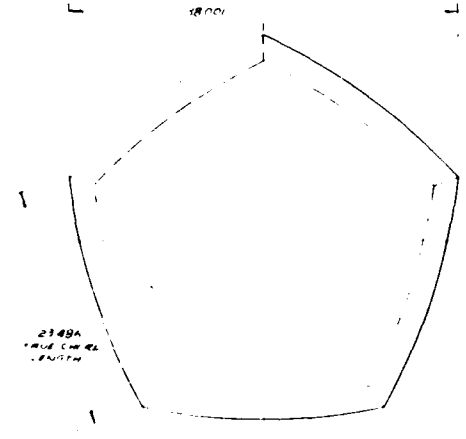

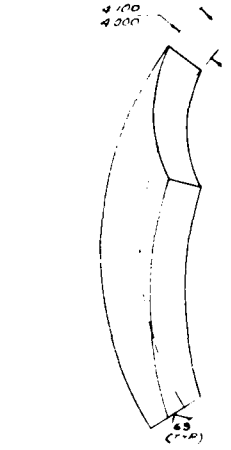

(2) SPHERICAL PENTAGON (10 REQ'D/ASSY)

NOTES.

1 MATERIAL TO BE ACRYLIC WITH THE FOLLOWING PHYSICAL PROPERTIES:

INDICATE	TYPICAL	TEST METHOD
HARDNESS ROCKWELL M	90	ASTM-D785-65
SPECIFIC GRAVITY	1.19 ± .01 (ETCHED WITH CROSS)	ASTM D792-66
REFRACTIVE INDEX	1.50 ± .01	ASTM D542-50
LUMINOUS TRANSMITTANCE	89% MIN	ASTM D1003-61
HAZE THICKNESS % OF SECTION	3% MAX	ASTM D1003-61
DISPLACEMENT FACTOR, THICKNESS OF SECTION	50% MAX	
○ TENSILE STRENGTH, RUPTURE	9000 PSI MIN	ASTM D638-68
○ TENSILE ELONGATION, RUPTURE	2% MIN	ASTM D638 68
○ MODULUS OF ELASTICITY, TENSION	400,000 PSI MIN	ASTM D638-68T
○ COMPRESSIVE STRENGTH	15,000 PSI MIN	ASTM D695-63
○ FLEXURAL STRENGTH RUPTURE	14,000 PSI MIN	ASTM D790-70
○ SHEAR STRENGTH, RUPTURE	8,000 PSI MIN	ASTM D732-46
IMPACT STRENGTH, IZOD	0.3 FT-LB/IN. MIN	ASTM-D256 70
○ COMPRESSIVE DEFORMATION	1% MAX	ASTM D621-64
WATER ABSORPTION IN 24 HR.	0.25% MAX	ASTM-D570-63

2 THE ABOVE MECHANICAL PROPERTIES MARKED ○ SHALL BE DETERMINED FOR EACH ACRYLIC SHEET BY MACHINING FROM THE SHEET TWO MATERIAL TEST SPECIMENS FOR EACH ASTM TEST METHOD SPECIFIED.

3 NUMBER EACH SEGMENT WITH APPROX. 1 INCH NUMERALS IN AT LEAST THREE (3) PLACES AFTER MACHINING (USE MARKS-A-LOT FELT TIP MARKER).

4 MEASURE & RECORD THE THICKNESS & THE OUTSIDE SPHERICAL RADIUS OF EACH SEGMENT. MEASURE AT THE CENTER AND AT EACH TIP.

5 TOLERANCE ON LINEAR DIMENSIONS AS ± .030 IN UNLESS OTHERWISE SPECIFIED.

		NAVAL UNDERSEA RESEARCH & DEVELOPMENT CENTER SAN DIEGO, CALIFORNIA 92132	
		TITLE: NUC NEMO MOLD 2003 SPHERICAL PENTAGONS	
		SIZE: D	CODE IDENT NO: 2003	REV: A

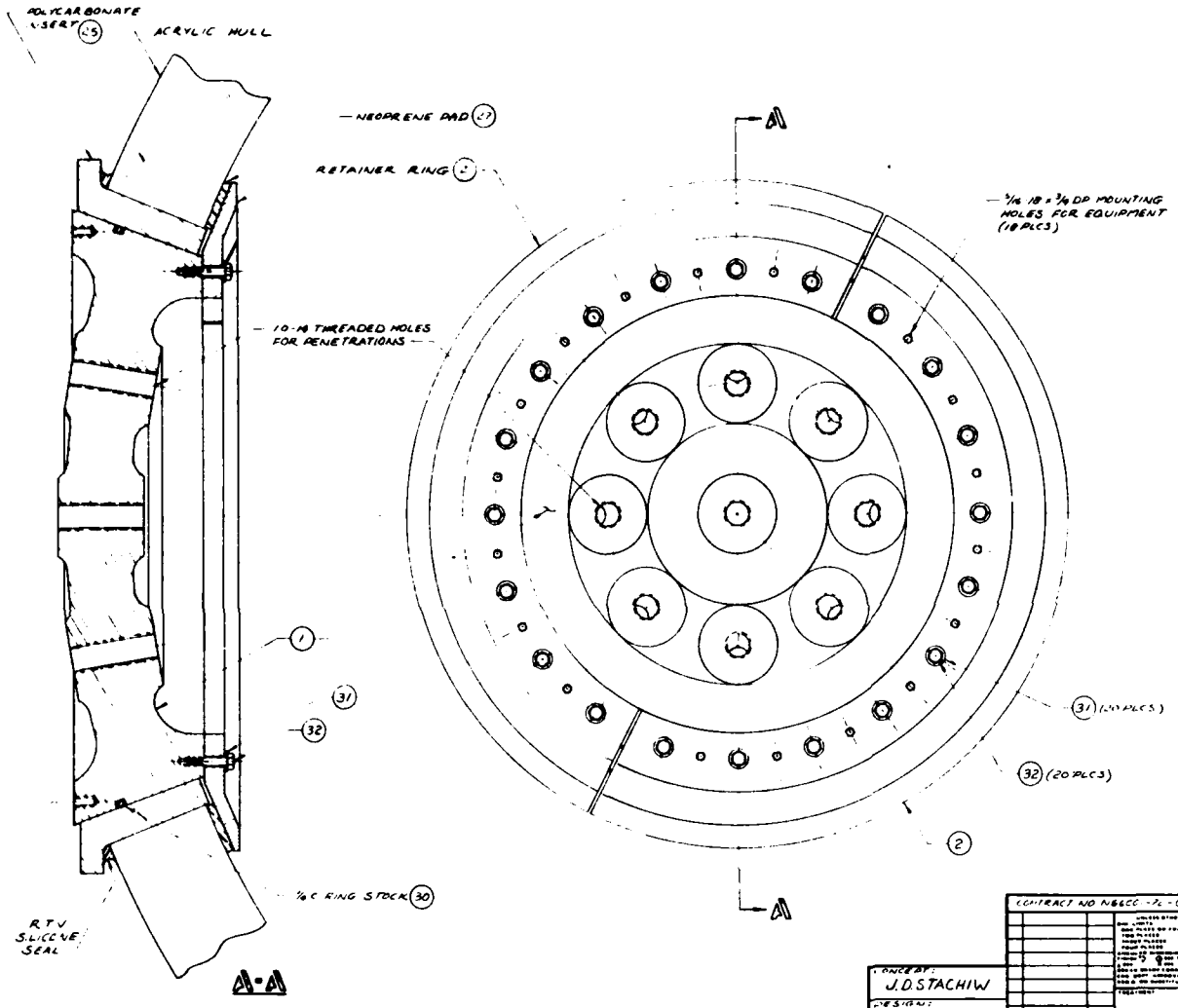

1	1/8 DIA x 1 1/4	PIN: MS17987-613	STEEL	46
3	3-5H-57N	BALL PLUNGER	VLIER ENG CORP	45
9	1/4 I.D.	WASHER	18-8 STAINLESS	44
3	1/4-20 x 3/8	SOCKET HD SCREW	" "	43
6	1/4 -12 x 1 3/8	" " "	" "	42
6	5/16-18 x 7/8	" " "	" "	41
2	1/4-20 x 2 1/4	" " "	" "	40
12	3/8-16 x 7/8	" " "	" "	39
6	#10-24 x 1/2	" " "	" "	38
3	3/4-18 NUT	FINISHED FULL	" "	37
3	5/8-18 NUT	MS35692-1030	" "	36
9	1/4-20 x 3/4	SOCKET HD SCREW	" "	35
3	C0350-006-17000	LATCH BUTTON SPRING	ASSOC SPRING CORP	34
6	3/32 DIA x 1/4	ROLL PIN	DRIV-LOK #35-156-1250	33
40	5/16-18 x 1 1/2	HEX. HEAD BOLT	18-8 STAINLESS	32
40	5/16 I.D.	WASHER	" "	31
20'	1/8 SECTION	O-RING STOCK	BUTYL	30
6	#2-14	O-RING 1/16 I.D. x 1/16 W	NITRILE (BUNA N)	29
3	2011-5	LIFTING EYE	4340 STEEL	28
2	2011-4	BOTTOM RETAINER PAD	60 DUR NEOPRENE	27
2	2011-3	TOP RETAINER PAD	" " "	26
1	2011-2	BOTTOM INSERT	LEXAN 9030 UV RESIST.	25
1	2011-1	TOP INSERT	"	24
1	2010-3	SPRING #AS42016	ASSOC. SPRING CORP	23
1	2010-2	SPRING #AS41878	" " "	22
2	2010-1	TOP RETAINER RING	6061 T6 ALUM	21
1	2009-6	HINGE PIN	17-4 PH STAINLESS	20
1	2009-5	SPRING RETAINER	6061-T6 ALUM.	19
2	2009-4	BUMPER PAD	60 DUR NEOPRENE	18
2	2009-3	HINGE BUSHING	17-4PH STAINLESS	17
1	2009-2	RIGHT HATCH HINGE	6061 T6 ALUM	16
1	2009-1	LEFT HATCH HINGE	" " "	15
1	2008-3	HINGE PLATE	" " "	14
1	2008-2	RIGHT STA. HINGE	" " "	13
1	2008-1	LEFT STA. HINGE	" " "	12
3	2007-8	INTERIOR HANDLE	" " "	11
3	2007-7	EXTERIOR HANDLE	" " "	10
3	2007-6	LATCH LUG	17-4PH STAINLESS	9
3	2007-5	STRIKER PLATE	" "	8
3	2007-4	LATCH BUTTON	6061-T6 ALUM	7
6	2007-3	THRUST WASHER	303 STAINLESS	6
3	2007-2	LATCH SHAFT	MONEL K-500	5
1	2007-1	HATCH	6061-T6 AL FORGING	4
1	2006	HATCH RING	" " "	3
2	2005-2	BOTTOM RETAINER RING	" " "	2
1	2005-1	BOTTOM PLATE	" " "	1
QTY	PART NO	NAME	MATERIAL	ITEM

CONTRACT NO N66CC-71-C-0122

DRAWN BY: J.D. STACHIW
DESIGN: J.J. LONES
PREPARED BY: ADROIT ENGINEERING

J. LONES 12-16-71
12-27-72
D. [illegible] 2-24-72

NAVAL UNDERSEA R & D CENTER

N.U.C. NEMO MODEL 2000
BOTTOM PLATE
ASSEMBLY

SIZE D | CODE 65C5 | SCALE HALF | DRAWING NO 2004 | REV | DATE 28 FEB 1972 | SHEET 1 OF 3

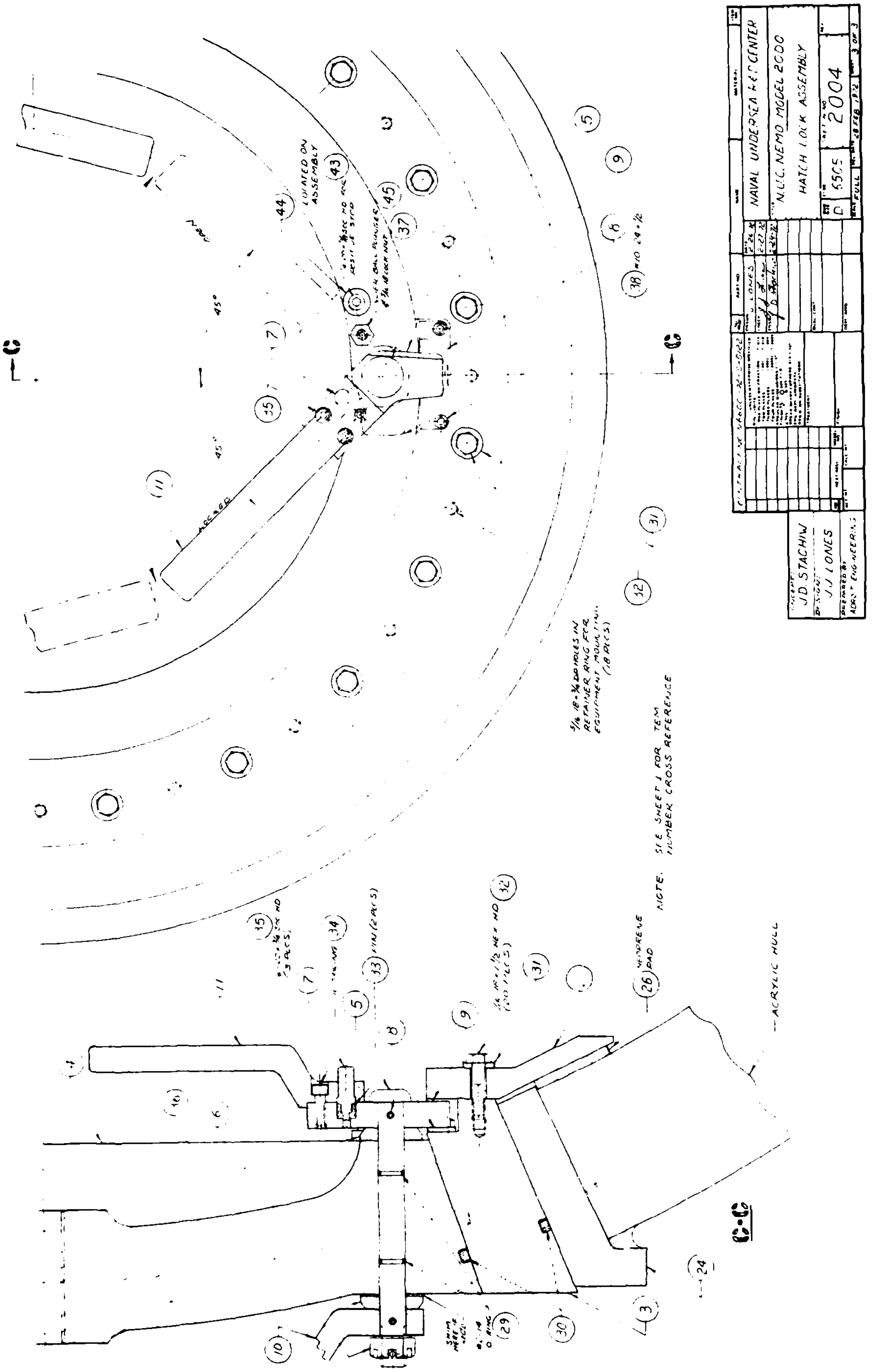
NAVAL UNDERSEA R&D CENTER
NUC NEMO MODEL 2000
HATCH LOCK ASSEMBLY
2004
FULL
3 OF 3
J.D. STACHIW
ACRYLIC HULL
NOTE. SEE SHEET 1 FOR ITEM NUMBER CROSS REFERENCE
NEOPRENE PAD
LOCATED ON ASSEMBLY
C-C

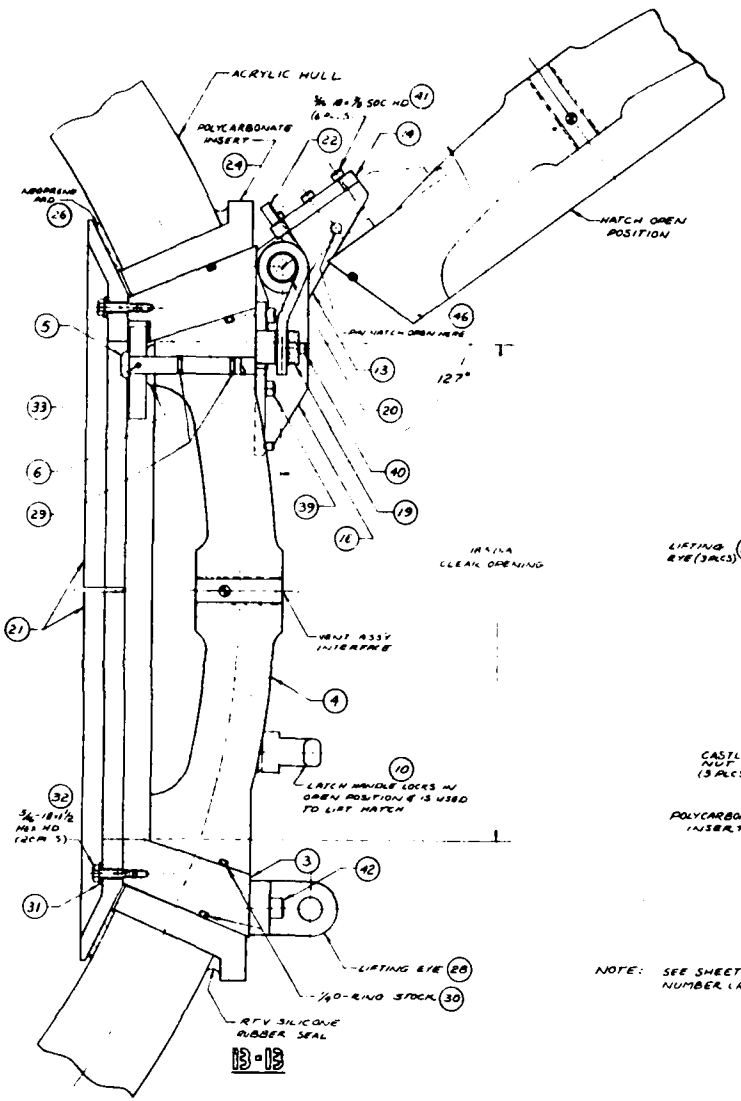

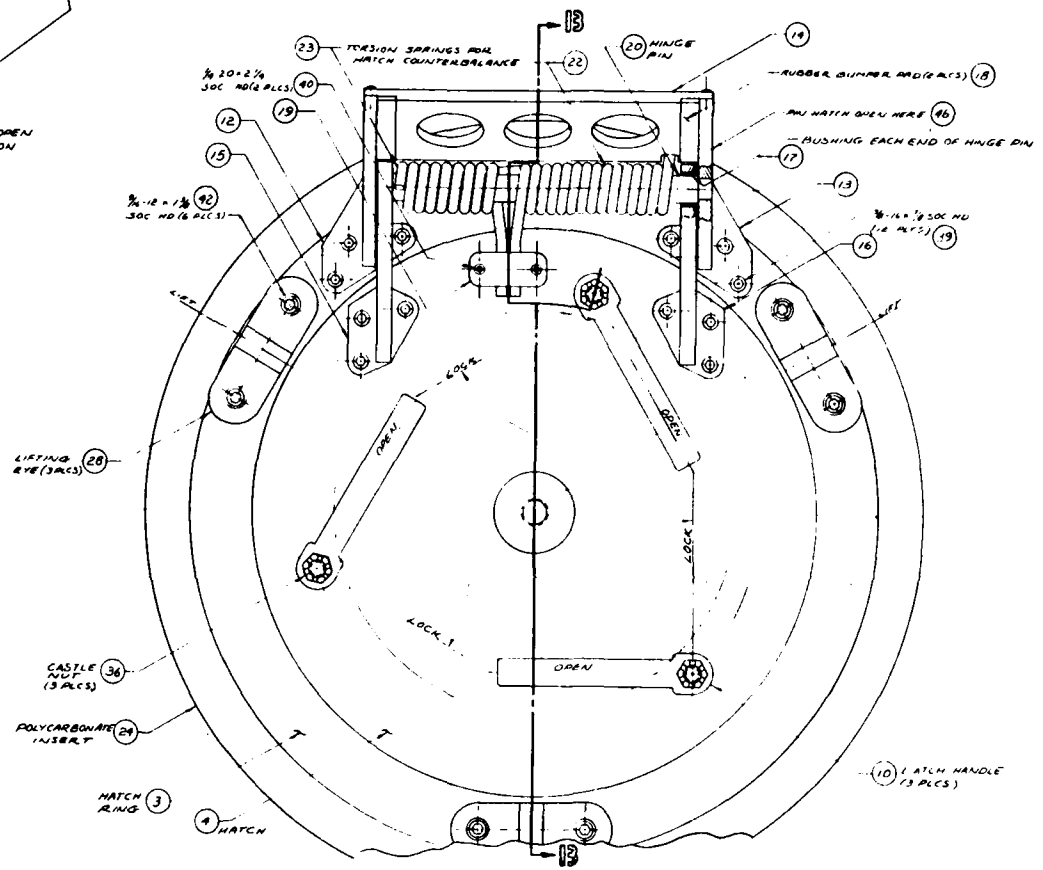

NOTE: SEE SHEET 1 FOR ITEM NUMBER CROSS REFERENCE

CONTRACT NO N66001-72-C-0122

DRAWN	J. LONES	2-24-72	NAVAL UNDERSEA R&D CENTER
CHECK		2-27-72	
ENGR		2-24-72	NUC. NEMO MODEL 2000
CONCEPT: J.D. STACHIW			HATCH ASSEMBLY
DESIGN: J.J. LONES			SIZE D / CODE 6505 / DRAWING NO. 2004
PREPARED BY: ADROIT ENGINEERING			SCALE HALF / DATE 08 FEB 1972 / SHEET 2 OF 3

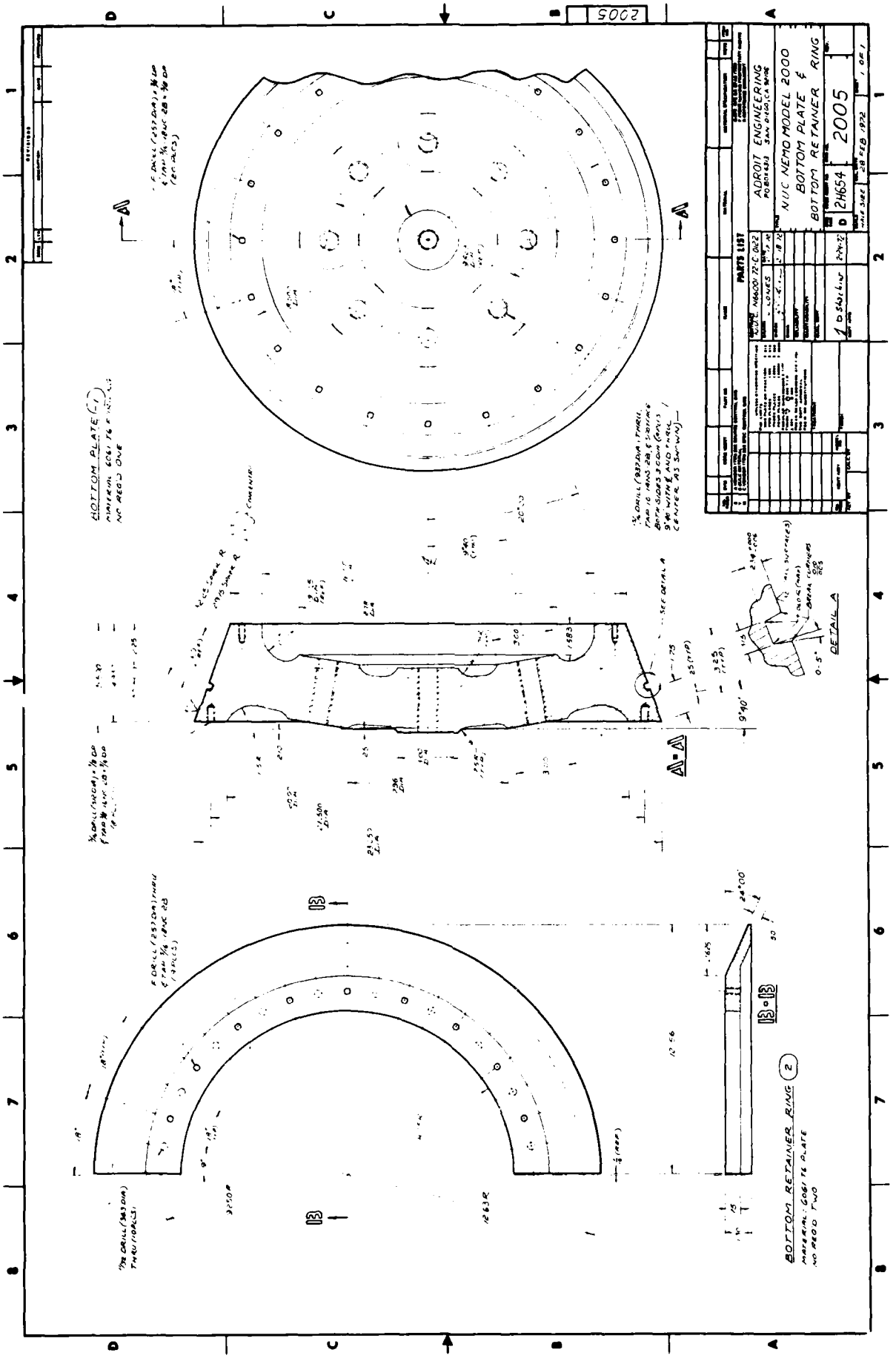
2005
AORDIT ENGINEERING
NUC NEMO MODEL 2000
BOTTOM PLATE &
BOTTOM RETAINER RING
2005
BOTTOM PLATE (1)
BOTTOM RETAINER RING (2)
DETAIL A

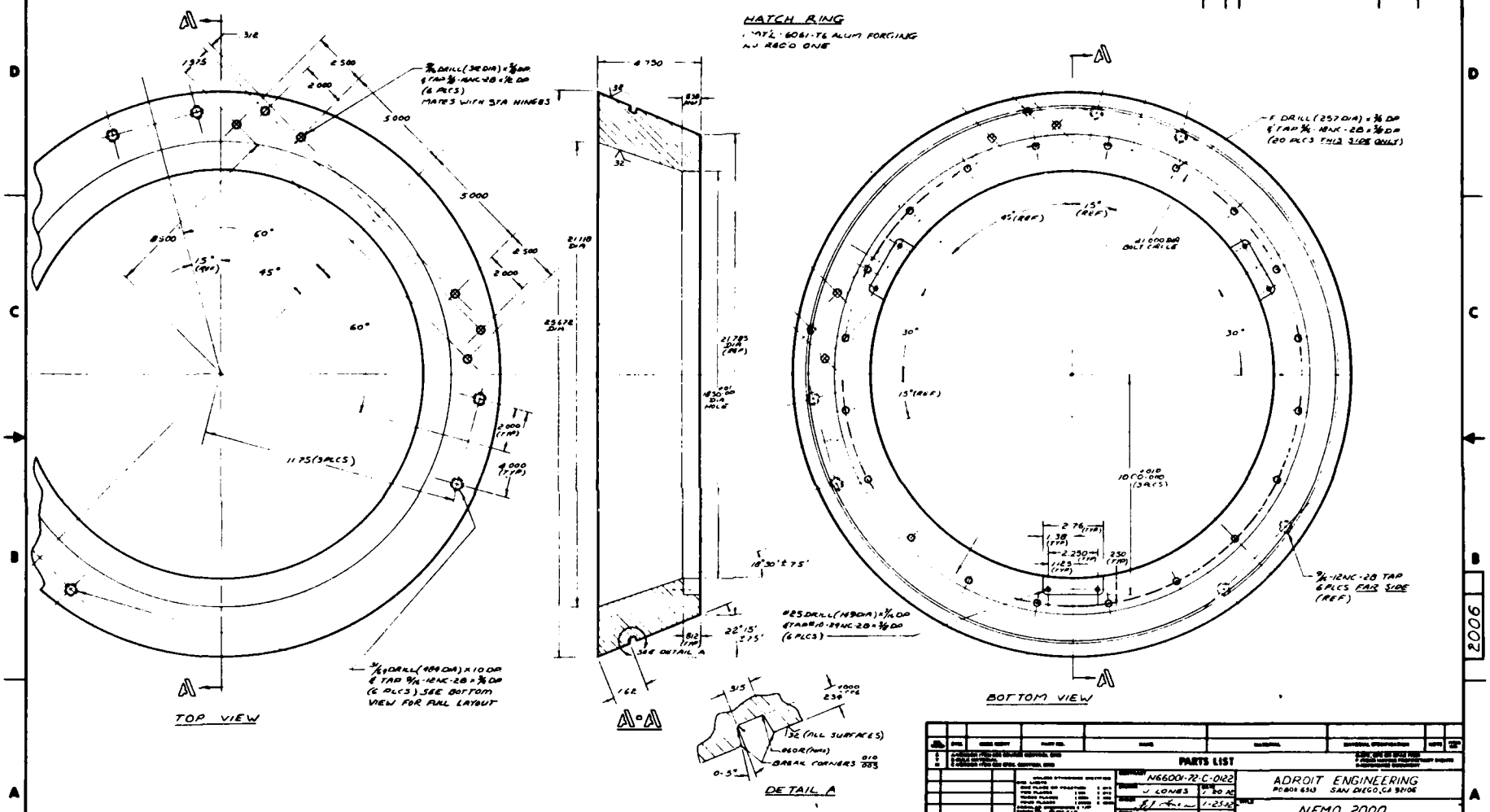
HATCH RING
MATL · 6061-T6 ALUM FORGING
NJ REGO ONE
TOP VIEW
BOTTOM VIEW
DETAIL A
PARTS LIST
ADROIT ENGINEERING
NEMO 2000
HATCH RING
2006
2H654
MATL · 6061-T6
ALUM FORGING
NONE
28 FEB 1972
1 OF 1

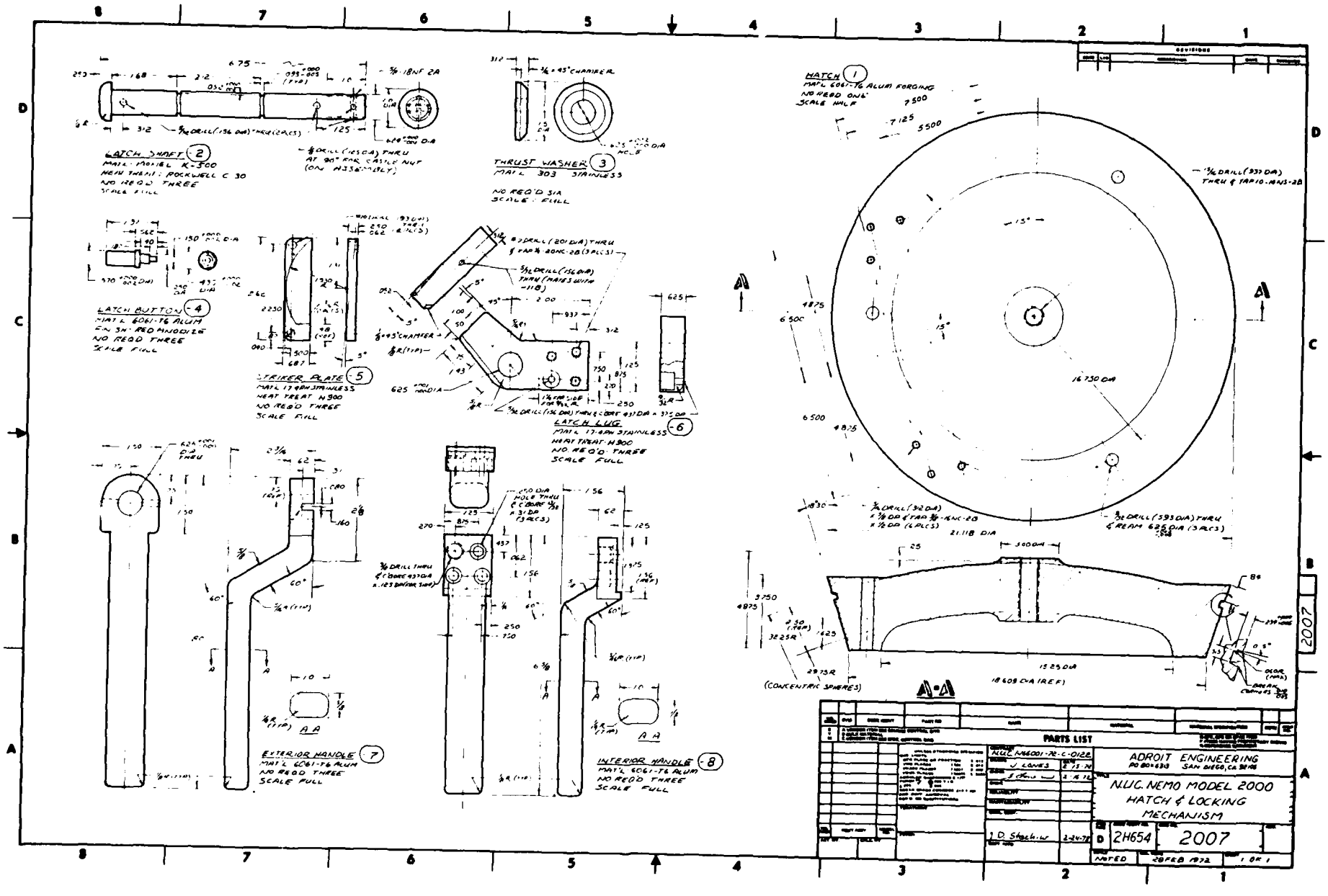
LATCH SHAFT (2)
MAT'L: MONEL K-500
HEAT TREAT: ROCKWELL C 30
NO REQ'D THREE
SCALE FULL
THRUST WASHER (3)
MAT'L 303 STAINLESS
NO REQ'D SIX
SCALE: FULL
LATCH BUTTON (4)
MAT'L 6061-T6 ALUM
FIN 3M: RED ANODIZE
NO REQ'D THREE
SCALE FULL
STRIKER PLATE (5)
MAT'L 17-4PH STAINLESS
HEAT TREAT H900
NO REQ'D THREE
SCALE FULL
LATCH LUG (6)
MAT'L 17-4PH STAINLESS
HEAT TREAT H900
NO REQ'D THREE
SCALE FULL
EXTERIOR HANDLE (7)
MAT'L 6061-T6 ALUM
NO REQ'D THREE
SCALE FULL
INTERIOR HANDLE (8)
MAT'L 6061-T6 ALUM
NO REQ'D THREE
SCALE FULL
HATCH (1)
MAT'L 6061-T6 ALUM FORGING
NO REQ'D ONE
SCALE HALF
PARTS LIST
ADROIT ENGINEERING
PO BOX 633 SAN DIEGO, CA 92112
N.U.C. NEMO MODEL 2000
HATCH & LOCKING MECHANISM
D 2H654 2007
NOTED 28 FEB 1972
1 OF 1
2007

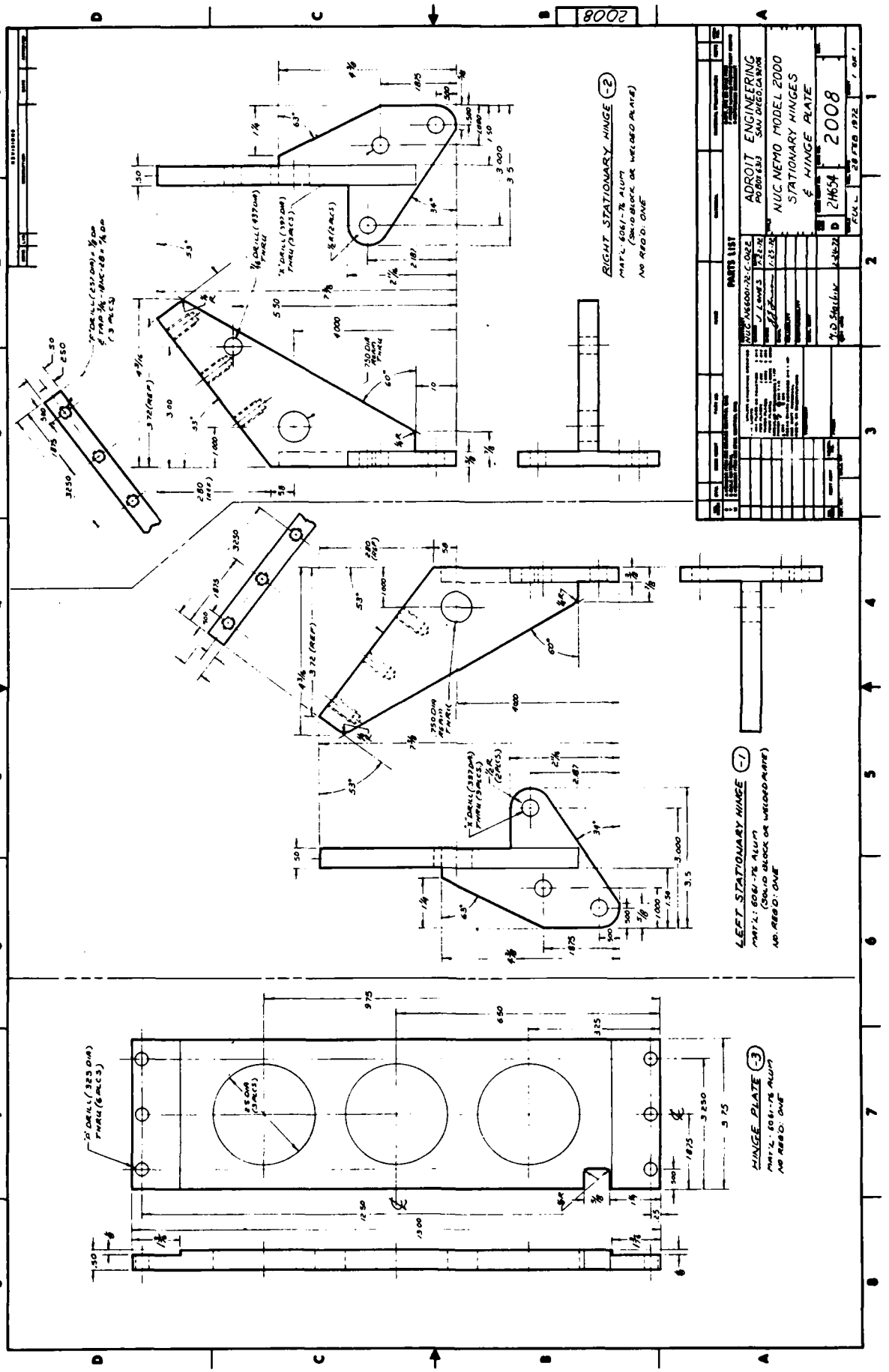
2008
RIGHT STATIONARY HINGE (-2)
MAT'L: 6061-T6 ALUM
(SOLID BLOCK OR WELDED PLATE)
NO REQ'D: ONE
LEFT STATIONARY HINGE (-1)
MAT'L: 6061-T6 ALUM
(SOLID BLOCK OR WELDED PLATE)
NO REQ'D: ONE
HINGE PLATE (-3)
MAT'L: 6061-T6 ALUM
NO REQ'D: ONE
PARTS LIST
ADROIT ENGINEERING
NUC NEMO MODEL 2000
STATIONARY HINGES
& HINGE PLATE
D 21654 2008
28 FEB 1972

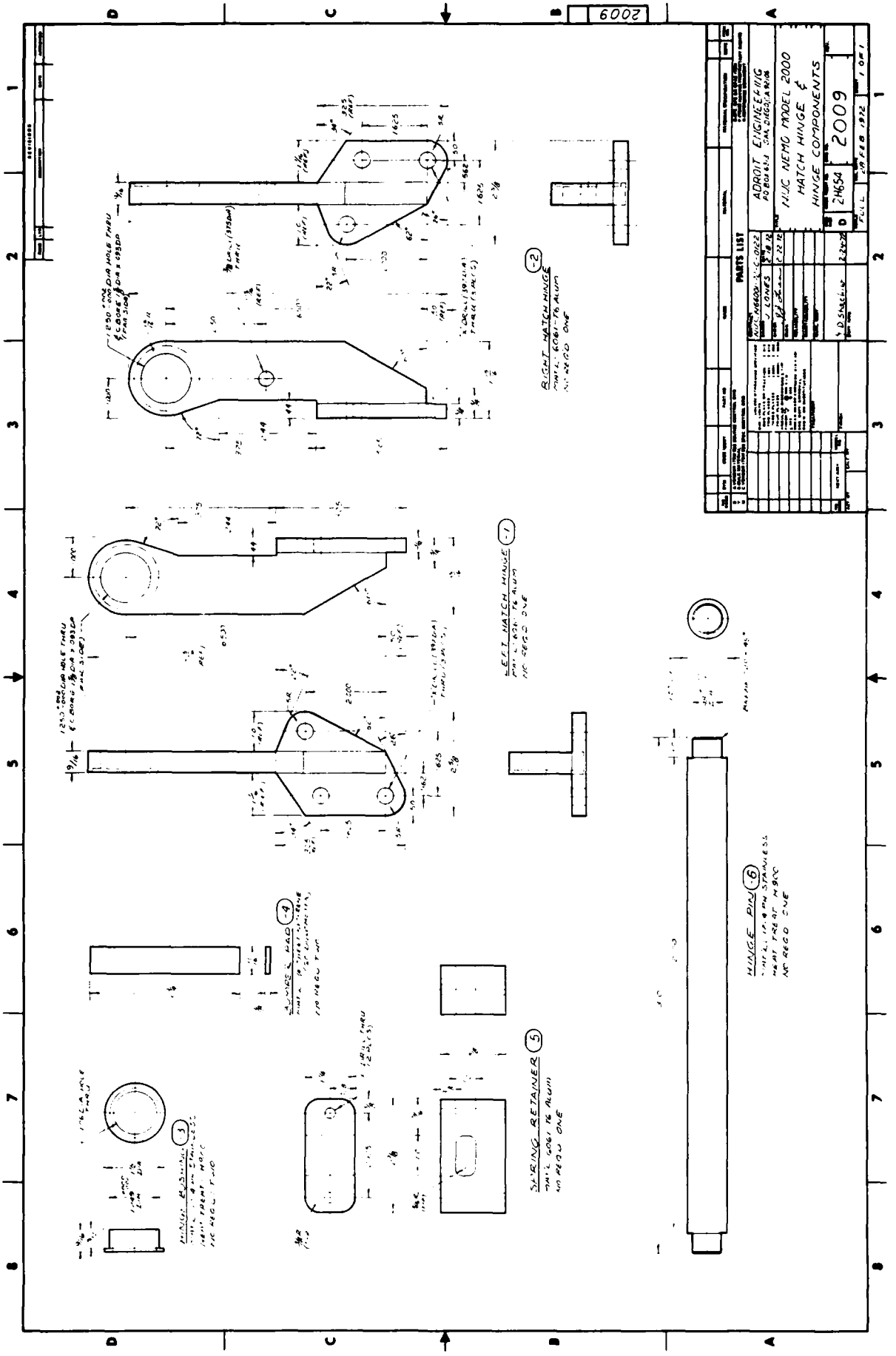
2009
PARTS LIST
ADROIT ENGINEERING
ROBOTICS SAN DIEGO, CA 92126
NUC NEMO MODEL 2000
HATCH HINGE & HINGE COMPONENTS
2009
RIGHT HATCH HINGE (2)
LEFT HATCH HINGE (1)
HINGE PIN (6)
SPRING RETAINER (5)
HINGE PIN (3)
SPRING RETAINER (4)

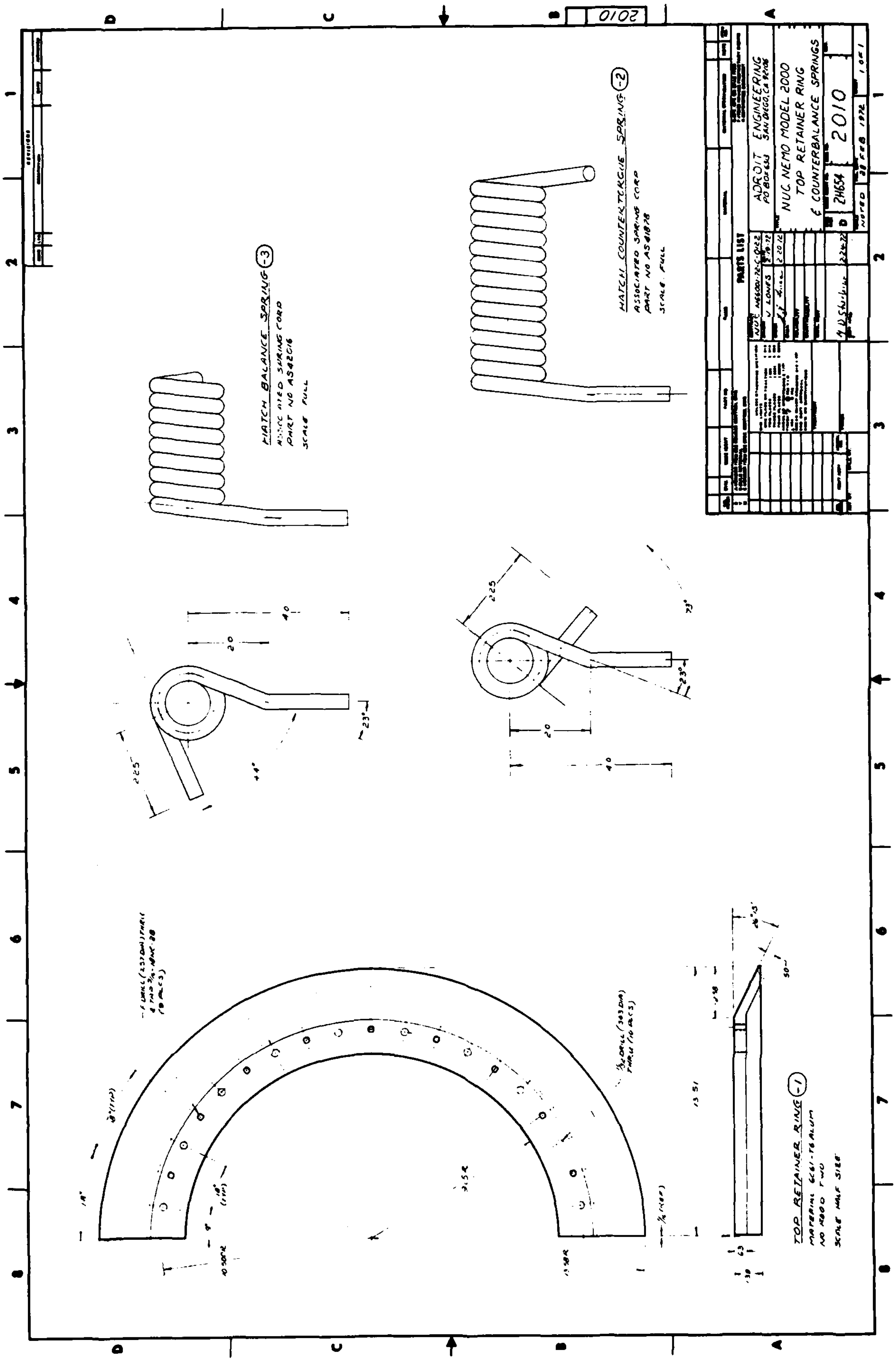
TOP RETAINER RING (-1)
MATERIAL 6061-T6 ALUM
NO REQD TWO
SCALE HALF SIZE
HATCH BALANCE SPRING (-3)
ASSOCIATED SPRING CORP
PART NO AS42016
SCALE FULL
HATCH COUNTERTORQUE SPRING (-2)
ASSOCIATED SPRING CORP
PART NO AS41878
SCALE FULL
PARTS LIST
ADROIT ENGINEERING
PO BOX 6513 SAN DIEGO, CA 92106
NUC NEMO MODEL 2000
TOP RETAINER RING
& COUNTERBALANCE SPRINGS
2H654
2010
NOTED
28 FEB 1972
1 OF 1

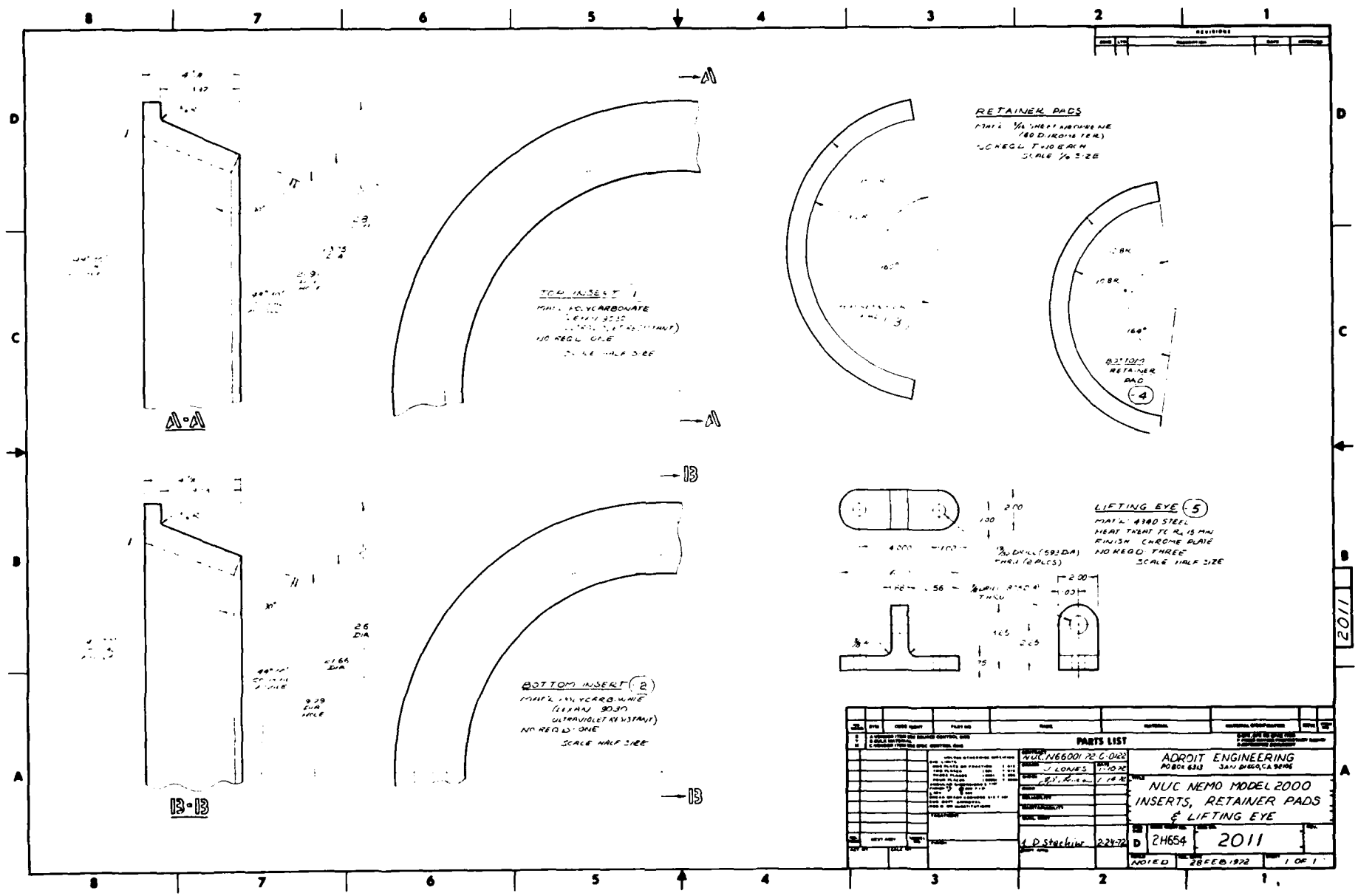
A-A
TOP INSERT (1)
MAT'L POLYCARBONATE
(LEXAN 9030
ULTRAVIOLET RESISTANT)
NO REQ'D ONE
SCALE HALF SIZE
RETAINER PADS
MAT'L 1/8 SHEET NEOPRENE
(60 DUROMETER)
NO REQ'D TWO EACH
SCALE 1/8 SIZE
BOTTOM RETAINER PAD (4)
B-B
BOTTOM INSERT (2)
MAT'L POLYCARBONATE
(LEXAN 9030
ULTRAVIOLET RESISTANT)
NO REQ'D ONE
SCALE HALF SIZE
LIFTING EYE (5)
MAT'L 4340 STEEL
HEAT TREAT TO Rc 15 MIN
FINISH CHROME PLATE
NO REQ'D THREE
SCALE HALF SIZE
PARTS LIST
NUC N66001 72 C-0122
J LONES
ADROIT ENGINEERING
PO BOX 6313 SAN DIEGO, CA 92106
NUC MEMO MODEL 2000
INSERTS, RETAINER PADS
& LIFTING EYE
D
2H654
2011
NOTED
28 FEB 1972
1 OF 1

NUC TP 451

NEMO MODEL 2000 ACRYLIC PLASTIC SPHERICAL HULL FOR MANNED SUBMERSIBLE OPERATION AT DEPTHS TO 3000 FEET

by

Jerry D. Stachiw
OCEAN TECHNOLOGY DEPARTMENT

December 1974

ADMINISTRATIVE INFORMATION

This report describes research performed between June 1972 and December 1974 as part of the investigation into man-rated transparent submersibles for maximum depth capabilities. Program efforts were requested by the Director of Navy Laboratories and were funded under a Project Order from the Naval Material Command through the Independent Research and Independent Exploratory Development program at the Naval Undersea Center under Subproject Task Area Number ZF-61-412-001.

Released by
H. R. TALKINGTON, Head
Ocean Technology Department

ACKNOWLEDGMENTS

The successful completion of an acrylic plastic hull for submersible mission operation to 3000 feet represents the combined effort of many individuals and companies. The hatches were designed by Adroit Engineering of San Diego, CA; the hull was fabricated by Swedlow Incorporated of Los Angeles, CA; and the finished assembly was tested by Southwest Research Institute of San Antonio, TX. This unified study result owes its achievement to the administrative and moral support of H. R. Talkington, Head – NUC Ocean Technology Department, and Dr. Wm. B. McLean, retired NUC Technical Director.

UNCLASSIFIED

SECURITY CLASSIFICATION OF THIS PAGE (When Data Entered)

REPORT DOCUMENTATION PAGE	READ INSTRUCTIONS BEFORE COMPLETING FORM
1 REPORT NUMBER TP 451	2 GOVT ACCESSION NO. / 3 RECIPIENT'S CATALOG NUMBER
4 TITLE (and Subtitle) Nemo Model 2000 Acrylic Plastic Spherical Hull for Manned Submersible Operation at Depths to 3000 Feet	5 TYPE OF REPORT & PERIOD COVERED TP – June 1972 to December 1974 6 PERFORMING ORG. REPORT NUMBER CNM – DLP
7 AUTHOR(s) Jerry D. Stachiw	8 CONTRACT OR GRANT NUMBER(s)
9 PERFORMING ORGANIZATION NAME AND ADDRESS Naval Undersea Center San Diego, CA 92132	10 PROGRAM ELEMENT, PROJECT, TASK AREA & WORK UNIT NUMBERS ZF-61-412-001
11 CONTROLLING OFFICE NAME AND ADDRESS Office of Naval Research Arlington, VA 22217	12 REPORT DATE December 1974 13 NUMBER OF PAGES
14 MONITORING AGENCY NAME & ADDRESS(if different from Controlling Office)	15 SECURITY CLASS (of this report) Unclassified 15a DECLASSIFICATION DOWNGRADING SCHEDULE

16 DISTRIBUTION STATEMENT (of this Report)

Approved for public release; distribution unlimited.

17 DISTRIBUTION STATEMENT (of the abstract entered in Block 20, if different from Report)

18 SUPPLEMENTARY NOTES

19 KEY WORDS (Continue on reverse side if necessary and identify by block number)

Plastics	Submersible Hulls	Transparent Materials
Structural Engineering	Acrylic Hull	Pressure Hulls
Submarine Engineering	Underwater Vehicles	
Acrylic Technology	Structural Materials	

20 ABSTRACT (Continue on reverse side if necessary and identify by block number)

Nemo Model 2000 acrylic plastic pressure hull assembly is described and represents the latest addition to the Nemo hull series represented by Nemo Model 600 and 1000 hull assemblies. The 66 inch OD X 58 inch ID spherical acrylic hull with aluminum hatches has successfully withstood 24 hour long external hydrostatic pressurizations to 450, 900, 1350 and 1800 psi. Pressure cycling and short term destructive testing of 15 inch OD X 13 inch ID scale models has shown that the crackfree fatigue life is in excess

DD FORM 1 JAN 73 1473 EDITION OF 1 NOV 65 IS OBSOLETE

UNCLASSIFIED

SECURITY CLASSIFICATION OF THIS PAGE (When Data Entered)

20. (Continued)

of 1000 pressure cycles at depths to 3000 feet and the short term implosion pressure is in the range of 10,000 to 11,000 feet. Stress wave emissions have been found to be a good indicator of incipient failure.

Nemo Model 2000 spherical pressure hulls with panoramic visibility are considered to be acceptable for manned submersibles with an operational depth capability to 3000 feet. The cyclic fatigue life of such hulls is conservatively predicted to be at least 12×10^6 feet hours.

SUMMARY

Problem

Manned submersibles with spherical acrylic plastic hulls have been known since the conception of the Nemo Hull in 1961 to provide greater panoramic vision at lower cost than steel hulls of the same shape and size equipped with many small portholes. To utilize this concept in Fleet design, the Nemo Hull was officially approved for minimum depth dives to 600 feet and demonstrated capabilities to 1000 feet in 1971. To further benefit Fleet operation, design and fabrication techniques were required to ameliorate fatigue factors inherent to structural joints between plastic and metal parts and thereby achieve the maximum operating depth allowed by the physical properties of acrylic plastic.

Results

Successive technological innovations have yielded three Nemo Hull designs that can be incorporated into existing or planned submersible systems for certified man-rated operation to ocean depths of 1000, 2000, and 3000 feet. New hatch design details have decreased bending moments at metallic hatch/acrylic hull interface and the use of polycarbonate gaskets in the acrylic plastic hatch seat has eliminated shear cracking. The latest of the Nemo Hull series, Model 2000, has a 66-inch outside diameter and a 58-inch inside diameter that yields a fatigue life of 12,000,000 feet hours over a projected 10-year life span and is capable of operation to the maximum depth allowed by the properties of acrylic plastic.

Recommendations

The Model 2000 Nemo Hull is recommended for manned operation at depths to 3000 feet. This latest design can now provide the Navy with a transparent hull for a wide variety of applications in undersea warfare, search, salvage, surveillance, and recovery missions.

DEFINITION OF TERMS

ASTM	American Society for Testing of Materials
critical pressure	external hydrostatic pressure at which catastrophic failure of the pressure hull takes place
ft	feet; equals 30.48 cm
hoop stress	principal membrane stress oriented at right angles to the longitudinal stress
ID	inside diameter of acrylic sphere
in	inches; equals 2.54 centimeters
longitudinal stress	principal membrane stress whose direction passes through poles of the sphere
NCEL	Naval Civil Engineering Laboratory, Port Hueneme, CA
Nemo Hull	Acrylic plastic hull with one atmosphere interior for manned submersibles with the following primary characteristics: (1) spherical shape (2) modular assembly of bonded pentagons (3) polar openings closed by inserts, a hatch at the top and a plate at the bottom (4) bearing surfaces on metallic hatch form a spherical angle whose apex is at the sphere
OD	outside diameter of acrylic sphere
PMR	Pacific Missile Range, Point Mugu, CA
psi	pounds per square inch; equals 0.070 kg/cm^2
R_i	inside diameter of acrylic sphere
R_o	outside diameter of acrylic sphere
short-term pressure	pressurization at 100 psi/minute rate
t	thickness of acrylic sphere

TABLE OF CONTENTS

INTRODUCTION

The idea of transparent pressure hulls for manned submersible operation became a reality in 1968 with the successful fabrication of the first full scale Nemo Hull shown in Figure 1. Since then, acrylic plastic pressure hulls of spherical shape have demonstrated competitive cost, unsurpassed panoramic visibility, and a large depth safety margin, which has given the Navy a cost-effective solution to submersible hull design.

Testing and evaluation of models and full scale Nemo Hulls continued until in 1970 the Model 600 Nemo Hull was officially approved by the U. S. Navy for manned operation to 600 feet,[1] although it demonstrated capabilities to 1000 feet, as pictured in operation in Figure 2. At that time, Nemo's endurance range beyond the standard 1000-foot minimum was inhibited by stress limitations inherent to joints between the acrylic hull and metallic hatches.[2-5] Further design studies were initiated to relieve this fatigue factor and extend the depth limit of the Nemo Hull to the maximum allowed by physical properties of the material for future work in deep ocean environments.

Subsequent work efforts during 1971-1972 resulted in the Model 1000 Nemo Hull with an optimized aluminum hatch and aluminum seating ring assembly. This model has been designed and stress analyzed for safe operations to 2000 feet. Both Models 600 and 1000 Nemo Hulls are recommended as cost-effective transparent hulls for submersible operations to, respectively, 1000 and 2000 feet.

The apex of development for the Nemo Hull culminated in 1974 with the Model 2000, the presentation of which is the purpose of this report. The results of experimental and analytical studies are presented for this acrylic plastic pressure hull, which is capable of manned submersible operation at depths to 3000 feet for at least 1000 times without fatigue cracks. The Model 2000 Nemo Hull provides the maximum safe operational depth with minimum weight to displacement and cost/depth ratios for use with manned submersibles in undersea warfare, search, salvage, surveillance and recovery missions to 3000 feet.

New design techniques and fabrication procedures are presented along with documented test results. The main body of the report is concise but terse to afford the reader a summary of study highlights. A more detailed description of design studies, fabrication procedures, and hydrostatic tests are presented in, respectively, Appendixes A, B, C, and D. The report documents a major breakthrough in technology for submersible hulls with panoramic visibility.

BACKGROUND

The failure of an acrylic plastic spherical Nemo Hull can occur in three ways. The hull can implode instantaneously because of overpressurization accompanying the catastrophic loss of the depth control system in a submersible; this type of failure is classified as *short term failure* and the pressure at which the failure occurs as short term critical pressure. The hull can also implode after it has been subjected for a long period of time to a

depth which is greater than the operational pressure, but less than the short term critical pressure. This type of failure is classified as *long term creep failure.* Finally, the failure of the hull can be initiated by cracks resulting from repeated dives to operational depth; this type of failure is classified as *fatigue failure.*

Previous experimental studies have already generated the data for prediction of short term and long term creep failures in Nemo Hulls with t/D_o ratios in the 0.015–0.017, 0.03, 0.047–0.05 and 0.064–0.67 ranges.[6] In conjunction with short term and long term implosion studies some data was also generated on the initiation of fatigue cracks in the acrylic bearing surfaces for metallic hatches on hulls with t/D_o ratios in the 0.03–0.035 range (references 2, 3, 4, 5). On the basis of that data it was concluded that for all practical applications in acrylic plastic Nemo Hulls the operational depth limitation is imposed primarily by the fatigue life of acrylic bearing surfaces supporting the metallic hatch. It is this fatigue life that imposes the 1000-foot operational depth limit on the 2.5-inch thick Model 600 Nemo Hull assembly and the 2000-foot limit on the nominally 4-inch thick Model 1000 Nemo Hull; the fatigue life being in both cases 1000 dives of 4 hour duration each to the maximum operational depth without initiation of fatigue cracks.

Since the short term collapse depth of the nominally 2.5-inch thick hull is 4150 feet and of the nominally 4-inch thick hull is 10,000 feet, there was no doubt that there existed a sufficient reservoir of potential structural strength to warrant research on improving the fatigue life of the hatch/hull interface. The effort to improve the fatigue life of Nemo Hulls was focused primarily on the Model 1000 Nemo Hull with a nominal 4-inch wall thickness,[7] as the potential operational depth improvement appeared to be higher here than in the Model 600 Nemo Hull with a nominal 2.5-inch thickness.

DISCUSSION

The objective of the study was to maximize the operational depth of the 66-inch diameter Nemo Hull with a 4-inch nominal wall thickness and maintain the minimum 1000 cycle fatigue life requirement specified for all acrylic plastic hulls.[5,6]

The approach selected was to (1) redesign the top and bottom aluminum inserts, (2) redesign the interface between the insert and the hull, and (3) improve the fabrication process for the hull. All of the modifications to the Nemo Hull design were to be evaluated experimentally and analytically.

The scope was to limit the study to two acrylic hull sizes; the 66-inch diameter, 4-inch thick, full scale operational hull and the 15-inch diameter, 1-inch thick model scale hull. The cyclic fatigue tests and the short term implosion tests were performed on the 15-inch diameter model scale hulls while the experimental determination of stress distribution and comparison with analytical stress calculations were conducted on the 66-inch diameter full scale operational hull.

DESIGN OF POLAR INSERTS

Although the existing design for polar inserts in the 66-inch diameter, nominally 4-inch thick Model 1000 Nemo Hull incorporated on the JOHNSON SEA-LINK submersible[7] was satisfactorily tested to a prooftest of 2000 feet, without yielding and probably could be used to greater depths, it contained a large number of undesirably high stress concentrations and thus was considered questionable for 3000-foot service. For a minimal cost, these hatches were modified for safe operation to 3000 feet.

The redesign of existing aluminum polar inserts for the 66-inch diameter, 4-inch thick hull (currently in service with the JOHNSON SEA-LINK submersible; see Ref. 7) consisted of redistributing the metal in the hatch and penetration plate so that the resultant of compressive membrane stresses in the acrylic hull would pass as close as possible to the centroid of the insert and thus generate only moderate bending moments in the insert; see Figure 3. A more detailed description of system design including schematic drawings is presented in Appendix A.

The new hull assembly was stress analyzed utilizing the finite element stress analysis program for arbitrary axisymmetric structures, called ZP-13,[8] as illustrated in Figure 4.

For this program the top hatch was idealized into 244 nodes and 399 elements, as shown in Figure 5, while the bottom plate was idealized into 228 nodes and 367 elements, shown in Figure 6. The maximum stresses in the aluminum hatch and bottom plate were calculated to occur at the central penetrations and at the junctions between the spherical aluminum shells and the circular flanges (again see Figs. 5 and 6). The highest stress in the plastic hull was predicted to occur on the interior surface at the point of contact between the aluminum flanges and the polycarbonate gasket.

The magnitude of the peak principal stresses in the top and bottom aluminum inserts when operating at a depth of 3000 feet was predicted to be 24,250 and 25,400 psi, respectively (values derived from extrapolation of stresses shown in Figs. 5 and 6). In both cases the peak principal stresses were located on the inside of the central hatch penetrations. These peak compressive hoop stresses were not considered dangerous at that location since the steel bulkhead penetrators would serve as reinforcements and carry some of the compressive stresses. The stresses at the juncture between the spherical surfaces on the hatch and bottom plate and their flanges were also substantial (20,000–23,000 psi), but they were well below the yielding point of aluminum. From an extrapolation of the stress values shown in Figures 7 and 8, the maximum compressive stress in the plastic hull was predicted to be longitudinal and of 10,900 psi magnitude. These stress levels were considered acceptable for operation of the manned Model 2000 Nemo Hull submersible to 3000 feet since the associated calculated safety factors, based on yielding of the aluminum and acrylic plastic, were approximately 1.5 for both materials.

DESIGN OF INSERT/HULL INTERFACE

The insert/hull interface successfully utilized in existing acrylic plastic submersibles NEMO, MAKAKAI, and JOHNSON SEA-LINK #1, consisted of direct contact between the metallic insert flange and the acrylic plastic.[2,9-11] Since the orientation of the interface was radial, shear stresses were minimized. Still, because of differences in structural rigidity

between the metallic inserts and the plastic hull, some differential movement between the inserts and the acrylic hull, as well as bending of the hull, takes place which causes shear cracks to appear in those areas of the acrylic plastic that come in contact with the metallic inserts.

There were two options available for elimination of the shear cracks. One feasible approach was to replace the metallic inserts with discs made of acrylic plastic with the same rigidity and compressibility as the plastic hull. The other approach was to place a compliant gasket between the rigid metallic insert and the limber plastic hull. Of these two approaches, the use of gaskets was operationally more appealing as it allowed the retention of operationally proven metallic inserts with the desirable high heat transfer coefficients. This left only the selection of the right type and thickness of gasket.

The gasket finally selected for the Model 2000 Nemo Hull assembly was one-inch thick polycarbonate plastic (see Fig. 3, Appendix A). Polycarbonate plastic was chosen because of its toughness, resistance to crack propagation, and modulus of elasticity that matches that of acrylic plastic. Because of the 1-inch wall thickness, the gasket possessed sufficient inherent structural strength to prevent it from being extruded into the hull interior by outside hydrostatic pressure. Also, the circumferential flange on the exterior edge of the gasket serves as a seal retainer, which keeps the water from entering the joint between the polycarbonate gasket and the acrylic plastic hull. The seal consisted of room temperature vulcanizing silicone rubber dispensed from a tube into the space between the gasket flange and the acrylic hull.

IMPROVEMENT OF FABRICATION PROCESS

The fabrication process[12] developed for the first acrylic plastic Nemo submersible[1] was also used in the fabrication of the acrylic plastic hulls for MAKAKAI[9] and the JOHNSON SEA-LINK[7] and focused primarily on the attainment of tight dimensional tolerances for the sphericity of the hull exterior. The variation in thickness of individual spherical pentagon modules remained a function of commercial casting tolerances for individual plates. Because of this dependency, the thickness of individual spherical pentagons varied as much as ±0.250 of an inch.

The large variation in thickness was acceptable so long as it was economically acceptable to rate the operational depth capability of a Nemo Hull on the basis of minimum hull thickness, and the mismatch in thickness between individual spherical pentagons was not considered optically objectionable. However, when emphasis was placed on cost effectiveness of the acrylic hull as a structure and as an optical system, it became economically untenable to tolerate such a large variation in wall thickness. The thicker portions of the hull would have constituted additional ballast that detracted from the payload and added nothing to the depth capability. In addition, the mismatches in thickness between individual spherical pentagons would have created a noticeable optical distortion for the crew of the vehicle.

Obviously, the key to uniformity of wall thickness was to use thick acrylic plastic spherical pentagons of uniform thickness in the construction of the hull. Basically, there were three techniques available for attainment of uniformly thick spherical pentagons: (1) custom casting of acrylic plates to very tight dimensional tolerances, (2) grinding

off-the-shelf acrylic plates to a uniform thickness, and (3) grinding spherical sectors to uniform curvature and thickness after thermoforming of plates. Of these three techniques the last one was found to produce the smallest thickness variation at approximately the same or less cost than required by the other techniques. The tolerances on hull thickness attained by grinding of formed spherical sectors were ±0.050 inches.

FABRICATION

Full Scale Assembly

Acrylic Hull

The 66-inch OD X 58-inch ID Model 2000 acrylic plastic Nemo Hull (see Figs. 9 and 10) was fabricated by Swedlow, Inc., basically in the same manner as the previously built Nemo Hulls.[12,13] The only improvements over the previous fabrication technique were the contour grinding of formed spherical sectors and placement of adhesive into the joints between spherical pentagons by means of hydrostatic pressure. Fabrication techniques, dimensional drawings, and relevant contract correspondence are presented in Appendix B.

Acrylite® plates manufactured by Monsanto served as basic construction material. The stringent material quality control procedures developed by NCEL and PMR for the prototype Model 600 Nemo Hull were applied here also.[2] Testing of material specimens showed that the 4.125 nominally thick Acrylite met the physical properties criteria listed in Table 1, as established by the Navy for acrylic plastic windows and pressure hulls in manned service.[2-5]

Because of improved fabrication techniques, not as many dimensional tolerances were required in building the Model 2000 Nemo Hull as were required for the Model 1000 Nemo Hull fabricated for the JOHNSON SEA-LINK submersible.[7] Thus, whereas the Model 1000 Nemo Hull thickness varied from 3.844 to 4.030 inches, the Model 2000 Nemo Hull varied only from 4.000 to 4.100 inches. Similarly, whereas the sphericity of Model 1000 Nemo Hull varied from 66.250 to 65.800, the Model 2000 Nemo Hull varied only from 66.095 to 65.900 inches. Assembly dimensions for the Nemo Model 2000 are listed in Table 2.

The only area that did not realize a significant improvement in the fabrication process was the bonding of joints between individual pentagons. A comparison of the 5456 to 7804 psi bond strength achieved for the 4-inch thick Model 1000 Nemo Hull[7] with that of the 5123 to 9116 psi bond strength attained for the Model 2000 Nemo Hull indicates that the strength of bonded joints in both hulls is about the same. This holds true also for the quality of the joint. Both the number and size of inclusions was about the same as shown in Figure 11 a and b. This indicates that although the technique of emplacing the adhesive into the joint and the polymerization regimen have been drastically changed since the fabrication of the first Model 600 Nemo Hull in 1968[2] the performance of the bonded joint has not. Since the entire Nemo Hull is under compression when submerged to operational depth, very little incentive exists to effect further improvements in the tensile qualities of the joints.

Table 1. Physical Properties of Acrylic Plastic Hull for 66 Inch OD X 58 Inch ID Nemo Model 2000

	Minimum	*Average*	*Maximum*
1. Properties of Plastic*			
ASTM D-638			
Ultimate Tensile Strength, psi	9,545	10,972	12,331
Elongation, percent	3.0	5.291	7.0
Modulus of Elasticity, psi	428,000	465,583	505,000
ASTM D-790			
Ultimate Flexural, psi	15,238	17,736	18,686
Modulus of Elasticity, psi	415,000	463,125	487,000
ASTM D-732			
Ultimate Shear Strength, psi	9,880	10,088	11,500
ASTM D-695			
Compressive yield, psi	17,700	18,416	19,600
Compressive modulus, psi	500,000	520,416	570,000
ASTM D-621			
Deformation under load; 4000 psi, 122°F for 24 hours	0.42	0.55	0.72
2. Properties of bonded joints**			
ASTM D-638			
Ultimate tensile strength, psi	5,123	7,815	9,116

*Total of 120 specimens taken from 12 acrylic plastic plates with 4.125 X 48 X 60 inches nominal dimensions.

**Total of 12 specimens taken from test blocks bonded for quality control purpose.

Table 2. Dimensions of the 66 Inch OD X 58 Inch ID Hull for Nemo Model 2000 Assembly

1. Individual Pentagons

	*Thickness**		*Contour Deviation***	
Pentagon	*Maximum*	*Minimum*	*Maximum*	*Minimum*
A	4.070	4.035	0.075	0.005
B	4.075	4.040	0.070	0.010
C	4.070	4.020	0.070	0.010
D	4.100	4.050	0.100	0.030
E	4.070	4.050	0.070	0.010
F	4.110	4.005	0.040	0.020
G	4.060	4.030	0.150	0.050
H	4.065	4.010	0.100	0.020
I	4.090	4.060	0.100	0.010
J	4.070	4.050	0.100	0.020
K	4.050	4.000	0.100	0.020
L	4.030	4.000	0.090	0.010

2. Sphere Assembly

Spherical Deviations	*Maximum*	*Minimum*
Total of 5 Measurements	-0.100	+0.095

*Total of 6 measurements per pentagon
**Total of 5 measurements per pentagon

Metallic Polar Inserts

The top hatch, top hatch ring, and bottom plate for the 66-inch OD hull were fabricated by machining 6061-T6 aluminum forgings, as pictured in Figures 12a, b and 13a, b (also see Appendix B). Material quality control of the aluminum forgings indicated a compressive yield strength of 36,300 psi and ultimate compressive strength of 43,100 psi. Special attention was paid to the machining of beveled seal seating surfaces to assure positive sealing and good bearing contact.

Polycarbonate Bearing Gasket

The bearing gaskets shown in Figure 14 between the metallic polar inserts and acrylic plastic hull were machined from polycarbonate plastic plates. Material quality control of the polycarbonate plates used as machining stock showed that the material was acceptable for this application. The physical properties are summarized in Table 3.

Table 3. Physical Properties of Polycarbonate Plastic Gaskets for 66 Inch OD X 58 Inch ID of Nemo Model 2000

	Minimum	*Average*	*Maximum*
ASTM D-638			
Ultimate Tensile Strength, psi	6,640	7,170	7,690
Elongation, percent	2.3	2.6	2.8
Modulus of Elasticity, psi	320,000	320,000	320,000
ASTM D-790			
Ultimate Flexural, psi	11,700	11,900	12,000
ASTM D-732			
Ultimate shear strength, psi	10,400	10,400	10,400
ASTM D-695			
Compressive yield, psi	12,500	12,800	13,000
Compressive modulus, psi	360,000	370,000	380,000
ASTM D-621			
Deformation under load, percent 4000 psi, 122°F for 24 hours	0.12	0.13	0.14
ASTM D-256			
Izod impact strength	0.67	0.76	0.85
ASTM D-570			
Water absorption, percent 24 hours	0.14	0.15	0.15

Since a polycarbonate plate of 6-inch thickness is currently not fabricated by industry, several half-inch thick plates were bonded together to form a 6-inch thick block. Although the bonding was performed by General Electric, the developer of polycarbonate plastic, the quality and strength of the joints were less than of the parent material. Additional efforts by Southwest Research Institute (SWRI) were made to improve the bonding technique, although these too failed to yield perfect joints. However, in view of the fact that the gasket is in compression when incorporated into the Model 2000 Nemo Hull assembly, less than perfect bonded joints were considered as acceptable for compressive loading service.

Scale Model Assembly

Acrylic Hull

The 15-inch OD X 13-inch ID acrylic plastic hulls were fabricated by the Technical Support Department of the Pacific Missile Range; Figure 15 pictures one of these hulls. The same thermoforming, machining, and bonding techniques were used to fabricate this scale model as were used in the fabrication of prototype models developed for the Nemo research program in 1965.[2] Quality control of acrylic plastic and of bonded joints showed that the scale model materials met the same specifications as did the full scale 66-inch diameter hull. Four scale models have been fabricated.

Metallic Polar Inserts

The polar inserts for the 15-inch OD model scale hulls were fabricated by machining aluminum and titanium forgings (see Appendix A). The 6061-T6 aluminum inserts were structural scale models of the aluminum polar inserts in the 66-inch diameter hull; see Figures 16a, b and 17a, b. The Ti-6Al-4V titanium inserts shown in Figure 18a, b, c, d represented simplified scale models of an alternate design for the 66-inch OD hull polar inserts, except that titanium was utilized instead of aluminum.

Polycarbonate Bearing Gaskets

The polycarbonate bearing gaskets (see Appendix A) were machined from 1-inch thick polycarbonate plates (Lexan CP-438). Common machine shop practices were used to achieve the desired finish and tolerances.

TEST PROGRAM

Model Scale Hulls

Static Tests

One 15-inch OD X 13-inch ID scale model hull, shown in Figure 19, was subjected to a series of hydrostatic tests which culminated in the implosion of the hull. The objectives of the static tests were to (1) establish the validity of aluminum hatch design for ocean depth operation to 3000 feet, (2) measure the stress wave emissions of the acrylic hull, (3) measure the creep of the hull at depths to 3000 feet, and (4) determine the short term implosion depth of the Model 2000 Nemo Hull assembly. To accomplish these objectives the scale model of the Model 2000 Nemo Hull was instrumented with 10 electric resistance strain gages and an acoustic transducer with a 160 kHz response capability, as shown in Figure 20.

Static tests were conducted at a room temperature range between 70–75°F in the pressure test facilities of the Southwest Research Institute, San Antonio, Texas.

1. Pressurize the 15-inch OD X 13-inch ID Nemo Model 34 to 1350 psi at 100 psi/minute rate, hold for 4 hours at that pressure, depressurize at 100 psi/minute rate to 0 psi, allow to relax for 4 hours prior to next test.
2. Pressurize the 15-inch OD X 13-inch ID Nemo Model 34 to 900 psi at 100 psi/minute rate, hold for 4 hours at that pressure, depressurize at 100 psi/minute rate to 0 psi, allow to relax for 4 hours prior to next test.
3. Pressurize the 15-inch OD X 13-inch ID Nemo Model 34 to implosion at 100 psi/minute rate.

Cyclic Tests

Three 15-inch OD X 13-inch ID Nemo Hull scale models were subjected to a series of pressure cycling tests. The objective of the pressure cycling tests was to establish (1) the fatigue life of bearing surfaces in acrylic plastic hulls that are in direct contact with metallic polar inserts and (2) the fatigue life of bearing surfaces in acrylic plastic hulls that are not in direct contact with the metallic polar inserts but interface through a polycarbonate bearing gasket; an assembly drawing of these contact points is shown in Figure 21. To achieve these objectives, the bearing surfaces of the acrylic hulls were to be inspected at the conclusion of the pressure cycle tests.

Pressure cycling of the scale model consisted of a series of tests conducted at a room temperature range between 70–75°F in the pressure test facilities of the Naval Civil Engineering Laboratory (NCEL), Port Hueneme, California, performed as follows.

1. Pressurize the 15-inch OD X 13-inch ID Nemo Model No. 35 to 500 psi at 100 psi/minute rate; hold at this pressure for 4 hours; depressurize at 100 psi/minute rate to zero and relax at that pressure for 4 hours before initiating the next pressure cycle. Repeat the pressure cycle 1000 times.

2. Pressurize the 15-inch OD X 13-inch ID Nemo Model No. 36 to 1000 psi at 100 psi/minute rate; hold at this pressure for 4 hours, depressurize at 100 psi/minute rate to zero and relax at that pressure for 4 hours before initiating the next pressure cycle. Repeat the pressure cycle 1000 times.
3. Pressurize the 15-inch OD X 13-inch ID Nemo Model No. 37 to 1500 psi at 100 psi/minute rate; hold at this pressure for 4 hours; depressurize at 100 psi/minute rate to zero and relax at this pressure for 4 hours before initiating the next pressure cycle. Repeat the pressure cycle 1000 times.

Full Scale Hull

Static Tests

The 66-inch OD X 58-inch ID full scale Model 2000 Nemo Hull assembly was subjected to a series of hydrostatic tests at SWRI, which culminated with a 4000-foot depth proof test; Figure 22 pictures the Model 2000 Nemo Hull with the SWRI pressure vessel. The objectives of the static tests were to (1) establish experimentally the strains and stresses imposed on the Model 2000 Nemo Hull assembly at a 3000-foot operational depth for comparison with the analytically generated data and (2) prove that the full scale Model 2000 Nemo Hull assembly could withstand pressures to a depth of 3000 feet without permanent deformation. To accomplish these objectives, strains were to be recorded during all of the tests at 20 locations; the location of the strain gages on the Model 2000 Nemo Hull is shown in Figure 23.

The static test series consisted of the following tests conducted at a room temperature which ranged between 65–75°F in the pressure test facilities of the Southwest Research Institute, San Antonio, Texas:

1. Pressurize to 450 psi at 100 psi/minute rate, hold at that pressure for 24 hours, depressurize to 0 psi at 100 psi/minute rate, and relax at that pressure for 24 hours prior to beginning of next test.
2. Pressurize to 900 psi at 100 psi/minute rate, hold at that pressure for 24 hours, depressurize to 0 psi at 100 psi/minute rate, and relax at that pressure for 24 hours prior to beginning of next test.
3. Pressurize to 1350 psi at 100 psi/minute rate, hold at that pressure for 24 hours, depressurize to 0 psi at 100 psi/minute rate, and relax at that pressure for 24 hours prior to beginning of next test.
4. Pressurize to 1800 psi at 100 psi/minute rate, hold at that pressure for 24 hours, depressurize to 0 psi at 100 psi/minute rate, and relax at that pressure for 24 hours prior to beginning of next test.

No cyclic tests were performed on the full scale Model 2000 Nemo Hull assembly.

TEST OBSERVATIONS

Model Scale Tests

Stresses

The 15-inch OD X 13-inch ID Nemo Model 34 assembly performed satisfactorily at simulated depths to 3000 feet. The highest measured principal stress of -5086 psi in the acrylic hull was on the interior, located at the edge of the top polar opening (0.500 inches away from aluminum hatch) and orientated along the meridian of the sphere; recorded stress values are listed in Table 4 (also see Figure 19). It is worth noting, however, that its magnitude was approximately only 10 percent larger than the average stress of -4642 psi measured at the equator on the interior of the sphere. This can be explained by the fact that the stress riser effect of the metallic insert decays rapidly with distance from the hatch. Since the strain gage was located approximately 3 degrees away from the edge it did not measure the peak stress but rather the tail end of it.

The maximum stress of -15,714 psi in the polar aluminum inserts was measured on the inside surface, adjacent to the flange, in the bottom plate, and its orientation was in the longitudinal direction.

The highest measured stresses, both on the acrylic hull and the aluminum inserts during the simulated dive to 3000 feet, were well below the yield points of their respective materials. All strains were observed to return to zero upon completion of the relaxation period following the simulated dive to 3000 feet (see Table 4). For both the acrylic plastic and aluminum, the apparent safety factors, based on the short term yielding of material, were well in excess of 2. On the basis of these stress measurements it was concluded that (1) the proposed design of hatches was adequate for dives to 3000 feet and that (2) the whole full scale Model 2000 Nemo Hull assembly could be safety tested at least at depths to 3000 feet.

Implosion Resistance

The 15-inch OD X 13-inch ID Model 34 Nemo Hull imploded under short term pressure loading at a simulated depth of 10,600 feet. The assembly failed by general plastic instability: the fragmented model is shown in Figure 24. The highest measured stresses in the aluminum hatches, prior to implosion, were found to be at locations #4 and #7 (see Figure 19), and their magnitude was in the -35,000 to -39,000 psi range, as shown in Figure 25. The 10,600-foot short term implosion depth of Model 34 gives the scale model a 3.5 safety margin for catastrophic dives. Data reduction of the hydrostatic tests is documented in Appendix C.

Acoustic Emission

The 15-inch OD X 13-inch ID Model 34 was a good source of acoustic emission during the first pressurization to 1350 psi; Figure 26 presented a histogram of stress wave

Table 4. Strains in 15 Inch OD X 13 Inch ID Nemo Model #34 during Simulated Dive at Depths to 3000 Feet

Gages			Strain micro inches/inch		Stress (psi)	
No.	*Location*		*Hoop*	*Longitudinal*	*Hoop*	*Longitudinal*
1a	Equator, outside	A	-5,900*	-5,700*	-3,345*	-3,284*
		B	-6,700	-6,300		
		C	0	-100		
1b	Equator, inside	A	-8,200*	-8,000*	-4,681*	-4,604*
		B	-9,550	-8,900		
		C	+10	+25		
2b	Edge of top polar opening, inside	A	-6,900*	-9,500*	-4,286*	-5,086*
		B	-7,700	-1,100		
		C	-50	-100		
3b	Lip of flange, bottom plate; inside	A	-900*	+150*	-9,386*	-1,319*
		B	-900	+150		
		C	0	0		
4a	Root of flange, bottom plate; outside	A	-275*	-50*	-3,187*	-1,456*
		B	-275	+100		
		C	0	0		
4b	Root of flange, bottom plate; inside	A	-600*	-1,250*	-10,714*	-15,714*
		B	-700	-1,350		
		C	0	0		
5a	Root flange, top hatch, outside	A	-100*	malfunc-	-1,099*	-330*
		B	-100	tioning		
		C	0	s. gage 0		
5b	Root of flange, top hatch, inside	A	-1,100*	-200*	-12,747*	-5,824*
		B	-1,100	-200		
		C	0	0		
6b	Edge of bottom, polar opening, inside	A	-8,300*	-6,900*	-4,558*	-4,127*
		B	-9,200	-7,800		
		C	0	+250		
7b	Lip of flange, top hatch, inside	A	-1,300*	+300*	-13,297*	-989*
		B	-1,300	+300		
		C	0	0		

Note A.* Immediately after pressurization to 3000 foot depth
B. After four (4) hours at 3000 foot depth
C. After 16 hours of relaxation at 0 depth

emissions. When, after relaxation at 0 psi, Model 34 was pressurized to 900 psi no further acoustic emission bursts were recorded which indicated that the acrylic hull exhibits a very marked Kaiser effect.

During the final pressure test to implosion, Model 34 emitted significant numbers of acoustic emissions, although only after the pressure passed the 9500-foot depth mark. Thus, between 0 and 9500 feet there were less than 50 emissions, as shown in Figure 27. Obviously then, the impending implosion of the acrylic hull could have been stopped during the simulated dive at about 500 feet above implosion depth on the basis of the acoustic emission recording (see Fig. 26).

Cyclic Fatigue Crazing

Observation of 15-inch OD X 13-inch ID Models 35, 36 and 37, after 1000 simulated 4-hour long dives, shown in Figure 28, revealed that only Model 37 which was pressure cycled to a depth of 3360 feet had slight indication of cyclic fatigue, whereas Models 35 and 36 which were pressure cycled to, respectively, 1120 and 2240 feet showed no signs of cyclic fatigue. The cyclic fatigue in Model 37 exhibited slight crazing of its conical bearing surface in the polar opening of the acrylic hull, which was exposed to direct contact with the metallic insert; see Figure 29. The other polar opening in Model 37, in which the acrylic bearing surface was not in direct contact with the metallic insert did not craze. From this, it can be concluded that at a cyclic history of less than 1000 dives the polycarbonate gasket has a significant effect only when the maximum pressure in a dive is 3360 feet or more. At lesser depths the polycarbonate gasket also increases the fatigue life of the acrylic hull, although more than 1000 dives are required to show experimentally the beneficial effect of the polycarbonate gasket.

It is important to point out here that even in Model 37 which was the only specimen with signs of cyclic fatigue on the acrylic bearing surface, the fatigue exhibited itself in the form of barely noticeable crazing. Based on past experience,[5] it can be conservatively predicted that it would take at least another 1000 dives to 3360 feet before the crazing would deteriorate into cracks 1/2-inch deep and thus require remachining of the bearing surface.

Creep

The creep observed during 4 hour sustained loading to 1350 psi was significantly higher than during sustained loading to 900 psi, as shown in Figures 30 and 31. The magnitude of creep in both cases was about 15 percent of short term strain. As expected (magnitude of creep is a function not only of time but also of short term strain), creep was more substantial at the edges of polar openings than at the equator. Similarly, it was larger on the interior of the hull than on its exterior.

The creep returned to zero after several hours of relaxation at zero pressure, indicating that the creep observed did not represent permanent deformation of plastic.

Full Scale Tests

General Performance

The 66-inch OD X 58-inch ID Nemo Model 2000 withstood successfully the four successive 24-hour hydrostatic pressure loadings to 450, 900, 1350 and 1800 psi without any appearance of cracks in the acrylic and only minor surface cracking in the polycarbonate plastic bearing surfaces at the polar openings.

Strains

The magnitude of strains observed during the 24-hour pressurization tests is shown in Figure 32; recorded stress values are listed in Table 5. Stress range was predicted by (1) the ZIP-13 finite element computer program and (2) strains generated during the hydrostatic testing of the 15-inch OD X 13-inch ID Model 34. The fact that the acrylic hull of Model 34 was approximately 10 percent thicker than required by the 1:4.4 scaling factor had to be taken into consideration during comparison of strains measured on the 15-inch and 66-inch diameter hulls.

The highest strains in acrylic plastic were measured on the interior of the hull at the edge of the top polar opening. The strains at the edge of the bottom polar opening were about 10 percent less, reflecting the fact that the bottom aluminum plate is significantly less stiff than the top hatch. The ratios between longitudinal and hoop strains at both locations were in the 3:1–4:1 range.

The interior longitudinal strain at the top polar opening was 100 percent greater than the interior longitudinal strain at the equator, while the interior hoop strain at the top polar opening was 50 percent less than the interior hoop strain at the equator. The exterior longitudinal strain at the top polar opening was only 20 percent greater than the exterior longitudinal strain at the equator, while the exterior hoop strain at the top polar opening was 70 percent less than the exterior hoop strain at the equator. On the aluminum polar inserts the highest strain was measured on the interior surfaces of (1) the bottom plate at location #6 in longitudinal direction and (2) the top plate at location #13 in longitudinal direction (see Fig. 23).

Magnitude of *Creep* at the equatorial surfaces of the hull was approximately the same as that recorded for Model 34. It was for all practical purposes absent during the 24 hour pressurizations to 450 and 900 psi, but it became noticeable (20–25 percent increase over short term strain) during 1350 psi pressurization and was significant (25–30 percent increase) during 1800 psi pressurization, as can be seen in Figure 32a through l. The numerical value of strains on the interior surface at the equator after 24 hours of sustained loading was in the 2500–3000, 5000–6000, 9000–11,000 and 13,000–15,000 micro inches/inch range for, respectively, 450, 900, 1350 and 1800 psi pressurizations. (See Figs. 32i and 32j.)

The numerical values of creep on the interior hull surface at the edges of top and bottom penetrations were higher than at the equator, but in terms of short term strain percentage they were not different from those at the equator. After 24 hours of sustained loading the longitudinal strains at penetrations were in the 4000–4500, 8000–10,000, 15,000–19,000 and 22,000–27,000 micro inches/inch range for, respectively, 450, 900, 1350 and 1800 psi

Table 5. Stresses in 66 Inch OD X 58 Inch ID Nemo Model 2000 Assembly During the 24 Hour Dive to a Depth of 3000 Feet

Gages		*Stress (psi)*	
Hull Location	*Orientation*	*Upon reaching 3000 feet*	*After 24 hours*
Inside #1	Hoop	-4,986	
	Longitudinal	-7,914*	
Outside #1	Hoop	-2,348	
	Longitudinal	-3,819	
Inside #2	Hoop	-5,476	
	Longitudinal	-5,290	
Outside #2	Hoop	-4,214	
	Longitudinal	-4,186	Stresses cannot be calculated because of creep in acrylic
Inside #3	Hoop	-4,486	
	Longitudinal	-6,714	
Outside #3	Hoop	-1,900	
	Longitudinal	-3,400	
Inside #4	Hoop	-5,595	
	Longitudinal	-5,438	
Outside #4	Hoop	-4,086	
	Longitudinal	-4,014	
Inside #5	Hoop	-10,495	-9,396
	Longitudinal	-11,648	-11,319
Outside #5	Hoop	-5,000	-4,835
	Longitudinal	-5,000	-4,451
Inside #6	Hoop	-13,626	-13,956
	Longitudinal	-17,088**	-18,187**
Outside #6	Hoop	-6,264	-5,549
	Longitudinal	-5,879	-5,165
Inside #7	Hoop	-13,297	-12,967
	Longitudinal	-10,989	-9,890
Outside #7	Hoop	-6,429	-6,429
	Longitudinal	-6,429	-6,429

*Highest stress in acrylic hull (during conversion of strains to stresses E = 400,000 psi and μ = 0.4 were applied).

**Highest stress in polar aluminum inserts (during conversion of strains to stresses E = 10,000,000 psi and μ = 0.3 were applied).

Table 5. (Continued).

Gages		*Stress (psi)*	
Hull Location	*Orientation*	*Upon reaching 3000 feet*	*After 24 hours*
Inside #8 Outside	Hoop	-13,022	-13,187
	Longitudinal	-3,407	-3,956
	Hoop	-3,516	-2,967
	Longitudinal	-55	+110
Inside #9 Outside	Hoop	-10,549	-9,341
	Longitudinal	-15,165	-12,802
	Hoop	-4,780	-4,780
	Longitudinal	-5,934	-5,934
Inside #10 Outside	Hoop	-10,549	-9,835
	Longitudinal	-10,165	-9,451
	Hoop	-4,670	-4,670
	Longitudinal	-3,901	-3,901
Inside #11 Outside	Hoop	-10,165	-9,066
	Longitudinal	-10,549	-10,220
	Hoop	-3,736	-3,736
	Longitudinal	-4,121	-4,121
Inside #12 Outside	Hoop	-11,429	-11,429
	Longitudinal	-11,429	-11,429
	Hoop	-3,956	-3,956
	Longitudinal	-3,187	-3,187
Inside #13 Outside	Hoop	-11,758	-13,352
	Longitudinal	-12,527	-14,505
	Hoop	-3,956	-6,813
	Longitudinal	-3,187	-6,044
Inside #14 Outside	Hoop	-12,692	-14,286
	Longitudinal	-12,308	-14,286
	Hoop	-4,670	-7,527
	Longitudinal	-3,901	-6,758

pressurizations (see Figs. 32b and 32f). Strains in acrylic returned essentially to zero after a 24-hour period of relaxation indicating that the creep in acrylic was not of a permanent nature even after the 24 hour sustained loading to 1800 psi hydrostatic pressure.

Stresses

The *maximum stress* measured on the *acrylic hull* (see Table 5) at the beginning of 24 hour pressurizations was -2339, -5043, -7914 and -10,962 psi at, respectively, 450, 900, 1350 and 1800 psi pressure loadings. The maximum stress, analyzed as typical for Nemo hulls,[14] was located on the interior surface of the hull at the edge of top polar opening and was oriented in the longitudinal direction. The stress on the interior equatorial surface was measured simultaneously as -1804, -3610, -5595 and -7757 psi. The magnitude of stress on the acrylic hull at the conclusion of the 24 hour pressurization periods is not known since there was considerable creep in the plastic which would make any classical stress calculations inaccurate.

The *maximum stress* on the aluminum inserts was measured on the interior of the bottom plate at location No. 6 in the longitudinal direction. The magnitude of the stress at the beginning of 24 hour pressurizations was -4967, -9890, -17,088 and -21,044 psi at, respectively, 450, 900, 1350 and 1800 psi loadings. At the conclusion of the 24-hour pressurization periods the magnitude of the stress had changed to -3198, -9890, -18,187 and -18,846 psi, respectively. After the 24-hour relaxation periods following pressurizations to 450, 900 and 1350 psi, all stresses in aluminum returned essentially to zero, as listed in Table 6. A different case presented itself at the conclusion of the relaxation period following the 24-hour pressurization to 1800 psi. Here the stresses at interior location Nos. 6, 13 and 14 on aluminum inserts not only failed to return to zero (see Table 6) but showed residual positive stresses of significant magnitude, and the reasons for their presence are not known. A more detailed listing of stresses is presented in Appendix C.

The *comparison* of stresses calculated on the basis of experimental data and the ZIP-13 finite element computer program show good agreement for all locations on the acrylic hull. For locations on aluminum inserts the agreement is not as good. It appears that for the locations on the exterior of aluminum inserts the calculated stresses are generally lower than measured values, whereas for locations on the interior of the inserts the calculated values are generally higher. However, since the highest stresses measured on aluminum inserts were on the interior surface, the calculated values tend to be conservative in nature and, thus, useful in the design of pressurized Nemo Hulls. A complete listing of computer generated strains and stresses for the Model 2000 Nemo Hull assembly is presented in Appendix D.

Table 6. Residual Strains in Aluminum Plates and Hatches of the 66 Inch OD X 58 Inch ID Nemo Model 2000 after Repeated 24 Hour Long Pressurizations

		Gage Locations					
		No. 6 Inside		*No. 13 Inside*		*No. 14 Inside*	
Test		*Hoop*	*Longitudinal*	*Hoop*	*Longitudinal*	*Hoop*	*Longitudinal*
450 psi	A	-240	-380	-190	-200	-250	-140
	B	-170	-240	-120	-140	-250	-140
	C	+120	+150	+100	+110	+10	+80
	D	+160	+180	+130	+210	+80	+60
900 psi	A	-500	-750	-450	-500	-500	-500
	B	-500	-750	-450	-500	-500	-500
	C	0	+100	+50	+0	+50	0
	D	+50	+150	+100	+0	+100	50
1350 psi	A	-850	-1300	-800	-900	-900	-850
	B	-850	-1400	-900	-1050	-1000	-1000
	C	0	0	+0	-100	-100	-150
	D	0	0	+0	-150	-200	-200
1800 psi	A	-1050	-1400	-1000	-1150	-1150	-1100
	B	-1050	-1400	-850	-1050	-1050	-1000
	C	+50	+300*	+200*	+100*	+50*	+500*
	D	-50	+2350*	+1450*	+1350*	+1350*	+1250*

A – Immediately after pressurization
B – After 24 hours of sustained pressurization
C – Immediately after pressure release
D – After 24 hours of relaxation
* – Questionable values, probably generated by malfunctioning bulkhead penetrators for instrumentation in Model 2000 Nemo Hull, or pressure vessel end closure.

TEST DATA DISCUSSION

Determination of Safe Operational Depth

In order for the chosen operational depth to be safe, many operational, as well as hull performance parameters, must be considered and carefully calculated.

Hull Performance Parameters

The *short term critical pressure* at which catastrophic implosion of the hull occurs in an uncontrolled dive is the best known and easiest to obtain performance parameter of an acrylic hull. The short term critical pressure represents the ultimate depth beyond which a submersible cannot descend at any time. For the Model 2000 Nemo Hull the short term critical pressure has been experimentally established at approximately 10,000 feet. The actual short term implosion test was performed on the 15-inch Model 34, which imploded at 4700 psi external hydrostatic pressure. Since the scale model is about ten percent thicker than required, the extrapolated short term implosion pressure for the full scale Model 2000 Nemo Hull is around 4000 psi if the same pressurization procedure is used as for the scale model. However, since the pressurization schedule for Model 34 did not correspond to the typical 100 psi/minute short term pressurization rate for acrylic hulls[2] (recording of strain data at 4500 and 4700 psi pressure levels delayed the pressurization by 5 minutes), the extrapolated short term collapse pressure for the Model 2000 Nemo Hull must be increased from 4000 psi to at least 4500. (Reference 6 indicates that the effect of delay in pressurization at pressures above 4500 psi is to reduce the short term implosion pressure of acrylic hull by about 100 psi for every minute of delay.) The 10,000-feet short term implosion depth gives the Model 2000 Nemo Hull the ability to bounce dive once under extreme emergency conditions probably to at least 8000 feet.

The *long term critical pressure of acrylic hulls* has been previously established[6] as a function of time and temperature. Because 100 hours is considered the maximum length of time that the crew of a submersible could survive under entrapment without new air support supplies, this time span will be used to establish a long term critical pressure. This pressure can be readily determined from a plot of experimental data generated by implosions of 15-inch OD X 13-inch ID Models 22, 23, 24, 25 and 34, as illustrated in Figure 33.[6] From the plot one can see that the implosion pressure of a scale model Nemo Hull under 2700 psi sustained loading at 70–75°F at ambient temperatures occurs after 100 hours. After application the 0.86 correction factor (based on plastic instability, takes into account the ten percent thicker hull of scale models), the projected 100 hour long term critical pressure of the Model 2000 Nemo Hull is 2320 psi in the 70–75°F ambient temperature range. In terms of depth it can then be stated that the Model 2000 Nemo Hull must be trapped for at least 100 hours at a depth of about 5000 feet before catastrophic failure occurs.

The *cyclic fatigue life* of acrylic hulls has been the subject of several studies since, as a rule, it is the determining factor in setting the safe operational depth of an acrylic hull. Since the cyclic fatigue life is not only a function of maximum pressure in the pressure cycle but also of duration and temperature, they all must be taken into consideration. Study of typical dive profiles for submersibles has established the fact that a submersible does not

stay at maximum operational depth longer than 4 hours. The rest of the typical dive is taken up by launching, descent, ascent, docking and retrieval. The temperature can vary widely during a dive but at operational depths it is usually below 50 degrees. Since pressure cycling at 70–75°F is not only more conservative, but also more economical, it was used to establish the cyclic fatigue life of the Model 2000 Nemo Hull.

The testing of 15-inch Models 35, 36 and 37 has conclusively shown that crazing appears in the acrylic hull at the polar openings without the polycarbonate gasket only after 1000 pressure cycles of 8-hour duration (4 hours loading followed by 4-hours relaxation) to 1500 psi. No crazing was observed in the polar opening of the acrylic hull protected by the polycarbonate gasket. Judging by these results the minimum crack-free fatigue life of the 15-inch OD X 13-inch ID Models is 1000 cycles to a maximum operational depth of 3350 feet. Based on the scale model data, the 66-inch OD X 58-inch ID Model 2000 Nemo Hull can perform 1000 dives to 3000 feet without initiation of cracks in the acrylic hull.

Operational Performance Parameters

In view of the fact that preservation of the crew is the major consideration in the design of pressure hulls it is considered mandatory that the short-term and long-term critical pressures be beyond the depth to which the submersible may be accidentally submerged. Furthermore, it is considered reasonable and customary that the implosion depth for a long term (no more than 100 hours) disabled submersible be at least 50 percent greater than the maximum operational depth (safety factor of 1.5). For a short term loss of control, the implosion depth should be at least 100 percent greater than the maximum operational depths (safety factor of 2).

In addition to preserving the crew there are also the economics of the hull life to be considered. If the fatigue life was set at 100 dives it would prove economically unsound since it would allow the submersibles to operate only for a period of time less than two years, although at greater depths. Similarly, if the fatigue life was stipulated as 10,000 cycles it would give the submersible unlimited life but at the cost of very shallow operational depth, which would significantly lower its operational usefulness. It is the author's opinion that a specified crack-free fatigue life of 1000 cycles represents a sound economical compromise between the operational depth and life of the submersible. For the full scale Model 2000 Nemo Hull the crack-free fatigue life has been experimentally established as 1000 dives to a maximum operational depth of 3000 feet. Since the 3000-foot fatigue life depth is based on 4-hour long simulated dives, there is no need to apply any pressure cycle duration discounting factor to the experimentally established fatigue life depth of 3000 feet.

Based on the factors discussed above, the maximum operational depths should not exceed 4000 feet (8000 feet/2) for short term disablement criterion, 3330 feet (5000 feet/1.5) for long term disablement criterion, and 3000 feet (3000 feet/1) for the fatigue life criterion. Since it is the least permissible operational depth, based on any of the above three criteria, that determines the actual depth rating of the hull, fatigue becomes the determining factor for establishing the operation depth rating of the Model 2000 Nemo Hull. As a result 3000 feet is considered as the maximum operational depth rating for the Model 2000 Nemo Hull.

FINDINGS

1. The 66-inch OD X 58-inch ID spherical capsule assembly, Model 2000 Nemo Hull, fabricated from commercial grade (Plexiglas G or equivalent) acrylic plastic and equipped with polycarbonate gaskets between aluminum hatches and the acrylic plastic will withstand a minimum of 1000 dives (4 hours at maximum depth, followed by 4 hours at the surface) from 0 to 3000 feet without initiation of cracks in the acrylic hull.

2. At the safe maximum operational depth of 3000 feet the maximum compressive stresses in aluminum hatches and acrylic plastic hull are only equal to 49 and 52 percent of, respectively, aluminum and acrylic plastic yield strengths.

3. Model 2000 Nemo capsule assembly will withstand accidental disablement at a depth of 5000 feet for at least 100 hours before catastrophic failure occurs. At greater depths the grace period prior to catastrophic failure is significantly shorter, as shown in Figure 33.

4. Model 2000 Nemo capsule assembly will withstand a temporary loss of control to a depth of 8000 feet for about 10 minutes before catastrophic failure occurs.

5. Model 2000 Nemo capsule assembly is an active acoustic stress wave emitter whose rate of acoustic emissions increases significantly just prior to short term implosion.

6. Permanent deformation of aluminum inserts (top hatch and bottom plate) takes place in areas of high stress concentrations when Model 2000 Nemo Hull is subjected to dives of 4000 feet.

7. Long term submersion of 24-hour duration, to 4000-foot depth, does not generate any cracks in the acrylic plastic hull or polycarbonate gaskets at the polar openings and the strains in acrylic plastic after a 24 hour relaxation period at atmospheric pressure return essentially to zero.

CONCLUSION

Spherical acrylic plastic hulls of Nemo Hull design with a $t/r_o = 0.123$ thickness can be man-rated for a minimum of 1000 operational dives to a maximum operational depth of 3000 feet.

OPERATIONAL RECOMMENDATIONS

1. The Model 2000 Nemo capsule assembly should, during its operational life, never be subjected to depths greater than 3300 feet. The proof test should preferably utilize a test depth of 3300 feet. Under no conditions should the magnitude of proof-test depth exceed 3600 feet unless stronger polar inserts are substituted for the standard Model 2000 Nemo Hull aluminum inserts.

2. The cyclic crack free fatigue life of the Model 2000 Nemo Hull should be *conservatively* considered to be in excess of 12,000,000-feet-hours (1000 cycles X 3000 foot depth X 4 hours duty). At the conclusion of each dive, the recorded feet-hours should be subtracted from the initial 12,000,000-feet-hour fatigue life. When the sum of feet hour subtotals generated by dives equals 12,000,000-feet-hours, inserts and gaskets should be removed from the capsule and the entire hull subjected to a detailed visual examination.

If no cracks are observed at the penetrations in the hull, the capsule should be strain gaged, reassembled, prooftested to 3300 feet and resulting strains compared to those generated during the first proof test conducted immediately after fabrication of the capsule. Significant differences in strain behavior will be considered important evidence of hull deterioration and should result in significantly reduced depth rating. Cracks in bonded joints originating at inclusions will be repaired if their length exceeds 0.5 inches. Cracked polycarbonate gaskets should be replaced with new gaskets.

If no significant difference in strain behavior is observed, the capsule assembly will be returned to service with a 3000 foot operational depth rating and an additional 12,000,000-foot-hour fatigue life. When the 12,000,000-foot-hour life is used up the capsule assembly will be subjected to the same inspection and prooftesting procedures conducted at conclusion of the first 12,000,000-foot-hour period. If the results of the new inspection and prooftesting are satisfactory, the capsule will again return to service with a 3,000-foot depth rating and additional 12,000,000-foot-hour life.

The recertification process will be repeated until either cracks are observed in the bearing surfaces of acrylic hull during one of the inspections or the strains change significantly. If cracks are observed they will either be repaired by routing and recasting with resin prior to retesting of the hull, or they will be left in place and the hull's depth rating will be reduced to 600 feet.

Subsequently, the hull will be inspected without disassembly for signs of crack propagation every 100 dives. When the depth of any crack exceeds 1 inch, as pictured in Figure 34, the capsule will be taken out of service immediately and the cracks repaired either by enlarging the polar opening or by recasting cracked areas. If not repaired, such a hull can be recertified for service to 120 feet. If, during periodic inspections conducted every 100 dives, the depth of the crack at the penetration is found to exceed 2 inches the acrylic hull will either be repaired or declared unfit for manned operation at any depth.

3. Attempts should be made to ensure that operators be seated inside the Nemo Hull as close as possible to the center of the sphere in order to minimize optical distortion.[15] Camera mounting should be located at the center of the hull if wide angle panning with the camera is to be performed during the mission.

Objects in hydrospace will appear smaller and closer to the hull than they are in reality.[15] Some experience on the part of the crew will be required to judge the distances correctly between the hull and the objects in hydrospace.

4. Many functions of the equipment mounted externally to the submersible can be controlled by modulated light beams projected from the interior of the hull by the crew.[16] This type of arrangement will eliminate many electrical penetrators in the bottom plate and make the control of externally stored scientific equipment an operationally easy matter.

Figure 1. Acrylic plastic hull with the typical Nemo polar penetrations, metallic hatches, and spherical pentagon modular construction.

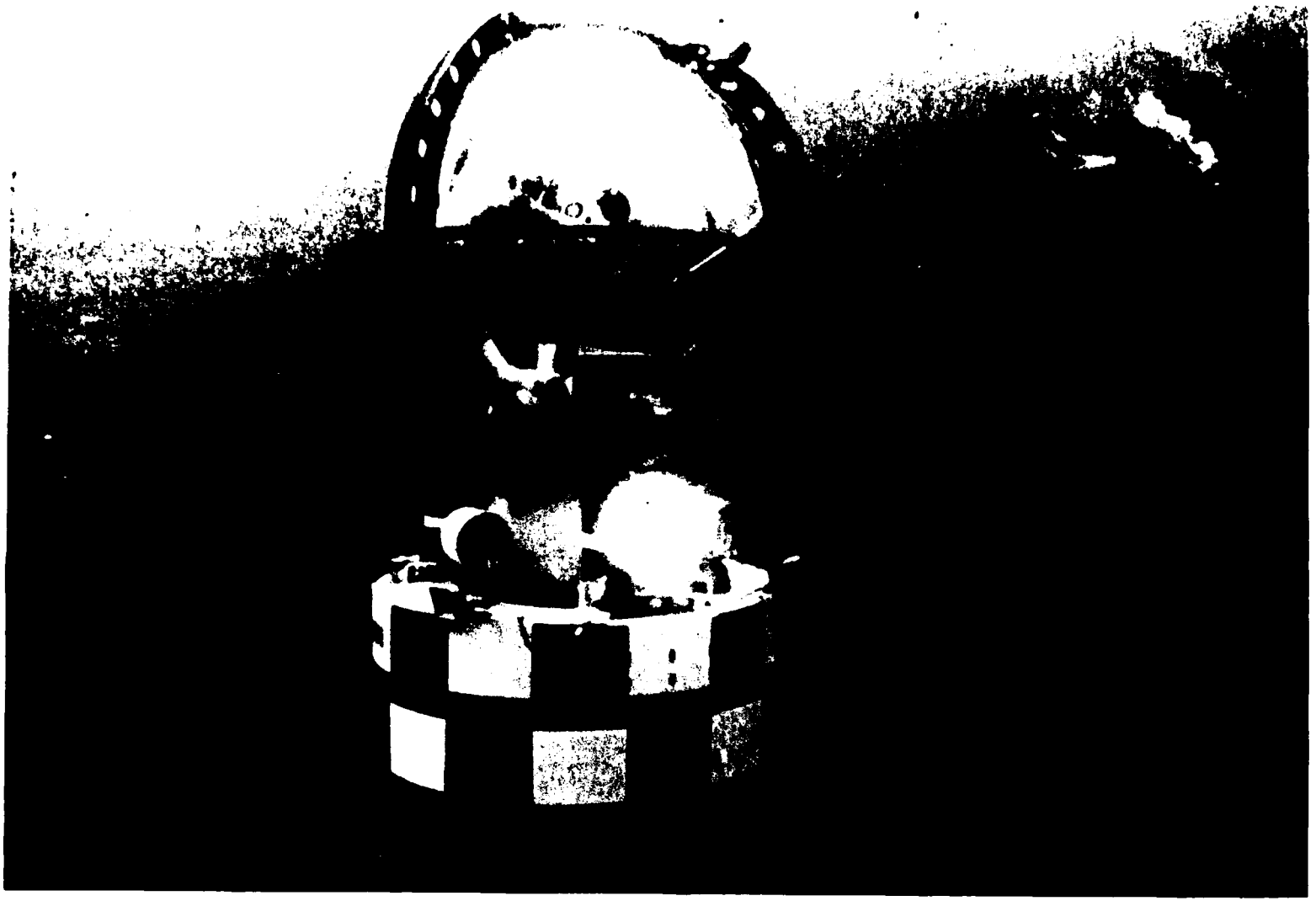

Figure 2. Nemo submersible, approved in 1970 by the U. S. Navy for manned operations to 600 feet.

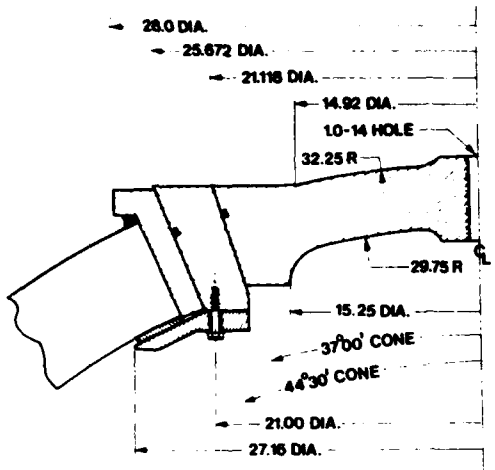

TOP HATCH DETAIL

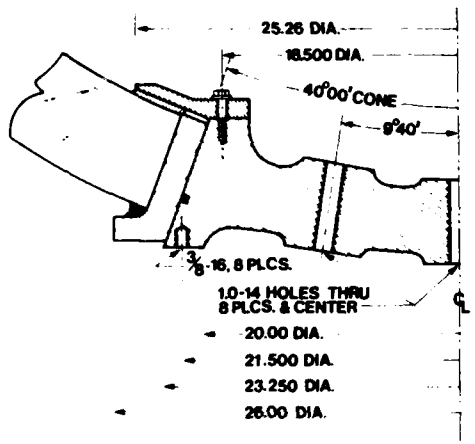

BOTTOM PLATE DETAIL

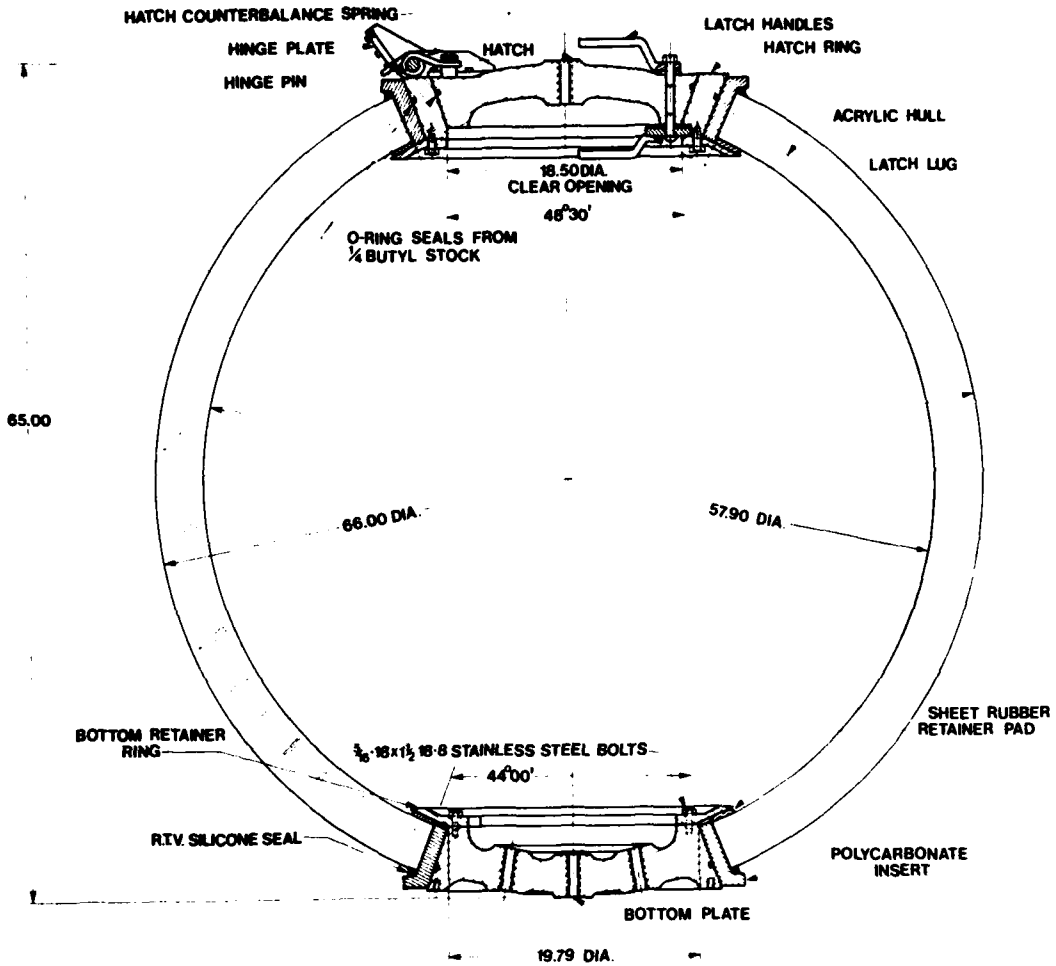

Figure 3. Schematic of the Model 2000 Nemo Hull.

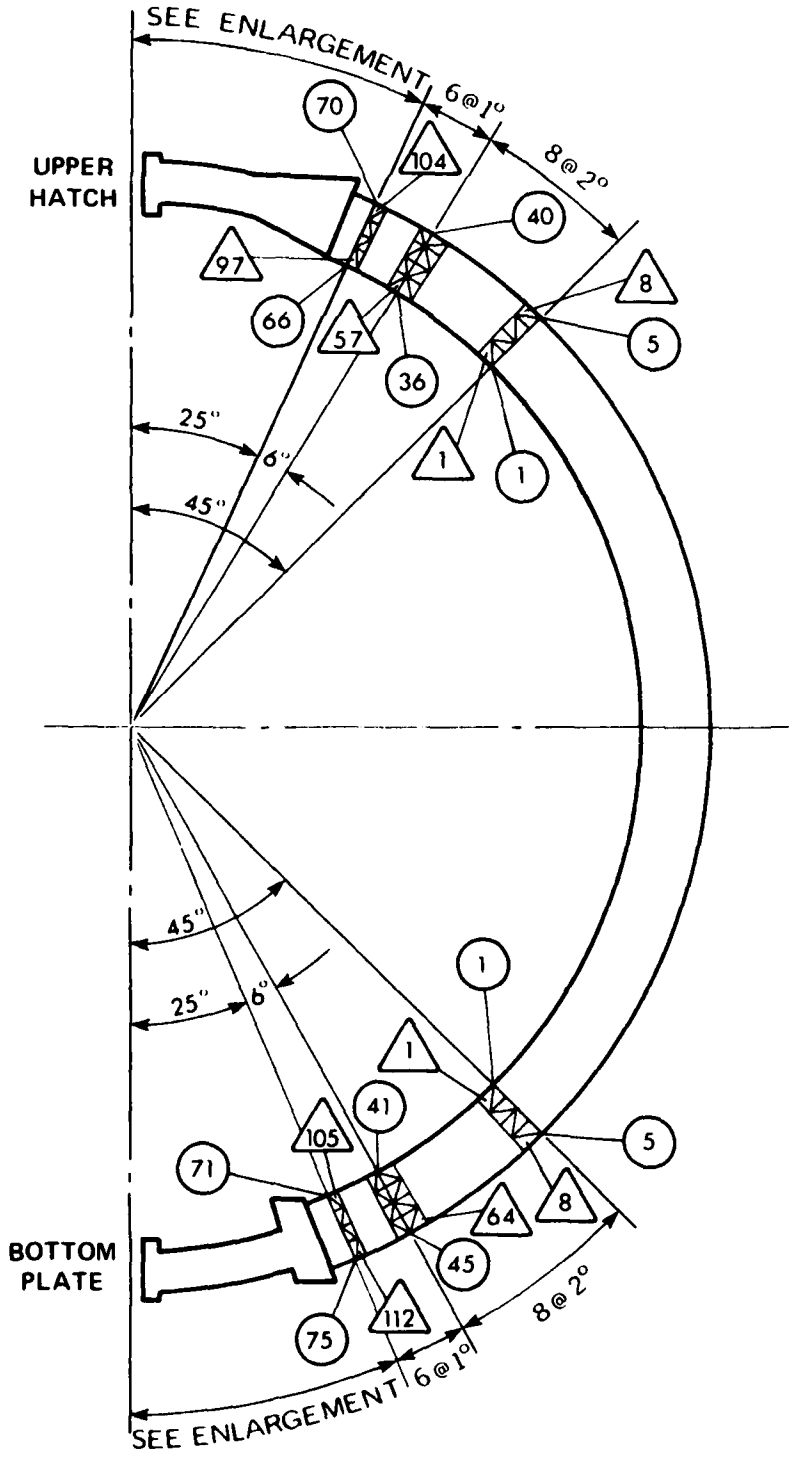

Figure 4. Idealized shape of the Model 2000 Nemo Hull assembly used in the ZP 13 finite element stress analysis.

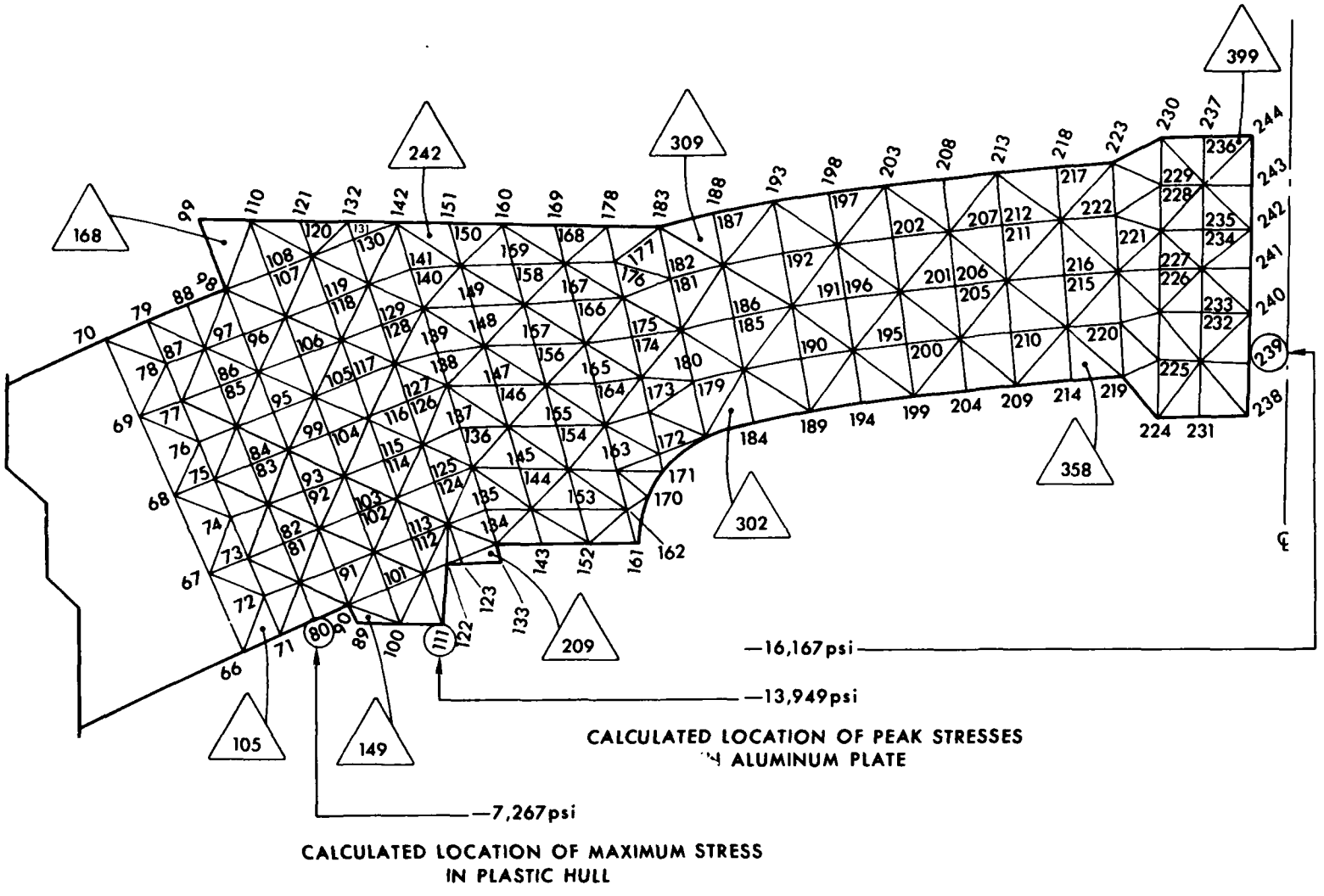

Figure 5. Idealized shape of the top hatch used in the ZP 13 finite element stress analysis of the Model 2000 Nemo Hull under simulated 900 psi external hydrostatic pressure.

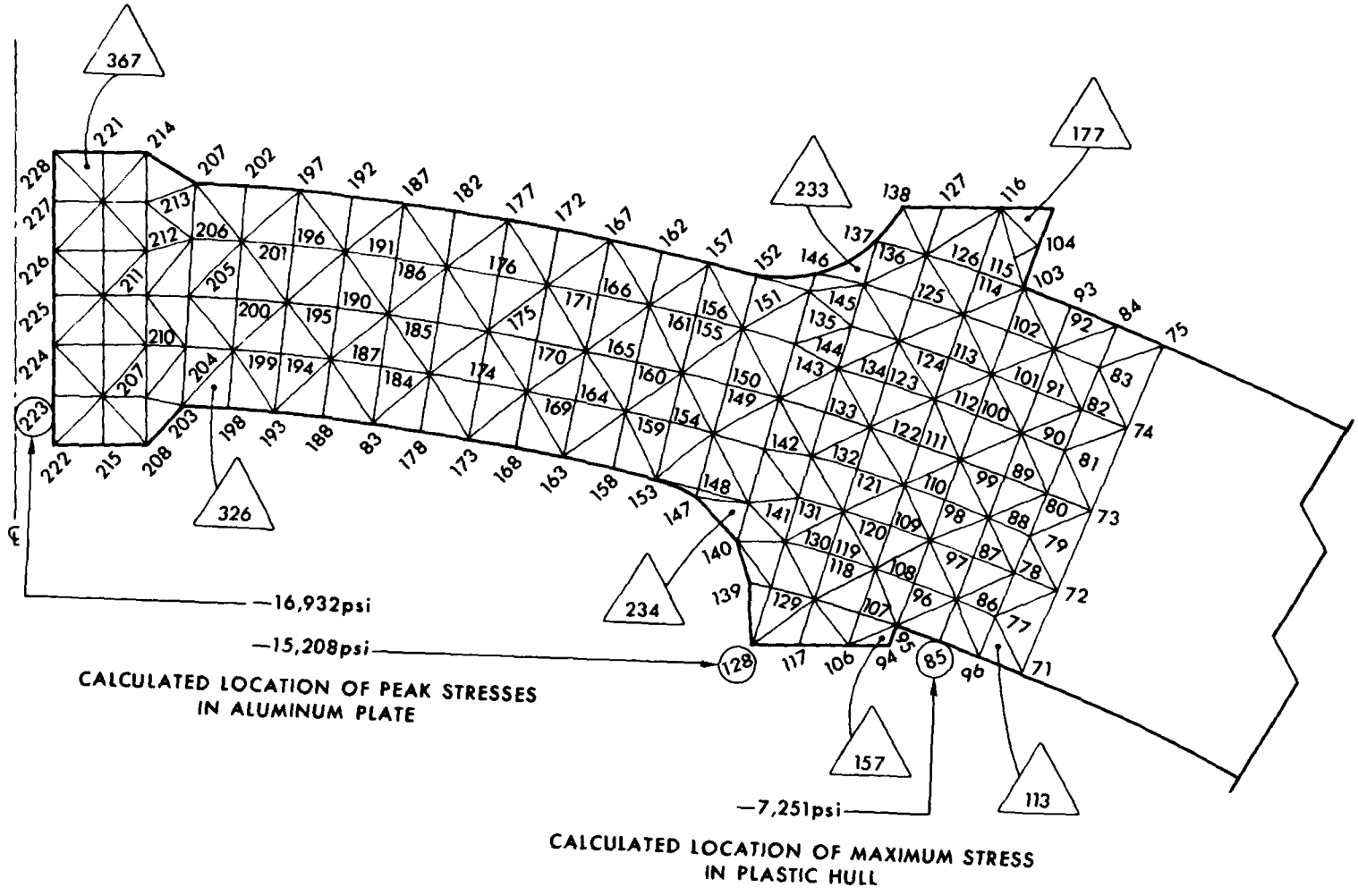

Figure 6. Idealized shape of the bottom plate used in the ZP 13 finite element stress analysis of the Model 2000 Nemo Hull under simulated 900 psi external hydrostatic pressure.

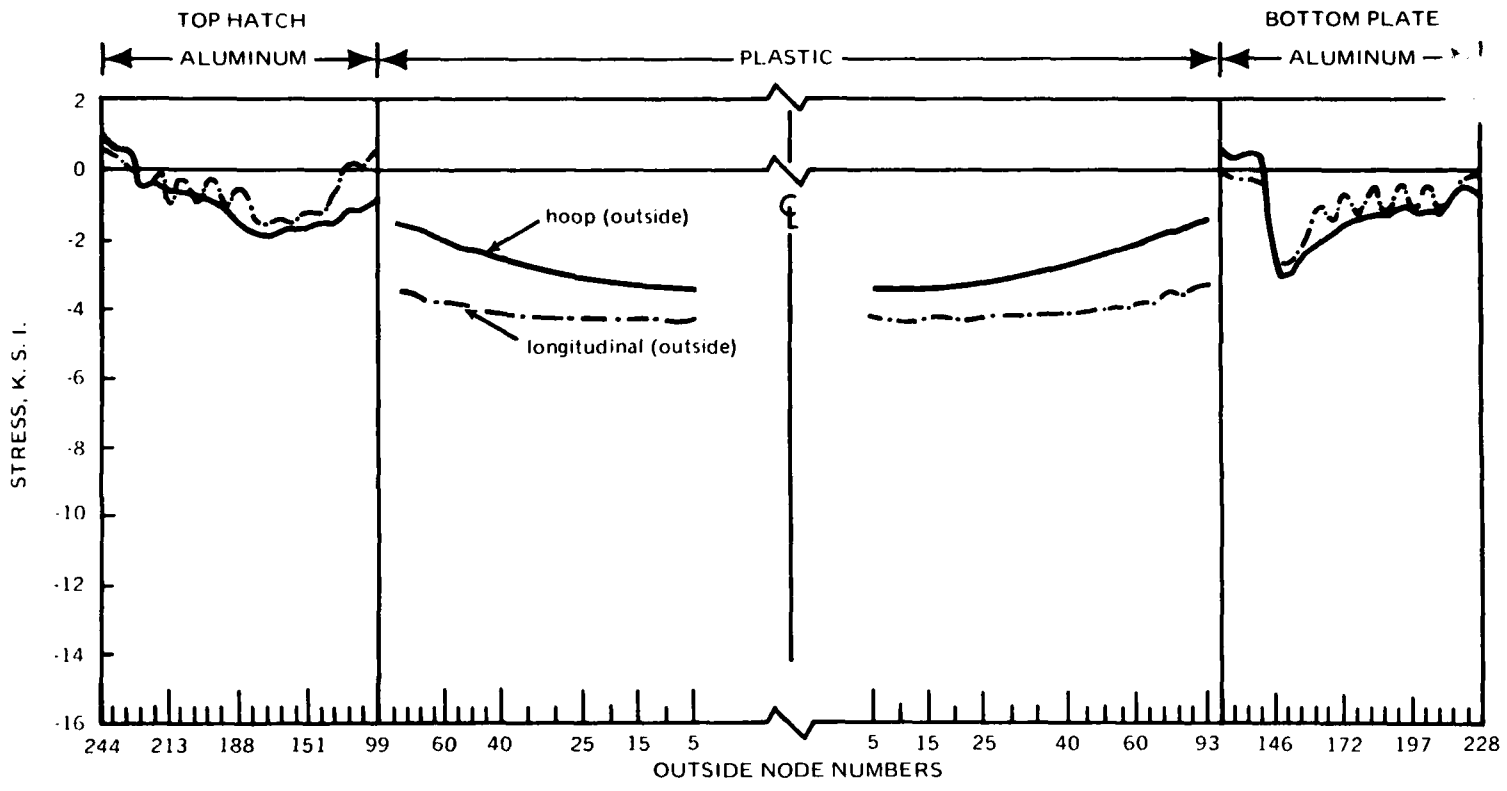

Figure 7. Calculated stress distribution in the Model 2000 Nemo Hull assembly under simulated 900 psi external hydrostatic pressure, outside surface.

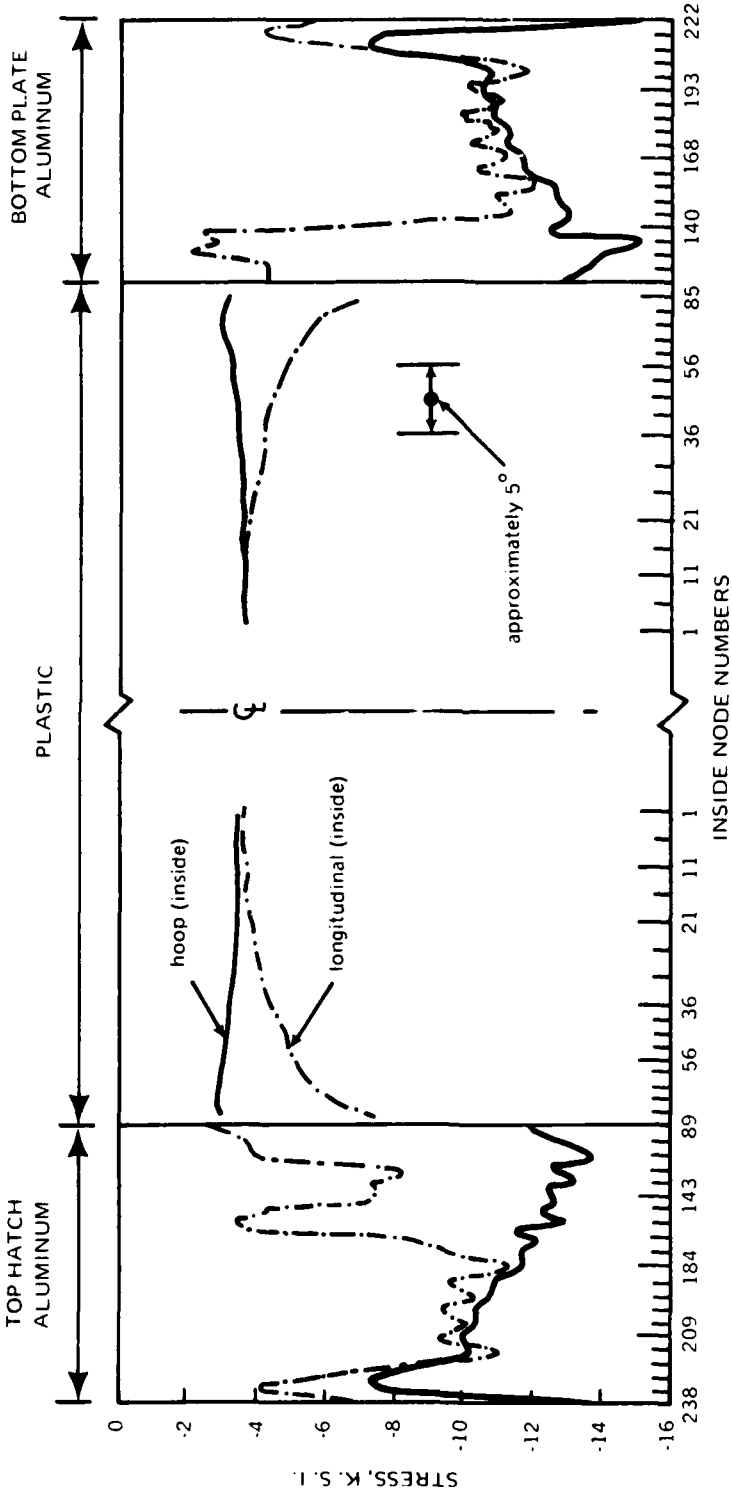

Figure 8. Calculated stress distribution in the Model 2000 Nemo Hull assembly under simulated 900 psi external hydrostatic pressure; inside surface.

Figure 9. Assembled Model 2000 Nemo Hull undergoing final polishing.

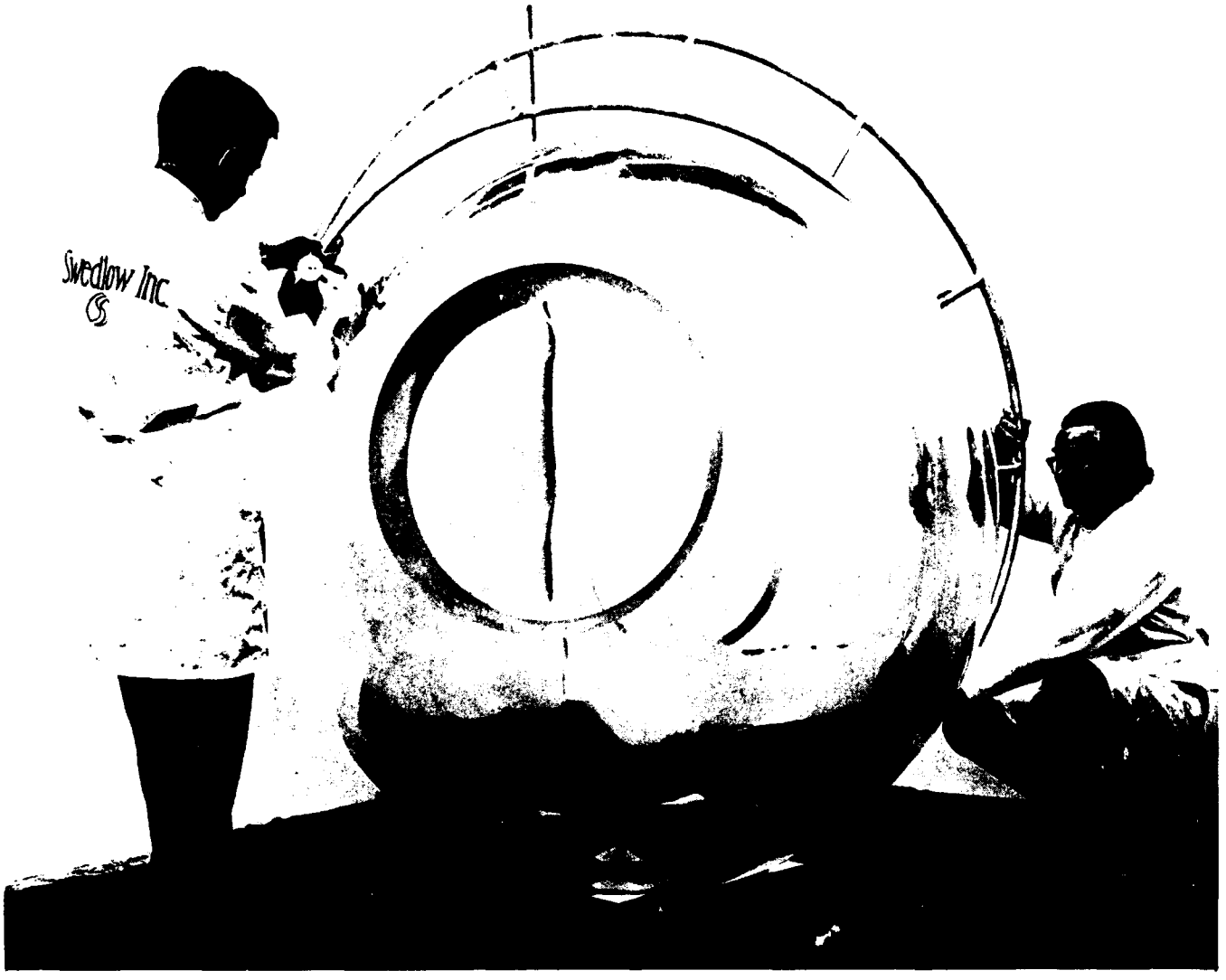

Figure 10. Inspection of Model 2000 Nemo Hull for out-of-roundness at Swedlow Inc.

Figure 11. Typical bonded joint between spherical pentagons.

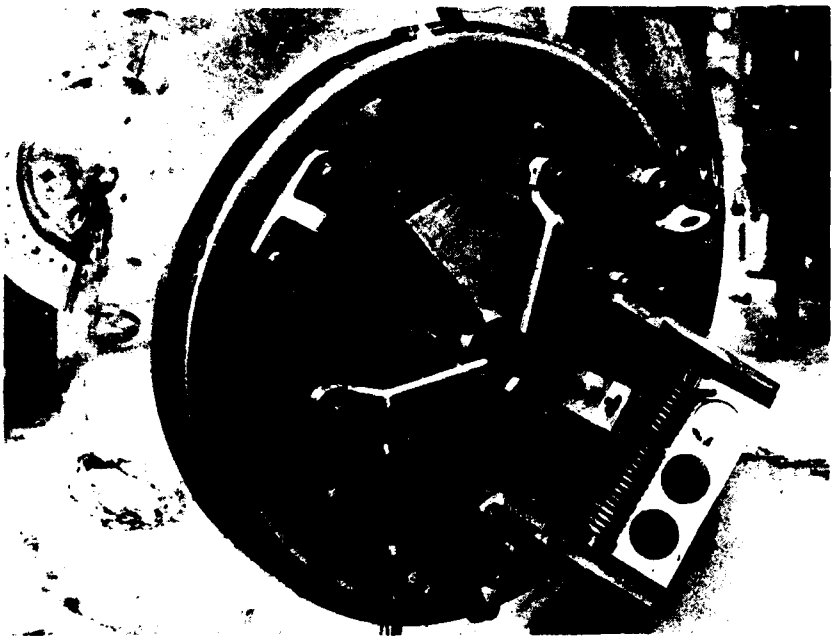

(a) outside view

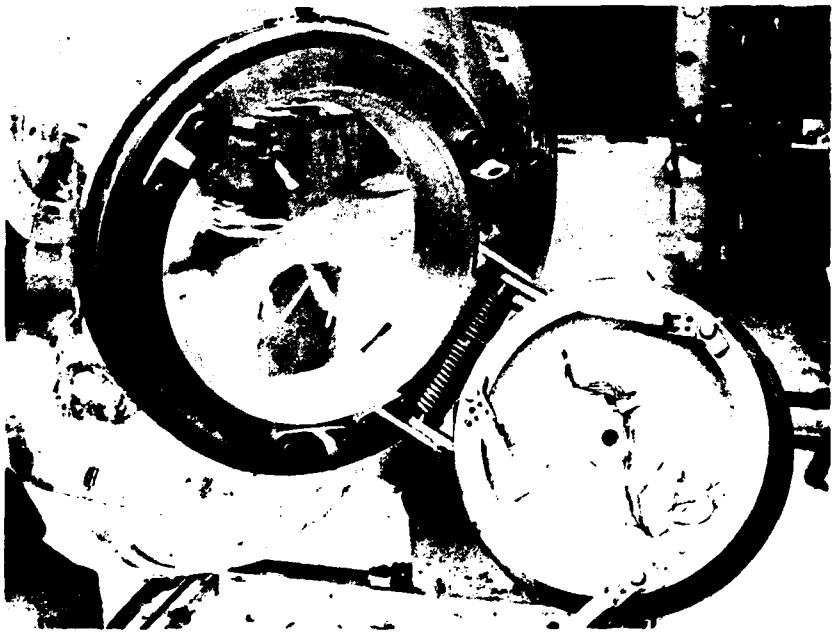

(b) inside view

Figure 12. Aluminum hatch for Model 2000 Nemo Hull.

(a) outside view

(b) inside view

Figure 13. Aluminum bottom plate for Model 2000 Nemo Hull.

Figure 14. Bearing gasket for polar openings in the hull fabricated from polycarbonate plastic plates.

Figure 15. 15 inch OD X 13 inch ID Model 34 serving as scale model of the Model 2000 Nemo Hull assembly.

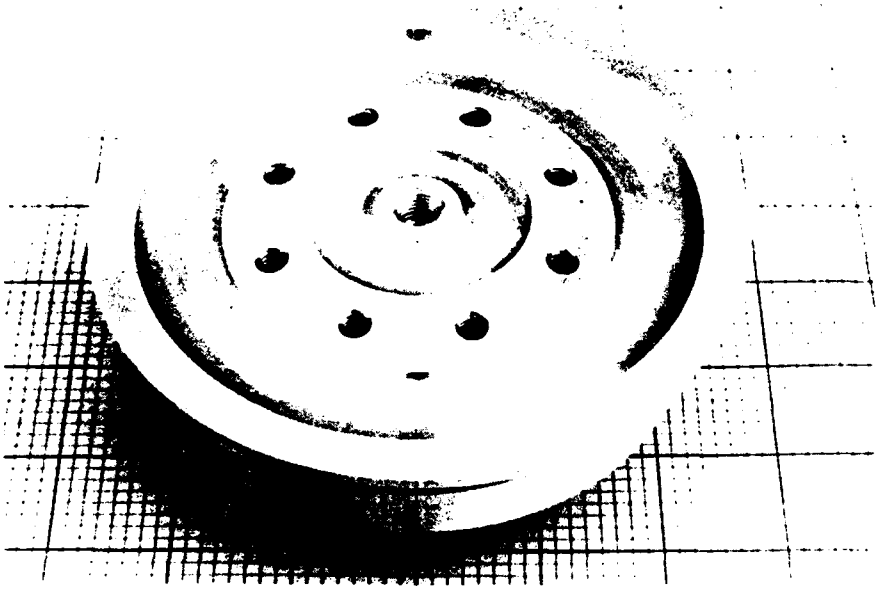

(a) outside view

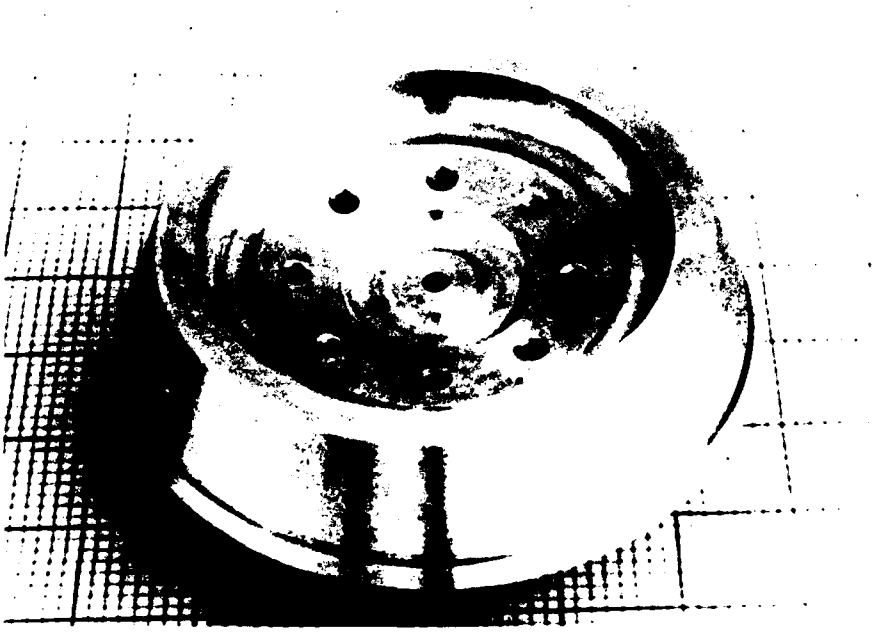

(b) inside view

Figure 16. Aluminum bottom plate for 15 inch OD X 13 inch ID Model 34 serving as scale model of Model 2000 Nemo Hull assembly.

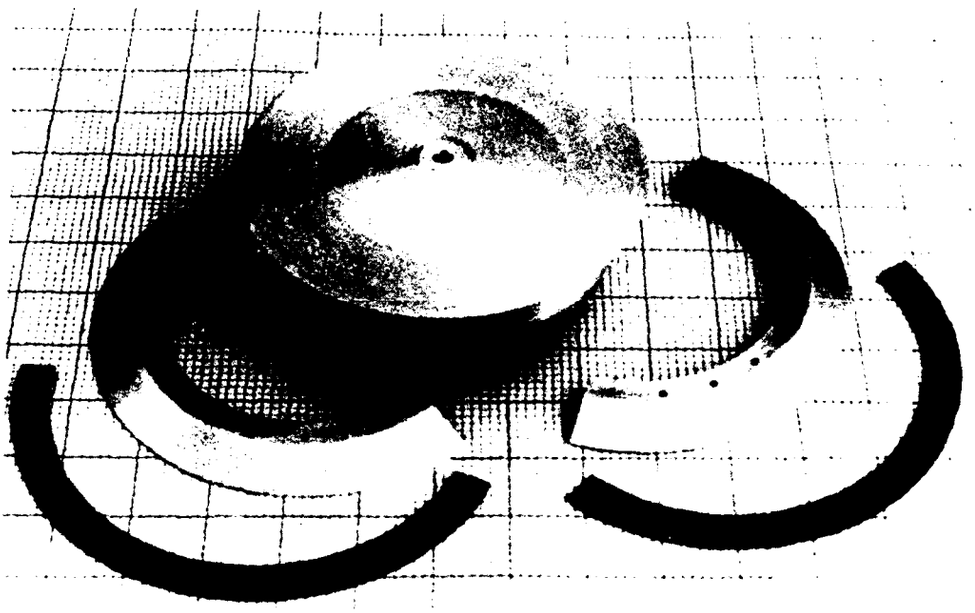

(a) outside view of hatch and retaining ring

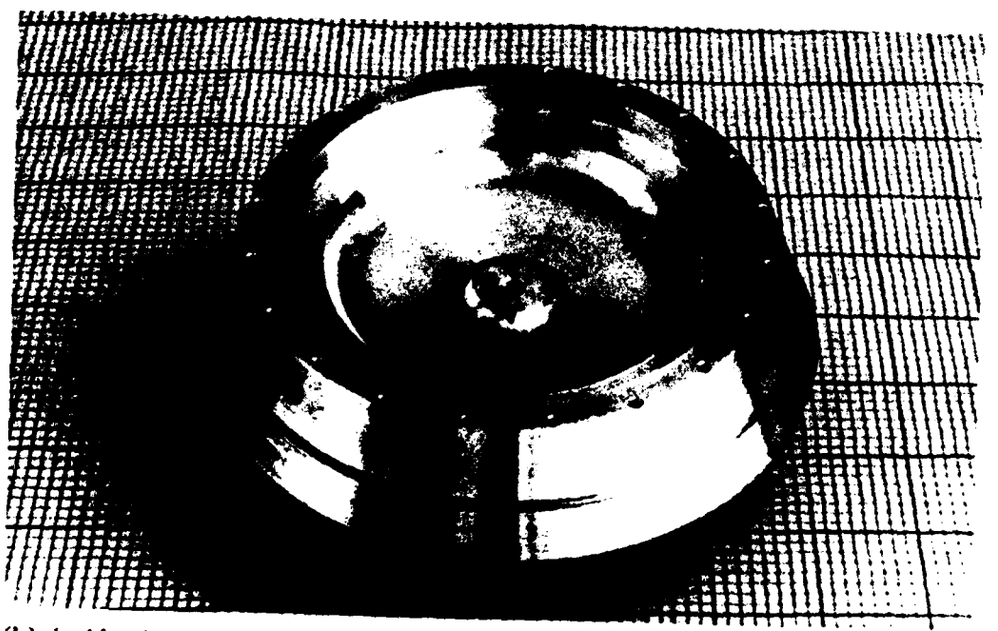

(b) inside view

Figure 17. Aluminum hatch for 15 inch OD X 13 inch ID Model 34 serving as scale model of Model 2000 Nemo Hull assembly.

(a) exterior view of hatch designed for service with polycarbonate gasket

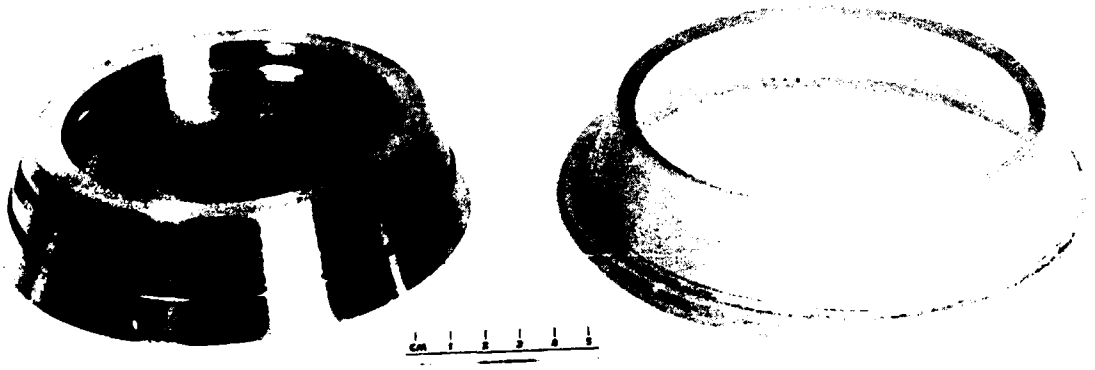

(b) interior view of hatch designed for service with polycarbonate gasket

Figure 18. Titanium hatch for 15 inch OD X 13 inch ID Models 35, 36 and 37.

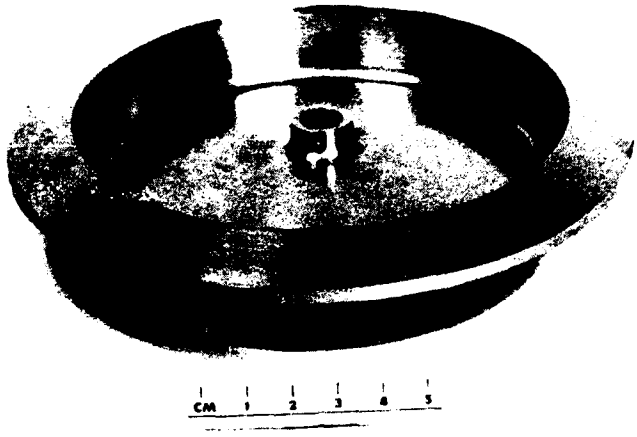

(c) exterior view of hatch designed for service without a polycarbonate gasket

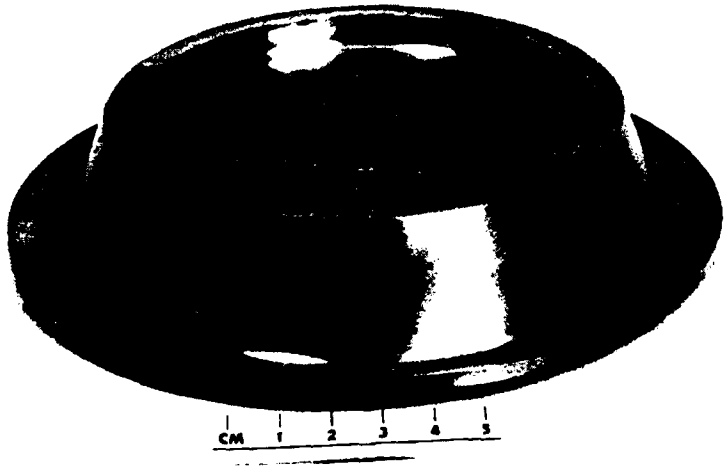

(d) interior view of hatch designed for service without a polycarbonate gasket

Figure 18. (Continued).

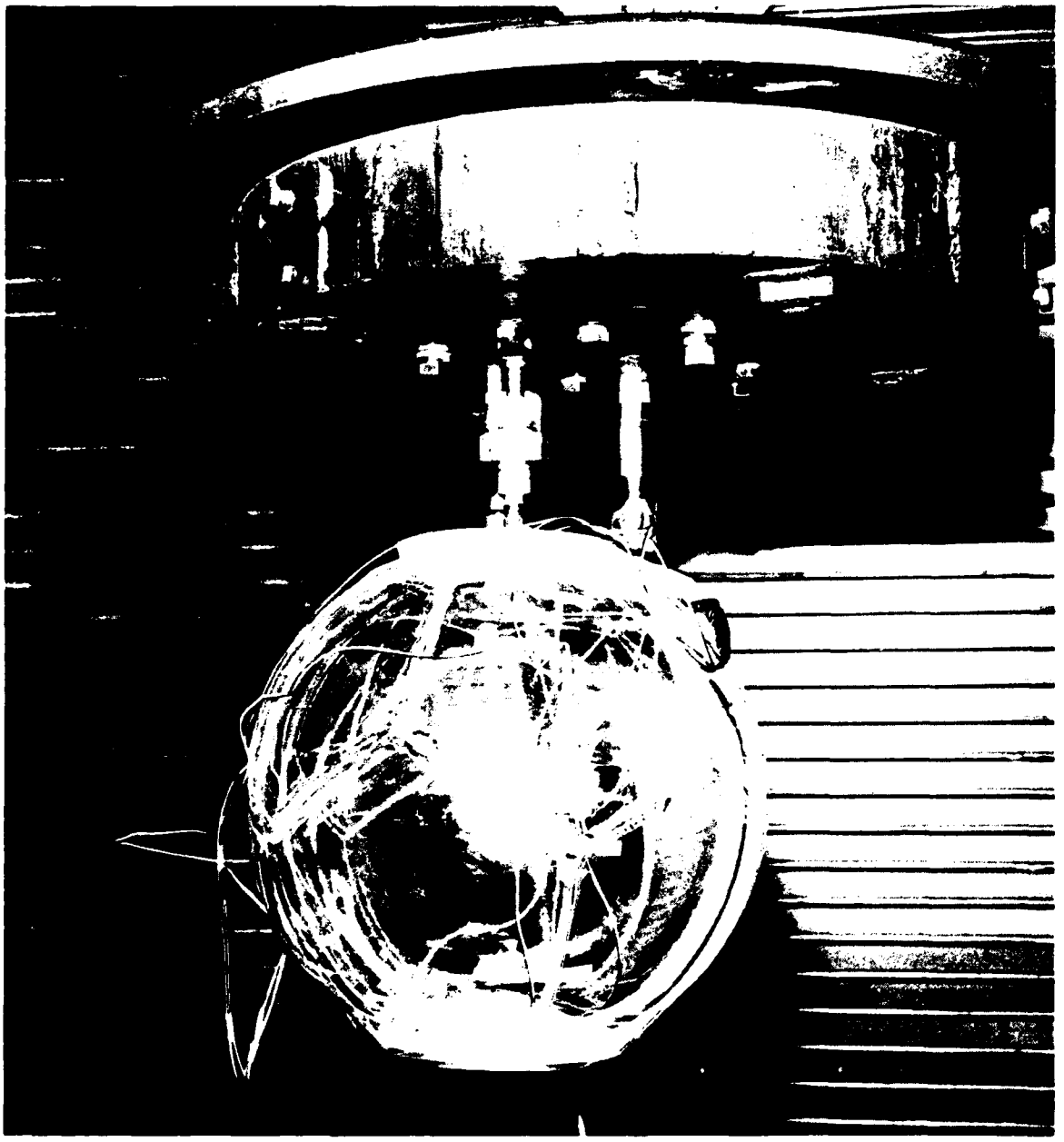

Figure 19. Test arrangement for hydrostatic testing of 15 inch OD X 13 inch ID Model 34 serving as scale model of Model 2000 Nemo Hull.

2b - 0.500 inches from edge of hatch
6b - 0.700 inches from edge of bottom plate

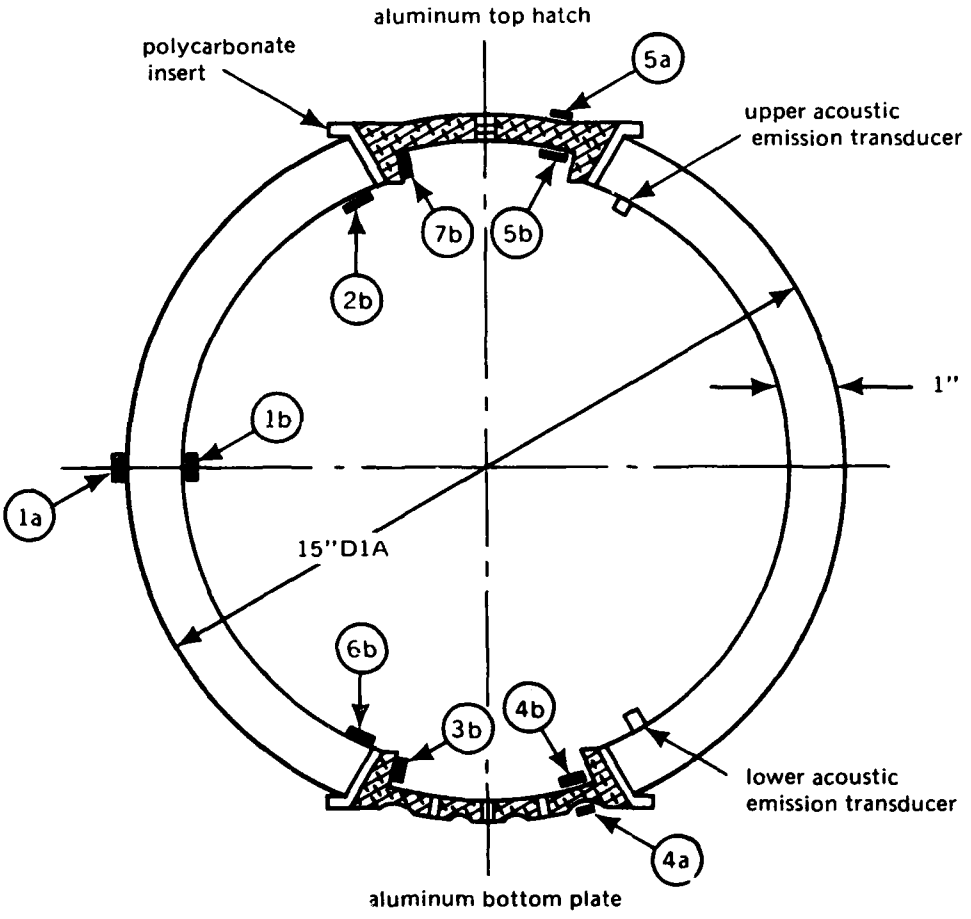

Note: Each number instrumented with 2 gage 90° rosettes

Figure 20. Location of strain gages on the 15 inch OD X 13 inch ID Model 34, serving as scale model of Model 2000 Nemo Hull.

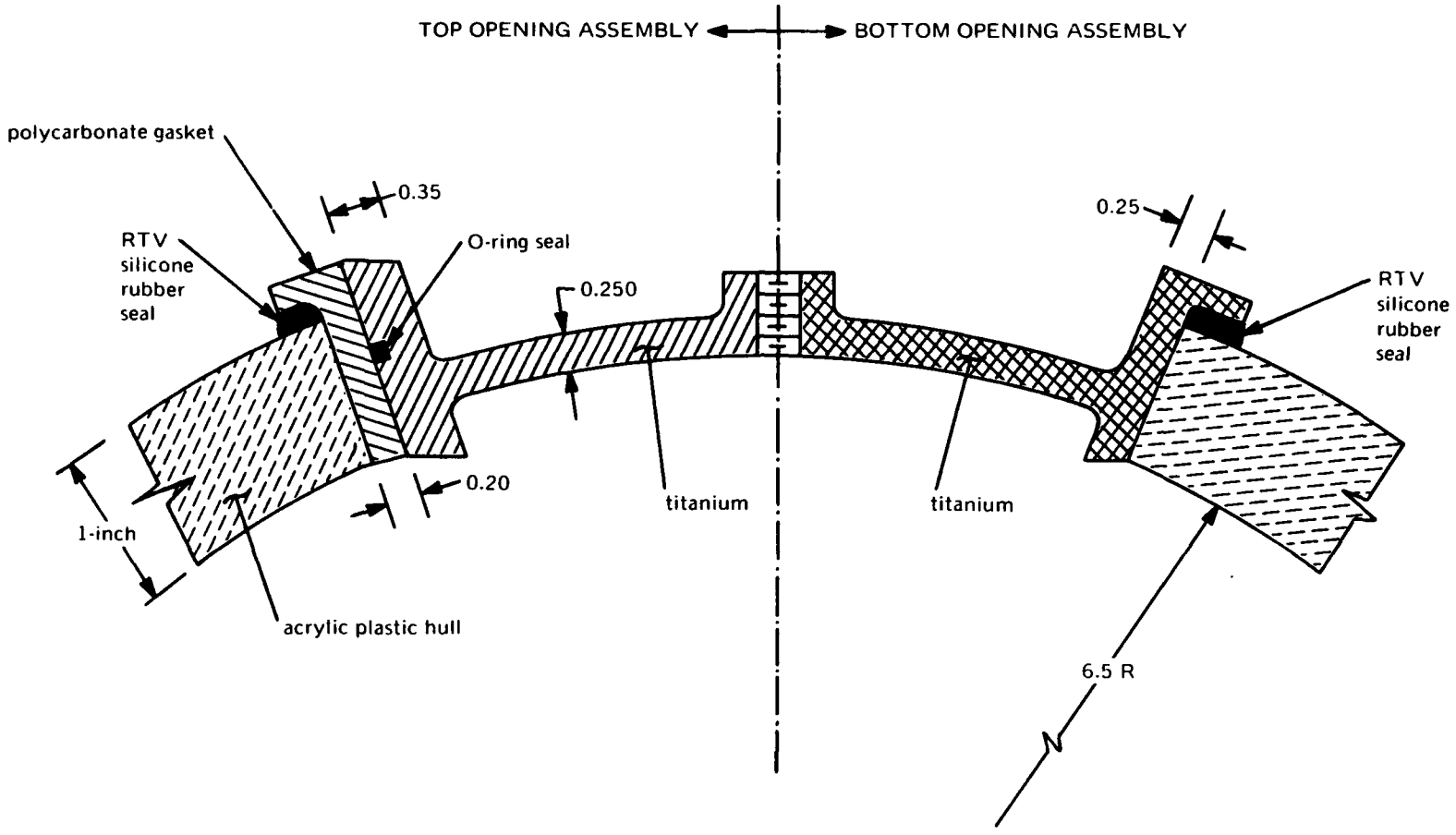

Figure 21. Typical hatches used in the 15 inch OD X 13 inch ID Models 35, 36 and 37 subjected to pressure cycling.

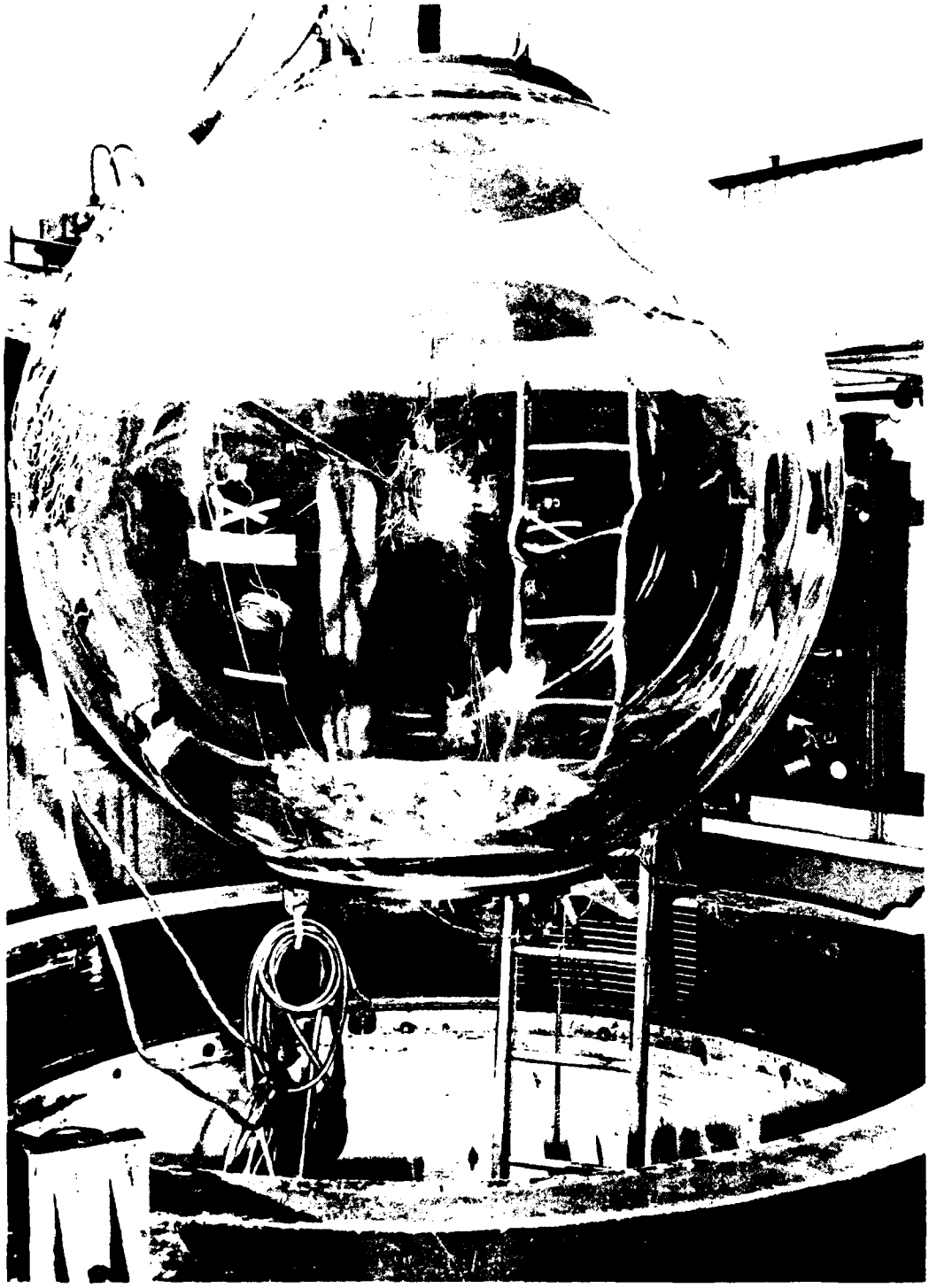

(a) instrumented assembly ready for placement in vessel

Figure 22. Testing of full scale Model 2000 Nemo Hull assembly in the 90 inch diameter pressure vessel at SWRI.

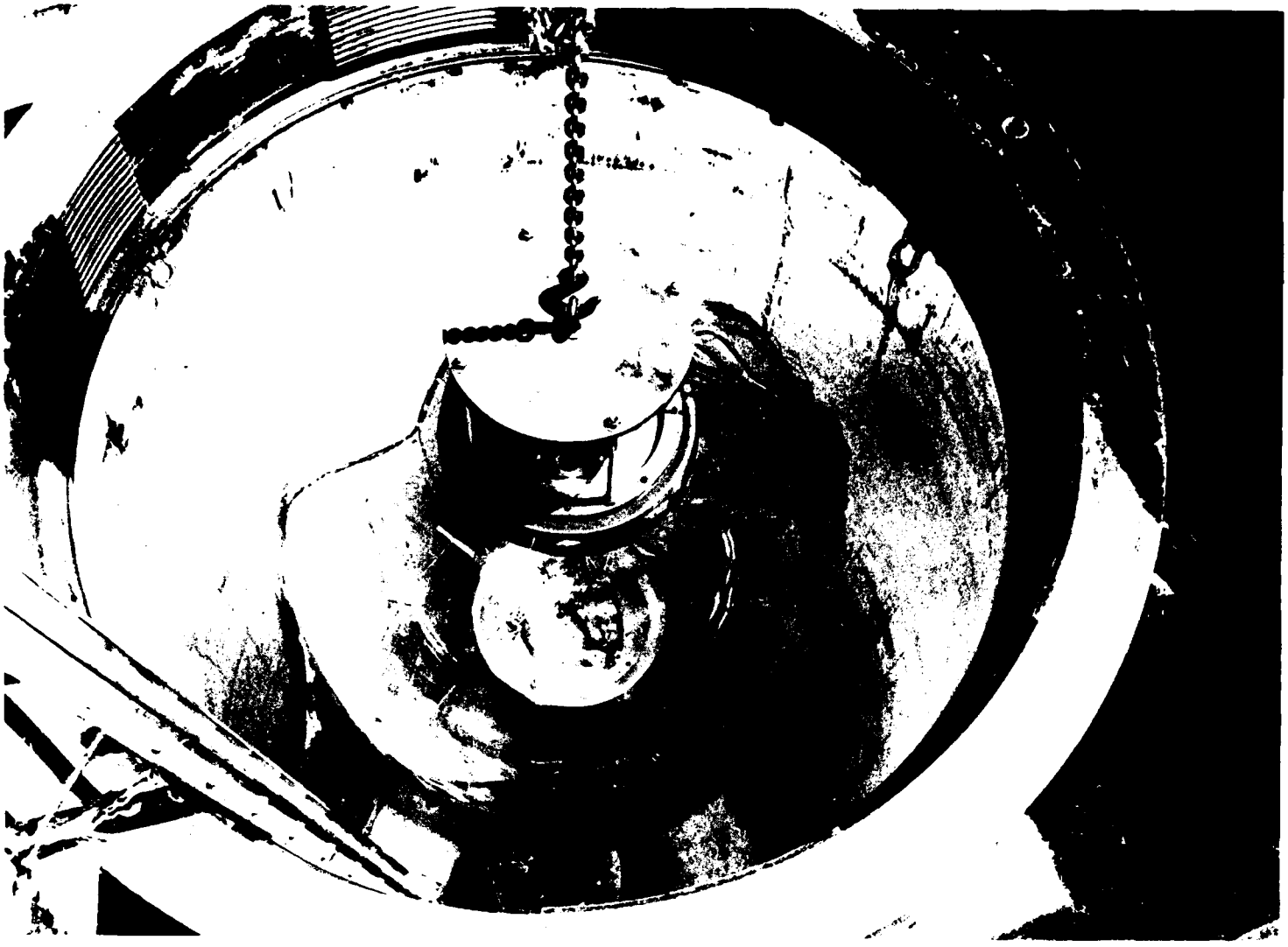

(b) Model 2000 Nemo Hull assembly in vessel

Figure 22. (Continued).

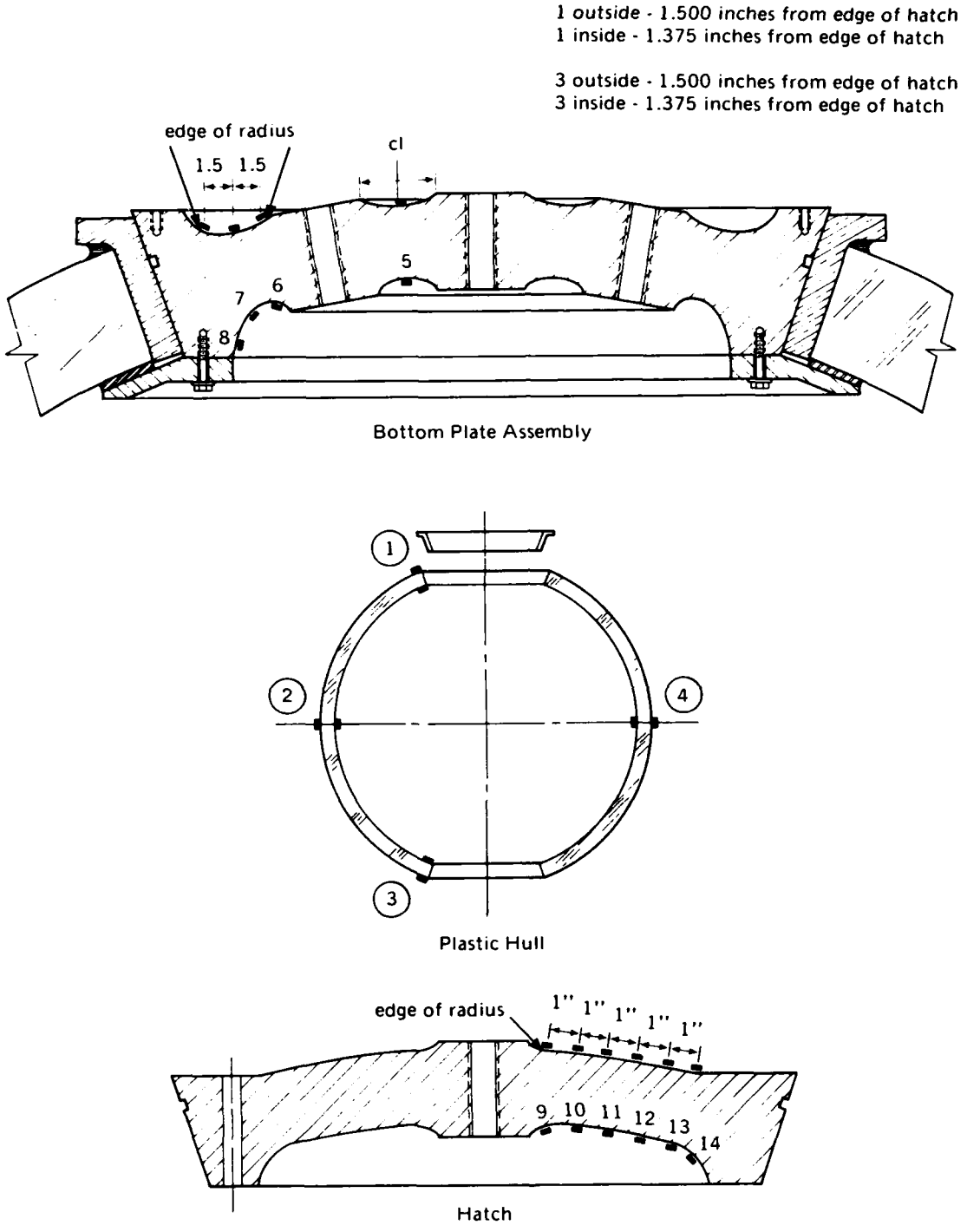

Figure 23. Location of strain gages on the 66 inch OD X 58 inch ID full scale Model 2000 Nemo Hull assembly.

Figure 24. Fragments of the 15 inch OD X 13 inch ID Model 34 after implosion at 4750 psi.

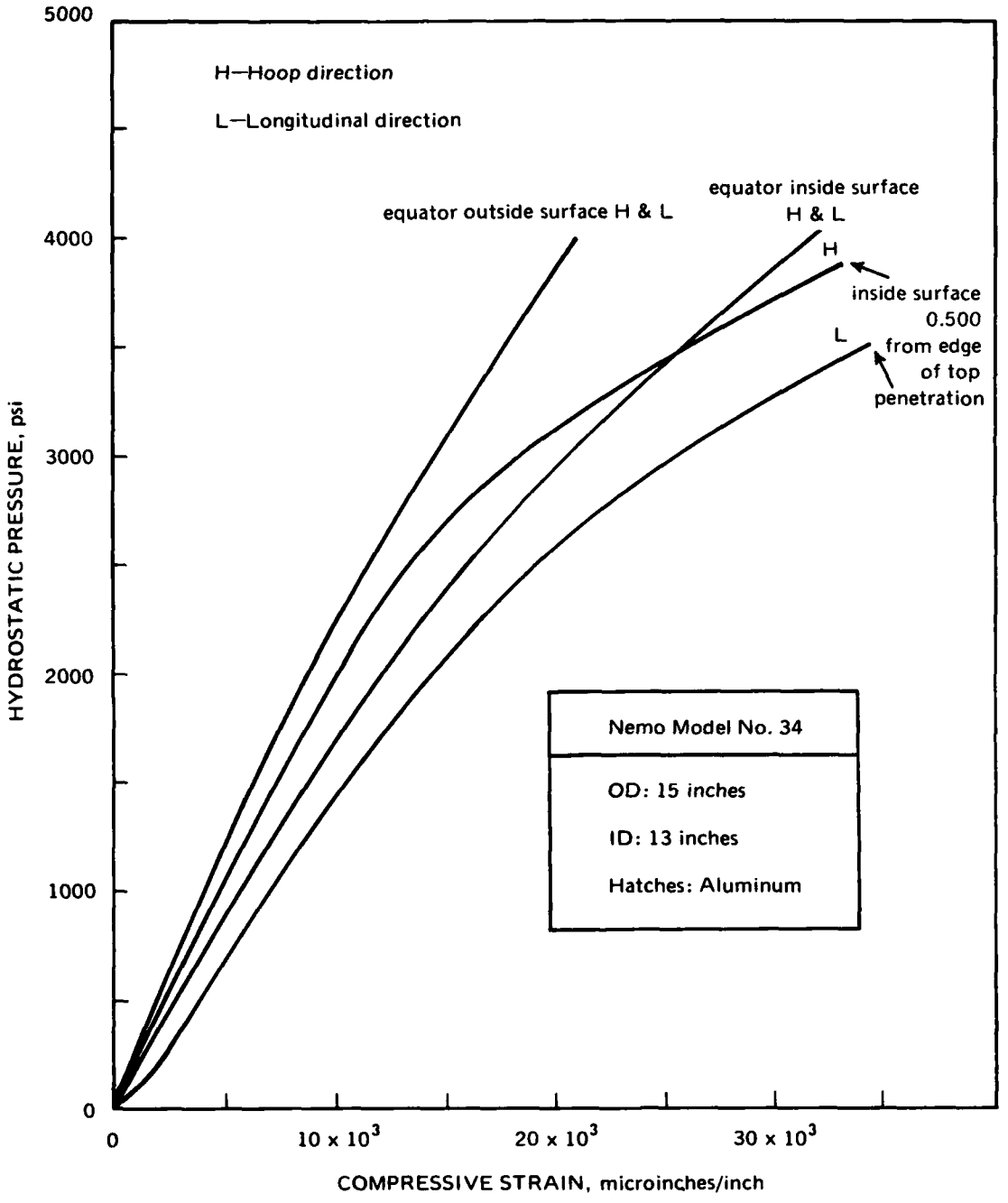

Figure 25. Strains in the 15 inch OD X 13 inch ID Model 34 serving as scale for Model 2000 Nemo Hull.

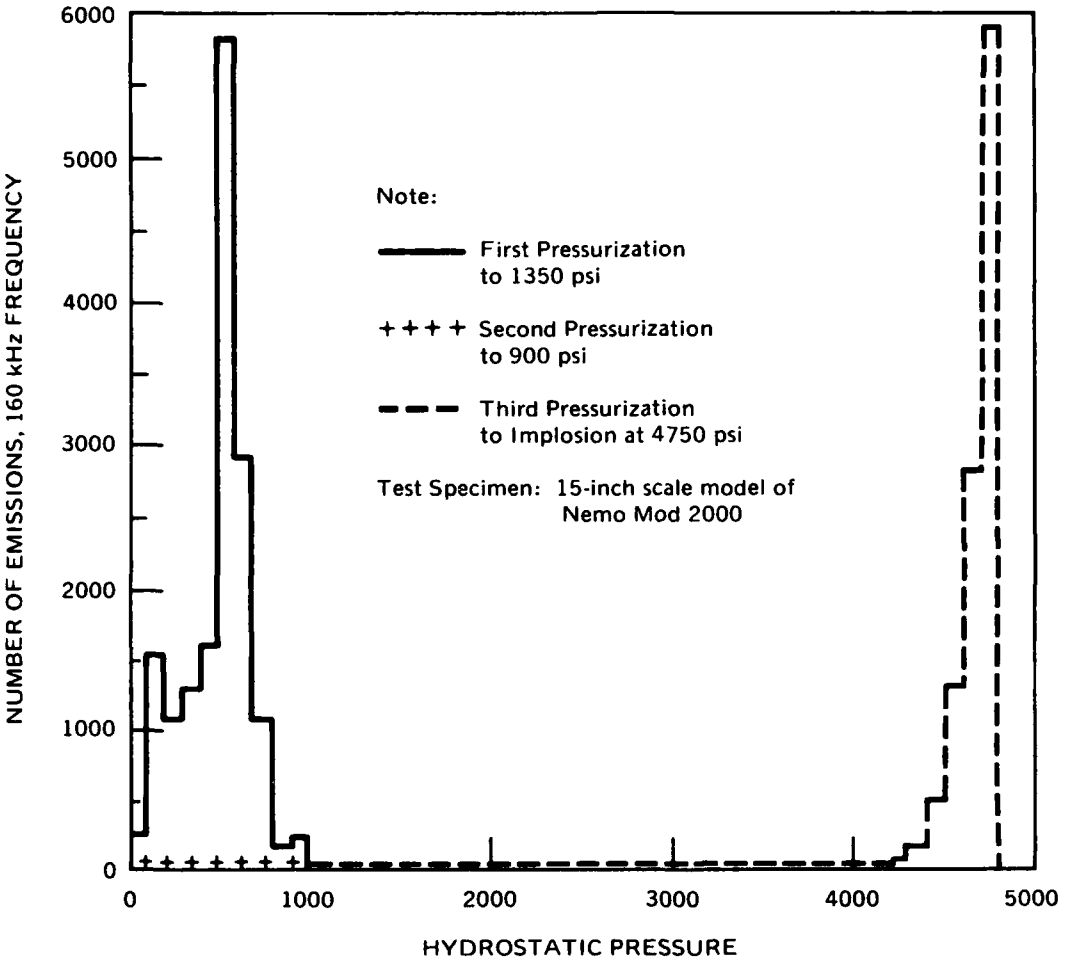

Figure 26. Histogram of stress wave emissions from 15 inch OD X 13 inch ID Model 34 of undergoing external pressure tests.

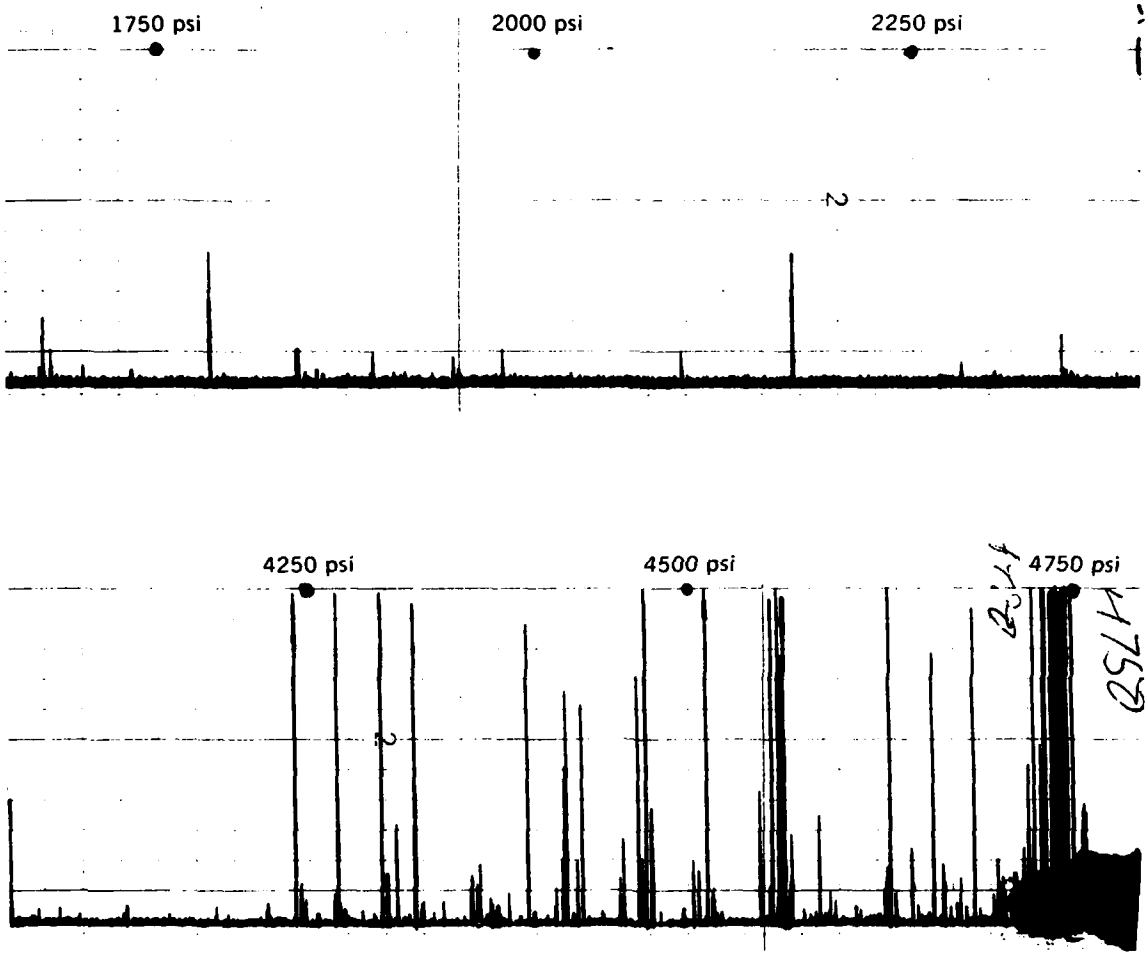

Figure 27. Recording of stress wave emissions preceding the short term implosion of 15 inch OD X 13 inch ID Model 34 assembly at 4750 psi external hydrostatic pressure.

Figure 28. Inspection of bearing surfaces on 15 inch OD X 13 inch ID Models 36 and 37 after 1000 pressure cycles to, respectively, 900 and 1500 psi hydrostatic pressure.

Figure 29. Fatigue crazing of the acrylic bearing surface of the Model 37 hull after 1000 pressurizations of 4 hour duration each to 1500 psi; this acrylic bearing surface was in direct contact with the metallic hatch.

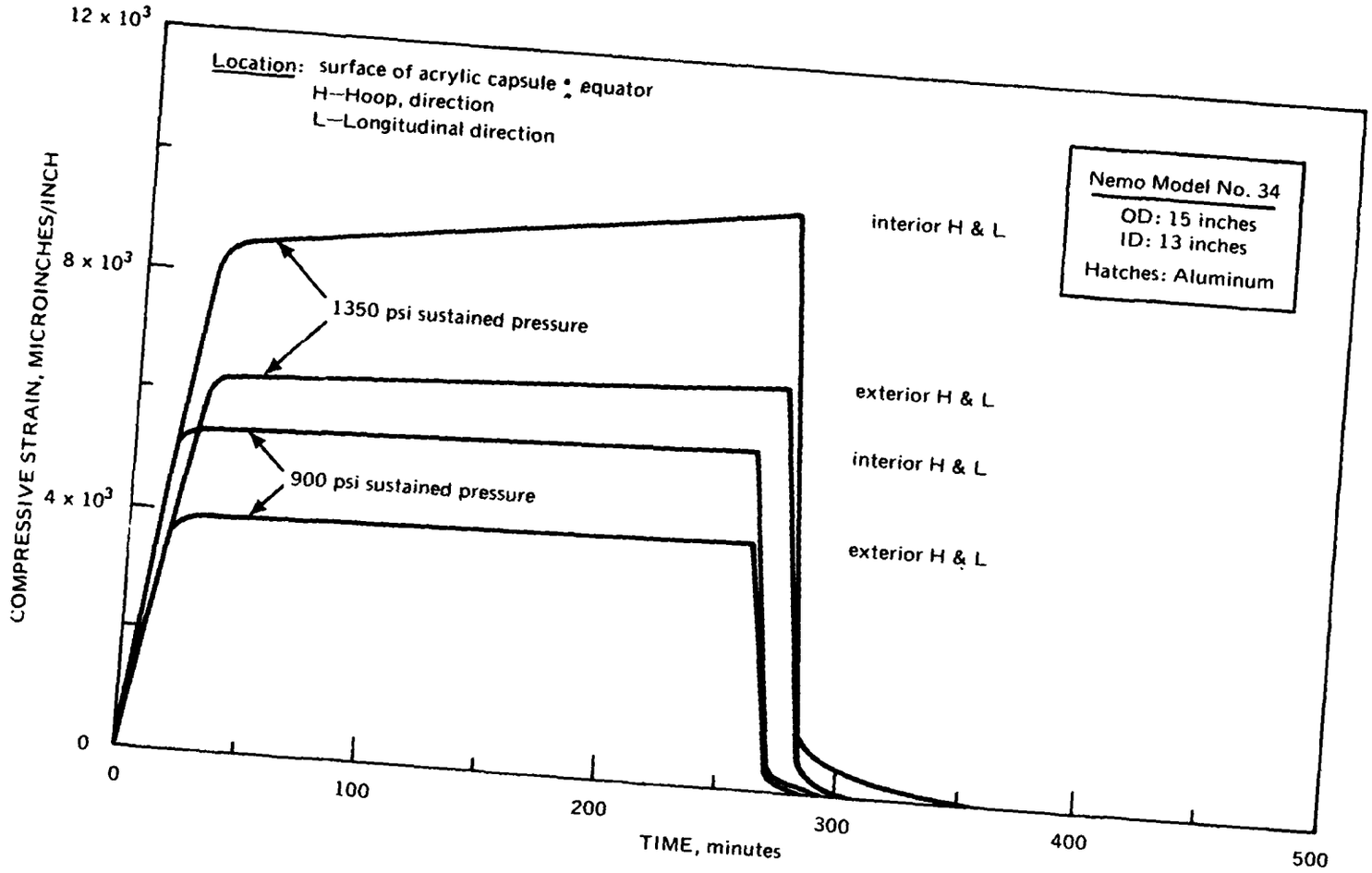

Figure 30. Creep of acrylic hull in 15 inch OD X 13 inch ID Model 34 under external hydrostatic pressure; measured on the interior and exterior surfaces at the equator.

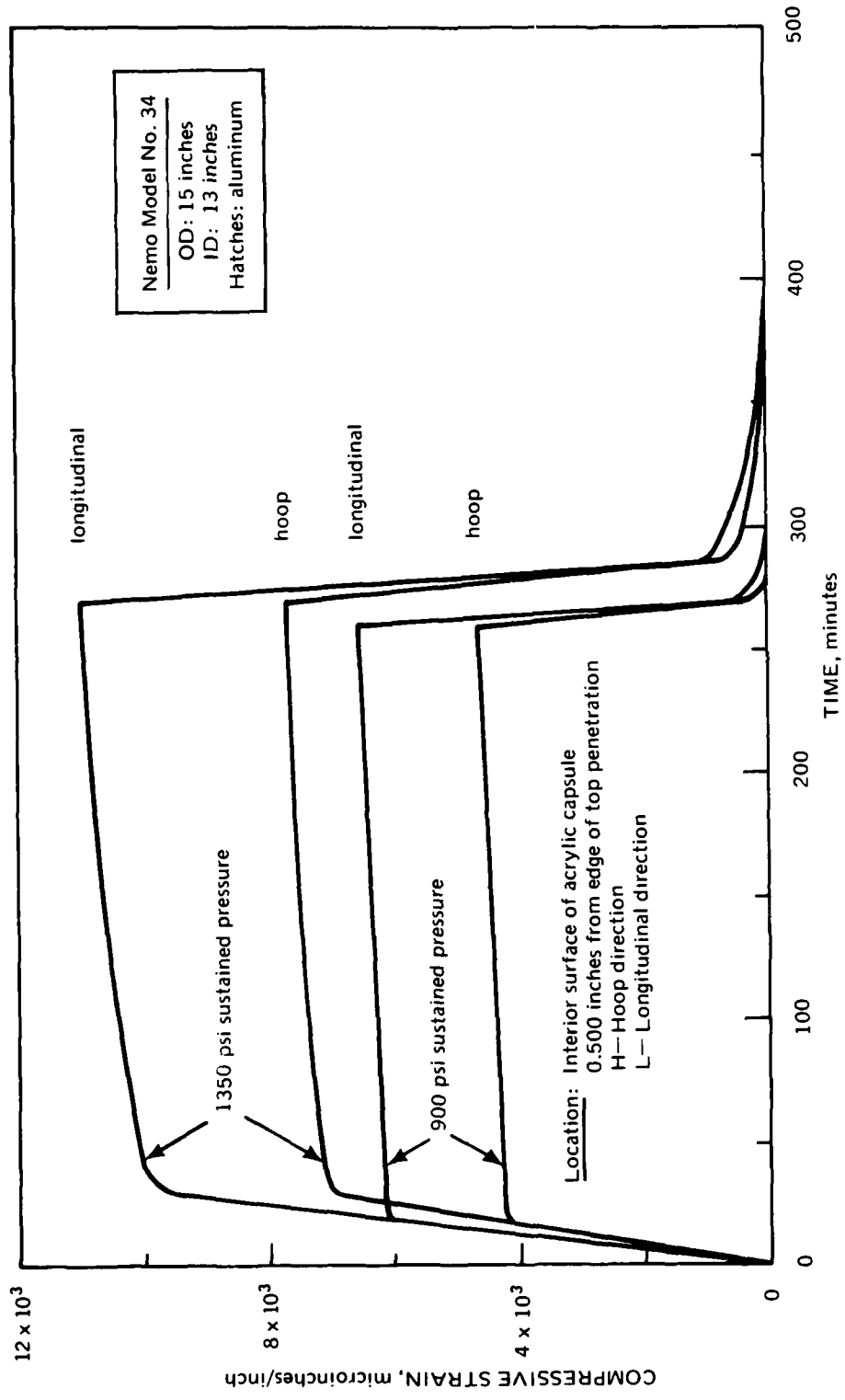

Figure 31. Creep of acrylic hull in 15 inch OD X 13 inch ID Model 34 under external hydrostatic pressure; measured on the interior surface at the edge of top polar penetration.

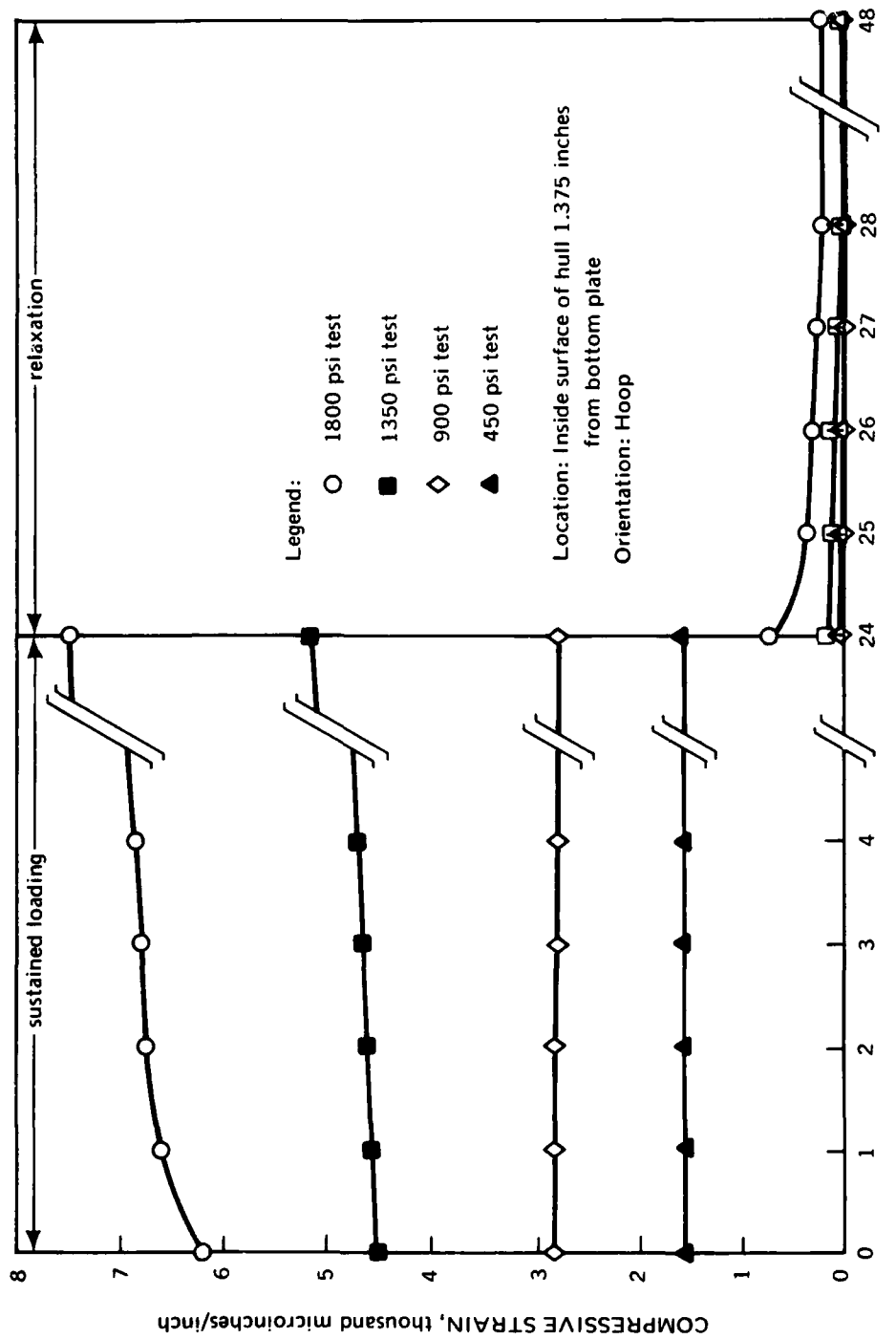

(a) inside surface; 1.375 inches from edge of bottom plate; *hoop*

Figure 32. Creep measured on the acrylic hull of the 66 inch OD X 58 inch ID Model 2000 Nemo Hull assembly during 24-hour long sustained loadings under external hydrostatic pressure.

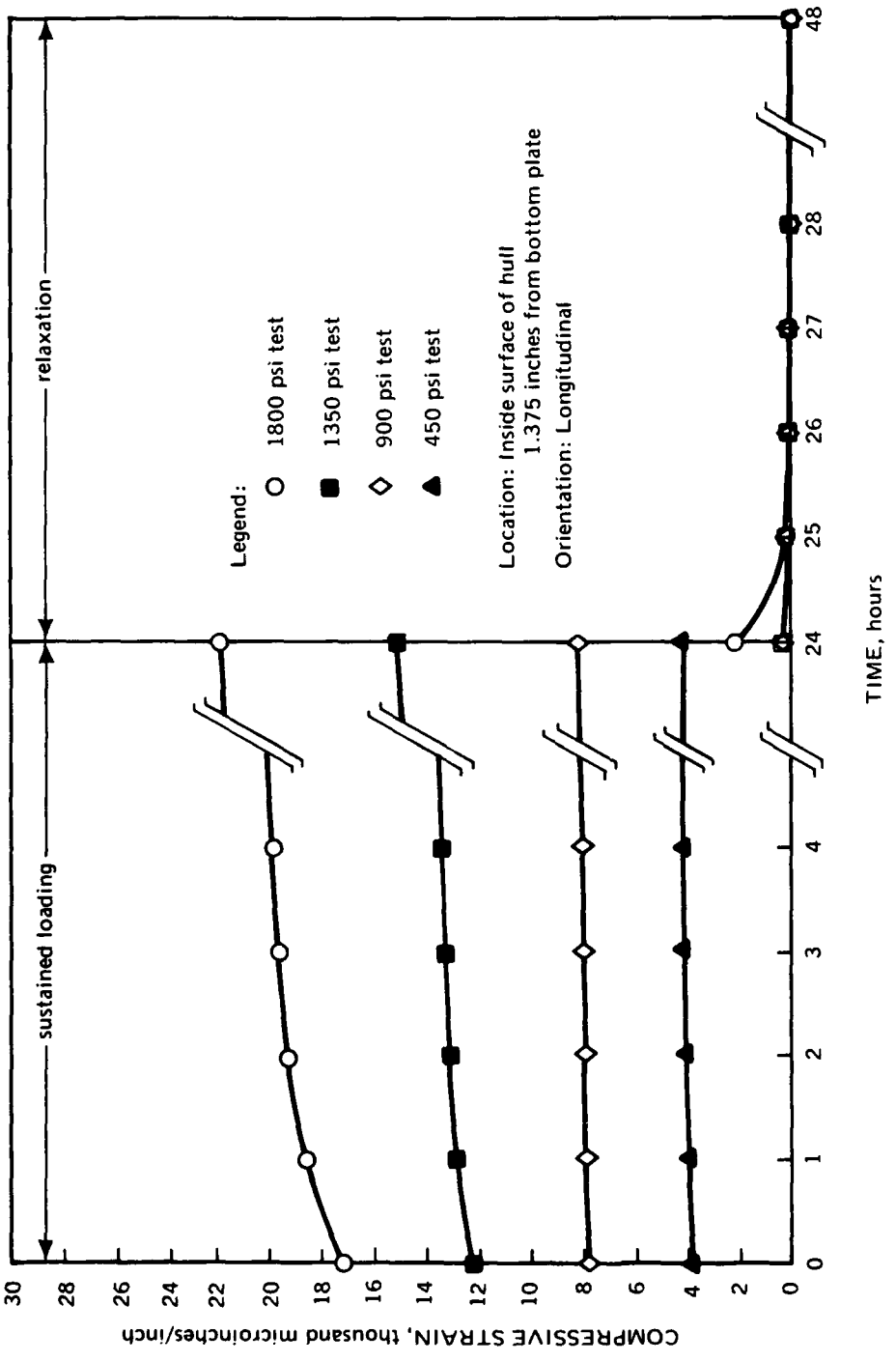

(b) inside surface; 1.375 inches from edge of bottom plate; *longitudinal*

Figure 32. (Continued).

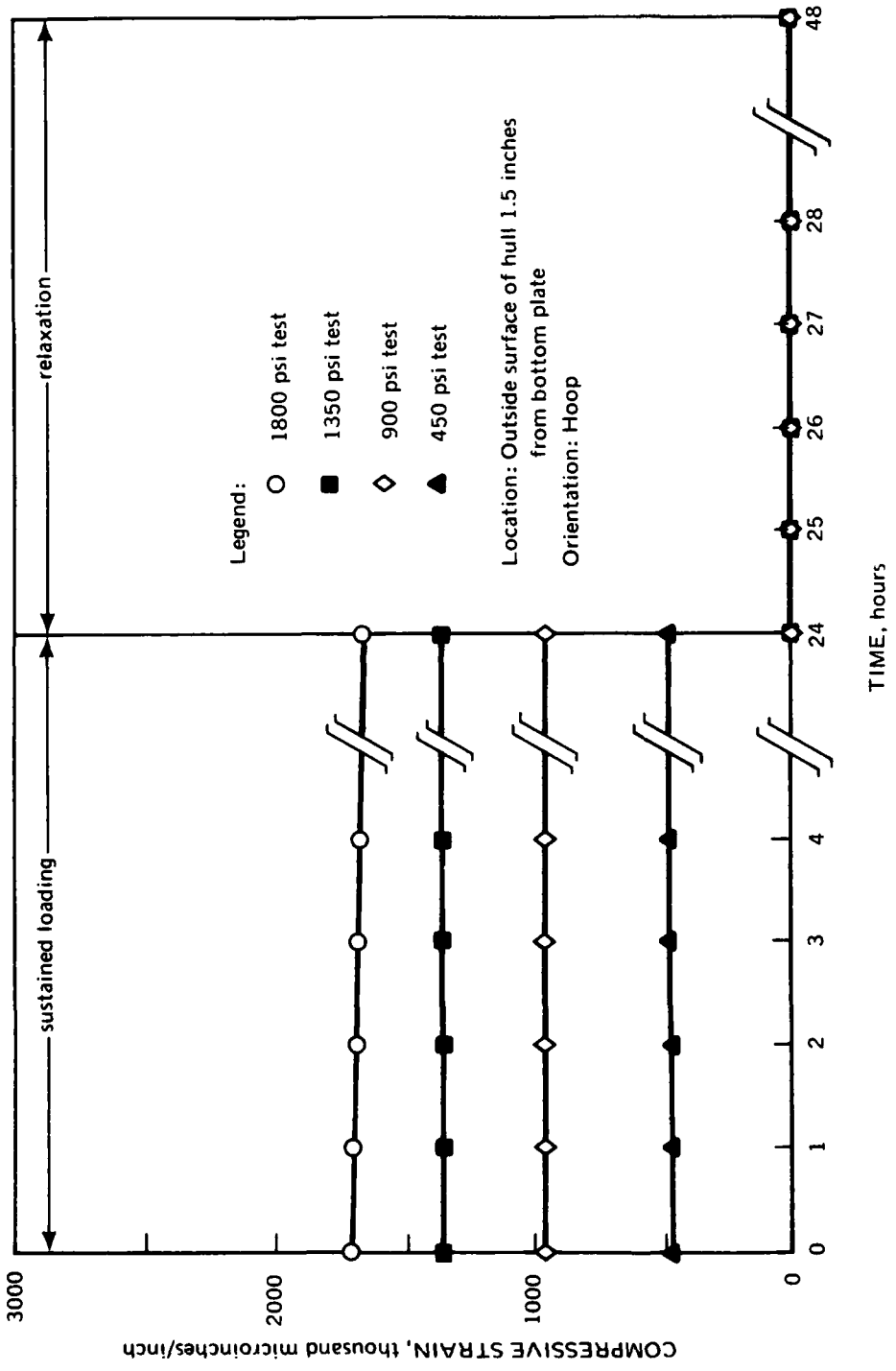

(c) outside surface; 1.500 inches from edge of bottom plate; *hoop*

Figure 32. (Continued).

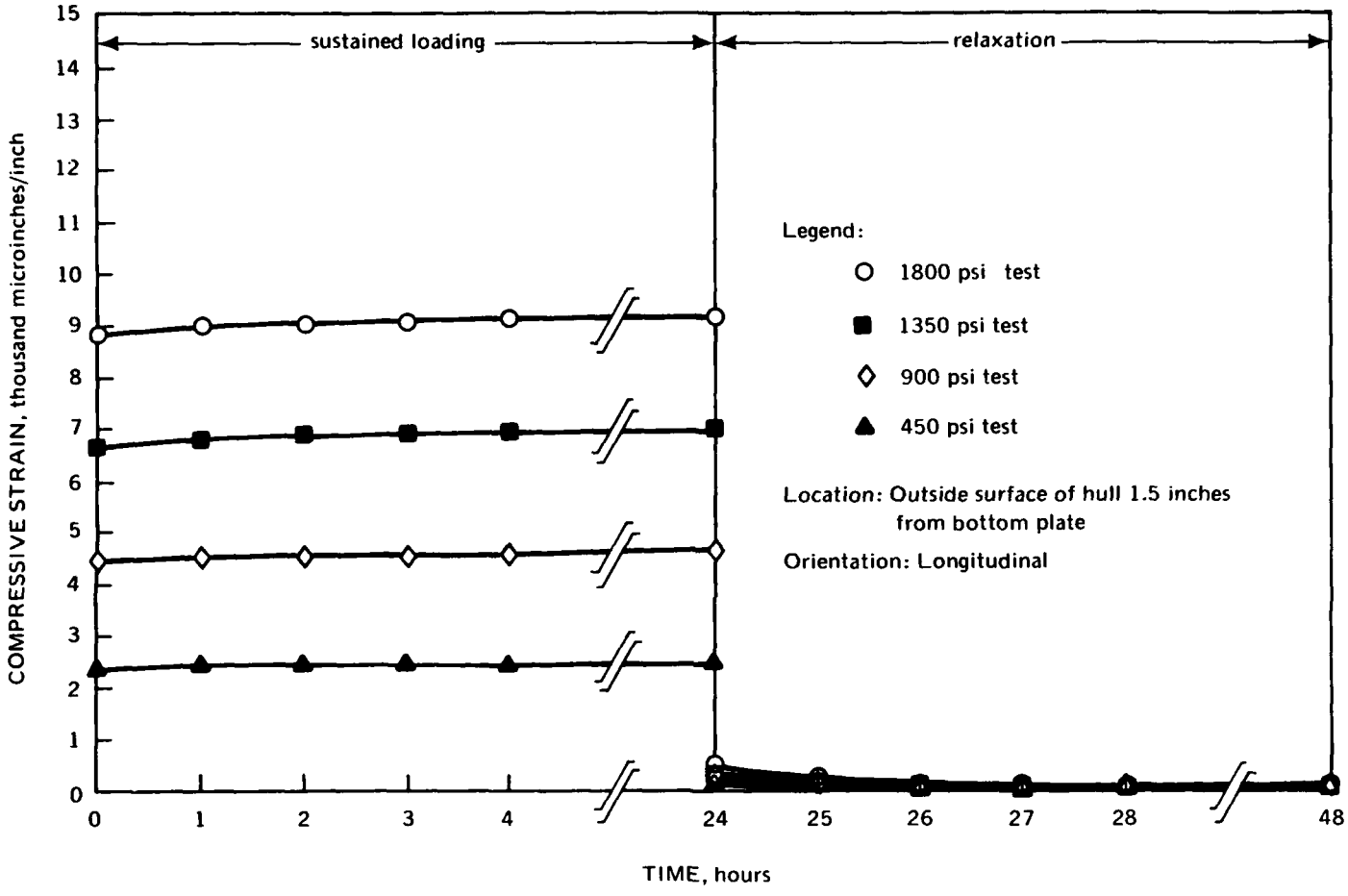

(d) outside surface; 1.500 inches from edge of bottom plate; *longitudinal*

Figure 32. (Continued).

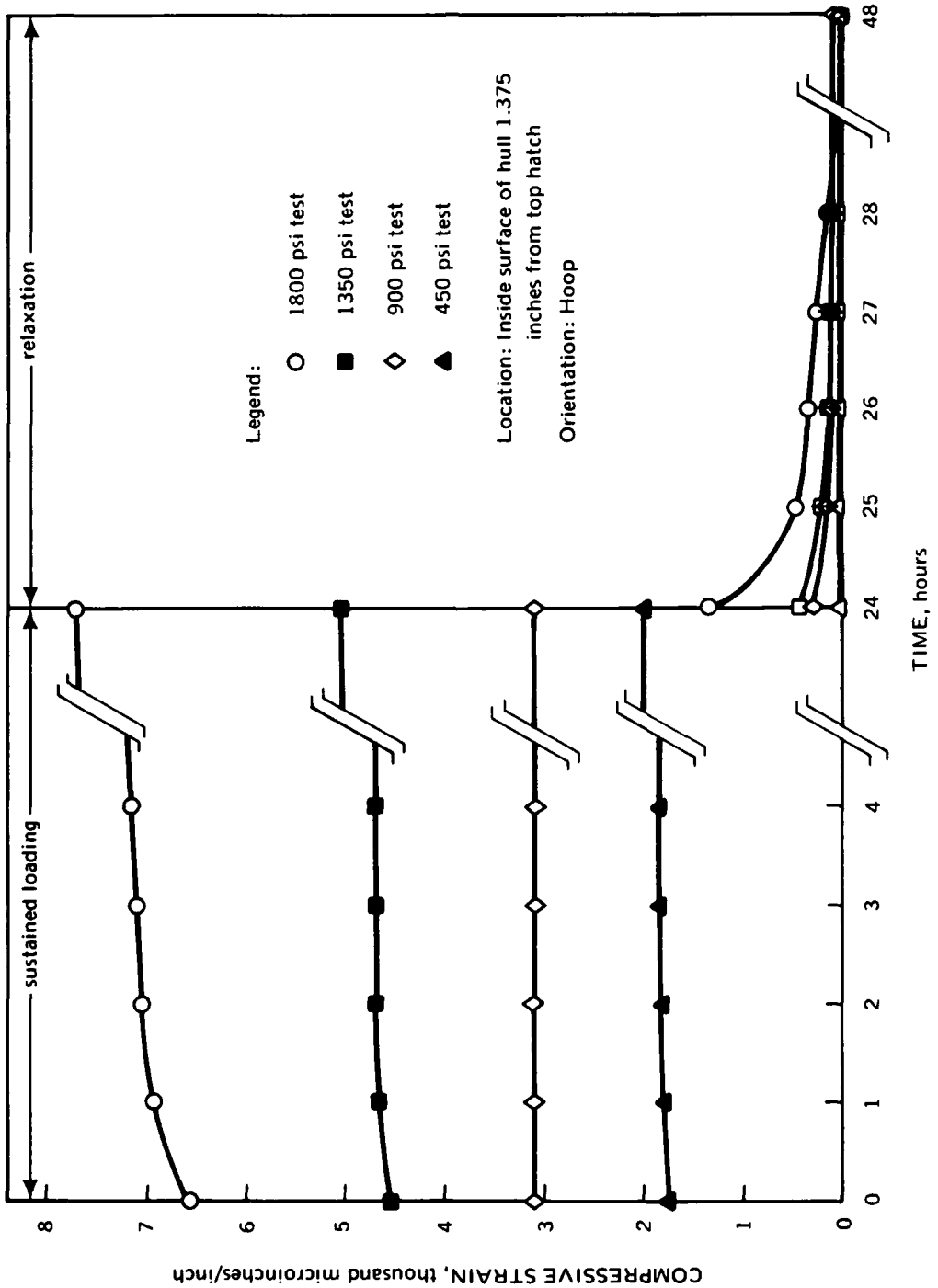

(e) inside surface; 1.375 inches from edge of top hatch; *hoop*

Figure 32. (Continued).

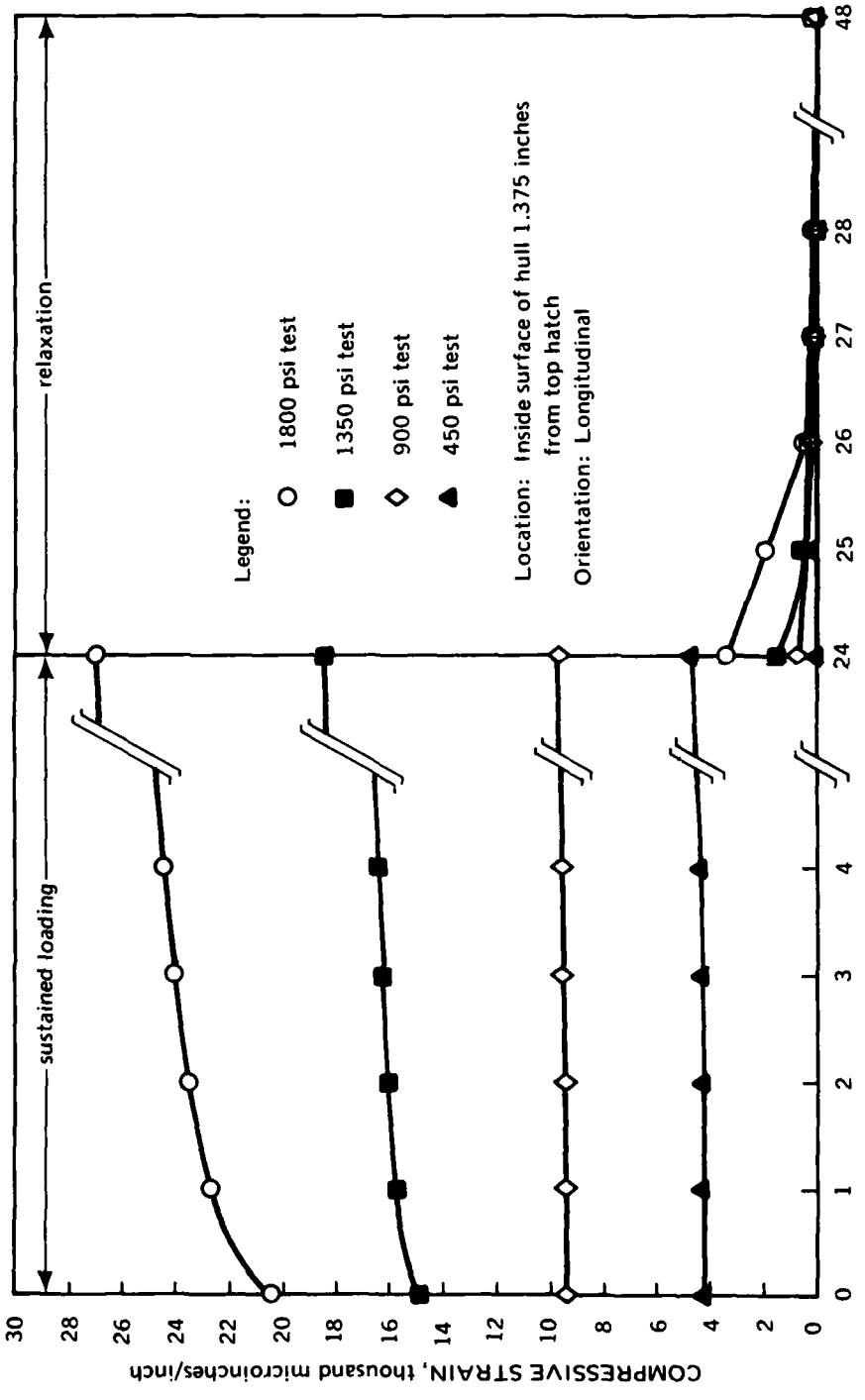

(f) inside surface; 1.375 inches from edge of top hatch; *longitudinal*

Figure 32. (Continued).

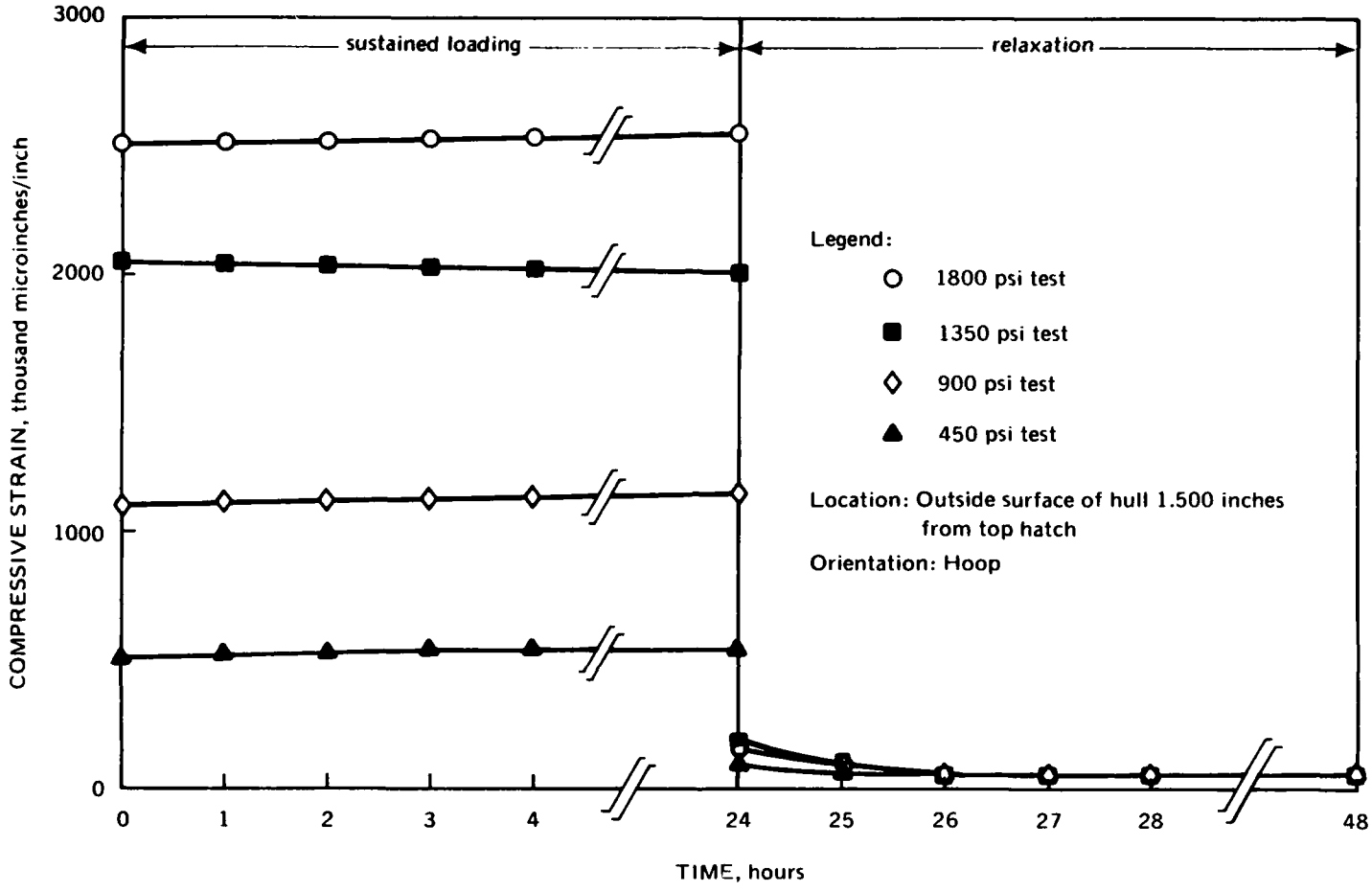

(g) outside surface; 1.500 inches from edge of top hatch; *hoop*

Figure 32. (Continued).

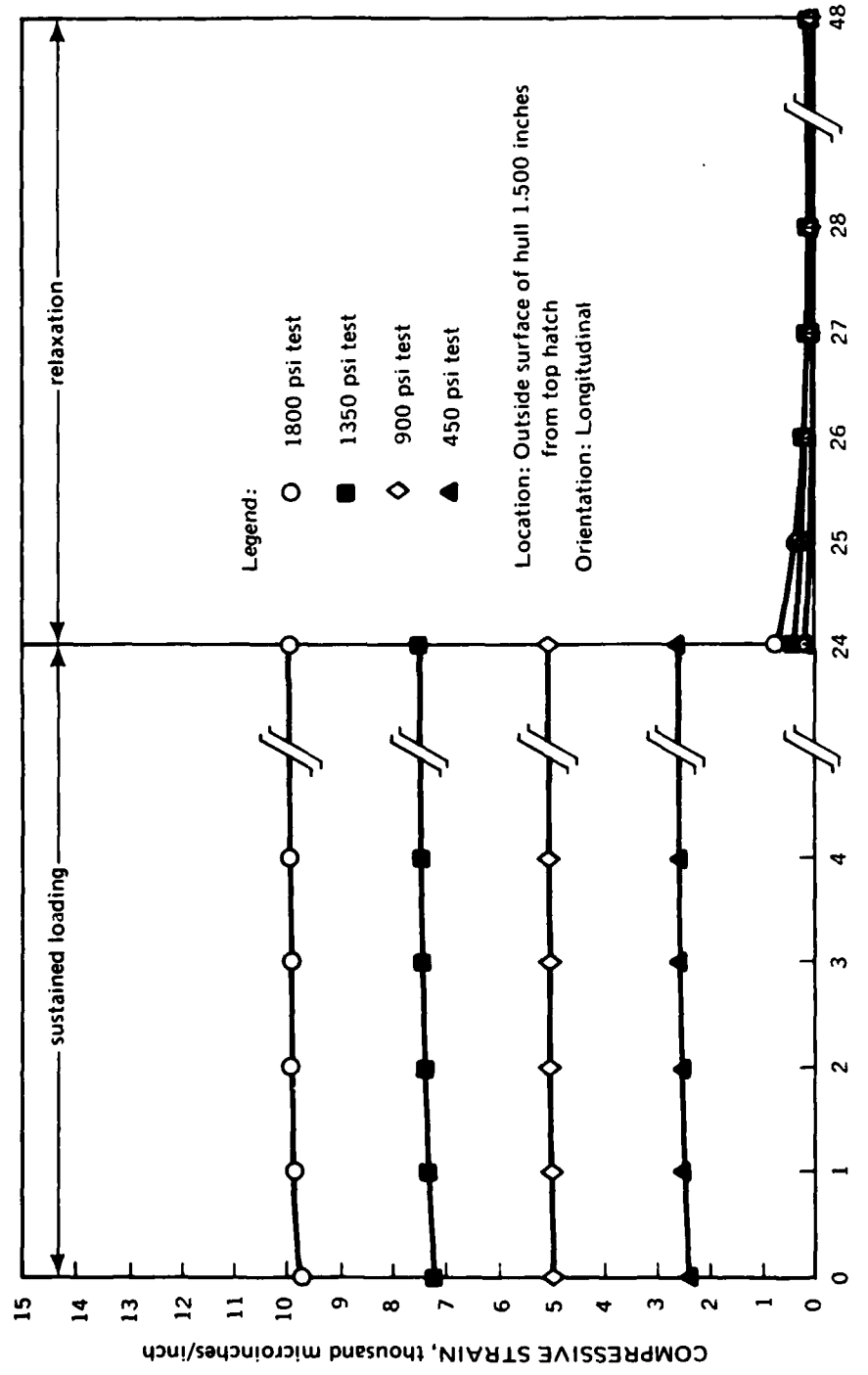

(h) outside surface; 1.500 inches from edge of top hatch; *longitudinal*

Figure 32. (Continued).

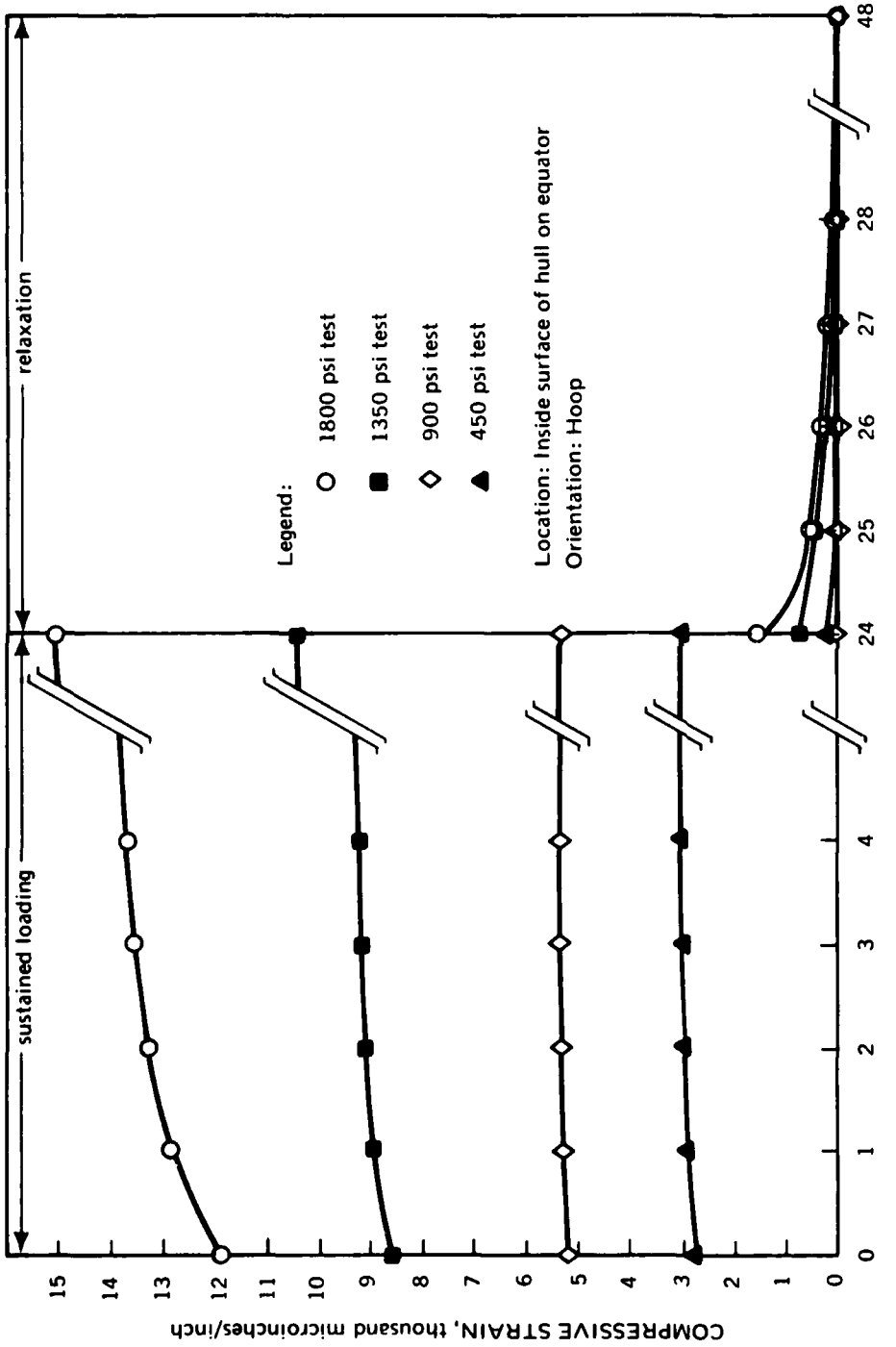

(i) inside surface; equator; *hoop*

Figure 32. (Continued).

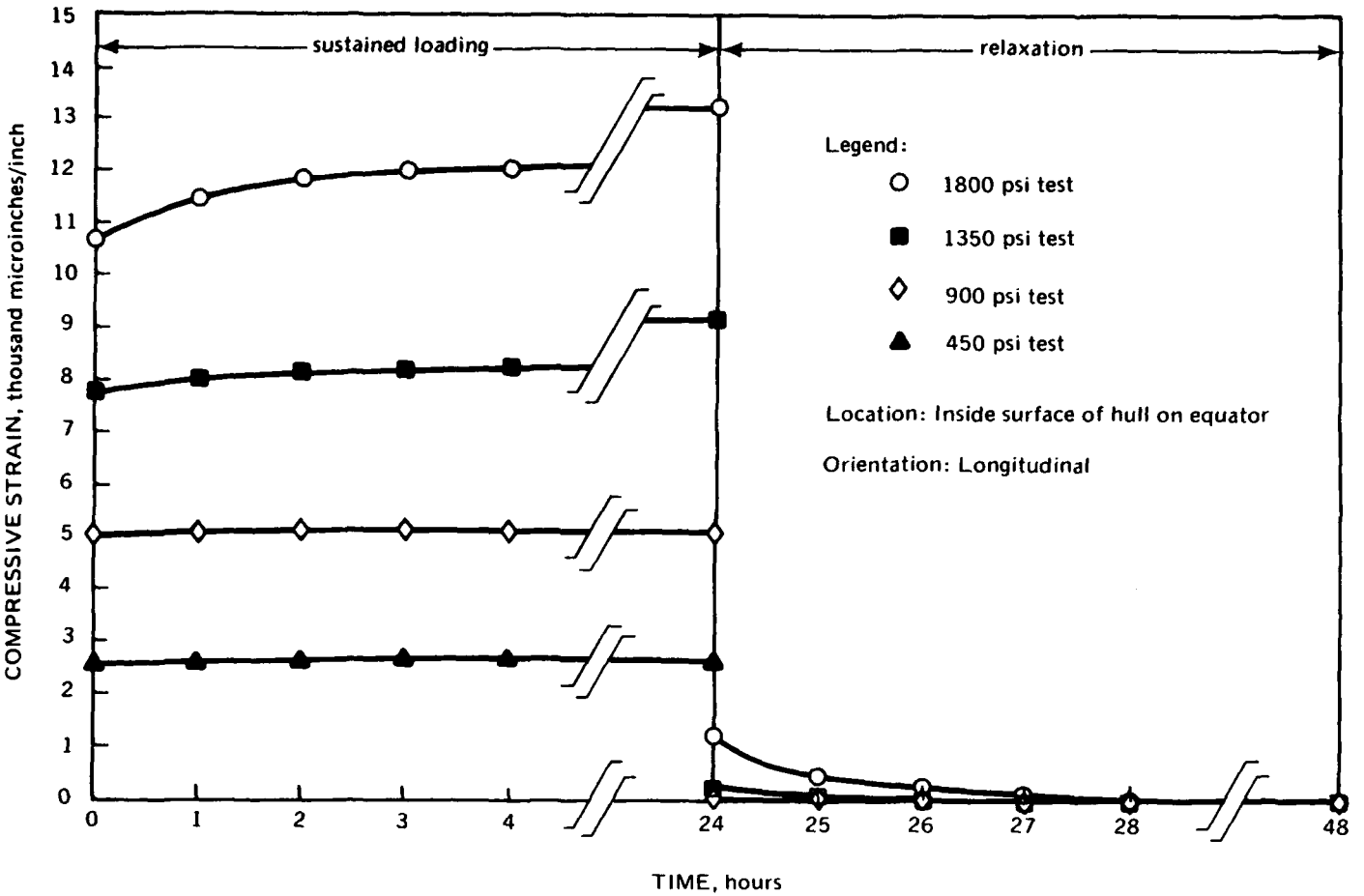

(j) inside surface; equator; *longitudinal*

Figure 32. (Continued).

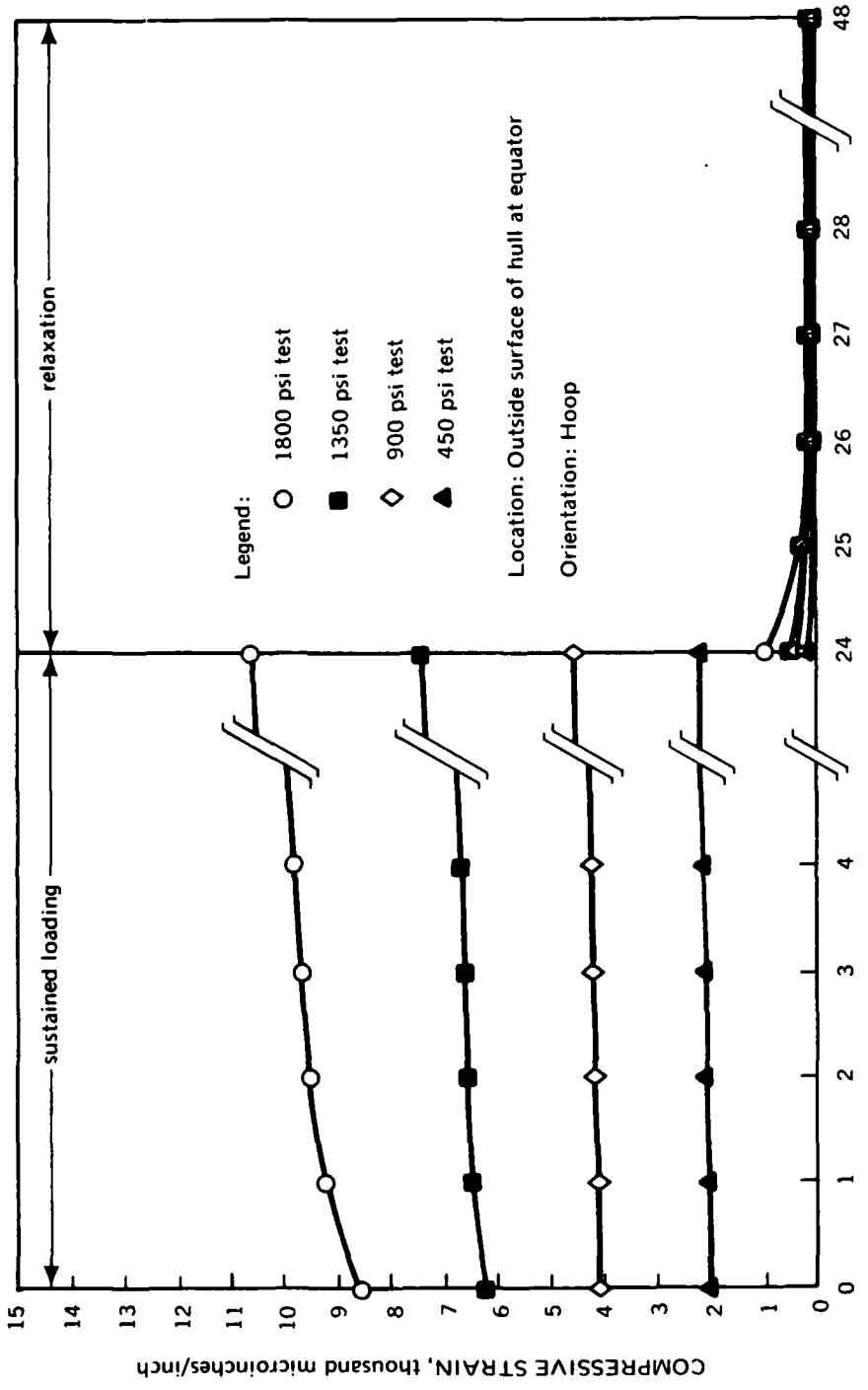

(k) outside surface; equator; *hoop*

Figure 32. (Continued).

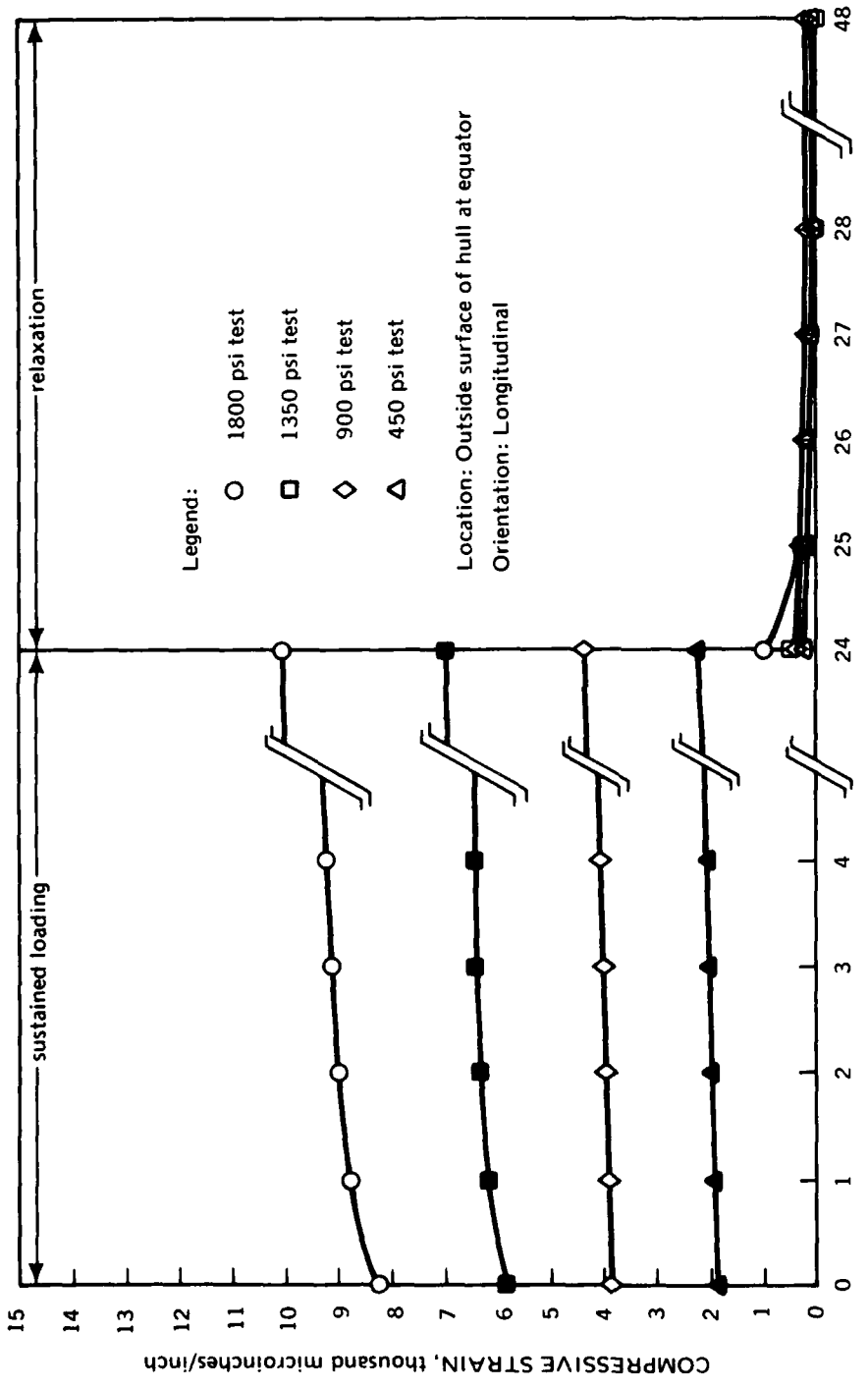

(l) outside surface; equator; *longitudinal*

Figure 32. (Continued).

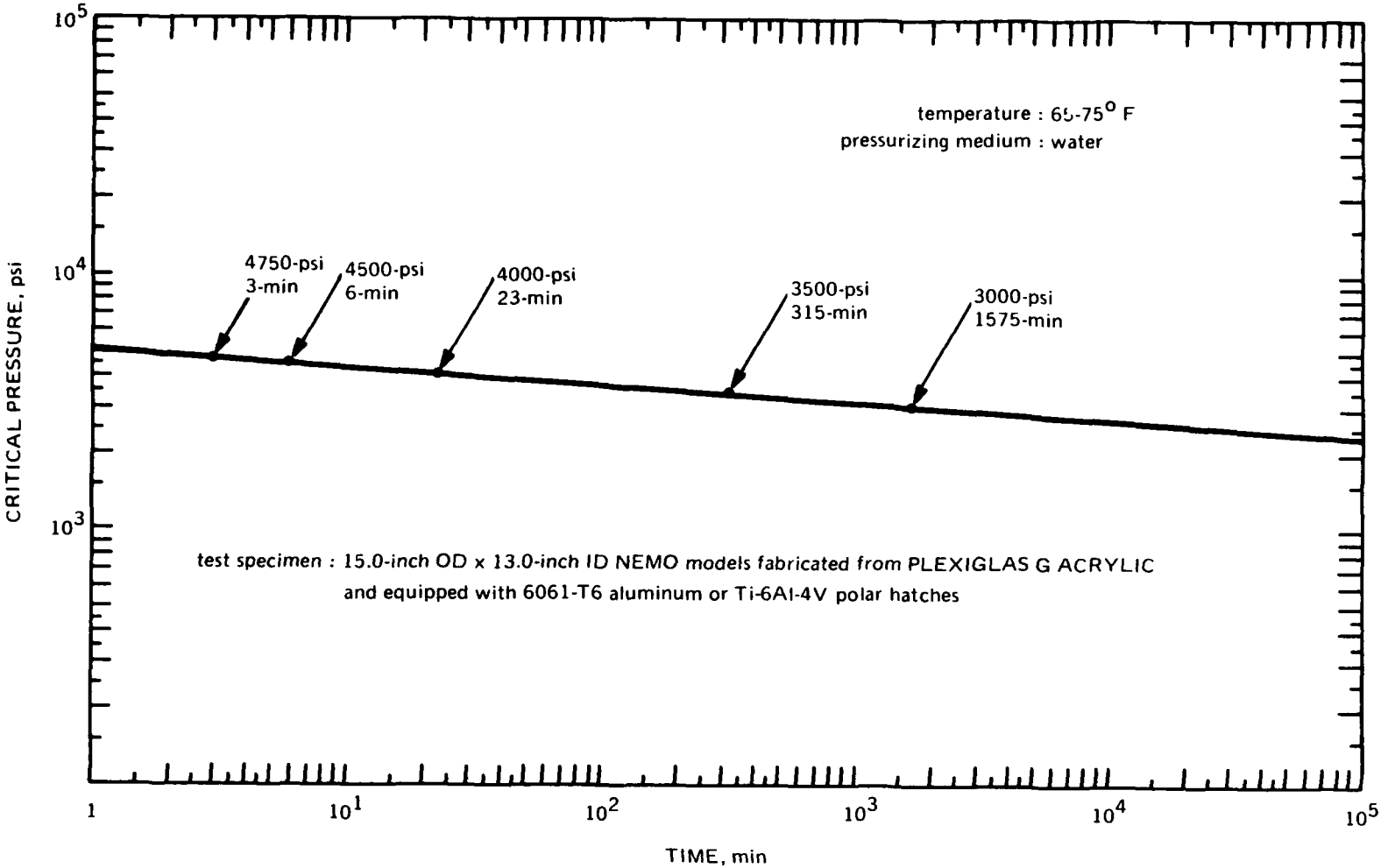

Figure 33. Long term critical pressure as a function of sustained loading duration.

Figure 34. Typical shear cracks in the bearing surface of an acrylic Nemo Hull generated by pressure cycling; when the cracks reach this size the acrylic hull should be removed from service and the bearing surface refinished. (Ref. 5. Nemo Hull Model 600 after pressure cycling to 2000 ft. depth.)

REFERENCES

1. Naval Civil Engineering Laboratory, Technical Report R-749, "NEMO, A New Concept in Submersibles," P. K. Rockwell, R. E. Elliott, M. R. Snoey, November 1971 (AD 735103).

2. Naval Civil Engineering Laboratory, Technical Report R-676, "Development of a Spherical Acrylic Plastic Pressure Hull for Hydrospace Applications," J. D. Stachiw, April 1970 (AD 707363)

3. Naval Civil Engineering Laboratory, Technical Note N-1113, "The Spherical Acrylic Pressure Hull for Hydrospace Application; Part 2. Experimental Stress Evaluation of Prototype NEMO Capsule," J. D. Stachiw and K. L. Mack, October 1970 (AD 715772)

4. Naval Civil Engineering Laboratory, Technical Note N-1094, "The Spherical Acrylic Pressure Hull for Hydrospace Application; Part 3. Comparison of Experimental and Analytical Stress Evaluations for Prototype NEMO Capsule." H. Ottsen, March 1970 (AD 709914)

5. Naval Civil Engineering Laboratory, Technical Note N-1134, "The Spherical Acrylic Pressure Hull for Hydrospace Application; Part 4. Cyclic Fatigue of NEMO Capsule #3," J. D. Stachiw, October 1970 (AD 715345)

6. American Society of Mechanical Engineers, Paper No. 70-WA/UnT-3, "Spherical Acrylic Pressure Hulls for Undersea Exploration," by J. D. Stachiw, *Journal of Engineering for Industry*, May 1971

7. American Society of Mechanical Engineers, Paper No. 71-WA/UnT-6, "Acrylic Pressure Hull for JOHNSON SEA-LINK Submersible," by J. R. Maison and J. D. Stachiw, December 1971

8. Naval Ship Research and Development Center, Technical Report 2641, "Finite Element Analysis for Arbitrary Axisymmetric Structures," L. N. Gifford, March 1968

9. American Society of Mechanical Engineers, Paper No. 72-WA/OCT-8, "Transparent Hull Submersible MAKAKAI," by D. W. Murphy and W. F. Mazzone, December 1972

10. American Society of Mechanical Engineers, Paper No. 70-WA/UnT-6, "The JOHNSON SEA-LINK – The First Deep Diving Welded Aluminum Submersible," by R. A. Kelsey and R. B. Dolan, December 1970

11. Naval Civil Engineering Laboratory, Technical Report R-716, "Structural Analysis of a Full Scale Spherical Acrylic Plastic Pressure Hull," M. R. Snoey and M. G. Katona, March 1971

12. American Society of Mechanical Engineers, Paper No. 70-WA/UnT-4, "Fabrication of NEMO-Type Spherical Acrylic Capsules for Underwater Vehicles," K. Tsuji and R. Shelton, December 1970

13. American Society of Mechanical Engineers, Paper No. 71-UnT-2, "Acrylic Pressure Hull for Submersible NEMO," by J. D. Stachiw, December 1970

14. American Society of Mechanical Engineers, Paper No. 70-UnT-B, "Stress Analysis of a Spherical Acrylic Pressure Hull," by M. R. Snoey and M. G. Katona, December 1970

15. American Society of Mechanical Engineers, Paper No. 70-UnT-A, "Optical Properties of a Spherical Plastic Underwater Observatory NEMO," by T. Trowbridge, December 1970

16. American Society of Mechanical Engineers, Paper No. 72-WA/OCT-11, "Modulated Light Beam Information Transmission System for Transparent Pressure Hulls," by J. E. Holzschuh and G. R. Beaman, December 1972

APPENDIX A

DESIGN DETAILS OF NEMO MODEL 2000

APPENDIX A. DESIGN DETAILS OF NEMO MODEL 2000

15-Inch OD X 13-Inch ID Scale Models

The acrylic hull of the 15-inch OD X 13-inch ID scale model 34 was designed to be a faithful copy of the 66-inch OD X 58-inch ID Model 2000 Nemo Hull both in proportions and in method of construction (Figures 1A and 2A). It was to be fabricated in the same manner as the 66-inch OD X 58-inch ID hull by thermoforming spherical sectors from flat discs, machining pentagons from sectors, and finally assembling the spherical pentagons into a sphere by bonding the joints between adjoining pentagons with PS-30 self-polymerizing adhesive (Figure 3A).

The aluminum plates (Figures 4A, 5A, and 6A) for top and bottom polar openings in the 15-inch OD X 13-inch ID Model 34 were not faithfully scaled down models of the hatches in the 66-inch OD X 58-inch ID diameter Model 2000 Nemo Hull. Although structurally the 6061-T6 aluminum plates in the 15-inch OD X 13-inch ID Model 34 behave identically to the hatches in the 66-inch OD X 58-inch ID hull, some operational features of the large hatches have been omitted in the scale model plates. Thus, for example, the top aluminum plate 15-inch OD X 13-inch ID Model 34 has the same rigidity and proportions as the top hatch in the 66-inch OD X 58-inch ID Model 2000 Nemo Hull but does not disassemble into separate hatch and hatch ring components.

The construction of the 15-inch OD X 13-inch ID Models 35, 36, and 37 was identical to that of Model 34. The only difference between Model 34 and the other models lay in the design of the polar plates. The polar plates for Models 35, 36, 37 were structurally idealized hatches designed in titanium Ti-6Al-4V (Figure 7A). Since these models were to be used in cyclic pressure tests to determine the effect of depth on the performance of the polycarbonate gasket between the hatch and the acrylic bearing surface, each model was equipped with the polycarbonate gasket only for the top plate while the bottom plate in each model was designed to operate without a gasket. In this manner each model was designed to operate both with and without a gasket around the titanium plates. In this manner, each model would provide the data on the performance of acrylic bearing surfaces at a given pressure with and without polycarbonate gaskets (Figure 8A).

66-Inch OD X 58-Inch ID Operational Model

The 66-inch OD X 58-inch ID operational Model 2000 Nemo Hull was designed for economical construction within tight dimensional tolerances to maximize the operational depth of the assembly. The acrylic hull was designed to be constructed from 12 spherical pentagons bonded together with PS 18, PS 30 or any other self-polymerizing adhesive with 5000 psi minimum tensile strength (Figures 9A and 10A).

The polar aluminum assemblies were designed, like the polar insert assemblies in the previous Model 600 and Model 1000 Nemo Hulls, to serve as hatches for personnel entry and feed through plates for electrical and hydraulic control cables. Aluminum was chosen as the

construction material because of its resistance to corrosion and attractive strength to weight ratio. The bottom feed through plate was equipped with 9 holes to accommodate 9 separate electrical or hydraulic feed throughs (Figure 11A). In addition, the feedthrough plate serves also as the foundation for any equipment contained within the capsule. The diameter of the top polar opening was selected to be ample enough even for a heavy set pilot or observer (Figure 12A). Because considerable exertion has been required of the crew in the past Nemo Hull designs to open the heavy hatch, a set of torsion springs was incorporated into the Model 2000 Nemo hatch assembly (Figure 12A). Also latch locks have been incorporated into the hatch handles to lock them securely in the open position when the hatch is open (Figure 13A).

All the parts of the hatch were made from 6061-T6 aluminum, except the Monel K-500 latch shafts, the 17-4 PH stainless hinge pin, steel counter balance springs, and polycarbonate plastic gaskets (Figures 14A, 15A, 16A, 17A, 18A, 19A and 20A). Materials chosen for these applications matched well with the galvanic potential of aluminum, thus preventing unduly severe galvanic corrosion. As a rule all the bevel angle tolerances on polar insert components were specified to be ±15 minutes, a readily attainable tolerance with standard shop machining practices. During the subsequent assembly of the Model 2000 Nemo Hull structure it was found, however, that the ±15-degree angle tolerances resulted in incomplete surface contact between matching beveled structural components. As a result of this finding, it is recommended that the angle tolerance be decreased to ±7.5 degrees in future Model 2000 Nemo Hull assemblies.

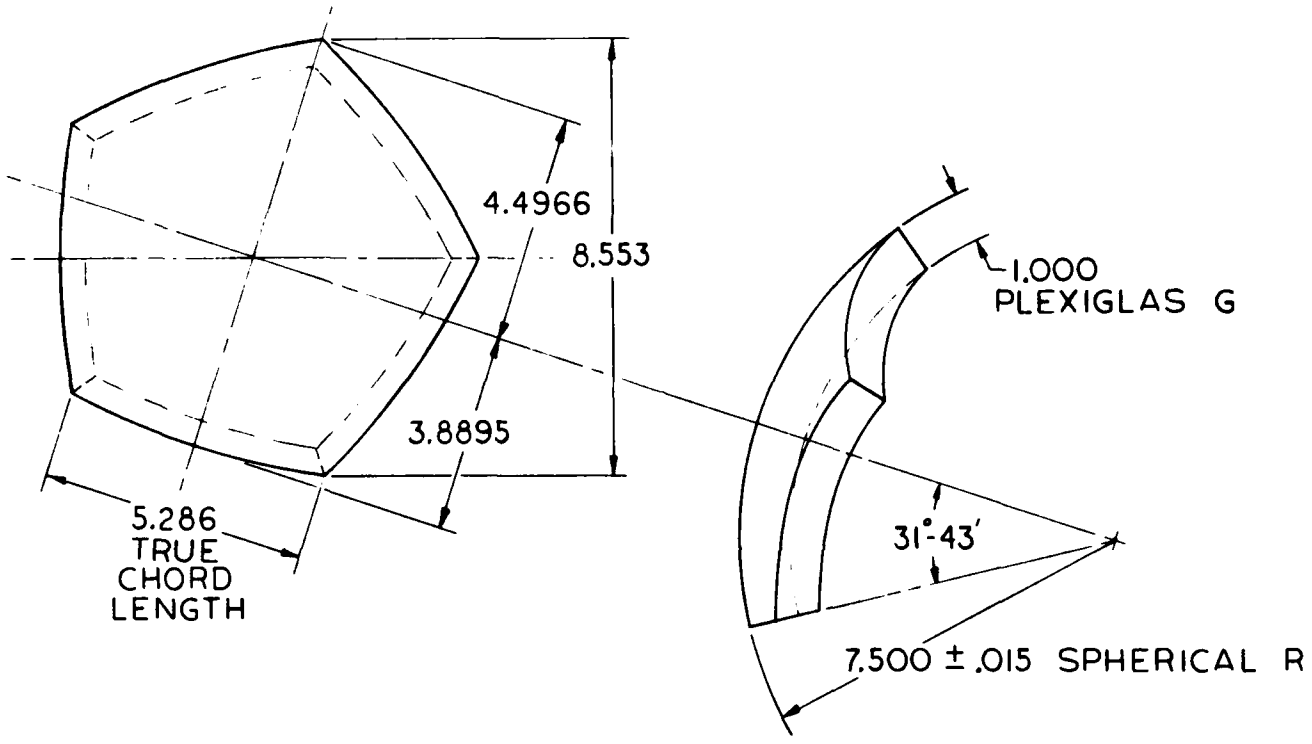

Figure 1A. Spherical pentagon for the 15-inch OD X 13-inch ID scale model of the Model 2000 Nemo Hull.

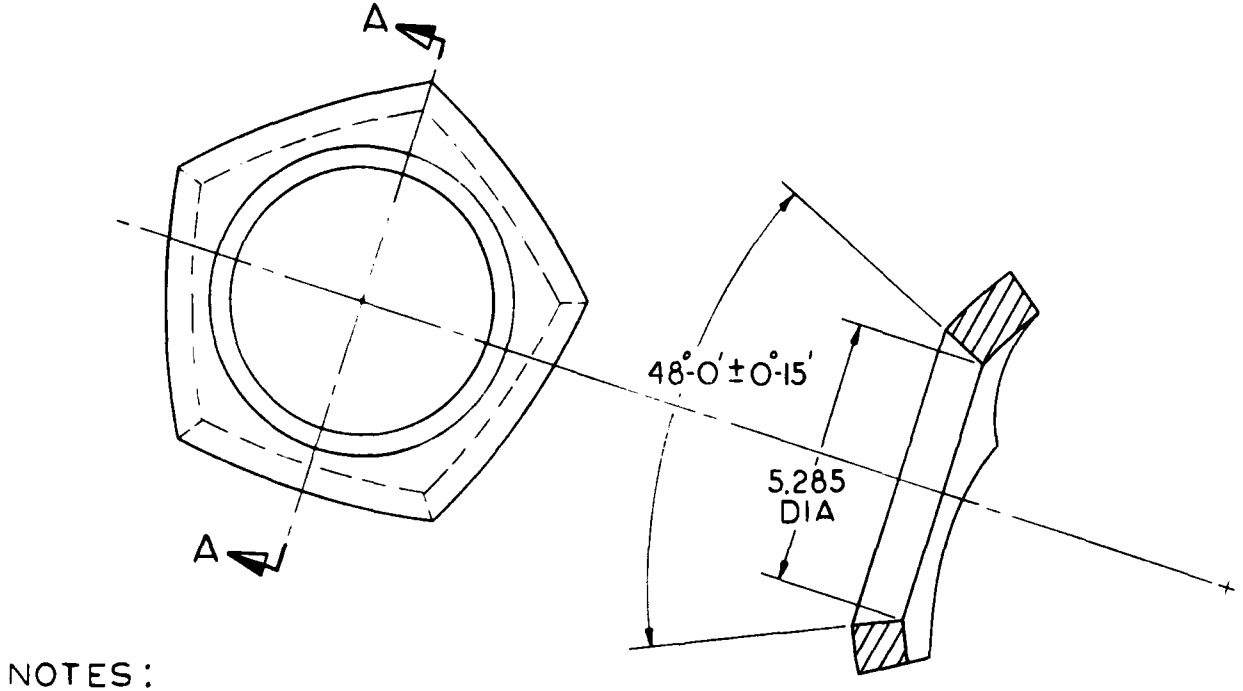

Figure 2A. Polar spherical pentagon for the 15-inch OD X 13-inch ID scale model of the Model 2000 Nemo Hull.

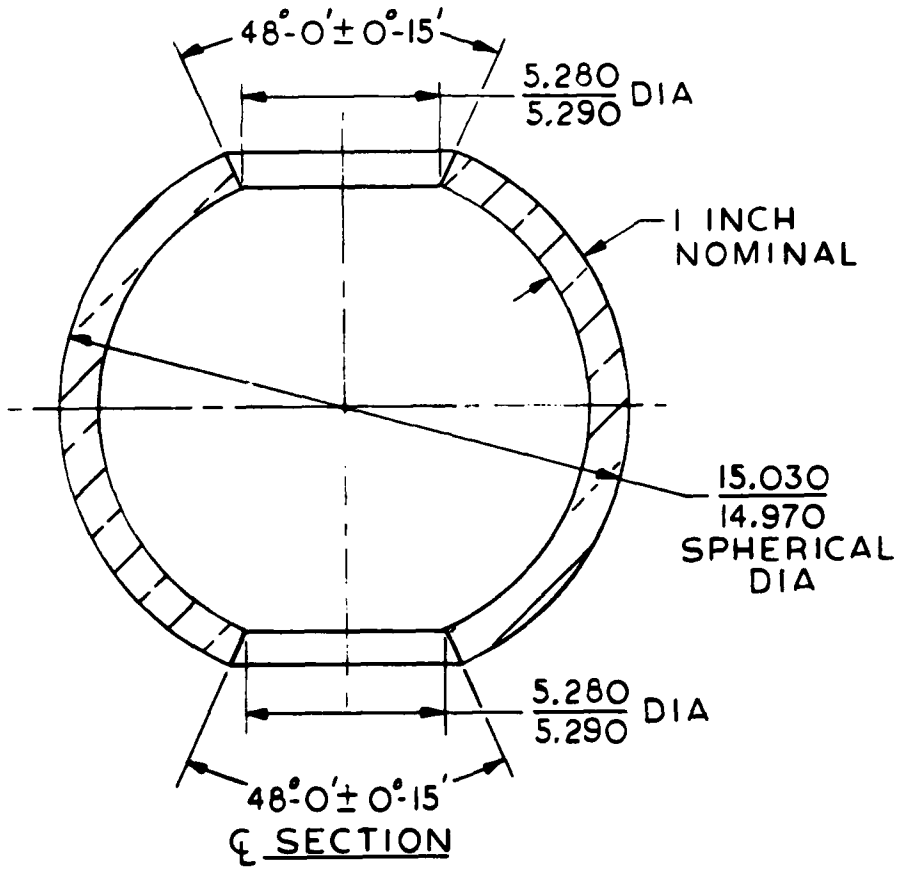

NOTES:
1. MATERIAL: PLEXIGLAS G, 1.0 INCH PLATE
2. ADHESIVE: PS-30
3. POLAR INSERTS: ALUMINUM HATCHES
PER DWG 701100-11
POLYCARBONATE GASKETS
PER DWG 701100-11

Figure 3A. Assembled hull of the 15-inch OD X 13-inch ID Model 34.

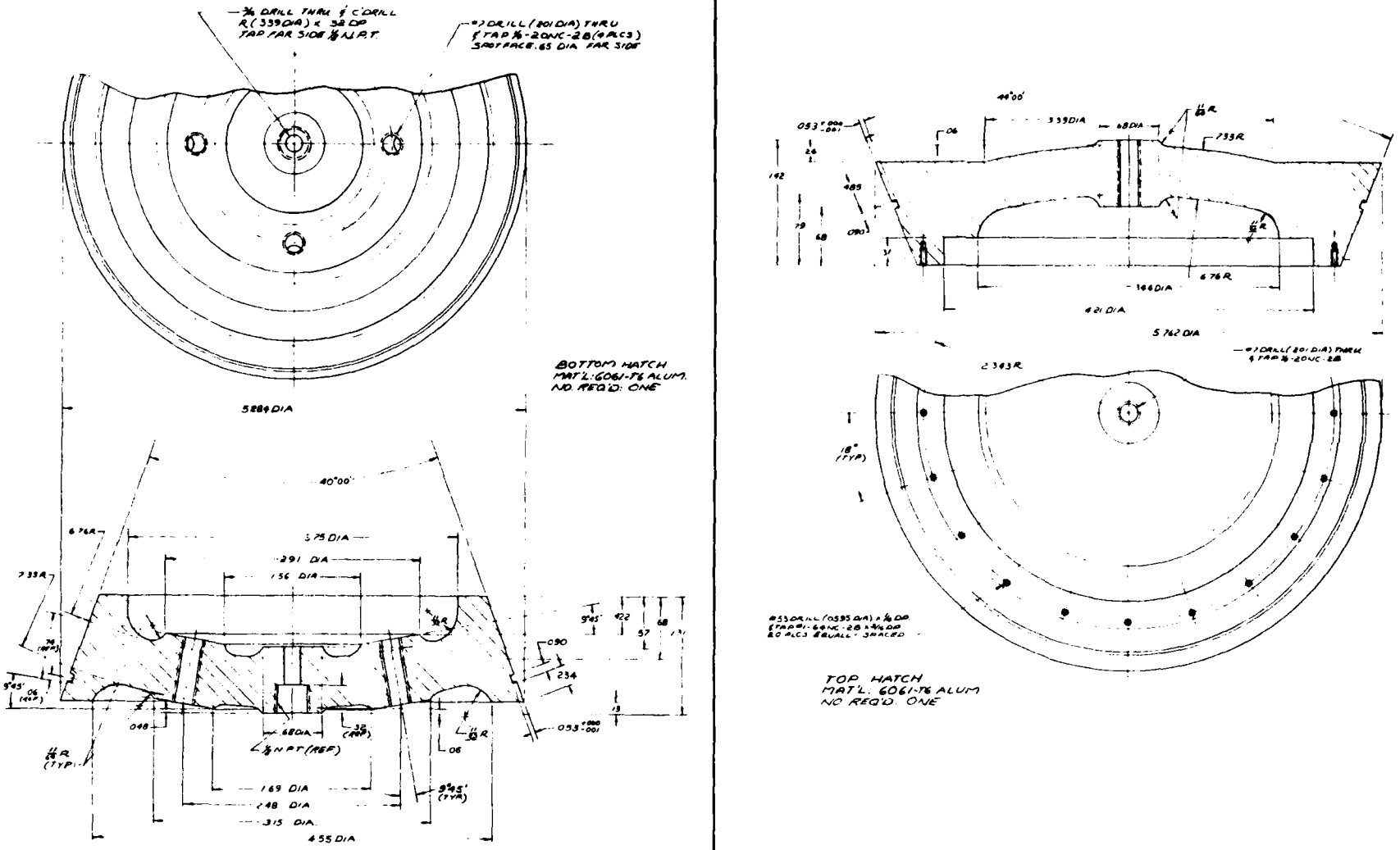

Figure 4A. Polar Aluminum Hatch Assemblies for the 15-inch OD X 13-inch ID Model 34.

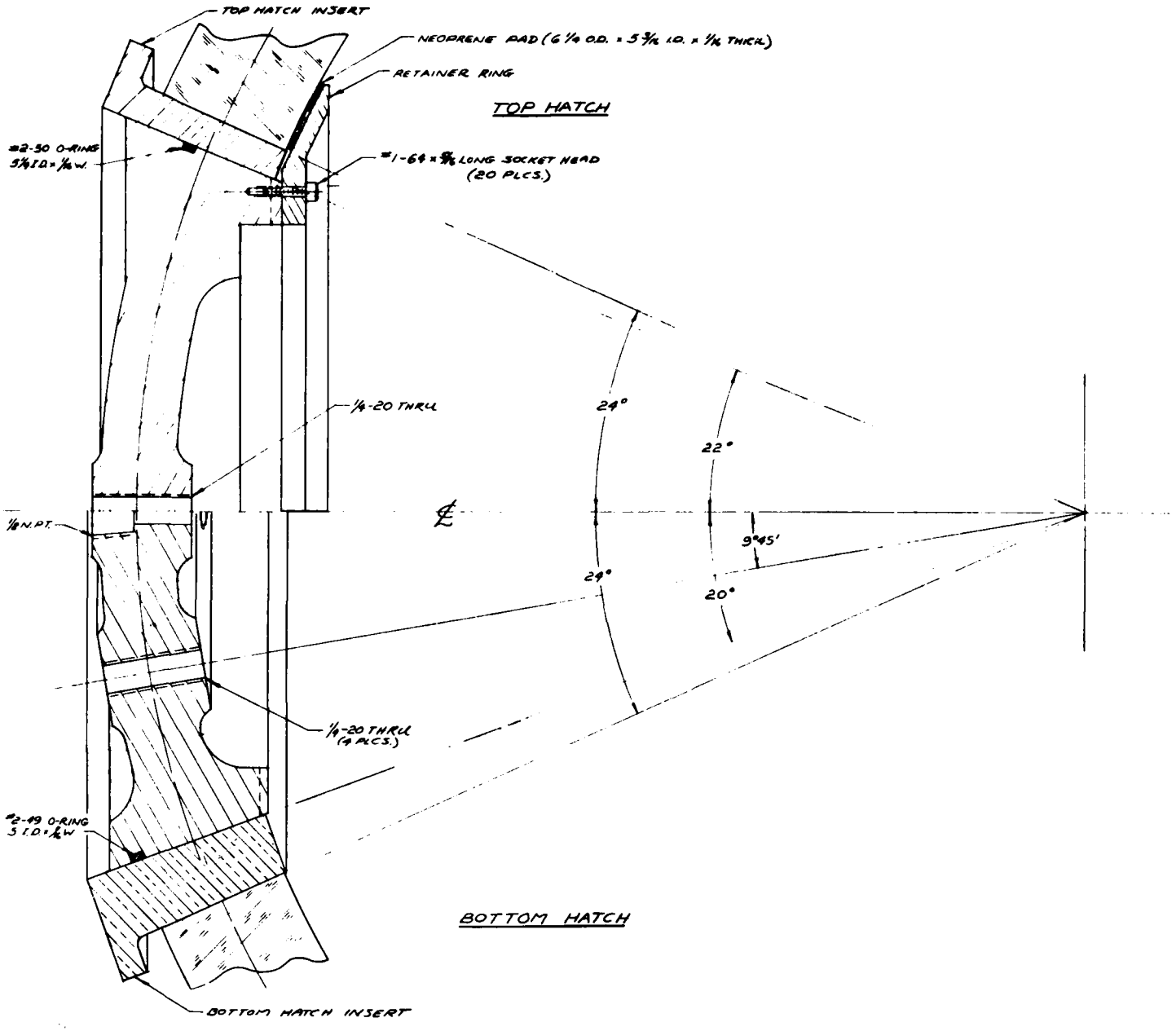

Figure 5A. Top and bottom aluminum hatches for the 15-inch OD X 13-inch ID Model 34.

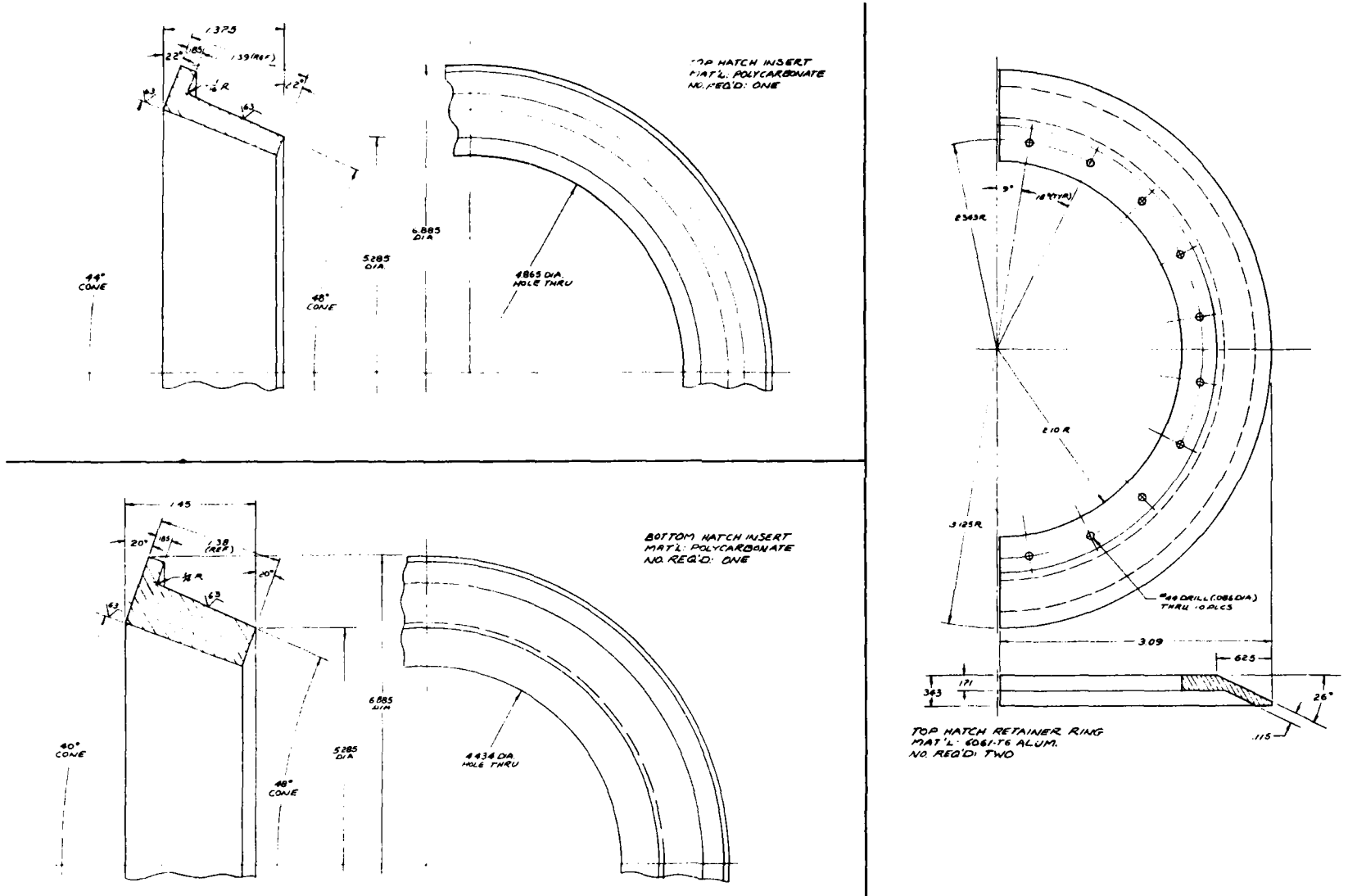

Figure 6A. Polycarbonate polar gaskets and top hatch retaining ring for the 15-inch OD X 13-inch ID Model 34.

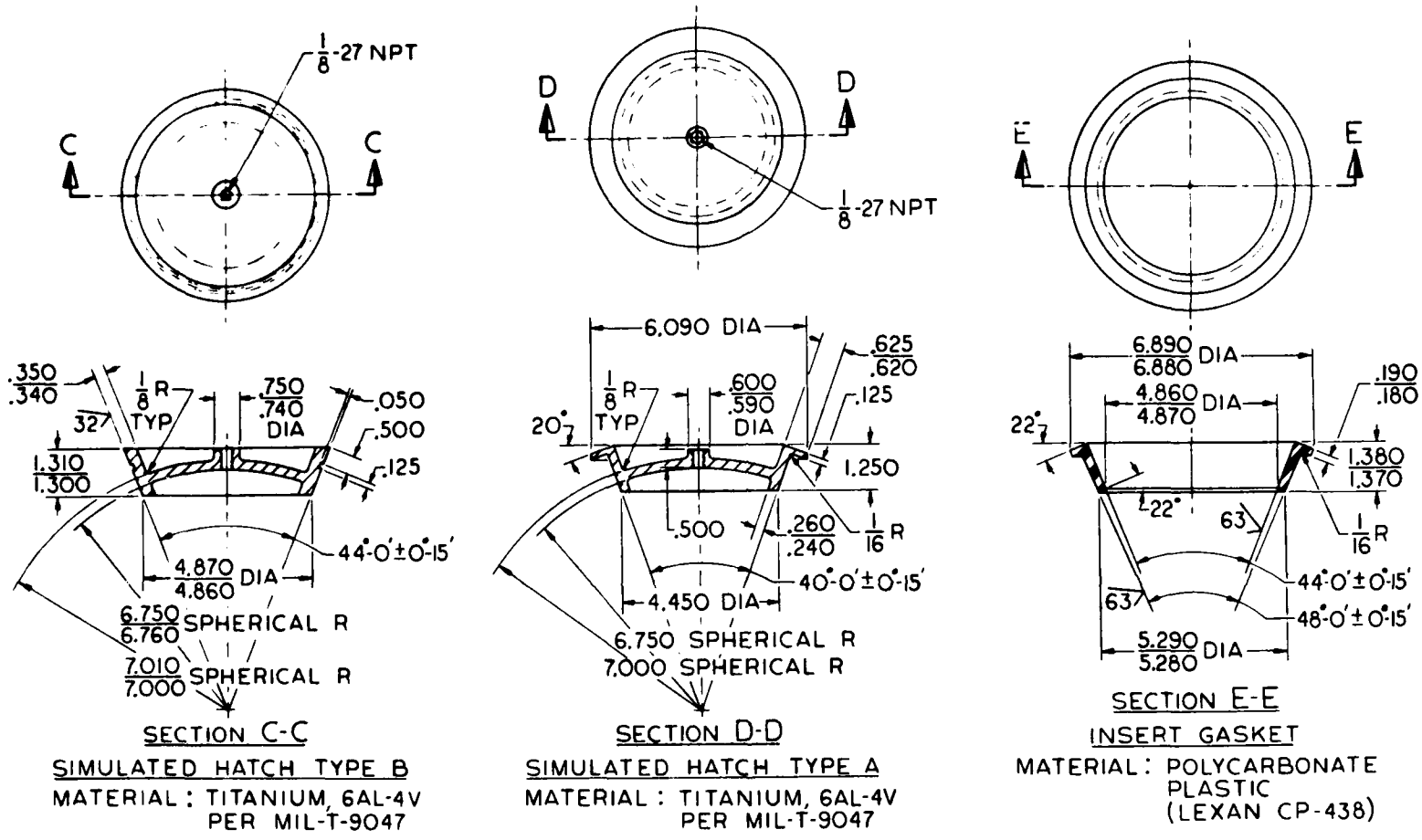

Figure 7A. Polar titanium hatches for service with 15-inch OD X 13-inch ID Models 35, 36 and 37. Note that Type A titanium hatch was designed for service without the polycarbonate gasket while Type B titanium hatch was designed to be used with a polycarbonate gasket.

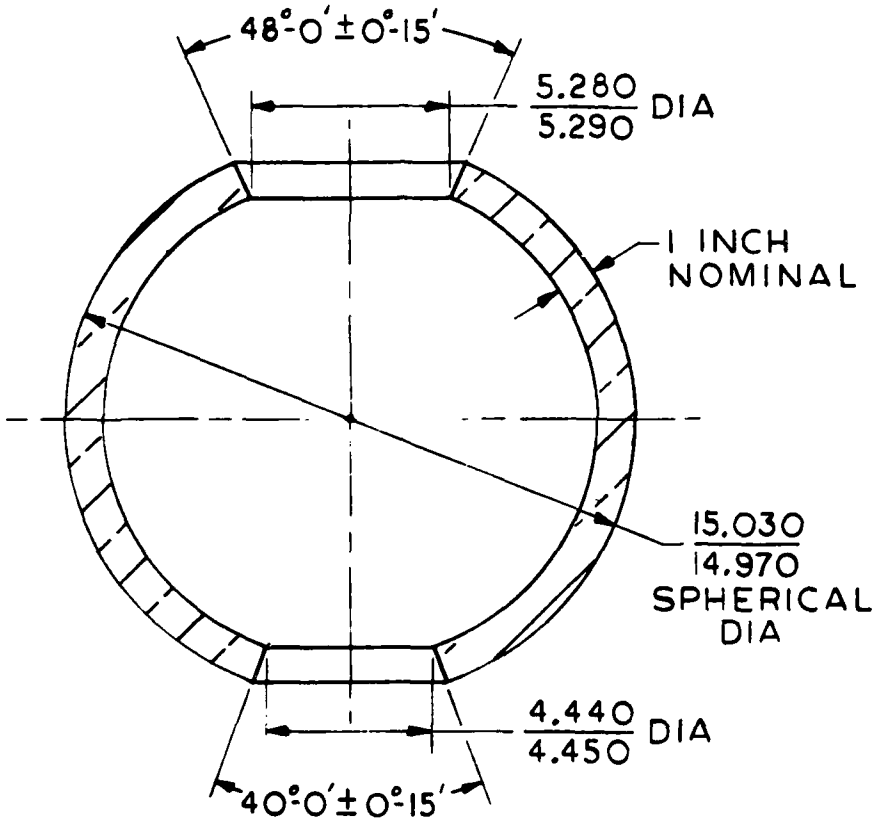

NOTES:

1. MATERIAL: PLEXIGLAS G, 1.0 INCH PLATE
2. ADHESIVE: PS-30
3. INSERTS: TOP OPENING - TYPE B TITANIUM HATCH WITH POLYCARBONATE GASKET
   BOTTOM OPENING - TYPE A TITANIUM HATCH WITHOUT GASKET

Figure 8A. Typical assembly of 15-inch OD X 13-inch ID Models 35, 36 and 37.

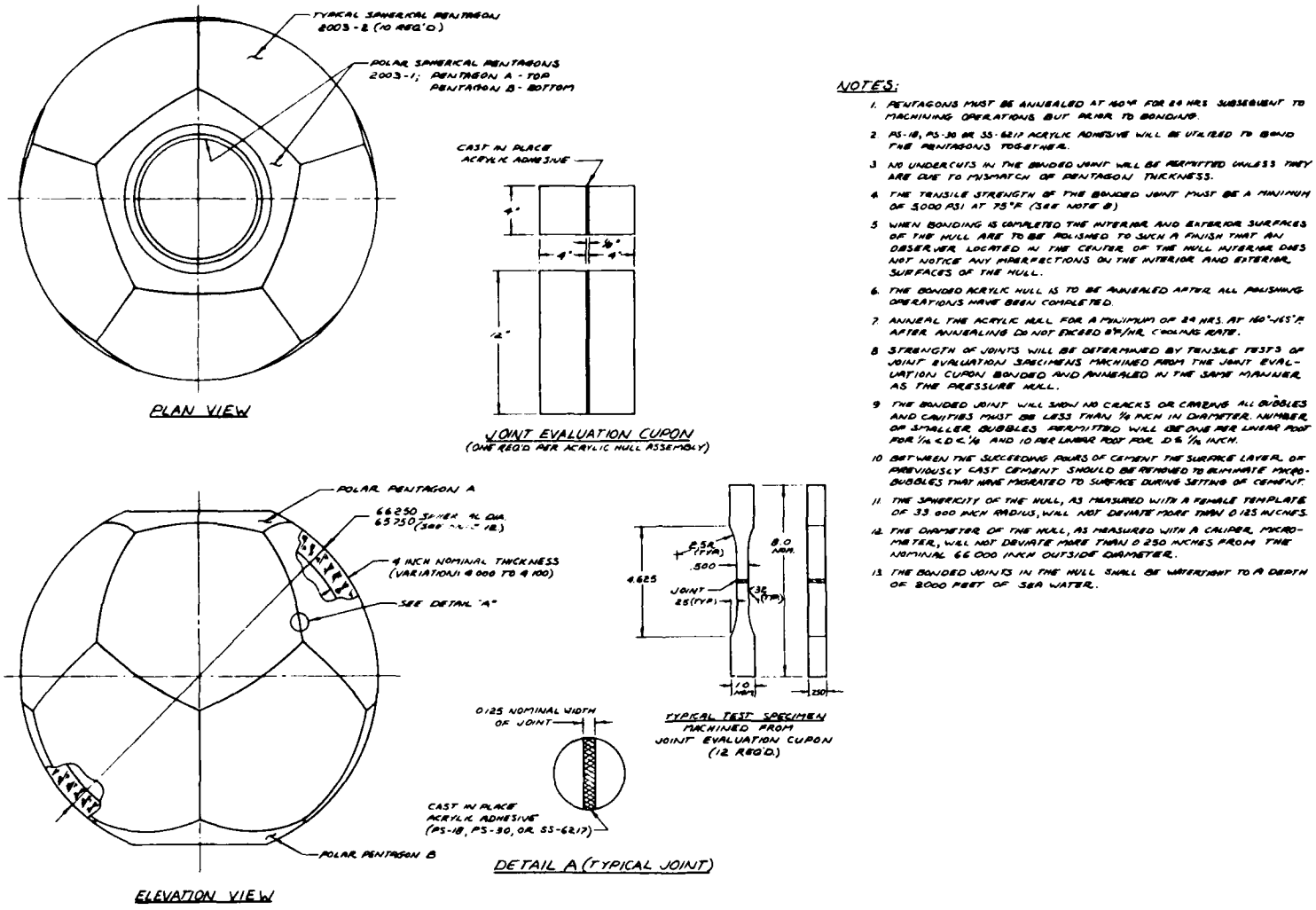

Figure 9A. Model 2000 acrylic Nemo Hull assembly, 66-inch OD X 58-inch ID.

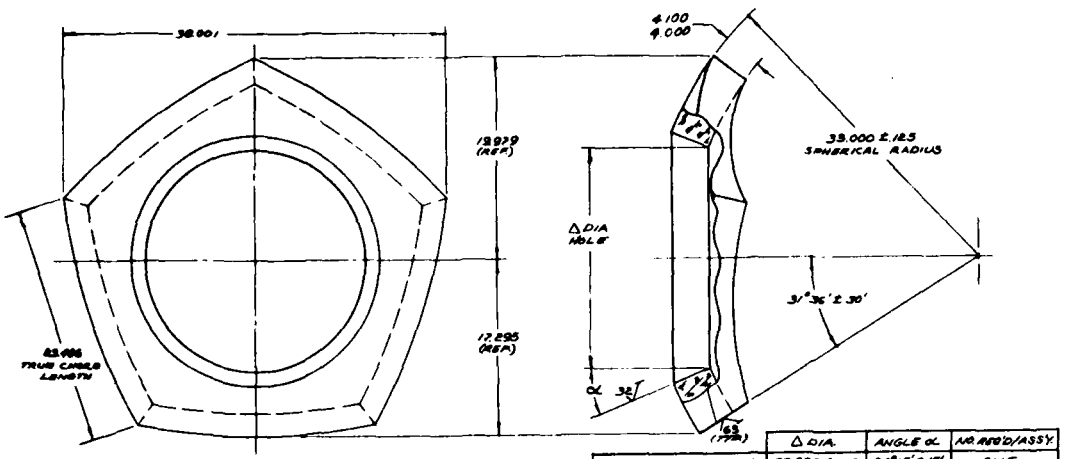

	Δ DIA.	ANGLE α	NO. REQ'D/ASS'Y.
POLAR PENTAGON A	23.822 ± .010	24°15' ± 15'	ONE
POLAR PENTAGON B	21.727 ± .010	22°00' ± 15'	ONE

(1) POLAR SPHERICAL PENTAGON

NOTES:

1. MATERIAL TO BE UNSHRUNK ACRYLIC WITH THE FOLLOWING PHYSICAL PROPERTIES:

PROPERTY	TYPICAL	TEST METHOD
HARDNESS, ROCKWELL M	90	ASTM-D785-65
SPECIFIC GRAVITY	1.19 ± 0.01 (2 PLACES WITHIN 0.005)	ASTM-D792-66
REFRACTIVE INDEX	1.50 ± .01	ASTM-D542-50
LUMINOUS TRANSMITTANCE; THICKNESS OF 0.5 INCH	89% MIN.	ASTM-D1003-61
HAZE; THICKNESS OF 0.6 INCH	3% MAX.	ASTM-D1003-61
DISPLACEMENT FACTOR; THICKNESS OF 0.5 INCH	50% MAX.	
○ TENSILE STRENGTH, RUPTURE	9,000 PSI MIN.	ASTM-D638-68
○ TENSILE ELONGATION, RUPTURE	2% MIN.	ASTM-D638-68
○ MODULUS OF ELASTICITY, TENSION	400,000 PSI MIN.	ASTM-D638-68T
○ COMPRESSIVE STRENGTH	13,000 PSI MIN.	ASTM-D695-69
○ FLEXURAL STRENGTH, RUPTURE	14,000 PSI MIN.	ASTM-D790-70
○ SHEAR STRENGTH, RUPTURE	8,000 PSI MIN.	ASTM-D732-46
IMPACT STRENGTH, IZOD	0.3 FT-LB/IN (MIN.)	ASTM-D256-70
○ COMPRESSIVE DEFORMATION UNDER LOAD (4000 PSI AT 122°F FOR 24 HR.)	1% MAX.	ASTM-D621-64
WATER ABSORPTION IN 24 HR.	0.25% MAX	ASTM-D570-63

2. THE ABOVE PHYSICAL PROPERTIES MARKED ○ SHALL BE DETERMINED FOR EACH ACRYLIC SHEET BY MACHINING FROM THE SHEET TWO MATERIAL TEST SPECIMENS FOR EACH ASTM TEST METHOD SPECIFIED.
3. NUMBER EACH SEGMENT WITH APPROX. .1 INCH NUMERALS IN AT LEAST THREE (3) PLACES AFTER MACHINING (USE "MARK-3-A-LOT" FELT TIP MARKER.)
4. MEASURE & RECORD THE THICKNESS & THE OUTSIDE SPHERICAL RADIUS OF EACH SEGMENT; MEASURE AT THE CENTER AND AT EACH TIP.
5. TOLERANCE ON LINEAR DIMENSIONS AS ± .030 IN. UNLESS OTHERWISE SPECIFIED.

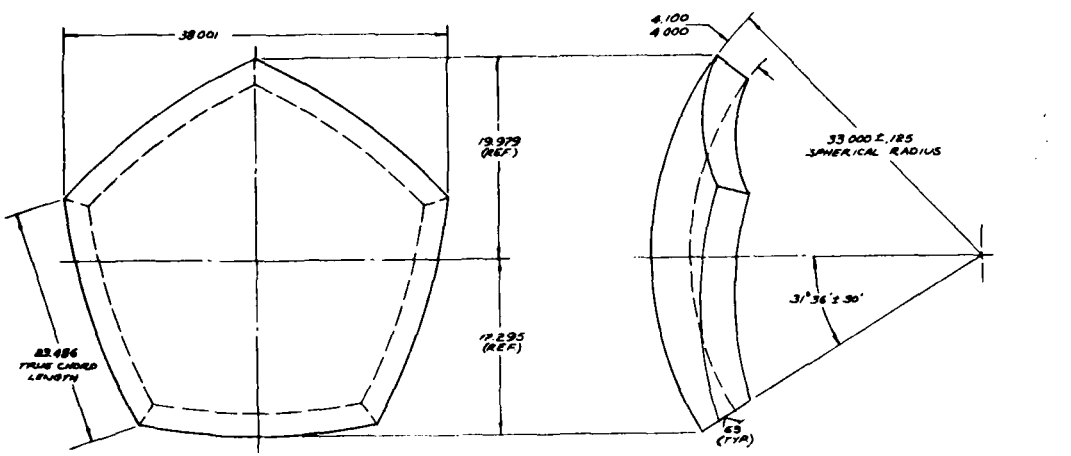

(2) SPHERICAL PENTAGON (10 REQ'D/ASS'Y.)

Figure 10A. Spherical pentagons for the 66-inch OD X 58-inch ID Model 2000 Nemo Hull.

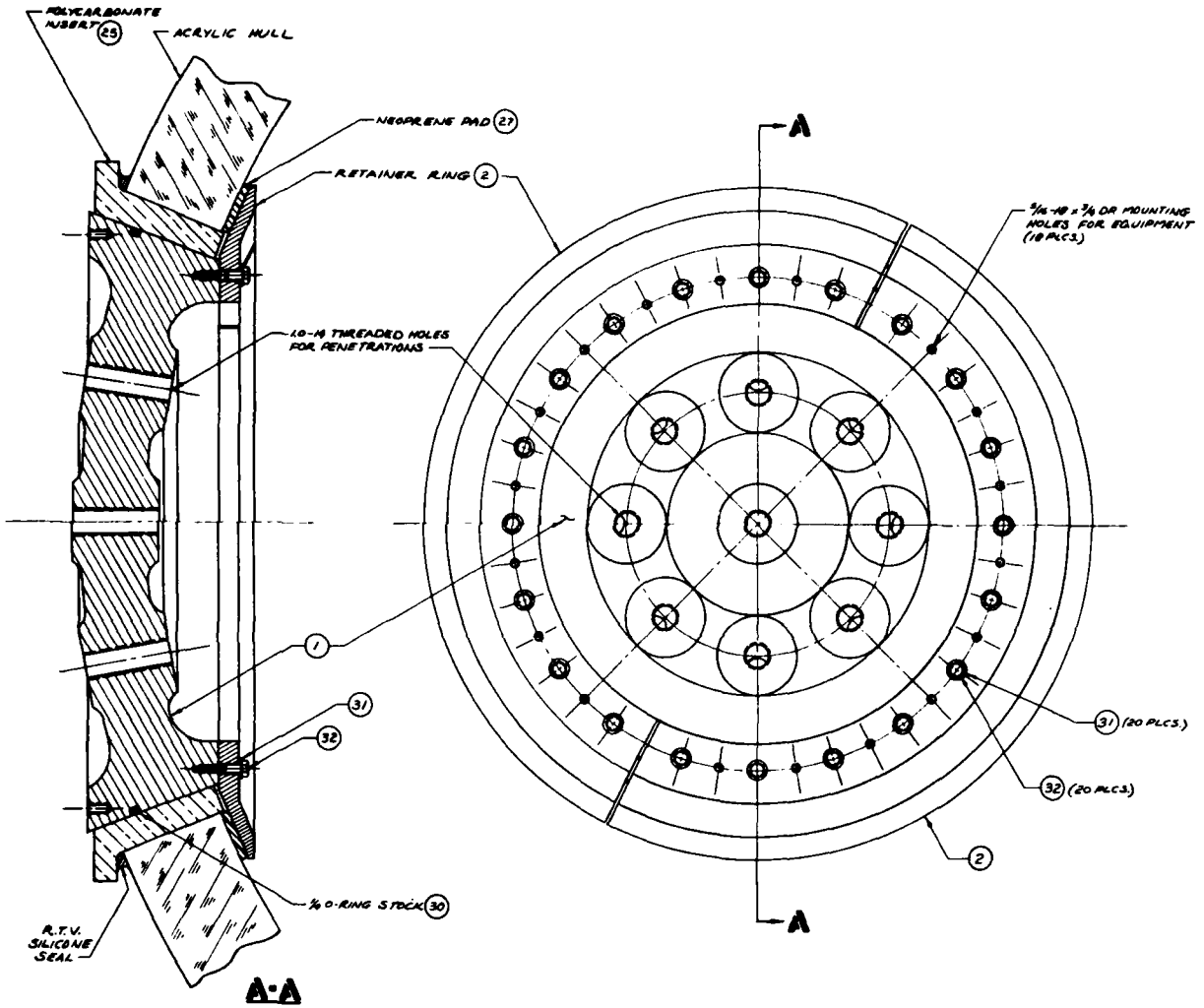

Figure 11A. Bottom plate assembly for the 66-inch OD X 58-inch ID Model 2000 Nemo Hull.

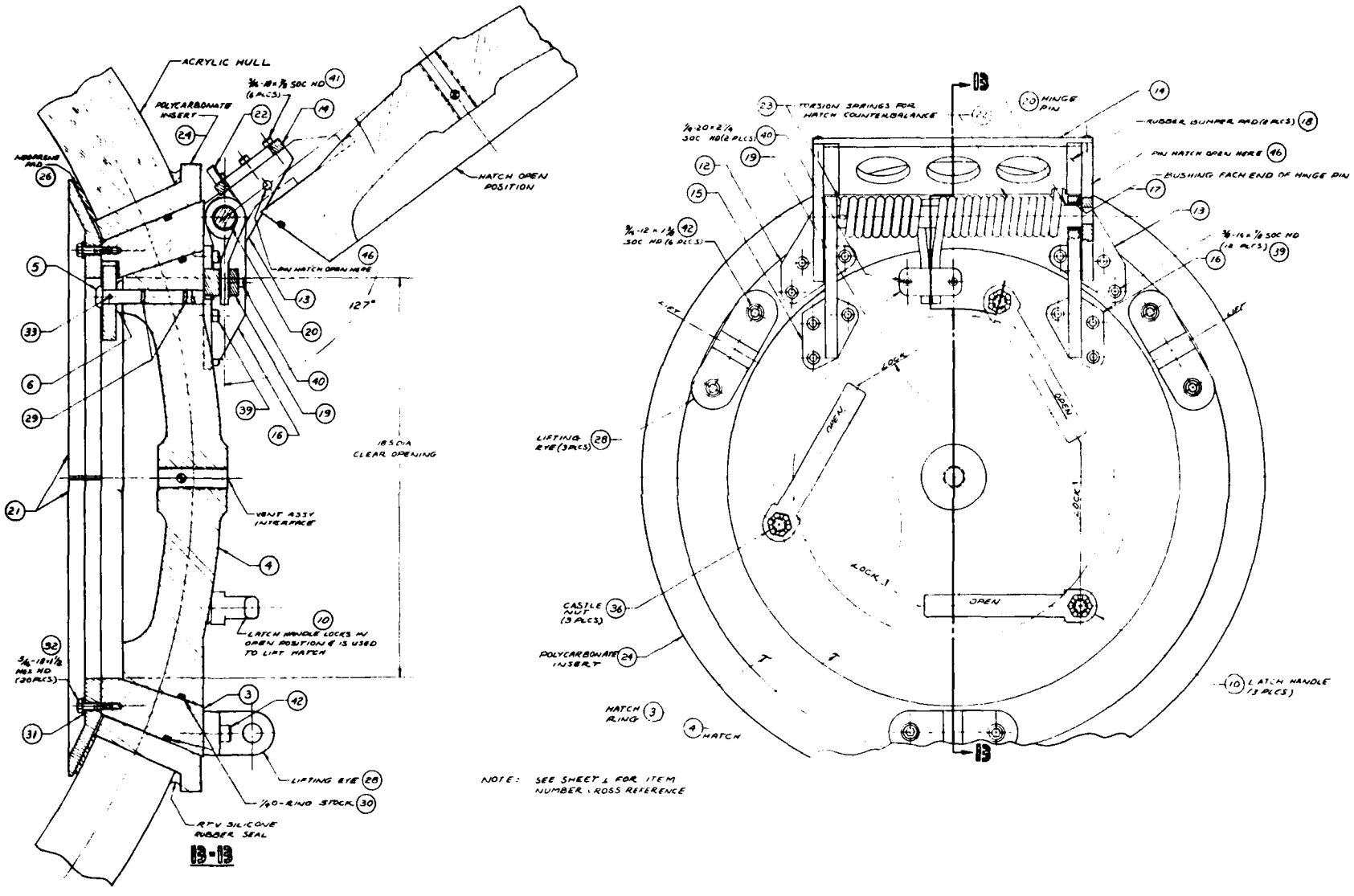

Figure 12A. Hatch assembly for the 66-inch OD X 58-inch ID Model 2000 Nemo Hull.

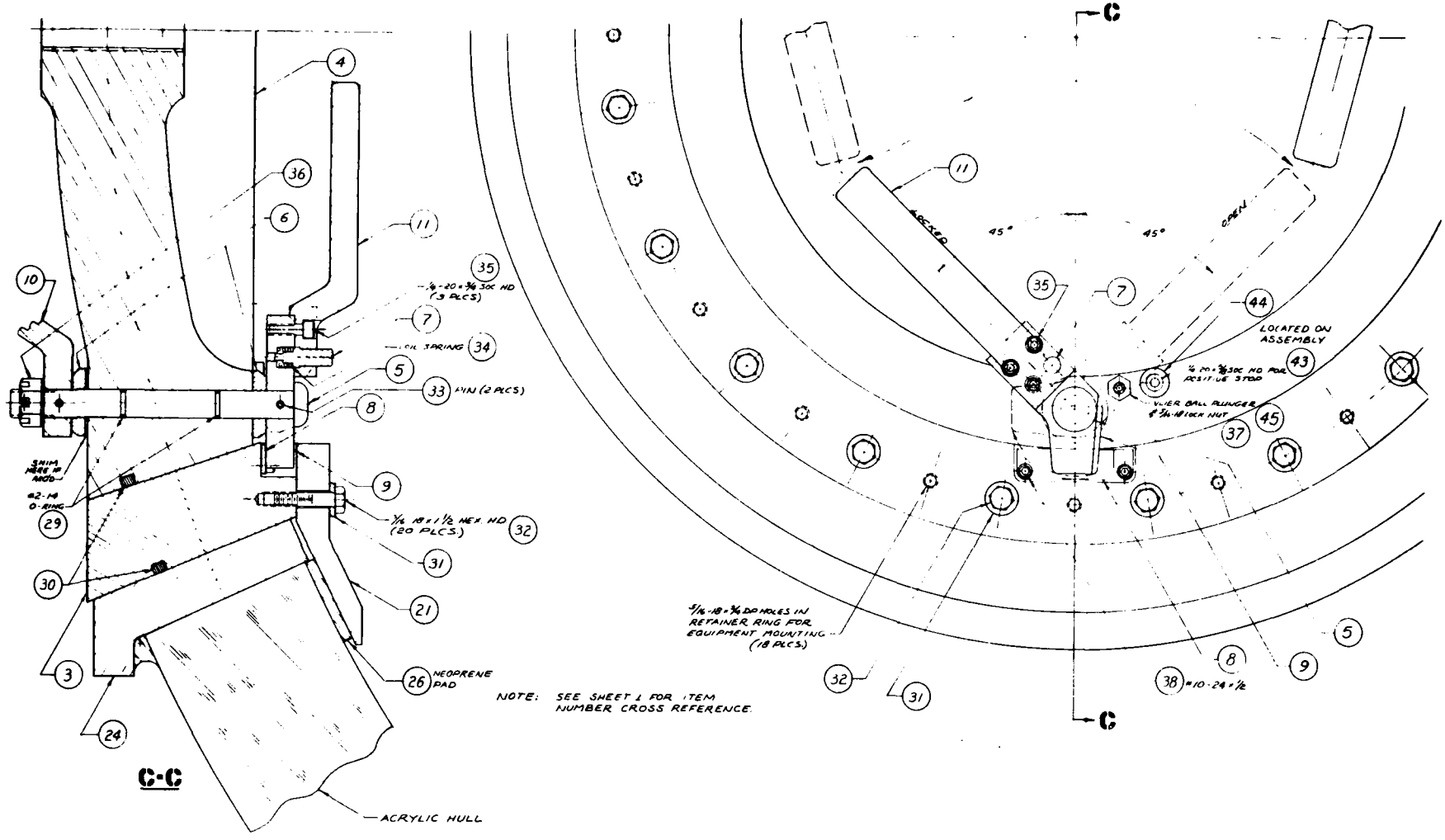

Figure 13A. Hatch lock assembly for the 66-inch OD X 58-inch ID Model 2000 Nemo Hull.

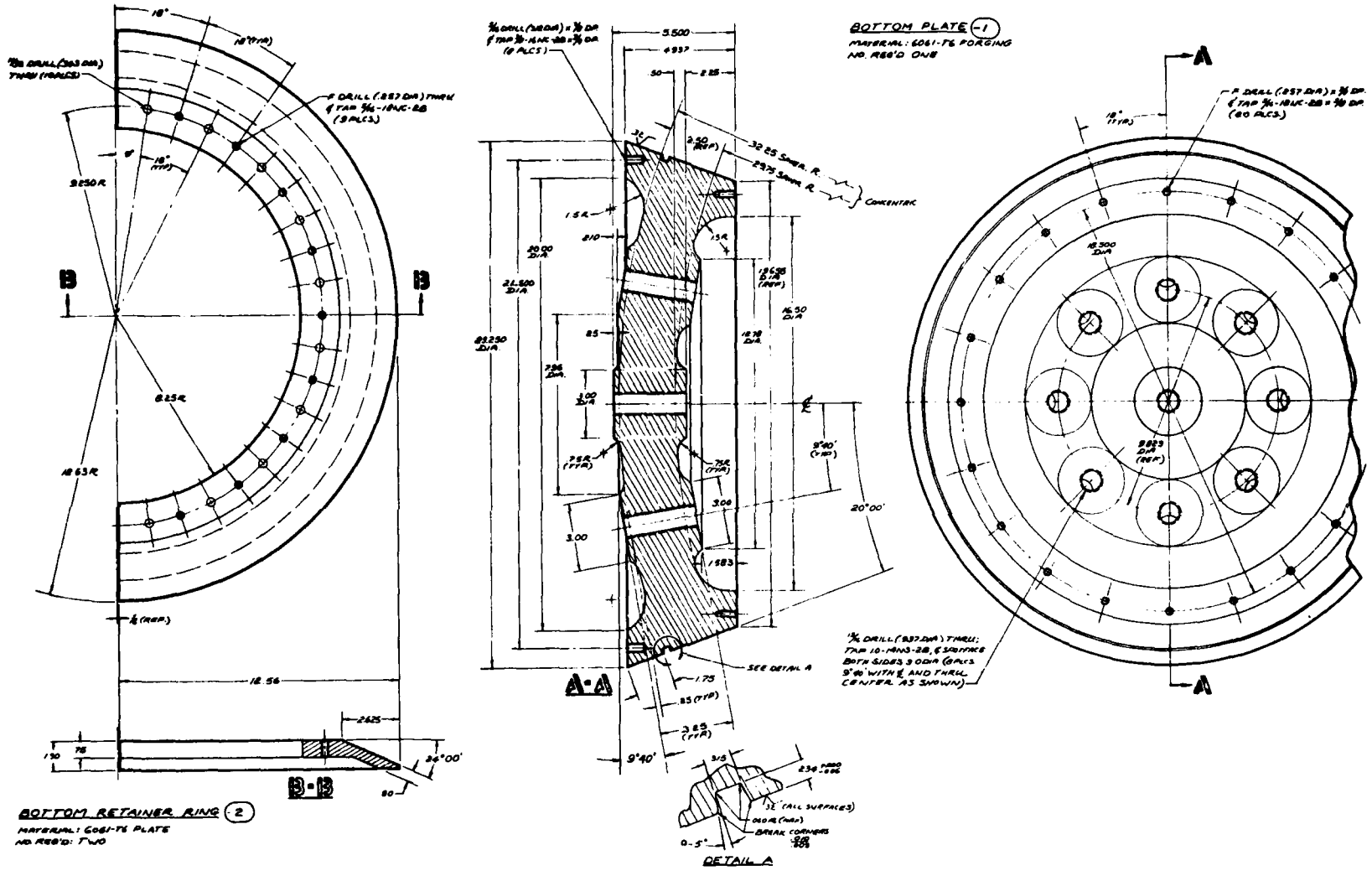

Figure 14A. Bottom plate and bottom retainer ring for the 66-inch OD X 58-inch ID Model 2000 Nemo Hull.

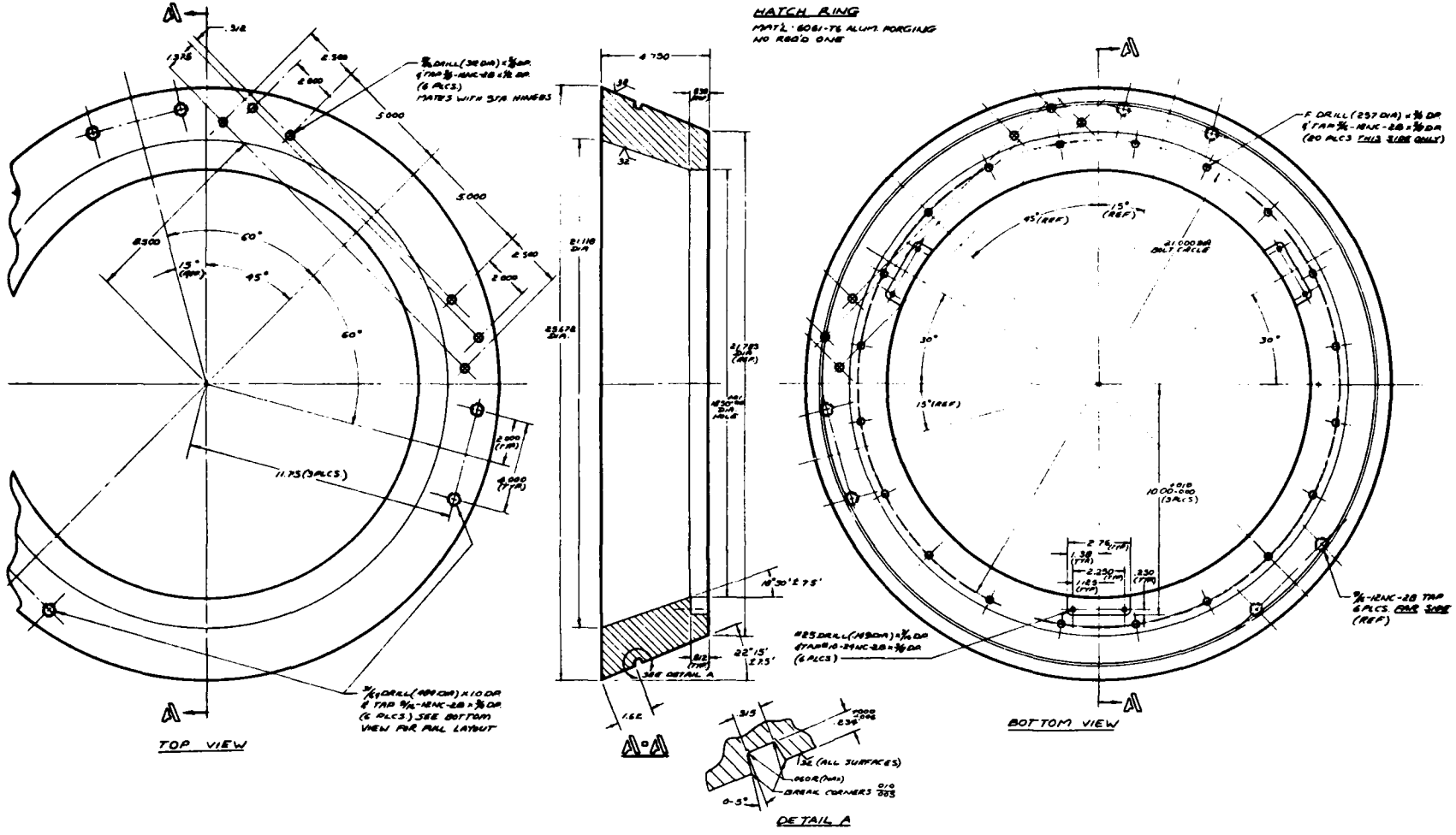

Figure 15A. Hatch ring for the 66-inch OD X 58-inch ID Model 2000 Nemo Hull.

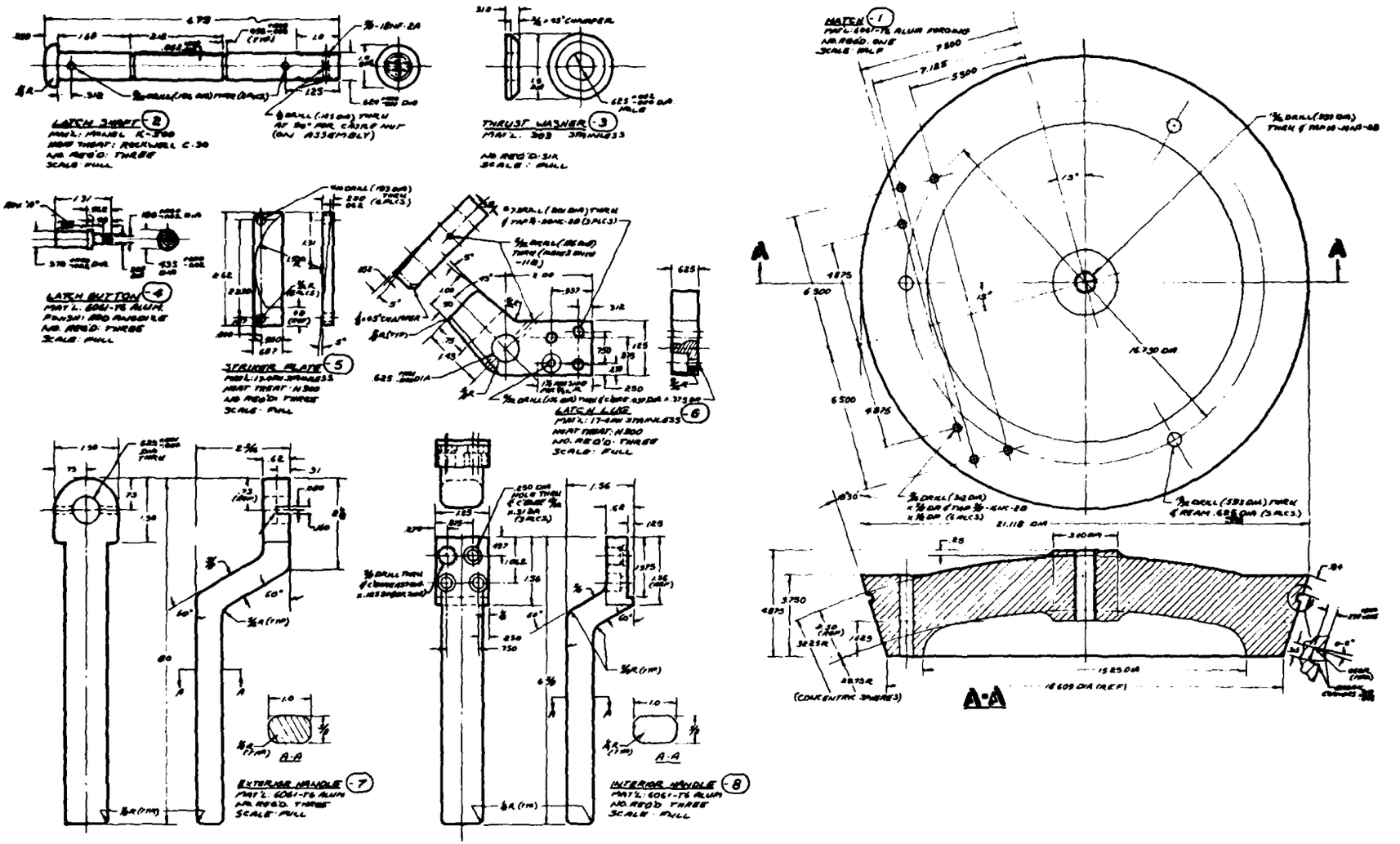

Figure 16A. Hatch and locking mechanism for the 66-inch OD X 58-inch ID Model 2000 Nemo Hull.

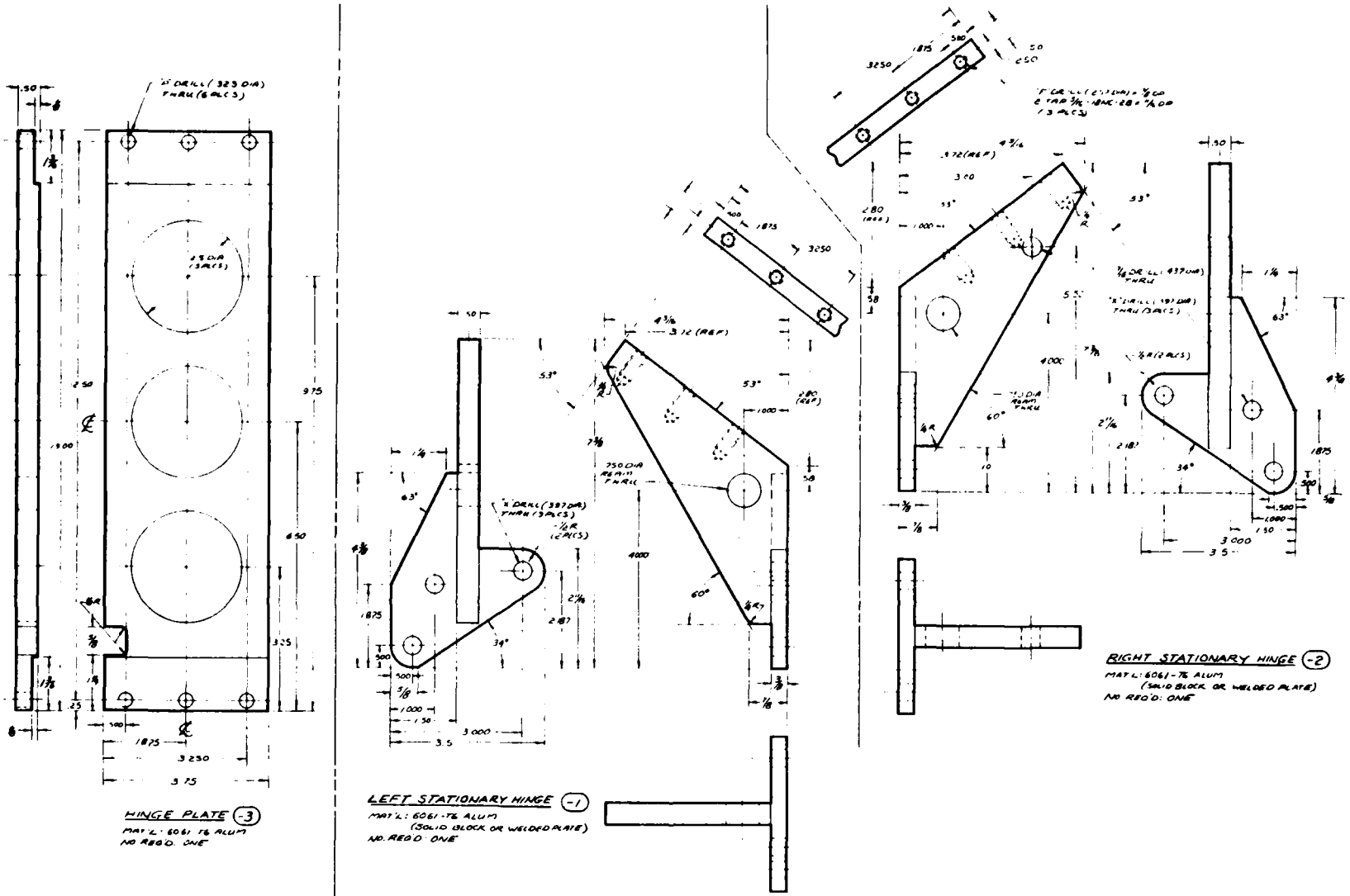

Figure 17A. Stationary hinges and hinge plate for the 66-inch OD X 58-inch ID Model 2000 Nemo Hull.

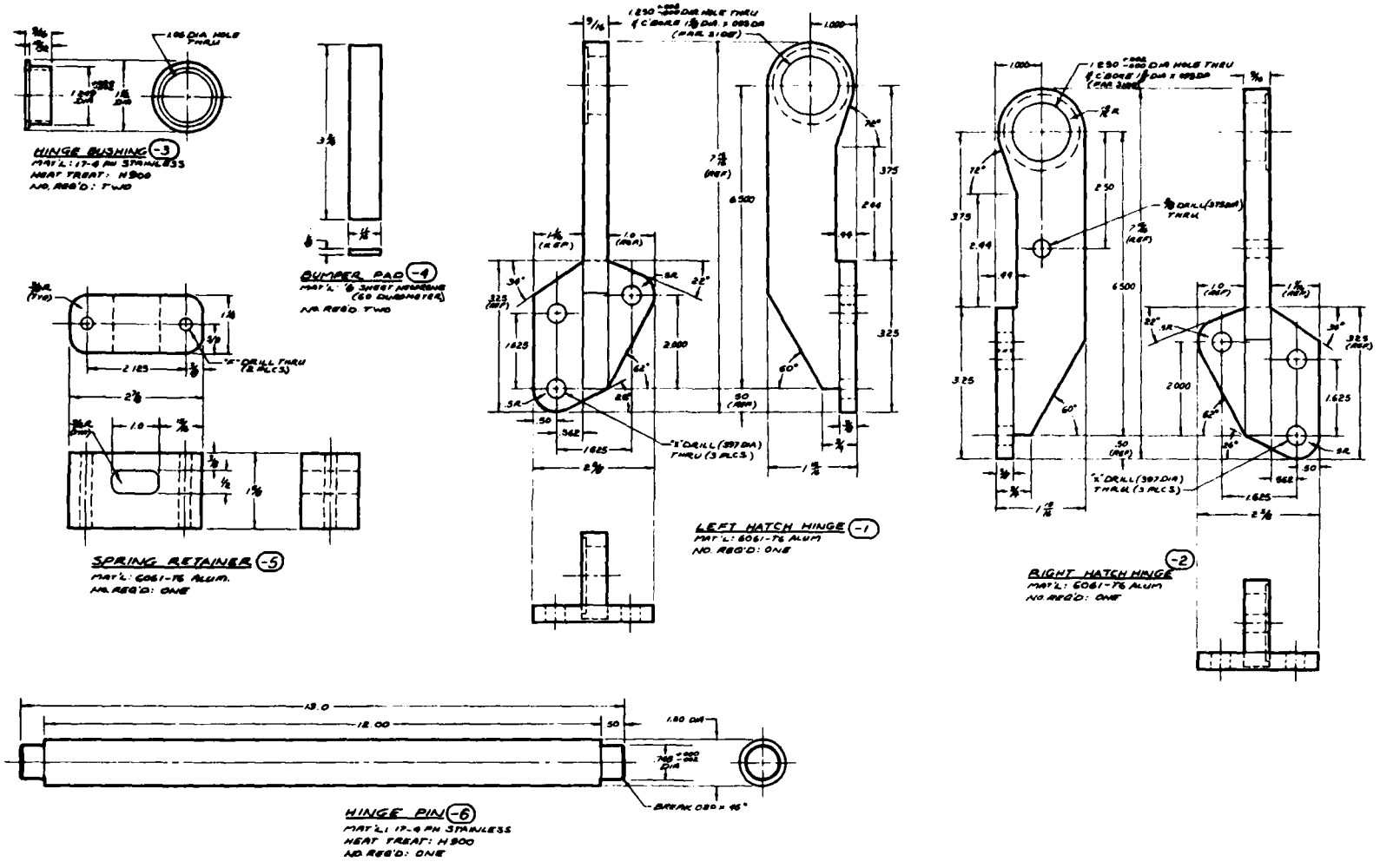

Figure 18A. Hatch hinge and hinge components for the 66-inch OD X 58-inch ID Model 2000 Nemo Hull.

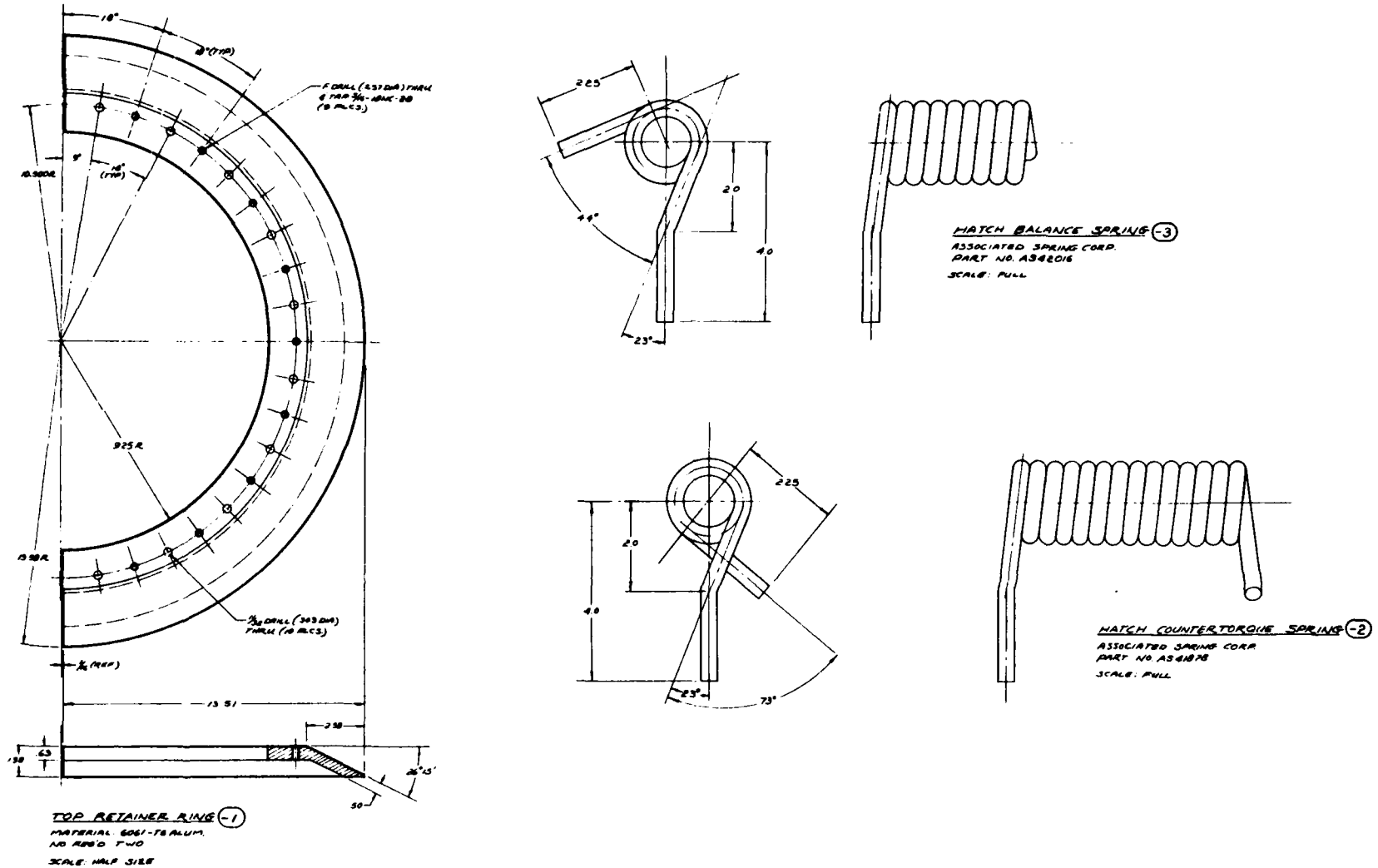

Figure 19A. Top retainer ring and counter balance springs for the 66-inch OD X 58-inch ID Model 2000 Nemo Hull.

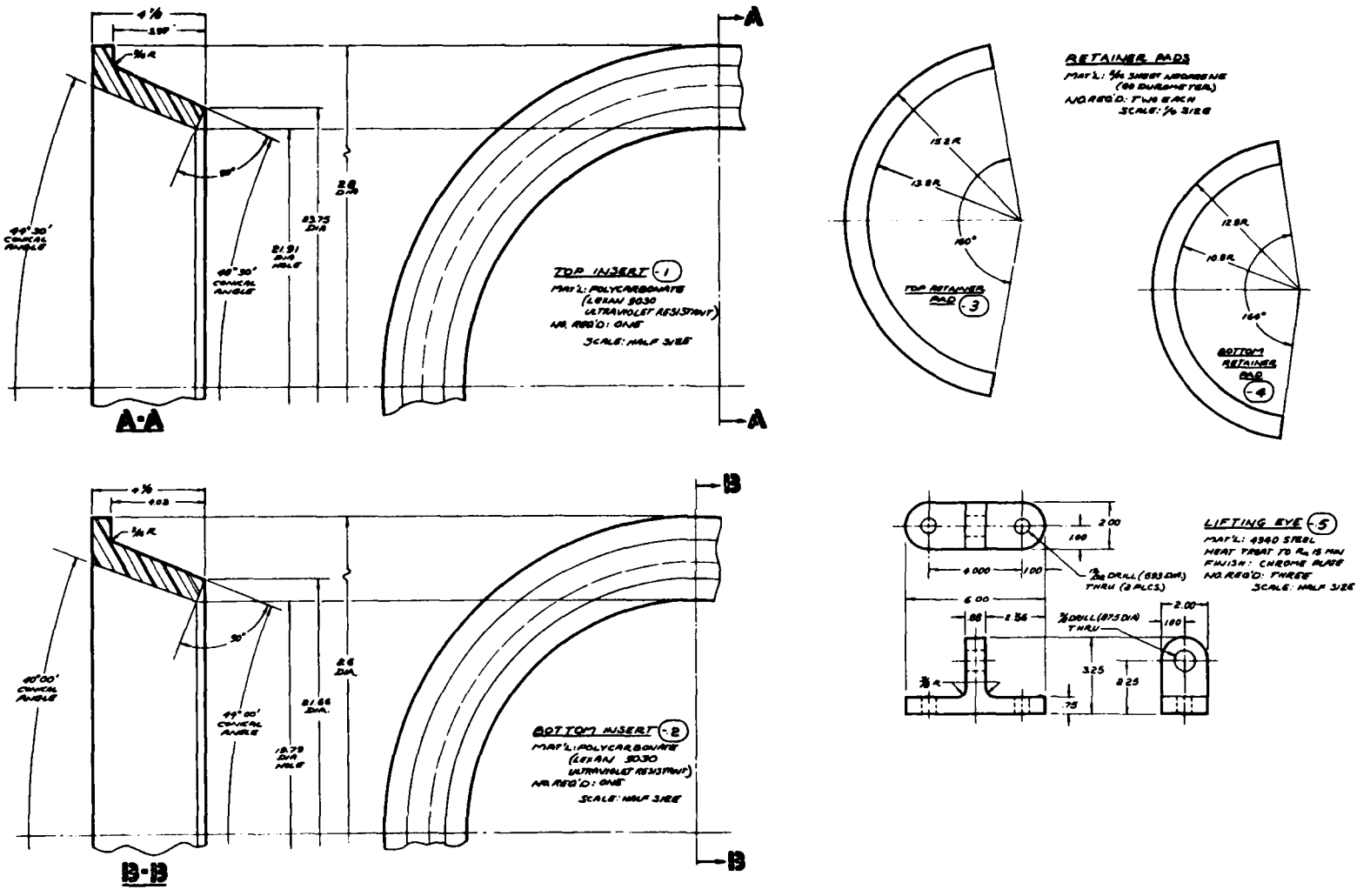

Figure 20A. Inserts, retainer pads, and lifting eye for the 66-inch OD X 58-inch ID Model 2000 Nemo Hull.

APPENDIX B

FABRICATION OF 66-INCH OD X 58-INCH ID MODEL 2000 NEMO HULL

APPENDIX B. FABRICATION OF 66-INCH OD X 58-INCH ID MODEL 2000 NEMO HULL

The 66-inch OD X 58-inch ID Model 2000 Nemo Hull assembly was fabricated basically in the same manner as the first 66-inch OD X 51-inch ID Model 600 Nemo Hull assembly built in 1968 by the Technical Services of Pacific Missile Range, Point Mugu, California. The cardinal features of that fabrication process are (1) cutting of discs from flat acrylic stock (Figure 1B), (2) thermoforming these discs into spherical sectors by means of metallic vacuum mold (Figure 2B), (3) cutting of spherical sectors into spherical pentagons (Figure 3B), (4) bonding of 12 spherical pentagons into a spherical shell (Figure 4B), (5) machining of metallic inserts in the form of top hatch and bottom penetration plate (Figure 5B), and placement of those inserts into polar hull openings (Figure 6B).

One phase of the fabrication process that has given trouble over the years to Nemo fabricators is that of the bonding of assembled 12 spherical pentagons. The problems associated with this phase of fabrication stem from the fact that the thickness of spherical pentagons bordering on a joint is not the same and that the width of joints between pentagons is not uniform. Because of the noncomformity in pentagon thickness and joint width it was difficult to seal the joint effectively so that it would contain the selfpolymerizing adhesive without leakage and yet assure a free flow of adhesive downwards and of displaced air upwards.

Steps were taken during fabrication of the Model 2000 Nemo Hull to eliminate the problems posed by nonuniform pentagon thicknesses and joint widths. These steps consisted of the following operations:

1. machining of all formed spherical sectors to uniform thickness in a lathe.

2. use of 0.125-inch thick X 0.25-inch diameter acrylic discs as spacers between individual pentagons during final assembly.

3. bonding of acrylic plastic strips to edges of joints for forming of pressure tight joint.

4. placement under pressure of selfpolymerizing adhesive into the joint cavities.

Because of these additional fabrication processing operations the resulting acrylic sphere is more uniform in thickness, sphericity, and diameter. As a result of this uniformity, the finished acrylic huil can be rated to higher operational pressure than was feasibly able prior to this time. Because the improved fabrication process may be of interest to others, a verbatim reproduction of shop fabrication instructions is attached as enclosure 1B at the end of this Appendix.

In parallel with the fabrication of the Model 2000 Nemo Hull, stringent quality control measures were a pted to assure a quality product and are attached as enclosures 2B through 9B. The qu y control measures consisted of:

1. performing destructive tests on material coupons cut from each sheet of acrylic plastic to ascertain the material properties of plastic (enclosure 2B).

2. performing destructive tests on bonded material coupons to ascertain strength of bonded joints (enclosure 3B).

3. performing dimensional checks on the spherical hull to ascertain its adherence to specified dimensional tolerances. Samples of dimensional checks are shown for thickness of discs before annealing (enclosure 4B), thickness of disc after annealing (enclosure 5B), thickness of disc after forming (enclosure 6B), sphericity of disc after forming (enclosure 7B), thickness of spherical pentagon after machining (enclosure 8B) and diameter of bonded sphere after annealing (enclosure 9B).

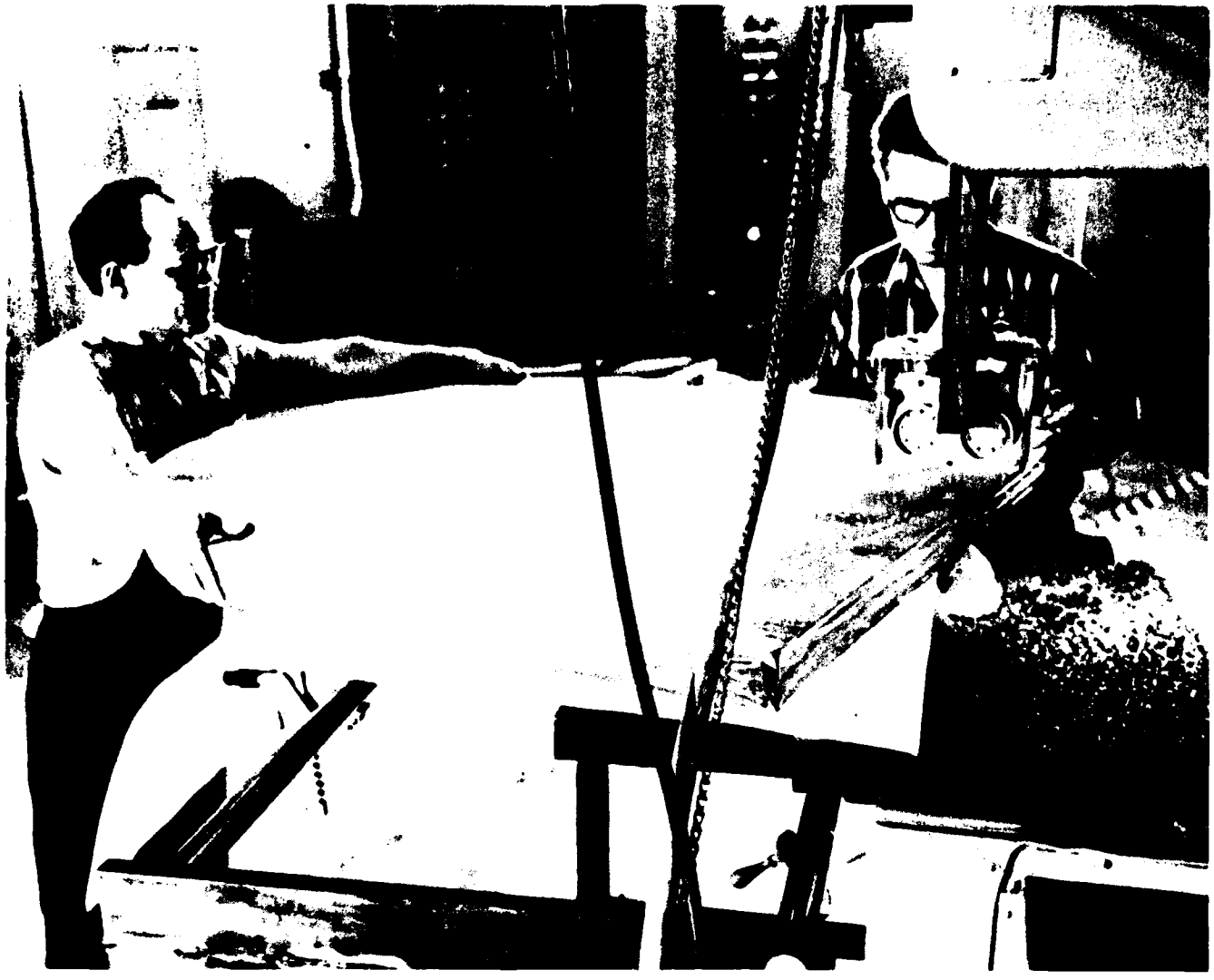

Figure 1B. Sawing of flat plates into circular discs of 46-inch diameter.

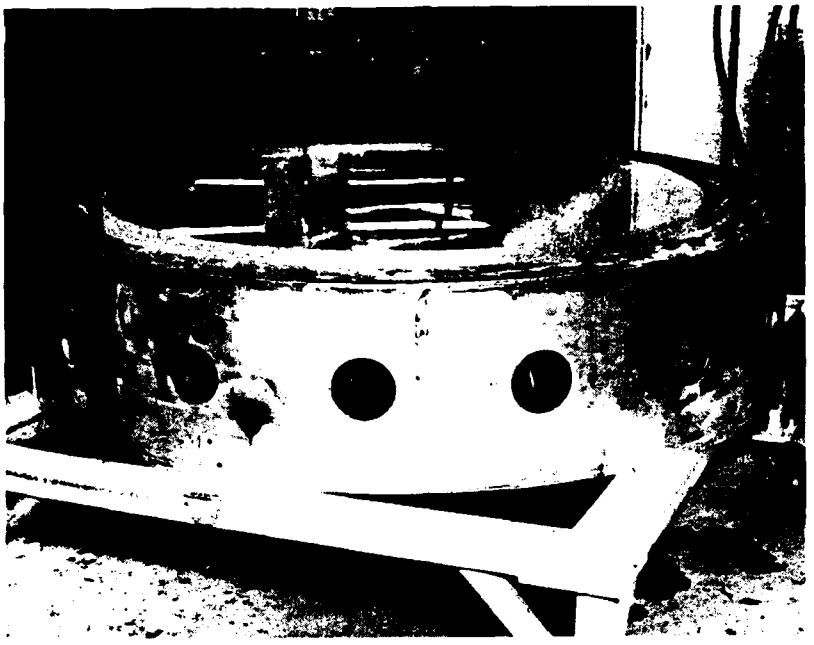

(a) Placement of disc into an aluminum female mold

(b) After forming the spherical sector is ready for removal from the mold

Figure 2B. Thermoforming of flat circular discs into spherical sectors.

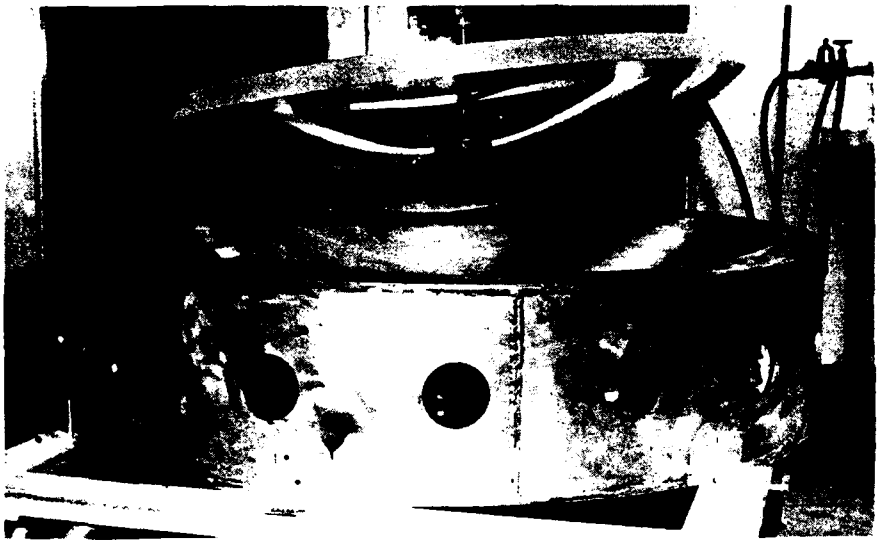

(c) The sector is picked up with a vacuum suction disc from the mold

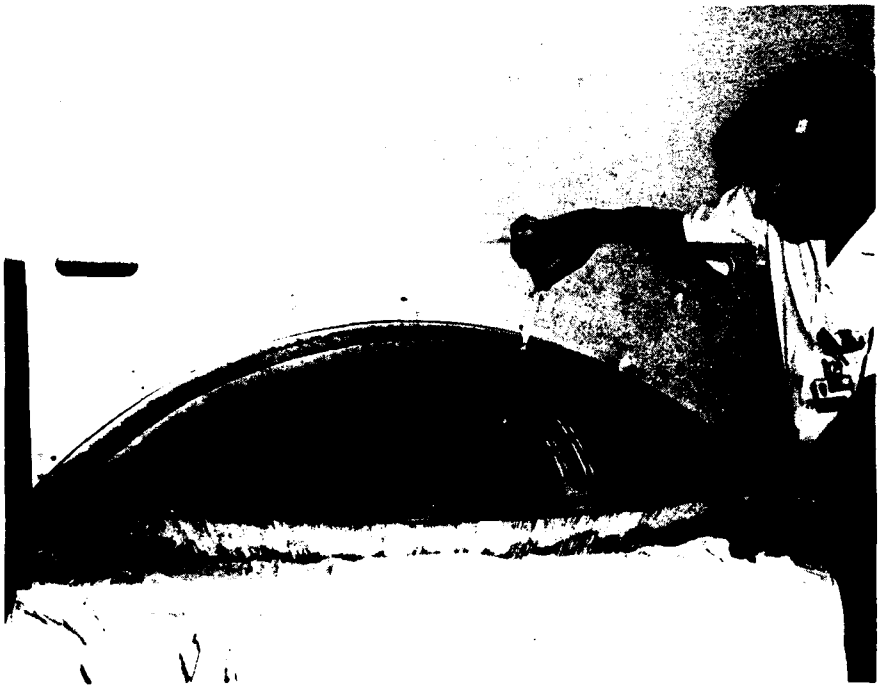

(d) Checking of sphericity on the formed sector

Figure 2B. (Continued).

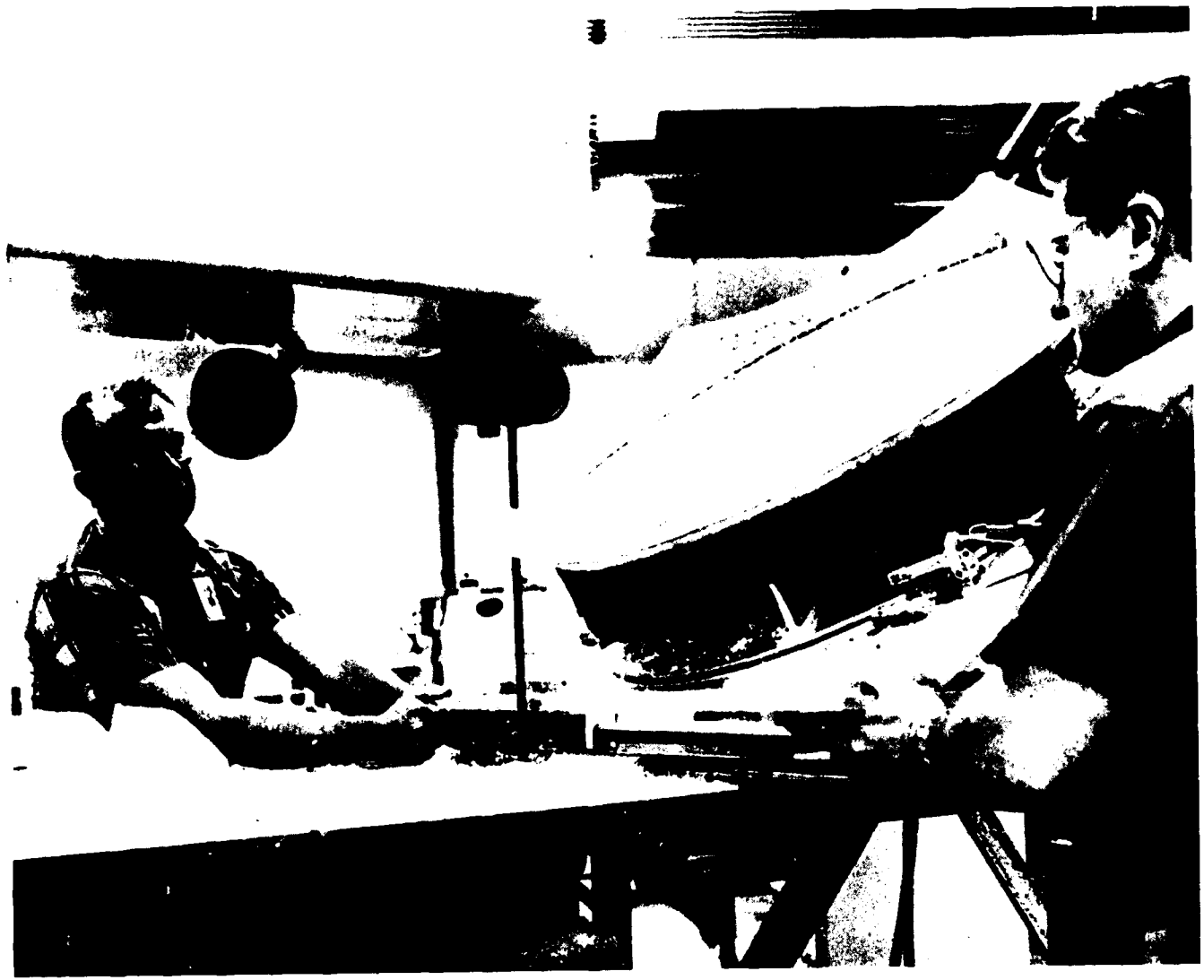

Figure 3B. Sawing the spherical sector into the form of a spherical pentagon.

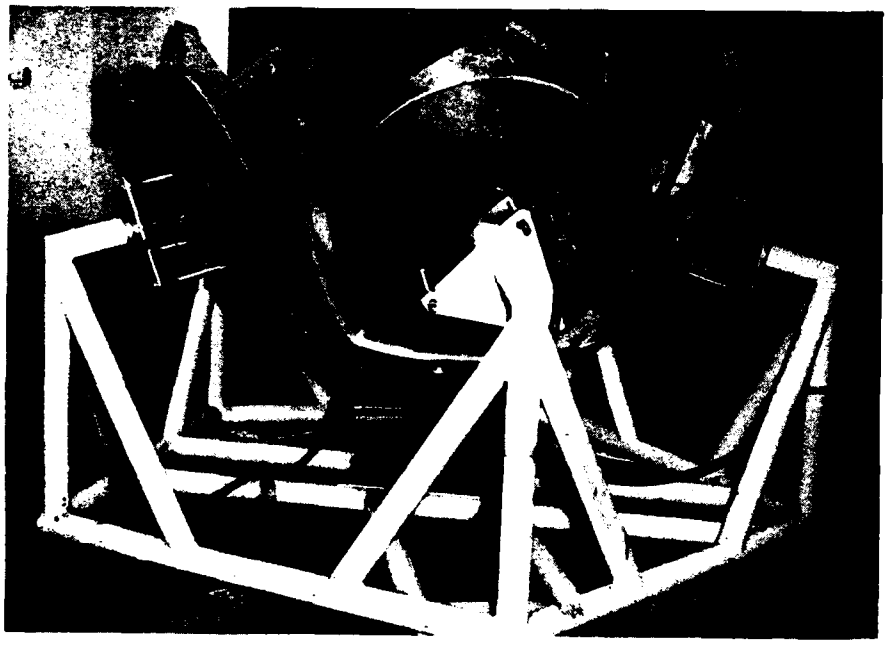

(a) Bonding of six pentagons to form a hemisphere

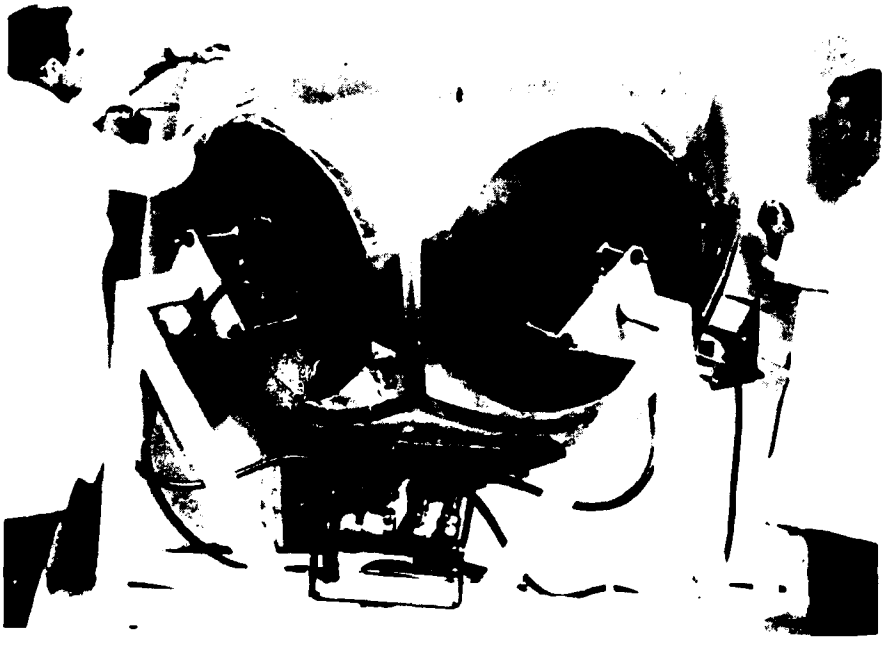

(b) Bonding of two hemispheres to form a sphere

Figure 4B. Holding fixture for bonding of spherical pentagons; note the large vacuum suction discs for holding of individual pentagons.

(c) Completed sphere after removal from bonding fixture

Figure 4B. (Continued).

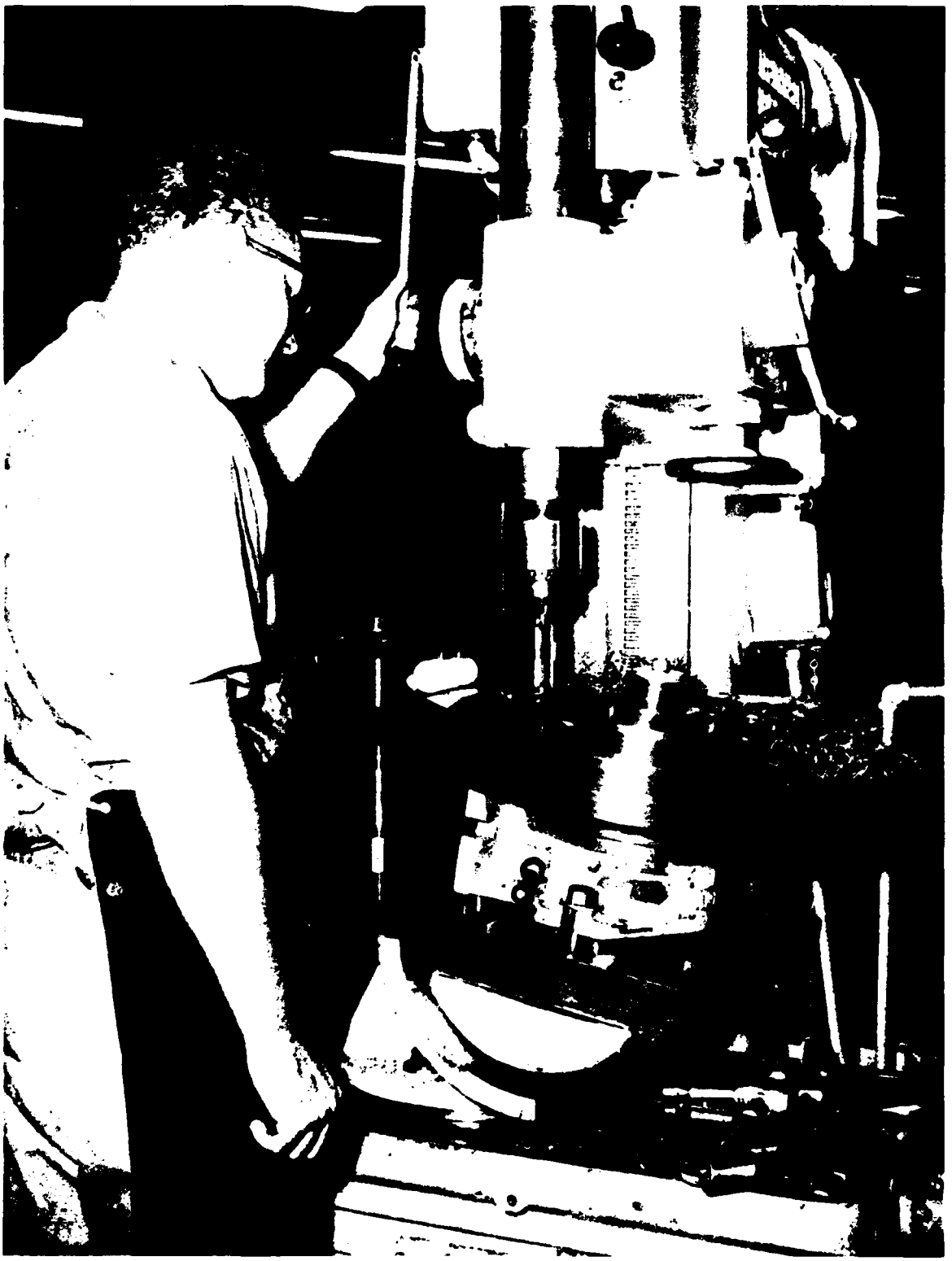

Figure 5B. Machining of metallic inserts for polar openings in the hull.

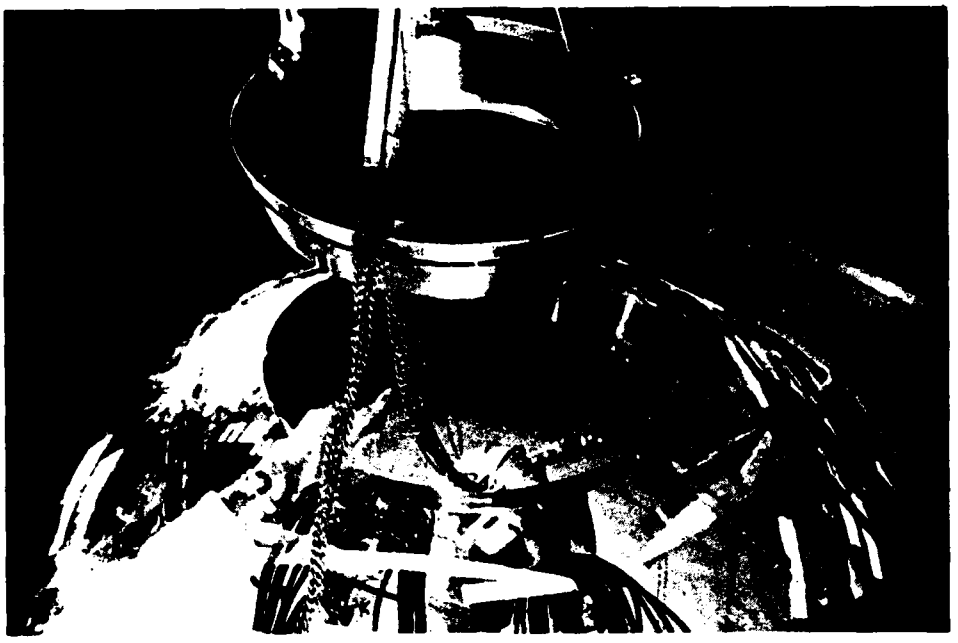

(a) Hatch seat being lowered in place

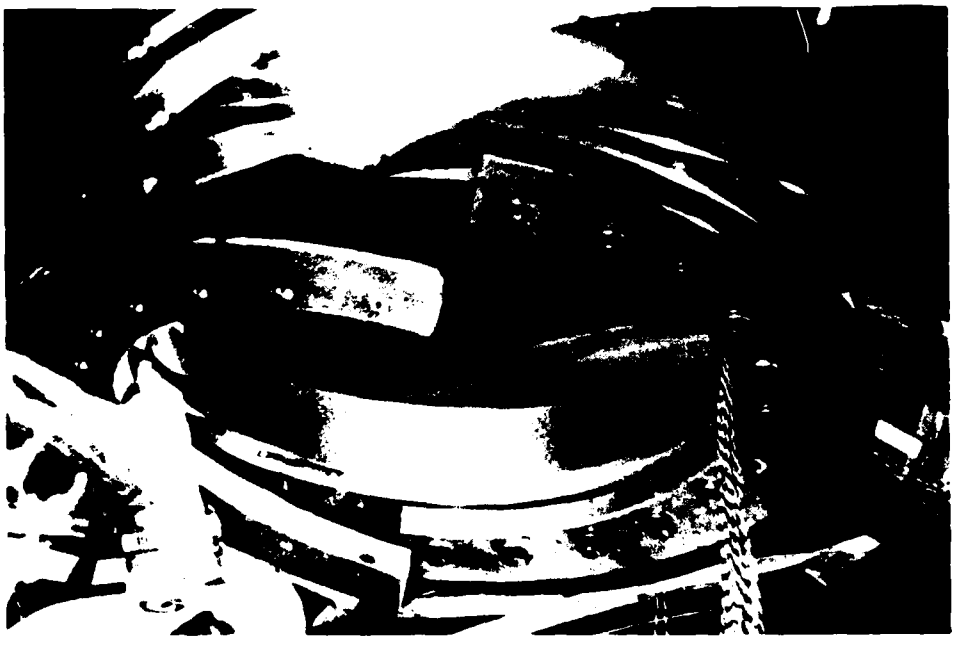

(b) Placement and bolting in place of hatch seat retaining flange

Figure 6B. Placement of metallic inserts into polar opening.

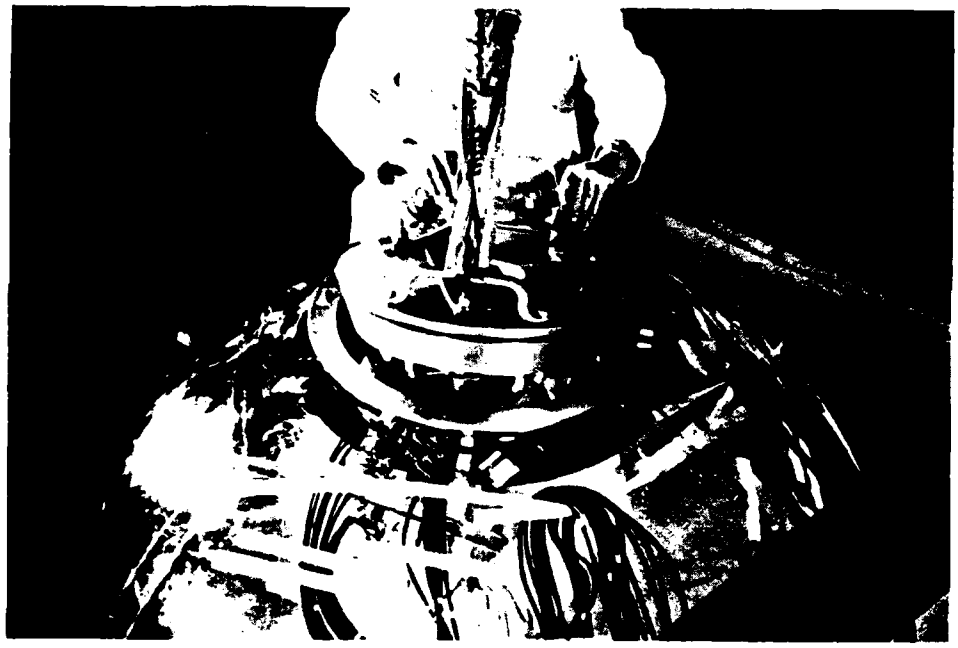

(c) Hatch assembly being attached to the hatch seat

(d) The hull being lowered onto the bottom penetration plate

Figure 6B. (Continued).

(e) Placement in place of retaining flange for bottom penetration plate

(f) Bolting of retaining flange for bottom penetration plate

Figure 6B. (Continued).

ENCLOSURE 1B

SWEDLOW's INSTRUCTIONS FOR WORKERS FABRICATING NEMO MOD 2000

1. Measure thickness of acrylic plate and chart at 12" intervals. Lay out a 46" diameter circle at the thickest part of the blank. Lay out nothing under 4.050 inches. Scribe SWU # on one cut off.
2. Bandsaw trim to line. Save one cut off that is scribed and send to C. Miller in Testing Lab.
3. Anneal the part at 325° F for 12 hours on a flat aluminum plate.
4. Inspect for thickness and chart at 12" intervals. Do not form plates under 4.170 inches.
5. Form per Forming Process Specification
6. Inspect for thickness (4.0 - 4.1) and contour.
7. Anneal @ 175° F for 24 hours.
8. Place part in machining fixture and align to marks. Drill three each 1/2" dia. holes and counterbore for 1/2" dia. Allen bolt. Bolt part down in three places.
9. Set up part and tracer template in Lucas lathe. Machine inside surface. Remaining thickness to be 4.050 minimum. Check contour readings to be sure part is 4.010 minimum at out of contour places. Part should be machined to 4.100 wherever possible and center section of part should not be cut as it will be under 4.100 thickness. Blend cut and uncut surfaces together with 360 grit wet sandpaper. This part must be polished to an optical finish after machining so the cut must be as smooth as possible.
10. Using vacuum lift place part in pentagon machine fixture and even up the edge of the part to the size of the fixture. Vacuum part into place on machining fixture. Make sure that hole in part comes out in the center of the piece to be cut off. Close air toggle clamps. Start saw and set feed at 25 inches per minute.
11. While cutting off first piece the saw may have a tendency to slow down or stop. If this happens, immediately press the return button, let the saw return and start the cut over. After cutting off the first piece, open

up the air toggle clamps and press the lever all the way to the left. This will lift the rotating part of the fixture slightly so that the index pin can be pulled and the part rotated to the next position. Continue this procedure until all five cuts have been made. Attach polar hole machining fixture to rotary table and place table on the milling machine. Two pentagons only. Place pentagon into machining fixture and bolt into place. Using a 7/8" dia. x 5" long end mill, cut a hole thru the part per the dimensions on NEMO Model 2000 Drawing #2003

12. Inspect for blueprint dimensions.
13. Anneal at 175^{O}F for 24 hours.
14. Clean up.
15. Take to assembly room.
16. Place one (1) Polar Pentagon in center of assembly fixture and using the large Starrett No. 656-441 indicator attached to extension, set against 1/2" ball situated in center of assembly pad.
17. Making sure indicator is laying flat against holding pad and measure distance from 1/2" ball to the inside of cut out in pentagon.
18. When pentagon is centered, place "L" shaped clamps to hold pentagon in place and bolt tightly to keep pentagon from moving during assembly.
19. Obtain 1/8" thick x 1/4" diameter acrylic spacers and bond approximately 4" from each corner centered.

    NOTE: Two (2) spacers are needed per side only. If one pentagon has these blocks, then omit blocks to mating side.

    Use PS-30 cement - for bonding spacers.
20. Using the vacuum hand lift, place five (5) pentagons into assembly fixture and align with polar pentagon.
21. After alignment obtain large micrometer with Brown and Sharpe No. 8241-941 dial indicator from inspection box. Obtain the three rods from box (1) 22" (2) 23" and (3) 21". Assemble together and set dial indicator to read zero.

NOTE: Dial indicator will not set at zero-zero dial, but will set at 600, so turn dial indicator to read zero to 600.

22. Using dial indicator measure the diameter of the hemisphere and shim where necessary to read 66" $\pm$ .25". Measure hemisphere.

NOTE: Each pentagon must be measured to one situated directly across from from one to the other.

23. When hemisphere is within spherical tolerance of 66" $\pm$ .250", obtain Plex G acrylic strips 3/4" thick or S310 material 0.750" wide by 36" long. Take to Machining and rout a groove down the center length 1/8" wide x 1/2" deep.

24. Form these strips to fit both outside and inside surfaces of set pentagons. Using methylene cloride, bond the strips to the pentagons.

25. After all strips have been bonded to hemisphere, place a bead of PS-18 resin around all strips to prevent leaks after hemisphere has been filled with S-49 casting cement.

26. Drill an "F" size hole at lowest point of hemisphere. Place a 1/4" OD aluminum tube 3" long into hole and cement into place between pentagons.

27. Obtain 2000 grams of basic S-49 resin from resin mixing room-in-a new, clean gallon can: Mix 4 grams of benzoin (.2%) and 10 grams of larurel peroxide (.5%). Place lid on container. Take resin to the NEMO room which is a temperature controlled room @ a constant 72^{o}F.

28. Place gallon can on converted edge attachment sander, and set atop the two (2) rollers. Turn switch on and let roll over night.

29. Place mixed S-49 as resin into pressure pot and attach nitrogen bottle to pot. Attach fill tube from pot to 1/4" OD Aluminum tube on sphere.

30. Apply five (5) pounds pressure.

31. Fill joints all around Polar Pentagon and allow resin to rise approximately one (1) inch above the upright joints. (This allows for shrinkage).

32. Clamp off tube.

33. Allow to cure in NEMO room until hard (approximately 24 hours). Room is

to be kept between 70°F and 75°F temperature.

34. Remove first hemisphere from cement fixture.
35. Rout joints on both outside and inside flush with pentagons.
36. Polish up all seams on both inner and outer surfaces.
37. Place six (6) new pentagons into assembly fixture and assemble same as first pentagon. Follow steps one (1) through twenty-two (36) above.
38. Place hemisphere Number one (1) on top of Number two (2) and check spherical diameter.
39. If hemispheres measure within tolerance of 66" ± .250", cut, fit and cement joint strips around equator of sphere leaving a funnel at the top of each bottom pentagon.
40. In obtaining and preparing S-49 resin, repeat Steps 27 and 28
41. To feed S-49 resin into the equator section of sphere, follow Steps 29 and 30 of Operation 5.
42. Allow resin to cure in NEMO room until hard (approximately 24 hours). Room is to be kept between 70°F and 75°F temperature.
43. Remove sphere from assembly fixture. Using the cell casting hoist, hook up lifting plate to hoist, fold lifting plate and insert into sphere. Making sure lifting plate will not damage sphere, lift sphere from fixture.
44. Machine, sand and polish all bonded areas.
45. Anneal sphere in a 175°F oven for 24 hours.
46. Inspect all cemented joints for voids larger than 1/4" in diameter.
47. Final clean up.
48. Final Inspection.
49. Wrap with Protec 10V.

12122 WESTERN AVENUE/GARDEN GROVE, CALIFORNIA 92645/714-893-7531 TELEX 678457

ENCLOSURE 2B

SWEDLOW, INC.

Reference: 45-74-121
Date: March 18, 1974

TEST REPORT

CUSTOMER: Disbursing Officer, DCASR, Los Angeles
11099 So. La Cienega Boulevard
Los Angeles, California 90045

PURCHASE ORDER NO.: N00123-73-C-1671

MATERIAL TESTED: Remnants from each sheet used in fabrication of NEMO Model 2000 Hull

Test specimens were cut to rough dimensions using a bandsaw and to final dimensions (with the exception of tensile specimens) by means of a vertical mill, with a six-flute, carbide-tipped shell end-mill. Tensile specimens were routed to the configuration of a template which complies with dimensions set forth in A.S.T.M. D-638 for Type I specimens. Sharp edges were broken to about .005 inch. Machined surfaces were sanded, first with 280 grit paper, and finally with 600 grit Wet-or-Dry paper to remove tool marks. All specimens were annealed to remove any residual stresses introduced during machining.

Test specimens were conditioned, at a temperature of 73.5 ± 2°F and relative humidity of 50 ± 5%, for a period of 40 hours prior to testing.

Tensile, compressive and flexural values were obtained by means of a Tinius-Olsen Elect-O matic Testing Machine. Deformation under load values were obtained on a Tinius-Olsen tester designed for that particular test.

Respectfully submitted,

SWEDLOW, INC.

C. A. Miller, Supervisor
Physical Testing Laboratory

SWEDLOW, INC.

TEST REPORT

Date: March 18, 1974

Purchase Order No.: N00123-73-C-1671

FOR: NEMO Model 2000 Hull

Sales Order No.: 3-5940

Page 1

TENSILE: Conditioned 40 hours at 73°F and 50 Percent R. H.

ASTM D-638 tested at 0.05 In/Min

SHEET NO.	SPECIMEN SIZE (INCH)	LOAD (LBS)	ULTIMATE (PSI)	ELONGATION (PERCENT)	MODULUS (PSI)
021	1- .236 x .483	1330	11,668	7.0	447,000
	2- .242 x .478	1365	11,800	6.0	465,000
023	1- .247 x .481	1465	12,331	6.0	467,000
	2- .251 x .476	1360	11,382	6.0	437,000
024	1- .255 x .479	1400	11,461	5.5	437,000
	2- .254 x .482	1420	11,600	5.5	485,000
025	1- .253 x .481	1425	11,709	5.5	473,000
	2- .252 x .479	1420	11,764	5.0	490,000
026	1- .251 x .483	1415	11,671	5.5	474,000
	2- .252 x .481	1355	11,179	5.5	456,000
027	1- .252 x .479	1315	10,893	5.5	446,000
	2- .253 x .477	1275	10,565	5.5	495,000
028	1- .248 x .472	1235	10,551	5.0	498,000
	2- .252 x .474	1270	10,632	5.5	492,000
029	1- .253 x .471	1200	10,070	4.0	446,000
	2- .247 x .474	1185	10,121	4.0	449,000
034	1- .254 x .475	1290	10,692	5.5	475,000
	2- .247 x .475	1265	10,781	5.0	478,000
035	1- .250 x .479	1250	10,440	5.0	505,000
	2- .246 x .477	1120	9,545	3.0	428,000
036	1- .250 x .476	1280	10,756	5.5	454,000
	2- .251 x .477	1275	10,649	5.0	465,000
037	1- .249 x .475	1250	10,570	5.5	465,000
	2- .248 x .474	1235	10,504	5.5	447,000

NEMO Model 2000 Hull
S. O. No. 3-5940
Test Report, Continued
Page 2

FLEXURAL - Conditioned 40 Hours at 73°F and 50 Percent R. H.

ASTM D-790 - 4 inch span, test speed 0.11 In/Min

SHEET NO.	SPECIMEN SIZE (INCH)	LOAD (LBS)	ULTIMATE (PSI)	MODULUS (PSI)
021	1- .500 x .258	95.8	17,261	415,000
	2- .500 x .258	95.5	17,207	443,000
023	1- .498 x .258	101.3	18,326	444,000
	2- .491 x .257	82.3	15,238	442,000
024	1- .500 x .258	103.1	18,577	452,000
	2- .494 x .258	101.3	18,474	457,000
025	1- .501 x .257	102.0	18,508	433,000
	2- .502 x .258	103.1	18,503	445,000
026	1- .501 x .258	101.1	18,180	460,000
	2- .498 x .257	101.3	18,492	463,000
027	1- .493 x .256	96.3	17,883	459,000
	2- .495 x .256	98.0	18,127	477,000
028	1- .493 x .249	93.1	18,258	478,000
	2- .493 x .247	93.7	18,686	474,000
029	1- .494 x .246	92.4	18,048	479,000
	2- .495 x .249	93.6	18,306	475,000
034	1- .492 x .247	88.1	17,588	475,000
	2- .493 x .246	82.5	16,624	480,000
035	1- .495 x .248	78.7	15,511	487,000
	2- .494 x .247	90.6	18,047	484,000
036	1- .494 x .247	77.0	15,326	473,000
	2- .493 x .248	92.1	18,210	484,000
037	1- .492 x .248	91.4	18,113	469,000
	2- .495 x .248	92.2	18,194	467,000

NEMO Model 2000 Hull
S. O. No. 3-5940
Test Report, Continued
Page 3

DEFORMATION UNDER LOAD

ASTM D 621 - Tested as received at 122°F for 24 hours under 4000 psi load
Test Specimens: 1/2 Inch Cube

SHEET NO.		DEFORMATION (INCH) 10 SEC.	24 HOURS	DIFFER (IN)	MICROMETER READING (IN)	CALC. ORIG. THICKNESS (IN)	DEFORM. (%)
021	1-	0.0863	0.0889	0.0026	0.4998	0.5024	0.52
	2-	0.0822	0.0848	0.0026	0.5025	0.5051	0.51
023	1-	0.0857	0.0886	0.0029	0.4985	0.5014	0.58
	2-	0.0813	0.0842	0.0029	0.5020	0.5049	0.57
024	1-	0.0819	0.0843	0.0024	0.5013	0.5037	0.48
	2-	0.0764	0.0788	0.0022	0.5025	0.5047	0.44
025	1-	0.0755	0.0778	0.0023	0.5036	0.5059	0.45
	2-	0.0763	0.0787	0.0024	0.5023	0.5047	0.48
026	1-	0.0765	0.0795	0.0030	0.5014	0.5044	0.60
	2-	0.0752	0.0774	0.0022	0.5007	0.5029	0.44
027	1-	0.0684	0.0708	0.0024	0.5029	0.5053	0.47
	2-	0.0676	0.0699	0.0023	0.5036	0.5039	0.46
028	1-	0.0738	0.0761	0.0023	0.4980	0.5003	0.46
	2-	0.0708	0.0735	0.0027	0.5003	0.5030	0.54
029	1-	0.0691	0.0712	0.0021	0.5014	0.5035	0.42
	2-	0.0707	0.0733	0.0026	0.4997	0.5023	0.52
034	1-	0.0709	0.0743	0.0034	0.4986	0.5020	0.67
	2-	0.0720	0.0751	0.0031	0.4983	0.5014	0.61
035	1-	0.0714	0.0745	0.0031	0.4990	0.5021	0.61
	2-	0.0711	0.0744	0.0033	0.4980	0.5013	0.65
036	1-	0.0715	0.0747	0.0032	0.4975	0.5007	0.63
	2-	0.0698	0.0734	0.0036	0.4996	0.5032	0.72
037	1-	0.0708	0.0740	0.0032	0.4991	0.5023	0.64
	2-	0.0707	0.0740	0.0033	0.4982	0.5015	0.66

SHEAR STRENGTH

ASTM D-732 Rate of Test: 0.05 In/Min
Punch Diameter: 0.999 In. (1.000 In. Dia. disc punched out)

SHEET NO.		THICKNESS (INCH)	MAXIMUM LOAD (LBS)	SHEAR STRENGTH (PSI)
021	1-	0.259	8,240	10,100
	2-	0.253	8,250	10,400
023	1-	0.255	8,190	10,200
	2-	0.254	8,220	10,300
024	1-	0.254	8,190	10,300
	2-	0.256	8,260	10,300
025	1-	0.257	8,220	10,200
	2-	0.258	8,340	10,300
026	1-	0.254	8,830	11,100
	2-	0.255	8,210	10,300
027	1-	0.250	7,800	9,930
	2-	0.245	7,770	10,100
028	1-	0.245	8,220	10,700
	2-	0.254	8,440	10,600
029	1-	0.250	8,200	10,400
	2-	0.253	8,690	10,900
034	1-	0.253	8,870	11,200
	2-	0.254	8,770	11,000
035	1-	0.252	9,130	11,500
	2-	0.253	8,450	10,600
036	1-	0.255	9,100	11,400
	2-	0.253	8,670	10,900
037	1-	0.254	8,340	10,500
	2-	0.256	7,950	9,880

NEMO Model 2000 Hull
S. O. No. 3-5940
Test Report, Continued

COMPRESSIVE PROPERTIES : Tested at Room Temperature

ASTM D-695 Rate of Test: 0.05 In/Min

SHEET NO.		SPECIMEN SIZE (INCH)	YIELD LOAD (LBS)	YIELD STRENGTH (PSI)	MODULUS (PSI)
021	1-	0.503 x 0.502 x 1.504	4,880	19,300	570,000
	2-	0.503 x 0.502 x 1.505	4,950	19,600	530,000
023	1-	0.500 x 0.503 x 1.502	4,630	18,400	520,000
	2-	0.501 x 0.503 x 1.502	4,590	18,200	500,000
024	1-	0.503 x 0.503 x 1.499	4,610	18,200	510,000
	2-	0.504 x 0.503 x 1.499	4,740	18,700	500,000
025	1-	0.505 x 0.505 x 1.502	4,660	18,300	510,000
	2-	0.504 x 0.504 x 1.500	4,780	18,800	510,000
026	1-	0.503 x 0.503 x 1.501	4,570	18,100	510,000
	2-	0.503 x 0.501 x 1.500	4,650	18,500	520,000
027	1-	0.504 x 0.506 x 1.502	4,650	18,200	510,000
	2-	0.506 x 0.504 x 1.504	4,690	18,400	520,000
028	1-	0.501 x 0.501 x 1.500	4,650	18,500	540,000
	2-	0.502 x 0.502 x 1.507	4,710	18,700	540,000
029	1-	0.502 x 0.502 x 1.506	4,810	19,100	530,000
	2-	0.502 x 0.502 x 1.506	4,610	18,300	500,000
034	1-	0.501 x 0.502 x 1.505	4,520	18,000	510,000
	2-	0.501 x 0.500 x 1.505	4,600	18,400	530,000
035	1-	0.502 x 0.501 x 1.506	4,650	18,500	520,000
	2-	0.503 x 0.503 x 1.506	4,480	17,700	530,000
036	1-	0.503 x 0.502 x 1.505	4,510	17,900	510,000
	2-	0.501 x 0.500 x 1.506	4,490	17,900	510,000
037	1-	0.501 x 0.502 x 1.505	4,640	18,400	530,000
	2-	0.503 x 0.502 x 1.503	4,510	17,900	530,000

ENCLOSURE 3B

SWEDLOW, INC.

Date: 21 May 1974

TEST REPORT

For: NEMO Model 2000 Hull

Purchase Order No. N00123-73-C-1671

BONDED JOINT TENSILE STRENGTH

(Required : 5000 psi)

Test specimens were machined from the joint evaluation coupon which had been bonded and annealedin the same manner as the pressure hull. Specimens were of the dimensional configuration set forth in Sketch No. 2002. The testing speed used was 0.05 inch per minute.

Specimen	Width (In)	Thickness (In)	Load (Lbs)	Ultimate Strength (psi)	Mode of Failure
1	0.744	0.529	3015	7661	Cohesive
2	0.747	0.532	3210	8074	Acrylic
3	0.750	0.485	2825	7766	Cohesive
4	0.746	0.547	3720	9116	Cohesive
5	0.750	0.540	2075	5123	Cohesive
6	0.749	0.534	3550	8876	Cohesive
7	0.747	0.531	2920	7362	Cohesive
8	0.748	0.526	3240	8235	Cohesive
9	0.742	0.519	2365	6141	Cohesive
10	0.748	0.536	3320	8281	Cohesive
11	0.745	0.536	3390	8489	Cohesive
12	0.744	0.534	3440	8659	Cohesive
			Average	7815	

C. A. Miller, Supervisor
Testing Laboratory

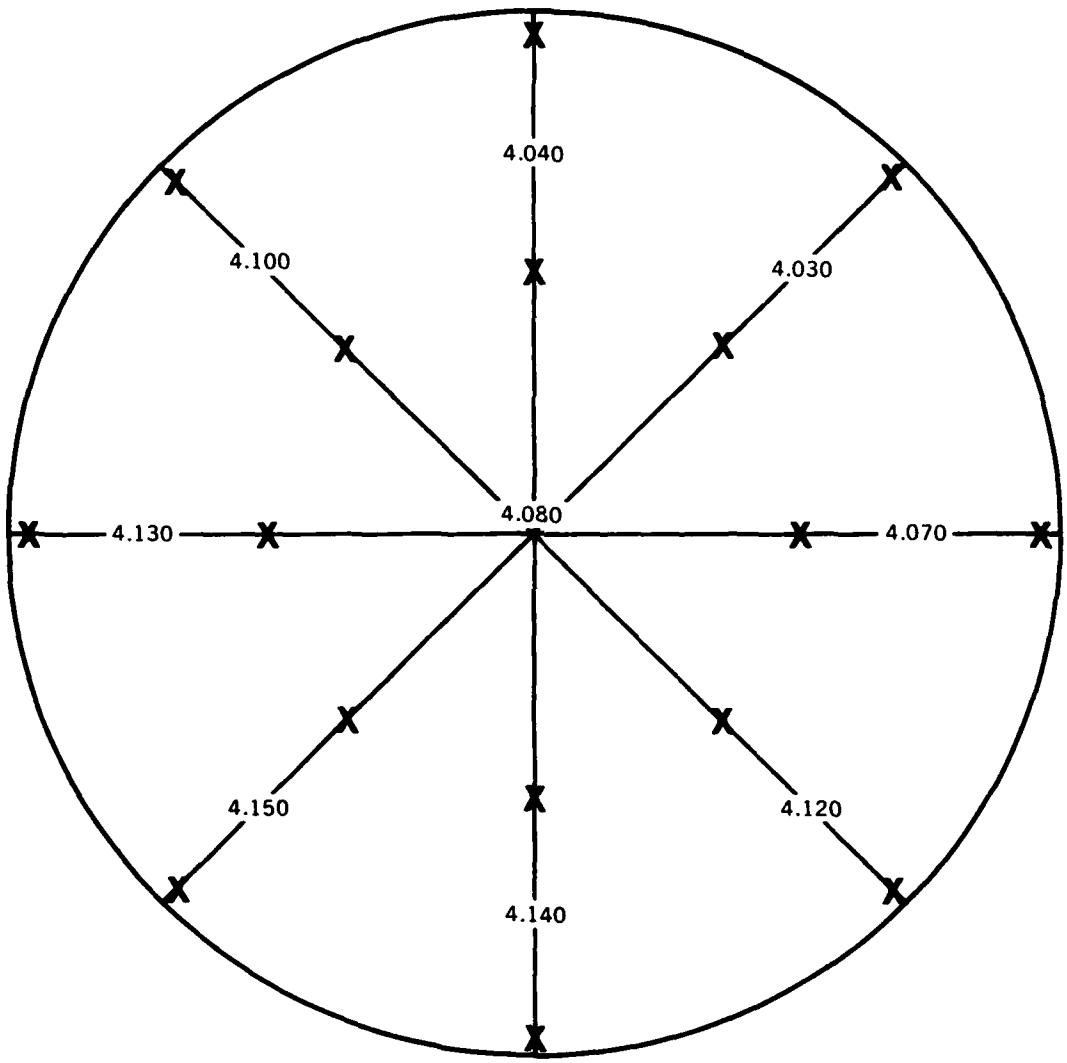

Thickness Before Annealing

Enclosure 5B

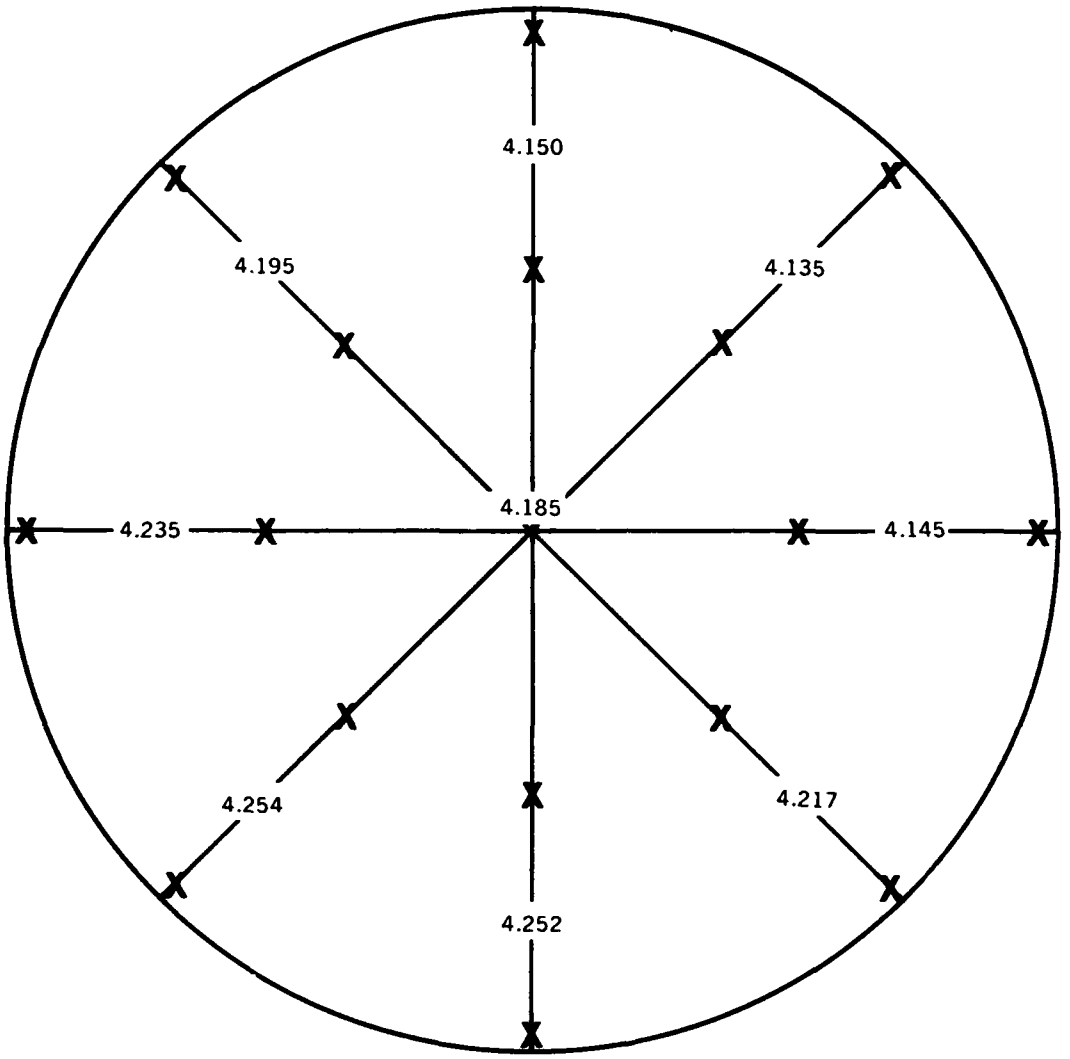

Thickness After Annealing

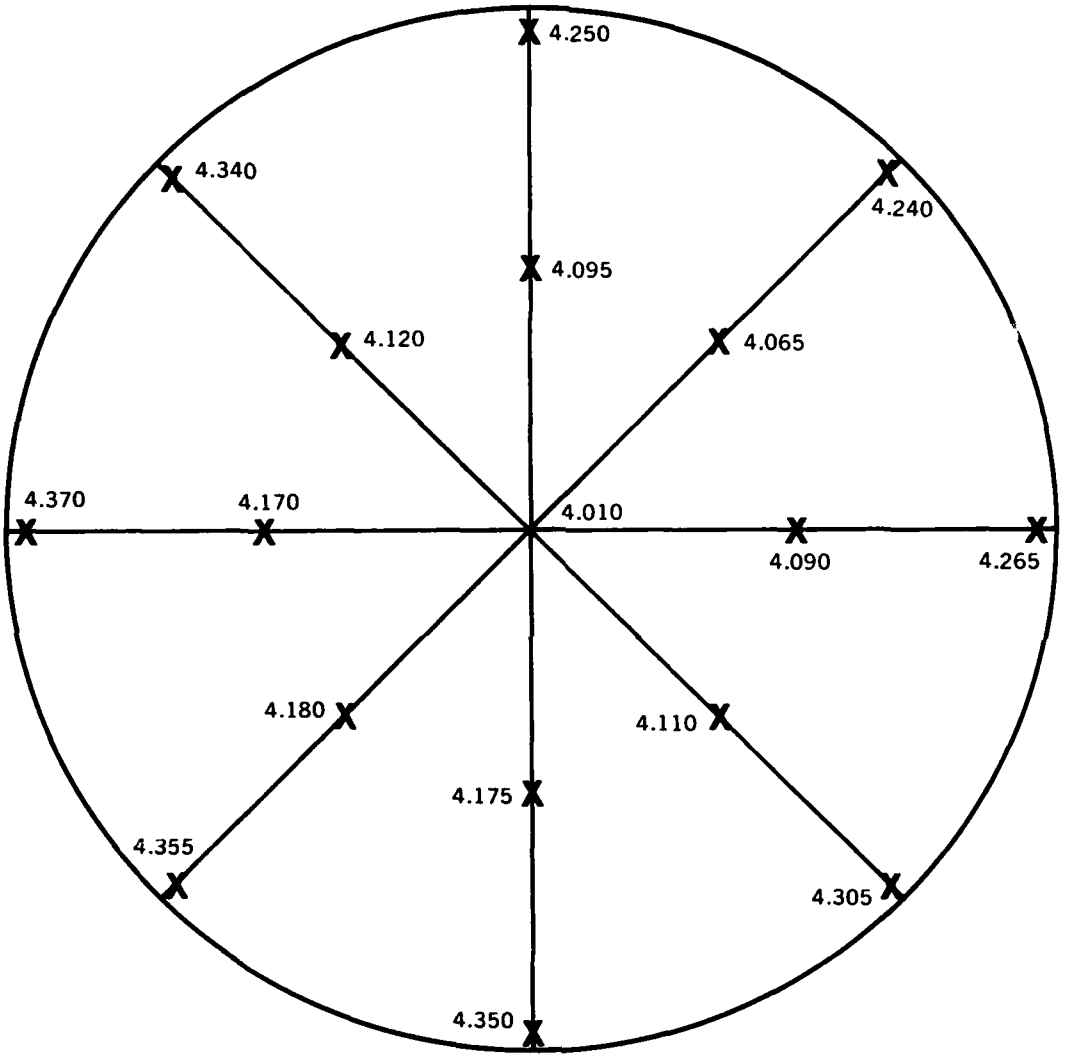

Thickness After Forming

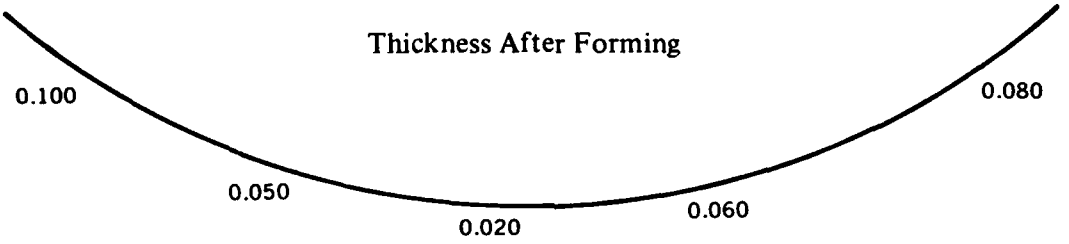

Sphericity After Forming

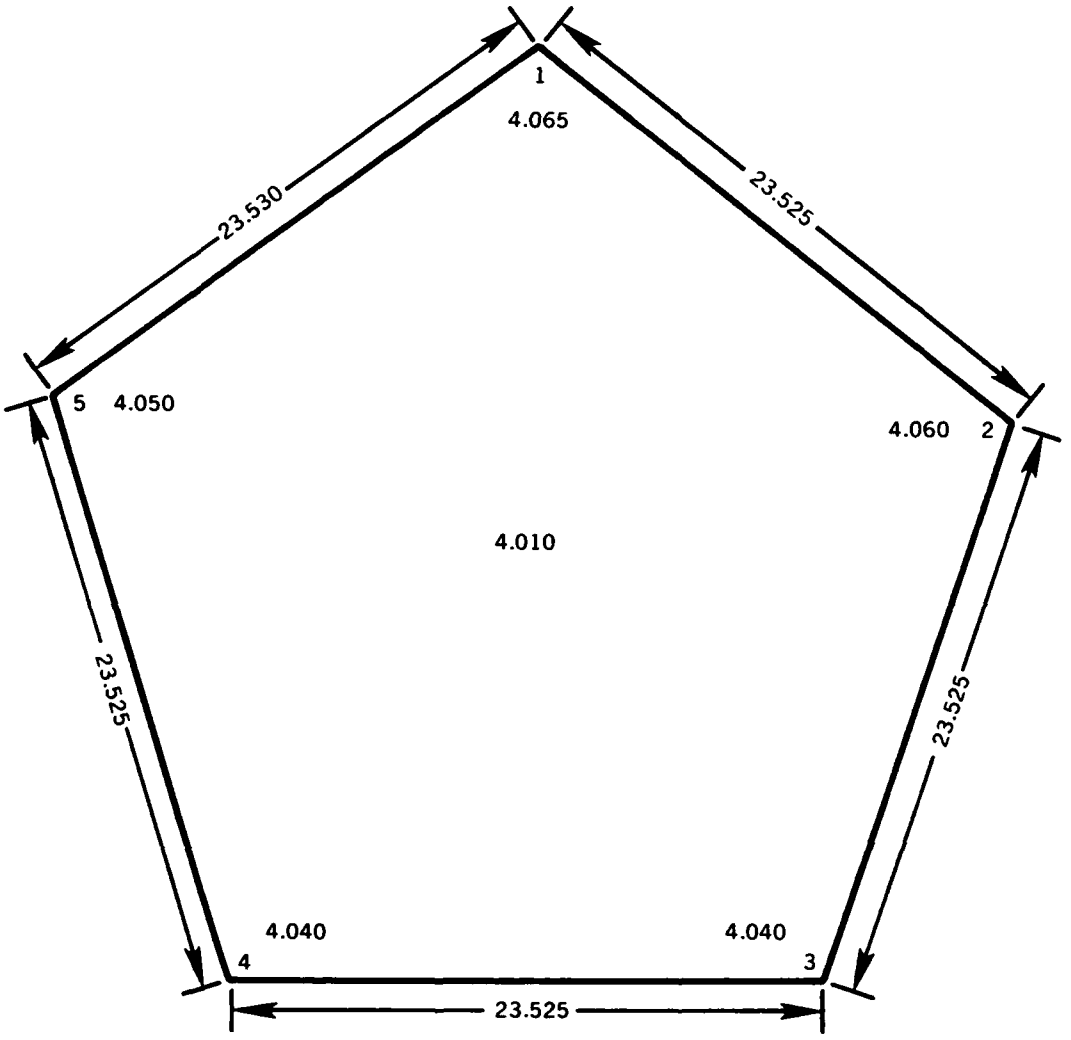

Thickness After Machining

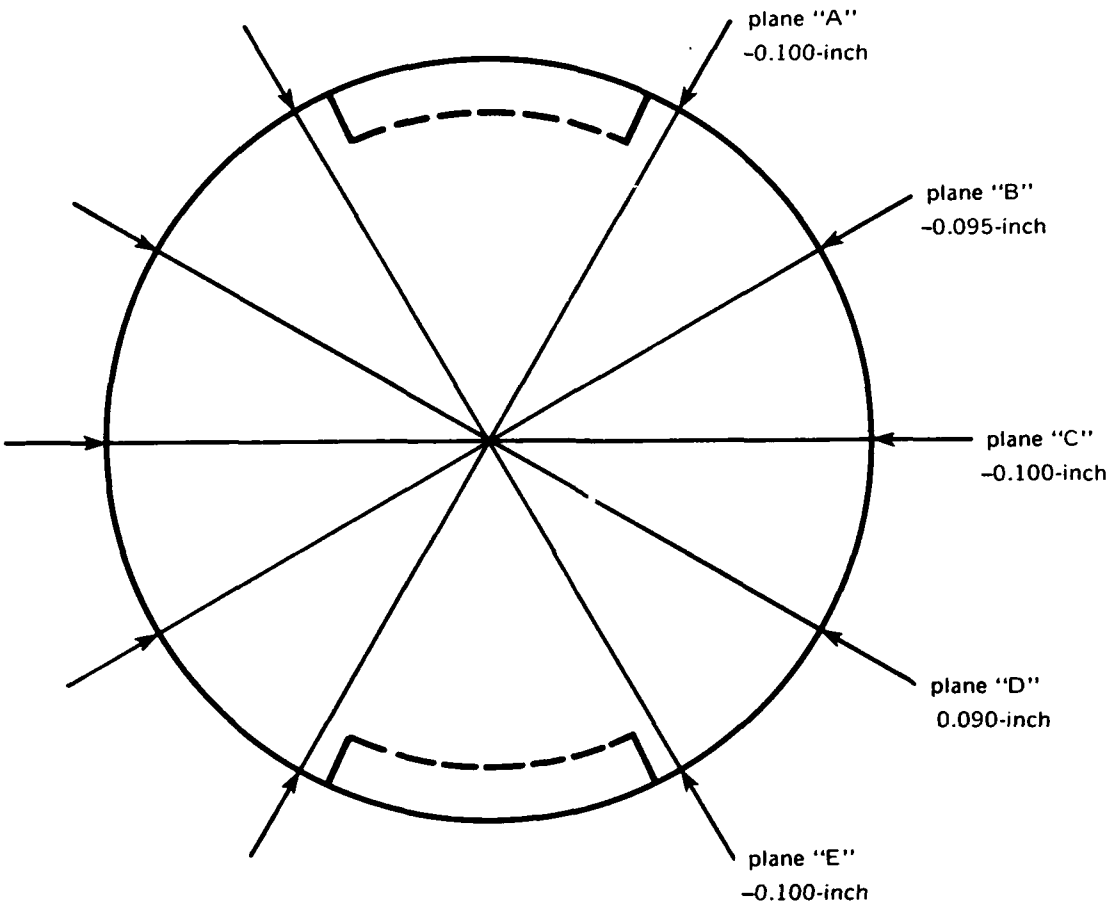

Diameter of the Finished Sphere

APPENDIX C

DATA FROM HYDROSTATIC TESTS

APPENDIX C. DATA FROM HYDROSTATIC TESTS

Both the 15-inch OD X 13-inch ID scale Model 34 and the 66-inch OD X 58-inch ID full scale Model 2000 Nemo Hulls were extensively instrumented with strain-gages (see Figs. 20 and 23 of main text) so that their structural performance under external hydrostatic pressure could be accurately measured and evaluated. Highlights of that data have been summarized (see Tables 4, 5 and 6) and discussed in the main body of the report.

Still, other researchers in the field of acrylic plastic pressure hulls may need to refer to some specific detail of that data not provided in the main body of the report. For this reason the data generated during some of the more severe hydrostatic tests has been selected for presentation here in Appendix C. For the 15-inch OD X 13-inch ID scale Model 34 the most severe as well as the most important test was pressurizing to implosion; this data is presented in Table 1C. The 66-inch OD X 58-inch ID full scale Model 2000 Nemo Hull has not been tested to implosion therefore this data is not available. Instead, the data from the long term pressurization cycles to 1350 and 1800 psi are shown in Tables 2C and 3C.

Data from 15-inch OD X 13-inch ID Model 34

Data Recording

The strain data was generated by subjecting the 15-inch OD X 13-inch ID Model 34 to external hydrostatic pressure rising at 100 psi/minute rate. During recording of strain data (which took about 2 minutes per recording) the pressure was held constant. The temperature of water used in pressurizing of Model 34 was in the 70–75°F range.

Data Interpretation

The most important observation that can be made of the strain data from Model 34 is that all the strains measured on the acrylic plastic as well as on aluminum were linear to well over 1400 psi, indicating that both materials were still in the elastic range when the simulated depth passed the 3000-foot mark. At simulated depth of 4000 feet most of the strains became markedly non-linear, and at 5000 feet the strains became exponential.

The linear behavior of strains to depths in the 3000–3300 foot range substantiates the postulate that the Model 2000 Nemo Hull design (and its scaled down version Nemo Model 34) is operationally safe to 3000 feet as all of the materials in the hull respond elastically in the 0–3000 foot range.

Data from 66-Inch OD X 58-Inch ID Model 2000 Nemo Hull

Data Recording

The strain data was generated by subjecting the 66-inch OD X 58-inch ID Model 2000 Nemo Hull to external hydrostatic pressure rising at 100 psi/minute rate. During recording of strain data (which took about 2 minutes per recording), the pressure was held constant. The temperature of water used in pressurizing of the Model 2000 Nemo Hull was in the 70–75°F range.

Once the maximum pressure was reached further pressurization was stopped and the maximum pressure maintained for 24 hours. Readings were taken at 6 hour intervals, but only the last reading (taken 24 hours after initiation of long term loading) is shown on the data printout.

Readings were taken also during the depressurization which took place at 100 psi/minute rate. Upon reaching 0 pressure the Model 2000 Nemo Hull assembly was allowed to relax for 24 hours while readings were taken every 6 hours (only the last relaxation reading is shown in the data printout).

Data Interpretation

The strains are linear to 3000 feet. The creep in acrylic plastic after 24 hours of sustained loading at 3000 feet was less than 20 percent of the short term strain at that depth. After reduction of pressure to 0 psi and 24 hour relaxation at 0 psi all strains returned to zero. Both the linearity of strain in the 0–3000 foot range and return of strains to zero at conclusion of the pressure cycle indicate that the Model 2000 Nemo Hull can be repeatedly pressurized without permanent deformation to 3000 feet.

When pressurized to 4000 feet there was some nonlinearity at depths beyond 3500 feet. The creep in acrylic plastic after 24 hours of sustained loading at 4000 feet was about 30 percent of the short term strain at that depth. After reduction of pressure to 0 and 24 hours of relaxation at 0 pressure most of the strains in acrylic and aluminum return essentially to zero (are within ±100 microinches of original zero). Only at some interior locations on aluminum components (location 6, 13, 14) were the remaining stresses positive and significantly high. No explanation has been found for their tensile character, or large magnitude.

The indications of nonlinearity during pressurization in the 3500–4000 foot depth range, excessive creep during long term pressurization at 4000 feet, and residual strains after relaxation at 0 depth indicate that pressurization of the Model 2000 Nemo Hull to 4000 feet subjects the assembly to excessive stresses. It is therefore postulated that the Model 2000 Nemo Hull assembly should not be prooftested in excess of 3600 feet for service at depths to 3300 feet.

Table 1C. Strains Measured on 15-Inch OD X 13-Inch ID Nemo Model 34

Load Psi	*Gage No. 1A-C*	*Gage No. 1A-L*	*Gage No. 1B-C*	*Gage No. 1B-L*	*Gage No. 2B-C*	*Gage No. 2B-L*	*Gage No. 3B-C*	*Gage No. 3B-L*	*Gage No. 4A-C*	*Gage No. 4A-L*
0	0	0	0	0	0	0	0	0	0	0
100	-500	-500	-550	-500	-1,800	-900	-80	0	-50	-50
200	-1,100	-1,000	-1,150	-1,100	-1,250	-2,100	-170	+10	-75	-75
300	-1,400	-1,500	-1,700	-1,800	-1,900	-2,700	-250	+20	-100	-100
400	-1,800	-1,900	-2,250	-2,350	-2,300	-3,300	-330	+30	-115	-120
500	-2,200	-2,250	-2,800	-2,900	-2,800	-3,950	-400	+50	-125	-130
600	-2,650	-2,650	-3,400	-3,500	-3,300	-4,600	-470	+70	-140	-150
700	-3,000	-3,050	-3,950	-4,000	-3,750	-5,100	-540	+90	-150	-150
800	-3,400	-3,400	-4,500	-4,500	-4,200	-5,750	-600	+110	-175	-150
900	-3,800	-3,800	-5,000	-5,100	-4,600	-6,400	-650	+130	-195	-120
1,000	-4,200	-4,200	-5,600	-5,700	-5,100	-7,050	-700	+150	-200	-100
1,100	-4,600	-4,600	-6,200	-6,200	-5,550	-7,650	-780	+150	-225	-75
1,200	-5,000	-5,000	-6,700	-6,800	-6,000	-8,350	-860	+150	-250	-50
1,300	-5,400	-5,400	-7,300	-7,300	-6,400	-8,950	-940	+150	-260	-30
1,400	-5,900	-5,800	-7,900	-7,900	-6,950	-9,700	-1,020	+130	-280	-20
1,500	-6,300	-6,200	-8,600	-8,500	-7,400	-10,400	-1,100	+110		
1,600	-6,700	-6,600	-9,100	-9,200	-7,900	-11,000	-1,190	+90		
1,700	-7,200	-7,000	-9,900	-9,900	-8,500	-11,850	-1,310	+70		
1,800	-7,750	-7,600	-10,600	-10,600	-9,200	-12,650	-1,400	+50		
1,900	-8,200	-8,000	-11,400	-11,500	-9,900	-13,600	-1,490	+30		
2,000	-8,800	-8,600	-12,200	-12,200	-10,500	-14,600	-1,600	+10		
2,200	-9,800	-9,500	-13,700	-13,800	-11,600	-16,500	-1,750	-10		
2,400	-10,000	-10,500	-15,200	-15,200	-12,800	-18,250	-1,900	-30		
2,600	-12,100	-11,700	-17,100	-17,800	-13,200	-21,000	-2,050	-50		
2,800	-13,400	-12,900	-18,600	-18,800	-15,800	-22,850	-2,150	-70		
3,200	-16,400	-15,600	-23,800	-22,700	-19,800	-28,900	-2,200	-90		
3,600	-18,600	-18,000	-27,100		-28,000	>-30,000	-2,250	-110		
4,000	-21,600	-20,200	>-30,000		>-30,000	>-30,000	-2,200	-120		

Location of gages shown on Figure 20, pg. 44.

Table 1C. (Continued).

Load Psi	*Gage No. 4B-C*	*Gage No. 4B-L*	*Gage No. 5A-C*	*Gage No. 5A-L*	*Gage No. 5B-C*	*Gage No. 5B-L*	*Gage No. 6B-C*	*Gage No. 6B-L*	*Gage No. 7B-C*	*Gage No. 7B-L*
0	0	0	0	0	0	0	0	0	0	0
100	-50	-180	-10	0	-80	-10	-800	-1,000	-90	90
200	-100	-300	-20	10	-160	-20	-1,500	-1,800	-210	150
300	-160	-400	-30	10	-240	-30	-2,000	-2,400	-300	150
400	-200	-500	-40	10	-330	-50	-2,500	-2,950	-400	190
500	-250	-590	-50	20	-410	-60	-3,000	-3,450	-490	190
600	-310	-700	-60	20	-490	-80	-3,600	-4,000	-590	220
700	-370	-790	-70	20	-570	-100	-4,100	-4,500	-600	230
800	-430	-900	-80	30	-650	-130	-4,600	-5,050	-710	230
900	-490	-1,010	-90	30	-710	-170	-5,100	-5,600	-900	240
1,000	-550	-1,100	-100	30	-780	-200	-5,700	-6,100	-1,000	240
1,100	-610	-1,190	-110	30	-840	-210	-6,150	-6,700	-1,110	240
1,200	-680	-1,270	-120	40	-920	-220	-6,800	-7,100	-1,220	250
1,300	-730	-1,350	-130	40	-1,000	-230	-7,200	-7,700	-1,330	250
1,400	-790	-1,430	-140	40	-1,090	-240	-7,800	-8,300	-1,440	250
1,500	-850	-1,520	-150	50	-1,180	-260	-8,250	-8,900	-1,550	270
1,600	-920	-1,620	-160	50	-1,280	-280	-8,750	-9,600	-1,600	290
1,700	-990	-1,710	-170	50	-1,320	-300	-9,300	-10,450	-1,720	320
1,800	-1,060	-1,800	-180	50	-1,370	-320	-9,900	-11,250	-1,830	350
1,900	-1,130	-1,950	-190	60	-1,550	-335	-10,600	-12,200	-1,900	430
2,000	-1,200	-2,050	-200	60	-1,630	-350	-11,200	-13,050	-2,020	500
2,200	-1,300	-2,400	-220	60	-1,800	-400	-12,500	-14,700	-2,270	600
2,400	-1,400	-2,600	-280	70	-2,000	-450	-13,900	-16,300	-2,470	700
2,600	-1,500	-2,800	-280	80	-2,200	-460	-15,700	-18,100	-2,700	850
2,800	-1,550	-2,900	-310	80	-2,340	-480	-17,550	-19,800	-2,860	900
3,200	-1,600	-3,100	-370	90	-2,500	-550	-23,100	-22,800	-3,250	1,000
3,600	-1,650	-3,250	-560	110	-2,500	-640	-27,500		-3,550	1,180
4,000	-1,600	-3,400	-530	120	-2,840	-550	>-30,000		-3,750	1,350

Table 2C. Strains Measured on the 66-Inch OD X 58-Inch ID Model 2000 Nemo Hull
Under 24-Hour Long Hydrostatic Loading of 1350 Psi

E= .40 POISSONS RATIO= .40 GAGE NO.= 1=OUTSIDE

	LOAD	EP1	EP2	SIGMA MAX	SIGMA MIN	TAU MAX
	0	0	0	0	0	0
	150	-300	-950	-324	-510	93
	300	-450	-1700	-538	-895	179
	450	-600	-2500	-762	-1305	271
	600	-800	-3300	-1010	-1724	357
	750	-950	-4100	-1233	-2133	450
	900	-1150	-4900	-1481	-2552	536
	1050	-1300	-5750	-1714	-2986	636
	1200	-1850	-6350	-2090	-3376	643
*[	1350	-2050	-7200	-2348	-3819	736
[	1350	-2000	-7500	-2381	-3952	786
	1350	-2000	-7500	-2381	-3952	786
	1200	-1850	-7300	-2271	-3829	779
	1050	-1650	-6550	-2033	-3433	700
	900	-1500	-5650	-1790	-2976	593
	750	-1300	-4700	-1514	-2486	486
	600	-1250	-3800	-1319	-2048	364
	450	-900	-2950	-990	-1576	293
	300	-700	-2000	-714	-1086	186
	150	-450	-1100	-424	-610	93
**[	0	-150	-350	-138	-195	29
[	0	0	0	0	0	0

*[denotes strains at the beginning and conclusion of 24 hour long sustained loading at 1350 psi

**[denotes strains at the beginning and conclusion of 24 hour long relaxation at 0 psi

EP1 – hoop orientation

EP2 – longitudinal orientation

Table 2C. (Continued).

STRAIN REDUCTION OF A TWO GAGE ROSETTE

E= .40 POISSONS RATIO= .40 GAGE NO.= 2=OUTSIDE

LOAD	EP1	EP2	SIGMA MAX	SIGMA MIN	TAU MAX
0	0	0	0	0	0
150	-700	-700	-467	-467	0
300	-1400	-1400	-933	-933	0
450	-2100	-2050	-1390	-1376	-7
600	-2750	-2700	-1824	-1810	-7
750	-3450	-3400	-2290	-2276	-7
900	-4150	-4100	-2757	-2743	-7
1050	-4850	-4800	-3224	-3210	-7
1200	-5600	-5500	-3714	-3686	-14
1350	-6350	-6250	-4214	-4186	-14
1450	-7550	-7550	-5033	-5033	0
1350	-7550	-7550	-5033	-5033	0
1200	-7350	-7300	-4890	-4876	-7
1050	-6550	-6500	-4357	-4343	-7
900	-5750	-5700	-3824	-3810	-7
750	-4900	-4850	-3257	-3243	-7
600	-4050	-4000	-2690	-2676	-7
450	-3050	-2950	-2014	-1986	-14
300	-2150	-2100	-1424	-1410	-7
150	-1300	-1300	-867	-867	0
0	-450	-400	-290	-276	-7
0	0	0	0	0	0

Location of gages shown on Figure 23, pg. 48.

Table 2C. (Continued).

STRAIN REDUCTION OF A TWO GAGE ROSETTE

E= .40 POISSONS RATIO= .40 GAGE NO.= 3=OUTSIDE

LOAD	EP1	EP2	SIGMA MAX	SIGMA MIN	TAU MAX
0	0	0	0	0	0
150	-200	-950	-276	-490	107
300	-400	-1650	-505	-862	179
450	-550	-2350	-710	-1224	257
600	-650	-3000	-881	-1552	336
750	-800	-3750	-1095	-1938	421
900	-950	-4500	-1310	-2324	507
1050	-1100	-5250	-1524	-2710	593
1200	-1200	-6000	-1714	-3086	686
1350	-1350	-6600	-1900	-3400	750
1350	-1350	-6950	-1967	-3567	800
1350	-1350	-6950	-1967	-3567	800
1200	-1300	-6800	-1914	-3486	786
1050	-1200	-6050	-1724	-3110	693
900	-1050	-5300	-1510	-2724	607
750	-850	-4500	-1262	-2305	521
600	-700	-3650	-1029	-1871	421
450	-600	-2800	-819	-1448	314
300	-450	-1900	-576	-990	207
150	-200	-1050	-295	-538	121
0	0	-250	-48	-119	36
0	0	0	0	0	0

Table 2C. (Continued).

STRAIN REDUCTION OF A TWO GAGE ROSETTE

E= .90 POISSONS RATIO= .30 GAGE NO.= 4=OUTSIDE

LOAD	EP1	EP2	SIGMA MAX	SIGMA MIN	TAU MAX
0	0	0	0	0	0
150	-750	-700	-490	-476	-7
300	-1400	-1350	-924	-910	-7
450	-2050	-1950	-1348	-1319	-14
600	-2750	-2600	-1805	-1762	-21
750	-3400	-3300	-2248	-2219	-14
900	-4050	-3900	-2671	-2629	-21
1050	-4800	-4600	-3162	-3105	-29
1200	-5500	-5250	-3619	-3548	-36
1350	-6200	-5950	-4086	-4014	-36
1350	-7400	-6950	-4848	-4719	-64
1350	-7400	-6950	-4848	-4719	-64
1200	-7250	-6800	-4748	-4619	-64
1050	-6450	-6150	-4243	-4157	-43
900	-5650	-5350	-3710	-3624	-43
750	-4800	-4500	-3143	-3057	-43
600	-3950	-3750	-2595	-2538	-29
450	-3100	-2900	-2029	-1971	-29
300	-2200	-2050	-1438	-1395	-21
150	-1350	-1200	-871	-829	-21
0	-500	-450	-324	-310	-7
0	0	0	0	0	0

Table 2C. (Continued).

STRAIN REDUCTION OF A TWO GAGE ROSETTE

E= 10,00 POISSONS RATIO= ,30 GAGE NO,= S=OUTSIDE

LOAD	EP1	EP2	SIGMA MAX	SIGMA MIN	TAU MAX
0	0	0	0	0	0
150	-50	-100	-879	-1264	192
300	-100	-150	-1593	-1978	192
450	-150	-150	-2143	-2143	0
600	-200	-200	-2857	-2857	0
750	-250	-200	-3407	-3022	-192
900	-300	-250	-4121	-3736	-192
1050	-300	-250	-4121	-3736	-192
1200	-300	-300	-4286	-4286	0
1350	-350	-350	-5000	-5000	0
1350	-350	-300	-4835	-4451	-192
1350	-350	-300	-4835	-4451	-192
1200	-300	-300	-4286	-4286	0
1050	-300	-300	-4286	-4286	0
900	-250	-250	-3571	-3571	0
750	-250	-200	-3407	-3022	-192
600	-200	-200	-2857	-2857	0
450	-150	-100	-1978	-1593	-192
300	-50	-100	-879	-1264	192
150	-50	-50	-714	-714	0
0	0	0	0	0	0
0	0	0	0	0	0

Table 2C. (Continued).

STRAIN REDUCTION OF A TWO GAGE ROSETTE

E= 30,00 POISSONS RATIO= ,30 GAGE NO,= 6=OUTSIDE

LOAD	EP1	EP2	SIGMA MAX	SIGMA MIN	TAU MAX
0	0	0	0	0	0
150	-50	-50	-714	-714	0
300	-100	-150	-1593	-1978	192
450	-150	-150	-2143	-2143	0
600	-200	-200	-2857	-2857	0
750	-250	-250	-3571	-3571	0
900	-300	-250	-4121	-3736	-192
1050	-350	-300	-4835	-4451	-192
1200	-400	-350	-5549	-5165	-192
1350	-450	-400	-6264	-5879	-192
1350	-400	-350	-5549	-5165	-192
1350	-400	-350	-5549	-5165	-192
1200	-400	-350	-5549	-5165	-192
1050	-400	-300	-5385	-4615	-385
900	-350	-300	-4835	-4451	-192
750	-300	-250	-4121	-3736	-192
600	-250	-200	-3407	-3022	-192
450	-150	-150	-2143	-2143	0
300	-50	-100	-879	-1264	192
150	-50	-50	-714	-714	0
0	0	0	0	0	0
0	0	0	0	0	0

Table 2C. (Continued).

STRAIN REDUCTION OF A TWO GAGE ROSETTE

E= 10.00 POISSONS RATIO= .33 GAGE NO.= 7=OUTSIDE

LOAD	EP1	EP2	SIGMA MAX	SIGMA MIN	TAU MAX
0	0	0	0	0	0
150	-100	-50	-1264	-879	-192
300	-150	-100	-1978	-1593	-192
450	-150	-150	-2143	-2143	0
600	-250	-200	-3407	-3022	-192
750	-300	-250	-4121	-3736	-192
900	-350	-300	-4835	-4451	-192
1050	-350	-350	-5000	-5000	0
1200	-400	-400	-5714	-5714	0
1350	-450	-450	-6429	-6429	0
1350	-450	-450	-6429	-6429	0
1350	-450	-450	-6429	-6429	0
1200	-400	-450	-5879	-6264	192
1050	-350	-350	-5000	-5000	0
900	-350	-300	-4835	-4451	-192
750	-300	-250	-4121	-3736	-192
600	-250	-200	-3407	-3022	-192
450	-150	-150	-2143	-2143	0
300	-100	-100	-1429	-1429	0
150	-50	-50	-714	-714	0
0	0	0	0	0	0
0	0	0	0	0	0

Table 2C. (Continued).

STRAIN REDUCTION OF A TWO GAGE ROSETTE

E= 10,00 POISSONS RATIO= ,30 GAGE NO.= 8=OUTSIDE

LOAD	EP1	EP2	SIGMA MAX	SIGMA MIN	TAU MAX
0	0	0	0	0	0
150	-50	50	-385	385	-385
300	-100	50	-934	220	-577
450	-150	100	-1319	604	-962
600	-200	100	-1868	440	-1154
750	-250	100	-2418	275	-1346
900	-300	100	-2967	110	-1538
1050	-300	150	-2802	659	-1731
1200	-350	100	-3516	-55	-1731
1350	-350	100	-3516	-55	-1731
1350	-300	100	-2967	110	-1538
1350	-300	100	-2967	110	-1538
1200	-300	100	-2967	110	-1538
1050	-300	100	-2967	110	-1538
900	-250	50	-2582	-275	-1154
750	-250	50	-2582	-275	-1154
600	-200	100	-1868	440	-1154
450	-150	50	-1484	55	-769
300	-100	50	-934	220	-577
150	-50	0	-549	-165	-192
0	0	0	0	0	0
0	0	0	0	0	0

Table 2C. (Continued).

STRAIN REDUCTION OF A TWO GAGE ROSETTE

E= 10.00 POISSONS RATIO= .30 GAGE NO.= 9=OUTSIDE

LOAD	EP1	EP2	SIGMA MAX	SIGMA MIN	TAU MAX
0	0	0	0	0	0
150	-50	-100	-879	-1264	192
300	-100	-150	-1593	-1978	192
450	-150	-200	-2308	-2692	192
600	-150	-250	-2473	-3242	385
750	-200	-300	-3187	-3956	385
900	-200	-350	-3352	-4505	577
1050	-250	-350	-3901	-4670	385
1200	-250	-400	-4066	-5220	577
1350	-300	-450	-4780	-5934	577
1350	-300	-450	-4780	-5934	577
1350	-300	-450	-4780	-5934	577
1200	-250	-400	-4066	-5220	577
1050	-200	-350	-3352	-4505	577
900	-200	-350	-3352	-4505	577
750	-150	-350	-2802	-4341	769
600	-150	-300	-2637	-3791	577
450	-150	-200	-2308	-2692	192
300	-100	-100	-1429	-1429	0
150	-50	-50	-714	-714	0
0	0	0	0	0	0
0	0	0	0	0	0

Table 2C. (Continued).

STRAIN REDUCTION OF A TWO GAGE ROSETTE

E= 10,00 POISSONS RATIO= ,30 GAGE NO,= 10=OUTSIDE

LOAD	EP1	EP2	SIGMA MAX	SIGMA MIN	TAU MAX
0	0	0	0	0	0
150	-50	-100	-879	-1264	192
300	-50	-150	-1044	-1813	385
450	-100	-150	-1593	-1978	192
600	-100	-150	-1593	-1978	192
750	-200	-200	-2857	-2857	0
900	-250	-200	-3407	-3022	-192
1050	-300	-250	-4121	-3736	-192
1200	-300	-250	-4121	-3736	-192
1350	-350	-250	-4670	-3901	-385
1350	-350	-250	-4670	-3901	-385
1350	-350	-250	-4670	-3901	-385
1200	-300	-250	-4121	-3736	-192
1050	-300	-250	-4121	-3736	-192
900	-300	-200	-3956	-3187	-385
750	-250	-150	-3242	-2473	-385
600	-150	-100	-1978	-1593	-192
450	-50	-100	-879	-1264	192
300	-50	-100	-879	-1264	192
150	-50	-50	-714	-714	0
0	0	0	0	0	0
0	0	0	0	0	0

Table 2C. (Continued).

STRAIN REDUCTION OF A TWO GAGE ROSETTE

E= 10.00 POISSONS RATIO= .30 GAGE NO.= 11=OUTSIDE

LOAD	EP1	EP2	SIGMA MAX	SIGMA MIN	TAU MAX
0	0	0	0	0	0
150	-50	-50	-714	-714	0
300	-100	-50	-1264	-879	-192
450	-150	-100	-1978	-1593	-192
600	-200	-150	-2692	-2308	-192
750	-200	-200	-2857	-2857	0
900	-200	-200	-2857	-2857	0
1050	-250	-250	-3571	-3571	0
1200	-250	-300	-3736	-4121	192
1350	-250	-300	-3736	-4121	192
1350	-250	-300	-3736	-4121	192
1350	-250	-300	-3736	-4121	192
1200	-250	-300	-3736	-4121	192
1050	-250	-250	-3571	-3571	0
900	-200	-200	-2857	-2857	0
750	-150	-150	-2143	-2143	0
600	-150	-100	-1978	-1593	-192
450	-100	-100	-1429	-1429	0
300	-100	-50	-1264	-879	-192
150	-60	-50	-714	-714	0
0	0	0	0	0	0
0	0	0	0	0	0

Table 2C. (Continued).

STRAIN REDUCTION OF A TWO GAGE ROSETTE

E= 10.00 POISSONS RATIO= .30 GAGE NO.= 12=OUTSIDE

LOAD	EP1	EP2	SIGMA MAX	SIGMA MIN	TAU MAX
0	0	0	0	0	0
150	-50	-50	-714	-714	0
300	-100	-100	-1429	-1429	0
450	-150	-100	-1978	-1593	-192
600	-150	-150	-2143	-2143	0
750	-200	-150	-2692	-2308	-192
900	-200	-200	-2857	-2857	0
1050	-250	-200	-3407	-3022	-192
1200	-250	-200	-3407	-3022	-192
1350	-300	-200	-3956	-3187	-385
1350	-300	-200	-3956	-3187	-385
1350	-300	-200	-3956	-3187	-385
1200	-300	-200	-3956	-3187	-385
1050	-250	-200	-3407	-3022	-192
900	-200	-200	-2857	-2857	0
750	-200	-150	-2692	-2308	-192
600	-150	-100	-1978	-1593	-192
450	-100	-50	-1264	-879	-192
300	-50	-50	-714	-714	0
150	-50	0	-549	-165	-192
0	0	0	0	0	0
0	0	0	0	0	0

Table 2C. (Continued).

STRAIN REDUCTION OF A TWO GAGE ROSETTE

E= 10,00 POISSONS RATIO= ,30 GAGE NO,= 13=OUTSIDE

LOAD	EP1	EP2	SIGMA MAX	SIGMA MIN	TAU MAX
0	0	0	0	0	0
150	-50	-100	-879	-1264	192
300	-100	-100	-1429	-1429	0
450	-100	-150	-1593	-1978	192
600	-150	-150	-2143	-2143	0
750	-150	-150	-2143	-2143	0
900	-200	-150	-2692	-2308	-192
1050	-250	-150	-3242	-2473	-385
1200	-250	-200	-3407	-3022	-192
1350	-300	-200	-3956	-3187	-385
1350	-500	-400	-6813	-6044	-385
1350	-500	-400	-6813	-6044	-385
1200	-450	-350	-6099	-5330	-385
1050	-350	-300	-4835	-4451	-192
900	-250	-250	-3571	-3571	0
750	-200	-150	-2692	-2308	-192
600	-150	-100	-1978	-1593	-192
450	-100	-50	-1264	-879	-192
300	-50	-50	-714	-714	0
150	-50	-50	-714	-714	0
0	0	0	0	0	0
0	0	0	0	0	0

Table 2C. (Continued).

STRAIN REDUCTION OF A TWO GAGE ROSETTE

E= 10,00 POISSONS RATIO= ,30 GAGE NO,= 14=OUTSIDE

LOAD	EP1	EP2	SIGMA MAX	SIGMA MIN	TAU MAX
0	0	0	0	0	0
150	-50	-100	-879	-1264	192
300	-100	-150	-1593	-1978	192
450	-150	-150	-2143	-2143	0
600	-200	-150	-2692	-2308	-192
750	-250	-200	-3407	-3022	-192
900	-250	-200	-3407	-3022	-192
1050	-300	-250	-4121	-3736	-192
1200	-300	-250	-4121	-3736	-192
1350	-350	-250	-4670	-3901	-385
1350	-550	-450	-7527	-6758	-385
1350	-550	-450	-7527	-6758	-385
1200	-500	-400	-6813	-6044	-385
1050	-400	-300	-5385	-4615	-385
900	-300	-200	-3956	-3187	-385
750	-250	-150	-3242	-2473	-385
600	-200	-150	-2692	-2308	-192
450	-100	-100	-1429	-1429	0
300	-50	-100	-879	-1264	192
150	-50	-50	-714	-714	0
0	0	0	0	0	0
0	0	0	0	0	0

Table 2C. (Continued).

STRAIN REDUCTION OF A TWO GAGE ROSETTE

E= .40 POISSONS RATIO= .40 GAGE NO.= 1=INSIDE

LOAD	EP1	EP2	SIGMA MAX	SIGMA MIN	TAU MAX
0	0	0	0	0	0
150	-800	-1150	-600	-700	50
300	-1250	-2550	-1081	-1452	186
450	-1750	-4450	-1681	-2452	386
600	-2200	-6100	-2210	-3324	557
750	-2700	-7650	-2743	-4157	707
900	-3100	-9550	-3295	-5138	921
1050	-3900	-11250	-3762	-6005	1121
1200	-4100	-12950	-4419	-6948	1264
1350	-4550	-14800	-4986	-7914	1464
1350	-5050	-18200	-5871	-9629	1879
1350	-5050	-18200	-5871	-9629	1879
1200	-4900	-17150	-5600	-9100	1750
1050	-4750	-15250	-5167	-8167	1500
900	-4100	-12500	-4333	-6733	1200
750	-3750	-10750	-3833	-5833	1000
600	-3300	-8200	-3193	-4533	700
450	-2900	-5450	-2419	-3148	364
300	-2350	-3450	-1776	-2090	157
150	-1500	-1950	-1086	-1214	64
0	-450	-1450	-490	-776	143
0	0	-50	-10	-24	7

Table 2C. (Continued).

E= .40 POISSONS RATIO= .40 GAGE NO.= 2=INSIDE

LOAD	EP1	EP2	SIGMA MAX	SIGMA MIN	TAU MAX
0	0	0	0	0	0
150	-1000	-900	-648	-619	-14
300	-1900	-1700	-1229	-1171	-29
450	-2800	-2550	-1819	-1748	-36
600	-3750	-3400	-2433	-2333	-50
750	-4600	-4250	-3000	-2900	-50
900	-5550	-5050	-3605	-3462	-71
1050	-6500	-5900	-4219	-4048	-86
1200	-7500	-6850	-4876	-4690	-93
1350	-8400	-7750	-5476	-5290	-93
1350	-10250	-9200	-6633	-6333	-150
1350	-10250	-9200	-6633	-6333	-150
1200	-9050	-8650	-5957	-5843	-57
1050	-7950	-7700	-5252	-5181	-36
900	-6900	-6750	-4571	-4529	-21
750	-5850	-5800	-3890	-3876	-7
600	-4700	-4900	-3171	-3229	29
450	-3550	-3850	-2424	-2510	43
300	-2600	-2700	-1752	-1781	14
150	-1650	-1450	-1062	-1005	-29
0	-600	-900	-343	-257	-43
0	-50	0	-24	-10	-7

Table 2C. (Continued).

STRAIN REDUCTION OF A TWO GAGE ROSETTE

E= .40 POISSONS RATIO= .40 GAGE NO.= 3=INSIDE

LOAD	EP1	EP2	SIGMA MAX	SIGMA MIN	TAU MAX
0	0	0	0	0	0
150	-600	-1300	-533	-733	100
300	-1100	-2550	-1010	-1424	207
450	-1550	-3900	-1481	-2152	336
600	-2000	-5250	-1952	-2881	464
750	-2450	-6600	-2424	-3610	593
900	-2950	-7900	-2910	-4324	707
1050	-3400	-9350	-3400	-5100	850
1200	-3950	-10850	-3948	-5919	986
1350	-4500	-12300	-4486	-6719	1114
1350	-5150	-15100	-5329	-8171	1421
1350	-5150	-15100	-5329	-8171	1421
1200	-4950	-14800	-5176	-7990	1407
1050	-4300	-13050	-4533	-7033	1260
900	-3750	-11250	-3929	-6071	1071
750	-3150	-9550	-3319	-5148	914
600	-2550	-7700	-2681	-4152	736
450	-2000	-5850	-2067	-3167	550
300	-1950	-4000	-1405	-2162	379
150	-750	-2150	-767	-1167	200
0	-150	-300	-129	-171	21
0	0	0	0	0	0

Table 2C. (Continued).

STRAIN REDUCTION OF A TWO GAGE ROSETTE

E= .40 POISSONS RATIO= .40 GAGE NO.= 4=INSIDI

LOAD	EP1	EP2	SIGMA MAX	SIGMA MIN	TAU MAX
0	0	0	0	0	0
150	-1000	-900	-648	-619	-14
300	-1950	-1750	-1262	-1205	-29
450	-2850	-2600	-1852	-1781	-36
600	-3750	-3500	-2452	-2381	-36
750	-4700	-4350	-3067	-2967	-50
900	-5650	-5250	-3690	-3576	-57
1050	-6550	-6100	-4281	-4152	-64
1200	-7550	-7100	-4948	-4819	-64
1350	-8550	-8000	-5595	-5438	-79
1350	-10400	-9500	-6762	-6505	-129
1350	-10400	-9500	-6762	-6505	-129
1200	-9950	-9350	-6519	-6348	-86
1050	-8900	-8300	-5819	-5648	-86
900	-7750	-7250	-5071	-4929	-71
750	-6600	-6100	-4305	-4162	-71
600	-5450	-5050	-3557	-3443	-57
450	-4350	-3900	-2814	-2686	-64
300	-3150	-2700	-2014	-1886	-64
150	-2050	-1500	-1262	-1105	-79
0	-700	-300	-390	-276	-57
0	-50	0	-24	-10	-7

Table 2C. (Continued).

STRAIN REDUCTION OF A TWO GAGE ROSETTE

E= 10.00 POISSONS RATIO= .30 GAGE NO.= 5=INSIDE

LOAD	EP1	EP2	SIGMA MAX	SIGMA MIN	TAU MAX
0	0	0	0	0	0
150	-50	-50	-714	-714	0
300	-150	-200	-2308	-2692	192
450	-200	-300	-3187	-3956	385
600	-300	-500	-4945	-6484	769
750	-400	-600	-6374	-7912	769
900	-450	-700	-7253	-9176	962
1050	-500	-750	-7967	-9890	962
1200	-650	-800	-9780	-10934	577
1350	-700	-850	-10495	-11648	577
1350	-600	-850	-9396	-11319	962
1350	-600	-850	-9396	-11319	962
1200	-600	-800	-9231	-10769	769
1050	-550	-750	-8516	-10055	769
900	-450	-650	-7088	-8626	769
750	-400	-550	-6209	-7363	577
600	-300	-450	-4780	-5934	577
450	-150	-300	-2637	-3791	577
300	-100	-200	-1758	-2627	385
150	-50	-50	-714	-714	0
0	0	0	0	0	0
0	0	0	0	0	0

Table 2C. (Continued).

STRAIN REDUCTION OF A TWO GAGE ROSETTE

E= 10,00 POISSONS RATIO= ,30 GAGE NO,= 6=INSIDE

LOAD	EP1	EP2	SIGMA MAX	SIGMA MIN	TAU MAX
0	0	0	0	0	0
150	-100	-100	-1429	-1429	0
300	-250	-350	-3901	-4670	385
450	-350	-500	-5495	-6648	577
600	-450	-650	-7088	-8626	769
750	-500	-800	-8132	-10440	1154
900	-600	-900	-9560	-11868	1154
1050	-700	-1050	-11154	-13846	1346
1200	-800	-1200	-12747	-15824	1538
1350	-850	-1300	-13626	-17088	1731
1350	-850	-1400	-13956	-18187	2115
1350	-850	-1400	-13956	-18187	2115
1200	-800	-1300	-13077	-16923	1923
1050	-700	-1150	-11484	-14945	1731
900	-600	-1000	-9890	-12967	1538
750	-500	-850	-8297	-10989	1346
600	-400	-700	-6703	-9011	1154
450	-350	-550	-5659	-7198	769
300	-250	-400	-4066	-5220	577
150	-100	-100	-1429	-1429	0
0	0	0	0	0	0
0	0	0	0	0	0

TABLE C-1 (Continued).

STRAIN REDUCTION OF A TWO GAGE ROSETTE

E= 10.00 POISSONS RATIO= .30 GAGE NO.= 7=INSIDE

LOAD	EP1	EP2	SIGMA MAX	SIGMA MIN	TAU MAX
0	0	0	0	0	0
150	-100	-100	-1429	-1429	0
300	-200	-200	-2857	-2857	0
450	-300	-300	-4286	-4286	0
600	-450	-350	-6099	-5330	-385
750	-600	-450	-8077	-6923	-577
900	-700	-500	-9341	-7802	-769
1050	-800	-550	-10604	-8681	-962
1200	-900	-650	-12033	-10110	-962
1350	-1000	-700	-13297	-10989	-1154
1350	-1000	-600	-12967	-9890	-1538
1350	-1000	-600	-12967	-9890	-1538
1200	-900	-600	-11868	-9560	-1154
1050	-800	-600	-10440	-8132	-1154
900	-700	-450	-9176	-7253	-962
750	-600	-400	-7912	-6374	-769
600	-500	-350	-6648	-5495	-577
450	-400	-300	-5385	-4615	-385
300	-250	-200	-3407	-3022	-192
150	-100	-100	-1429	-1429	0
0	0	0	0	0	0
0	0	0	0	0	0

Table 2C. (Continued).

STRAIN REDUCTION OF A TWO GAGE ROSETTE

E= 10,00 POISSONS RATIO= .30 GAGE NO.= 8-INSIDE

LOAD	EP1	EP2	SIGMA MAX	SIGMA MIN	TAU MAX
0	0	0	0	0	0
150	-100	50	-934	220	-577
300	-250	50	-2582	-275	-1154
450	-400	100	-4066	-220	-1923
600	-550	100	-5714	-714	-2500
750	-700	200	-7033	-110	-3962
900	-800	250	-7967	110	-4038
1050	-950	300	-9451	165	-4808
1200	-1050	100	-11209	-2363	-4423
1350	-1200	50	-13022	-3407	-4808
1350	-1200	0	-13187	-3956	-4615
1350	-1200	0	-13187	-3956	-4615
1200	-1100	100	-11758	-2527	-4615
1050	-1000	350	-9835	549	-6198
900	-850	300	-8352	495	-4423
750	-700	250	-6868	440	-3684
600	-550	150	-5549	-165	-2692
450	-400	150	-3901	330	-2115
300	-250	100	-2418	275	-1346
150	-100	50	-934	220	-877
0	0	0	0	0	0
0	0	0	0	0	0

Table 2C. (Continued).

STRAIN REDUCTION OF A TWO GAGE ROSETTE

E= 10,00 POISSONS RATIO= ,30 GAGE NO,= 9-INSIDE

LOAD	EP1	EP2	SIGMA MAX	SIGMA MIN	TAU MAX
0	0	0	0	0	0
150	-50	-50	-714	-714	0
300	-150	-200	-2308	-2692	192
450	-200	-300	-3187	-3956	385
600	-300	-450	-4780	-5934	577
750	-350	-600	-5824	-7747	962
900	-400	-750	-6868	-9560	1346
1050	-450	-850	-7747	-10824	1538
1200	-500	-1050	-8956	-13187	2115
1350	-600	-1200	-10549	-15165	2308
1350	-550	-1000	-9341	-12802	1731
1350	-550	-1000	-9341	-12802	1731
1200	-550	-1000	-9341	-12802	1731
1050	-450	-900	-7912	-11374	1731
900	-400	-800	-7033	-10110	1538
750	-350	-650	-5989	-8297	1154
600	-300	-500	-4945	-6484	769
450	-250	-350	-3901	-4670	385
300	-150	-200	-2308	-2692	192
180	-80	-100	-879	-1264	192
0	0	0	0	0	0
0	0	0	0	0	0

Table 2C. (Continued).

STRAIN REDUCTION OF A TWO GAGE ROSETTE

E= 10.00 POISSONS RATIO= .30 GAGE NO.= 10=INSIDE

LOAD	EP1	EP2	SIGMA MAX	SIGMA MIN	TAU MAX
0	0	0	0	0	0
150	-100	-50	-1264	-879	-192
300	-200	-100	-2527	-1758	-385
450	-300	-200	-3956	-3187	-385
600	-350	-300	-4835	-4461	-192
750	-400	-400	-5714	-5714	0
900	-500	-500	-7143	-7143	0
1050	-550	-550	-7857	-7857	0
1200	-650	-650	-9286	-9286	0
1350	-750	-700	-10549	-10165	-192
1350	-700	-650	-9835	-9451	-192
1350	-700	-650	-9835	-9451	-192
1200	-650	-650	-9286	-9286	0
1050	-550	-650	-7857	-7857	0
900	-500	-500	-7143	-7143	0
750	-400	-450	-5879	-6264	192
600	-350	-350	-5000	-5000	0
450	-300	-250	-4121	-3736	-192
300	-200	-150	-2692	-2308	-192
150	-100	-50	-1269	-879	-192
0	0	0	0	0	0
0	0	0	0	0	0

Table 2C. (Continued).

STRAIN REDUCTION OF A TWO GAGE ROSETTE

E= 10.00 POISSONS RATIO= .30 GAGE NO.= 11=INSIDE

LOAD	EP1	EP2	SIGMA MAX	SIGMA MIN	TAU MAX
0	0	0	0	0	0
150	-50	-50	-714	-714	0
300	-100	-200	-1758	-2527	385
450	-200	-250	-3022	-3407	192
600	-300	-350	-4451	-4835	192
750	-400	-450	-5879	-6264	192
900	-500	-550	-7308	-7692	192
1050	-550	-600	-8022	-8407	192
1200	-650	-700	-9451	-9835	192
1350	-700	-750	-10165	-10549	192
1350	-600	-750	-9066	-10220	577
1350	-600	-750	-9066	-10220	577
1200	-600	-700	-8901	-9670	385
1050	-550	-650	-8187	-8956	385
900	-500	-550	-7308	-7692	192
750	-450	-450	-6429	-6429	0
600	-350	-350	-5000	-5000	0
450	-250	-250	-3571	-3571	0
300	-150	-150	-2143	-2143	0
150	-50	-50	-714	-714	0
0	0	0	0	0	0
0	0	0	0	0	0

Table 2C. (Continued).

STRAIN REDUCTION OF A TWO GAGE ROSETTE

E= 10,00 POISSONS RATIO= ,30 GAGE NO,= 12=INSIDE

LOAD	EP1	EP2	SIGMA MAX	SIGMA MIN	TAU MAX
0	0	0	0	0	0
150	-50	-50	-714	-714	0
300	-150	-200	-2308	-2692	192
450	-250	-250	-3571	-3571	0
600	-300	-350	-4451	-4835	192
750	-400	-450	-5879	-6264	192
900	-500	-550	-7308	-7692	192
1050	-600	-650	-8736	-9121	192
1200	-700	-700	-10000	-10000	0
1350	-800	-800	-11429	-11429	0
1350	-800	-800	-11429	-11429	0
1350	-800	-800	-11429	-11429	0
1200	-750	-750	-10714	-10714	0
1050	-650	-650	-9286	-9286	0
900	-550	-550	-7857	-7857	0
750	-450	-450	-6429	-6429	0
600	-350	-350	-5000	-5000	0
450	-250	-250	-3571	-3571	0
300	-150	-150	-2143	-2143	0
150	-50	-50	-714	-714	0
0	0	0	0	0	0
0	0	0	0	0	0

Table 2C. (Continued).

STRAIN REDUCTION OF A TWO GAGE ROSETTE

E= 10,00 POISSONS RATIO= ,30 GAGE NO,= 13=INSIDE

LOAD	EP1	EP2	SIGMA MAX	SIGMA MIN	TAU MAX
0	0	0	0	0	0
150	-100	-100	-1429	-1429	0
300	-200	-200	-2857	-2857	0
450	-300	-300	-4286	-4286	0
600	-400	-400	-5714	-5714	0
750	-500	-500	-7143	-7143	0
900	-550	-600	-8022	-8407	192
1050	-600	-700	-8901	-9670	385
1200	-700	-800	-10330	-11099	385
1350	-800	-900	-11758	-12527	385
1350	-900	-1050	-13352	-14505	577
1350	-900	-1050	-13352	-14505	577
1200	-800	-900	-11758	-12527	385
1050	-700	-750	-10165	-10549	192
900	-600	-600	-8571	-8571	0
750	-500	-500	-7143	-7143	0
600	-400	-400	-5714	-5714	0
450	-300	-300	-4286	-4286	0
300	-200	-150	-2692	-3308	-192
150	-50	-50	-714	-714	0
0	0	0	0	0	0
0	0	0	0	0	0

Table 2C. (Continued).

STRAIN REDUCTION OF A TWO GAGE ROSETTE

E= 10.00 POISSONS RATIO= .30 GAGE NO.= 14=INSIDE

LOAD	EP1	EP2	SIGMA MAX	SIGMA MIN	TAU MAX
0	0	0	0	0	0
150	-100	-50	-1264	-879	-192
300	-200	-150	-2692	-2308	-192
450	-300	-200	-3956	-3187	-385
600	-400	-300	-5385	-4615	-385
750	-500	-400	-6813	-6044	-385
900	-600	-500	-8242	-7473	-385
1050	-700	-600	-9670	-8901	-385
1200	-800	-750	-11264	-10879	-192
1350	-900	-850	-12692	-12308	-192
1350	-1000	-1000	-14286	-14286	0
1350	-1000	-1000	-14286	-14286	0
1200	-900	-850	-12692	-12308	-192
1050	-750	-650	-10385	-9615	-385
900	-650	-550	-8956	-8187	-385
750	-500	-400	-6813	-6044	-385
600	-400	-300	-5385	-4615	-385
450	-300	-200	-3956	-3187	-385
300	-150	-100	-1978	-1593	-192
150	-50	-50	-714	-714	0
0	0	0	0	0	0
0	0	0	0	0	0

E= .40 POISSONS RATIO= .40 GAGE NO.= 1=OUTSIDE

LOAD	EP1	EP2	SIGMA MAX	SIGMA MIN	TAU MAX
0	0	0	0	0	0
100	.250	.800	.271	.429	79
200	.300	.1250	.381	.652	136
300	.400	.1750	.524	.910	193
400	.450	.2250	.643	.1157	257
500	.550	.2750	.786	.1414	314
600	.650	.3250	.929	.1671	371
700	.750	.3850	.1090	.1976	443
800	.900	.4400	.1267	.2267	500
900	.1050	.4950	.1443	.2557	557
1000	.1100	.5450	.1562	.2805	621
1100	.1200	.6050	.1724	.3110	693
1200	.1350	.6500	.1881	.3352	736
1300	.1850	.6900	.2195	.3638	721
1400	.2000	.7400	.2362	.3905	771
1500	.2150	.8000	.2548	.4219	836
1600	.2300	.8700	.2752	.4581	914
1700	.2400	.9250	.2905	.4862	979
*[1800	.2500	.9750	.3048	.5119	1036
1800	.2500	.10000	.3095	.5238	1071
1800	.2500	.10000	.3095	.5238	1071
1700	.2400	.9650	.2981	.5052	1036
1600	.2350	.9250	.2881	.4852	986
1500	.2300	.8900	.2790	.4676	943
1400	.2200	.8500	.2667	.4467	900
1300	.2100	.8100	.2543	.4257	857
1200	.2000	.7700	.2419	.4048	814
1100	.1950	.7200	.2300	.3800	750
1000	.1900	.6600	.2162	.3505	671
900	.1750	.6000	.1976	.3190	607
800	.1700	.5500	.1857	.2943	543
700	.1600	.4950	.1705	.2662	479
600	.1500	.4400	.1552	.2381	414
500	.1400	.3800	.1390	.2076	343
400	.1300	.3250	.1238	.1795	279
300	.1250	.2700	.1110	.1524	207
200	.1100	.2000	.905	.1162	129
100	.950	.1250	.690	.776	43
**[0	.150	.750	.219	.386	86
. 0	.50	150	5	62	.29

* denotes strains at the beginning and conclusion of 24 hour long sustained loading at 1900 psi

** denotes strains at the beginning and conclusion of 24 hour long sustained loading at 0 psi

Table 3C. (Continued).

STRAIN REDUCTION OF A TWO GAGE ROSETTE

E= .40 POISSONS RATIO= .40 GAGE NO.= 2=OUTSIDE

LOAD	EP1	EP2	SIGMA MAX	SIGMA MIN	TAU MAX
0	0	0	0	0	0
100	-450	-480	-300	-300	0
200	-850	-900	-576	-590	7
300	-1350	-1350	-900	-900	0
400	-1750	-1750	-1167	-1167	0
500	-2250	-2250	-1500	-1500	0
600	-2700	-2650	-1790	-1776	-7
700	-3150	-3150	-2100	-2100	0
800	-3600	-3600	-2400	-2400	0
900	-4150	-4050	-2748	-2719	-14
1000	-4550	-4500	-3024	-3010	-7
1100	-5100	-5000	-3381	-3352	-14
1200	-5500	-5450	-3657	-3643	-7
1300	-6050	-5950	-4014	-3986	-14
1400	-6550	-6450	-4348	-4319	-14
1500	-7050	-7000	-4640	-4676	-7
1600	-7650	-7550	-5081	-5052	-14
1700	-8200	-8100	-5448	-5419	-14
1800	-8650	-8600	-5757	-5743	-7
1800	-10900	-10640	-7219	-7148	-36
1800	-10900	-10650	-7219	-7148	-36
1700	-10550	-10300	-6986	-6914	-36
1600	-10080	-9850	-6662	-6605	-29
1500	-9650	-9500	-6405	-6362	-21
1400	-9200	-9060	-6105	-6062	-21
1300	-8800	-8650	-5838	-5795	-21
1200	-8350	-8200	-5538	-5495	-21
1100	-7900	-7750	-5238	-5195	-21
1000	-7300	-7150	-4838	-4795	-21
900	-6700	-6550	-4438	-4395	-21
800	-6200	-6050	-4105	-4062	-21
700	-5650	-5550	-3748	-3719	-14
600	-5000	-4900	-3314	-3286	-14
500	-4400	-4350	-2924	-2910	-7
400	-3800	-3950	-2562	-2605	21
300	-3200	-3300	-2152	-2181	14
200	-2500	-2600	-1686	-1714	14
100	-1800	-1950	-1229	-1271	21
0	-990	-1100	-662	-705	21
0	50	0	24	10	7

STRAIN REDUCTION OF A TWO GAGE ROSETTE

E= .40 POISSONS RATIO= .40 GAGE NO.= 3=OUTSIDE

LOAD	EP1	EP2	SIGMA MAX	SIGMA MIN	TAU MAX
0	0	0	0	0	0
100	-100	-600	-162	-305	71
200	-200	-1100	-305	-562	129
300	-300	-1600	-448	-819	186
400	-400	-2000	-571	-1029	229
500	-500	-2500	-714	-1286	286
600	-600	-3000	-857	-1543	343
700	-700	-3450	-990	-1776	393
800	-770	-3900	-1110	-2009	447
900	-870	-4400	-1252	-2261	504
1000	-950	-4900	-1386	-2514	564
1100	-1050	-5450	-1538	-2795	629
1200	-1100	-5900	-1648	-3019	686
1300	-1200	-6400	-1790	-3276	743
1400	-1300	-6900	-1933	-3533	800
1500	-1400	-7400	-2076	-3790	857
1600	-1500	-7900	-2219	-4048	914
1700	-1600	-8400	-2362	-4305	971
1800	-1700	-8800	-2486	-4514	1014
1800	-1650	-9150	-2529	-4671	1071
1800	-1650	-9150	-2529	-4671	1071
1700	-1550	-8800	-2414	-4486	1036
1600	-1500	-8400	-2319	-4286	986
1500	-1400	-8000	-2190	-4076	943
1400	-1350	-7650	-2100	-3900	900
1300	-1250	-7200	-1967	-3667	850
1200	-1200	-6850	-1876	-3490	807
1100	-1100	-6400	-1743	-3257	757
1000	-1000	-5900	-1600	-3000	700
900	-900	-5450	-1467	-2767	650
800	-850	-5000	-1357	-2543	593
700	-750	-4550	-1224	-2310	543
600	-650	-4100	-1090	-2076	493
500	-550	-3600	-948	-1819	436
400	-450	-3100	-805	-1562	379
300	-350	-2600	-662	-1305	321
200	-200	-1950	-467	-967	250
100	-100	-1250	-286	-614	164
0	50	-450	-62	-205	71
0	0	300	57	143	-43

Table 3C. (Continued).

STRAIN REDUCTION OF A TWO GAGE ROSETTE

E= .90 POISSONS RATIO= .40 GAGE NO.= 4=OUTSIDE

LOAD	EP1	EP2	SIGMA MAX	SIGMA MIN	TAU MAX
0	0	0	0	0	0
100	-450	-460	-300	-300	0
200	-850	-860	-667	-567	0
300	-1350	-1250	-881	-852	-14
400	-1750	-1700	-1157	-1143	-7
500	-2250	-2150	-1481	-1452	-14
600	-2650	-2600	-1757	-1743	-7
700	-3150	-3100	-2090	-2076	-7
800	-3600	-3450	-2371	-2329	-21
900	-4050	-3900	-2671	-2629	-21
1000	-4450	-4300	-2938	-2895	-21
1100	-5000	-4800	-3295	-3238	-29
1200	-5450	-5250	-3595	-3538	-29
1300	-5950	-5750	-3929	-3871	-29
1400	-6400	-6200	-4229	-4171	-29
1500	-6900	-6650	-4552	-4481	-36
1600	-7500	-7200	-4943	-4857	-43
1700	-8050	-7750	-5310	-5224	-43
1800	-8550	-8200	-5633	-5533	-50
1800	-10600	-10000	-6952	-6781	-86
1800	-10600	-10000	-6952	-6781	-86
1700	-10250	-9700	-6729	-6571	-79
1600	-9800	-9250	-6429	-6271	-79
1500	-9400	-8900	-6171	-6029	-71
1400	-9000	-8450	-5895	-5738	-79
1300	-8500	-8050	-5581	-5452	-64
1200	-8150	-7650	-5338	-5195	-71
1100	-7650	-7200	-5014	-4886	-64
1000	-7050	-6700	-4633	-4533	-50
900	-6500	-6100	-4257	-4143	-57
800	-6000	-5650	-3933	-3833	-50
700	-5450	-5150	-3576	-3490	-43
600	-4850	-4550	-3176	-3090	-43
500	-4300	-4000	-2810	-2724	-43
400	-3700	-3450	-2419	-2348	-36
300	-3100	-2850	-2019	-1948	-36
200	-2400	-2200	-1562	-1505	-29
100	-1750	-1600	-1138	-1095	-21
0	-950	-800	-605	-562	-21
0	150	50	81	52	14

STRAIN REDUCTION OF A TWO GAGE ROSETTE

E= 10.00 POISSONS RATIO= .30 GAGE NO.= 5=OUTSIDE

LOAD	EP1	EP2	SIGMA MAX	SIGMA MIN	TAU MAX
0	0	0	0	0	0
100	-50	-50	-714	-714	0
200	-50	-50	-714	-714	0
300	-100	-100	-1429	-1429	0
400	-100	-100	-1429	-1429	0
500	-150	-150	-2143	-2143	0
600	-200	-150	-2692	-2308	-192
700	-200	-150	-2692	-2308	-192
800	-200	-200	-2857	-2857	0
900	-200	-200	-2857	-2857	0
1000	-250	-200	-3407	-3022	-192
1100	-300	-250	-4121	-3736	-192
1200	-300	-250	-4121	-3736	-192
1300	-300	-250	-4121	-3736	-192
1400	-350	-300	-4835	-4451	-192
1500	-350	-300	-4835	-4451	-192
1600	-400	-350	-5549	-5165	-192
1700	-400	-350	-5549	-5165	-192
1800	-400	-350	-5549	-5165	-192
1800	-400	-350	-5549	-5165	-192
1800	-400	-350	-5549	-5165	-192
1700	-350	-300	-4835	-4451	-192
1600	-350	-300	-4835	-4451	-192
1500	-350	-300	-4835	-4451	-192
1400	-300	-250	-4121	-3736	-192
1300	-300	-250	-4121	-3736	-192
1200	-350	-250	-4670	-3901	-385
1100	-300	-200	-3956	-3187	-385
1000	-300	-200	-3956	-3187	-385
900	-250	-150	-3242	-2473	-385
800	-200	-150	-2692	-2308	-192
700	-200	-150	-2692	-2308	-192
600	-150	-150	-2143	-2143	0
500	-150	-100	-1978	-1593	-192
400	-100	-100	-1429	-1429	0
300	-100	-50	-1264	-879	-192
200	-50	0	-549	-165	-192
100	0	0	0	0	0
0	50	100	879	1264	-192
0	-50	0	-549	-165	-192

Table 3C. (Continued).

STRAIN REDUCTION OF A TWO GAGE ROSETTE

E= 10.00 POISSONS RATIO= .30 GAGE NO.= 6=OUTSIDE

LOAD	EP1	EP2	SIGMA MAX	SIGMA MIN	TAU MAX
0	0	0	0	0	0
100	-50	-100	-879	-1264	192
200	-50	-100	-879	-1264	192
300	-100	-150	-1593	-1978	192
400	-100	-150	-1593	-1978	192
500	-150	-150	-2143	-2143	0
600	-200	-200	-2857	-2857	0
700	-200	-200	-2857	-2857	0
800	-250	-250	-3571	-3571	0
900	-250	-250	-3571	-3571	0
1000	-300	-250	-4121	-3736	-192
1100	-300	-300	-4286	-4286	0
1200	-350	-300	-4835	-4451	-192
1300	-350	-300	-4835	-4451	-192
1400	-400	-350	-5549	-5165	-192
1500	-450	-350	-6099	-5330	-385
1600	-450	-400	-6264	-5879	-192
1700	-500	-400	-6813	-6044	-385
1800	-500	-450	-6978	-6593	-192
1900	-500	-450	-6978	-6593	-192
1800	-500	-450	-6978	-6593	-192
1700	-450	-400	-6264	-5879	-192
1600	-450	-400	-6264	-5879	-192
1500	-450	-400	-6264	-5879	-192
1400	-400	-350	-5549	-5165	-192
1300	-350	-350	-5000	-5000	0
1200	-350	-350	-5000	-5000	0
1100	-300	-350	-4451	-4835	192
1000	-250	-300	-3736	-4121	192
900	-250	-250	-3571	-3571	0
800	-250	-250	-3571	-3571	0
700	-200	-250	-3022	-3407	192
600	-150	-250	-2473	-3242	385
500	-100	-200	-1758	-2527	385
400	-100	-150	-1593	-1978	192
300	-50	-150	-1044	-1813	385
200	-50	-100	-879	-1264	192
100	0	-50	-165	-549	192
0	100	50	1264	879	192
0	50	0	549	165	192

STRAIN REDUCTION OF A TWO GAGE ROSETTE

E= 10,00 POISSONS RATIO= ,30 GAGE NO,= 7=OUTSIDE

LOAD	EP1	EP2	SIGMA MAX	SIGMA MIN	TAU MAX
0	0	0	0	0	0
100	-50	-50	-714	-714	0
200	-100	-50	-1264	-879	-192
300	-150	-100	-1978	-1593	-192
400	-150	-100	-1978	-1593	-192
500	-200	-150	-2692	-2308	-192
600	-250	-200	-3407	-3022	-192
700	-250	-250	-3571	-3571	0
800	-300	-250	-4121	-3736	-192
900	-300	-250	-4121	-3736	-192
1000	-300	-250	-4121	-3736	-192
1100	-350	-350	-5000	-5000	0
1200	-350	-350	-5000	-5000	0
1300	-400	-400	-5714	-5714	0
1400	-400	-400	-5714	-5714	0
1500	-450	-400	-6264	-5879	-192
1600	-500	-450	-6978	-6593	-192
1700	-500	-500	-7143	-7143	0
1800	-550	-500	-7692	-7308	-192
1800	-550	-450	-7527	-6758	-385
1800	-550	-450	-7527	-6758	-386
1700	-500	-400	-6813	-6044	-385
1600	-500	-350	-6648	-5495	-577
1500	-500	-350	-6648	-5495	-577
1400	-400	-300	-5385	-4615	-385
1300	-400	-300	-5385	-4615	-385
1200	-400	-300	-5385	-4615	-386
1100	-350	-300	-4835	-4451	-192
1000	-300	-250	-4121	-3736	-192
900	-300	-200	-3956	-3187	-385
800	-250	-150	-3242	-2473	-386
700	-200	-150	-2692	-2308	-192
600	-200	-100	-2527	-1758	-385
500	-150	-50	-1813	-1044	-386
400	-100	-50	-1264	-879	-192
300	-100	0	-1099	-330	-385
200	-50	50	-385	385	-385
100	-50	50	-385	385	-385
0	50	150	1044	1813	-386
0	-50	50	-385	385	-385

Table 3C. (Continued).

STRAIN REDUCTION OF A TWO GAGE ROSETTE

E= 10,00 POISSONS RATIO= ,30 GAGE NO.= B=OUTSIDE

LOAD	EP1	EP2	SIGMA MAX	SIGMA MIN	TAU MAX
0	0	0	0	0	0
100	-50	50	-385	385	-385
200	-100	100	-769	769	-769
300	-150	100	-1319	604	-962
400	-150	100	-1319	604	-962
500	-150	100	-1319	604	-962
600	-200	100	-1868	440	-1154
700	-200	100	-1868	440	-1154
800	-250	100	-2418	275	-1346
900	-250	150	-2253	824	-1538
1000	-250	150	-2253	824	-1538
1100	-300	150	-2802	659	-1731
1200	-300	200	-2637	1209	-1923
1300	-300	200	-2637	1209	-1923
1400	-350	200	-3187	1044	-2115
1500	-350	250	-3022	1593	-2308
1600	-400	200	-3736	879	-2308
1700	-450	200	-4286	714	-2500
1800	-450	200	-4286	714	-2500
1800	-400	250	-3571	1429	-2500
1800	-400	250	-3571	1429	-2500
1700	-350	200	-3187	1044	-2115
1600	-350	200	-3187	1044	-2115
1500	-300	150	-2802	659	-1731
1400	-250	200	-2088	1374	-1731
1300	-250	200	-2088	1374	-1731
1200	-250	200	-2088	1374	-1731
1100	-200	200	-1538	1538	-1538
1000	-200	200	-1538	1538	-1538
900	-150	200	-989	1703	-1346
800	-150	200	-989	1703	-1346
700	-150	200	-989	1703	-1346
600	-100	200	-440	1868	-1154
500	-100	200	-440	1868	-1154
400	-50	200	110	2033	-962
300	-50	150	-55	1484	-769
200	0	150	495	1648	-577
100	50	100	879	1264	-192
0	150	100	1978	1593	192
0	50	0	549	165	192

STRAIN REDUCTION OF A TWO GAGE ROSETTE

E= 10,00 POISSONS RATIO= ,30 GAGE NO,= 9=OUTSIDE

LOAD	EP1	EP2	SIGMA MAX	SIGMA MIN	TA
0	0	0	0	0	0
100	-50	-50	-714	-714	0
200	-50	-100	-879	-1264	192
300	-100	-150	-1593	-1978	192
400	-150	-150	-2143	-2143	0
500	-150	-200	-2308	-2692	192
600	-150	-200	-2308	-2692	192
700	-150	-200	-2308	-2692	192
800	-200	-250	-3022	-3407	192
900	-250	-250	-3571	-3571	0
1000	-250	-250	-3571	-3571	0
1100	-250	-300	-3736	-4121	192
1200	-250	-300	-3736	-4121	192
1300	-300	-350	-4451	-4835	192
1400	-300	-350	-4451	-4835	192
1500	-350	-400	-5165	-5549	192
1600	-350	-400	-5165	-5549	192
1700	-350	-450	-5330	-6099	385
1800	-400	-450	-5879	-6264	192
1800	-400	-450	-5879	-6264	192
1800	-400	-450	-5879	-6264	192
1700	-400	-400	-5714	-5714	0
1600	-400	-350	-5549	-5165	-192
1500	-400	-350	-5549	-5165	-192
1400	-350	-350	-5000	-5000	0
1300	-300	-350	-4451	-4835	192
1200	-300	-300	-4286	-4286	0
1100	-300	-250	-4121	-3736	-192
1000	-250	-250	-3571	-3571	0
900	-250	-200	-3407	-3022	-192
800	-200	-150	-2692	-2308	-192
700	-200	-150	-2692	-2308	-192
600	-200	-100	-2527	-1758	-385
500	-100	-100	-1429	-1429	0
400	-100	-50	-1264	-879	-192
300	-100	-50	-1264	-879	-192
200	-50	0	-549	-165	-192
100	0	50	165	549	-192
0	50	150	1044	1813	-385
0	0	50	165	549	-192

Table 3C. (Continued).

STRAIN REDUCTION OF A TWO GAGE ROSETTE

E= 10,00 POISSONS RATIO= ,30 GAGE NO,= 10=OUTSIDE

LOAD	EP1	EP2	SIGMA MAX	SIGMA MIN	TAU MAX
0	0	0	0	0	0
100	-50	-50	-714	-714	0
200	-50	-100	-879	-1264	192
300	-100	-100	-1429	-1429	0
400	-100	-100	-1429	-1429	0
500	-100	-100	-1429	-1429	0
600	-150	-100	-1978	-1593	-192
700	-150	-150	-2143	-2143	0
800	-200	-150	-2692	-2308	-192
900	-200	-200	-2857	-2857	0
1000	-200	-150	-2692	-2308	-192
1100	-250	-200	-3407	-3022	-192
1200	-250	-200	-3407	-3022	-192
1300	-300	-200	-3956	-3187	-385
1400	-300	-200	-3956	-3187	-385
1500	-300	-200	-3956	-3187	-385
1600	-350	-250	-4670	-3901	-385
1700	-400	-250	-5220	-4066	-577
1800	-400	-250	-5220	-4066	-577
1800	-400	-250	-5220	-4066	-577
1700	-350	-200	-4505	-3352	-577
1600	-350	-200	-4505	-3352	-577
1500	-350	-200	-4505	-3352	-577
1400	-300	-150	-3791	-2637	-577
1300	-300	-150	-3791	-2637	-577
1200	-300	-150	-3791	-2637	-577
1100	-200	-100	-2527	-1758	-385
1000	-200	-100	-2527	-1758	-385
900	-200	-100	-2527	-1758	-385
800	-200	-100	-2527	-1758	-385
700	-100	-50	-1264	-879	-192
600	-100	-50	-1264	-879	-192
500	-100	-50	-1264	-879	-192
400	-100	-50	-1264	-879	-192
300	-100	0	-1099	-330	-385
200	-50	50	-385	385	-385
100	0	50	165	549	-192
0	50	100	879	1264	-192
0	-50	50	-385	385	-385

Table 3C. (Continued).

STRAIN REDUCTION OF A TWO GAGE ROSETTE

E= 10,00 POISSONS RATIO= ,30 GAGE NO,= 11=OUTSIDE

LOAD	EP1	EP2	SIGMA MAX	SIGMA MIN	TAU MAX
0	0	0	0	0	0
100	-50	-50	-714	-714	0
200	-100	-50	-1264	-879	-192
300	-100	-100	-1429	-1429	0
400	-100	-50	-1264	-879	-192
500	-100	-100	-1429	-1429	0
600	-150	-150	-2143	-2143	0
700	-100	-150	-1593	-1978	192
800	-150	-150	-2143	-2143	0
900	-200	-200	-2857	-2857	0
1000	-150	-200	-2308	-2692	192
1100	-200	-250	-3022	-3407	192
1200	-200	-250	-3022	-3407	192
1300	-200	-250	-3022	-3407	192
1400	-200	-250	-3022	-3407	192
1500	-200	-250	-3022	-3407	192
1600	-250	-300	-3736	-4121	192
1700	-250	-350	-3901	-4670	385
1800	-250	-400	-4066	-5220	577
1800	-250	-350	-3901	-4670	385
1800	-250	-350	-3901	-4670	385
1700	-250	-300	-3736	-4121	192
1600	-200	-300	-3187	-3956	385
1500	-250	-300	-3736	-4121	192
1400	-200	-250	-3022	-3407	192
1300	-200	-250	-3022	-3407	192
1200	-200	-200	-2857	-2857	0
1100	-150	-200	-2308	-2692	192
1000	-100	-150	-1593	-1978	192
900	-100	-150	-1593	-1978	192
800	-100	-150	-1593	-1978	192
700	-100	-50	-1264	-879	-192
600	-50	-50	-714	-714	0
500	-50	-50	-714	-714	0
400	-50	-50	-714	-714	0
300	-50	0	-549	-165	-192
200	0	0	0	0	0
100	50	50	714	714	0
0	100	100	1429	1429	0
0	150	0	1648	495	577

Table 3C. (Continued).

STRAIN REDUCTION OF A TWO GAGE ROSETTE

E= 10,00 POISSONS RATIO= ,30 GAGE NO,= 12=OUTSIDE

LOAD	EP1	EP2	SIGMA MAX	SIGMA MIN	TAU MAX
0	0	0	0	0	0
100	-50	-150	-1044	-1813	385
200	-100	-150	-1593	-1978	192
300	-150	-150	-2143	-2143	0
400	-100	-150	-1593	-1978	192
500	-150	-200	-2308	-2692	192
600	-200	-200	-2857	-2857	0
700	-200	-200	-2857	-2857	0
800	-200	-200	-2857	-2857	0
900	-250	-200	-3407	-3022	-192
1000	-200	-200	-2857	-2857	0
1100	-250	-250	-3571	-3571	0
1200	-300	-200	-3956	-3187	-385
1300	-300	-250	-4121	-3736	-192
1400	-300	-250	-4121	-3736	-192
1500	-350	-250	-4670	-3901	-385
1600	-400	-250	-5220	-4066	-577
1700	-400	-300	-5385	-4615	-385
1800	-400	-300	-5385	-4615	-385
1800	-400	-300	-5385	-4615	-385
1800	-400	-300	-5385	-4615	-385
1700	-400	-250	-5220	-4066	-577
1600	-350	-250	-4670	-3901	-385
1500	-350	-250	-4670	-3901	-385
1400	-300	-200	-3956	-3187	-385
1300	-300	-200	-3956	-3187	-385
1200	-300	-200	-3956	-3187	-385
1100	-250	-200	-3407	-3022	-192
1000	-250	-200	-3407	-3022	-192
900	-200	-150	-2692	-2308	-192
800	-200	-150	-2692	-2308	-192
700	-150	-150	-2143	-2143	0
600	-150	-150	-2143	-2143	0
500	-100	-100	-1429	-1429	0
400	-100	-100	-1429	-1429	0
300	-100	-100	-1429	-1429	0
200	-50	-100	-879	-1264	192
100	0	-50	-165	-549	192
0	0	50	165	549	-192
0	-50	-50	-714	-714	0

Table 3C. (Continued).

STRAIN REDUCTION OF A TWO GAGE ROSETTE

E= 10,00 POISSONS RATIO= ,30 GAGE NO,= 13=OUTSIDE

LOAD	EP1	EP2	SIGMA MAX	SIGMA MIN	TAU MAX
0	0	0	0	0	0
100	-50	-100	-879	-1264	192
200	-100	-100	-1429	-1429	0
300	-150	-150	-2143	-2143	0
400	-100	-150	-1593	-1978	192
500	-150	-150	-2143	-2143	0
600	-200	-150	-2692	-2308	-192
700	-200	-200	-2857	-2857	0
800	-200	-200	-2857	-2857	0
900	-250	-200	-3407	-3022	-192
1000	-250	-200	-3407	-3022	-192
1100	-300	-200	-3956	-3187	-385
1200	-300	-200	-3956	-3187	-385
1300	-350	-200	-4505	-3352	-577
1400	-350	-200	-4505	-3352	-577
1500	-350	-200	-4505	-3352	-577
1600	-400	-200	-5055	-3516	-769
1700	-400	-200	-5055	-3516	-769
1800	-400	-250	-5220	-4066	-577
1800	-400	-200	-5055	-3516	-769
1800	-400	-200	-5055	-3516	-769
1700	-400	-200	-5056	-3516	-769
1600	-400	-200	-5055	-3516	-769
1500	-400	-150	-4890	-2967	-962
1400	-350	-150	-4341	-2802	-769
1300	-300	-150	-3791	-2637	-577
1200	-300	-150	-3791	-2637	-577
1100	-300	-150	-3791	-2637	-577
1000	-250	-100	-3077	-1923	-577
900	-200	-100	-2527	-1758	-385
800	-200	-100	-2527	-1758	-385
700	-200	-50	-2363	-1209	-577
600	-150	-50	-1813	-1044	-385
500	-150	-50	-1813	-1044	-385
400	-150	-50	-1813	-1044	-385
300	-100	0	-1099	-330	-385
200	-100	0	-1099	-330	-385
100	-50	50	-385	385	-385
0	0	100	330	1099	-385
0	100	100	1429	1429	0

Table 3C. (Continued).

STRAIN REDUCTION OF A TWO GAGE ROSETTE

E= 10,00 POISSONS RATIO= ,30 GAGE NO,= 14=OUTSIDE

LOAD	EP1	EP2	SIGMA MAX	SIGMA MIN	TAU MAX
0	0	0	0	0	0
100	-50	-100	-879	-1264	192
200	-100	-100	-1429	-1429	0
300	-150	-150	-1593	-1978	192
400	-100	-150	-1593	-1978	192
500	-150	-200	-2308	-2692	192
600	-200	-700	-4505	-8358	1923
700	-200	-200	-2857	-2857	0
800	-200	-200	-2857	-2857	0
900	-250	-200	-3407	-3022	-192
1000	-250	-200	-3407	-3022	-192
1100	-300	-200	-3956	-3187	-385
1200	-300	-200	-3956	-3187	-385
1300	-300	-250	-4121	-3736	-192
1400	-300	-250	-4121	-3736	-192
1500	-350	-250	-4670	-3901	-385
1600	-400	-250	-5220	-4066	-577
1700	-400	-250	-5220	-4066	-577
1800	-400	-300	-5385	-4615	-385
1800	-450	-250	-5769	-4231	-769
1800	-450	-250	-5769	-4231	-769
1700	-400	-250	-5220	-4066	-577
1600	-400	-250	-5220	-4066	-577
1500	-350	-250	-4670	-3901	-385
1400	-350	-200	-4505	-3352	-577
1300	-300	-200	-3956	-3187	-385
1200	-300	-150	-3791	-2637	-577
1100	-250	-150	-3242	-2473	-385
1000	-250	-150	-3242	-2473	-385
900	-200	-100	-2527	-1758	-385
800	-200	-100	-2527	-1758	-385
700	-200	-100	-2527	-1758	-385
600	-150	-50	-1813	-1044	-385
500	-100	-50	-1264	-879	-192
400	-100	-50	-1264	-879	-192
300	-50	0	-549	-165	-192
200	-50	0	-549	-165	-192
100	0	50	165	549	-192
0	0	100	330	1099	-385
0	50	0	549	165	192

Table 3C. (Continued).

STRAIN REDUCTION OF A TWO GAGE ROSETTE

E= ,*0 POISSONS RATIO= ,*0 GAGE NO,= 1=INSIDE

LOAD	EP1	EP2	SIGMA MAX	SIGMA MIN	TAU MAX
0	0	0	0	0	0
100	-600	-700	-919	-998	19
200	-950	-1750	-786	-1019	119
300	-1200	-2750	-1095	-1538	221
400	-1500	-3850	-1498	-2119	336
500	-1850	-5000	-1833	-2733	450
600	-2100	-6100	-2162	-3305	571
700	-2450	-7350	-2567	-3967	700
800	-2750	-8450	-2919	-4598	819
900	-2850	-9550	-3176	-5090	957
1000	-3850	-11050	-3938	-5995	1029
1100	-3900	-12300	-4200	-6600	1200
1200	-3950	-13150	-4386	-7019	1319
1300	-4600	-14150	-4838	-7595	1379
1400	-4750	-15350	-5186	-8219	1519
1500	-5150	-16800	-5652	-8981	1664
1600	-5800	-17350	-6067	-9367	1650
1700	-6150	-19100	-6567	-10267	1850
1800	-6550	-20400	-7005	-10962	1979
1800	-7700	-26950	-8800	-14300	2750
1800	-7700	-26950	-8800	-14300	2750
1700	-7550	-26150	-8576	-13890	2657
1600	-7250	-25100	-8233	-13333	2550
1500	-6950	-23950	-7871	-12729	2429
1400	-6650	-23150	-7576	-12290	2357
1300	-6400	-22100	-7257	-11743	2243
1200	-6150	-21050	-6938	-11195	2129
1100	-5900	-19850	-6590	-10676	1993
1000	-5550	-18350	-6138	-9795	1829
900	-5400	-16950	-5800	-9100	1650
800	-5200	-15750	-5476	-8490	1507
700	-4950	-14550	-5129	-7871	1371
600	-4700	-13000	-4810	-7129	1157
500	-4650	-10250	-4167	-5767	800
400	-4150	-8850	-3662	-5005	671
300	-3550	-7600	-3138	-4295	579
200	-3400	-5850	-2733	-3433	350
100	-3250	-4750	-2452	-2881	214
0	-1350	-3450	-1300	-1900	300
0	50	250	71	129	-29

Table 3C. (Continued).

STRAIN REDUCTION OF A TWO GAGE ROSETTE

E= .40 POISSONS RATIO= .40 GAGE NU,= 2=INSIDE

LOAD	EP1	EP2	SIGMA MAX	SIGMA MIN	TAU MAX
0	0	0	0	0	0
100	-650	-600	-929	-910	-7
200	-1200	-1100	-781	-752	-14
300	-1800	-1650	-1171	-1129	-21
400	-2400	-2200	-1562	-1505	-29
500	-3000	-2800	-1962	-1905	-29
600	-3600	-3350	-2362	-2281	-36
700	-4300	-3950	-2800	-2700	-50
800	-4900	-4550	-3181	-3062	-64
900	-5500	-5050	-3581	-3452	-64
1000	-6100	-5600	-3971	-3829	-71
1100	-6850	-6300	-4462	-4305	-79
1200	-7400	-6800	-4819	-4648	-86
1300	-8100	-7450	-5276	-5090	-93
1400	-8750	-8050	-5700	-5500	-100
1500	-9500	-8700	-6181	-5952	-114
1600	-10300	-9400	-6695	-6438	-129
1700	-11000	-10050	-7152	-6881	-136
1800	-11700	-10650	-7600	-7300	-150
1800	-14800	-13250	-9571	-9129	-221
1800	-14800	-13250	-9571	-9129	-221
1700	-14350	-12800	-9271	-8829	-221
1600	-13750	-12300	-8890	-8476	-207
1500	-13200	-11750	-8529	-8110	-207
1400	-12650	-11250	-8167	-7767	-200
1300	-12000	-10700	-7752	-7381	-186
1200	-11400	-10150	-7362	-7005	-179
1100	-10800	-9550	-6962	-6605	-179
1000	-9950	-8800	-6419	-6086	-164
900	-9200	-8150	-5933	-5633	-150
800	-8550	-7500	-5500	-5200	-150
700	-7850	-6850	-5043	-4757	-143
600	-7100	-6100	-4543	-4257	-143
500	-6200	-5400	-3981	-3752	-114
400	-5400	-4700	-3467	-3267	-100
300	-4600	-3900	-2933	-2733	-100
200	-3600	-3050	-2295	-2138	-79
100	-2700	-2250	-1719	-1586	-64
0	-1600	-1250	-1000	-900	-50
0	-150	-50	-81	-52	-14

TABLE D-1. (CONTINUED).

STRAIN REDUCTION OF A TWO GAGE ROSETTE

E= .90 POISSONS RATIO= .90 GAGE NO.= 3-INSIDE

LOAD	EP1	EP2	SIGMA MAX	SIGMA MIN	TAU MAX
0	0	0	0	0	0
100	-400	-900	-362	-805	71
200	-700	-1650	-648	-919	136
300	-1050	-2450	-967	-1367	200
400	-1300	-3300	-1248	-1819	286
500	-1650	-4200	-1586	-2314	364
600	-1950	-5100	-1900	-2800	450
700	-2300	-6100	-2259	-3343	543
800	-2600	-7000	-2571	-3829	629
900	-2900	-7900	-2886	-4314	714
1000	-3250	-8850	-3233	-4833	800
1100	-3450	-10000	-3643	-5457	907
1200	-3950	-10850	-3948	-5919	986
1300	-4300	-11900	-4314	-6486	1086
1400	-4650	-12850	-4662	-7005	1171
1500	-5050	-14000	-5071	-7629	1279
1600	-5400	-15050	-5438	-8198	1379
1700	-5850	-16200	-5871	-8829	1479
1800	-6200	-17250	-6238	-9395	1579
1900	-7500	-21900	-7743	-11857	2057
1800	-7500	-21900	-7743	-11857	2057
1700	-7250	-21200	-7490	-11476	1993
1600	-6900	-20300	-7152	-10981	1914
1500	-6650	-19450	-6871	-10529	1829
1400	-6400	-18650	-6600	-10100	1750
1300	-6050	-17800	-6271	-9629	1679
1200	-5750	-16950	-5967	-9167	1600
1100	-5400	-16050	-5629	-8671	1521
1000	-5000	-14900	-5219	-8048	1414
900	-4600	-13450	-4848	-7619	1336
800	-4250	-12450	-4490	-6976	1243
700	-3850	-11900	-4100	-6400	1150
600	-3450	-10750	-3690	-5776	1043
500	-3050	-9550	-3271	-5129	929
400	-2600	-8250	-2810	-4424	807
300	-2200	-7050	-2390	-3776	693
200	-1700	-5400	-1838	-2895	529
100	-1250	-3750	-1310	-2024	357
0	-700	-2100	-733	-1133	200
0	-200	550	10	224	-107

Table 3C. (Continued).

STRAIN REDUCTION OF A TWO GAGE ROSETTE

E= ,*0 POISSONS RATIO= ,*0 GAGE NO,= *=INSIDE

LOAD	EP1	EP2	SIGMA MAX	SIGMA MIN	TAU MAX
0	0	0	0	0	0
100	*600	*600	*900	*900	0
200	*1200	*1100	*781	*758	*19
300	*1800	*1700	*1181	*1152	*14
400	*2550	*2200	*1633	*1533	*50
500	*3050	*2800	*1986	*1914	*36
600	*3650	*3400	*2386	*2314	*36
700	*4350	*4000	*2833	*2733	*50
800	*4950	*4550	*3224	*3110	*57
900	*5550	*5150	*3629	*3510	*57
1000	*6200	*5750	*4048	*3919	*64
1100	*6900	*6450	*4514	*4386	*64
1200	*7500	*7000	*4905	*4762	*71
1300	*8200	*7650	*5362	*5205	*79
1400	*8850	*8300	*5796	*5638	*79
1500	*9550	*8950	*6252	*6081	*86
1600	*10350	*9700	*6776	*6590	*93
1700	*11150	*10400	*7290	*7076	*107
1800	*11850	*11100	*7757	*7543	*107
1800	*15050	*13850	*9805	*9462	*171
1800	*15050	*13860	*9805	*9462	*171
1700	*14550	*13360	*9471	*9129	*171
1600	*13950	*12800	*9081	*8752	*164
1500	*13350	*12250	*8690	*8376	*157
1400	*12850	*11750	*8357	*8043	*157
1300	*12250	*11150	*7957	*7643	*157
1200	*11600	*10600	*7543	*7257	*143
1100	*10950	*10000	*7119	*6848	*136
1000	*10050	*9200	*6538	*6295	*121
900	*9350	*8500	*6071	*5829	*121
800	*8650	*7860	*5614	*5386	*114
700	*7900	*7150	*5124	*4910	*107
600	*7050	*6350	*4567	*4367	*100
500	*6250	*5550	*4033	*3833	*100
400	*5450	*4800	*3510	*3324	*93
300	*4600	*4050	*2962	*2805	*79
200	*3600	*3100	*2305	*2162	*71
100	*2650	*2200	*1681	*1552	*64
0	*1500	*1150	*933	*838	*50
0	0	150	29	71	*21

STRAIN REDUCTION OF A TWO GAGE ROSETTE

E= 10.00 POISSONS RATIO= .30 GAGE NO.= 6-INSIDE

LOAD	EP1	EP2	SIGMA MAX	SIGMA MIN	TAU MAX
0	0	0	0	0	0
100	-50	-50	-714	-714	0
200	-60	-100	-879	-1484	192
300	-100	-150	-1593	-1978	192
400	-200	-250	-3022	-3407	192
500	-250	-300	-3736	-4121	192
600	-300	-400	-4615	-5385	385
700	-350	-450	-5330	-6099	385
800	-400	-550	-6209	-7363	577
900	-500	-600	-7473	-8242	385
1000	-550	-700	-8352	-9505	577
1100	-600	-800	-9231	-10769	769
1200	-650	-850	-9945	-11484	769
1300	-700	-900	-10659	-12198	769
1400	-750	-950	-11374	-12912	769
1500	-800	-1050	-12253	-14176	962
1600	-850	-1100	-12967	-14890	962
1700	-900	-1150	-13681	-15604	962
1800	-950	-1250	-14560	-16868	1154
1800	-950	-1250	-14560	-16868	1154
1800	-950	-1250	-14560	-16868	1154
1700	-900	-1200	-13846	-16154	1154
1600	-850	-1100	-12967	-14890	962
1500	-800	-1050	-12253	-14176	962
1400	-750	-1000	-11538	-13462	962
1300	-700	-900	-10659	-12198	769
1200	-650	-800	-9780	-10934	577
1100	-550	-750	-8516	-10055	769
1000	-500	-650	-7637	-8791	577
900	-450	-600	-6923	-8077	577
800	-400	-500	-6044	-6813	385
700	-350	-450	-5330	-6099	385
600	-250	-400	-4066	-5220	577
500	-200	-300	-3187	-3956	385
400	-150	-200	-2308	-2692	192
300	-100	-150	-1593	-1978	192
200	0	-50	-165	-549	192
100	50	0	549	165	192
0	50	0	549	165	192
0	0	-100	-330	-1099	385

Table 3C. (Continued).

STRAIN REDUCTION OF A TWO GAGE ROSETTE

E= 10.00 POISSONS RATIO= .30 GAGE NO.= 6=INSIDE

LOAD	EP1	EP2	SIGMA MAX	SIGMA MIN	TAU MAX
0	0	0	0	0	0
100	-50	-100	-879	-1264	192
200	-150	-150	-2193	-2193	0
300	-150	-250	-2973	-3242	385
400	-200	-350	-3352	-4505	577
500	-300	-500	-4945	-6484	769
600	-350	-550	-5659	-7198	769
700	-400	-700	-6703	-9011	1154
800	-450	-750	-7418	-9725	1154
900	-550	-860	-8846	-11154	1154
1000	-600	-950	-9725	-12418	1346
1100	-700	-1050	-11154	-13846	1346
1200	-750	-1100	-11868	-14560	1346
1300	-750	-1150	-12033	-15110	1538
1400	-800	-1250	-12912	-16374	1731
1500	-900	-1350	-14341	-17802	1731
1600	-950	-1400	-15055	-18516	1731
1700	-1000	-1500	-15934	-19780	1923
1800	-1050	-1600	-16813	-21044	2115
1800	-1050	-1400	-16154	-18846	1346
1800	-1050	-1400	-16154	-18846	1346
1700	-1000	-1300	-15276	-17582	1154
1600	-950	-1200	-14396	-16319	962
1500	-850	-1100	-12967	-14890	962
1400	-800	-950	-11923	-13077	577
1300	-750	-850	-11044	-11813	385
1200	-650	-750	-9615	-10385	385
1100	-600	-650	-8736	-9121	192
1000	-550	-550	-7857	-7857	0
900	-450	-450	-6429	-6429	0
800	-400	-350	-5549	-5165	-192
700	-350	-250	-4670	-3901	-385
600	-300	-150	-3791	-2637	-577
500	-200	0	-2198	-659	-769
400	-150	100	-1319	604	-962
300	-50	200	110	2033	-962
200	0	300	989	3297	-1154
100	50	400	1868	4560	-1346
0	50	300	1538	3462	-962
0	-50	2350	7198	25659	-9231

Table 3C. (Continued).

STRAIN REDUCTION OF A TWO GAGE ROSETTE

E= 10,00 POISSONS RATIO= ,30 GAGE NO,= 7=INSIDE

LOAD	EP1	EP2	SIGMA MAX	SIGMA MIN	TAU MAX
0	0	0	0	0	0
100	-50	-50	-714	-714	0
200	-100	-100	-1429	-1429	0
300	-200	-150	-2692	-2308	-192
400	-250	-200	-3407	-3022	-192
500	-350	-250	-4670	-3901	-385
600	-400	-300	-5385	-4615	-385
700	-500	-350	-6648	-5495	-577
800	-550	-400	-7363	-6209	-577
900	-600	-400	-7912	-6374	-769
1000	-700	-450	-9176	-7253	-962
1100	-800	-550	-10604	-8681	-962
1200	-850	-600	-11319	-9396	-962
1300	-900	-650	-12033	-10110	-962
1400	-950	-700	-12747	-10824	-962
1500	-1000	-750	-13462	-11538	-962
1600	-1050	-850	-14341	-12802	-769
1700	-1150	-850	-15440	-13132	-1154
1800	-1200	-900	-16154	-13846	-1154
1800	-1250	-950	-16868	-14560	-1154
1800	-1250	-950	-16868	-14560	-1154
1700	-1150	-850	-15440	-13132	-1154
1600	-1050	-750	-14011	-11703	-1154
1500	-1000	-700	-13297	-10989	-1154
1400	-950	-600	-12418	-9725	-1346
1300	-850	-550	-11154	-8846	-1154
1200	-800	-500	-10440	-8132	-1154
1100	-650	-400	-8462	-6538	-962
1000	-600	-350	-7747	-6824	-962
900	-550	-300	-7033	-6110	-962
800	-450	-250	-5769	-4231	-769
700	-400	-200	-5055	-3516	-769
600	-250	-150	-3242	-2473	-385
500	-200	-100	-2527	-1758	-385
400	-150	-50	-1813	-1044	-385
300	-100	0	-1099	-330	-385
200	0	50	165	549	-192
100	50	50	714	714	0
0	50	100	879	1264	-192
0	0	50	165	549	-192

Table 3C. Continued).

STRAIN REDUCTION OF A TWO GAGE ROSETTE

E= 10,00 POISSONS RATIO= ,30 GAGE NO,= 8=INSIDE

LOAD	EP1	EP2	SIGMA MAX	SIGMA MIN	TAU MAX
0	0	0	0	0	0
100	-50	50	-385	385	-385
200	-150	100	-1319	604	-962
300	-250	150	-2253	824	-1538
400	-300	150	-2802	659	-1731
500	-400	200	-3736	879	-2308
600	-500	250	-4670	1099	-2885
700	-600	250	-5769	769	-3269
800	-650	300	-6159	1154	-3654
900	-750	350	-7088	1374	-4231
1000	-850	350	-8187	1044	-4615
1100	-950	350	-9286	714	-5000
1200	-1050	350	-10385	385	-5385
1300	-1100	100	-11758	-2527	-4615
1400	-1150	100	-12308	-2692	-4808
1500	-1250	0	-13736	-4121	-4808
1600	-1300	-50	-14951	-4835	-4808
1700	-1350	-50	-15000	-5000	-5000
1800	-1450	-50	-16099	-5330	-5385
1800	-1450	-150	-16429	-6429	-5000
1800	-1450	-150	-16429	-6429	-5000
1700	-1400	100	-15055	-3516	-5769
1600	-1350	200	-14176	-2253	-5962
1500	-1250	200	-14077	-1923	-5577
1400	-1200	200	-12527	-1758	-5385
1300	-1050	250	-10714	-714	-5000
1200	-950	250	-9615	-385	-4615
1100	-800	300	-7802	659	-4231
1000	-700	350	-6538	1538	-4038
900	-600	400	-5275	2418	-3846
800	-550	400	-4725	2582	-3654
700	-500	450	-4011	3297	-3654
600	-450	450	-3462	3462	-3462
500	-350	450	-2363	3791	-3077
400	-300	450	-1813	3956	-2885
300	-200	400	-879	3736	-2308
200	-100	400	220	4066	-1923
100	-50	350	604	3681	-1538
0	-100	400	220	4066	-1923
0	0	400	1319	4396	-1538

STRAIN REDUCTION OF A TWO GAGE ROSETTE

E= 10,00 POISSONS RATIO= ,30 GAGE NO,= 9=INSIDE

LOAD	EP1	EP2	SIGMA MAX	SIGMA MIN	TAU MAX
0	0	0	0	0	0
100	-50	-50	-714	-714	0
200	-100	-100	-1429	-1429	0
300	-100	-200	-1758	-2527	385
400	-150	-300	-2637	-3791	577
500	-200	-400	-3516	-5055	769
600	-250	-500	-4396	-6319	962
700	-300	-600	-5275	-7582	1154
800	-350	-700	-6154	-8846	1346
900	-400	-800	-7033	-10110	1538
1000	-450	-900	-7912	-11374	1731
1100	-500	-950	-8626	-12088	1731
1200	-550	-1050	-9505	-13352	1923
1300	-600	-1150	-10385	-14615	2115
1400	-650	-1300	-11429	-16429	2500
1500	-700	-1350	-12143	-17143	2500
1600	-750	-1450	-13022	-18407	2692
1700	-750	-1550	-13352	-19505	3077
1800	-800	-1650	-14231	-20769	3269
1800	-800	-1500	-13736	-19121	2692
1800	-800	-1500	-13736	-19121	2692
1700	-750	-1450	-13022	-18407	2692
1600	-750	-1300	-12527	-16758	2115
1500	-700	-1200	-11648	-15495	1923
1400	-650	-1100	-10769	-14231	1731
1300	-600	-1050	-10055	-13516	1731
1200	-550	-1000	-9341	-12802	1731
1100	-500	-850	-8297	-10989	1346
1000	-450	-800	-7582	-10275	1346
900	-400	-650	-6538	-8462	962
800	-350	-600	-5824	-7747	962
700	-350	-500	-5495	-6648	577
600	-250	-400	-4066	-6220	577
500	-200	-350	-3352	-4505	577
400	-150	-200	-2308	-2692	192
300	-150	-150	-2143	-2143	0
200	-100	-100	-1429	-1429	0
100	-50	0	-549	-165	-192
0	-50	0	-549	-165	-192
0	-150	0	-1648	-495	-577

Table 3C. (Continued).

STRAIN REDUCTION OF A TWO GAGE ROSETTE

E= 10.00 POISSONS RATIO= .30 GAGE NO.= 10=INSIDE

LOAD	EP1	EP2	SIGMA MAX	SIGMA MIN	TAU MAX
0	0	0	0	0	0
100	-50	-50	-714	-714	0
200	-100	-100	-1429	-1429	0
300	-150	-150	-2143	-2143	0
400	-200	-200	-2857	-2857	0
500	-250	-250	-3571	-3571	0
600	-300	-300	-4286	-4286	0
700	-350	-350	-5000	-5000	0
800	-450	-400	-6264	-5879	-192
900	-500	-450	-6978	-6593	-192
1000	-550	-550	-7857	-7857	0
1100	-650	-600	-9121	-8736	-192
1200	-650	-650	-9286	-9286	0
1300	-700	-700	-10000	-10000	0
1400	-750	-750	-10714	-10714	0
1500	-800	-800	-11429	-11429	0
1600	-850	-850	-12143	-12143	0
1700	-900	-950	-13022	-13407	192
1800	-950	-1000	-13736	-14121	192
1800	-900	-900	-12857	-12857	0
1800	-900	-900	-12857	-12857	0
1700	-850	-800	-11978	-11593	-192
1600	-800	-750	-11264	-10879	-192
1500	-750	-700	-10549	-10165	-192
1400	-700	-650	-9835	-9451	-192
1300	-650	-600	-9121	-8736	-192
1200	-600	-550	-8407	-8022	-192
1100	-550	-500	-7692	-7308	-192
1000	-500	-450	-6978	-6593	-192
900	-460	-350	-6099	-5330	-385
800	-400	-300	-5385	-4615	-385
700	-350	-250	-4670	-3901	-385
600	-250	-200	-3407	-3022	-192
500	-250	-150	-3242	-2473	-385
400	-150	-100	-1978	-1593	-192
300	-100	-50	-1264	-879	-192
200	-100	0	-1099	-330	-385
100	-50	50	-385	385	-385
0	0	0	0	0	0
0	0	-150	-495	-1648	577

Table 3C. (Continued).

STRAIN REDUCTION OF A TWO GAGE ROSETTE

E= 10.00 POISSONS RATIO= .30 GAGE NO.= 11=INSIDE

LOAD	EP1	EP2	SIGMA MAX	SIGMA MIN	TAU MAX
0	0	0	0	0	0
100	-50	0	-549	-165	-192
200	-50	-50	-714	-714	0
300	-100	-100	-1429	-1429	0
400	-200	-150	-2698	-2308	-192
500	-250	-200	-3407	-3022	-192
600	-300	-250	-4121	-3736	-192
700	-350	-300	-4835	-4451	-192
800	-400	-400	-5714	-5714	0
900	-450	-450	-6429	-6429	0
1000	-550	-500	-7698	-7308	-192
1100	-650	-550	-8956	-8187	-385
1200	-650	-600	-9121	-8736	-192
1300	-700	-650	-9835	-9451	-192
1400	-750	-700	-10549	-10165	-192
1500	-750	-800	-10879	-11264	192
1600	-850	-850	-12143	-12143	0
1700	-850	-900	-12308	-12692	192
1800	-900	-950	-13022	-13407	192
1800	-900	-900	-12857	-12857	0
1800	-900	-900	-12857	-12857	0
1700	-800	-850	-11593	-11978	192
1600	-750	-800	-10879	-11264	192
1500	-700	-750	-10165	-10549	192
1400	-650	-700	-9451	-9835	192
1300	-600	-650	-8736	-9121	192
1200	-550	-600	-8022	-8407	192
1100	-500	-550	-7308	-7692	192
1000	-450	-450	-6429	-6429	0
900	-350	-400	-5165	-5549	192
800	-300	-350	-4451	-4835	192
700	-250	-300	-3736	-4121	192
600	-200	-250	-3022	-3407	192
500	-150	-150	-2143	-2143	0
400	-100	-100	-1429	-1429	0
300	-50	-50	-714	-714	0
200	0	0	0	0	0
100	50	50	714	714	0
0	50	50	714	714	0
0	50	0	549	165	192

Table 3C. (Continued).

STRAIN REDUCTION OF A TWO GAGE ROSETTE

E= 10,00 POISSONS RATIO= ,30 GAGE NO,= 12=INSIDE

LOAD	EP1	EP2	SIGMA MAX	SIGMA MIN	TAU MAX
0	0	0	0	0	0
100	-50	-50	-714	-714	0
200	-100	-50	-1264	-879	-192
300	-150	-100	-1978	-1593	-192
400	-250	-150	-3242	-2473	-385
500	-300	-200	-3956	-3187	-385
600	-350	-250	-4670	-3901	-385
700	-400	-350	-5549	-5165	-192
800	-450	-400	-6264	-5879	-192
900	-500	-450	-6978	-6593	-192
1000	-600	-500	-8242	-7473	-385
1100	-700	-600	-9670	-8901	-385
1200	-700	-650	-9835	-9951	-192
1300	-750	-700	-10549	-10165	-192
1400	-800	-750	-11264	-10379	-192
1500	-850	-850	-12143	-12143	0
1600	-900	-900	-12857	-12857	0
1700	-950	-950	-13571	-13571	0
1800	-1000	-1000	-14286	-14286	0
1800	-1000	-950	-14121	-13736	-192
1800	-1000	-950	-14121	-13736	-192
1700	-950	-900	-13407	-13022	-192
1600	-850	-850	-12143	-12143	0
1500	-800	-800	-11429	-11429	0
1400	-750	-750	-10714	-10714	0
1300	-700	-650	-9835	-9951	-192
1200	-650	-600	-9121	-8736	-192
1100	-600	-550	-8407	-8022	-192
1000	-550	-500	-7692	-7308	-192
900	-500	-450	-6978	-6593	-192
800	-450	-400	-6264	-5879	-192
700	-400	-300	-5385	-4615	-385
600	-300	-250	-4121	-3736	-192
500	-250	-200	-3407	-3022	-192
400	-150	-150	-2143	-2143	0
300	-100	-100	-1429	-1429	0
200	-50	0	-549	-165	-192
100	0	0	0	0	0
0	0	50	165	549	-192
0	50	50	714	714	0

Table 3C. (Continued).

STRAIN REDUCTION OF A TWO GAGE ROSETTE

E= 10,00 POISSONS RATIO= ,30 GAGE NO,= 13=INSIDE

LOAD	EP1	EP2	SIGMA MAX	SIGMA MIN	TAU MAX
0	0	0	0	0	0
100	-50	-50	-714	-714	0
200	-50	-50	-714	-714	0
300	-100	-100	-1429	-1429	0
400	-150	-150	-2143	-2143	0
500	-250	-250	-3571	-3571	0
600	-350	-300	-4836	-4951	192
700	-350	-400	-5165	-5549	192
800	-400	-450	-5879	-6264	192
900	-450	-500	-6593	-6978	192
1000	-550	-600	-8022	-8407	192
1100	-600	-700	-8901	-9670	385
1200	-650	-750	-9615	-10385	385
1300	-700	-800	-10330	-11099	385
1400	-750	-900	-11209	-12363	577
1500	-800	-950	-11923	-13077	577
1600	-900	-1000	-13187	-13956	385
1700	-950	-1050	-13901	-14670	385
1800	-1000	-1150	-14780	-15934	577
1800	-850	-1050	-12802	-14341	769
1800	-850	-1050	-12802	-14341	769
1700	-800	-1000	-12088	-13626	769
1600	-750	-900	-11209	-12363	577
1500	-700	-800	-10330	-11099	385
1400	-600	-750	-9066	-10220	577
1300	-550	-700	-8352	-9505	577
1200	-500	-650	-7637	-8791	577
1100	-400	-600	-6374	-7912	769
1000	-350	-500	-5495	-6648	577
900	-300	-450	-4780	-5934	577
800	-250	-350	-3901	-4670	385
700	-200	-300	-3187	-3956	385
600	-150	-250	-2473	-3242	385
500	-50	-150	-1044	-1813	385
400	0	-100	-330	-1099	385
300	50	-50	385	-385	385
200	100	0	1099	330	385
100	200	50	2363	1209	577
0	200	100	2527	1758	385
0	1450	1350	20385	19615	385

Table 3C. (Continued).

STRAIN REDUCTION OF A TWO GAGE ROSETTE

E= 10,00 POISSONS RATIO= ,30 GAGE NO,= 14=INSIDE

LOAD	EP1	EP2	SIGMA MAX	SIGMA MIN	TAU MAX
0	0	0	0	0	0
100	-50	0	-549	-165	-192
200	-100	0	-1099	-330	-385
300	-150	-50	-1813	-1044	-385
400	-200	-100	-2527	-1758	-385
500	-250	-150	-3242	-2473	-385
600	-350	-250	-4670	-3901	-385
700	-450	-300	-5934	-4780	-577
800	-500	-400	-6813	-6044	-385
900	-550	-450	-7527	-6758	-385
1000	-650	-500	-8791	-7637	-577
1100	-750	-600	-10220	-9066	-577
1200	-800	-650	-10934	-9780	-577
1300	-890	-700	-11648	-10495	-577
1400	-900	-800	-12527	-11758	-385
1500	-950	-900	-13407	-13022	-192
1600	-1000	-950	-14121	-13736	-192
1700	-1050	-1000	-14835	-14451	-192
1800	-1150	-1100	-16264	-15879	-192
1800	-1050	-1000	-14835	-14451	-192
1800	-1050	-1100	-15165	-15549	192
1700	-1000	-1050	-14451	-14835	192
1600	-900	-950	-13022	-13407	192
1500	-850	-850	-12149	-12149	0
1400	-800	-800	-11429	-11429	0
1300	-700	-750	-10165	-10549	192
1200	-650	-650	-9286	-9286	0
1100	-600	-600	-8571	-8571	0
1000	-550	-550	-7857	-7857	0
900	-450	-450	-6429	-6429	0
800	-400	-400	-5714	-5714	0
700	-350	-300	-4835	-4451	-192
600	-250	-250	-3571	-3571	0
500	-200	-190	-2692	-2308	-192
400	-150	-100	-1978	-1593	-192
300	-50	-50	-714	-714	0
200	0	0	0	0	0
100	50	50	714	714	0
0	50	50	714	714	0
0	1350	1250	18956	18187	385

APPENDIX D

DATA FROM FINITE ELEMENT STRESS ANALYSIS OF 66-INCH OD X 58-INCH ID MODEL 2000 NEMO HULL ASSEMBLY

APPENDIX D. DATA FROM FINITE ELEMENT STRESS ANALYSIS OF 66-INCH OD X 58-INCH ID MODEL 2000 NEMO HULL ASSEMBLY

Although the results of the finite element stress analysis for 66-inch OD X 58-inch ID Model 2000 Nemo Hull under 900 psi hydrostatic loading have been summarized in the text of the report (Figures 4 to 8) it was considered desirable to publish this data for the benefit of other plastic hull investigators. The data details the predicted stress and strains for both the top hatch (Figures 1D) and bottom penetration plate (Figure 2D). To correlate the stresses and strains shown on Figures 1D and 2D with physical locations on the Model 2000 Nemo Hull one has only to locate the corresponding node numbers on finite element meshes for top hatch (Figure 5) and bottom penetration plate (Figure 6).

Since the finite element stress analysis was based on the assumption that the stress-strain relationship of acrylic plastic is linear under short term loading in the 0–10,000 psi stress range, the calculated values for 900 psi hydrostatic loading (Figure 1D and 2D) can be extrapolated with reasonable confidence to 1350 psi hydrostatic loading representing the 3000 foot operational depth of the Model 2000 Nemo Hull. For hydrostatic loadings in excess of 1500 psi the extrapolation of values calculated for 900 psi is not recommended as the stress-strain relationship for acrylic plastic becomes non-linear at the stress values encountered in this loading range.

NODAL COORDINATES

UPPER HATCH NEMO 2000

NODE	R	Z	Longitudinal Strain	Longitudinal Stress	Hoop Stress	Hoop Strain
1	20.5061	20.5061	-5.9876E-03	-3474.627	-3508.1689	-5.88876E-03
2	21.2132	21.2132	-6.2279E-03	-3771.071	-3420.7828	-5.53927E-03
3	21.9203	21.9203	-6.4793E-03	-4114.766	-3440.6879	-5.23011E-03
4	22.6274	22.6274	-7.0177E-03	-4238.333	-3462.9044	-4.94818E-03
5	23.3345	23.3345	-7.2358E-03	-4337.637	-3417.2559	-4.69806E-03
6	19.7780	21.2094	-5.7767E-03	-3523.897	-3470.0490	-5.87311E-03
7	20.4600	21.9906	-6.2462E-03	-3773.153	-3404.9458	-5.49853E-03
8	21.1419	22.6720	-6.4653E-03	-4013.519	-3411.7487	-5.15843E-03
9	21.8239	23.3533	-7.0681E-03	-4246.639	-3427.5842	-4.85680E-03
10	22.5059	24.1347	-7.4818E-03	-4429.069	-3392.0766	-4.57652E-03
11	19.0252	21.8866	-6.1935E-03	-3738.698	-3505.5841	-5.82443E-03
12	19.6818	22.6413	-6.3758E-03	-3812.255	-3383.0278	-5.40935E-03
13	20.3378	23.3960	-6.7456E-03	-4040.638	-3375.1728	-5.04529E-03
14	20.9939	24.1507	-7.1939E-03	-4252.325	-3372.6919	-4.71227E-03
15	21.6499	24.9055	-7.3521E-03	-4341.998	-3299.3659	-4.41075E-03
16	18.2503	22.5372	-6.1128E-03	-3701.828	-3450.8131	-5.72414E-03
17	18.8796	23.3149	-6.5307E-03	-3863.799	-3344.1192	-5.27717E-03
18	19.5089	24.0915	-6.8962E-03	-4070.431	-3317.5995	-4.87794E-03
19	20.1383	24.8682	-7.2982E-03	-4273.547	-3301.9317	-4.52102E-03
20	20.7676	25.6458	-7.6219E-03	-4429.152	-3235.4173	-4.18648E-03
21	17.4526	23.1604	-6.6142E-03	-3911.609	-3460.3127	-5.57817E-03
22	18.0595	23.9591	-6.7894E-03	-3998.935	-3293.8848	-5.08613E-03
23	18.6663	24.7577	-7.0700E-03	-4111.610	-3242.9213	-4.65891E-03
24	19.2581	25.5563	-7.3334E-03	-4249.159	-3200.5057	-4.27928E-03
25	19.8599	26.3550	-7.4986E-03	-4323.724	-3092.7178	-3.91029E-03
26	16.6337	23.7549	-6.8602E-03	-3974.415	-3391.8324	-5.36602E-03
27	17.2073	24.5796	-7.1004E-03	-4094.894	-3223.1976	-4.83779E-03
28	17.7809	25.3937	-7.2830E-03	-4154.490	-3144.6667	-4.37725E-03
29	18.3544	26.2129	-7.4663E-03	-4227.325	-3080.9465	-3.96283E-03
30	18.9280	27.0320	-7.6881E-03	-4356.546	-2966.5721	-3.57166E-03
31	15.7995	24.3219	-7.4851E-03	-4227.141	-3363.8781	-5.08764E-03
32	16.3392	25.1601	-7.5943E-03	-4191.180	-3139.2086	-4.51636E-03
33	16.8838	25.9988	-7.5734E-03	-4227.376	-3025.5010	-4.02865E-03
34	17.4284	26.8375	-7.5686E-03	-4258.609	-2926.0287	-3.59016E-03
35	17.9731	27.6761	-7.6226E-03	-4251.412	-2773.3637	-3.17269E-03
36	15.9361	24.8529	-8.0377E-03	-4403.599	-3259.8574	-4.71970E-03
37	15.4511	25.7150	-7.9882E-03	-4318.816	-3012.2989	-4.11453E-03
38	15.9662	26.5722	-7.8850E-03	-4290.561	-2871.5295	-3.60496E-03
39	16.4812	27.4294	-7.7323E-03	-4249.920	-2740.1880	-3.14716E-03
40	16.9963	28.2865	-7.6503E-03	-4189.999	-2569.7764	-2.70965E-03
41	14.5000	25.1147	-8.4781E-03	-4577.978	-3234.0671	-4.49926E-03
42	15.0000	25.9808	-8.4287E-03	-4481.399	-2970.3833	-3.87785E-03
43	15.5000	26.8468	-8.1473E-03	-4366.960	-2796.4451	-3.35750E-03
44	16.0000	27.7128	-7.8018E-03	-4239.827	-2641.1248	-2.89982E-03
45	16.5000	28.5788	-7.6796E-03	-4153.290	-2454.1230	-2.45324E-03
46	14.0595	25.3640	-9.0098E-03	-4772.311	-3187.7027	-4.24987E-03
47	14.5993	26.2386	-8.7575E-03	-4583.480	-2892.5861	-3.61115E-03
48	15.0291	27.1132	-8.4082E-03	-4437.898	-2711.0947	-3.09058E-03
49	15.5139	27.9878	-7.9154E-03	-4244.114	-2537.2415	-2.62849E-03
50	15.9987	28.8625	-7.4843E-03	-4026.184	-2313.5971	-2.18631E-03
51	13.4197	25.6055	-9.3679E-03	-4894.012	-3118.0388	-3.96641E-03
52	13.8891	26.4844	-9.2991E-03	-4758.817	-2830.5456	-3.31646E-03
53	14.5536	27.3714	-8.6629E-03	-4508.434	-2615.2823	-2.79114E-03
54	15.0231	28.2543	-7.9767E-03	-4226.631	-2417.0431	-2.34386E-03

UPPER HATCH
NODES 1-54

Figure 1D. Predicted stress and strains for the top hatch.

Node	R	Z	LONGITUDINAL STRAIN	LONGITUDINAL STRESS	HOOP STRESS	HOOP STRAIN
95	15.9926	29.1373	-7.6994E-03	-4049.644	-2204.3193	-1.89930E-03
96	13.1657	25.8392	-1.0066E-02	-5157.696	-3066.2076	-3.64699E-03
97	13.6197	26.7302	-9.6261E-03	-4841.319	-2736.9161	-2.98171E-03
98	14.0737	27.6212	-9.0116E-03	-4636.569	-2525.6225	-2.47114E-03
99	14.5277	28.5122	-8.0743E-03	-4229.887	-2300.5618	-2.03004E-03
60	14.9817	29.4032	-7.1869E-03	-3797.984	-2017.1828	-1.61076E-03
61	12.7128	24.0650	-1.0964E-02	-5293.186	-2971.6538	-3.28238E-03
62	13.1511	24.9438	-1.0294E-02	-5139.059	-2680.1239	-2.61093E-03
63	13.5895	25.8626	-9.2604E-03	-4702.989	-2431.3093	-2.10831E-03
64	14.0279	28.7619	-8.1151E-03	-4211.351	-2177.7783	-1.71039E-03
65	14.4662	29.6602	-7.5452E-03	-3911.747	-1929.2457	-1.30196E-03
66	12.2559	24.2829	-1.1621E-02	-5796.839	-2947.3187	-2.86572E-03
67	12.6785	25.1442	-1.0722E-02	-5311.072	-2599.5985	-2.18107E-03
68	13.1012	28.0955	-9.9644E-03	-4823.934	-2385.1660	-1.73158E-03
69	13.5238	29.0018	-8.1114E-03	-4195.047	-2060.5552	-1.35982E-03
70	13.9464	29.9082	-6.8286E-03	-3569.629	-1725.8002	-1.00250E-03
71	11.8337	24.9757	-1.2628E-02	-6116.993	-2877.4438	-2.42162E-03
72	12.0378	26.9322	-1.2144E-02	-5873.993	-2675.6839	-2.04019E-03
73	12.2418	27.8887	-1.1229E-02	-5430.769	-2659.3011	-1.75483E-03
74	12.4458	27.8451	-1.0332E-02	-5186.963	-2425.6255	-1.54480E-03
75	12.6498	28.3016	-9.4204E-03	-4874.155	-2345.3813	-1.36016E-03
76	12.8539	28.7581	-8.7845E-03	-4492.508	-2106.8106	-1.19239E-03
77	13.0579	29.2146	-7.9894E-03	-4196.625	-2005.1022	-1.04022E-03
78	13.2619	29.6710	-7.2611E-03	-3787.640	-1769.5195	-8.84263E-04
79	13.4660	30.1275	-6.6252E-03	-3488.422	-1627.6608	-7.35561E-04
80	11.4085	24.6617	-1.5270E-02	-7267.283	-3067.3956	-1.86414E-03
81	11.6052	27.1219	-1.2966E-02	-6424.979	-2847.7177	-1.47647E-03
82	11.8019	27.5811	-1.1070E-02	-5419.018	-2563.9970	-1.30016E-03
83	11.9986	28.0408	-1.0064E-02	-5209.293	-2414.2018	-1.11040E-03
84	12.1953	28.5004	-9.1491E-03	-4801.126	-2240.6718	-9.86493E-04
85	12.3920	28.9601	-8.9155E-03	-4652.619	-2071.4554	-8.36370E-04
86	12.5887	29.4198	-7.7716E-03	-4120.972	-1897.4569	-7.26895E-04
87	12.7854	29.8795	-7.0996E-03	-3784.990	-1720.7316	-5.88949E-04
88	12.9821	30.3392	-6.9872E-03	-3650.933	-1545.5401	-4.86175E-04
89	10.8861	24.6093	1.3319E-04	-2511.124	-11703.3153	-1.08919E-03
90	10.9808	26.8907	-5.0654E-03	-5555.699	-8859.9858	-1.03869E-03
91	11.1701	27.3034	-6.4923E-03	-6382.016	-6888.6165	-9.23464E-04
92	11.3595	27.7662	-5.6866E-03	-5559.935	-5979.6645	-8.05639E-04
93	11.5488	28.2290	-4.9991E-03	-5187.220	-5366.5999	-7.00035E-04
94	11.7381	28.6918	-4.6007E-03	-4723.239	-4768.5030	-5.98509E-04
95	11.9274	29.1545	-4.1327E-03	-4418.068	-4298.7406	-5.05053E-04
96	12.1168	29.6173	-3.8807E-03	-4025.544	-3748.6515	-4.14169E-04
97	12.3061	30.0801	-3.5067E-03	-3654.709	-3289.7120	-3.24933E-04
98	12.4954	30.5428	-2.3223E-03	-2548.735	-2762.7734	-2.32185E-04
99	12.6847	31.0056	1.2085E-04	578.281	-869.0213	-7.16596E-05
100	10.3766	24.5925	6.7541E-05	-3701.262	-12886.3614	-1.15397E-03
101	10.5502	27.0167	-1.3400E-04	-5018.653	-11782.8561	-1.03538E-03
102	10.7219	27.4826	-2.3218E-04	-5498.123	-10594.6768	-9.09697E-04
103	10.8936	27.9484	-2.5469E-04	-5335.120	-9373.6264	-7.91488E-04
104	11.0654	28.4142	-2.4806E-04	-4988.739	-8242.5875	-6.80573E-04
105	11.2371	28.8800	-2.2868E-04	-4540.262	-7195.7768	-5.78924E-04
106	11.4088	29.3458	-2.1227E-04	-4214.484	-6239.9361	-4.81477E-04
107	11.5805	29.8116	-1.9069E-04	-3727.979	-5215.7389	-3.88320E-04
108	11.8123	30.2774	-1.2978E-04	-2934.105	-4186.1647	-2.96107E-04
109	11.9940	30.7432	-6.9422E-05	-1788.589	-2839.3518	-2.03982E-04
110	12.2302	31.3987	7.1810E-05	76.116	-1111.2789	-8.61692E-05
111	9.0878	26.4231	1.0332E-04	-3998.291	-13949.7961	-1.21986E-03
112	10.1191	27.2325	-2.2715E-05	-4580.733	-11724.3149	-1.02243E-03
113	10.2882	27.7012	-2.3800E-04	-5806.569	-10694.9814	-8.87791E-04
114	10.4623	28.1699	-2.3334E-04	-5292.473	-9293.8147	-7.64605E-04
115	10.6364	28.6386	-2.2582E-04	-4894.662	-8109.7783	-6.53311E-04
116	10.8105	29.1073	-2.1537E-04	-4620.899	-6919.4907	-5.47545E-04

UPPER HATCH
NODES 55-116

Figure 1D. (Continued).

NODE	R	Z	LONGITUDINAL STRAIN	LONGITUDINAL STRESS	HOOP STRESS	HOOP STRAIN
117	10.9895	29.5760	-2.0223E-04	-4015.157	-5858.4428	-4.48591E-04
118	11.1586	30.0998	-1.6810E-04	-3339.626	-4723.0310	-3.51961E-04
119	11.3327	30.5135	-1.3327E-04	-2686.093	-3631.0662	-2.58782E-04
120	11.5068	30.9822	-5.4326E-05	-1075.945	-2314.8754	-1.65752E-04
121	11.6635	31.4049	8.4780E-05	203.479	-1070.1167	-8.46414E-05
122	9.8692	27.3290	-1.9822E-04	-6470.883	-12692.1512	-1.02499E-03
123	9.6672	27.3993	-3.7863E-04	-8319.721	-13155.3484	-1.02087E-03
124	9.8336	27.8658	-2.4965E-04	-6201.142	-10929.8497	-8.78126E-04
125	10.0000	28.3373	-2.0759E-04	-5277.629	-9382.9120	-7.53353E-04
126	10.1664	28.8088	-2.0725E-04	-4804.601	-8035.2280	-6.36105E-04
127	10.3328	29.2803	-1.9426E-04	-4259.807	-6772.3109	-5.28311E-04
128	10.4992	29.7518	-1.7752E-04	-3729.830	-5587.0043	-4.24479E-04
129	10.6655	30.2233	-1.4743E-04	-3048.723	-4396.0653	-3.26533E-04
130	10.8319	30.6948	-9.7525E-05	-2224.533	-3220.4543	-2.29886E-04
131	10.9983	31.1663	-3.7217E-05	-1205.759	-1965.2098	-1.38154E-04
132	11.0649	31.3549	3.8444E-05	-957.879	-1514.8464	-1.02225E-04
133	9.2179	27.3905	-2.8335E-04	-7365.231	-13312.5389	-1.07331E-03
134	9.2643	27.6911	-3.0593E-04	-7976.556	-12472.5415	-9.69813E-04
135	9.4200	28.1534	-2.4302E-04	-6205.543	-10670.2603	-8.36411E-04
136	9.5757	28.6157	-2.1690E-04	-5295.661	-8965.5090	-7.11345E-04
137	9.7294	29.0780	-1.9918E-04	-4855.359	-7678.9275	-5.96147E-04
138	9.8830	29.5403	-1.8412E-04	-4025.336	-6303.2062	-4.86955E-04
139	10.0387	30.0026	-1.6172E-04	-3492.996	-5173.9170	-3.84548E-04
140	10.1934	30.4649	-1.2284E-04	-2726.098	-3911.9743	-2.85496E-04
141	10.3481	30.9272	-8.6161E-05	-2040.177	-2830.9965	-1.91296E-04
142	10.5028	31.3895	-5.7704E-05	-1205.061	-1520.6954	-9.96428E-05
143	8.7295	27.6849	-3.1235E-04	-7500.299	-12723.6517	-1.00679E-03
144	8.8761	28.1513	-2.4925E-04	-6270.792	-11013.9649	-8.79685E-04
145	9.0227	28.6177	-2.3004E-04	-5544.430	-9427.2468	-7.46097E-04
146	9.1693	29.0812	-2.1541E-04	-4906.057	-7966.9447	-6.22253E-04
147	9.3159	29.5462	-1.9194E-04	-4282.550	-6642.4110	-5.05706E-04
148	9.4625	30.0111	-1.6150E-04	-3558.133	-5330.9095	-3.97208E-04
149	9.6091	30.4760	-1.2364E-04	-2813.602	-4092.6445	-2.93714E-04
150	9.7556	30.9410	-8.6906E-05	-2086.158	-2900.9968	-1.95262E-04
151	9.9022	31.4059	-4.8771E-05	-1234.723	-1620.1791	-1.00028E-04
152	8.1967	27.6715	-3.2531E-04	-7400.113	-12188.6716	-1.06822E-03
153	8.3351	28.1390	-1.2450E-04	-4796.838	-10853.5830	-9.33713E-04
154	8.4736	28.6064	-2.3908E-04	-5614.973	-9750.3437	-7.88652E-04
155	8.6121	29.0738	-2.6048E-04	-5408.068	-8357.3207	-6.52812E-04
156	8.7505	29.5412	-2.1926E-04	-4620.856	-6949.5901	-5.28819E-04
157	8.8890	30.0087	-1.8256E-04	-3867.471	-5600.9527	-4.13043E-04
158	9.0274	30.4761	-1.3614E-04	-3009.121	-4277.7891	-3.04856E-04
159	9.1659	30.9435	-9.9019E-05	-2206.908	-3013.8203	-2.01401E-04
160	9.3043	31.4109	-7.6681E-05	-1690.763	-1680.1903	-1.01874E-04
161	7.6697	27.6562	1.2016E-04	-3426.961	-13080.6782	-1.16347E-03
162	7.8000	28.1260	-1.0591E-05	-3759.375	-11203.7331	-1.00094E-03
163	7.9303	28.5957	-2.3244E-04	-5462.829	-10026.8617	-8.38721E-04
164	8.0606	29.0655	-2.7854E-04	-5759.164	-8825.0017	-6.85943E-04
165	8.1909	29.5353	-2.6196E-04	-5164.758	-7346.5747	-5.51988E-04
166	8.3211	30.0050	-2.0120E-04	-4185.439	-5906.9394	-4.30114E-04
167	8.4514	30.4748	-1.5253E-04	-3259.697	-4484.2198	-3.16055E-04
168	8.5817	30.9446	-1.0332E-04	-2341.003	-3131.1328	-2.08404E-04
169	8.7120	31.4144	-6.1733E-05	-1397.974	-1712.9714	-1.03627E-04
170	7.5329	28.2116	-3.5029E-05	-1139.999	-11515.9302	-1.01550E-03
171	7.3239	28.5248	-4.5154E-04	-8659.361	-12283.3669	-9.32336E-04
172	7.3612	28.6701	-4.5778E-04	-8686.857	-11779.1073	-8.68046E-04
173	7.4760	29.1173	-3.9841E-04	-7439.519	-9844.3459	-7.04454E-04
174	7.5909	29.5645	-2.7655E-04	-5655.962	-7846.3750	-5.67726E-04
175	7.7057	30.0116	-2.1403E-04	-4578.999	-6288.5936	-4.46433E-04
176	7.8205	30.4588	-1.6323E-04	-3528.736	-4805.2147	-3.32990E-04
177	7.9353	30.9060	-9.8816E-05	-2391.422	-3344.8567	-2.25621E-04
178	8.0501	31.3532	-7.2821E-05	-1550.659	-1918.9998	-1.21807E-04

UPPER HATCH
NODES 117-178

Figure 1D. (Continued).

NODE	R	Z	LONGITUDINAL STRAIN	LONGITUDINAL STRESS	HOOP STRESS	HOOP STRAIN
179	6.8990	28.9521	-5.3956E-04	-9207.409	-11648.0897	-7.96889E-04
180	6.9829	29.5603	-3.6477E-04	-6892.977	-8553.8148	-5.93983E-04
181	7.1315	30.1685	-2.3811E-04	-4759.154	-6141.5092	-4.21900E-04
182	7.2753	30.7768	-1.2514E-04	-2913.777	-3986.9996	-2.67924E-04
183	7.4191	31.3850	-7.1133E-05	-1443.609	-1810.8570	-1.19974E-04
184	6.2342	29.0891	-7.3795E-04	-11487.664	-11713.3930	-7.67031E-04
185	6.3672	29.7002	-4.6286E-04	-7726.435	-8571.4227	-5.75093E-04
186	6.4982	30.3113	-2.5264E-04	-4852.279	-5986.1443	-4.02673E-04
187	6.6292	30.9224	-1.2101E-04	-2743.093	-3667.1222	-2.43893E-04
188	6.7602	31.5335	2.0371E-05	-495.969	-1369.0072	-9.58498E-05
189	5.6254	29.2133	-5.7555E-04	-9853.238	-10883.1070	-7.38880E-04
190	5.7438	29.8220	-4.6414E-04	-7540.752	-8218.3180	-5.56067E-04
191	5.8620	30.4307	-2.8491E-04	-5035.219	-5775.5263	-3.83251E-04
192	5.9801	31.0394	-1.2323E-04	-2667.152	-3430.5924	-2.24728E-04
193	6.0983	31.6482	-4.8318E-05	-988.665	-1181.4694	-7.39453E-05
194	5.0124	29.3247	-6.6994E-04	-10395.955	-10811.3092	-7.19448E-04
195	5.1179	29.9907	-4.7342E-04	-7500.457	-7968.8309	-5.35560E-04
196	5.2232	30.6568	-2.9160E-04	-5477.575	-5539.8412	-3.66285E-04
197	5.3285	31.3229	-1.2881E-04	-2622.391	-3201.6344	-2.05800E-04
198	5.4338	31.9889	2.4532E-05	-207.801	-868.0566	-5.82826E-05
199	4.3923	29.4232	-5.6558E-04	-9362.916	-10368.8906	-6.99245E-04
200	4.4893	30.0919	-4.7148E-04	-7410.912	-7770.4775	-5.19660E-04
201	4.5821	30.7605	-2.9586E-04	-5439.593	-5337.2792	-3.48676E-04
202	4.6745	31.4276	-1.2847E-04	-2560.825	-3037.2705	-1.91794E-04
203	4.7663	32.8958	-5.1436E-05	-903.993	-836.4157	-4.26254E-05
204	3.7802	29.5089	-6.6306E-04	-10245.477	-10404.2624	-6.84076E-04
205	3.8596	30.1288	-4.7317E-04	-7360.194	-7580.6033	-5.02411E-04
206	3.9390	30.7487	-2.9094E-04	-4848.813	-5191.3118	-3.36440E-04
207	4.0184	31.3687	-1.2922E-04	-2513.956	-2879.1635	-1.77769E-04
208	4.0978	31.9886	2.5591E-05	-153.864	-588.8716	-3.22653E-05
209	3.1614	29.5816	-5.7783E-04	-9377.036	-10034.1657	-6.65178E-04
210	3.2278	30.2030	-4.6760E-04	-7281.917	-7457.0311	-4.90844E-04
211	3.2942	30.8245	-2.8679E-04	-4771.446	-5052.0155	-3.24026E-04
212	3.3606	31.4459	-1.1990E-04	-2399.996	-2780.2388	-1.70451E-04
213	3.4270	32.0674	-4.8654E-05	-295.581	-598.5164	-2.24288E-05
214	2.5412	29.6413	-7.4888E-04	-11078.427	-10257.0314	-6.39618E-04
215	2.5995	30.2640	-4.7608E-04	-7389.857	-7396.5972	-4.77633E-04
216	2.6579	30.8867	-2.6252E-04	-4539.073	-4988.1084	-3.22220E-04
217	2.7013	31.5094	-1.1749E-04	-2316.181	-2679.5993	-1.65804E-04
218	2.7547	32.1321	2.7879E-05	-76.995	-431.9118	-1.93926E-05
219	1.9198	29.6880	-5.4616E-04	-8429.722	-8994.5422	-5.75574E-04
220	1.9602	30.3117	-4.0302E-04	-6536.064	-7144.6089	-4.83954E-04
221	2.0005	30.9354	-2.5155E-04	-4296.990	-4888.8967	-3.30241E-04
222	2.0408	31.5591	-1.0111E-04	-2074.924	-2598.4038	-1.70705E-04
223	2.0812	32.1828	-3.0940E-05	-474.983	-396.4596	-1.98068E-05
224	1.5000	29.3500	-4.2814E-04	-6385.529	-7146.7916	-5.29306E-04
225	1.5000	29.9910	-4.4531E-04	-7340.752	-8375.5391	-5.82920E-04
226	1.5000	30.6320	-3.0898E-04	-5260.498	-6614.7672	-4.89082E-04
227	1.5000	30.9730	-2.2610E-04	-3993.883	-4894.3954	-3.52477E-04
228	1.5000	31.5140	-1.3867E-04	-2425.834	-2938.7720	-2.06832E-04
229	1.5000	32.0550	-4.5290E-05	-810.040	-909.3383	-5.83982E-05
230	1.5000	32.5960	1.0110E-05	233.031	557.7692	5.32980E-05
231	1.0000	29.3500	-1.6232E-04	-4088.217	-8040.8563	-6.87980E-04
232	1.0000	29.9910	-1.9529E-04	-4311.314	-7956.3047	-6.80060E-04
233	1.0000	30.6320	-2.0456E-04	-4201.828	-7065.7673	-5.89464E-04
234	1.0000	30.9730	-1.2604E-04	-2807.250	-5086.2821	-4.29122E-04
235	1.0000	31.5140	-7.2510E-05	-1895.844	-3248.5306	-2.57385E-04
236	1.0000	32.0550	-2.8388E-05	-712.440	-1066.0179	-7.53408E-05
237	1.0000	32.5960	3.9017E-05	915.417	566.6736	5.90629E-05
238	.5000	29.3500	-6.8484E-05	-6736.985	-15835.9041	-1.27860E-03
239	.5000	29.8910	-2.3950E-05	-6292.109	-16167.6661	-1.33739E-03
240	.5000	30.4320	-7.0878E-05	-5483.216	-12860.7786	-1.05209E-03

UPPER HATCH
NODES 179-240

Figure 1D. (Continued).

NODE	R	Z	LONGITUDINAL STRAIN	LONGITUDINAL STRESS	HOOP STRESS	HOOP STRAIN
241	.5000	30.9730	-9.0822E-06	-3955.348	-10302.9407	-8.53292E-04
242	.5000	31.5140	-1.9234E-05	-2591.412	-6043.8953	-4.78373E-04
243	.5000	32.0550	4.7102E-05	-744.258	-2497.5735	-1.86135E-04
244	.5000	32.5960	3.5745E-05	669.091	1029.2964	8.36687E-05

UPPER HATCH
NODES 241-244

Figure 1D. (Continued).

NODAL COORDINATES — LOWER PLATE NEMO 2000

NODE	R	Z	Longitudinal Strain	Longitudinal Stress	Hoop Stress	Hoop Strain
1	20.5061	20.5061	-5.8484E-03	-3671.763	-3676.4302	-6.31204E-03
2	21.2132	21.2132	-6.0453E-03	-3751.949	-3577.2228	-5.94492E-03
3	21.9203	21.9203	-6.4328E-03	-3971.937	-3584.4522	-5.61919E-03
4	22.6274	22.6274	-6.7910E-03	-4189.406	-3596.0460	-5.32294E-03
5	23.3345	23.3345	-6.9880E-03	-4270.739	-3540.1721	-5.05924E-03
6	19.7780	21.2093	-5.6478E-03	-3576.233	-3648.8519	-6.31812E-03
7	20.4600	21.9406	-6.0725E-03	-3752.318	-3570.0445	-5.92599E-03
8	21.1419	22.6720	-6.4572E-03	-3974.803	-3565.4069	-5.57055E-03
9	21.8239	23.4033	-6.8288E-03	-4190.593	-3569.6790	-5.25458E-03
10	22.5059	24.1347	-7.2071E-03	-4355.982	-3524.6634	-4.96247E-03
11	19.0257	21.8866	-5.9980E-03	-3715.048	-3686.1243	-6.29603E-03
12	19.6818	22.6913	-6.1613E-03	-3782.072	-3555.5094	-5.86588E-03
13	20.3378	23.3960	-6.5303E-03	-3993.372	-3537.5025	-5.48620E-03
14	20.9939	24.1507	-6.8891E-03	-4198.631	-3525.9738	-5.13963E-03
15	21.6499	24.9054	-7.0823E-03	-4273.136	-3444.2123	-4.82618E-03
16	18.2503	22.5372	-5.8711E-03	-3661.119	-3641.6826	-6.23128E-03
17	18.8796	23.3144	-6.2710E-03	-3812.950	-3525.9564	-5.76900E-03
18	19.5089	24.0915	-6.6287E-03	-4014.419	-3491.5672	-5.35463E-03
19	20.1383	24.8687	-6.9730E-03	-4210.809	-3467.7744	-4.98334E-03
20	20.7676	25.6458	-7.3331E-03	-4358.201	-3394.6239	-4.63768E-03
21	17.4526	23.1604	-6.2836E-03	-3837.068	-3658.9880	-6.21862E-03
22	18.0545	23.9491	-6.4615E-03	-3872.850	-3486.0376	-5.62226E-03
23	18.6563	24.7377	-6.7611E-03	-4042.708	-3430.2237	-5.17831E-03
24	19.2581	25.5263	-7.0471E-03	-4207.498	-3383.4606	-4.77425E-03
25	19.8599	26.3550	-7.2151E-03	-4260.329	-3269.6393	-4.40229E-03
26	16.6337	23.7559	-6.4144E-03	-3859.667	-3599.1075	-5.97170E-03
27	17.2073	24.5746	-6.6922E-03	-3990.893	-3428.4066	-5.42715E-03
28	17.7809	25.3937	-6.9256E-03	-4075.651	-3348.4152	-4.94726E-03
29	18.3544	26.2129	-7.1595E-03	-4213.858	-3282.6041	-4.51476E-03
30	18.9280	27.0320	-7.4229E-03	-4308.697	-3168.6544	-4.10934E-03
31	15.7995	24.3219	-6.9396E-03	-4069.804	-3585.3381	-5.76046E-03
32	16.3392	25.1601	-7.0296E-03	-4095.938	-3358.1778	-5.17031E-03
33	16.8838	25.9988	-7.1982E-03	-4124.169	-3247.8314	-4.65846E-03
34	17.4284	26.8375	-7.2980E-03	-4197.883	-3150.5676	-4.19596E-03
35	17.9731	27.6761	-7.3990E-03	-4207.823	-2996.4109	-3.76068E-03
36	14.9361	24.8579	-7.4069E-03	-4220.322	-3509.3322	-5.47581E-03
37	15.4511	25.7150	-7.4343E-03	-4172.659	-3266.0988	-4.84604E-03
38	15.9662	26.5722	-7.4189E-03	-4183.568	-3123.1644	-4.30396E-03
39	16.4812	27.4294	-7.4068E-03	-4202.491	-2998.9216	-3.81403E-03
40	16.9963	28.2865	-7.4425E-03	-4189.508	-2830.8200	-3.35056E-03
41	14.0595	25.3640	-7.4522E-03	-4416.341	-3429.6796	-5.10823E-03
42	14.5443	26.2386	-7.4151E-03	-4316.163	-3143.3912	-4.43923E-03
43	15.0291	27.1132	-7.7331E-03	-4293.040	-2962.8800	-3.87092E-03
44	15.5139	27.9878	-7.5155E-03	-4169.591	-2805.0892	-3.36390E-03
45	15.9987	28.8625	-7.4576E-03	-4098.352	-2599.6923	-2.87392E-03
46	13.6197	25.6055	-8.5116E-03	-4628.835	-3402.7965	-4.88617E-03
47	14.0891	26.4889	-8.2848E-03	-4442.808	-3085.9731	-4.19696E-03
48	14.5536	27.3714	-8.0019E-03	-4323.240	-2891.3813	-3.62342E-03
49	15.0231	28.2543	-7.6473E-03	-4187.699	-2710.6170	-3.10717E-03
50	15.4926	29.1373	-7.3699E-03	-4025.044	-2483.5073	-2.61463E-03
51	13.1667	25.8392	-8.8256E-03	-4733.921	-3337.6310	-4.63183E-03
52	13.6147	26.7302	-8.6993E-03	-4583.706	-3022.0703	-3.92902E-03
53	14.0737	27.6212	-8.2908E-03	-4383.485	-2798.1215	-3.34580E-03
54	14.5277	28.5122	-7.7011E-03	-4163.590	-2593.8571	-2.83544E-03

LOWER PLATE
NODES 1-54

Figure 2D. Predicted stress and strains for bottom penetration plate.

NODE	R	Z	LONGITUDINAL STRAIN	LONGITUDINAL STRESS	HOOP STRESS	HOOP STRAIN
55	14.9817	29.4032	-7.9815E-03	-4029.979	-2368.1943	-2.33432E-03
56	12.7128	26.0650	-9.4785E-03	-4977.742	-3291.9706	-4.34486E-03
57	13.1511	26.9638	-9.0653E-03	-4700.856	-2935.1585	-3.62443E-03
58	13.5895	27.8626	-8.5515E-03	-4369.491	-2705.6408	-3.04676E-03
59	14.0279	28.7614	-7.8284E-03	-4175.173	-2480.4011	-2.53534E-03
60	14.4662	29.6602	-7.1745E-03	-3843.514	-2201.8182	-2.04616E-03
61	12.2559	26.2829	-9.8165E-03	-5083.806	-3198.4056	-4.01608E-03
62	12.6785	27.1842	-9.6249E-03	-4904.796	-2867.0120	-3.28631E-03
63	13.1012	28.0855	-8.8244E-03	-4550.547	-2601.6770	-2.70821E-03
64	13.5238	29.0018	-7.9947E-03	-4159.351	-2352.3312	-2.22237E-03
65	13.9464	29.9082	-7.4410E-03	-3913.653	-2100.0426	-1.73561E-03
66	11.7954	26.4928	-1.0646E-02	-5394.113	-3138.0859	-3.64338E-03
67	12.2021	27.4064	-1.0035E-02	-5038.336	-2759.9626	-2.89662E-03
68	12.6088	28.3199	-9.1836E-03	-4664.294	-2505.0667	-2.34724E-03
69	13.0156	29.2335	-7.9877E-03	-4160.339	-2227.6479	-1.87458E-03
70	13.4223	30.1470	-6.8233E-03	-3600.308	-1892.3343	-1.42946E-03
71	11.3312	26.6996	-1.1228E-02	-5595.557	-3035.1541	-3.21224E-03
72	11.7219	27.6151	-1.0874E-02	-5409.871	-2751.4027	-2.45929E-03
73	12.1127	28.5357	-9.3997E-03	-4764.554	-2416.1246	-1.93505E-03
74	12.5034	29.4562	-7.9850E-03	-4159.980	-2126.6255	-1.52273E-03
75	12.8941	30.3767	-7.0300E-03	-3640.688	-1771.5039	-1.10184E-03
76	10.8636	26.8883	-1.2620E-02	-6129.473	-2994.2539	-2.71028E-03
77	11.0509	27.3519	-1.2135E-02	-5882.632	-2775.6018	-2.28787E-03
78	11.2382	27.8155	-1.1279E-02	-5648.477	-2735.1007	-1.96314E-03
79	11.4255	28.2791	-1.0340E-02	-5163.021	-2461.6637	-1.71860E-03
80	11.6128	28.7427	-9.4288E-03	-4868.589	-2392.5822	-1.50948E-03
81	11.8001	29.2063	-8.7529E-03	-4485.706	-2155.8415	-1.32306E-03
82	11.9874	29.6699	-7.9906E-03	-4162.041	-2029.1135	-1.14601E-03
83	12.1747	30.1335	-7.1481E-03	-3711.582	-1762.6422	-9.64454E-04
84	12.3620	30.5971	-6.4789E-03	-3412.631	-1624.4482	-7.94959E-04
85	10.3927	27.0738	-1.5298E-02	-7251.659	-3136.2059	-2.06682E-03
86	10.5719	27.5406	-1.3033E-02	-6466.471	-2921.6216	-1.63034E-03
87	10.7510	28.0074	-1.1165E-02	-5641.309	-2614.2474	-1.42822E-03
88	10.9302	28.4742	-1.0121E-02	-5222.125	-2447.7751	-1.20814E-03
89	11.1094	28.9410	-9.2168E-03	-4806.994	-2264.5843	-1.06828E-03
90	11.2886	29.4078	-8.9518E-03	-4955.312	-2091.8193	-8.99796E-04
91	11.4678	29.8746	-7.7366E-03	-4085.230	-1896.9618	-7.74425E-04
92	11.6470	30.3414	-6.9733E-03	-3708.254	-1702.0973	-6.17725E-04
93	11.8261	30.8082	-6.2936E-03	-3349.163	-1519.2830	-5.02206E-04
94	9.8331	27.0162	-8.9827E-06	-4334.719	-12904.3074	-1.14847E-03
95	9.9186	27.2511	-5.1039E-03	-5918.467	-9424.8996	-1.09603E-03
96	10.0896	27.7209	-6.5671E-03	-6389.380	-7186.4579	-9.69679E-04
97	10.2606	28.1908	-5.7356E-03	-5564.630	-6122.3294	-8.36668E-04
98	10.4316	28.6606	-4.9914E-03	-5218.370	-5405.0885	-7.16721E-04
99	10.6026	29.1305	-4.6470E-03	-4747.523	-4713.2604	-6.01837E-04
100	10.7736	29.6003	-4.1890E-03	-4459.062	-4191.2160	-4.98137E-04
101	10.9446	30.0702	-3.8775E-03	-3999.153	-3601.1412	-3.97636E-04
102	11.1157	30.5400	-3.4509E-03	-3556.013	-3102.0460	-3.00313E-04
103	11.2867	31.0099	-2.2659E-03	-2475.584	-2514.4309	-1.98499E-04
104	11.4577	31.4797	9.7966E-05	-36.196	-1519.7179	-9.98621E-05
105	11.6287	31.9495	9.2617E-05	622.465	- 109.3408	-4.73497E-06
106	9.3178	27.0607	2.7093E-05	-4327.590	-13601.2316	-1.20629E-03
107	9.4415	27.4200	-8.1995E-05	-4703.387	-12378.8248	-1.10271E-03
108	9.6043	27.8928	-1.4360E-04	-5266.758	-11052.4048	-9.62755E-04
109	9.7670	28.3656	-2.5401E-04	-5379.510	-9675.8467	-8.25726E-04
110	9.9298	28.8383	-2.6625E-04	-5071.719	-8319.2223	-6.97888E-04
111	10.0926	29.3111	-2.5806E-04	-4724.427	-7158.6530	-5.81623E-04
112	10.2554	29.7838	-2.4022E-04	-4304.016	-6051.7859	-4.72541E-04
113	10.4182	30.2566	-2.1234E-04	-3773.673	-4958.3352	-3.69785E-04
114	10.5810	30.7294	-1.3494E-04	-2820.945	-3830.5302	-2.69106E-04
115	10.7437	31.2021	-5.3436E-05	-1577.430	-2441.1379	-1.68171E-04
116	10.9879	31.9113	5.8405E-05	256.719	-318.5787	-1.81227E-05

LOWER PLATE
NODES 55-116

Figure 2D. (Continued).

NODE	R	Z	LONGITUDINAL STRAIN	LONGITUDINAL STRESS	HOOP STRESS	HOOP STRAIN
117	8.7761	27.0100	2.6118E-04	-2215.533	-14022.0108	-1.30900E-03
118	8.9615	27.5806	5.3100E-05	-3364.573	-12176.6055	-1.11863E-03
119	9.1160	28.0562	-1.7012E-04	-5142.670	-11110.2074	-9.63350E-04
120	9.2705	28.5317	-2.3664E-04	-5336.300	-9689.1365	-8.15197E-04
121	9.4250	29.0072	-2.6918E-04	-5287.017	-8391.3637	-6.81830E-04
122	9.5795	29.4828	-2.5672E-04	-4799.935	-7074.0331	-5.59052E-04
123	9.7340	29.9583	-2.3857E-04	-4266.199	-5837.0761	-4.47431E-04
124	9.8885	30.4338	-1.9600E-04	-3519.686	-4602.4514	-3.39962E-04
125	10.0431	30.9093	-1.4267E-04	-2628.266	-3348.1486	-2.38362E-04
126	10.1976	31.3849	-3.7295E-05	-1102.753	-1932.1793	-1.36846E-04
127	10.3675	31.9079	7.7618E-05	496.759	-273.9907	-2.48937E-05
128	8.2791	27.0634	2.5619E-04	-2808.321	-15208.8778	-1.39295E-03
129	8.4788	27.7328	1.0638E-04	-3115.490	-12547.6457	-1.14761E-03
130	8.6250	28.2110	-1.4602E-04	-5086.431	-11271.6440	-9.68043E-04
131	8.7712	28.6891	-2.7467E-04	-6090.337	-10089.5583	-8.06163E-04
132	8.9173	29.1673	-2.7075E-04	-5504.263	-8461.9845	-6.63952E-04
133	9.0635	29.6454	-2.5828E-04	-4961.469	-7066.4837	-5.38178E-04
134	9.2097	30.1236	-2.2892E-04	-4180.650	-5626.9861	-4.20749E-04
135	9.3559	30.6018	-1.7624E-04	-3340.192	-4361.5820	-3.12078E-04
136	9.5021	31.0799	-1.1967E-04	-2278.993	-2934.0408	-2.06787E-04
137	9.6483	31.5581	-4.9613E-05	-1099.896	-1528.7493	-1.06564E-04
138	9.9383	31.9081	9.3807E-05	183.149	-363.8600	-2.89866E-05
139	8.2364	27.8058	5.2430E-04	311.939	-12406.6078	-1.16769E-03
140	8.0900	28.2130	-2.2086E-04	-6561.645	-12722.4868	-1.03925E-03
141	8.2002	28.5975	-3.6661E-04	-7655.984	-11515.2820	-8.79033E-04
142	8.3725	29.1983	-2.8837E-04	-6035.366	-8999.7878	-6.82391E-04
143	8.5448	29.7991	-2.4825E-04	-5032.705	-7041.3076	-5.15351E-04
144	8.7170	30.3999	-1.9296E-04	-3882.859	-5201.7506	-3.68363E-04
145	8.8893	31.0007	-1.5684E-04	-2891.222	-3439.9188	-2.29811E-04
146	8.9944	31.1929	-1.2577E-04	-2502.897	-2976.9305	-1.88807E-04
147	7.6740	28.6397	-6.7664E-04	-11277.611	-13077.4914	-9.14419E-04
148	7.6999	28.7363	-6.1301E-04	-10618.975	-12575.2348	-8.71900E-04
149	7.8616	29.3400	-3.7218E-04	-7194.293	-9409.1195	-6.66415E-04
150	8.0234	29.9437	-2.4162E-04	-5170.548	-7089.9932	-4.96855E-04
151	8.1852	30.5474	-1.8727E-04	-3840.269	-5012.9351	-3.43232E-04
152	8.3469	31.1511	-1.4652E-04	-2730.647	-3134.1199	-2.00172E-04
153	7.1821	28.8701	-6.1896E-04	-10980.659	-12731.9406	-8.50584E-04
154	7.3329	29.4766	-4.2126E-04	-7659.662	-9386.6405	-6.56606E-04
155	7.4838	30.0831	-2.7965E-04	-5481.309	-6965.2212	-4.76917E-04
156	7.6347	30.6896	-1.6530E-04	-3558.511	-4725.6134	-3.20516E-04
157	7.7856	31.2961	-1.2285E-04	-2198.446	-2554.4933	-1.70203E-04
158	6.6619	28.9995	-7.6983E-04	-12131.119	-12550.7194	-8.25149E-04
159	6.8019	29.6036	-5.0229E-04	-8367.919	-9344.1831	-6.31884E-04
160	6.9418	30.2128	-2.9528E-04	-5534.379	-6763.2408	-4.58596E-04
161	7.0818	30.8219	-1.6124E-04	-3397.466	-4425.9522	-2.98043E-04
162	7.2218	31.4310	-3.0086E-05	-1184.554	-2070.2821	-1.47877E-04
163	6.1397	29.1096	-6.1889E-04	-10386.796	-11747.2758	-7.99523E-04
164	6.2686	29.7211	-5.0585E-04	-8206.895	-9021.3042	-6.13920E-04
165	6.3976	30.3327	-3.2406E-04	-5686.955	-6556.8679	-4.39623E-04
166	6.5266	30.9442	-1.6097E-04	-3296.413	-4189.4720	-2.79689E-04
167	6.6556	31.5558	-8.4802E-05	-1591.532	-1908.6411	-1.26952E-04
168	5.6159	29.2152	-7.1803E-04	-11268.305	-11738.6278	-7.80317E-04
169	5.7339	29.8240	-5.1821E-04	-8228.645	-8800.4791	-5.94060E-04
170	5.8513	30.4328	-3.3027E-04	-5630.285	-6328.9360	-4.23064E-04
171	5.9693	31.0565	-1.6902E-04	-3225.452	-3956.6594	-2.61206E-04
172	6.0873	31.6703	-2.5653E-06	-732.831	-1554.2827	-1.11804E-04
173	5.0893	29.3115	-6.1554E-04	-10158.338	-11243.0807	-7.59624E-04
174	5.1962	29.9272	-5.1725E-04	-8138.325	-8596.4122	-5.78009E-04
175	5.3032	30.5430	-3.3684E-04	-5610.815	-6128.3382	-4.05558E-04
176	5.4101	31.1588	-1.6900E-04	-3163.893	-3789.3467	-2.47132E-04
177	5.5170	31.7746	-8.2696E-05	-1494.258	-1553.8145	-9.65694E-05
178	5.5616	29.3982	-7.1311E-04	-11056.922	-11286.5408	-7.43480E-04

LOWER PLATE
NODES 116-178

Figure 2D. (Continued).

NODE	R	Z	LONGITUDINAL STRAIN	LONGITUDINAL STRESS	HOOP STRESS	HOOP STRAIN
179	4.6574	30.0158	-5.2090E-04	-8102.076	-8399.8929	-5.60377E-04
180	4.7533	30.6339	-3.3514E-04	-5590.226	-5970.5157	-3.92278E-04
181	4.8991	31.2510	-1.6606E-04	-3122.003	-3622.7174	-2.32604E-04
182	4.9999	31.4684	9.1168E-06	-599.483	-1266.3934	-8.62531E-05
183	4.0324	29.4755	-6.1728E-04	-10092.206	-10854.1564	-7.25150E-04
184	4.1171	30.0997	-5.1832E-04	-8033.372	-8250.6367	-5.47119E-04
185	4.2018	30.7139	-3.3684E-04	-5503.543	-5813.6615	-3.78010E-04
186	4.2865	31.3331	-1.6690E-04	-3059.811	-3511.8340	-2.22975E-04
187	4.3713	31.9529	-8.2490E-05	-1375.699	-1326.8182	-7.59141E-05
188	3.5019	29.5932	-7.2909E-04	-11061.230	-10954.2003	-7.09756E-04
189	3.5755	30.1638	-5.2149E-04	-8023.108	-8101.8961	-5.31900E-04
190	3.6490	30.7345	-3.3011E-04	-5416.808	-5709.4614	-3.68978E-04
191	3.7226	31.4051	-1.6260E-04	-3021.293	-3402.8076	-2.13304E-04
192	3.7962	32.0258	6.9758E-06	-517.703	-1105.8061	-7.12623E-05
193	2.9703	29.6019	-6.3097E-04	-10068.432	-10504.8771	-6.88970E-04
194	3.0327	30.2232	-5.1219E-04	-7912.092	-7983.8346	-5.21684E-04
195	3.0951	30.8451	-3.2516E-04	-5353.927	-5613.5132	-3.59646E-04
196	3.1575	31.4670	-1.5996E-04	-2938.437	-3357.7620	-2.10194E-04
197	3.2199	32.0889	-7.9703E-05	-1321.762	-1232.6316	-6.78192E-05
198	2.4377	29.6500	-6.0812E-04	-11881.483	-10772.3298	-6.60573E-04
199	2.4889	30.2729	-5.1557E-04	-8013.731	-7967.2592	-5.09371E-04
200	2.5401	30.8957	-2.9826E-04	-5112.742	-5583.8795	-3.60872E-04
201	2.5913	31.5187	-1.5953E-04	-2899.668	-3315.7473	-2.09821E-04
202	2.6425	32.1416	1.8870E-05	-471.473	-1148.9319	-7.12947E-05
203	1.9043	29.6899	-5.9679E-04	-9339.456	-9332.6632	-5.95814E-04
204	1.9493	30.3127	-3.9917E-04	-6658.136	-7600.0851	-5.19438E-04
205	1.9943	30.9369	-2.8837E-04	-4977.158	-5603.2436	-3.71572E-04
206	2.0293	31.5601	-1.6238E-04	-2995.500	-3365.4120	-2.18169E-04
207	2.0643	32.1839	-7.1233E-05	-1305.172	-1352.8593	-7.75265E-05
208	1.5000	29.3500	-4.9160E-04	-6527.462	-7230.7929	-5.35042E-04
209	1.5000	29.8910	-4.6072E-04	-7634.899	-8753.4221	-6.09471E-04
210	1.5000	30.4320	-3.4175E-04	-5746.471	-7206.6853	-5.35879E-04
211	1.5000	30.9730	-2.5457E-04	-4587.928	-5647.4558	-3.97421E-04
212	1.5000	31.5140	-1.4995E-04	-2800.879	-3625.0875	-2.54526E-04
213	1.5000	32.0550	-7.6823E-05	-1596.271	-1934.8245	-1.21811E-04
214	1.5000	32.5960	-2.8052E-05	-690.165	-583.5689	-2.05240E-05
215	1.0000	29.3500	-1.6316E-04	-4091.399	-8096.3900	-6.95792E-04
216	1.0000	29.8910	-2.0521E-04	-4535.508	-8356.0300	-7.13328E-04
217	1.0000	30.4320	-2.3197E-04	-4649.579	-7749.5426	-6.43757E-04
218	1.0000	30.9730	-1.9006E-04	-3203.989	-5810.2507	-4.86650E-04
219	1.0000	31.5140	-8.3669E-05	-2298.554	-4084.0242	-3.21114E-04
220	1.0000	32.0550	-2.7995E-05	-1129.930	-2093.7648	-1.55660E-04
221	1.0000	32.5960	6.3853E-06	-296.079	-552.9774	-2.77829E-05
222	.5000	29.3500	-7.0267E-05	-4767.431	-15976.4860	-1.29502E-03
223	.5000	29.8910	-2.6529E-05	-4593.325	-16932.6708	-1.40165E-03
224	.5000	30.4320	-7.7342E-05	-5993.329	-14035.9815	-1.14701E-03
225	.5000	30.9730	-6.9011E-06	-4518.922	-11785.9885	-9.72891E-04
226	.5000	31.5140	-1.6045E-05	-3261.710	-7694.6621	-6.05593E-04
227	.5000	32.0550	2.5800E-05	-1714.554	-4539.8330	-3.49656E-04
228	.5000	32.5960	3.0162E-05	-173.179	-956.8047	-7.40681E-05

LOWER PLATE
NODES 179-228

Figure 2D. (Continued).